

307216

38/1995

Acta Geologica Hungarica

VOLUME 38, NUMBER 1, 1995

18.

EDITOR-IN-CHIEF

J. HAAS

EDITORIAL BOARD

**GY. BÁRDOSSY (Chairman), G. CSÁSZÁR, G. HÁMOR,
T. KECSKEMÉTI, GY. PANTÓ, GY. POGÁCSÁS,
T. SZEDERKÉNYI, Á. KRIVÁN-HORVÁTH (Co-ordinating Editor),
H. M. LIEBERMAN (Language Editor)**

ADVISORY BOARD

**K. BIRKENMAJER (Poland), M. BLEAHU (Romania),
P. FAUPL (Austria), M. GAETANI (Italy), S. KARAMATA (Serbia),
M. KOVAČ (Slovakia), J. PAMIĆ (Croatia)**



Akadémiai Kiadó, Budapest

ACTA GEOL. HUNG. 38 (1) 1-93 (1995) HU ISSN 0236-5278

ACTA GEOLOGICA HUNGARICA

A QUARTERLY OF THE HUNGARIAN ACADEMY OF SCIENCES

Acta Geologica Hungarica publishes original studies on geology, crystallography, mineralogy, petrography, geochemistry, and paleontology.

Acta Geologica Hungarica is published in yearly volumes of four numbers by

AKADÉMIAI KIADÓ
Publishing House of the Hungarian Academy of Sciences

H-1117 Budapest Prielle Kornélia u. 19-35

Manuscripts and editorial correspondence should be addressed to the

ACTA GEOLOGICA HUNGARICA

Dr. János Haas
Academical Research Group, Department of Geology, Eötvös Loránd University of Sciences
H-1088 Budapest, Múzeum krt. 4/a, Hungary
E-mail: haas@ludens.elte.hu

Orders should be addressed to

AKADÉMIAI KIADÓ
H-1519 Budapest, P.O. Box 245, Hungary

Subscription price for Volume 38 (1995) in 4 issues US\$ 92.00, including normal postage, airmail delivery US\$ 20.00.

Acta Geologica Hungarica is abstracted/indexed in Bibliographie des Sciences de la Terre, Chemical Abstracts, Hydro-index, Mineralogical Abstract

© Akadémiai Kiadó, Budapest 1995

38
1995

507216

Facies characteristics of the Lofer cycles in the Upper Triassic platform carbonates of the Transdanubian Range, Hungary

János Haas,

*Geological Research Group,
Eötvös Loránd University, Budapest*

Anna Balog

*Department of Geol. Sciences, Virginia Polytechnic
Institute and State University, USA*

Lofer cycles are metre-scale peritidal-subtidal (lagoonal) cycles within platform carbonates. Based on observations of Upper Triassic sequences of Lofer cyclicity in the Transdanubian Range, this paper summarizes fundamental features of the basic facies and subfacies which make up the cycles. Assumed environments of deposition of the distinguished facies types are also presented.

Key words: carbonate platform, metre-scale cyclicity, facies analysis, paleoenvironment, peritidal, lagoonal, Upper Triassic, Transdanubian Range

Introduction

Due to their extension and thickness, Upper Triassic (Upper Carnian–Norian–Rhaetian) carbonate formations play a fundamental role in the construction of the Transdanubian Range. These particular formations, primarily the Main Dolomite (Fődolomit in Hungarian, which shows close similarity with the South Alpine Dolomia Principale and the Austroalpine Dachstein Dolomite, but differs from the typically bituminous, thin-bedded Hauptdolomit) and the Dachstein Limestone, extend far beyond the area of the Transdanubian Range. One can follow them all along the broad shelf of the former Tethys, from the West Carpathians, through the Eastern and the Southern Alps and also in the Dinarides and Hellenides. Even in the Himalaya and on Timor Island, the Upper Triassic formations show amazing similarity with the above-mentioned ones.

The most spectacular feature of these platform carbonates is a meter-scale cyclicity, since, due to different colour and potential for weathering of the individual members of the cycles, this feature is well visible both in the natural outcrops and the quarry exposures (Fig. 1). Rapid and long-lasting subsidence of the Tethys shelf and development of an extremely broad and level tidal flat were particularly favourable for accumulation and preservation of thick cyclic peritidal–lagoonal sequences. Considering these facts it is understandable why these formations became classic examples of cyclic shallow marine carbonates,

Addresses: J. Haas: H-1088 Budapest, Múzeum krt. 4/a, Hungary

A. Balogh: Blacksburg, Virginia, 24061-0420, USA

Received: 2 January, 1995

0236-5278/95/\$ 5.00 © 1995 Akadémiai Kiadó, Budapest

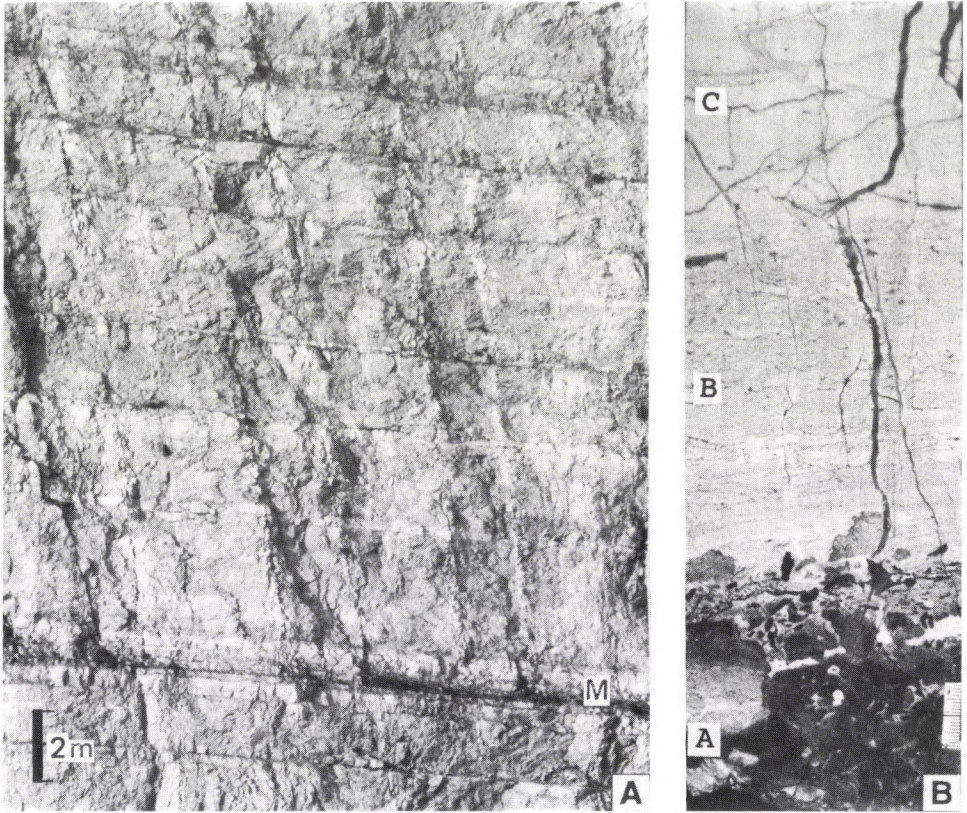


Fig. 1

Lofer cycles in the Dachstein Limestone Formation. A) Cyclic sequence in the Kecskekő quarry (Gerecse Mts) Anomalously thick facies A is indicated by letter M; B) Basal part of a Lofer cycle in core. A = member A; B = member B; C = member C; Core Porva Po-89 (Bakony Mts) 246.2–246.5 m (polished slab)

and why they form a part of almost every textbook dealing with cyclic sedimentation.

The study of these sequences was initiated as early as the last century and already in the 1930s they were the subject of pioneering sedimentological investigations (Sander 1936); in the 1960s studies on the Dachstein Limestone paved the way for the modern analysis and interpretation of cyclic carbonates (Fischer 1964); nevertheless, problems of facies interpretation and early diagenesis have not yet been completely solved, and further, more detailed, studies are necessary.

The relatively simple structure of the Transdanubian Range, with only subordinate tectonic deformation of its Triassic formations, and continuous drill-core sequences made possible a very detailed observation of the

sedimentological features, which could not be attained even in the much better exposed Alpine, Carpathian and Dinaridic sections. The results of our studies in the Transdanubian Range, mainly concerning the characteristics and cause of the cyclicity and the platform evolution, have been published in several papers (Haas and Dobosi 1982; Schwarzacher and Haas 1986; Haas 1982, 1987, 1988, 1991, 1994). The aim of the present paper is to characterize the facies which make up the cycles, and to display various types and subtypes of the basic facies. Based on facies analysis of the studied formations a general facies model was compiled, showing sites of deposition of the distinguished facies types.

Previous sedimentological description and genetic interpretation of the Lofer cycles

Sander (1936) first described the cyclothem of Dachstein Limestone as the alternation of laminated dolomitic limestone and thick-bedded limestone, to which he gave the name "Lofer facies" after the Loferer Steinberg. Sander considered the cycles as caused by sea level changes, but he did not find any evidence of subaerial exposures. He thought that the dolomitic laminae formed below wave base, at a depth of more than 200 m.

Schwarzacher (1948, 1954) investigated the characters of cyclicity and recognized the megacyclic organization of the elementary cycles.

Fischer's study (1964) on Triassic Lofer cyclothem in the Alps provided new ideas for the investigation of Upper Triassic carbonate formations. He defined the basic features of Lofer cyclothem as follows:

1. Disconformity at the base
2. Clayey red or green basal layer, which is often found only in solution cavities in the underlying rock (A-member)
3. Intertidal member consisting of algal mats and formations with shrinkage phenomena (B-member)
4. Thick-bedded subtidal member consisting of calcarenite and calcilutite with a rich marine biota (C-member).

Fischer identified the genetic features of cycle members and interpreted them on the basis of carbonate sedimentological observations in the Persian Gulf. He stated that the typical structural and textural elements of cyclothem were formed by near surface diagenesis (dolomitization, desiccation, weathering).

He described shrinkage structures (prism-cracks, sheet-cracks, birdseye pores). For a type of carbonate rock characterized by shrinkage pores ordered in lines, shrinkage cracks and sheet cracks he introduced the term "loferite", of which he recognized four different subtypes: algal mat loferite, pellet loferite, homogeneous loferite and loferite conglomerates.

Analyzing the reasons for cyclicity Fischer confirmed Sander's and Schwarzacher's theory about the annual rhythmicity of mm-thick laminae of

algal mat origin. According to his calculation each lofer cyclothem represents about 50 thousand years. Therefore he correlated Lofer cyclothem with the 41 thousand year long obliquity cycles of the Earth. He pointed out that oscillations of sea level of a few meters to 10–15 m are the direct cause for cyclic sedimentation.

In Hungary Fülöp (1976) first applied these new ideas about cyclothem in his monograph "The Mesozoic basement horst blocks of Tata".

Based on observations on cores in the Bakony Mountains Haas (1982) suggested that the ideal Lofer cycle is symmetric, in other words that, above the deepening upward A, B and C succession described by Fischer, B facies may appear again (B' member), and occasionally an in situ weathering crust (paleosol layer) may also occur (A' member). Of course, in reality, the development or preservation of the complete ideal cycle is relatively rare and the cycles are made up of various combinations of the basic facies types (Haas 1994).

Facies characteristics of the cycle members

Some of the characteristic facies types of the cycle members were described by Fischer (1964). In particular he discussed the "loferites" of member B in detail. On the basis of our own observations in the Transdanubian Range, together with the works of Fischer and others on Alpine Lofer cycles, we attempted to work out a more detailed classification for the facies types. For the classification macrotextural features (intra-breccias, microbial structure, sheet cracks etc.) and microtextural and microfacies characters were equally taken into account. The classification is shown in Fig. 2, where, beside the macroscopically distinguishable facies of the ideal Lofer cycle, the subtypes and variants are also displayed.

Facies A (members A and A')

Facies A is of red, pink, tan or greyish green colour and consists of argillaceous and/or carbonate rocks. Its thickness varies from a few cm to 30–40 cm and only rarely exceeds this figure. In some cases the thickness of facies A can reach a few metres. However, detailed observation of these beds generally revealed internal, subaerial disconformity surfaces and among them altered thin layers of facies B or C (considered to be altered "mini-cycles"). In many cases facies A fills shrinkage cracks or solution cavities.

The following subfacies can be distinguished:

A.1 *Marl* (or dolomitic marl), argillaceous marl, silty marl (Fig. 3)

A.2 *Argillaceous micritic limestone* (or dolomite)

A.2.1 *Mudstone* – containing no or only few per cent of grains (pellets, bioclasts, intraclasts). The original texture may have been pelletal, but, due to early diagenetic homogenization, it is no longer recognizable.

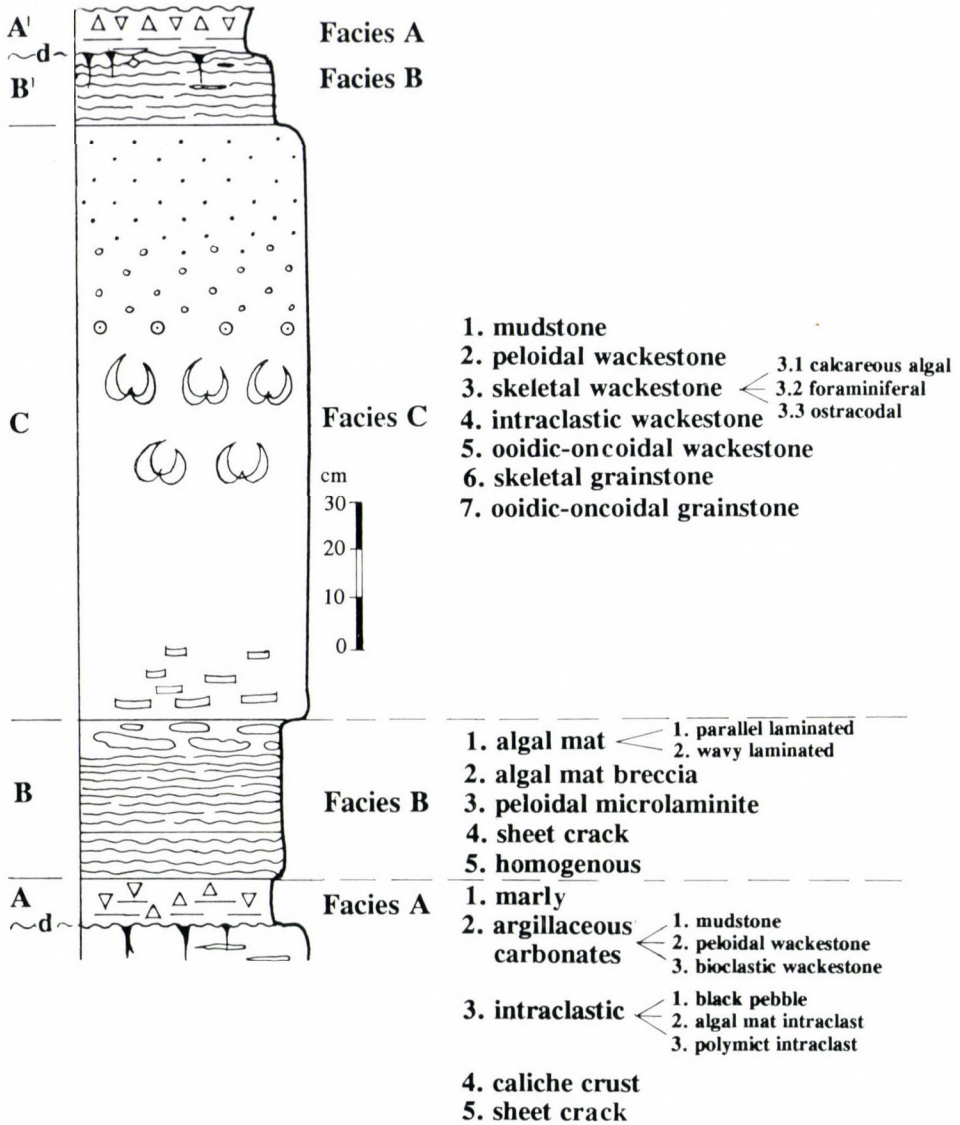


Fig. 2
The ideal Lofer cycle and facies types and variations of the cycle members. d – disconformity

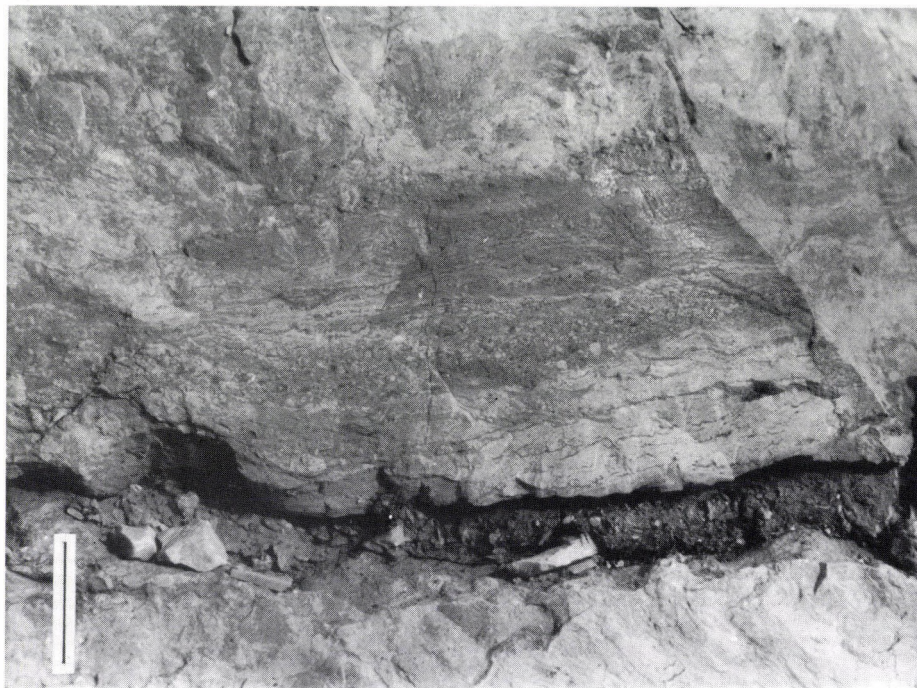


Fig. 3
Basal marl layer (A.1) above an uneven, subaerial disconformity surface. It is covered by facies B of algal mat development. Dachstein Limestone; Gorba quarry (Gerecse Mts), Scale bar = 10 cm

A.2.2 *Peloidal wackestone facies (pelmicrite)* – with pellets or peloids in a micritic matrix; bioclasts or intraclasts are scarce.

A.2.3 *Bioclastic wackestone facies (biomicrite, biopelmicrite)* – containing a significant amount of bioclasts (as much as 50%) in a micritic matrix.

The foraminiferal and the ostracodal biofacies types are particularly common.

As a rule, all the above-mentioned types of the A.2 subfacies are macroscopically unrecognizable.

A.3 *Intraclastic facies*

This lithologic type is characterized by a significant amount of intraclasts (5%) in an argillaceous micritic limestone matrix. Intraclasts can generally be seen with the naked eye. On the basis of the genetic characteristics of the predominant intraclasts the following subtypes can be distinguished:

A.3.1 *Black pebble facies* (Fig. 4, 5)

The black pebbles are dark grey or black-coloured carbonate intraclasts. Their sizes range from a few mm to a few cm. Microscopic studies revealed that the

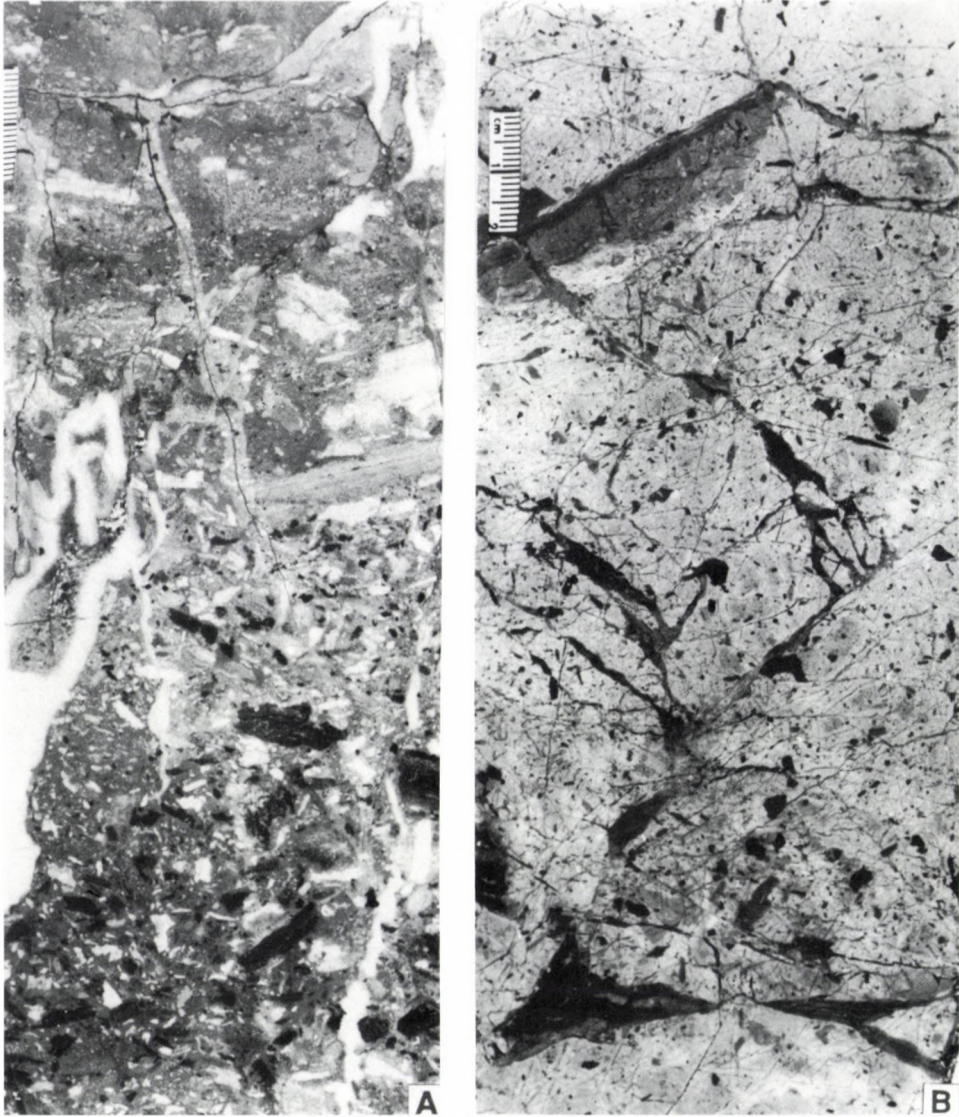


Fig. 4
Black pebble facies (A.3.1). A) Blackened algal mat rip-ups in the lower part of the layer grading upward into a polymict intrabreccia (A.3.3), Dachstein Limestone, Core Porva Po-89 202.4–202.6 m (polished slab); B) Scattered small-size black intraclasts, Main Dolomite–Dachstein Limestone transitional unit, Core Porva Po-89 492.5–492.7 m (polished slab)

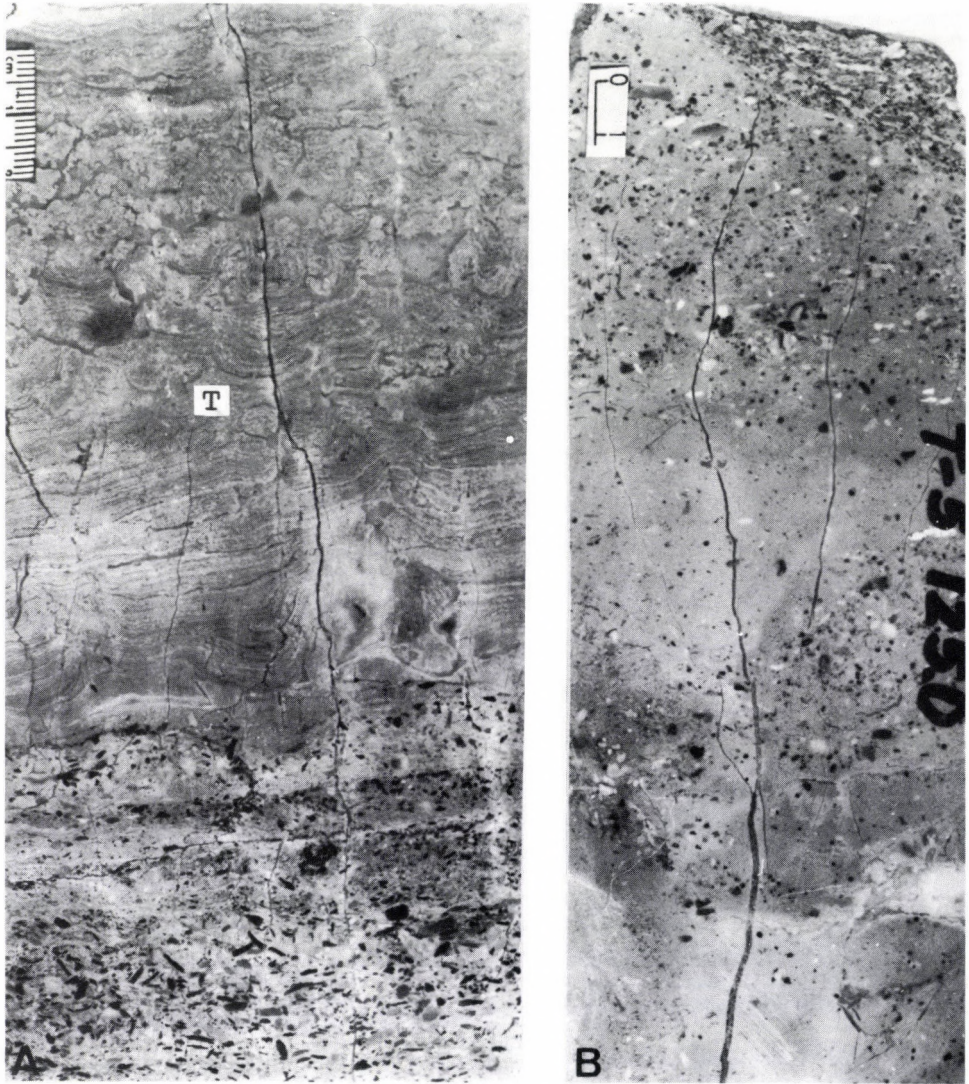


Fig. 5
Black pebble facies (A.3.1). A) Scattered tiny black intraclasts at the base of a cycle and an algal mat facies (B.1.2) above it. Note micro-tepee structures (T) close to the top of the core, Dachstein Limestone, Core Porva Po-89 343.5–343.7 m (polished slab); B) Scattered tiny black and white intraclasts in mudstone matrix. Inhomogenous distribution of the clasts may be a result of bioturbation, Dachstein Limestone, Core Tata T-5 125.0 m (polished slab)

grains are of "algal mat" origin as a rule (Fig. 6). Occasionally tiny black grains also appear among caliche crusts.

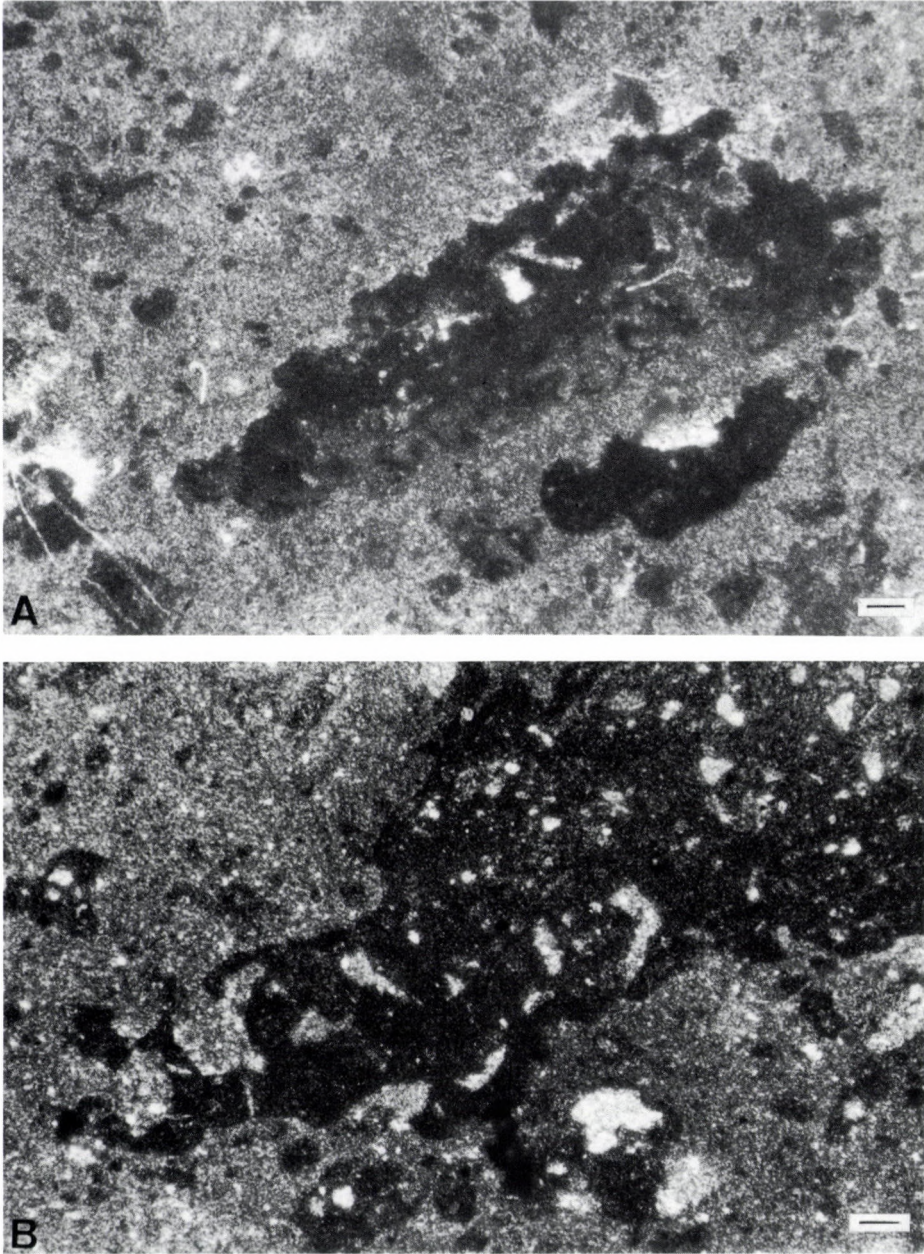


Fig. 6
Photomicrographs of black pebbles. A) Peloidal micrite intraclasts, Dachstein Limestone, Core Porva Po-89 144.0 m Scale bar = 0.1 mm; B) Micrite (mudstone) intraclast. Note traces of bioerosion around the rims and in the inside of the clast, Dachstein Limestone, Core Porva Po-89. 202.4 m Scale bar = 0.1 mm

A.3.2 Algal mat intraclast facies (Fig. 7)

This rock type contains intraclasts generated by desiccation and tearing up of algal mats (commonly it represents the transition between members A and B).

A.3.3 Polymict intraclast facies (Figs 8, 9, 10a). In many cases intraclasts originate from the previously consolidated cycles which were also reworked; in such cases, clasts of facies A, B and C occur together with black pebbles and semi-consolidated fragments of algal mats, giving these rocks a multicoloured hue.

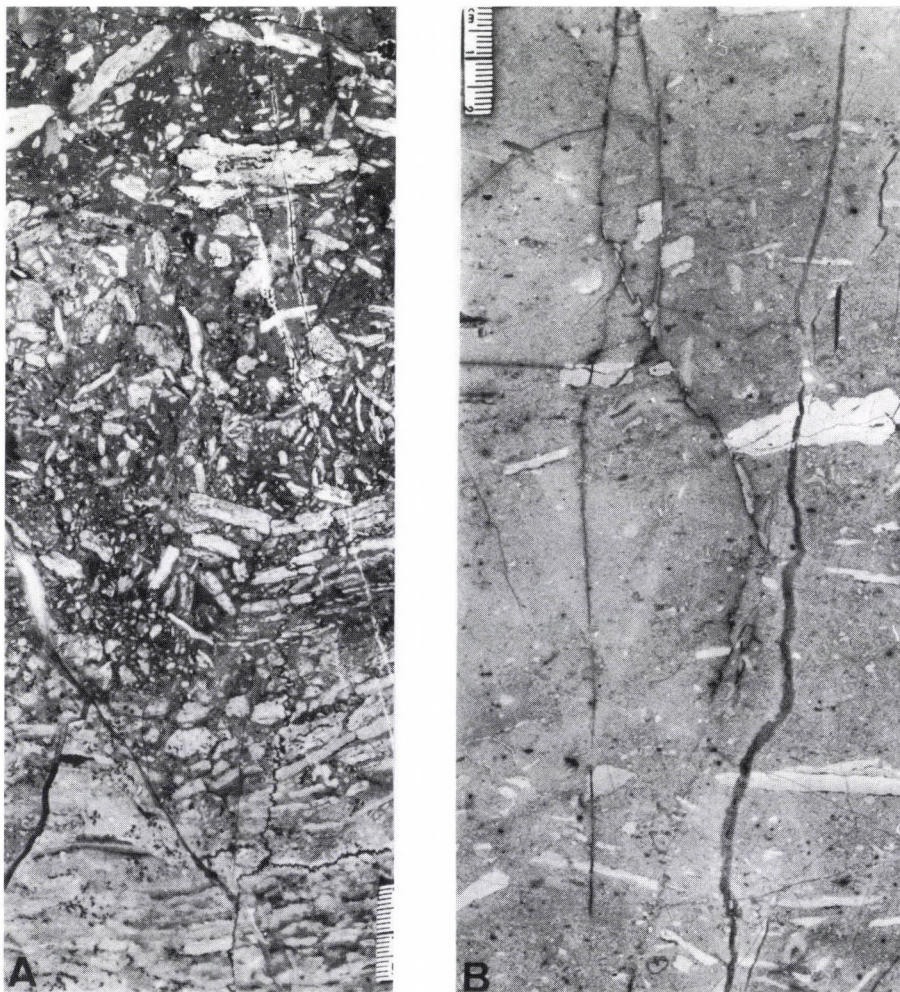


Fig. 7

Algal mat intraclast facies (A.3.2). A) Densely packed algal mat rip-ups in argillaceous carbonate matrix, Dachstein Limestone, Core Porva Po-89 100.0–100.3 m (polished slab); B) Algal mat rip-ups in carbonate matrix, Dachstein Limestone, Core Porva Po-89 153.1–153.5 m (polished slab)

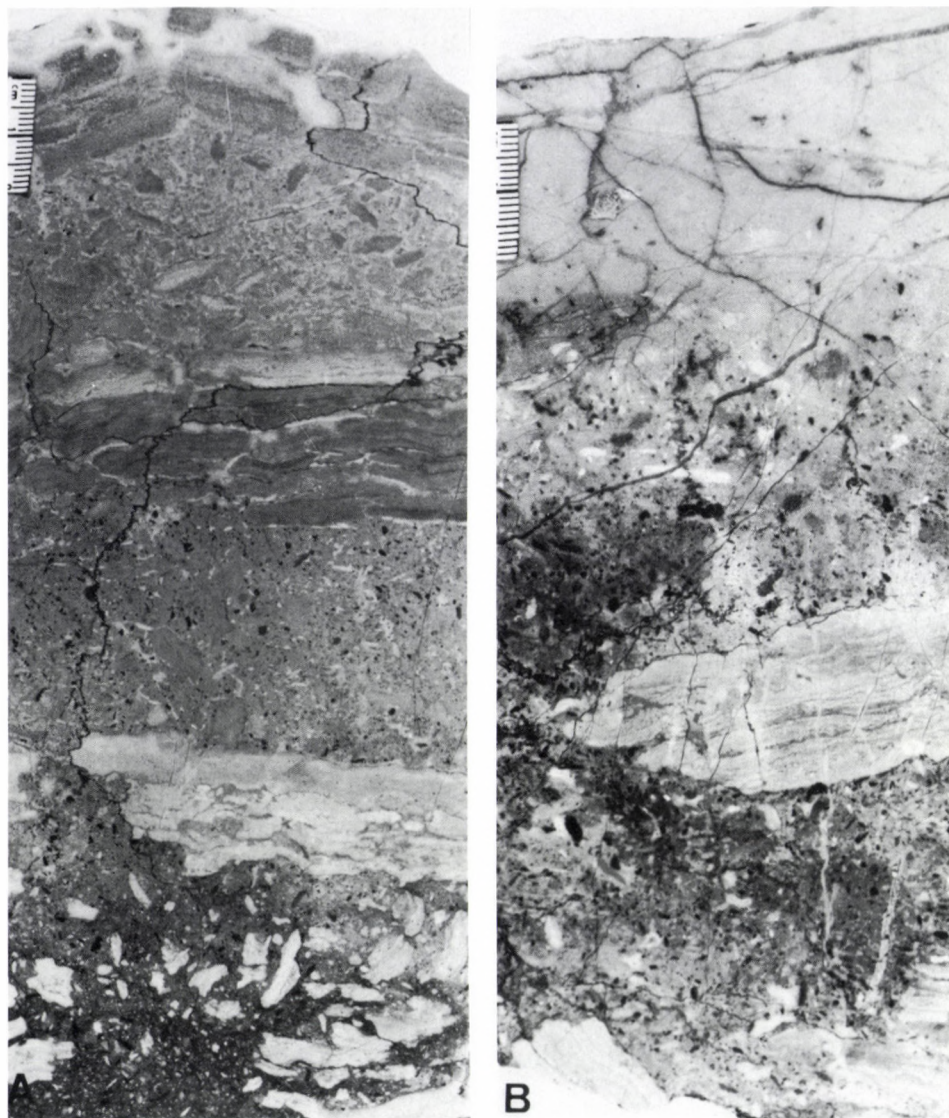


Fig. 8
Polymict intraclast facies (A.3.3). A) Algal mat rip-ups and tiny black intraclast in the lower part, para-autochthonous brecciation of the algal mat in the upper part of the core, Dachstein Limestone, Core Porva Po-89 225.8–226.0 m (polished slab); B) Small-size black pebbles and algal mat rip-ups: Note, continuous upward transition of facies A into a subtidal C facies, Dachstein Limestone, Core Porva Po-89 243.3–243.5 m (polished slab)



Fig. 9
Polymict intraclast facies. Storm breccia. It consists of rip-ups of diverse origins in a greenish grey mudstone matrix, Dachstein Limestone, Kecskékő quarry (Gerecse Mts)

A.4 Caliche-type crusts (Fig. 11a)

Yellowish, tan or pink, laminitic, occasionally pisoidic and/or intraclastic layers. They occur as a rule in the dolomitized sections.

A.5 Layers with sheet cracks and early cavity infillings (Figs 11b, 12)

All of the above rock types may contain sheet cracks, and stromatolite-like, drusy or isopachous cavity infillings which formed during early diagenesis. Their origin can be attributed to microkarstic solution on desiccation of the mud or the activity of burrowing organisms.

Beds of facies A are ascribed to this category if the greater part of the layer consists of infilled cavities of early diagenetic origin.

Intermediate rock types between facies A and facies B or C are fairly common. These types may form either by reworking of facies A or by subaerial weathering of previously deposited sediments.

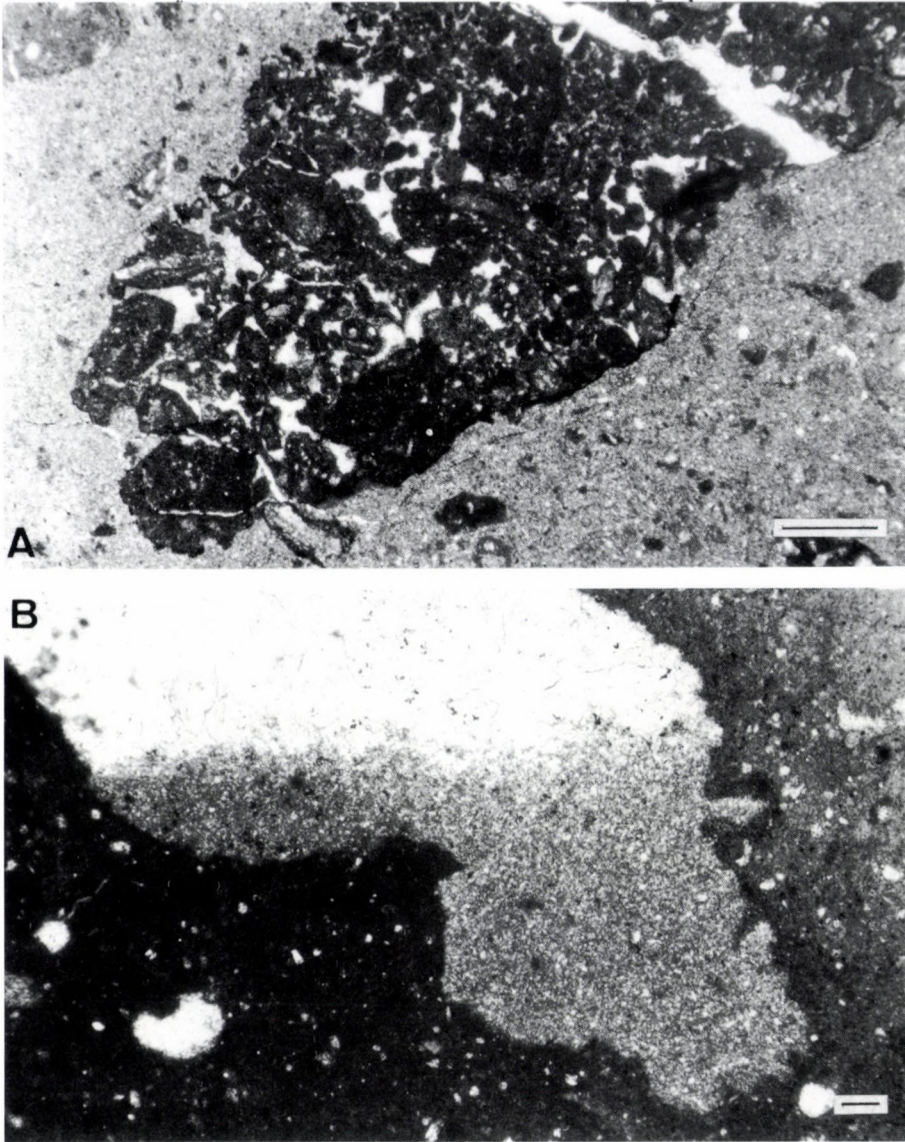


Fig. 10
Photomicrographs of facies A. A) Peloidal dolomicrite with fenestral pores in an intraclast of cm-size. Dolomitization and cementation of the pores and fractures took place prior to reworking. The matrix is carbonate silt with minor amount of quartz silt, Dachstein Limestone, Core Porva Po-89 349.6 m Scale bar = 0.5 mm; B) Geopetal cavity fill: crystal silt at the base, coarse sparry calcite at the top. The matrix is red micrite with intraclasts, Dachstein Limestone, Core Porva Po-89. 331.8 m Scale bar = 0.1 mm

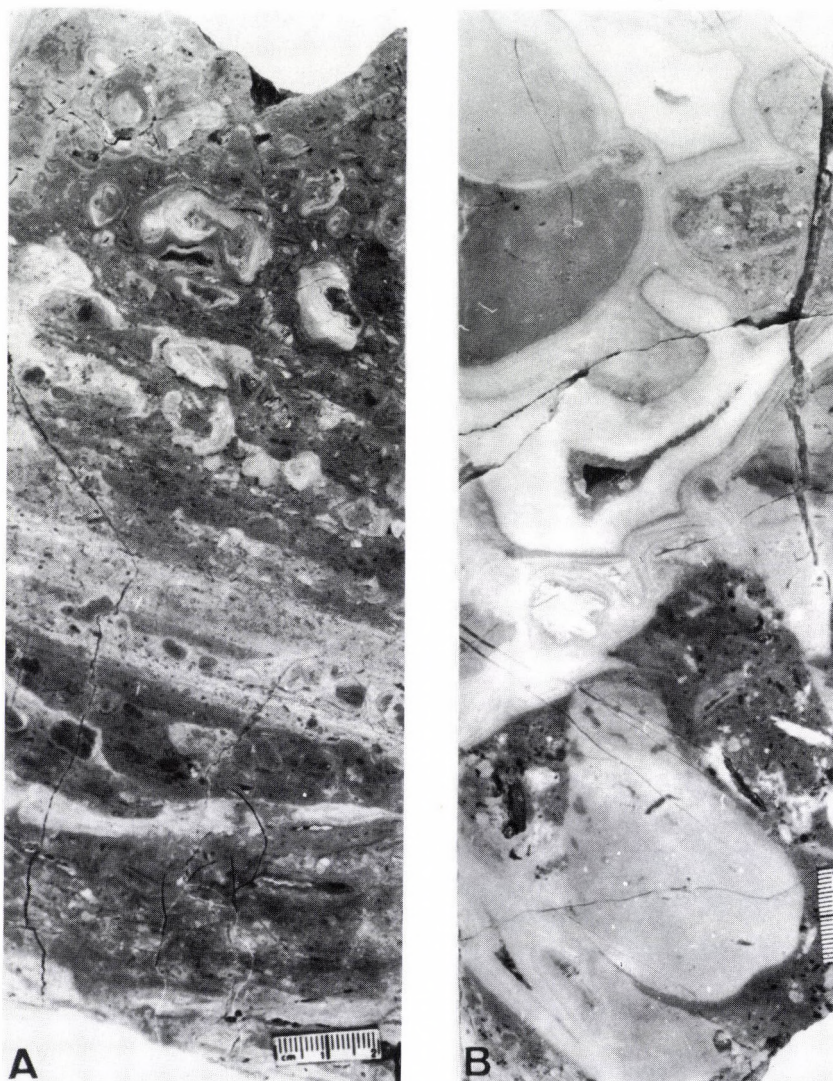


Fig. 11
Subfacies of facies A. A) Caliche-type crust (A.4) with para-autochthonous brecciation at the base and cm-size vadose pisolites at the top of the core, Main Dolomite–Dachstein Limestone transitional unit, Core Ugod Ut-8 92.0–92.2 m (polished slab); (B) Large solution cavities in an A bed, filled by isopachous calcite cement (A.5), Dachstein Limestone, Core Porva Po-89 159.8–160.0 m (polished slab)

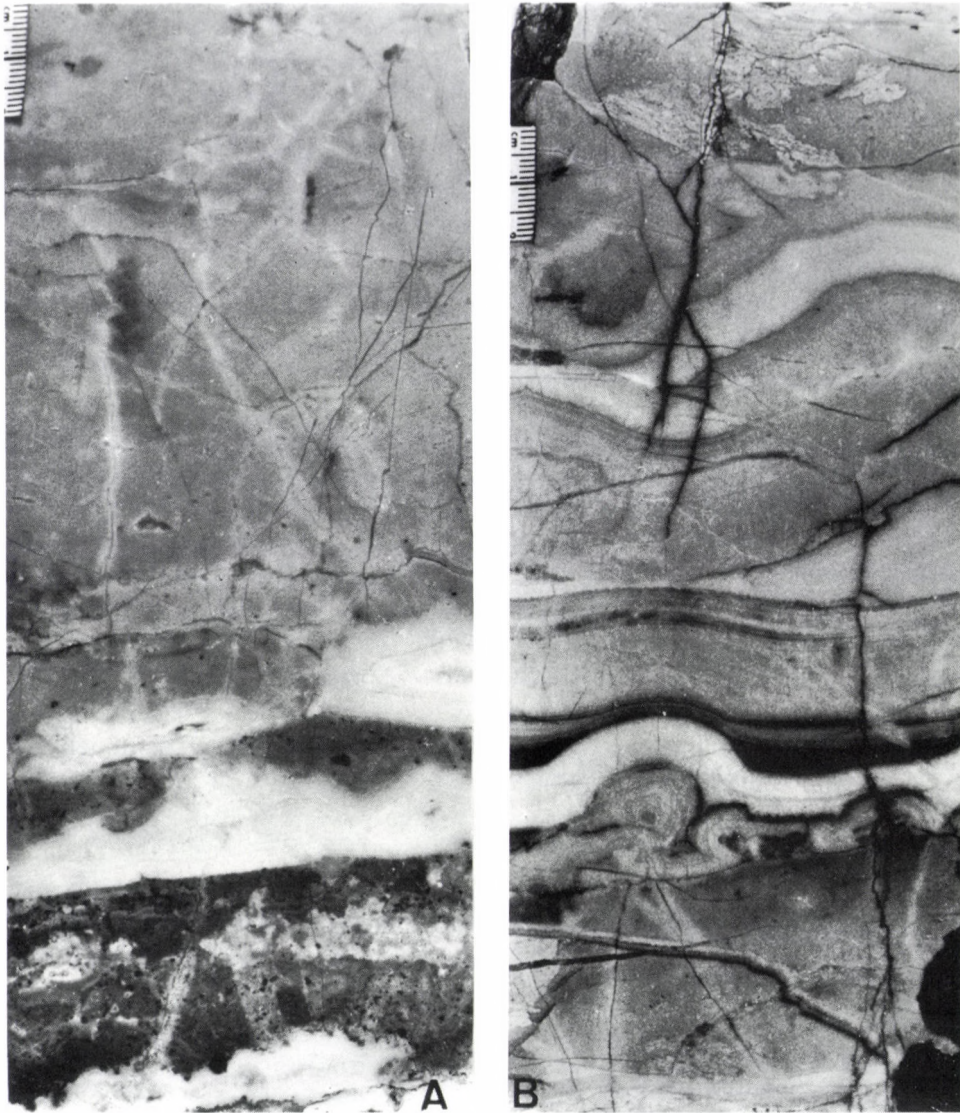


Fig. 12

Sheet cracks (A.5). A) Sheet cracks filled by isopachous calcite in a black pebble facies at the base of the core, Dachstein Limestone, Core Porva Po-89 105.8–106.0 m (polished slab); B) Large sheet cracks filled partly by fine intrasediment and partly by isopachous calcite cement. At the topmost part of the core algal mat rip-ups are visible, Dachstein Limestone, Core Porva Po-89 199.5–199.7 m (polished slab)

Facies B (members B and B')

According to Fischer's (1964) definition, B beds are characterized primarily by the presence of shrinkage pores (fenestra, bird-eye structures). As a rule they are microlaminated and stromatolitic.

Even in the Dachstein Limestone member B is generally dolomitic, containing 5 to 8% dolomite of early diagenetic origin. It is worth mentioning that, mainly in the dolomitized sections, the laminitic rock-types are partially caliche-type crusts. However, distinction of the microbial crusts and caliche crusts is frequently difficult and we had neglected to distinguish them previously. Detailed analysis of this problem is under way (Balog et al. 1993).

According to our observation in the Transdanubian Range the colour of member B is chiefly pale, greyish white, yellowish, or locally pinkish.

Beds of facies B are normally 0.1–1.5 m thick; rarely they can reach 2–3 m. In the latter case the regressive B' and the transgressive B members are not distinguishable as a rule, i.e. they are amalgamated.

Fischer recognized the fenestral laminated B beds as loferites and subdivided them into algal mat, pelleted, homogenous and conglomeratic facies. His classification can also be applied to facies B of the Transdanubian Range, with minor modification.

B.1 Algal mat (stromatolitic) facies (Fig. 13)

Microlaminated, with laminae of fenestral pores. Remnants of algal filaments are locally observable under the microscope, but generally only peloids, bioclasts or less frequently intraclasts and oncoids trapped in the algal mat can be seen. Two variants can be distinguished:

B.1.1 parallel laminated (Fig. 14)

B.1.2 wavy laminated (Fig. 15). Teepee-structures occasionally occur (Fig. 15b).

B.2 Algal mat breccia (intraclastic facies) (Figs 16, 17)

Slightly reworked (para-autochthonous) rip-ups, slabs, fragments of desiccated algal mats.

B.3 Peloidal microlaminite

Definite algal mat structure is not apparent; laminations are due to alternation of micritic and sparitic microlayers. Sparitic laminae are amalgamated birds-eye pores or very thin and small sheet cracks, but occasionally micrite and biopel-sparite laminae alternate.

B.4 Sheet crack facies (Figs 18, 19)

The bulk of these rocks consists of sheet cracks or cm to tens of cm size stromatolite-like and isopachous sparitic (bull's eye-type) cavity infillings. In the case of geopetal-type cavity fillings the lower parts of the cavities are filled with carbonate silts or muds, which are either continental or marine. The latter is indicated by tiny bioclasts (mainly ostracods). The upper part of the geopetal

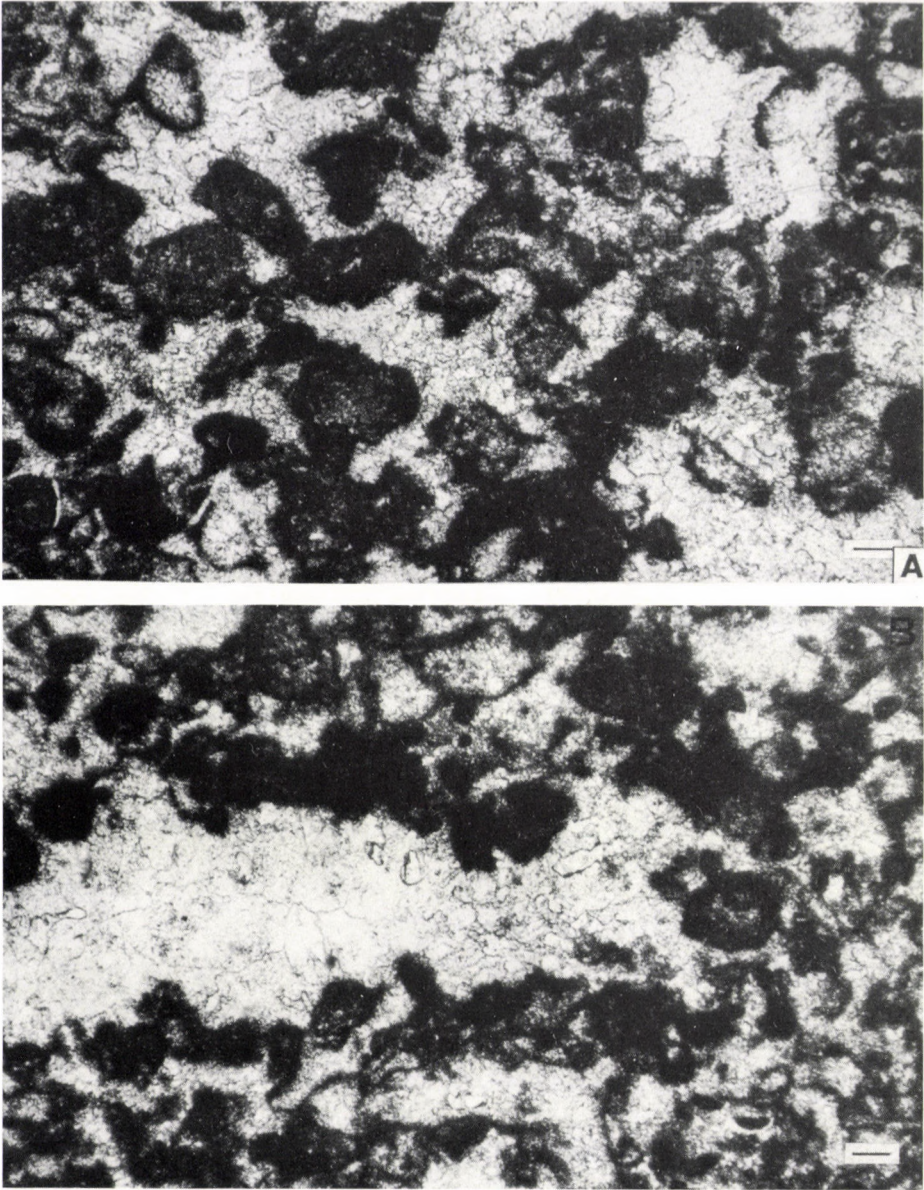


Fig. 13
Fenestral pores in the algal mat facies (B.1). A) Peloidal texture with fenestral pores, filled by sparry calcite. The pores are probably of shrinkage-pore origin, Dachstein Limestone, Core Porva Po-89 145.5 m Scale bar = 0.1 mm; B) Amalgamated fenestral pores, Dachstein Limestone, Core Porva Po-89 145.5 m Scale bar = 0.1 mm

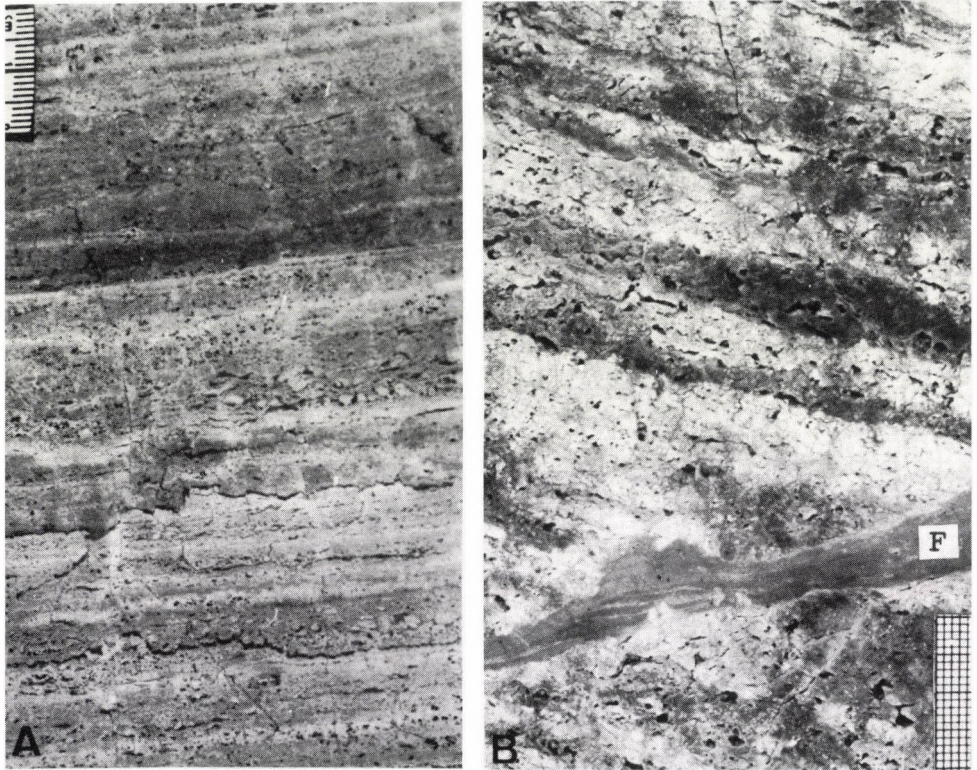


Fig. 14

Algal mat (stromatolitic) facies, parallel laminated type (B.1.1). A) Main Dolomite–Dachstein Limestone transitional unit, Core Porva Po-89 476.0–476.3 m (polished slab); B) Main Dolomite–Dachstein Limestone transitional unit, Core Epöl E-5 (Gerecse Mts) 479.1–479.2 m (polished slab); F – younger fracture fill

cavities are filled with isopachous, fine-crystalline, occasionally fibrous sparite as well as, in their internal part, blocky sparite.

B.5 Homogenous facies (Fig. 20)

Definite lamination is lacking. Pelmicrite texture with indistinct sparite from disorganized shrinkage pores, sheet cracks, and druses are characteristic. In some cases an originally microlaminated structure has been destroyed by bioturbation (Fig. 21a); in other cases transitional developments occur, towards either facies A or C.

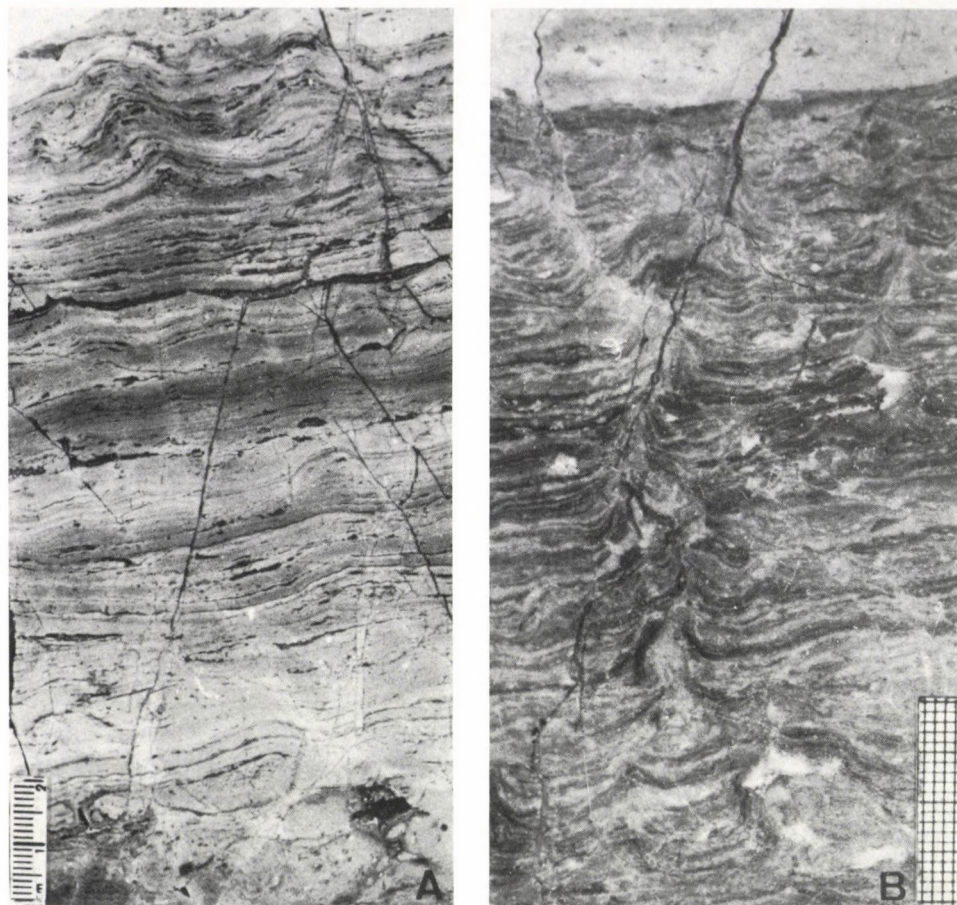


Fig. 15

Algal mat (stromatolitic) facies, wavy laminated facies (B.1.2). A) Dolomitized algal laminite, Main Dolomite–Dachstein Limestone transitional unit, Core Ugod Ut-8 111.0–111.2 m (polished slab); B) Microtepee-structure (T), Main Dolomite–Dachstein Limestone transitional unit, Core Tatabánya Tbt-8 82.7–83.0 m (polished slab)

Facies C (member C)

Facies C is not very diversified on a macroscopic scale, and consists of light to mid-grey, or yellowish, brownish, microcrystalline or peloidal, ooidic, oncoidic, bioclastic limestones, as well as dolomite, typically with megalodonts (Fig. 22). The thickness of this member is 1 to 3 m as a rule.

Several types can be distinguished on the basis of microfacies. Generally these are also characterized by particular biota (Hohenegger and Piller 1975; Oravec-Scheffer 1987). However, although we must emphasize that within an

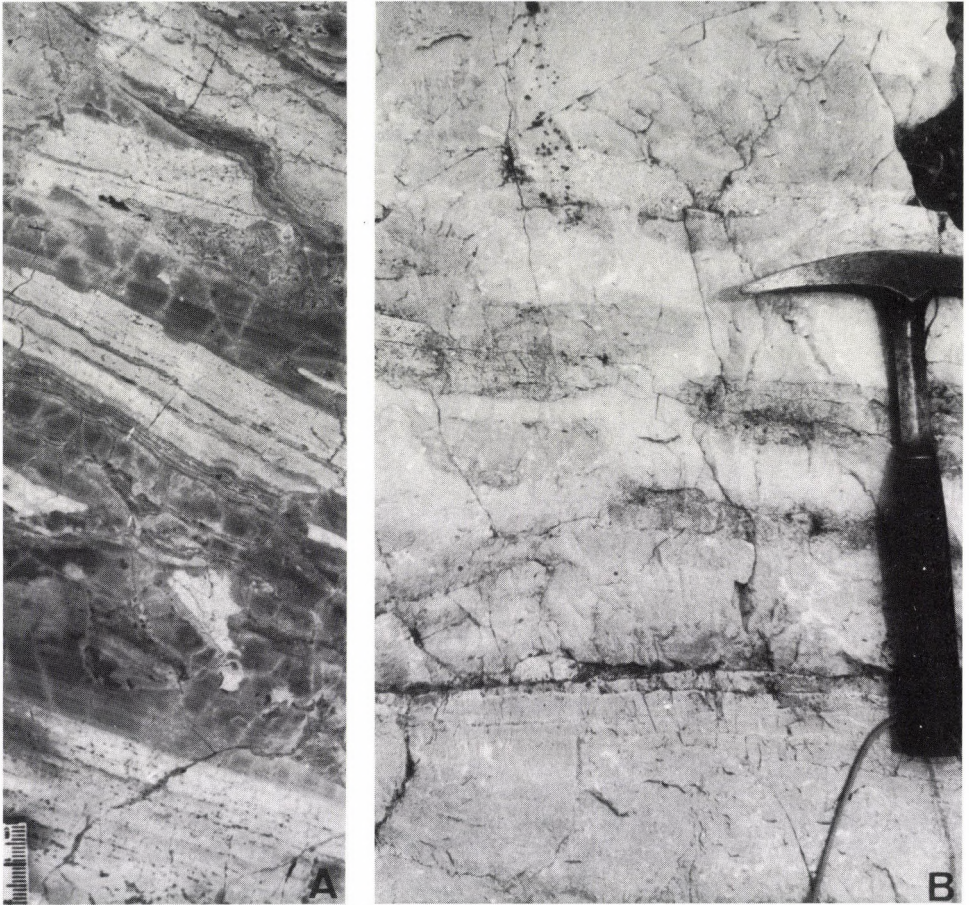


Fig. 16
Algal mat breccia (B.2). A) Slightly reworked slabs of algal mat origin, Main Dolomite–Dachstein Limestone transitional unit, Core Ugod Ut-8 92,7–92,8 m (polished slab); B) Large rip-up slabs of algal mat origin, Dachstein Limestone, Ugod Szár-hegy quarry

individual C bed different microfacies-types may occur, no trend was found in their distribution.

The most frequent types are:

C.1 mudstone (micrite – with *Involutina* and *Nodosaria* assemblage)

C.2 peloidal wackestone, packstone (pelmicrite (Fig. 23) – with *Trochammina*, *Glomospira*, *Agathammina*, and *Paleospiroplectammina* assemblage)

C.3 skeletal wackestone, packstone (biomicrite, biopelmicrite – Fig. 24a). Subtypes are as follows.

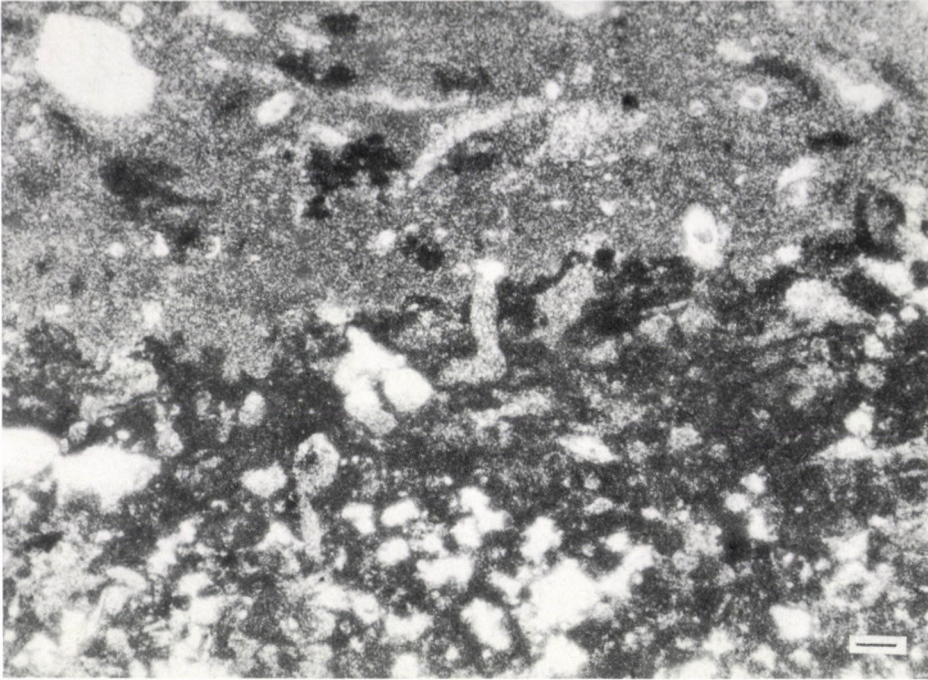


Fig. 17

Intraclast of algal mat origin. Note trace of bioerosion at the margin of the clast, Dachstein Limestone, Core Porva Po-89 148,1 m Scale bar = 0,1 mm

C.3.1 calcareous algal (dasycladacean – Fig. 24b)

C.3.2 foraminiferal (with *Aulotortus* and *Nodosaridae* assemblage – Fig. 25a)

C.3.3 ostracodal (Fig. 25b)

C.4 intraclastic wackestone, packstone (intramicrite – Fig. 26a)

C.5 ooidic-oncoidal wackestone, packstone (oomicrite, oncoid or grapestone micrite - with miliolids)

C.6 skeletal grainstone (biosparite – Fig. 26b)

C.7 ooidic-oncoidal grainstone (oosparite, oncoidal sparite - with *Tetrataxis* and *Duostomina* assemblage – Figs 27, 28)

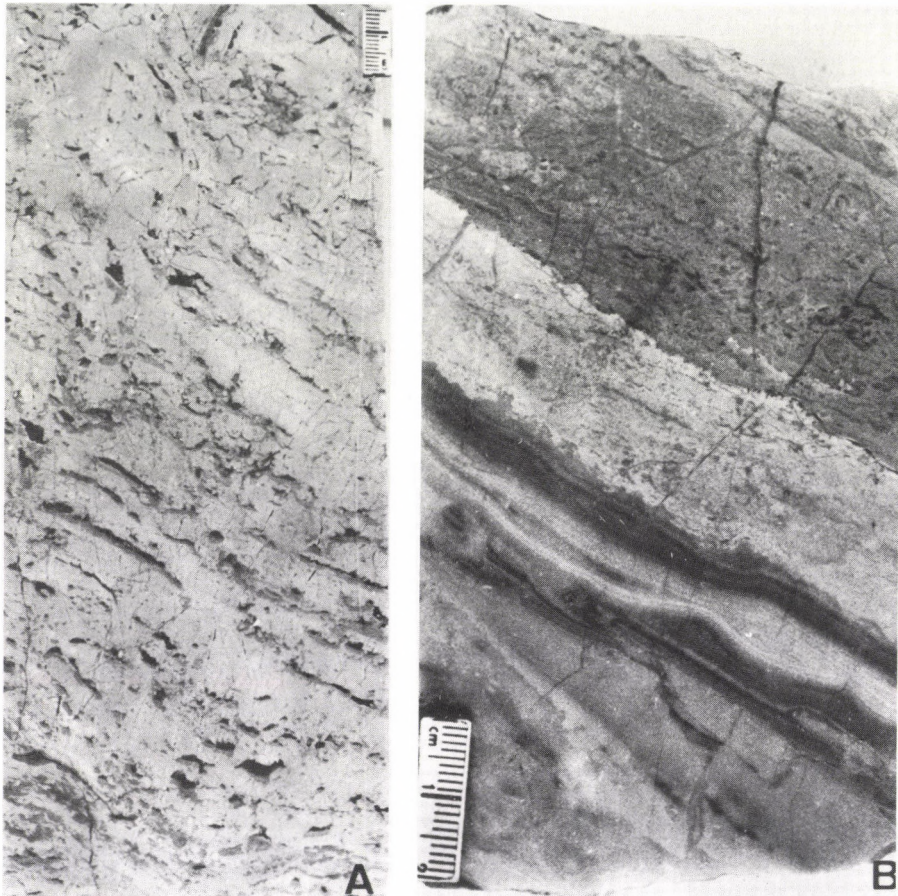
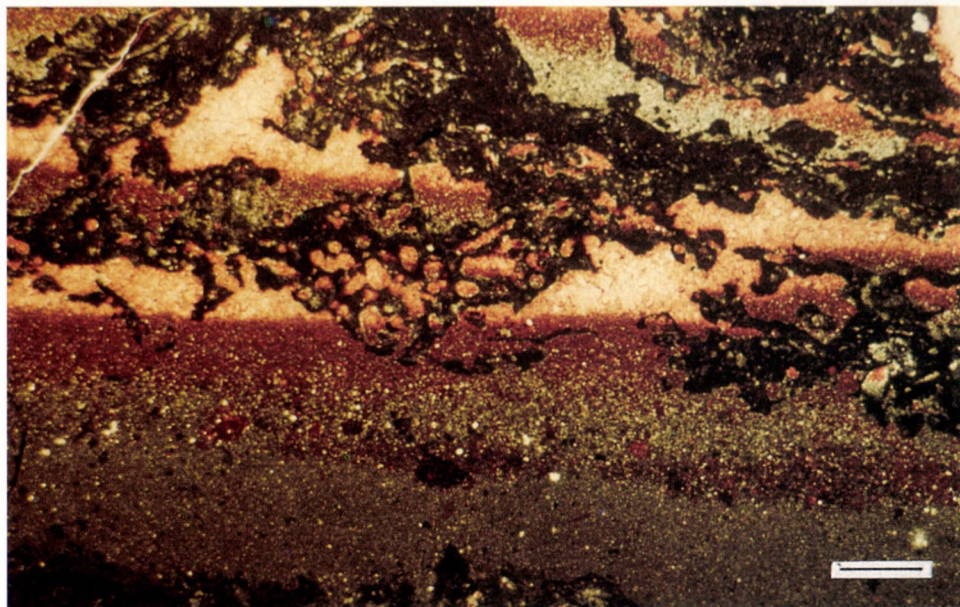


Fig. 18

Sheet crack facies (B.4). A) Sheet cracks of cm-size. They may have formed by amalgamation of fenestral pores. Basal part of the cracks is filled with intrasediment. Their top part is generally empty as result of secondary dissolution, Main Dolomite–Dachstein Limestone transitional unit, Core Ugod Ut-8. 82,7–83,0 m (polished slab); B) Large sheet-cracks within an algal mat layer, Main Dolomite–Dachstein Limestone transitional unit, Core Ugod Ut-8 166.6–166.8 m (polished slab)

Fig. 19 →

Sheet crack facies (B.4). A) Cm-size sheet cracks with geopetal cavity-fill. In the basal part, microlayers consisting of calcite and dolomite silt and mud alternate. The upper part of the sheet cracks are filled with sparry calcite, Dachstein Limestone, Core Porva Po-89 409.0 m, Scale bar = 0.5 mm; B) Cm-size sheet cracks with geopetal cavity-fill. Dolomite mud in the basal part and sparry calcite in the upper part of the pores, Dachstein Limestone, Core Porva Po-89 440.8 m, Scale bar = 0.5 mm



B

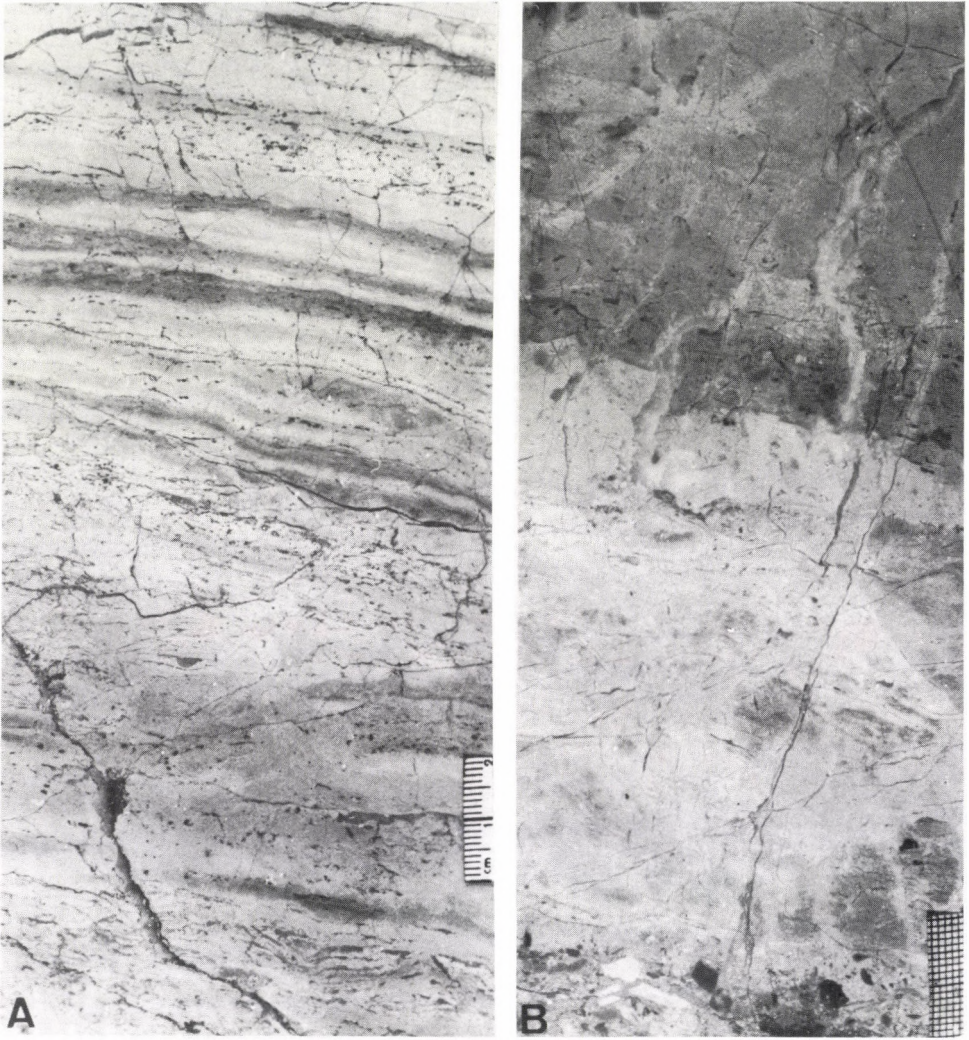


Fig. 20

Homogenous facies (B.5). A) Homogenization of the originally laminated structure is well visible in the middle part of the core. In the upper part lamination is vague, Dachstein Limestone, Core Porva Po-89 411.8–412.0 m (polished slab); B) Multicoloured, mixed breccia (A.3.3) at the base, bioturbated, homogenized B facies in the middle, and facies C at the top of the core, Dachstein Limestone, Core Zirc Zt-62 220.1–220.3 m (polished slab)

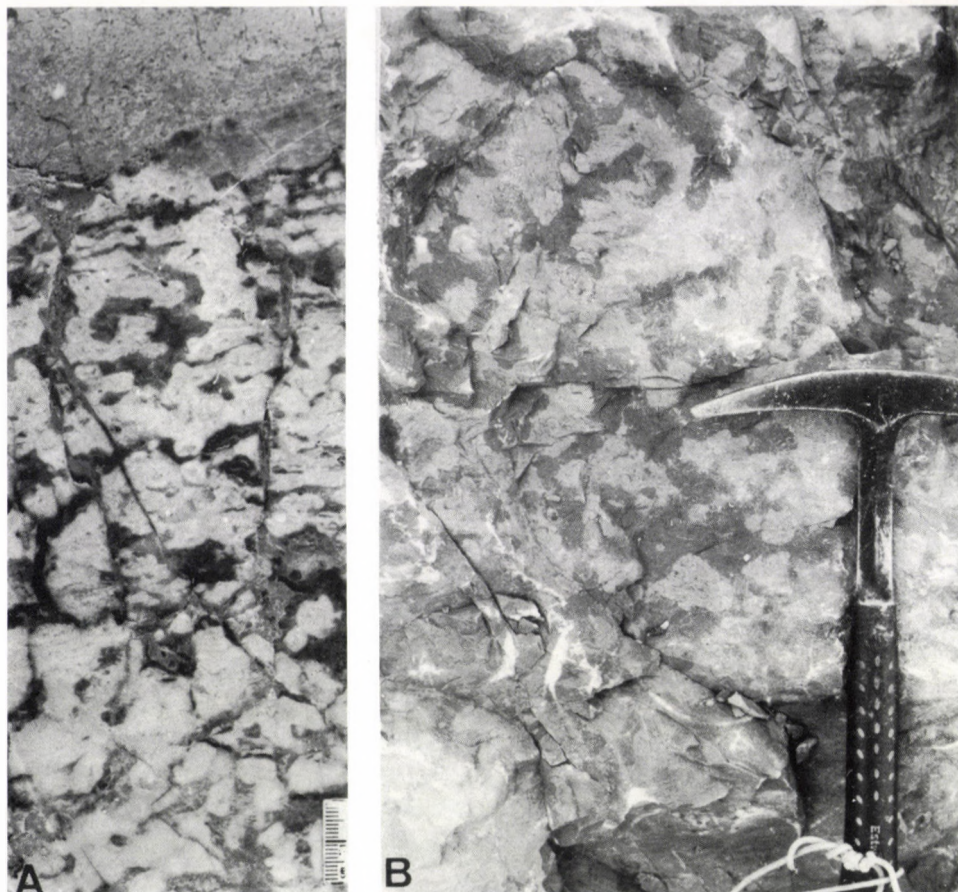


Fig. 21
Bioturbation (burrowing). A) Bioturbation in facies B led to almost complete devastation of the originally laminated structure, Main Dolomite–Dachstein Limestone transitional unit, Core Ugod Ut-8 92.7–93.0 m (polished slab); B) Bioturbation in facies C, Dachstein Limestone, Kecskekő quarry

Characteristic facies development of the lithostratigraphic units

Lithostratigraphic (lithogenetic) units showing Lofer cyclicity differ from one other not only in the stacking pattern of the individual cycles but also in the facies character of the cycle members. Characteristic macro- and microtextural features can be summarized as follows:

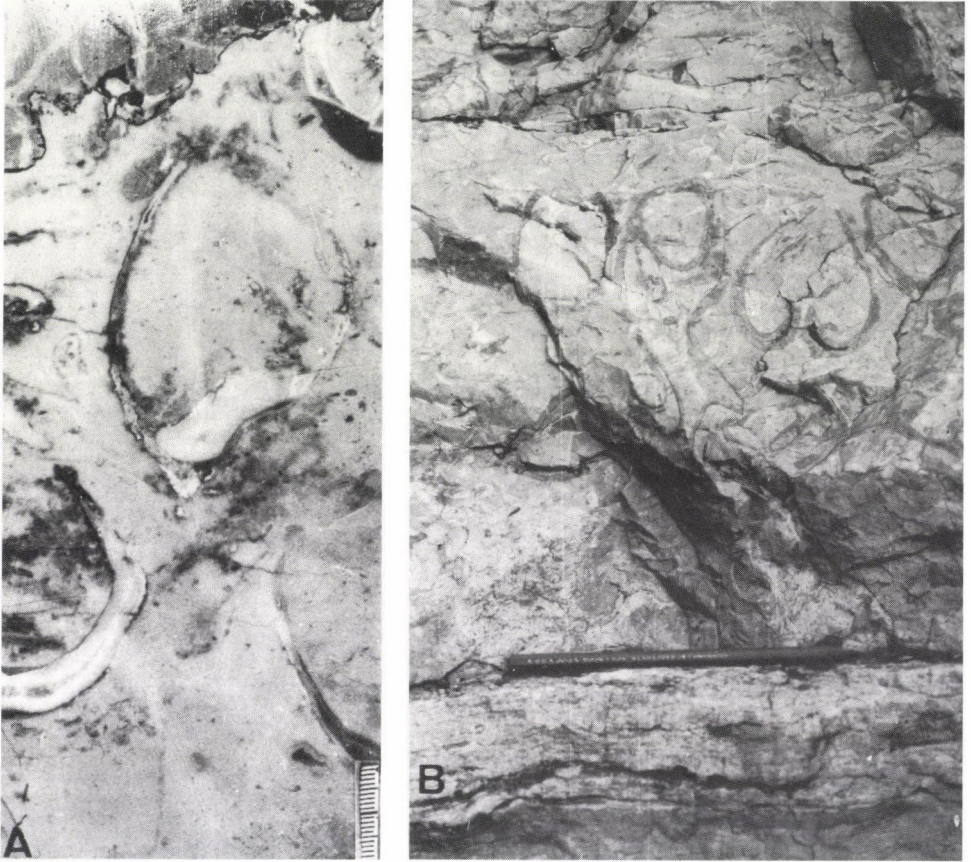


Fig. 22
Megalodont banks in facies C. A) Dachstein Limestone, Core Porva Po-89 272.9–273.1 m (polished slab); B) Dachstein Limestone, Tata Kálvária-hill quarry

Main Dolomite

In the Main Dolomite Formation microfabric features are frequently obscured by diagenetic processes, and only relicts of the original texture can be observed. However, the main facies types are usually distinguishable.

Facies A only rarely appears and if it does, it is represented by a few cm-thick reddish or greenish stripes and/or brecciated horizons, as a rule. Caliche crusts (A.4) may fall within this category also, but their comprehensive distinction from microbial laminites of facies B has not yet been finalized.

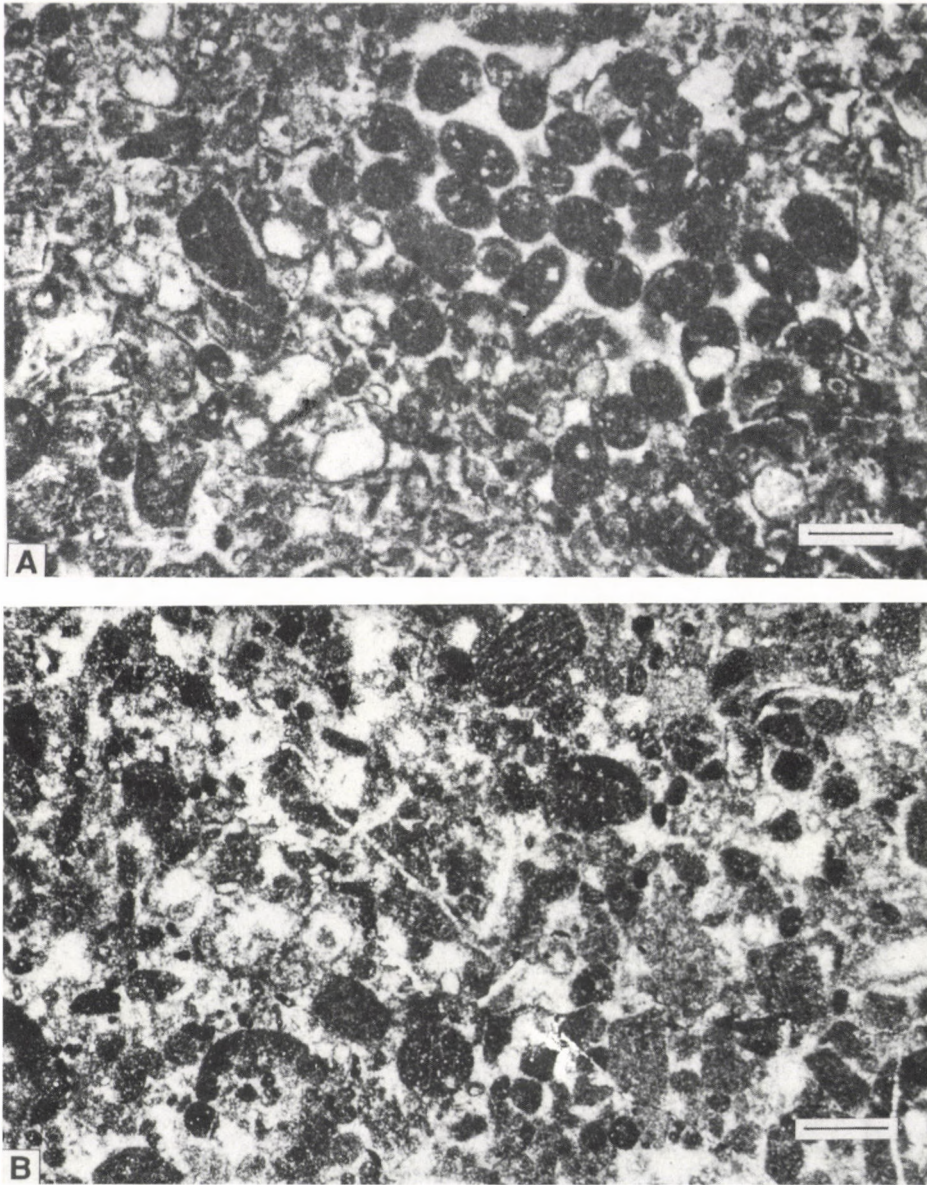


Fig. 23
Peloidal facies (C.2). A) Pelmicrosparite with fecal pellets, Main Dolomite–Dachstein Limestone transitional unit, Core Porva Po-89 461.7 m, Scale bar = 0.5 mm; B) Pelmicrosparite with Favreina-type fecal pellets and biomolds, Main Dolomite–Dachstein Limestone transitional unit, Core Ugod Ut-8 122.5 m, Scale bar = 0.5 mm

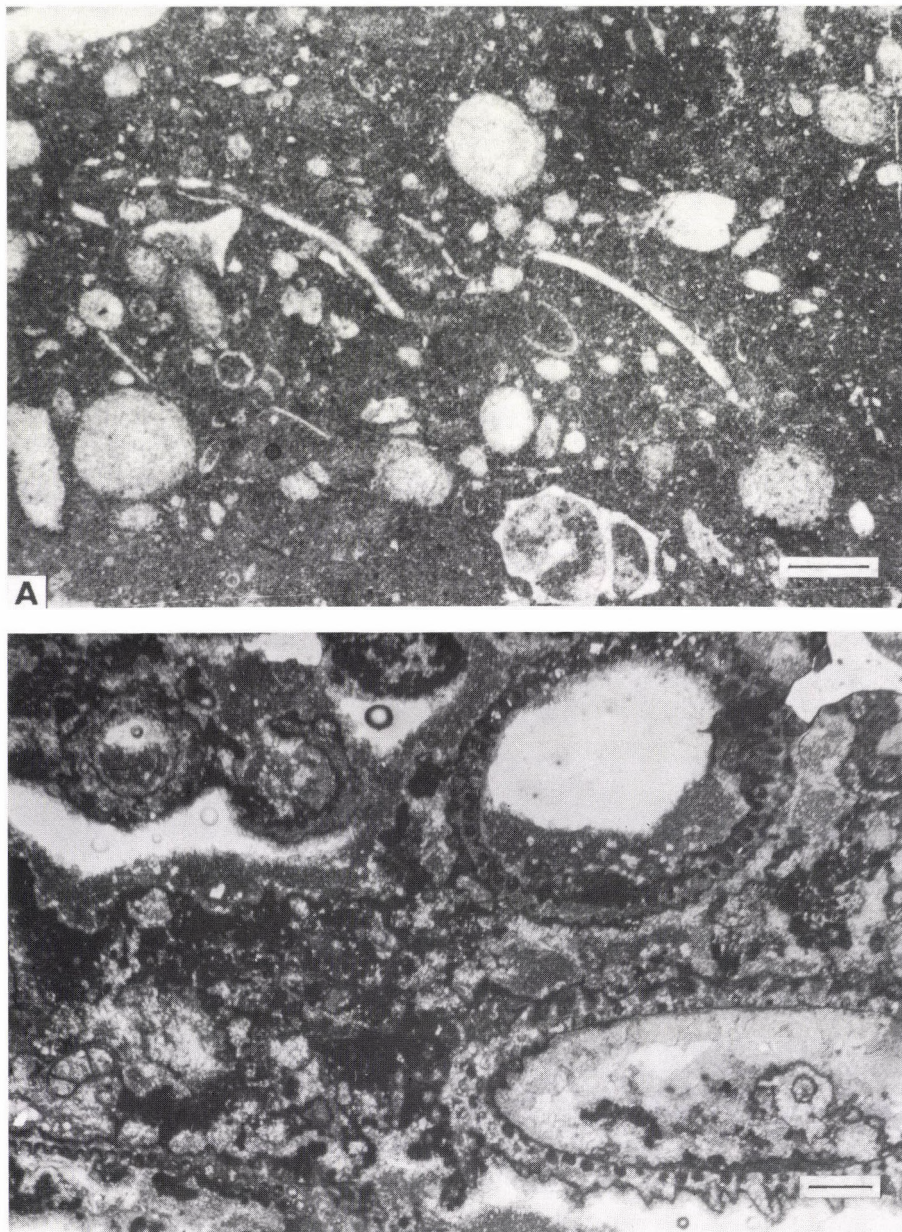


Fig. 24
Skeletal facies (C.3). A) Biomicrite (wackestone) with foraminifer and mollusc shell fragments, Core Tardosbánya Tba-1 69.3 m, Scale bar = 0.5 mm; B) Dasycladacean packstone (C.3.1), molds and solution cavities are filled by geopetal cement: carbonate silt in the basal part and sparry dolomite in the upper part of the pores (the later is partially dissolved), Main Dolomite, Sümeg Szőlő-hill, Scale bar = 1.0 mm

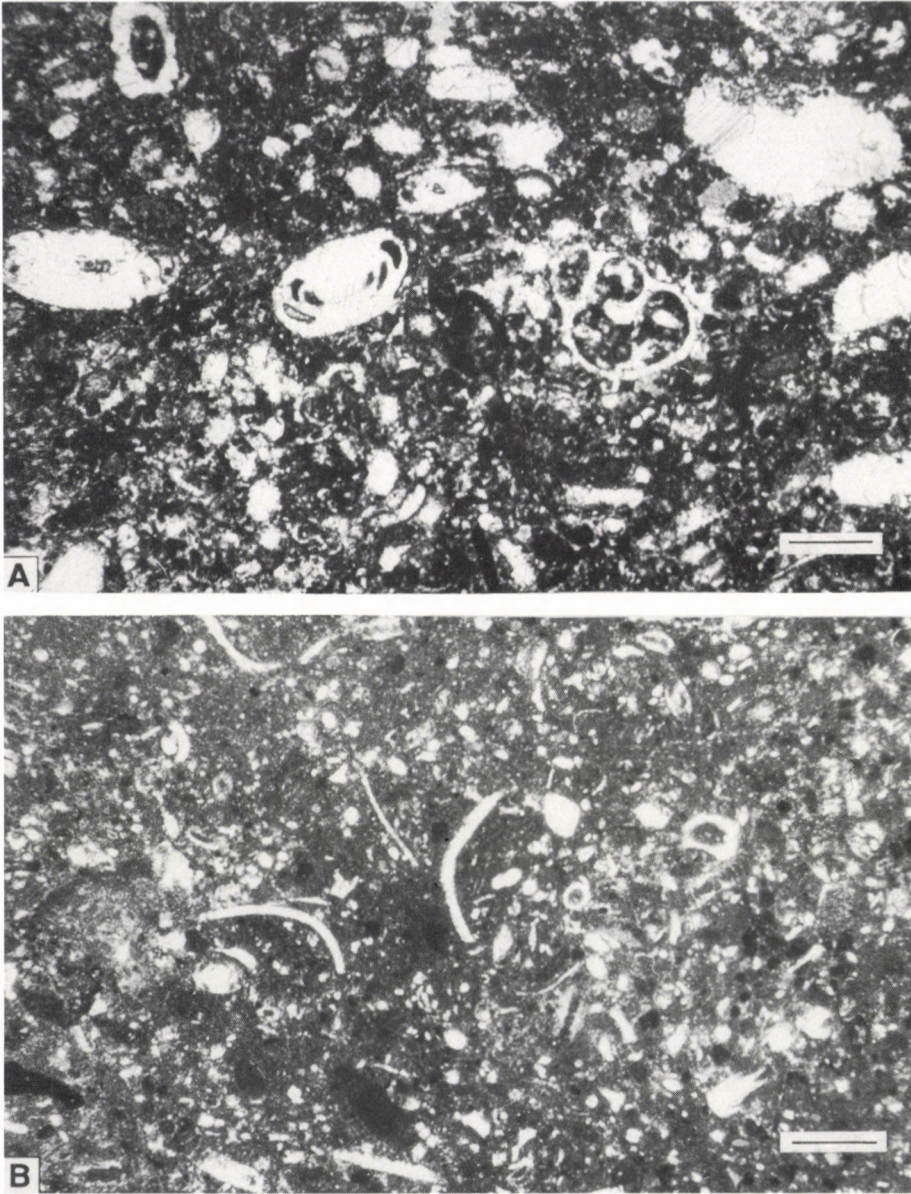


Fig. 25
Skeletal facies (C.3). A) Foraminiferal packstone (pelbiomicrite) (C.3.2). Dachstein Limestone, Core Tardosbánya Tba-2 84.7 m, Scale bar = 0.5 mm; B) Ostracodal packstone (biopelmicrite) (C.3.3), Dachstein Limestone, Core Tardosbánya Tba-2 93.9 m, Scale bar = 0.5 mm

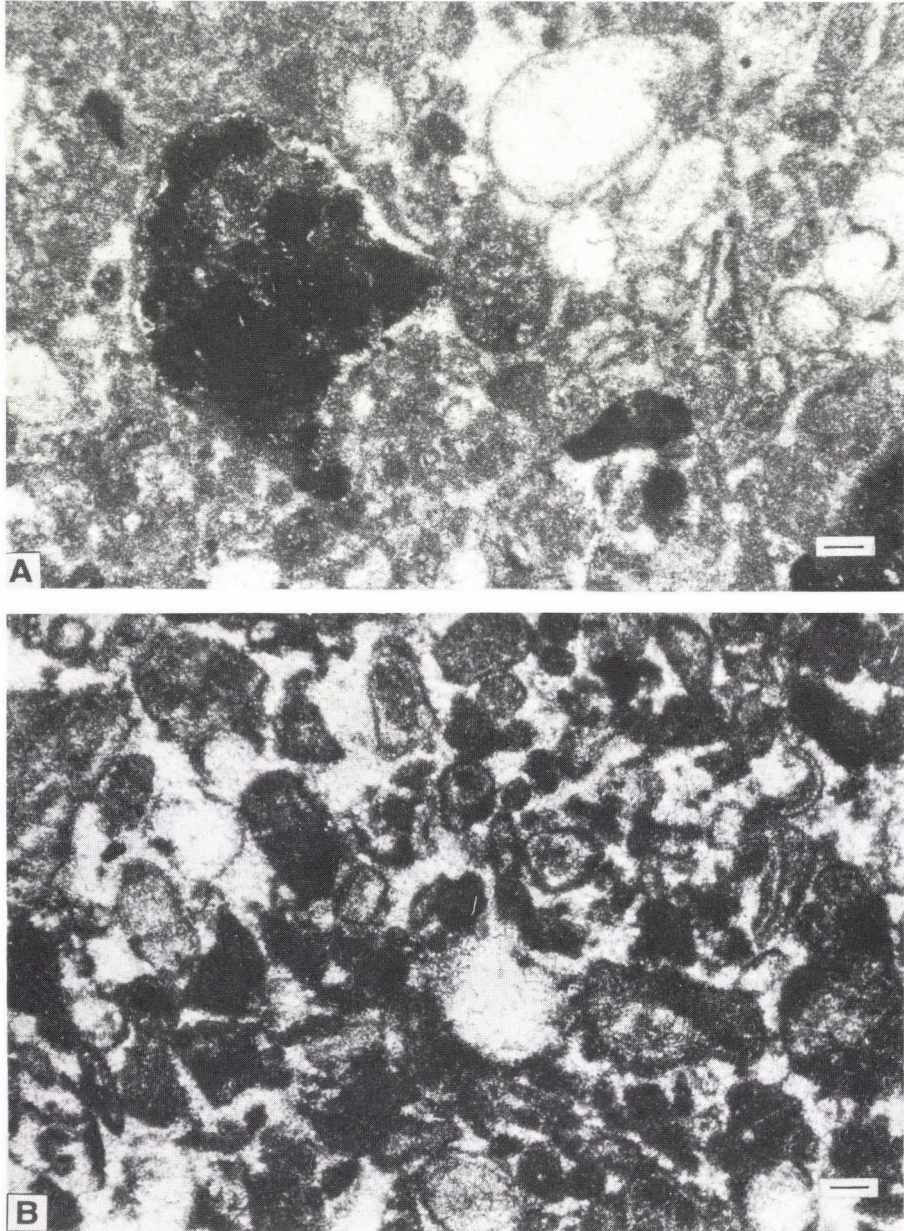


Fig. 26
Intraclastic (C.4) and skeletal grainstone (C.6) facies. A) Intraclastic skeletal packstone, the intraclasts are "blackened" grains, reworked from facies A, Dachstein Limestone, Core Porva Po-89 331.4 m, Scale bar = 0.1 mm; B) Skeletal grainstone (biopelsparite), substantial part of the skeletal grains are dissolved and replaced by sparry calcite (biomold), Dachstein Limestone, Core Porva Po-89 150.2 m, Scale bar = 0.1 mm

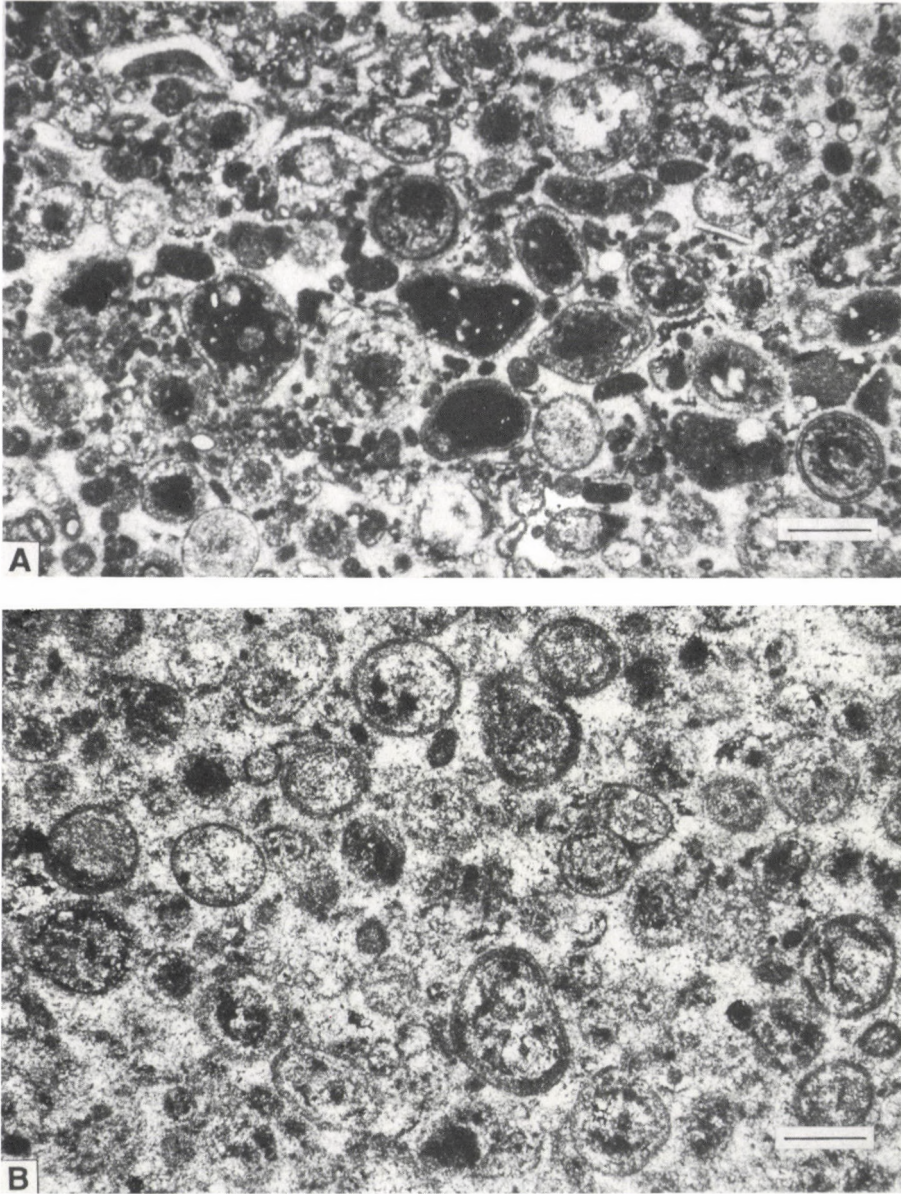


Fig. 27
Ooidic-oncoidal grainstone facies (C.7). A) Ooidic grainstone (oosparite), in addition to the typical multilayered ooids, grains coated by a single layer (cortoids) are common, Dachstein Limestone, Core Tardosbánya Tba-2 98.0 m, Scale bar = 0.5 mm; B) Ooidic grainstone (oosparite), internal part of some of the ooid grains are dissolved and filled with sparry calcite (oomolds), Dachstein Limestone, Core Tardosbánya Tba-3 46.0 m, Scale bar = 0.5 mm

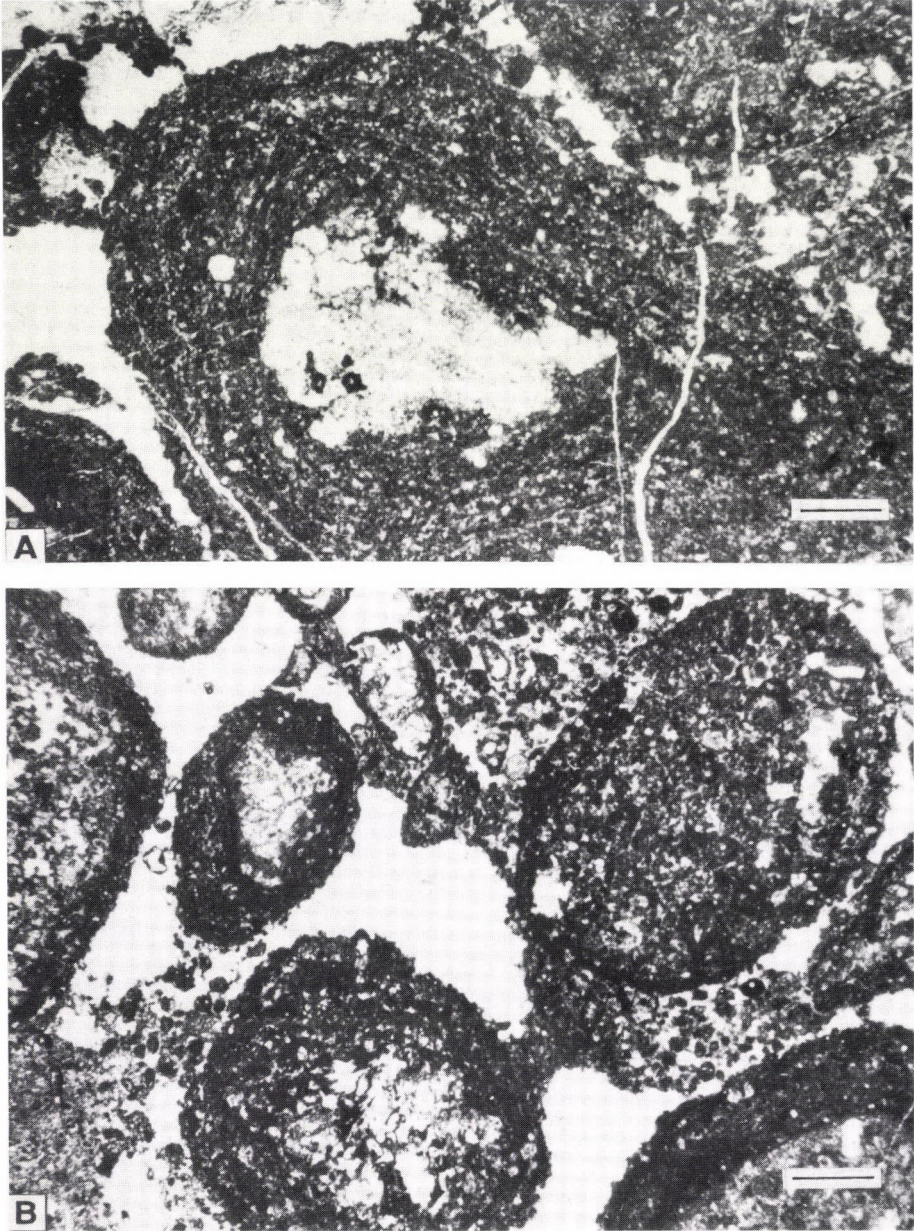


Fig. 28

Ooidic- oncoidal grainstone facies (C.7). A) Oncoid grain, Dachstein Limestone, Core Vác-2 1191.0 m, Scale bar = 0.5 mm; B) Oncoidal grainstone, Empty interparticle pores are result of secondary dissolution, Dachstein Limestone, Core Vác-21 58.0 m, Scale bar = 0.5 mm

Among facies B the parallel and wavy laminated algal mat (B.1) and the algal mat breccia (B.2) types are the most frequent, but peloidal microlaminite (B.3) and the homogenous (B.5) development are also recognizable.

As far as member C is concerned, mud-supported (micritic) textural types are predominant (C.1; C.2; C.3) although they are frequently recrystallized. Particularly characteristic is the intraclastic type (C.4). Intraclasts a few cm in size generally originated from facies B and C. In the latter case they are mainly storm breccias. The thickness of these beds may exceed significantly the mean value of the C beds.

Main Dolomite–Dachstein Limestone transitional unit

In the Main Dolomite–Dachstein Limestone transitional unit, in facies A the micritic (A.2) and all of the three subfacies of the intraclastic (A.3) texture types occur, including storm breccias. Types A.1 and A.2 appear as a rule as fissure fillings. Within member B the algal mat (B.1), the brecciated (B.2) and the massive (B.5) facies are common. In member C the intraclastic (C.4) and the pelmicritic (C.2) facies are predominant.

Dachstein Limestone

Texture in the lower part of the Dachstein Limestone is particularly varied. Every type of facies A and B appears. Within A beds the intraclastic (A.3) and within B beds the algal mat (B.1) facies are predominant. Within member C the mudstone (C.1), the peloidic (C.2), the skeletal (C.3) and the oolitic-oncoidal, packstone (C.5) texture types are common. The intraclast facies is less common although intraclasts of algal-mat origin can usually be observed in the basal part of the C beds.

In the north-eastern part of the Transdanubian Range (blocks on the east side of the Danube; Buda Hills) where Lofer cyclic development of the Dachstein Limestone is generally subordinate, oolitic-oncoidal grainstone (C.7) texture is characteristic, in many cases appearing as lenses within skeletal layers.

No significant difference in the facies characteristics was detectable between the upper and lower parts of the Dachstein Limestone. However, in the upper part facies A is frequently missing, or extremely thin, although anomalously thick A beds also occur. Black pebble facies is particularly common and conspicuous. In a few places black limestone lenses also occur as intercalations within facies A.

In facies B the parallel laminated B.1.1 type is predominant; the algal mat breccia is also common, and the peloidal facies occurs rarely. B beds are frequently missing or are thin.

Within member C the peloidal (C.2) and the mud-supported skeletal facies (C.3) prevail but the skeletal grainstone (C.6) facies is also present, generally in lenses. Oolitic-oncoidal packstones (C.5) as well as skeletal grainstones (C.6) can be seen locally. Intraclasts of algal-mat origin are usually present in the lower part of the C beds.

Paleoenvironmental interpretation

A paleoenvironmental interpretation of the facies described above is shown in Fig. 29. The model is based on observations from the Bahamas Bank (Ginsburg and Hardie 1975), Shark Bay Australia (Hagan and Lagon 1975; Woods and Brown 1975), and the Persian Gulf (Shinn 1973; Purser and Evans 1973). The most important aspects of this interpretation are described below.

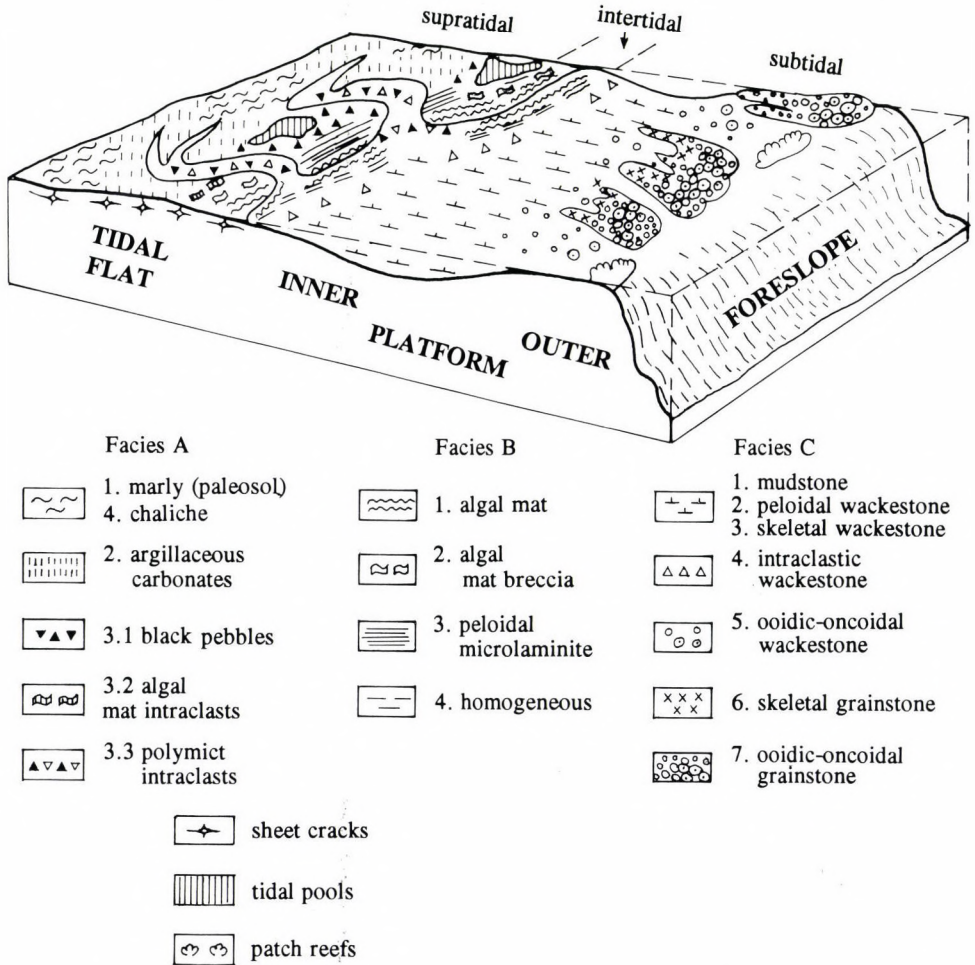


Fig. 29
Paleoenvironmental model, showing assumed sites of formation of the distinguished facies and subfacies

Rock types of facies A were formed in the supratidal zone of the tidal flat, and some of them show features of the onset of pedogenesis. In situ paleosol is considered to belong to the regressive wing of the cycle. It also appears as infillings in paleokarst cavities and fissures. In all subfacies of member A the terrigenous material was generally mixed with carbonate mud of marine origin. They were formed either by subaerial weathering (pedogenic alteration) of marine sediments or by reworking of paleosols in the subsequent transgressive phase. In the latter case they appear at the base of the cycle.

Authigenic breccias of subfacies A.3 (mainly the mixed facies A.3.3) are predominantly storm sediments. Channel fill sediment are also intraclastic as a rule.

The black pebbles (A.3.1) are formed from carbonate sediments deposited in small tidal flat pools and impregnated by organic matter (Strasser and Davaud 1983; Császár 1989). These rapidly lithified carbonate sediments were brecciated and eroded, as a rule during the subsequent transgressional phases, reworked and deposited, occasionally together with other intraclasts, in the basal layer of the cycles.

Rock types of facies B are tidal flat sediments. In the intertidal and lower part of the supratidal zone, microbial (algal-mat) coatings are common. Subfacies B.1.1 is characteristic mainly of the lower intertidal zone, whereas types B.1.2 and B.3 may indicate the middle and the upper part of the supratidal zone. The subfacies characterized by sheet cracks (B.4) and algal-mat breccias (B.2) may have been formed in the upper part of the intertidal and the lower part of the supratidal zone, where sediments desiccated and ripped up regularly.

Peloidal and bioclastic micrites of the C beds (C.1, C.2, C.3) were accumulated in a lagoon or inner shelf of low energy. The grainstones (oolitic, oncoidal, bioclastic) indicate the agitated environment of the shelf margin. The oolitic and oncoidal micrites (C.5) could have been deposited in the lee of the ooid mounds.

The rocks of intraclastic type (C.4) are partly storm generated and partly basal lag sediments, formed during transgressions, when more or less consolidated sediments of the substratum were ripped up and reworked.

Acknowledgements

The studied cores were drilled mainly within the framework of the Key-Section Program of the Hungarian Geological Survey. The authors wish to thank Mrs. László Pellérdy for the core photographs. We thank Géza Császár and László Korpás for reviewing the manuscript and their valuable comments and suggestions. Financial support was provided by the Hungarian National Science Fund (2671) and the Hungarian-US Joint Fund (JFNo 212)

References

- Balog, A., J.F. Read, J. Haas 1993: Climate controlled dolomitization of a Late Triassic platform, Hungary. – (Abstract) SEPM Meeting 1993, August 8-12, 1993 Pennsylvania.
- Császár, G. 1989: Transgressive Urganian sequence with black "pebbles" from the Villány Mountains, Hungary. – *Acta Geol. Hung.*, 32, 1-2, pp. 3-29.

- Fischer, A. G. 1964: The Lofer cyclothems of the Alpine Triassic. – *Kansas Geol. Survey Bull.*, 169, 1, pp. 102–149.
- Fülöp, J. 1976: The Mesozoic basement horst blocks of Tata. – *Geol. Hung. Ser. Geol.*, 16, pp. 1–225.
- Ginsburg, R.N., L.A. Hardie 1975: Tidal and storm deposits, Northwestern Andros Island, Bahamas. – In: R.N. Ginsburg (Ed.): *Tidal Deposits*. Springer Verlag Berlin, Heidelberg, New York, pp. 201–208.
- Haas, J. 1982: Facies analysis of the cyclic Dachstein Limestone Formation (Upper Triassic) in the Bakony Mountains, Hungary. – *Facies*, 6, pp. 75–84.
- Haas, J. 1987: Felső-triász szelvények korrelációja a lofer-ciklusok alapján (Gerecse hegység) (Correlation of Upper Triassic profiles on the basis of Lofer cycles [Gerecse Mts.]) – *Földt.Közl., Bull. of the Hungarian Geol. Soc.*, 117, pp. 375–383.
- Haas, J. 1988: A Dunántúli-középhegység felső-triász karbonátos kőzeteinek fácieselemzése a Lofer ciklusok jellegei alapján (Upper Triassic carbonate rocks of the Transdanubian Mid-Mountains: facies analysis based on Lofer cycle features). – *Földt. Közl.*, 118, pp. 101–108.
- Haas, J. 1991: A basic model for Lofer cycles. – In: G. Einsele, W. Ricken, A. Seilacher (Eds): *Cycles and Events in Stratigraphy*. Springer-Verlag Berlin, Heidelberg, New York, London, Paris, Tokyo, Hong-Kong, Barcelona, Budapest, pp. 722–732.
- Haas, J. 1994: Lofer cycles of the Upper Triassic Dachstein platform in the Transdanubian Mid-Mountains, Hungary. – *Spec. Publs Int. Ass. Sediment.* 19, pp. 303–322. Blackwell Scientific, Oxford.
- Haas, J., K. Dobosi 1982: Felső-triász ciklusos karbonátos kőzetek vizsgálata bakonyi alapszelvényeken (Investigation of Upper Triassic cyclic carbonate rocks in key sections in the Bakony). – *MÁFI Évi Jel. 1980-ról*, pp. 135–168.
- Hagan, G.M., B.W. Logan 1975: Prograding tidal-flat sequences: Hutchison Embayment, Shark Bay, Western Australia. – In: R.N. Ginsburg (ed.): *Tidal Deposits*, Springer-Verlag, Berlin, Heidelberg, New York, pp. 215–222.
- Hohenegger, J., W. Piller 1975: Ökologie und systematische Stellung der Foraminiferen in gebanktem Dachsteinkalk (Obertrias) des nördlichen Toten Gebirges (Oberösterreich). – *Palaeogeogr. Palaeoclimatol. Palaeoecol.*, 18, pp. 241–276.
- Oravecz-Scheffer, A. 1987: A Dunántúli-középhegység triász képződményeinek foraminiferái () – *Geol. Hung. Ser. Pal.*, 50, pp. 1–331.
- Purser, B.H., G. Evans 1973: Regional sedimentation along the Trucial Coast, SE Persian Gulf. – In: Purser, B.H (ed.): *The Persian Gulf; Holocene Carbonate Sedimentation and Diagenesis in a Shallow Epicontinental Sea*. Springer Verlag, New York, pp. 211–232.
- Sander, B. 1936: Beiträge zur Kenntnis der Anlagerungsgefüge (Rhythmischer Kalke und Dolomite aus der Trias). I. und II. – *Tschermak Mineral. Petr. Mittl.*, 48, pp. 27–139, pp. 141–209.
- Schwarzacher, W. 1948: Sedimentpetrografische Untersuchungen kalkalpiner Gesteine. Hallstätterkalk von Hallstatt und Ischl. – *Jb. Geol. B.-A.*, 91, pp. 1–48.
- Schwarzacher, W. 1954: Die Grossrhythmik des Dachsteinkalkes von Lofer. – *Tschermaks Mineral Petrogr. Mitt.*, 4, pp. 44–54.
- Schwarzacher, W., J. Haas 1986: Comparative statistical analysis of some Hungarian and Austrian Upper Triassic peritidal carbonate sequences. – *Acta Geol. Hung.*, 29, pp. 175–196.
- Shinn, E.A. 1973: Recent Intertidal and Nearshore Carbonate Sedimentation around Rock Highs, E. Qatar, Persian Gulf. – In: B.H. Purser (Ed.): *The Persian Gulf*, Springer-Verlag, Berlin, Heidelberg, New York, pp. 193–198.
- Strasser, A. and E. Davaud 1983: Black pebbles of the Purbeckian (Swiss and French Jura): lithology, geochemistry and origin. – *Eclogae geol. Helv.*, 76/3, pp. 551–580, Basel.
- Woods, P.J., R.G. Brown 1975: Carbonate sedimentation in an Arid Zone Tidal Flat, Nilemah Embayment, Shark Bay, Western Australia. – In: R.N. Ginsburg (Ed.): *Tidal Deposits*, pp. 223–232.

Environmental significance of the Anisian Ostracoda fauna from the Forrás Hill near Felsőörs (Balaton Highland, Transdanubia, Hungary)

Miklós Monostori

*Department of Palaeontology,
Eötvös Loránd University, Budapest*

The quantitative palaeoecological analysis of the Anisian Felsőörs Limestone Formation in the type locality shows a deepening basin with one or more submerging platforms from which material slumped into the basin from time to time. In the systematical part there are some remarks on the known species and description of five new species and subspecies: *Reubenella angulata*, *Bairdia cassiana rotundidorsata*, *Bairdia humilis*, *Bairdia (Urobairdia) angusta recta*, *Bairdia (Urobairdia) lata*.

The indicator character of the species follows from their previous data, quantitative distribution and coexistence.

Key words: Triassic, Ostracoda, paleoecology

Introduction

The first publication about Triassic ostracods of the Balaton Highland is the work of Méhes (1911) in the great scientific series "Resultate der wissenschaftlichen Erforschung des Balatonsees". Many new species were described in this work, without any statistical or quantitative data. After a long hiatus Kozur (1970, 1971, 1972, in Bunza and Kozur 1971) gave a modern description of many known and new species from the Forráshegy (Forrás Hill) section, with paleoecological remarks but without a quantitative evaluation of the fauna.

The microfaunal evaluation of the Forrás Hill section with its stratigraphic column was published in the excursion guide of the 21st European Micropaleontological Colloquium. (Oravecz-Scheffer 1989), again without quantitative data.

A bed by bed sampling was carried out in 1992 with the aid of the Hungarian Geological Institute. This paper contains the results of the quantitative evaluation of ostracods, supported by OTKA project N T 7631.

Address: M. Monostori: H-1083 Budapest, Ludovika tér 2, Hungary

Received: 24 April, 1995

Geology, Sampling

The Forrás Hill section (Fig. 1) contains Anisian dolomites without microfauna in its lower part (Megyehegy Dolomit Formation). The middle (main) part of the section consists of marl and limestone layers (Felsőörs Limestone Formation), with some tuff in its upper half. The upper part of the section is of Ladinian age (Nemesvámos Limestone Member of the tuffaceous Buchenstein Formation).

All the Anisian ostracods are from the Felsőörs Limestone Formation; samples (Fig. 1) are from Bed 45 to Bed 100c.

Altogether 31 samples yielded ostracodes, from the loose marls by washing and from the hard marls and limestones by dissolving in concentrated acetic acid. The number of picked specimens is 1603, of which 1502 are determinable.

We have in the section three zones suitable for quantitative evaluation (see on Fig. 1):

Samples 46–52

Samples 76–83

Samples 86–99c.

Systematical part

Subclass Ostracoda Latreille, 1806

Order Myodocopida Sars, 1866

Suborder Cladocopa Sars, 1866

Family Polycopidae Sars, 1866

Genus *Polycope* Sars, 1866

Polycope sp.

Dimensions: carapace: L = 0.35 mm, H = 0.31 mm, L/H = 1.12

Remarks: The unornamented casts are indeterminable on the species level.

Material: 7 specimens in samples No. 75, 76, 83, 80, and 78.

Order Podocopida G. W. Müller, 1894

Suborder Platycopa Sars, 1866

Family Cytherellidae Sars, 1866

Genus *Reubenella* Sohn, 1968

Reubenella angulata n. sp.

Plate I, fig. 1.

Derivatio nominis: after its quadrangular character.

Locus typicus: Felsőörs, Forrás Hill.

Stratum typicum: Bed 83, Anisian (Illyrian).

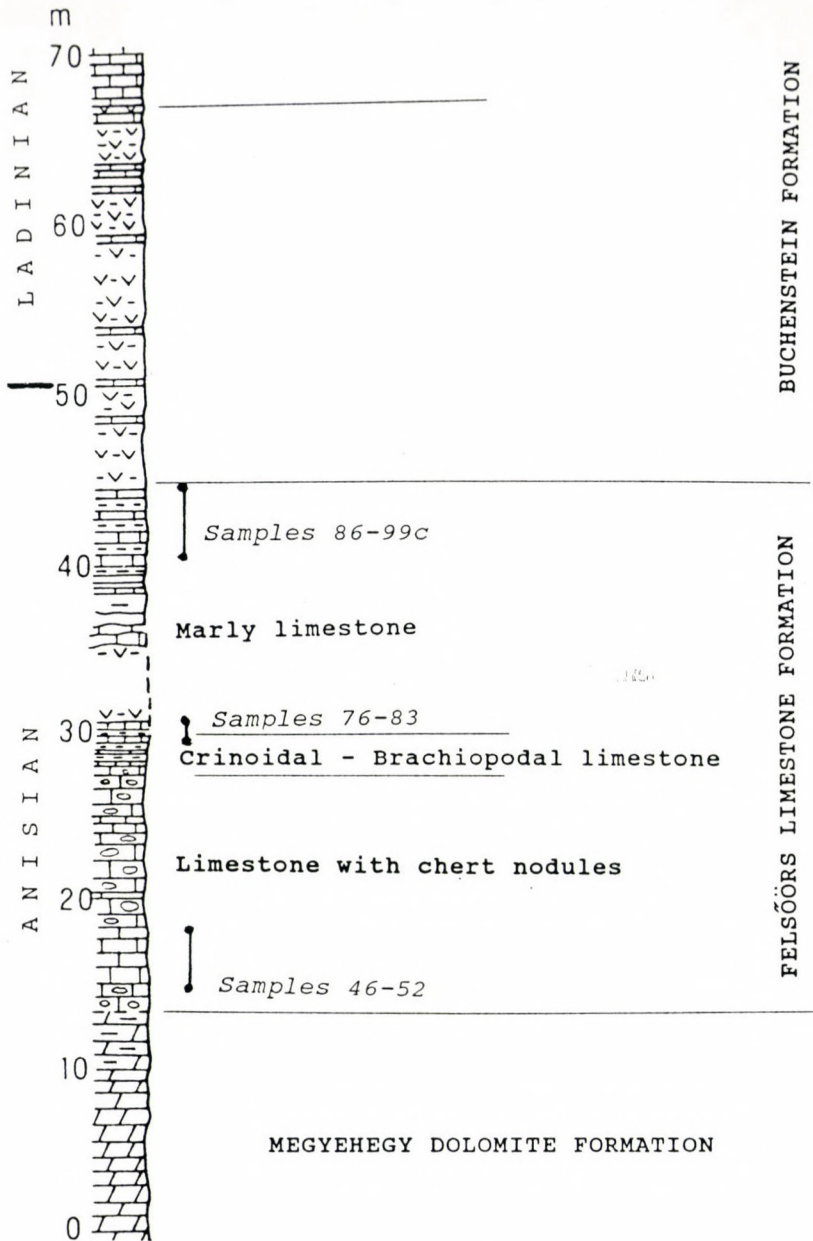


Fig. 1
Position of the quantitatively evaluated ostracod samples in the Forrás Hill section. Stratigraphic column after Oravecz-Scheffer 1989

Diagnosis: Elongated form with quadrangular shape and strong break of the ventral part of the lateral surface.

Description: The anterior outline of the right valve is broadly and symmetrically rounded. It turns into the straight dorsal outline at 0.2 of length. After 0.8 of length follows the slightly asymmetrical posterior outline. There is a break on the posterior outline at level of 0.3 height, the lower part has a larger radius. It turns gradually into the slightly convex ventral outline. Height is at 0.3 of length. The left valve has a similar outline, its dorsal outline is very slightly convex. In ventral view after a short flattened marginal part the anterior surface of the valves emerges at about 40–45° to 0.15 length, then they are nearly parallel, at 0.9 length they slope at about 80° and end with a short posterior part with 30–40°. The less elongated specimens are less angulate in ventral view with more gradual anterior and posterior transitions. There is a depressed area on the left valve at the anterior margin. A deep triangular depression is on the dorsal part, a smaller depression is posteroventral. The ventral and posterior lateral surface parts slope abruptly after a break.

Dimensions: carapaces: L = 0.77–0.81 mm; H = 0.41–0.43 mm, L/H = 1.88.

Comparison: *Reubenella avnimelechi* Sohn, 1968 is similar in ventral view, but less quadrangular in lateral view and it has a characteristic reticulation on its surface. *R. subcylindrica* (Sandberger 1866) is more rounded both in lateral and ventral views.

Material: 8 specimens, in samples No. 52; 83 and between 99 and 99a.

Suborder Metacopa Sylvester-Bradley, 1967

Superfamily Healdiacea Harlton, 1963

The family Healdiacea has the second position in the Triassic of the Balaton Highland in terms of the number of specimens. The genus *Hungarella* of Méhes (1911) does not have any type material, nor even has not any locality name on plate captions, and has a rather wide range of stratigraphical and locality notes in the description. The very important muscle scars are rarely and hardly visible, so it is necessary to make a revision of all Balaton Highland sections.

In the present paper I give the specimen number of the 3 species in Kozur's work (1970) placed in the genus "*Hungarella*".

"*Hungarella*" *felsooersensis* (Kozur 1970)

Plate I, fig. 2

1970. *Healdia* (*Heladia*) *felsooersensis* n. sp. – Kozur, p. 21, Pl. 3, f. 13, Pl. 4, f. 1–6.

Dimensions: carapace: L = 0.50–0.78 mm; H = 0.38–0.56 mm; L/H = 1.32–1.47; W = 0.26–0.41.

Remarks: The spines are usually broken from the right valves. The overlap of the left valve sometimes is very high dorsally. The anterior end of the right

valve is pointed, its upper part somewhat concave, its lower part distinctly convex.

Material: 297 specimens in samples No. 76, 83, 86, 90, 92, 96, 97, 97/98, 98, 98/99, 99/99a, 99a, 99b, and 99c.

"*Hungarella*" *reniformis* (Méhes, 1911)

Plate I, fig. 3.

1911. *Bairdia* ? *problematica* n. sp. var. *reniformis* n. var. Méhes, p. 21, Pl. II, f. 19–23.

1970. *Healdia* (*Hungarella*) *reniformis* (Méhes 1911) Kozur, pp. 22–23, Pl. 4, f. 15–17.

Dimensions: L = 0.40–0.50 mm; H = 0.26–0.33 mm; L/H = 1.48–1.55.

Remarks: Kozur's remarks relating to figs 21–22 of Méhes are not acceptable because they are obviously drawn from the right valve. These dorsally more rounded forms sometimes have a rather strong posterior spine on the right valve. It is probable, from the material, that this form is not a different species but it belongs to the instars of *felseoersensis* with gradual transitions.

Material: 275 specimens in samples No. 83, 86, 90, 92, 93/94, 96, 97, 97/98, 98, 99/99a, 99a, 99b, and 99c.

"*Hungarella*" *anisica* (Kozur, 1970)

Plate I, f. 4.

1970. *Healdia* (*Healdia*) *anisica* n. sp. Kozur, pp. 21–22, Pl. 4, f. 7–14.

1972. *Healdia anisica* Kozur, 1970 Kozur, Pl. 1, f. 4.

?1984. *Healdia anisica* Kozur, 1970 Salaj et Jendrejakova, 1984, Pl. 1, f. 1.

Dimensions: L = 0.34–0.51 mm; H = 0.20–0.29 mm; L/H = 1.65–1.68.

Remarks: Salaj et Jendrejakova's photo is made from the inner side of left valve, so we cannot observe the features characteristic of the species. The rather high outline is not common in this species. Only a few specimens have the posterior vertical edge, on the most of the similar little and elongated forms there is only a distinct break posteriorly in the dorsal and ventral view of the carapace.

Material: 69 specimens in samples No. 83, 86, 92, 96, 98, 99/99a, 99a, and 99b.

"*Hungarella*" sp.

Material: 16 poorly preserved specimens in samples No. 80, 97, 97/98, 98/99, and 100/c/3

Suborder Podocopa Sars, 1866

Superfamily Bairdiacea Sars, 1866

Family Bairdididae Sars, 1888

Genus *Bairdia* McCoy, 1844

Bairdia balatonica Méhes, 1911

Plate I, fig 5., Plate II, fig. 1.

1911. *Bairdia balatonica* n. sp. Méhes, pp. 13–14, Pl. I, f. 8–11.

1911. *Bairdia dadayi* Méhes, 1911 Méhes, pp. 17–18., Pl. I, f. 29–30.

?1965. *Bairdia balatonica* Méhes var. 1911 Széles, p. 414, fig. 4.

1965. *Bairdia dadayi* Méhes, 1911 Széles, pp. 412–413, fig. 1.

1978. *Bairdia* cf. *balatonica* Méhes, 1911 Kristan-Tollmann, p. 81, Pl. 1, f. 1–3.

Dimensions: carapaces: L = 0.81–1.09 mm, H = 0.52–0.69 mm, L/H = 1.47–1.58.

Remarks: In 1994 (p. 315) I believed that Kristan-Tollmann's material represented a new species.

In the Forrás Hill material the typical *balatonica* and the high form (with extreme dorsal overlap), as in Kristan-Tollmann's material, are in the same sample, with transition.

These high forms have a distinct short swelling along the top part of dorsal outline. On Kristan-Tollmann's Carnian form the dorsal part of the anterior outline on the right valve is more concave and the posterior outline is more elongated; it is questionable whether it is a new subspecies or not. It is problematical to put the *balatonica* var. of Széles into the species owing to its strong dorsal asymmetry.

Material: 57 specimens in samples No. 97, 99b, 99c, and 99/99a.

Bairdia cassiana rotundidorsata n. ssp.

Plate II, figs 2–3.

Derivatio nominis: after the symmetrically arched dorsal outline.

Locus typicus: Felsőörs, Forrás Hill.

Stratum typicum: Bed 83, Anisian (Illyrian).

Diagnosis: the form has a symmetrically arched dorsal margin on the left valve.

Comparison: An elongated form with somewhat acute and upward directed posterior end at about 1/3 height level. Somewhat variable are the L/H, the convexity of lower part, the concavity of upper part of posterior outline and the overlap. The symmetrically arched dorsal outline of the left valve as contrasted with the nominate subspecies (Kristan-Tollmann and Hamedani 1973), is characteristic.

Dimensions: carapaces: L = 0.72–1.00 mm, H = 0.38–0.59 mm, L/H = 1.64–1.92.

Material: 501 specimens in samples No. 78, 80, 81, 82, 83, 86, 92, 96, 97, 98, 98/99, 99/99a, 99a, and 99b.

Bairdia finalyi (Méhes 1911)

Plate III, fig. 1.

1911. *Cytherideis finalyi* n. sp. Méhes, pp. 27–28, Pl. IV, f. 11 (non f. 12–13).

1971. *Bairdia finalyi* (Méhes, 1911) Kozur, p. 4, f. 2D

1984. *Bairdia finalyi* (Méhes) Salaj, Jendrejakova, Pl. 1, f. 3.

Remarks: the specimens correspond to the species revised by Kozur 1971.

Dimensions: carapaces: L = 0.66–0.88 mm, H = 0.29–0.38 mm, L/H = 2.28–2.32.

Material: 20 carapaces in samples No. 78, 80, 83, 99/99a, 99b, 99a, 81, 86, and 92.

Bairdia humilis n. sp.

Plate III, fig. 2.

Derivatio nominis: after its low carapace height.

Locus typicus: Felsőörs, Forrás Hill.

Stratum typicum: Bed No. 83, Anisian (Illyrian).

Diagnosis: elongated form with little overlapping, the median straight element of the dorsal outline is short.

Description: The anterior outline of the left valve is very asymmetrically rounded, the radius of the lower part is large, then becomes gradually smaller and after a break turns into the dorsal outline. It is nearly symmetrically trapezoidal, the long anterior and posterior parts are nearly straight, hardly concave and go at angles of 150–160° to the short and hardly convex median element. The posterior outline, after a break, is very asymmetrical, its radius rapidly increasing towards the ventral outline. The ventral outline is hardly concave.

On the right valve the dorsal outline is more angular, the ventral outline is more concave.

Dimensions: (carapace): L = 0.71 mm, H = 0.30 mm, L/H = 2.37.

Comparison: This species is similar to *B. finalyi* (Méhes, 1911), but more symmetrical with a very characteristic outline.

Material: 1 carapace from Bed No. 83.

Bairdia (Urobairdia) angusta recta n. ssp.

Plate III, figs 3–4.

Derivatio nominis: after the nearly horizontal caudal process.

Locus typicus: Felsőörs, Forrás Hill.

Stratum typicum: Bed No. 99/99a, Anisian (Illyrian).

Diagnosis: the caudal process is only slightly curved upward.

Comparison: elongated form with distinct caudal process. As compared to the type subspecies (*U. angusta angusta* Kollmann 1963) the caudal process is shorter and is not so much directed upward, the lower part of the caudal process is hardly convex or nearly straight and the posterodorsal outline is less depressed.

Dimension: carapace: L = 0.81–1.0 mm, H = 0.46–0.58 mm, L/H = 1.72–1.76.

Material: 13 specimens in samples No. 92, 96, 97, 99/99a, and 99b.

Bairdia (Urobairdia) lata n. sp.

Plate IV, fig. 1.

Derivatio nominis: after the great height among the Urobairdiae.

Locus typicus: Felsőörs, Forrás Hill.

Stratum typicum: Bed No. 92, Anisian (Illyrian).

Diagnosis: it is a high form.

Description: The anterior outline of the left valve is broadly and asymmetrically rounded, its upper part is nearly straight. From the 0.25 to 0.6 length the dorsal outline is nearly straight, after a break it slopes straight to 0.9 length where there is a short depression of the caudal process. The caudal process ends narrowly, its lower side has a slowly curved outline turning to the asymmetrically rounded ventral outline.

There is a slight depression under the middle part of the trapezoidal dorsal outline.

The right valve is more angular both dorsally and ventrally, the ventral and dorsal overlappings are quite moderate.

Dimensions: carapace: L = 1.00 mm, H = 0.65 mm, L/H = 1.54

Comparison: there is not any similarly high form among the Triassic Urobairdia species.

Material: 8 specimens in samples No. 92, 97/98, 99/99a, and 99b.

Urobairdia sp. 1.

Plate IV, figs 2–3.

Remarks: casts of mostly juvenile forms similar to *U. angusta recta*.

Material: 63 specimens in beds No. 61, 75, 76, 77, 78, 80, 81, 82, and 99b.

Genus Bairdiolites Croneis et Gale, 1939

Bairdiolites cf. *compactus* Kristan-Tollmann, 1970

Plate IV, fig. 5.

Dimensions: L = 0.86 mm

Remarks: the specimen from Felsőörs is somewhat incomplete, but the main sculptural elements are similar to *compactus*. Figures 9–10 on plate 2 in Salaj-Jendrejakova (1984) obviously belong to another taxa.

Material: 1 specimen in sample 81.

Genus Lobobairdia Kollmann, 1963

Lobobairdia zapfei Kozur, 1971

Plate IV, fig. 4.

1971. *Lobobairdia?* *zapfei* n. sp. Kozur, pp. 6–7, fig. 1 H

Dimensions: left valves: L = 1.00–1.30 mm, H = 0.57 mm, L/H = 1.75.

Remarks: the shape and ornamentation are characteristic for the mostly fragmented specimens collected from the type locality.

Material: 20 specimens in samples No. 76, 80, 81, and 82.

Genus *Nodobairdia* Kollmann, 1963

Nodobairdia? *martinssoni* (Kozur, 1971)

Plate V, fig. 1.

Dimensions: carapace: L = 0.70 mm, H = 0.46 mm, L/H = 1.52.

Remarks: the typical ventral far-off-margin longitudinal costa, the antero- and posterodorsal elongated knots and the central little knots are typical for the species.

Material: 1 specimen in sample 80.

Nodobairdia sp.

Remarks: posterior fragment with two distinct nodes from sample 82.

Genus *Ptychobairdia* Kollmann, 1960

Ptychobairdia cf. *bolzi* Kozur, 1971

cf. 1971. *Triebelina bolzi* n. sp. Kozur, pp. 8–10, Fig. 2B, D, E.

Dimensions: carapace: L = 0.94 mm, H = 0.51 mm, L/H = 1.84.

Remarks: the characteristic four longitudinal swellings are well visible on the fairly well preserved specimens.

Material: 2 specimens in samples 86 and 99/99a.

Ptychobairdia? *veghae* Kozur, 1971

Plate V, fig. 2.

1971. *Triebelina veghae* n. sp. Kozur, pp. 14–15, fig. 1D.

Dimensions: carapace: L = 0.73 mm, H = 0.41 mm.

Remarks: The longitudinal costae have characters typical for this species. The dimensions are much larger than on the type material. Probably Kozur's type material contains instar specimens.

Material: 1 specimen in sample No. 99b.

Genus *Acratia* Delo, 1930

Acratia cf. *goemoeryi* Kozur, 1970

Dimensions: carapace: L = 0.80 mm, H = 0.36 mm, L/H = 2.22 mm.

Remarks: The shallow anteroventral sinus reminds one of *A. goemoeryi* Kozur, 1970, but the dorsal outline is more convex than that on the *goemoeryi* type material.

Material: 1 carapace in sample No. 92. ? 3 juv. carapace in sample 45.

Genus *Bairdiacypris* Bradfield, 1935

Bairdiacypris anisica Kozur, 1971

Plate V, fig. 3.

1911. *Cytherideis finalyi* n. sp. Méhes, pp. 27–28, Pl. IV, f. 12–15.

1911. *Bairdiacypris anisica* n. sp. Kozur, pp. 4–5, Fig. 2B–C, E–G.

Dimensions: carapaces: L = 0.60–0.98 mm, H = 0.32–0.45 mm, L/H = 1.82–2.35.

Remarks: the outline is rather variable. The instars are shorter (at L 0.60–0.62 L/H are 1.82–1.94). The dorsal arch sometimes somewhat higher, also variable are the breakings of posterior and anterior outlines. Figures 12–13 of *Cytherideis finalyi* n. sp. on Pl. IV in Méhes (1911) represent this species.

Material: 67 carapaces in samples No. 76, 78, 79, 80, 81, 83, 86, 99/99a, 99b, and 99c.

Superfamily Cytheracea Baird 1850

Family Bythocytheridae Sars 1866

Genus *Monoceratina* Roth 1928

Monoceratina n. sp. B Kozur, 1970

Remarks: a single fragmental valve in sample 99c.

Superfamily Cypridacea Baird, 1845

Genus *Spinocypris* Kozur, 1971

?*Spinocypris vulgaris* Kozur, 1971

Plate V, fig. 4.

Dimensions: carapaces: L = 0.37–0.57 mm, H = 0.22–0.36 mm, H/L = 1.56–1.98.

Remarks: The material is rather poorly preserved without distinct posterior spine. The posterior end is always damaged. The outline and the dimensions are very similar to this species but also similar to *Paracypris loferensis* Kristan-Tollmann, 1991 (from the Rhaetian).

Material: 57 specimens in samples No. 45, 46, 47, 50, 52, 53, 64, 78, 79, 80, 86, and 99b.

Environmental evaluation

The lower part of the Felsőörs Limestone consists of gray limestones with chert nodules. The main part of the section consists of spiculiferous biomicrite (samples 45–64) with foraminifers and conodonts. The ostracoda association is simple, with 87% of the specimens falling within one species: ?*Spinocypris vulgaris* with rare *Reubenella*, *Bairdia* (*Urobairdia*), *Bairdiacypris*, ?*Acratia*. The

fauna is rather poorly preserved. The association suggests an environment below the storm-wave base (Fig. 2).

The middle part of the Felsőörs Limestone is a crinoidal-brachiopodal limestone with a rich benthos assemblage, sessile foraminifers on macrofauna and conodonts (samples 65–82). The presence of some shallow-water ostracods (ornate Bairdiids) is characteristic: Bairdiolites, Lobobairdia, and Nodobairdia. The percentage of their specimens alternates between 10 and 50, indicating, in Kozur's opinion, an agitated, shallow water depositional environment. However, their percentage in the total specimen number of these beds is only 16. The main part of the fauna consists of forms which are the main elements in the overlying deepwater sediments (elongated Bairdia, caudally acuted Bairdia (Urobairdia – 46 % of the total specimen number belongs to the latter!), Bairdiacypris (Fig. 3). The crinoidal-brachiopodal limestone contains mixed material of shallow-water, near-platform sediments and deeper slope sediments. It was formed by transportation of shallow-water sediments down the slope. This is in agreement with the opinion of Budai and Vörös about the Triassic sedimentation of the Balaton Highland (Budai and Vörös 1992, Fig. 3).

The upper part of the Felsőörs Limestone is a brownish-grey marly limestone with ammonites, Daonella, foraminifers, radiolarians, conodonts and ostracods. Among the ostracods there are no shallow water forms. The main elements are the elongated Bairdia species (*B. cassiana rotundidorsata*, *B. finalyi*), the "Hungarella", the posteriorly acuted Bairdia (Urobairdia) (Fig. 4), and occasionally Bairdiacypris. Kozur has found some characteristic psychrosphaeric forms as *Acantoscapa*, *Nagyella*, and *Triceratina* underlining the deep water character of the sedimentation. Investigating a 0.5 kg sample from each bed we were unable to obtain a single specimen of these forms: their total proportion in the ostracod fauna is less than one percent. The ostracods are sometimes very numerous in the samples. There is a remarkable shift in dominance of elongate Bairdia to "Hungarella" from sample No. 93/94 upwards (Fig. 4). The rare *Ptychobairdia* of the Felsőörs Limestone (upper part) are the only ornate Bairdiidae in the deep water environment. It is possible that they lived on the submerged platform and were carried into the deep basin.

The quantitative evaluation of the Upper Anisian ostracods supports the paleogeographic picture of a deepening basin with one or more submerged platforms supplying the basin with redeposited material from time to time.

Indicator character of species:

We can connect some species with their probable environment:

1) Shallow sublittoral normal marine periplatform territories:

Lobobairdia zapfei Kozur

Nodobairdia martinsoni (Kozur)

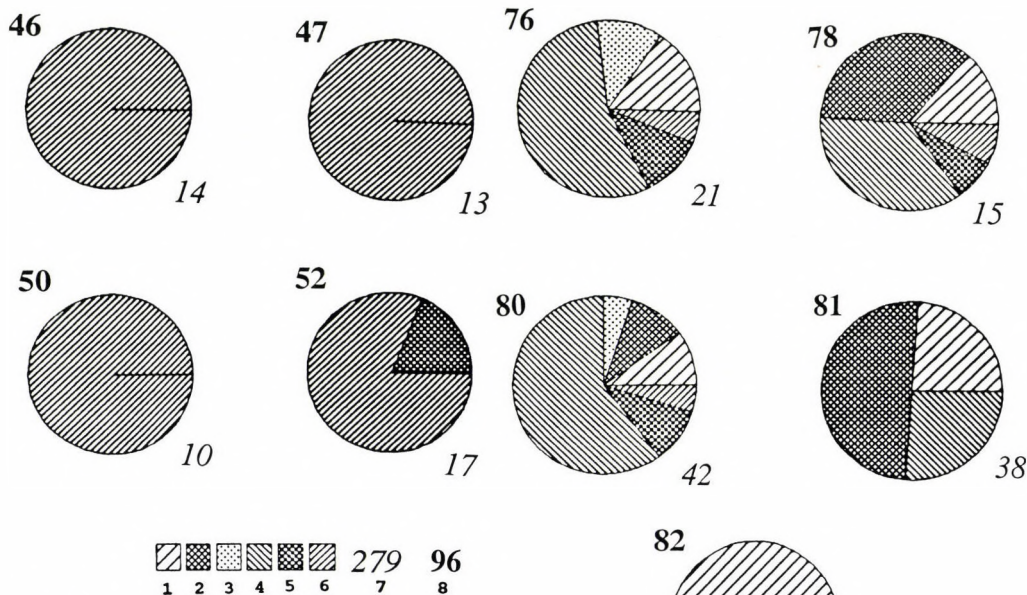


Fig. 2
Quantitative distribution of ostracods in cherty nodular limestone. 1. Bairdiolites + Lobobairdia + Nodobairdia; 2. Bairdia; 3. "Hungarella"; 4 Bairdia (Urobairdia); 5. Bairdiacypris; 6. Spinocypris; 7. specimen number; 8. sampling number. The 0 % is in right position and the percentage is anticlockwise

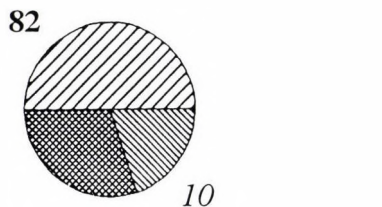


Fig. 3
Quantitative distribution of ostracods in samples of the crinoid-brachiopod limestone. For legend see Fig. 2

2) Deep sublittoral marine environment (below the stormwave base):

Bairdia (Urobairdia) sp.

?*Spinocypris vulgaris* Kozur

and all the species dominating in the bathyal environment.

3) Bathyal marine environment:

Dominating forms:

"*Hungarella*" *felseoersensis* Kozur

"*Hungarella*" *reniformis* Méhes

"*Hungarella*" *anisica* Kozur

Bairdia cassiana rotundidorsata n. ssp. (elongated form)

Occasionally frequent forms:

Bairdiacypris anisica Kozur

Bairdia balatonica Méhes

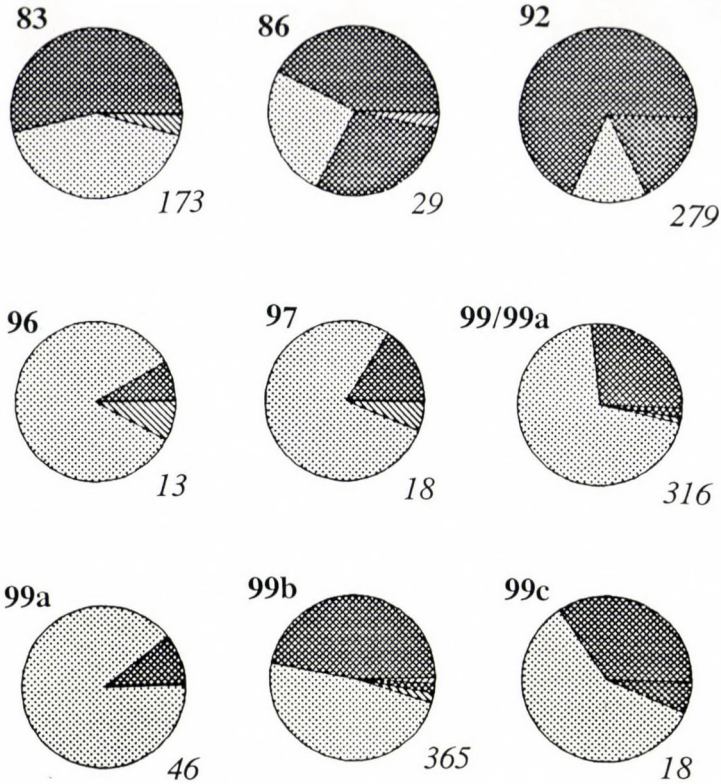


Fig. 4
Quantitative distribution of the ostracods in samples of the marly limestone. For legend see Fig 2.

Rare, but characteristic forms:

Bairdia finalyi Méhes (elongated form)

Bairdia humilis n. sp. (elongated form)

Bairdia (Urobairdia) angusta recta n. ssp.

Bairdia (Urobairdia) lata n. sp.

Acratia cf. *goemoeryi* Kozur

Monoceratina n. sp. B. Kozur and all psychrosphaeric forms described by Kozur (1971), but not found during the present investigations.

The species *Ptychobairdia bolzi* Kozur and *Ptychobairdia veghae* Kozur may be deep sublittoral forms of the submerged platforms carried into the basin.

Plate I

1. *Reubenella angulata* n. sp. Carapace from the left valve. Sample 83. M = 100x.
- 2-4. "*Hungarella*" *felsoeoersensis* (Kozur 1970). Carapaces from the right valves. 2. Sample 92. M = 75x. 3-4. Sample 99a. M = 90x, 70x.
5. "*Hungarella*" *anisica* (Kozur 1970). Carapace from right valve. Sample 83. M = 120x.
6. "*Hungarella*" *reniformis* Méhes, 1911. Carapace from right valve. Sample 92. M = 120x

Plate II

- 1-3. *Bairdia balatonica* Méhes 1911. Carapaces from right valves. Sample 99b. M = 70x, 53x, 60x.
- 4-5. *Bairdia cassiana rotundidorsata* n. sp. Carapaces from right valves. Sample 92. M = 90x

Plate III

1. *Bairdia finalyi* Méhes 1911. Carapace from right valve. Sample 80. M = 108x.
2. *Bairdia humilis* n. sp. Carapace from right valve. Sample 83. M = 120x.
- 3-4. *Bairdia* (*Urobairdia*) *angusta recta* n. ssp. Carapaces from right valves. 3. Sample 96. M = 95x. 4. Sample 99/99a. M = 80x

Plate IV

1. *Bairdia* (*Urobairdia*) *lata* n. sp. Left valve. Sample 92. M = 70x.
- 2-3. *Bairdia* (*Urobairdia*) sp.1. Casts from right side. 2. Sample 76. M = 100x. 3. Sample 81. M = 105x.
4. *Lobobairdia zapfei* Kozur 1971. Posterior part of right valve. Sample 82. M = 68x.
5. *Bairdiolites* cf. *complanatus* Kristan-Tollman, 1970, Left valve. Sample 81. M = 80x

Plate V

1. *Nodobairdia?* *martinsoni* (Kozur 1971). Carapace from right valve. Sample 80. M = 80x.
2. *Ptychobairdia veghae* Kozur 1971. Left valve. Sample 99b. M = 110x.
3. *Bairdiacypris anisica* Kozur 1971. Carapace from right valve. Sample 99b. M = 80x.
4. ?*Spinocypris vulgaris* Kozur 1971, Carapace from right valve. Sample 47. M = 165x

Plate I

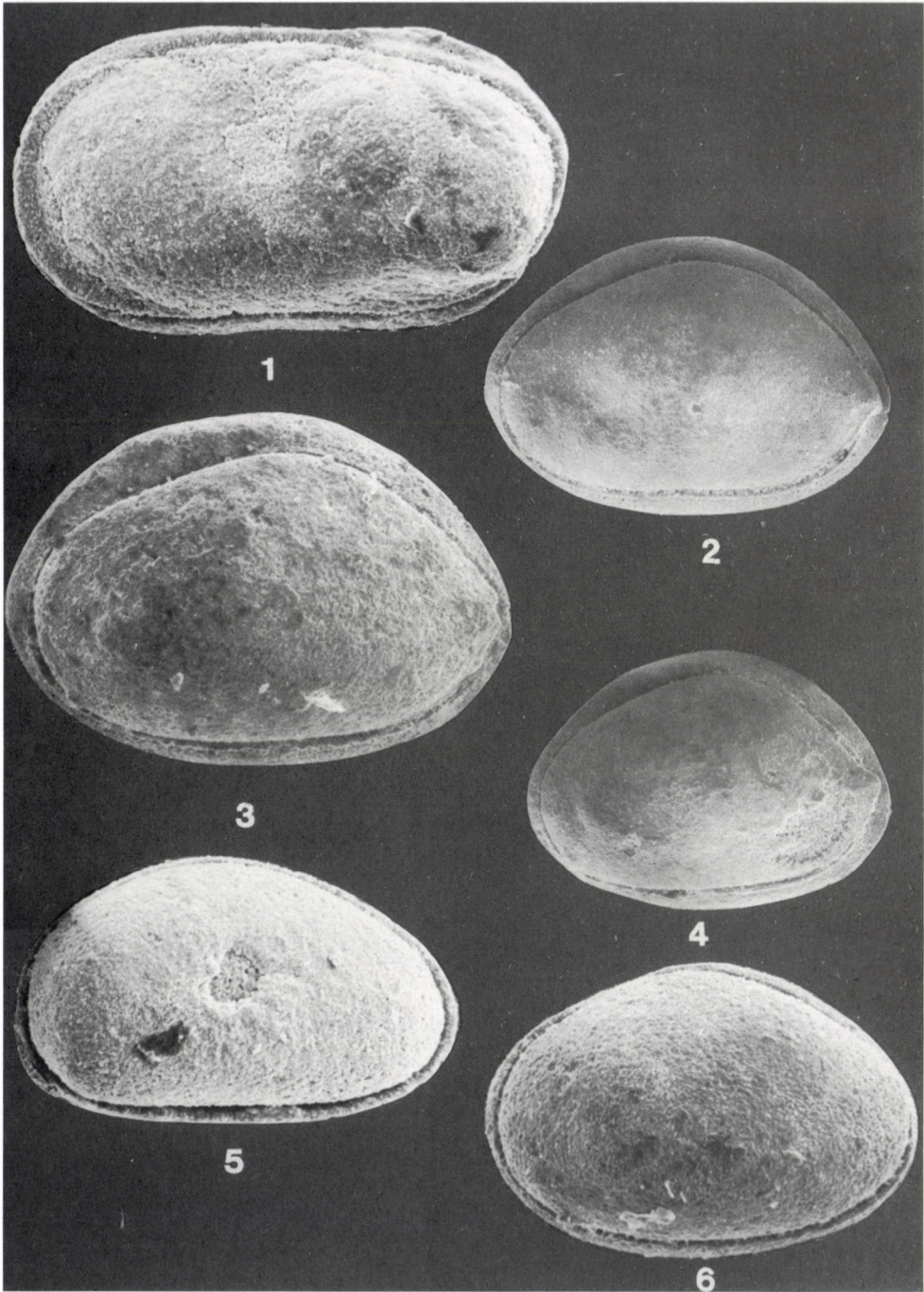


Plate II

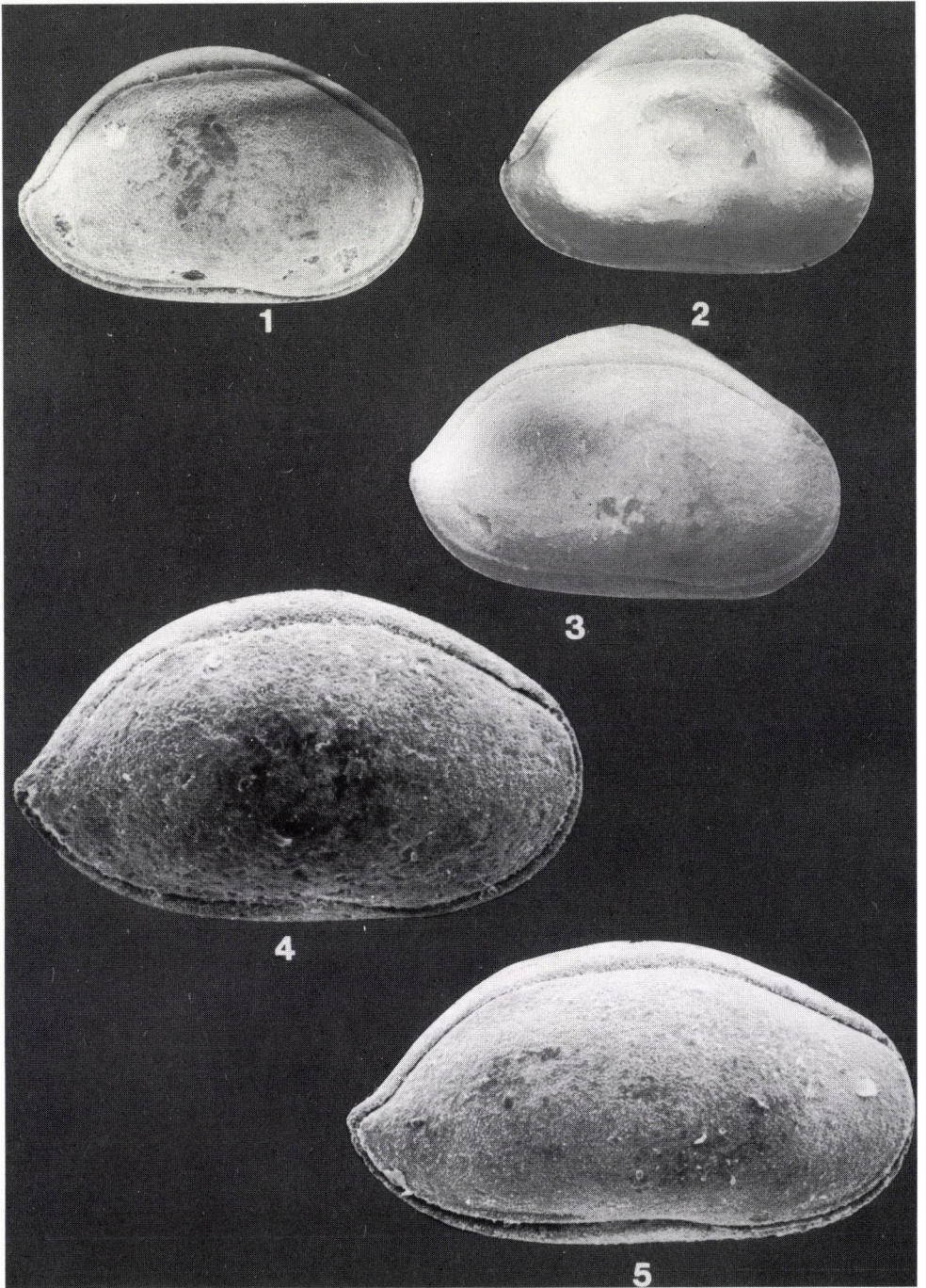


Plate III

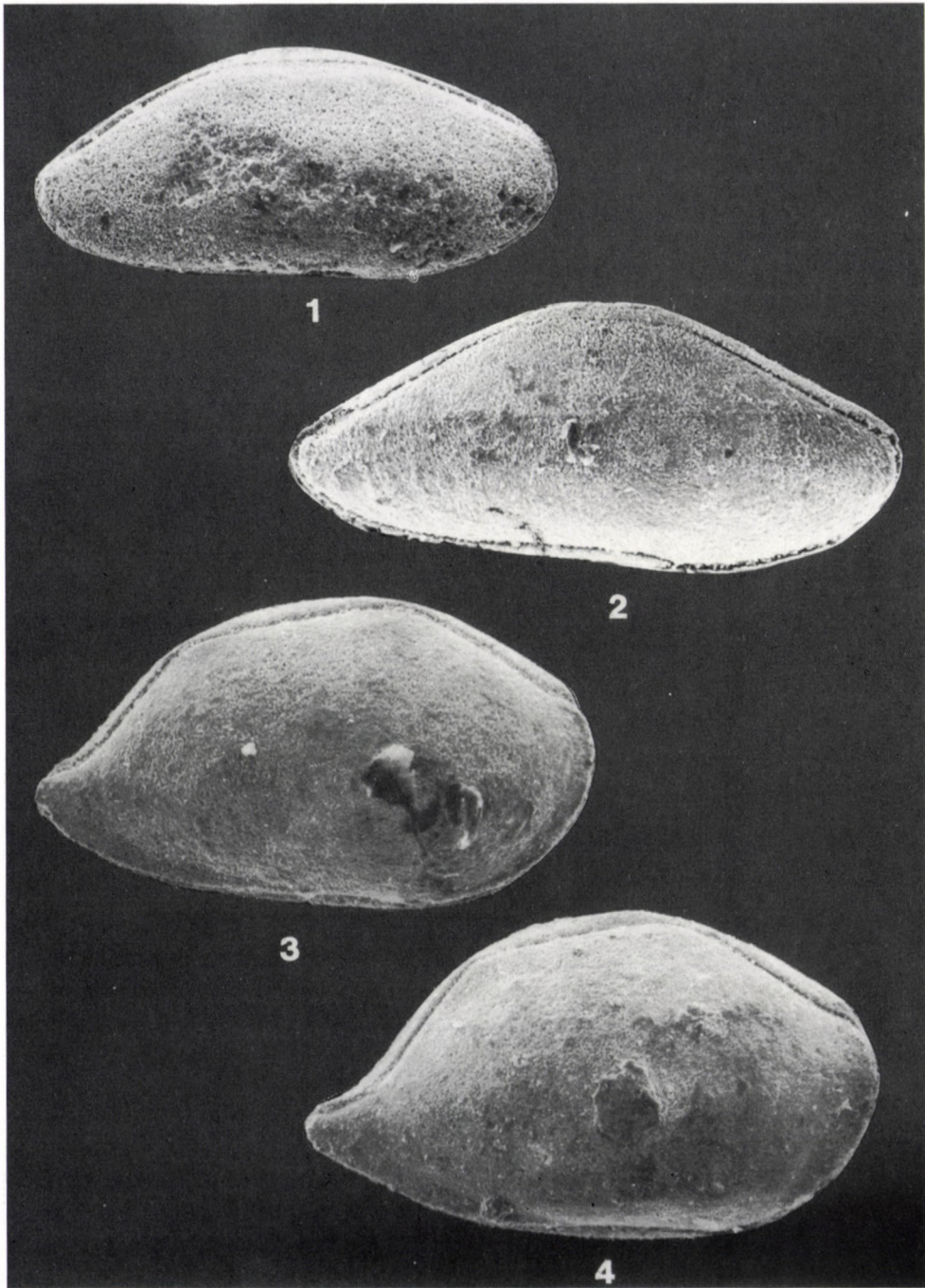


Plate IV

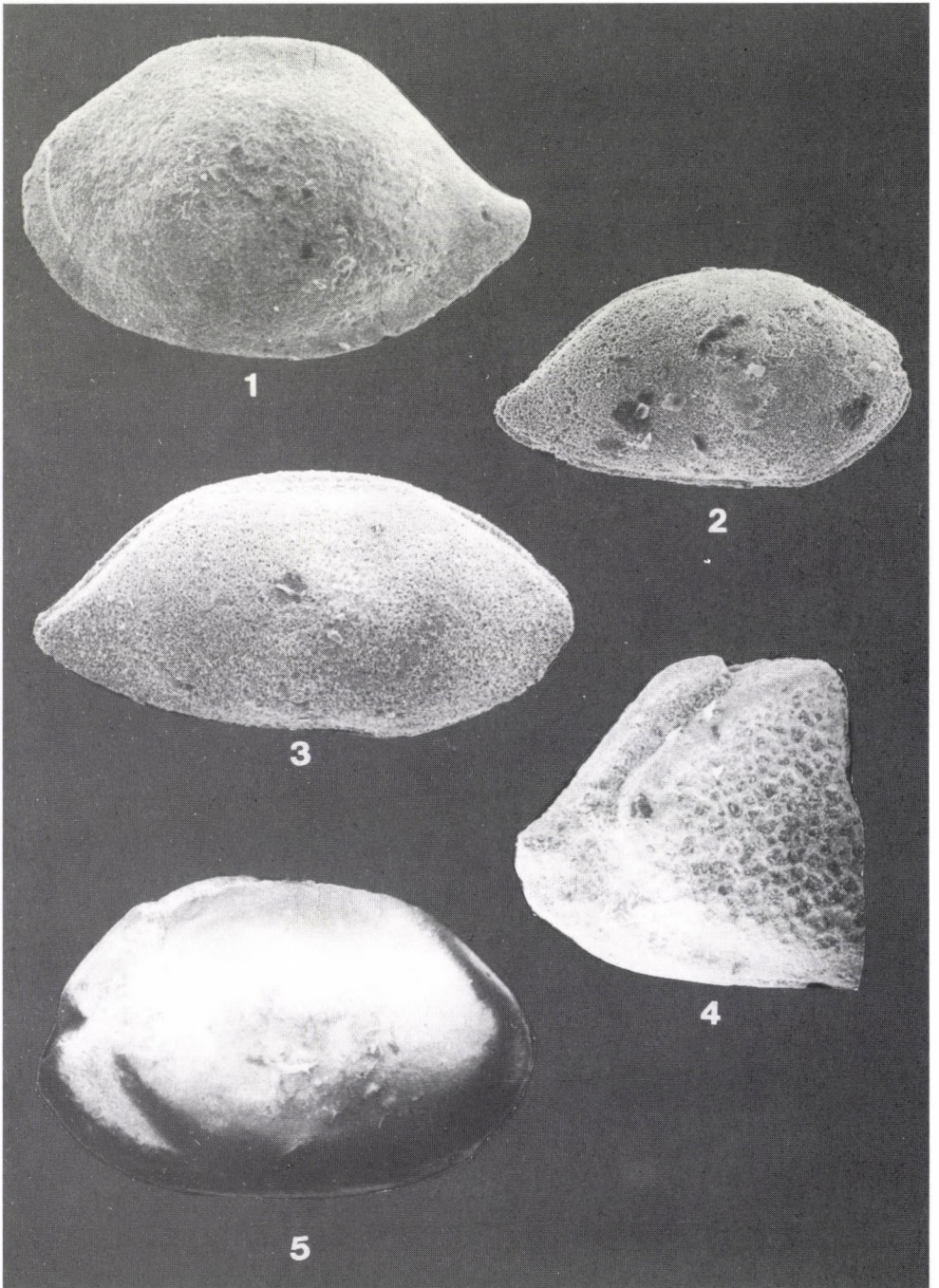
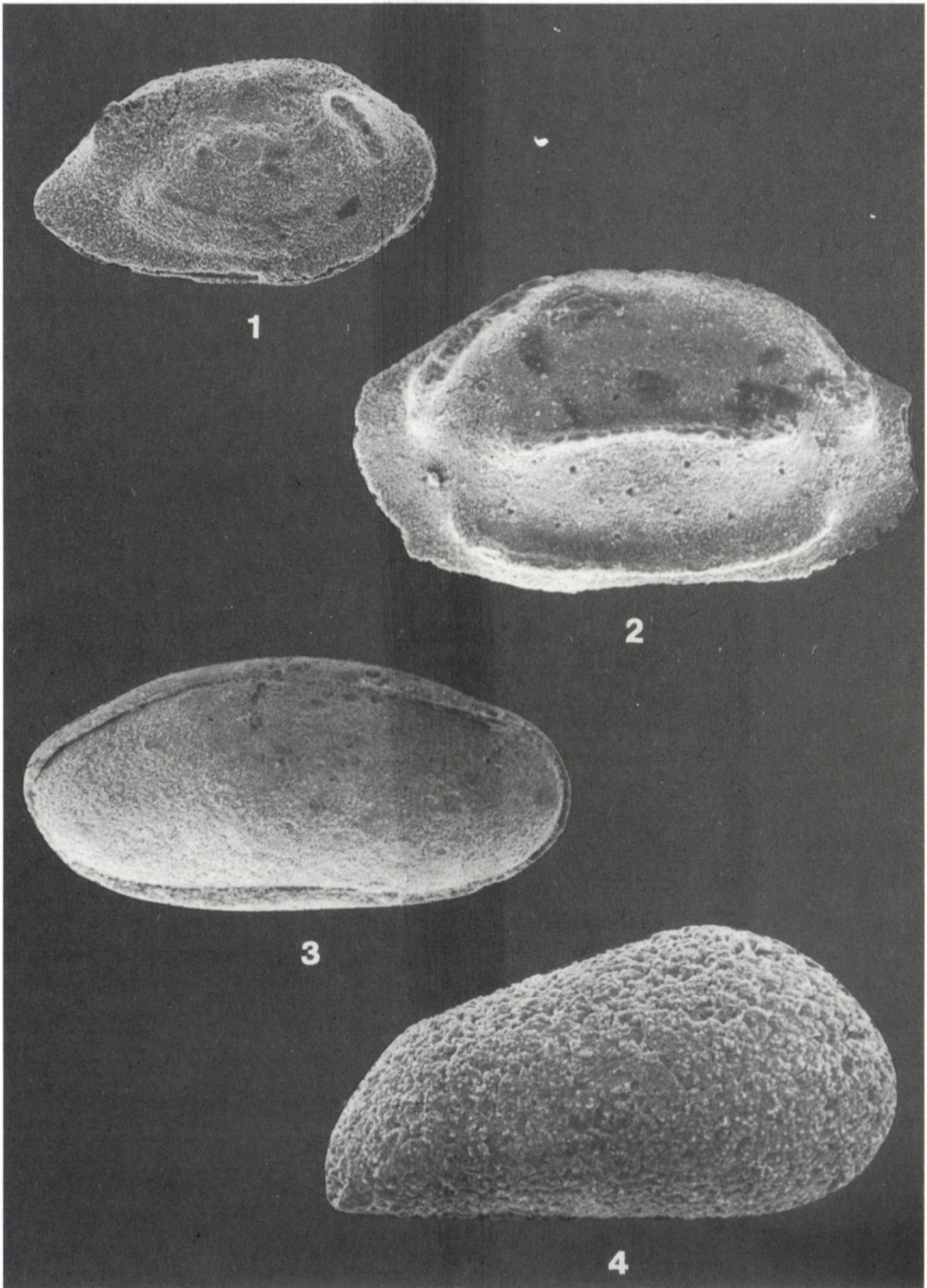


Plate V



References

- Budai, T. 1992: Middle Triassic formations of the Balaton Highland and of the Southern Alps: Stratigraphic correlation. – *Acta Geol. Hung.*, 35, 3, pp. 217–236.
- Budai, T., Gy. Lelkes, O. Piros 1993: Evolution of Middle Triassic shallow marine carbonates in the Balaton Highland (Hungary). – *Acta Geol. Hung.*, 36, 1, pp. 145–165.
- Budai, T., A. Vörös 1992: Middle Triassic history of the Balaton Highland: extensional tectonics and basin evolution. – *Acta Geol. Hung.*, 35, 3, pp. 237–250.
- Budai, T., A. Vörös 1993: The Middle Triassic events of the Transdanubian Central Range in the frame of the Alpine evolution. – *Acta Geol. Hung.*, 36, 1, pp. 3–13.
- Bunza, G., H. Kozur 1971: Beiträge zur Ostracodenfauna der tethyalen Trias. – *Geol. Paläont. Mitt. Innsbruck*, 1, 2, pp. 1–76, T. 1–8.
- Kollmann, K. 1963: Ostracoden aus der alpinen Trias Österreichs. – 2. Jahrb. geol. Bundesanst., Wien, 106, pp. 121–204, T. 1–11.
- Kozur, H. 1970: Neue Ostracoden-Arten aus dem Obersten Anis des Bakonyhochlandes (Ungarn). – *Berichte Nat.-Med. Ver. Innsbruck*, 58, pp. 1–40, T. 1–4.
- Kozur, H. 1971: Die Bairdiacea der Trias. I–III. – *Geol.-Paläontol. Mitt. Innsbruck*, 1, 3, pp. 1–27, Pl. 1–3, 6; pp. 1–18, T. 1–2.
- Kozur, H. 1972: Die bedeutung triassischer Ostracoden für stratigraphische und paläoökologische Untersuchungen Mitteilungen Ges. Geol. Bergbaustud., 211, pp. 623–660, T. 1–3.
- Kristan-Tollmann, E. 1970: Einige neue Bairdien (Ostracoda) aus der alpinen Trias. – *N. Jahrb. Geol. Paläont. Abh.*, 135, pp. 268–310, T. 33–37.
- Kristan-Tollmann, E. 1973: Zur Ausbildung des Schliessmuskelfeldes bei triadischen Cytherellidae (Ostracoda). – *Neues Jahrbuch Geol. Paläont. Monatsh.*, pp. 351–373.
- Kristan-Tollmann, E. 1978: Bairdiidae (Ostracoda) aus den Obertriadischen Cassianer Schichten der Ruones-Wiesen bei Corvara in Südtirol. – *Schriftenreihe Erdwiss. Kom. Österr. Akad. Wiss.*, Wien, 4, pp. 74–104.
- Kristan-Tollmann, E., A. Hamedani 1973: Eine spezifische Mikrofaunen-Vergesellschaftung aus den Opponitzer Schichten des Oberkarn der niederösterreichischen Kalkvoralpen. – *N. Jahrb. Geol. Paläont. Abh.*, 143, pp. 193–222.
- Kristan-Tollmann, E., H. Lobitzer, G. Sotti, Cs. Ravasz, A. Bruckner-Wein, L.A. Kodina, P. Klein, B. Schwaighofer, I. Draxler, R. Surenian, H. Stradner 1991: Mikropaläontologie und Geochemie der Kössener Schichten des Karbonat-Plattform-Becken-Komplexes, Kammerköhralm-Steinplatte (Tirol/Salzburg). – *Jubiläumsschrift 20 Jahre Geol. Zusammenarbeit Österreich-Ungarn*, Wien, 1, pp. 153–191, T. 1–9.
- Méhes, Gy. 1911: Über Trias-Ostracoden aus dem Bakony. – *Resultate wiss. Erforsch. Balatonsee*. 1. Anh. Paläontologie Umgeb. Balatonsee, 3, N 6, pp. 1–15, T. 1–4.
- Monostori, M. 1994: Ostracod evidence of the Carnian Salinity Crisis in the Balaton Highland, Hungary. – *N. Jahrb. Geol. Paläont. Abh.*, 143, pp. 193–222.
- Oravecz-Scheffer, A. 1989: Felsőörs, Forrás Hill, Malomvölgy section. – *XXIst European Micropalaeontological Colloquium, Guidebook*, Hungarian Geological Society, Budapest, pp. 326–336.
- Salaj, J., O. Jendrejakova 1984: Ecology and facial relation of some groups of Triassic Foraminifers and Ostracods of stratigraphic importance. – *Geol. Carpathica*, 35, 2, pp. 231–240, Pl. 1–3.
- Sohn, I.G. 1968: Triassic Ostracodes from Makhtesh Ramon, Israel. – *Geological Surv. of Israel, Bulletin N 44*, Jerusalem, pp. 1–71, Pl. 1–4.
- Széles, M. 1965: Ostracoden aus oberkarnischen Schichten in Nosztori-Tal. – *Földtani Közlöny*, 95, pp. 412–417, 7 Abb.

Crystallization conditions of pegmatites from the Velence Mts, western Hungary, on the basis of thermobarometric studies

Ferenc Molnár

*Department of Mineralogy,
Eötvös Loránd University, Budapest*

Kálmán Török

*Department of Petrology and Geochemistry,
Eötvös Loránd University, Budapest*

Peter Jones

*Department of Earth Sciences,
Carleton University*

The pegmatite nests and myrolitic cavities occurring in the Variscan (280 Ma.) biotitic monzogranite of the Velence Mts are characterized by simple mineralogy (K-feldspar, plagioclase, quartz, mica). The fluid inclusion studies carried out on quartz revealed that the pegmatites were formed from high temperature, relatively dilute (less than 10 NaCl equiv. wt. %) solutions. The composition of these fluids was determined by microprobe analyses of opened inclusions, and the results show that the parent solutions had a NaCl–CaCl₂–H₂O-type composition with variable Na/Ca atomic proportions. The combination of two-feldspar thermometry and fluid inclusion data indicates that the pegmatites were formed in two temperature ranges, between 500 and 600 °C and 300 to 400 °C, at about 2 kbars pressure. Studies of secondary fluid inclusions also yield data about the character of post-pegmatite, more saline hydrothermal fluids. The occurrence of very dilute, boiling fluids related to Eocene volcanic activity was also detected in the quartz crystals of pegmatites, and the data suggest that the depth of the granite intrusion was about 1700–1900 m at the time of that igneous activity.

Key words: Variscan granite, pegmatite, microthermometry of fluid inclusions, composition of fluid inclusions, two feldspar thermometry

Introduction

Several postmagmatic formations are known in the monzogranite intrusion of the Velence Mts. The earlier studies were mostly focused on the economically important vein-type polymetallic (Zn–Pb–Cu) and fluorite deposits (Jantsky 1957). Pegmatite bodies occur in subordinate amount in the Velence Mts and none of them are of economic interest. However, the understanding of the physicochemical characteristics of the earliest pegmatitic fluids related to the crystallization of the granite intrusion is crucial to the reconstruction of ore-forming processes.

Addresses: F. Molnár: H-1088, Budapest Múzeum krt. 4/A, Hungary

K. Török: H-1088 Budapest, Múzeum krt. 4/A, Hungary

P. Jones: Dept. Earth Sciences, Carleton University, Ottawa K1S 5B6, Canada

Received: 15 April, 1995

Earlier studies were restricted to the mineralogical characterization of the pegmatites (Jantsky 1957; Nagy 1967; Buda 1993). Thus conclusions formed about the temperature and pressure conditions during the formation of the pegmatites were based on two-feldspar thermometry (Buda 1985; Buda 1993). The purpose of this study was to determine the crystallization conditions of these bodies, and to outline the earliest stage of the evolution of the hydrothermal system related to the granite intrusion, on the basis of thermobarometric studies.

Geology of the studied area and mineralogy of pegmatites

The main mass of the Velence Mts is composed of a Variscan (280 Ma.) biotitic monzogranite intrusion (Fig. 1). The average modal-composition of the rock is the follows: Q – 34%, A – 28%, P – 31%, M – 6%. The igneous body crystallized from a low-temperature, vapour-saturated eutectic melt, and the estimated pressure of magmatic crystallization is about 2 kbars (Buda 1985). The monzogranite intrusion is transected by syngenetic or slightly younger granite-porphphy and aplite dikes (Fig. 1).

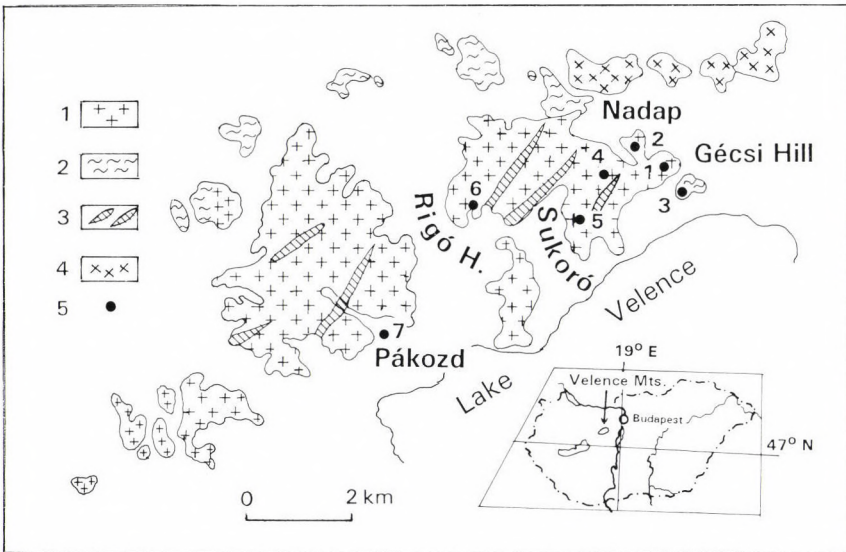


Fig. 1
Geological sketch-map of the Velence Mts (after Buda 1993). 1. monzogranite; 2. metamorphic shale; 3. granite-porphphy; 4. andesite; 5. sampling points: 1, Gécsi Hill-1; 2, Gécsi Hill-2; 3, Gécsi Hill-3; 4, Nadap-Sukoró; 5, Sukoró, Ingókő; 6, Rigó Hill; 7, Pákozd Quarry

The intrusion is hosted by metamorphic shales characterized by thermal metamorphic alteration (andalusite hornfels, spotted shales) along the contact with the intrusion. The contact zones also contain tectonic breccia bodies. The granite-porphry and aplite dikes intruded not only the monzogranite but the metamorphic host rocks, as well (Jantsky 1957; Mikó 1964).

The monzogranite body is bordered by Eocene andesitic rocks in the eastern part of the Velence Mts (Fig. 1). Although there is a fault zone between the granite and andesitic rocks outcropping on the surface, several andesite dikes related to the Eocene volcanic activity transect the intrusion (Jantsky 1957).

The most important formations related to the postmagmatic regime of the granite intrusion are the beresitic zones and quartz-fluorite-barite veins carrying polymetallic mineralization (Kiss 1954; Mikó 1964). Rare pegmatites occur in two forms: lensoid or nest-like rounded-elongated bodies (up to 1–2 m³) and small myarolitic cavities (max. 0.001 m³). The structure of the lensoid pegmatitic bodies is quite simple. Generally, their marginal zones are fine-grained, followed by coarse-grained, graphic-textured zones of quartz-K-feldspar. The central parts of these lenses are filled with subhedral or anhedral quartz crystals, or less frequently by K-feldspar. Plagioclase and biotite occur in subordinate amounts in these lenses; the amount of biotite (usually chloritized) and muscovite is usually less than 1 vol. %. Biotite is enriched in Sc and Nb (up to 1000–3000 ppm; Kubovics 1960). This type of pegmatite is represented by the Gécsi Hill-1, Gécsi Hill-2, Gécsi Hill-3, Nadap-Sukoró, and Pákozd Quarry samples (Fig. 1).

The myarolitic cavities are characterized by the presence of euhedral quartz (amethyst in some places), K-feldspar and albite. Rarely biotite was also observed. The occurrence of fayalite in the area of Rigó Hill, as well as tourmaline (elbaite and indigolite) and garnet (pyrope) between Nadap and Sukoró (Fig. 1) was also reported in these formations (Nagy 1967; Buda 1993). The myarolitic cavities are represented by the Sukoró-Ingókő and Rigó Hill samples (Fig. 1).

Methodology

The homogenization temperatures, eutectic temperatures and melting temperatures of ice data of the frozen inclusions were determined by means of a Chaixmeca-type microthermometry apparatus (Poty et al. 1976) on double-polished, 0.1–0.5 mm thick sections of quartz (Eötvös Loránd University, Department of Mineralogy).

The microprobe analyses on opened inclusions were carried out on a Jeol 6400 SEM equipped with a Link eXL L24 X-ray analyzer and Oxford Instruments CT 1500 cryogenic system (Carleton University, Department of Earth Sciences). Qualitative energy-dispersive X-ray analyses were carried out at 15 kV with a beam current of 0.50 nA. For cryogenic studies, specimens were first frozen in liquid nitrogen, transferred to the cryopreparation chamber of the SEM, held

at -180°C , fractured and coated with a conductive film (200 \AA) of aluminium. The fractured specimens were then transferred to the cryogenic stage of the SEM where the inclusions were observed and analyzed at -170°C . All analyses were made using the ultrathin window mode on the X-ray analyzer to improve light element (Na) detection.

The feldspar compositions were measured by an AMRAY 1830I scanning electron microprobe, equipped with an EDAX PV 9800 EDS detector (Eötvös Loránd University, Department of Petrology and Geochemistry). The analyses were performed with 15KV acceleration potential, 1.5 nA beam current and counting time of 30 seconds. Due to the presence of albite exsolution lamellae in potassium feldspar, analyses were completed with defocused beam on areas of about $100\text{ }\mu\text{m}^2$, to cover the chosen feldspar grain (Kroll et al. 1993). All results were normalized to $\text{Or} + \text{Ab} + \text{An} = 100\text{ mol \%}$.

Results

Fluid inclusion petrography

The fluid inclusion studies were carried out on quartz occurring in pegmatites. Both types of quartz (anhedral and euhedral) contain a large number of inclusions. According to their phase composition at room temperature, the inclusion types can be classified as follows:

1. Monophase inclusions

a) Solid inclusions. The occurrence of various minerals as inclusions uncommon in the studied pegmatitic quartz. Feldspar, mica and rutile crystals were observed in a few samples only. However, the quartz crystals from Rigó Hill contain opaque inclusions with hexahedral habit (pyrite or magnetite), and some greenish, orthorhombic and needle-like phases. These latter crystallites can be identified as fayalite and grünerite (Buda 1993).

b) Liquid inclusions. The fluid inclusions without a vapour phase at room temperature occur along the healed fractures of quartz (secondary fluid inclusions; Roedder 1984). The vapour phase appeared within these inclusions during the freezing studies, and their reproducible homogenization took place in the temperature range of two-phase inclusions. Thus the absence of a vapour phase before freezing can be explained by the metastable state of the inclusion liquid.

2. Two-phase inclusions

Most of these inclusions also occur in healed fractures of quartz. However, some of them are encountered as relatively large ($20\text{--}30\text{ }\mu\text{m}$) single inclusions. These inclusions are probably primary in origin. The volume of vapour phase is highly variable. Most commonly the liquid/vapour ratio is between $95 : 5$

and 70 : 30. Besides these inclusions, the Gécsi Hill-1 sample contains two-phase inclusions, with a liquid/vapour ratio of 30 : 70 (Fig. 2). The presence of vapour-rich inclusions can be indicative of a boiling fluid regime. All of these vapour-rich inclusions were observed along the healed fractures of quartz; thus their trapping occurred after the deposition of the host mineral.

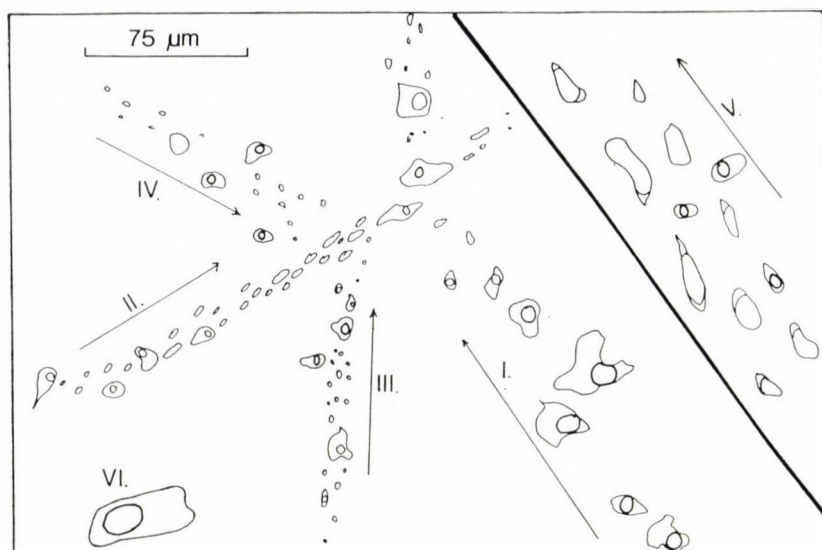


Fig. 2

Distribution of the various generations of fluid inclusions in the Gécsi Hill-1 sample. The microthermometry data of these generation are as follows: I. Th = 318–340 °C, C = 0.17–1.2 NaCl equiv. wt. %; II. Th = 204–223 °C, C = 2.3–3.1 NaCl equiv. wt. %; III. Th = 333–336 °C, C = 0.3–0.6 NaCl equiv. wt. %; IV. Th = 324–344 °C, C = 0.17 NaCl equiv. wt. %; V. Th = 336–345 °C, C = 0.3–0.6 NaCl equiv. wt. %; VI. possibly primary inclusion, Th = 365 °C, C = 2.1 NaCl equiv. wt. %

3. Polyphase inclusions

This rare type of inclusion contains solid phase(s) beside the liquid and vapour phases. The crystallites characterized by optical anisotropy did not dissolve during heating. These properties suggest that the solid phases are accidentally trapped particles, and not daughter minerals. SEM observations carried out on opened inclusions identified the solid phases as potassium feldspar, calcite and mica.

Microthermometry data

The frequency distribution diagram of homogenization temperatures for all studied samples is shown in Fig. 3. The polymodal character of the frequency diagram is related to the presence of several generations of fluid inclusions in

the studied samples. These generations are characterized by homogenization temperatures between 310 and 370 °C, 190 and 245 °C, 145 and 185 °C and 95 and 140 °C, respectively.

Figure 4 shows the frequency distribution of homogenization temperatures within different samples. The highest temperature values occur in the Gécsi Hill-1 sample only. Detailed petrographic studies on this sample revealed that the inclusions homogenizing between 350 and 370 °C are probably primary in origin (single, relatively large inclusions), while the others with homogenization temperatures between 310 and 350 °C are definitively secondary in origin (see Fig. 2). On the other hand, almost all of the studied samples contain an inclusion generation with homogenization temperatures between 190 °C and 245 °C. The exception is the Nadap–Sukoró sample, in which all the measured homogenization temperatures are lower than 180 °C.

The frequency distribution diagram of eutectic melting temperatures of fluid inclusions measured during the freezing studies is shown in Fig. 5. The eutectic melting temperatures between –50 °C and –60 °C suggest that the composition of these inclusions can be modeled by the NaCl–CaCl₂–H₂O system (the eutectic temperature of this system is –55 °C; Ermakov and Dolgov 1979). However, the FeCl₃–H₂O binary system also has its eutectic temperature in this range (Roedder 1984). The possibility of the presence of iron-rich solutions is supported by the fayalite-bearing paragenesis of the Rigó Hill sample (Buda 1993). The appearance of the liquid phase in the frozen inclusions between –20 °C and –40 °C (Fig. 5) also indicates a mixed, NaCl–CaCl₂–H₂O-type fluid composition, but with a relative low Ca content (Haynes 1985). In some cases, the eutectic melting of ice was observed well below –55 °C. These very low values would be the indicator of a LiCl–H₂O-type fluid composition (the eutectic temperature of this system is probably between –75 °C and –78 °C; Roedder 1984).

The most frequent melting temperature values of ice are distributed between 0 °C and –5 °C, as well as –10 °C and –15 °C (Fig. 6). These values correspond to 0–8 and 14–19 NaCl equiv. wt. %, the most frequent concentration values of inclusion liquid (Potter et al. 1978). The last ice crystal was also observed to melt well below –21.2 °C, the eutectic temperature of the NaCl–H₂O system (Bodnar and Vityk 1994). This observation also indicates that these inclusions may contain Ca (or Fe-, Li-) rich solutions.

Figure 7 shows that the fluids with Ca-depleted, NaCl–CaCl₂–H₂O-type model composition (eutectic melting data between –20 °C and –40 °C) are characteristic either of the high or of the lower temperature inclusion generations. Lower eutectic melting temperatures (from –50 to –60 °C) also occur in the fluid inclusions homogenized at a temperature lower than 240 °C. A similar distribution is seen on the "homogenization temperature – melting temperature of ice" plot (Fig. 8). The high temperature fluids are characterized by a relatively high melting temperature of ice. Otherwise, the low-temperature fluids have relatively low melting temperatures.

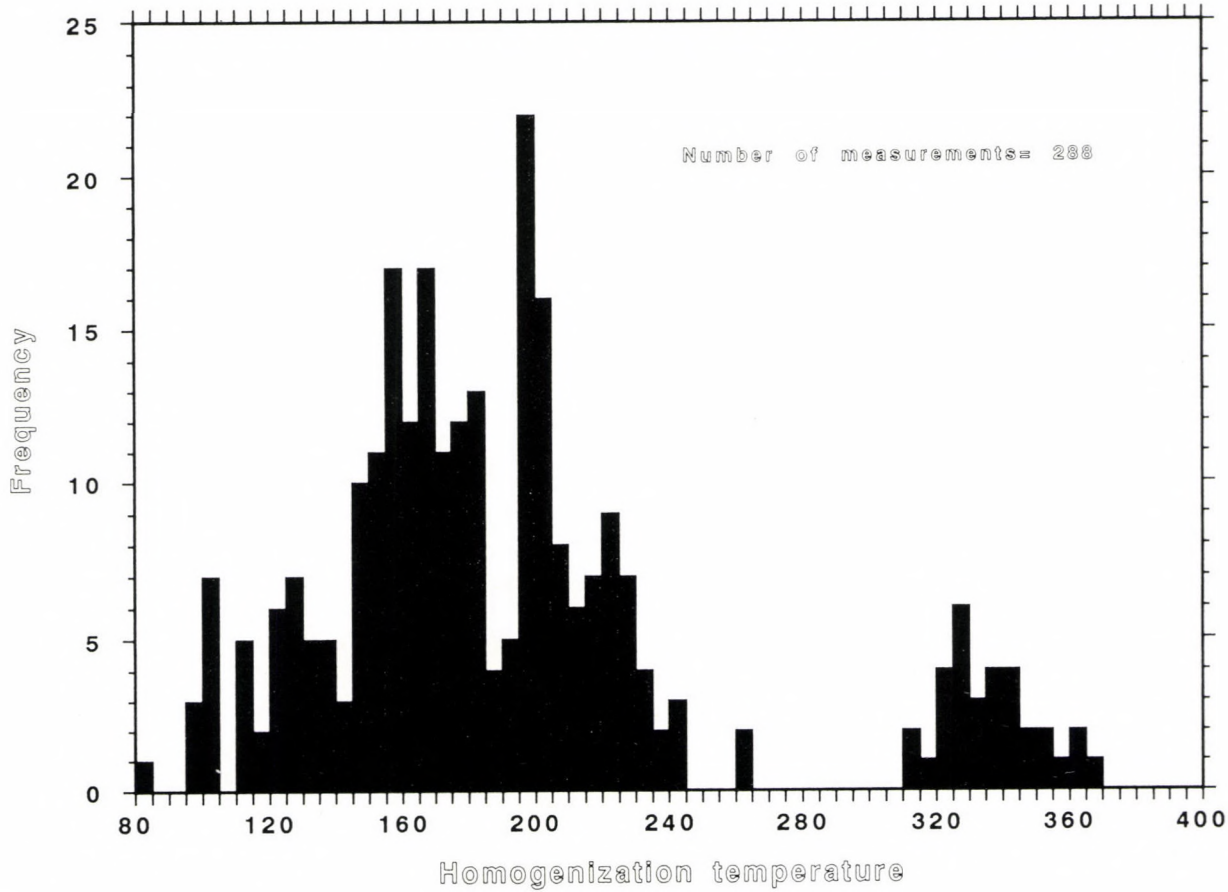


Fig. 3
Frequency distribution diagram of homogenization temperatures

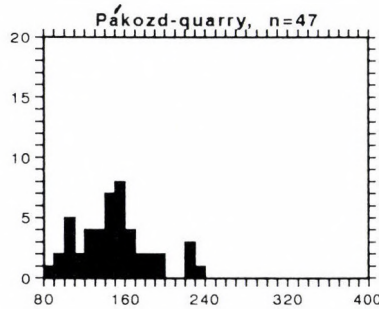
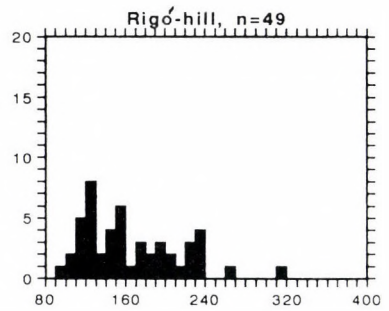
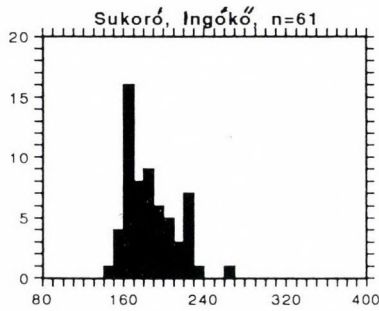
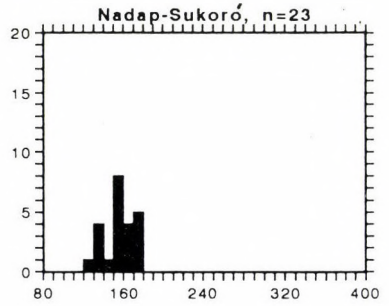
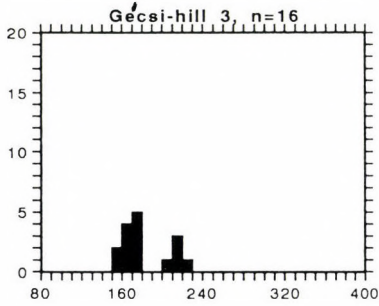
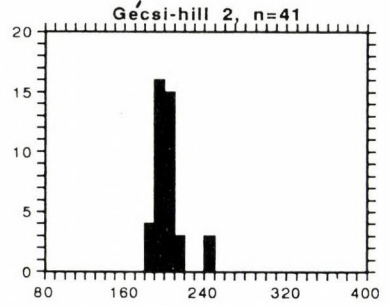
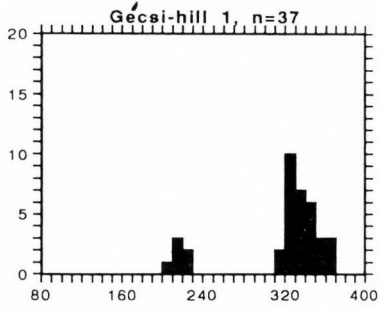


Fig. 4
Frequency distribution diagram of homogenization temperatures in various samples

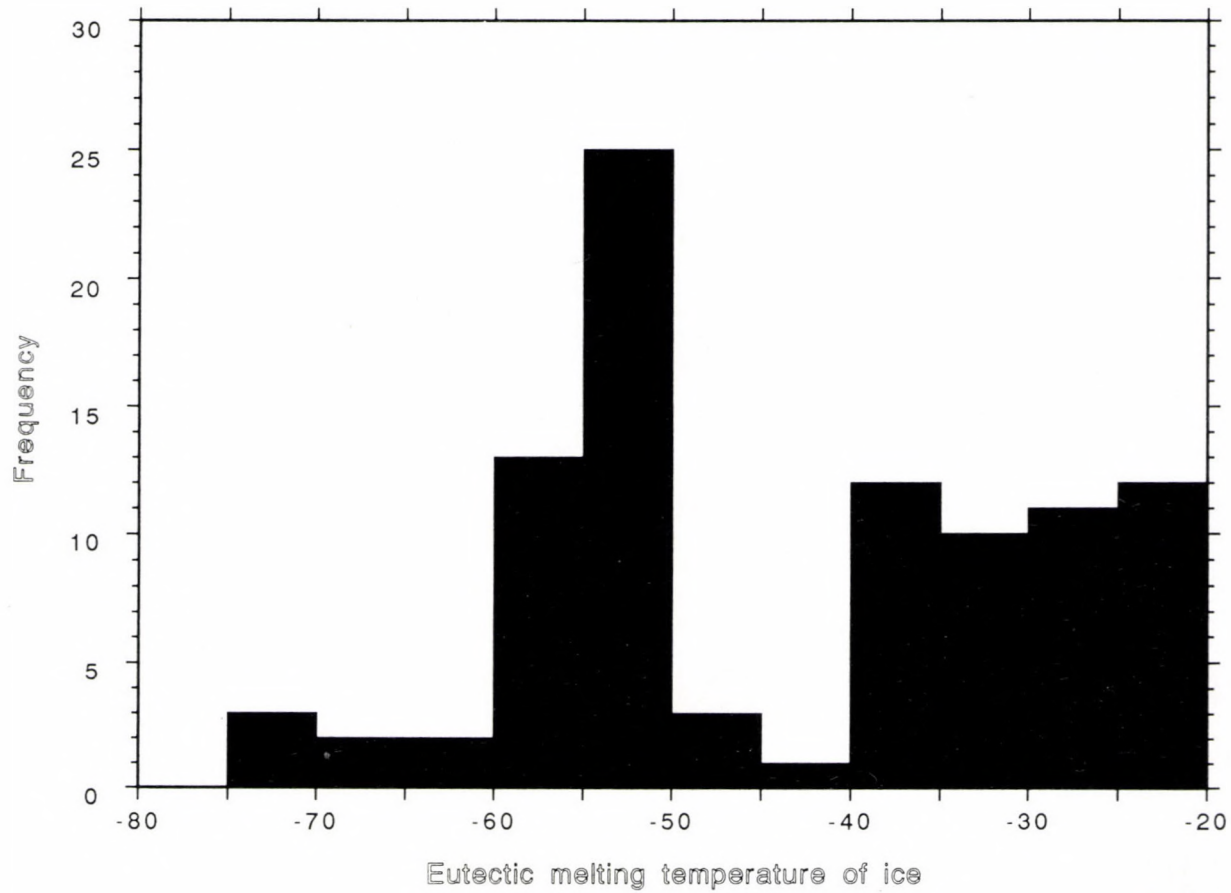


Fig. 5
Frequency distribution diagram of eutectic melting temperatures

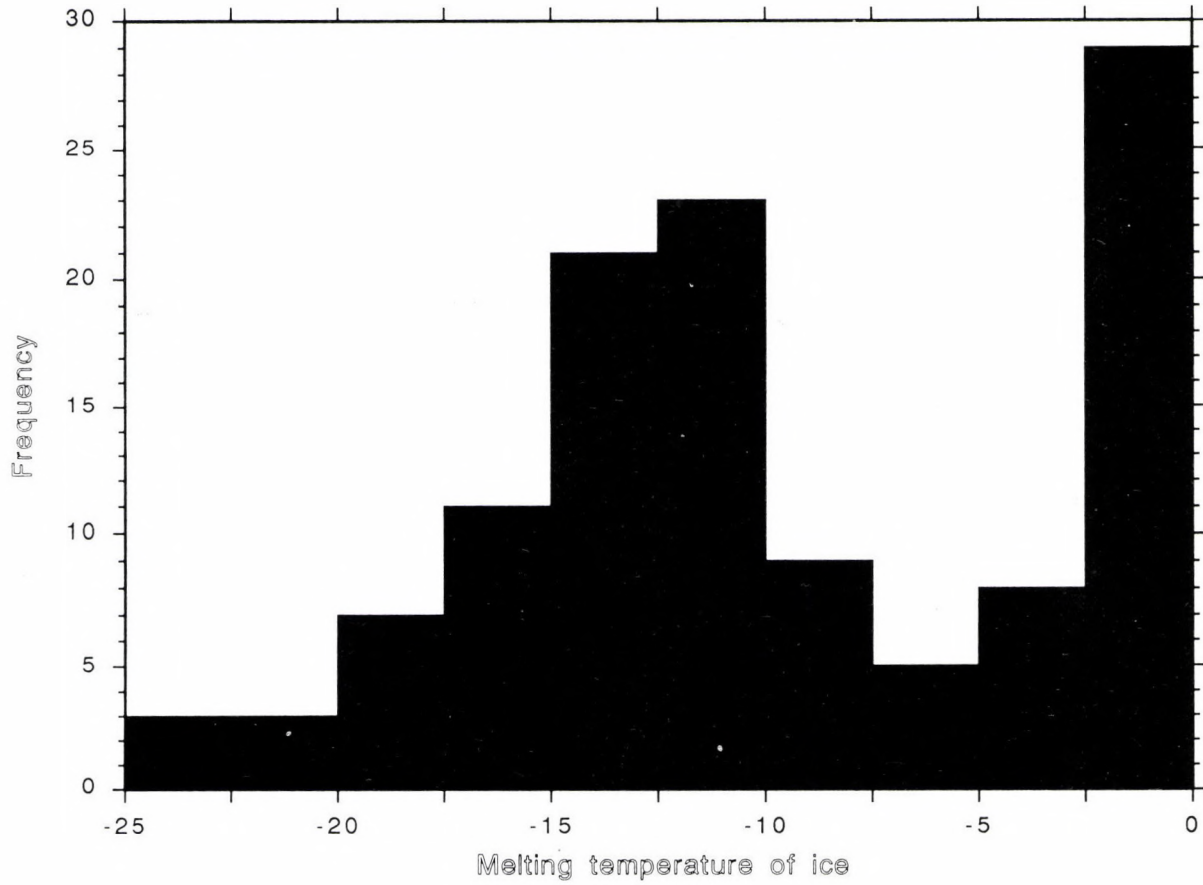


Fig. 6
Frequency distribution diagram of melting temperature of ice data

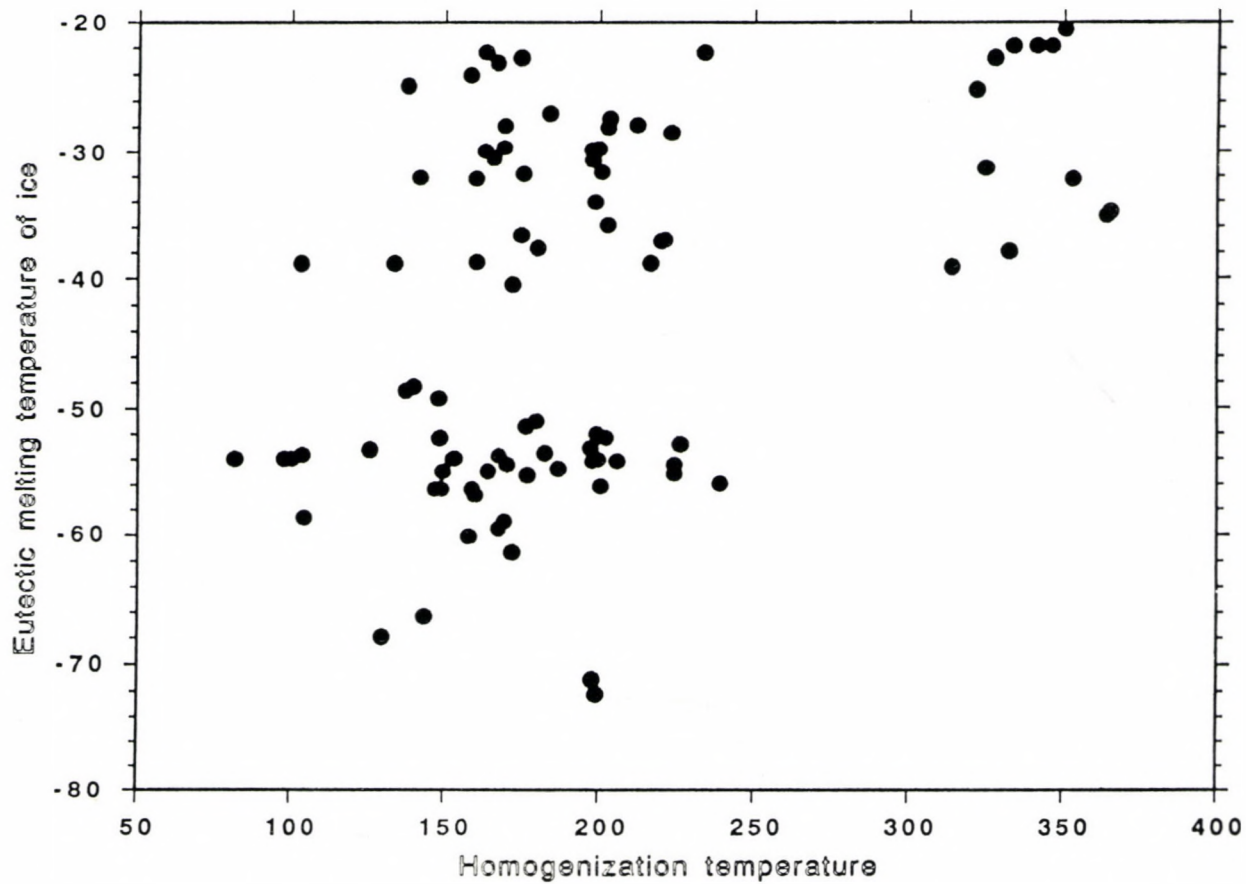


Fig. 7
Distribution of the eutectic melting temperature data as a function of homogenization temperatures

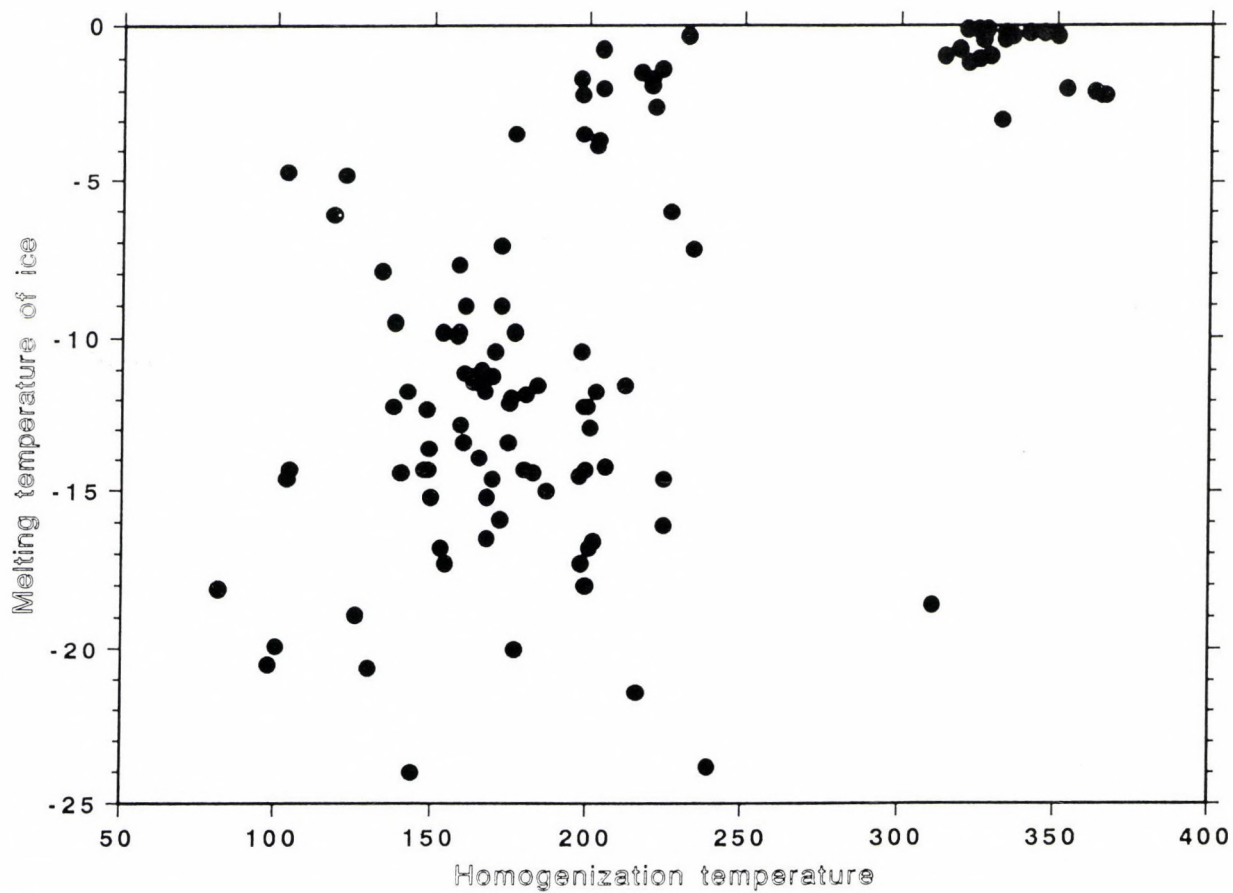


Fig. 8
Distribution of the melting temperature of ice data as a function of homogenization temperatures

On the basis of the petrographic studies and microthermometric data, several generations of inclusions can be distinguished in the pegmatitic quartz of the Velence Mts. The characteristics of these generations are summarized in Table 1.

Table 1

Microthermometry data of fluid inclusion generations in the pegmatitic quartz crystals from the Velence Mts

Inclusion type	Homogenization temperature °C (Th)	First (eutectic) melting temperature °C (Tm1)	Ice-melting temperature °C (Tm ice)
Primary	350–370	–30– –40	–2– –3
Secondary	310–350	–20– –26	0– –1
Secondary (primary)	190–245	–20– –40 –20– –40 –50– –80	0– –4 –7– –14 –10– –24
Secondary	145–185	–20– –40 –48– –68	–7– –14 –4– –24
Secondary	95–140	–20– –40 –54– –68	–5– –9 –14– –24

Results of microprobe analyses on opened fluid inclusions

According to test measurements on synthetic fluid inclusions (Haynes et al. 1988), the composition of solutions can be determined semi-quantitatively by SEM/EDX analyses of solid residue produced during the opening of inclusions. More than 30 analyses were made on the solid precipitates in and around the opened precipitates in quartz from the Velence Mts. These data were compared to analyses of the ice crystals in the frozen fluid inclusions of the same sample.

The analytical totals of the elements analyzed were low due to the small size of the inclusions relative to the much larger interaction volume of the electron beam. However, analyses showing considerable mass balance between Cl and cations are believed to be acceptable, and representative of inclusion composition. These results are listed in Tables 2 and 3.

The most abundant cation detected in fluid inclusions is sodium. The presence of calcium was also observed in the majority of analyses. Less frequently the occurrence of potassium, iron and magnesium was also recorded. The solid precipitates found on the wall of fluid inclusion cavities usually had a hexahedral habit. However, their composition is not pure NaCl (Plate I/1), and they are relatively enriched in Ca. On the other hand, the anhedral splashes of evaporites precipitated from the fluids released from the inclusions display a pure NaCl composition (Plate I/2).

Similar compositional characteristics have been observed on the frozen inclusions. Some of results show pure NaCl–H₂O fluid composition, while in the majority of studied inclusions a mixed, NaCl–CaCl₂–H₂O-type fluid composition was detected (Table 2).

Table 2

Results of electron microprobe analyses on solid evaporites of opened fluid inclusions

Sample	Na wt%	K wt%	Ca wt%	Mg wt%	Cl wt%	Σ
Gécsi Hill-1	4.85	0.00	0.00	0.00	6.32	10.90
	2.35	0.00	0.00	0.00	3.16	5.51
	4.72	0.00	0.00	0.00	6.62	11.34
	4.55	0.00	0.98	0.00	7.69	13.22
	4.29	0.00	2.28	0.00	8.23	14.80
	2.17	0.00	0.84	0.00	3.80	6.81
Pákozd-quarry	15.24	0.00	2.91	0.00	24.84	42.99
	9.84	0.00	1.14	0.00	14.25	25.23
	29.81	1.04	1.91	0.34	46.64	79.74
	15.63	2.46	6.14	0.89	31.70	56.82
	19.95	0.14	0.5	0.00	29.78	50.37
	13.92	0.10	4.74	0.00	24.23	42.99
	22.72	0.00	1.74	0.00	34.24	58.70
Rigó Hill	17.20	0.00	0.74	0.00	25.48	43.42
	13.34	0.00	2.35	0.00	23.24	38.93
	6.29	0.00	1.28	0.00	11.74	19.31
	9.15	0.00	5.36	0.00	19.11	33.62
	24.12	0.14	4.45	0.00	38.53	67.24

on the basis of 2 atoms

Sample	Na	K	Ca	Mg	Σ cations	Σ Cl
Gécsi Hill-1	1.056	0.000	0.000	0.000	1.056	0.944
	1.068	0.000	0.000	0.000	1.068	0.932
	1.047	0.000	0.000	0.000	1.047	0.953
	0.902	0.000	0.111	0.000	1.013	0.987
	0.785	0.000	0.239	0.000	1.024	0.976
	0.849	0.000	0.189	0.000	1.038	0.962
Pákozd-quarry	0.923	0.000	0.101	0.000	1.024	0.976
	0.997	0.000	0.066	0.000	1.063	0.937
	0.960	0.020	0.035	0.010	1.025	0.974
	0.744	0.069	0.168	0.040	1.021	0.979
	1.007	0.004	0.015	0.000	1.026	0.975
	0.859	0.004	0.168	0.000	1.031	0.970
	0.990	0.000	0.043	0.000	1.033	0.967
	1.007	0.000	0.025	0.000	1.032	0.968
Rigó Hill	0.897	0.000	0.090	0.000	0.987	1.013
	0.860	0.000	0.100	0.000	0.960	1.040
	0.743	0.000	0.250	0.000	0.993	1.007
	0.932	0.000	0.099	0.000	1.034	0.966
	0.932	0.000	0.099	0.000	1.034	0.966

On the basis of the relative amount of the main cations (Na and Ca), the results of analyses of solid precipitates are in agreement with the results carried out on the frozen inclusions (Fig. 9). According to these data three compositionally different solutions can be distinguished in the studied inclusions:

- 1. Almost pure NaCl-H₂O-type composition with Ca content lower than 0.07 atomic percent.
- 2. NaCl-CaCl₂-H₂O-type fluids with enhanced (0.08-0.2 atomic percent) Ca content.
- 3. NaCl-CaCl₂-H₂O-type fluids with Ca content higher than 0.24 atomic percent.

Table 3

Results of electron microprobe analyses on the ice crystals of frozen and opened inclusions

Sample	Na wt%	K wt%	Ca wt%	Fe wt%	Cl wt%	Σ
Pákozd	0.51	0.00	0.40	0.00	1.29	2.20
quarry	0.93	0.07	0.29	0.18	2.13	3.60
Gécsi Hill-2	1.86	0.00	0.48	0.00	3.21	5.55
	2.10	0.00	0.71	0.00	3.80	6.61
	2.26	0.00	0.54	0.00	4.38	7.18
	1.91	0.09	0.47	0.28	3.69	6.44
	1.83	0.00	0.78	0.00	4.01	6.62
	3.38	0.00	0.00	0.00	5.18	8.56
	2.35	0.00	0.00	0.00	3.82	6.17
	2.69	0.00	0.00	0.00	4.42	7.11
	1.61	0.00	0.41	0.31	3.40	5.73
	3.01	0.00	0.00	0.00	4.05	7.06
on the basis of 2 atoms						
Sample	Na	K	Ca	Fe	Σ cations	Σ Cl
Pákozd	0.651	0.000	0.289	0.000	0.940	1.060
quarry	0.720	0.030	0.127	0.057	0.934	1.067
Gécsi Hill-2	0.881	0.000	0.131	0.000	1.012	0.987
	0.844	0.000	0.164	0.000	1.008	0.992
	0.835	0.000	0.114	0.000	0.949	1.051
	0.805	0.021	0.115	0.048	0.989	1.011
	0.751	0.000	0.183	0.000	0.934	1.066
	1.003	0.000	0.000	0.000	1.003	0.997
	0.973	0.000	0.000	0.000	0.973	1.027
	0.968	0.000	0.000	0.000	0.968	1.032
	0.770	0.000	0.114	0.060	0.944	1.055
	1.068	0.000	0.000	0.000	1.068	0.932

These solution compositions are in agreement with the microthermometry data. The solutions of the first group probably represent the fluid inclusions with a relatively high (close to -20 °C) eutectic melting temperature. The other two groups with elevated Ca content are the fluid inclusions having relatively depressed (close to, or within the -50 °C to -60 °C temperature range) eutectic melting temperatures.

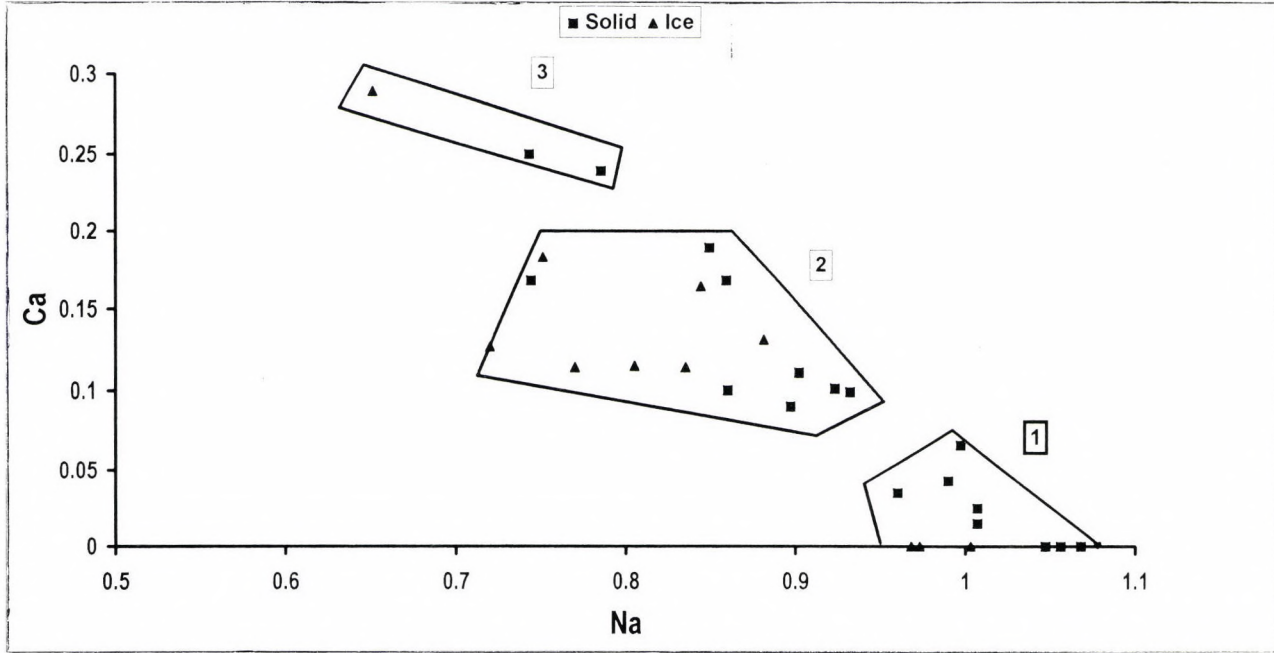


Fig. 9
Ca mole fraction vs. Na mole fraction of solid precipitates and ice in opened fluid inclusions. 1, 2 and 3 – compositionally different inclusion generations (see text)

Pressure correction for homogenization temperatures

The homogenization temperatures listed in Table 1 are not the trapping temperatures of fluid inclusions, because of the high pressure conditions of the crystallization of pegmatites. The difference between the trapping temperature and homogenization temperature is proportional to the difference between the pressure of trapping and the inner pressure of fluid inclusions at the temperature of homogenization. Therefore the calculation of isochores (the constant density curves in the p - T space) is indispensable for each inclusion type. The trapping of inclusion liquid occurred along its isochore, and the trapping conditions are determined by the temperature value of the estimated pressure condition on the isochore (Roedder 1984).

For the calculation of isochores it is essential to know the homogenization temperature, composition and salinity data of fluid inclusions. The homogenization temperatures and salinity data were determined by the microthermometry studies, and the composition of fluids were estimated on the basis of eutectic melting temperatures and microprobe analyses of fluid inclusions. According to the latter data most of the fluids trapped in inclusions of quartz are characterized by a NaCl-CaCl₂-H₂O-type solution, and some of inclusions are enriched in Ca ions.

Isochores of inclusions were calculated on the basis of equations published by Zhang and Frantz (1987). The test calculations proved that the differences in isochore parameters for inclusions with the same homogenization temperature and melting temperature data, but different composition (e.g. NaCl-H₂O and CaCl₂-H₂O) are negligible. Therefore the isochores calculated with the assumption of a NaCl-H₂O fluid composition are also useable for the Ca-bearing solutions, if the melting temperature of ice is higher than -21.2 °C, the eutectic temperature of the NaCl-H₂O system. In the opposite case (e.g. melting temperatures lower than -21.2 °C) the equation for the CaCl₂-H₂O system (Zhang and Frantz 1987) was used for the calculation of isochores.

The crystallization pressure of the monzogranite intrusion of the Velence Mts was estimated by Buda (1985, 1993) on the basis of the mineralogy of the intrusive body and its enclaves. These studies revealed that the monzogranite intrusion crystallized at about 2 kilobars pressure. Using this data, the pressure correction for the homogenization temperatures measured in the pegmatitic quartz is between 100 and 250 °C. Thus the possibly primary fluid inclusions of the Gécsi Hill-1 sample were trapped at about 600°C (between 595 and 625 °C) and the trapping temperature of fluid inclusions (with homogenization temperatures between 190 and 245 °C) is between 300 and 385 °C (Fig. 10).

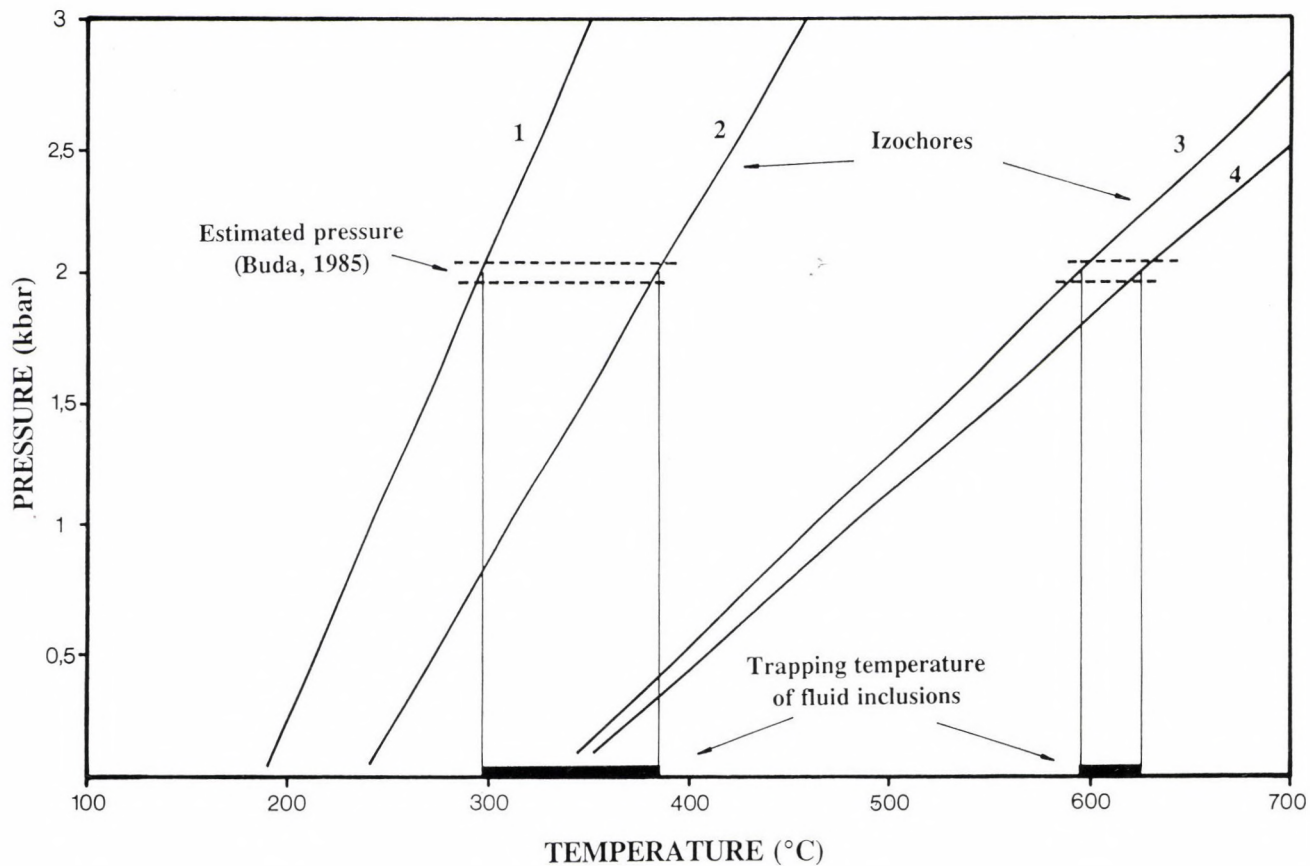


Fig. 10

Estimation of trapping conditions of fluid inclusions. The estimated pressure of trapping is 2 kbars (Buda 1985). The intersection of isochores and this pressure value yields a 595–625 °C as well as a 295–385 °C temperature range. Parameters of the isochores: 1. $T_h = 190^\circ\text{C}$, $T_{m \text{ ice}} = -18^\circ\text{C}$; 2. $T_h = 240^\circ\text{C}$, $T_{m \text{ ice}} = -0.5^\circ\text{C}$; 3. $T_h = 350^\circ\text{C}$, $T_{m \text{ ice}} = -2^\circ\text{C}$; 4. $T_h = 360^\circ\text{C}$, $T_{m \text{ ice}} = -2^\circ\text{C}$

Two-feldspar thermometry

The concentration of the albite component in a coexisting plagioclase and alkali feldspar mineral pair depends on the temperature, and less extensively on the pressure of crystallization (Stormer 1975). Using this peculiarity of coexisting feldspars, the crystallization temperature of pegmatites from the Velence Mts was estimated by Buda (1985, 1993) in the earlier studies. According to that data, the formation of pegmatites took place at around 520 ± 35 °C.

During the sample collection related to this study, small myarolitic cavities with euhedral K-feldspar and albite were found in the eastern part of Velence Mts, between Nadap and Sukoró (Fig. 1). The microscopic texture of these parageneses suggests that albite occurs in syntaxial intergrowth with potassium feldspar (Plate I/3); thus their crystallization was probably contemporaneous.

Coexisting feldspar compositions were determined by microprobe analyses and two compositionally different K-feldspar and plagioclase pairs have been found (Table 4):

- potassium feldspar with depleted albite content (Ab = 4.5–9.5%) and plagioclase with low K-feldspar content (Or = 0–4%).
- potassium feldspar with high albite content (Ab = 24–31%) and pure albite.

Table 4

Composition of coexisting feldspars determined by microprobe analyses. n – number of measurements on the same crystal. The temperatures of crystallization at 2 kbars were calculated on the basis of an equation published by Stormer (1975)

n	Plagioclase			K-feldspar			Temperature at 2 kbars (°C)
	Albite	Anorthite	Orthoclase	n	Albite	Orthoclase	
5	98.2	1.8	0.0	7	8.6	91.4	383
4	96.0	0.00	4.0	4	9.5	90.5	398
3	97.4	1.6	1.0	4	9.2	90.8	392
3	98.8	0.0	1.2	3	9.5	90.5	393
3	94.9	2.1	2.9	3	7.4	92.6	371
3	97.8	1.0	1.2	3	8.9	91.1	386
2	99.9	0.0	0.1	3	4.5	95.5	313
3	100.0	0.0	0.0	3	31.0	69.0	542
3	100.0	0.0	0.0	3	24.0	76.0	514

According to these data the two-feldspar thermometer outlines two temperature ranges for the crystallization of the pegmatites. Using the equation

published by Stormer (1975), these are between 510 and 540 °C, as well as between 310 and 400 °C at 2 Kbar pressure (Table 4).

The high temperature range is in very good agreement with the earlier data (Buda 1985, 1993), and it is close to the estimated trapping temperature (at about 600 °C) of fluid inclusions found in the Gécsi Hill-1 sample. On the other hand, the lower temperature range determined by the two-feldspar thermometer is the same as the trapping conditions (between 300 and 385 °C) of the highest-temperature inclusion generation found in the other samples.

Discussion

The combination of the fluid inclusion data with the two-feldspar thermometry revealed that the crystallization of pegmatites took place at two different temperature ranges. The high-temperature regime probably represents the earliest stage of the postmagmatic fluid system, because the temperatures of these fluids were very close to the crystallization temperature (between 600 and 700 °C; Buda 1985) of the monzogranite. The other temperature range of the formation of the small myarolitic cavities was between 310 and 400 °C according to the two-feldspar thermometer. However, the two-feldspar thermometer is not calibrated below 400 °C (Stormer 1975), therefore the determined crystallization temperature range can only be accepted with great caution. On the other hand, this temperature interval is in good agreement with the fluid inclusion data, suggesting that two-feldspar thermometry may be extended below 400 °C.

The temporal evolution of a volatile phase fractionated from a granitic melt is highly dependent on the geologic setting and composition (water content) of the intrusion. In some cases there has been shown a continuous transition between the melt and fluid regimes on the basis of the occurrence of hydrosaline and hypersaline fluid inclusions (e.g. Volnin pegmatite, Ukraine, Weisbrod 1981; Cathelineau et al. 1988). However, there are other observations showing that low salinity solutions (concentration lower than 10 NaCl equiv. wt. %) can also be the parent fluids of pegmatites (Taylor et al. 1979; Weisbrod 1981; Chakoumakos et al. 1982; London 1986a, b).

The salinity of fluids fractionated from a crystallizing granitic intrusion is determined by the water content of the melt and the pressure conditions of crystallization. At a given pressure the fractionating fluid has quite a low salinity if the water content of the melt is relatively high. The occurrence of highly saline fluids (fluid inclusions with halite daughter minerals) is indicative of a relatively low-pressure regime in which the primary magmatic fluid, separated from the melt, underwent boiling, forming hypersaline solutions (Strong 1981; Bodnar and Cline 1991).

The fluid inclusion data from the pegmatitic quartz of the Velence Mts demonstrate the existence of a low-salinity fluid regime during the high-temperature stage of crystallization. The pressure of this system (2 kbars) was

much higher than the boiling conditions for dilute solutions. Therefore the absence of highly saline fluids in the early stage of the postmagmatic system can be related to the relatively deep position of crystallization.

The presence of vapour-rich secondary fluid inclusions in the Gécsi Hill-1 sample indicates the penetration of boiling fluids into this pegmatite lens after its crystallization. Taking into account the homogenization temperature (about 340 °C) and salinity data (0–3 NaCl equiv. wt. %) of liquid-rich inclusions coexisting with the vapour-rich inclusions, the boiling occurred between 110 and 150 bars pressure (Haas 1971). These values are much lower than the estimated crystallization pressure of the pegmatites (2 kbars). However, an andesitic dike of Eocene age cuts the granite intrusion very close to the locality (approximately 20 m from it). Thus the boiling fluids were probably related to the thermal regime of that dike. The pressure data of boiling suggests that the depth of the eastern part of the granite intrusion was at a depth between 1700 and 1900 m in the time of the Eocene volcanic activity.

The secondary fluid inclusions of pegmatitic quartz with very low homogenization temperatures (less than 180 °C) are probably related to the hydrothermal activity following the pegmatitic stage of the evolution of the granite-related fluid system. These low temperature hydrothermal solutions were different from the earlier pegmatitic fluids, considering their composition (very deep eutectic and melting temperatures of fluid inclusions, see Fig. 5). The enhanced Ca content and salinity is characteristic of deep basinal fluids (Fyfe et al. 1978). Thus the change of fluid composition probably reflects the penetration of the deep basinal fluids into the cooling postmagmatic fluid system of the Velence Mts. The detailed study of this hydrothermal activity is the topic of further fluid inclusion studies.

Conclusions

The combination of the results of fluid inclusion studies and two-feldspar thermometry suggests two stages for the formation of pegmatites in the Velence Mts. The high-temperature (500–600 °C) phase was followed by a low-temperature (300–400 °C) pegmatite crystallization. These results suggest that the formation of lensoid or nest-like pegmatites and myarolitic cavities was an extended process, before the opening of the hydrothermal veins. The high-temperature fluid regime was characterized by relatively dilute solutions (e.g. concentration lower than 5 NaCl equiv. wt. %). The composition of these fluids was NaCl–CaCl₂–H₂O-type, with a predominance of sodium. Beside these fluids, more saline solutions also appeared in the postmagmatic system during the lower temperature stage (300–400 °C). These highly saline solutions were characterized by an elevated Ca content. The occurrence of these fluids probably reflects the mixing between the magmatic and deep basinal fluid regime. Some secondary generations of fluid inclusions of pegmatitic quartz recorded a low-pressure boiling system, which was probably related to the Eocene igneous activity recognized in the eastern part of the Velence Mts.

Acknowledgements

This study has benefited from discussions with Dr. Gy. Buda and Dr. I. Gatter. A portion of this work was completed during F. Molnár's visit to Ottawa, supported by Carleton University and the Education Ministry of Hungary. This study was also supported by HNRF (OTKA) No. 1/3 2299 grant to Gy. Buda and HNRF (OTKA) No. F 007597 grant to F. Molnár.

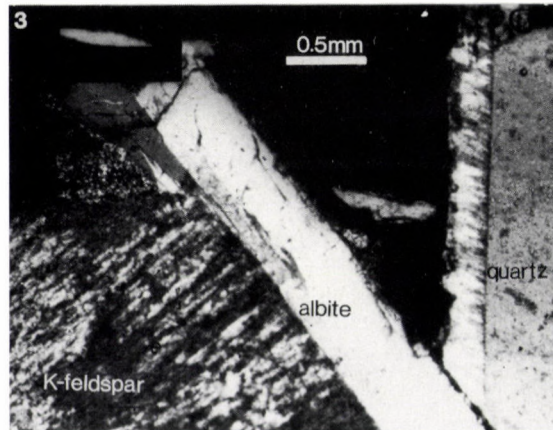
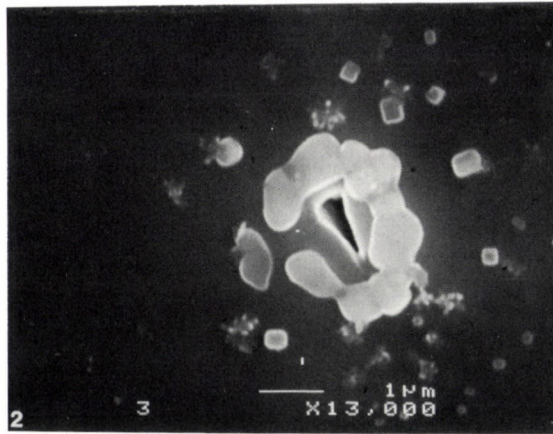
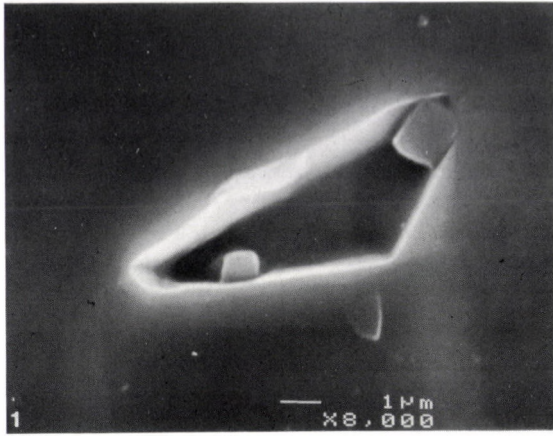
Plate I

1. Solid precipitates with hexaedral habit in an opened fluid inclusion. Sample locality: Gécsi Hill-1. SEM photograph.
2. Anhedral splashes of evaporites precipitated from the fluids released from an opened inclusion. Sample locality: Gécsi Hill-1. SEM photograph.
3. Syntaxial intergrowth of albite with potassium feldspar. Sample locality: between Nadap and Sukoró. Polarizing microscopic photograph taken with crossed Nicols.

References

- Bodnar, R.J., J.S. Cline 1991: Fluid inclusion petrography of porphyry copper deposits revisited: re-interpretation of observed characteristics based on recent experimental and theoretical data. – *Plinius*, 5, pp. 24–25.
- Bodnar, R.J., M.O. Vityk 1994: Interpretation of microthermometric data for H₂O–NaCl fluid inclusions. – In: De Vivo B., Frezotti M.L. (Eds) Fluid inclusions in minerals: methods and applications. Short course of the working group of IMA. pp. 117–130.
- Buda, Gy. 1985: Origin of collision-type Variscan granitoids in Hungary, West Carpathian and Central Bohemian Pluton. – Unpublished Ph.D. Thesis. (in Hungarian), 95 p.
- Buda, Gy. 1993: Enclaves and fayalite-bearing pegmatitic "nests" in the upper part of the granite intrusion of the Velence Mts., Hungary. – *Geol. Carpathica*, 44, pp. 143–153.
- Cathelineau, M., J. Marignac, J. Dubessy, B. Poty, A. Weisbrod, C. Ramboz, J. Leroy 1988: Fluids in granitic environment. – *Rendic. Soc. Italiana. Min. Petr.*, 43, pp. 263–274.
- Chakoumakos, B.C., D.G. Brookins, R.C. Ewing, G.P. Landis, M.E. Register 1982: The Harding - pegmatite: A summary of recent research. – *Amer. Miner.*, 67, pp. 182–183.
- Ermakov, N.P., J.A. Dolgov 1979: Thermobarogeochemistry. – Nedra, Moscow, 271 p. (in Russian).
- Fyfe, W.S., N.J. Price, A.B. Thompson 1978: Fluids in the Earth's crust. – Elsevier, Amsterdam, Oxford, New York, 383 p.
- Haas, J.L. 1971: The effect of salinity on the maximum thermal gradient of a hydrothermal system at hydrostatic pressure. – *Econ. Geol.*, 66, pp. 941–946.
- Haynes, F.M. 1985: Determination of fluid composition by sequential freezing. – *Econ. Geol.*, 80, pp. 1436–1439.
- Haynes, F.M., M. Sterner, R.J. Bodnar 1988: Synthetic fluid inclusions in quartz. IV. Chemical analyses of fluid inclusions by SEM/EDA: Evaluation of method. – *Geochim. Cosmochim. Acta*, 52, pp. 969–979.
- Jantsky, B. 1957: A Velencei-hegység földtana (Geology of Velence Mts). – *Geol. Hung. Ser. Geol.*, 10, 166 p.
- Kiss, J. 1954: A Velencei-hegység északi peremének hidrotermális ércesedése (The hydrothermal mineralization of the Northern part of the Velence Mts). – *MÁFI Évi Jel. 1953.-ről*, pp. 111–127.
- Kroll, H., C. Evangelakakis, G. Voll 1993: Two-feldspar geothermometry: a review and revision for slowly cooled rocks. – *Contrib. Miner. Petrol.*, 114, pp. 510–518.
- Kubovics, I. 1960: Trace element analysis of the post-magmatic formations of the Velence Mountains. – *Földt. Közl.*, 90, pp. 273–292.

Plate I



- London, D. 1986a: Magmatic–hydrothermal transition in the Tanco rare element pegmatite: evidence from fluid inclusions and phase equilibrium experiments. – *Amer. Miner.*, 71, pp. 376–395.
- London, D. 1986b: Formation of tourmaline-rich gem pockets in miarolitic pegmatites. – *Amer. Miner.*, 71, pp. 396–405.
- Mikó, L. 1964: A Velence-hegységi kutatás újabb földtani eredményei (New results of research in the Velence Mts). – *Földt. Közl.*, 94, pp. 66–74.
- Nagy, B. 1967: A sukurói turmalinos pegmatit ásvány-kőzettani, geokémiai vizsgálata (Mineralogical, petrologic and geochemical studies of the tourmaline-bearing pegmatite at Sukoró). – *MÁFI Évi Jel.* 1965-ről, pp. 507–515.
- Potter, R.W., M.A. Clyne, D.L. Brown 1978: Freezing point depression of aqueous sodium chloride solutions. – *Econ. Geol.*, 73, pp. 284–285.
- Poty, B., J. Leroy, L. Jachimowitz 1976: A new device for measuring temperatures under the microscope: the Chaixmeca microthermometry apparatus. – *Fluid Inc. Res.*, 9, pp. 173–178.
- Roedder, E. 1984: Fluid inclusions. – *Rev. Miner.*, 12, 644 p.
- Stormer, J.C. 1975: A practical two-feldspar geothermometer. – *Am. Mineral.*, 60, pp. 667–674.
- Strong, D.F. 1981: A model for granophile mineral deposits. – In: *Ore deposit models*. Geosci. Canada Reprint, Ser., 3, pp. 59–66.
- Taylor, B.E., E.E. Foord, H.D. Holland 1979: Stable isotope and fluid inclusion studies on gem-bearing pegmatite–aplite dikes, San Diego Co., California. – *Contrib. Mineral. Petrol.*, 68, pp. 187–205.
- Weisbrod, A. 1981: Fluid inclusions in shallow intrusives. – In: *Short course in fluid inclusions: application to petrology*. Min. Assoc. Canada Short Course Handbook, 6, pp. 241–272.
- Zhang, Y.G., J.D. Frantz 1987: Determination of the homogenization temperatures and densities of supercritical fluids in the system NaCl–KCl–CaCl₂–H₂O using synthetic fluid inclusions. – *Chem. Geol.*, 64, pp. 335–350.

Results of the research of the abiotic component of the environment in the Bratislava area



Jozef Hricko,
Geocomplex, Bratislava

Jozef Viskup,
Comenius University, Bratislava

Jaroslav Vozár
EL Ltd., Spišská Nová Ves

In the 1991–93 period, the project named "Bratislava-environment, abiotic component" was carried out in the Bratislava region. This area covers approx. 500 km² and is a typical product of the period of dynamic and extensive economic development, with all its secondary factors and disdain for the environment.

In order to determine the present state of the abiotic component of the environment, the following activities were performed within the scope of the project: remote sensing; various geologic maps; radioactive pollution maps; radon risk maps; seismic hazard; magnetic field maps; geochemical survey (litho, hydro, snow); electromagnetic smog map; risk geofactors map; hygienic–toxic–medical analysis.

Key words: remote sensing, radon and seismic risk, geochemistry, hygienic–toxic analysis

Introduction

The Bratislava region has an areal extent of about 500 km². The environment is primarily defined by its geographical position along the Danube river and at the contact of the Malé Karpaty Mts with the Podunajská Nízina Lowland (to the SE) and with the Slovak part of the Vienna Basin (to the NW) – see Fig. 1. The Malé Karpaty Mts are made up of a Paleozoic–Mesozoic complex, while sedimentary areas are covered by Quaternary–Neogene complexes.

The tectonic predisposition is a typical feature of the area in question. Young, deep-seated and partly still active fault systems represent a suitable environment for the rising up of metals in molecular form (lead, zinc, etc.) and radon emanations to the surface. The tectonic predisposition also increases the level of seismic hazard. A very thin and permeable surface layer above the Zitny Ostrov groundwater basin permits the contamination of water by industrial and agricultural pollutants.

Addresses: J. Hricko: Geocomplex a.s., Geologická 21, 822 07 Bratislava, Slovak Republic

J. Viskup: Comenius University, Bratislava, Slovak Republic

J. Vozár: EL Ltd., Spišská Nová Ves, Slovak Republic

Received: 20 October, 1993

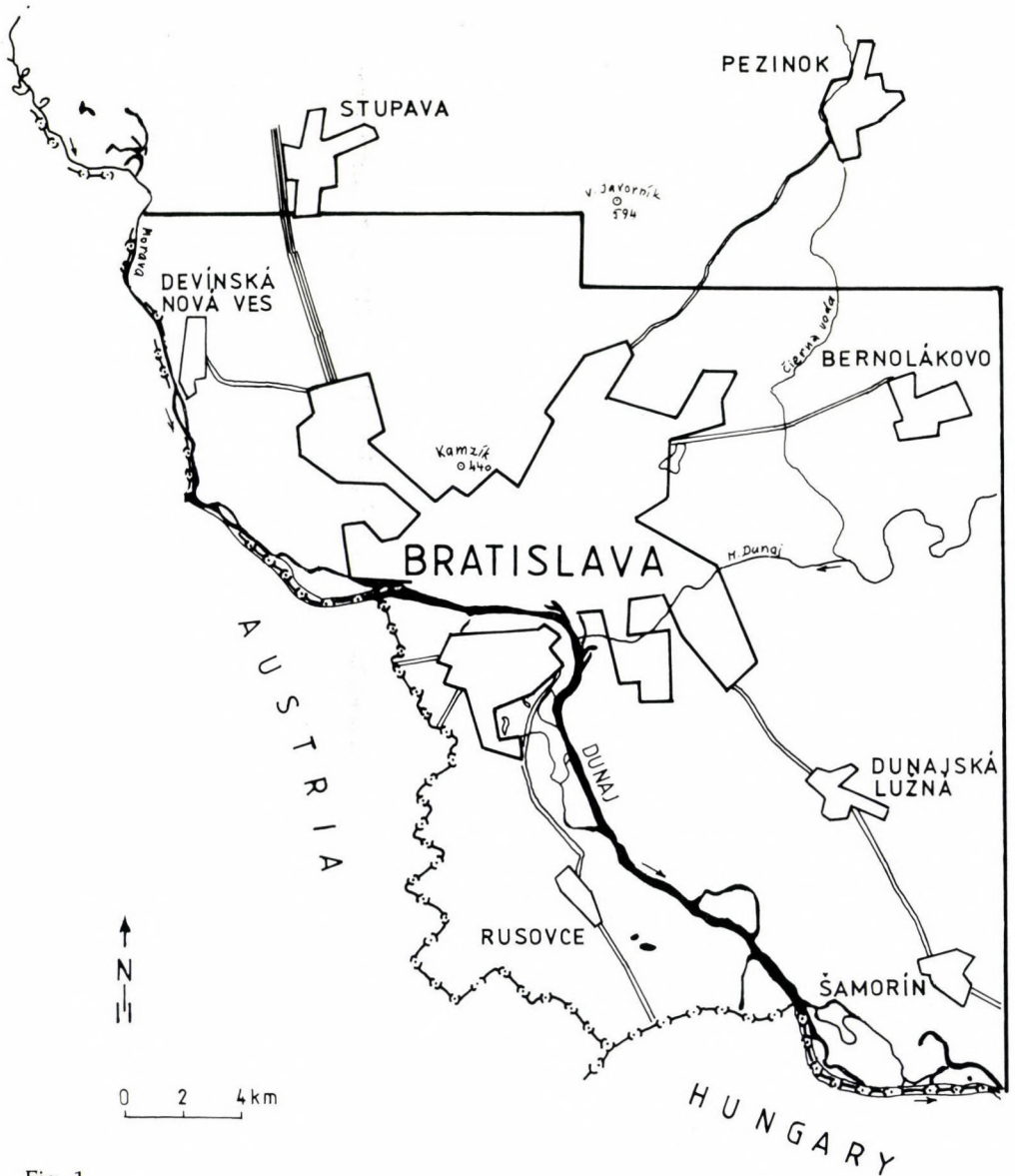


Fig. 1
Project area

The Bratislava economic-urban agglomeration is a typical product of the period of dynamic and extensive development, with all its secondary negative factors and ignorance of environmental concerns. This region is, according to WHO methodology, regarded as an area of high potential for environmental

pollution. The main polluters are huge chemical plants and agricultural producers. The inorganic and organic pollutants penetrate the soil, water and atmosphere.

In order to define the present state of the abiotic component of the environment in the Greater Bratislava region, various activities have been performed within an environmental project, financed by the Ministry of Environment of the Slovak Republic, geologic research and survey section. The main results obtained are presented in this article.

Remote sensing

Multispectral air photos at an approximate scale of 1:10 000, with follow-up field testing, allowed us to update the basic topographic maps at 1:10 000 scale. All maps have been digitized for future use. By means of air photo interpretation, the state of the vegetation and the character of waste dumps were studied.

On the basis of Landsat image interpretation, the tectonic system of the area in question was compiled. It served to construct a more detailed tectonic map (Fig. 2).

Research of the lithosphere

All parts of the lithosphere were studied in the Bratislava region.

To assess the permeability of the surface layer, thickness and resistivity maps at 1:50 000 scale were compiled, using electric sounding, geologic mapping and drilling results.

Thickness and resistivity maps of the Quaternary–Neogene sandy–gravely sediments were also compiled.

The deep geologic structures were studied by geoelectric and gravity surveys, by using results of older geologic, drilling and seismic work. Macroseismic observations, magneto-telluric and deep seismic sounding information was also taken into consideration.

The deep geologic pattern of SW Slovakia is shown in Fig. 3.

Radioactive pollution and radon risk maps

The project area was covered by airborne gamma-ray spectrometry. As a result, K, U, Th, Cs (134) and Cs (137) content maps at 1:50 000 scale were compiled. They served to analyze the level of radioactive pollution of the area observed by interpretation of the derived maps. They are: total count of equivalent gamma-ray radiation (K+U+Th+Cs-134+Cs-137) from ground surface (in nSv per hour) and total count of gamma-ray radiation in the air, 1 m above the surface (in nGy per hour).



Fig. 2
Landsat image of Malé Karpaty Mts

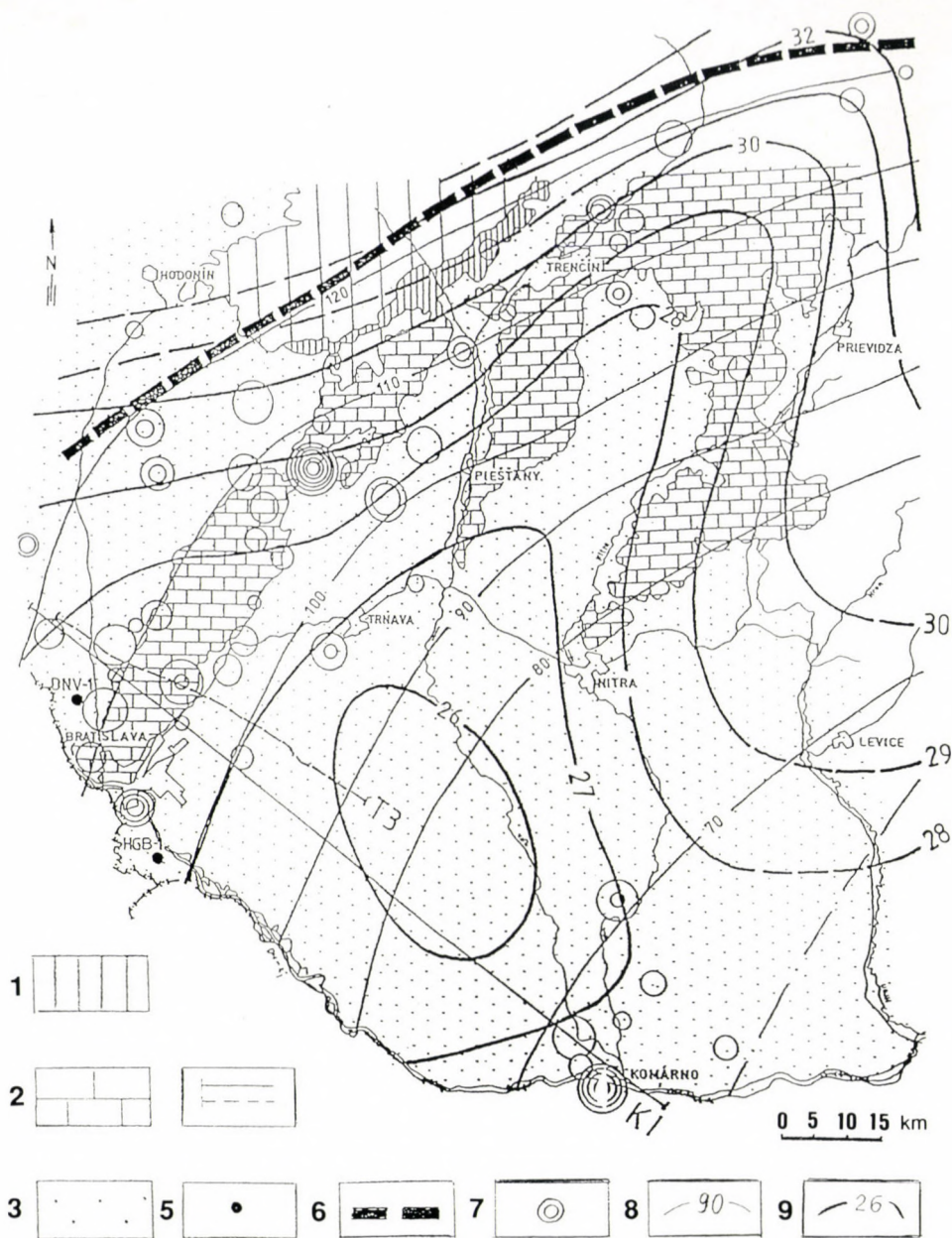


Fig. 3
 Deep geological pattern of the SW Slovakia (by Šefara 1993). 1. Magura flysch; 2. Tatricum;
 3. Cenozoic; 4. location of the seismic profiles; 5. deep borehole; 6. Carpathian conductive zone;
 7. registered earthquakes; 8. thickness of lithosphere; 9. thickness of terrestrial crust

As a result of this work, we can state that the radio-hygienic situation in the Bratislava region is favourable.

To understand the distribution of the radioactive gas radon (222) in the subsurface, the volume activity of Rn (222) was detected in holes 80 cm deep. The standard SAN method was used in the radon survey. Radon risk maps at 1:25 000 and 1:50 000 scales were compiled. To define the category of the radon risk, additional data (soil grain-size and permeability; geotechnical, geologic and tectonic conditions, etc.) were taken into consideration.

By means of gamma-ray spectrometry "in situ", the K, U and Th contents on the surface were also calculated.

According to survey results, 56.8% of the region lies in a low radon risk, 37.6% in a medium radon risk and 5.6% in a high radon risk area. This means that 43% of the Bratislava region lies above limits values of Notice No. 406/92 of the Ministry of Health of the Slovak Republic.

Table of radon risk assessment

Category of radon risk	Volume activity of Rn (222) in kBq.m ⁻³		
	Permeability of soil		
	small	medium	high
low – I	< 30	< 20	< 10
medium – II	30–100	20–70	10–30
high – III	> 100	> 70	> 30

The surface layer radioactivity is low to medium.

Seismic hazard

To define the behaviour of the project area during possible earthquakes, macroseismic observations (using long-term data), seismo-tectonic analysis and microseismic zoning were carried out there.

According to the regional map of seismic zoning, the Bratislava region lies in 7^o of expected intensity on the MSK-64 scale. In microseismic zoning, the maximum expected seismic intensity (I_o) lies in the interval of 4.5–7.0^o of the MSK-64 scale. The lowest values have been observed in granitic rocks of the Malé Karpaty Mts (except in areas located along young fault zones). The highest values were detected along fault zones and in areas made up of thick, sandy-gravelly Quaternary sediments.

Geomagnetic activity

Present research shows the relation between the number of bronchial asthma and epilepsy cases and changes of the geomagnetic field. A certain relationship has been observed between accidents of sportsmen and magnetic activity

(Túnyi 1991). For this reason, geomagnetic observations were performed in the Bratislava region.

As a result of these observations, two maps were compiled. The first is a map of increased geomagnetic activity Δk , using long-term data from the Hurbanovo station and our own systematic measurements over 2 years. The second map is isolines map of the Z-component of the magnetic field (Zd), caused by electrical city traffic. The maximum values of Zd were observed in the central part of the city of Bratislava, with prolongation to the NW and NE.

Electromagnetic smog

The negative influence of the electromagnetic field of VSW and USW radio-transmitters on the human brain and nervous systems is well-known. The measuring of the electromagnetic smog level in the Bratislava region has shown that in some city areas, observed parameters reach values many times higher than valid Czechoslovak and Slovak limits of the Ministry of Health.

Geochemical survey

The geochemical survey consisted of four types of works:

a) *Atmogeochemistry*

With this method, deep-seated fault zones were detected. Along these zones, some metals in molecular form rise up to the surface. By laboratory analysis of air samples, taken 0.5 m above the surface, the contents of Ca, K, Pb and Zn were determined. The sampling was performed on sections located along streets, roads and paths of the city agglomeration. In some places, Zn and Pb contents are many times higher than valid limits. The atmogeochemical results also served to compile the tectonic map.

b) *Geochemical-ecological research of snow*

During the 1990-91 and 1991-92 winter seasons, snow samples were taken at carefully selected sites. A total of 603 snow samples were analyzed for pH, NH_4 , NO_3 , SO_4 , SiO_2 , Li, Na, K, Mg, Ca, Sr, Cl, F, Mn, Fe, Al, Zn, Cu, Pb, Cd, Ni, Co, Cr, Hg, As, Sb, Se, and Tl. The map series were compiled for individual elements and for components distribution.

c) *Lithogeochemistry*

The lithogeochemical survey consisted of sampling and analysis of hard rocks, stream sediments and soil samples for metals, organic and inorganic pollutants. The map series at 1:50 000 scale were constructed to show the distribution of the individual elements and components.

In several areas of the Bratislava region, the contents are higher than Slovak standards allow.

d) Hydrogeochemistry

Samples of surface and ground water were analyzed for a great number of metals and other pollutants. The results of the chemical analyses are presented on distribution maps at 1:50 000 scale, and on water quality maps.

Conclusions

The data obtained during the execution of the project served as a basis for the compilation of summary maps in which the main geofactors negatively influencing the environment of the Bratislava region are shown.

At present, the data are analyzed from a hygienic-toxic-medical point of view. The results of this analysis will be used for planning the steps which will reduce negative factors to an acceptable level.

For instance, in cooperation with the hygienic-medical authorities, a monitoring of the radon level in the houses and flats was carried out in the sub-areas with high radon risk. The observations showed that in several cases the values of equivalent volume radon activity are higher than the Slovak limits.

Reference

- Hricko, J., I. Túnyi, et al. 1993: The Bratislava-environment, abiotic component. Final report. – Manuscript, Geocomplex a.s. Bratislava (in press).
- Šefara, J. 1993: The Bratislava-environment, abiotic component. Final report. – Manuscript, Geocomplex a.s. Bratislava (in press).

The main tasks of ecogeologic research in Bulgaria



Todor A. Todorov

*Geological Institute, Bulgarian Academy of Sciences
Sofia*

In Bulgaria, the environment in a number of areas is in a bad and even critical situation. It follows from this that ecological, including ecogeologic, studies are increasing in importance and rapidly becoming a matter of priority. The most pressing ecogeologic problems are the following: the effects of human activity on the Black Sea and the Danube River; the protection of ground, surficial, mineral, and thermal water resources; the effects of engineering geology in protecting the environment; the geochemical evaluation of the effects of human presence in both urban and rural areas; a review of the country's mineral base from a ecogeologic point of view; activation of recent seismic-tectonic processes by human agency; monitoring of geologic processes affecting the environment; ecological mapping, and the protection of natural monuments.

Key words: environmental geology, Bulgaria

Introduction

The quantity of available ecogeologic data increases constantly (Todorov 1991). According to this wealth of information, the following conclusion may be drawn concerning the present state of global ecogeologic research:

– The methodology of ecogeologic mapping as a whole is still being experimented with, and no agreement on a single, globally accepted method has yet been reached. This leads to confusion and misunderstanding;

– Considerable experience has been gained in engineering geologic and hydrogeologic aspects of ecogeology. Considerable concrete results have been achieved in estimating the alteration of engineering geologic conditions in areas of intensive agricultural activity, as well as evaluating the appearance of recent exogenous and endogenous geologic processes. Consensus also exists on the issues of protecting surface, ground, mineral, and thermal waters against pollution and exhaustion;

– By and large, mineral resources are still viewed as being renewable. The high probability of their exhaustion under the present conditions of rapacious exploitation demands that they be utilized in a rational way; this in turn touches upon the problems of the process of extraction, and the subsequent complexities of their use. A separate but related matter here is that of the ecological state

Address: Todor A. Todorov: Acad. G. Bonchev Str. 24, Sofia 1113, Bulgaria

Received: 20 October, 1993

of the mineral deposits, and of the environmental consequences arising from the exploration, exploitation and processing thereof;

– Recently a good deal of attention has been paid to lithomonitoring (geological monitoring) of the geological environment. According to one concept for the future, lithomonitoring would replace the current practice of estimative research on the state of the geologic medium. The element of prospection should play a more important role in this next stage of improvement;

– Ecogeologic studies are covering a wider realm of subjects, with particular emphasis placed upon the danger of radiation, and upon the geochemical impact on various population centers, such as urban regions, mining areas, resorts, etc. In addition, another geochemical aspect of mineral resource study is that of understanding their toxicity, and the *a priori* study establishing the danger of environmental pollution in their exploration, exploitation and especially in their processing. The same concerns have prompted studies on human waste products, since they represent not only a potential source of raw materials but also a substantial environmental contaminator, when viewed in terms of their interaction with natural agents (wind, water, etc.);

– Particular attention is being paid to natural monuments, also known as geophenomena; these are now being viewed as irreplaceable natural resources, as well as being sites of scientific, recreational and esthetic interest.

Ecogeologic trends in Bulgaria

At this point, it is worth comparing the status of ecogeologic studies in Bulgaria with the global trend.

The lack of ecogeologic awareness in a large number of agricultural complexes has had a sharp and negative effect on the environment and on human health, on the reliability and safety of equipment, and on the protection of fauna and flora. In some areas, the environmental situation is in a bad, even critical, situation. This leads to the conclusion that ecological, including ecogeologic, studies are becoming increasingly important, and in some areas are a matter of urgency. The prospects for such studies have improved, ever since the subject of ecology has been more widely included in the curricula of universities and higher centers of study; also, ecological awareness has been made mandatory for industry.

It is suggested that the Geological Institute of the Bulgarian Academy of Sciences be a center to coordinate research in the sphere of ecogeology. Another leading role in this area could be played by the Committee of Geology and Mineral Resources, with the assistance of their subsidiary departments throughout the nation. This suggestion rests upon the premise that such work can only be competently performed by organizations with the elaborate and complex technical equipment it would require.

In terms of the direction such work should take, the following general guidelines are offered:

- Estimating the present state, and establishing a prognosis, of the human effect upon the Black Sea and the Danube River. Within the scope of this item are included all geological problems pertaining to the protection of these two large bodies of water which are partially located within Bulgarian territory. These problems are not only a national concern, but an international one. This makes it to an even greater degree incumbent upon Bulgaria to set up a well-defined program to address this issue. Such a program should be submitted to UNESCO via the International Geologic Correlation Program (IGCP), the International Geosphere-Biosphere Program (IGBP), or through the United Nations Program for the Protection of the Environment (UNEP), with the aim of receiving financial support from these organizations and of securing the participation of foreign experts to assist in solving the problems. This item is a critical one, since the waters of the Danube and the Black Sea primarily "wash" the Bulgarian coast, and thereafter that of the neighboring countries;
- Reviewing the geologic component of protecting ground, surface, mineral and thermal waters. This complex matter includes the degree of pollution and the protection of the resource against exhaustion, with a prognosis on expected danger in the closer and more distant future;
- Understanding the engineering geologic aspects of the protection of the geologic medium. This problem was the reason for the establishment of the currently undertaken project named "Earth Environment on the Territory of Bulgaria-Protection and Rational Usage (geotechnical aspects)". This project is complex in nature and its aims are diverse, but as a whole the intention is to estimate the state of the geologic medium (Earth) within the territory of Bulgaria at the present time, and to make prognoses on possible changes resulting from human influence and of natural endogenous and exogenous processes; it deals with the future of lithomonitoring over the entire territory of Bulgaria;
- Performing ecologically designed geochemical studies to evaluate the environmental status of various landscapes and human settlement centers, based upon human and natural effects. This would include special geochemical studies on Sofia, other larger and smaller towns, villages, mining and industrial centers, agricultural complexes, resorts, etc.;
- Review, on a new ecological and scientific basis, the mineral resource base of Bulgaria. This is suggested as the realization of a completely new estimation of the storage condition of mineral raw materials (bearing in mind that these are non-renewable resources) as well as of a prognosis on their protection in the near and distant future. Part of this should also be a study on the widening of the range (mineral types) and quantity of resources by means of the inclusion of non-traditional types of raw materials, on a more rational utilization and, at the same time, on the protection of these resources against exhaustion. Within the sphere of this study would fall the ecological estimation of already available and of new resources, i.e. their toxicity, and that of the quantity and composition of human-derived waste material;

this should include the elucidation of the possible uses of such waste as a source of raw materials, without neglecting their simultaneous consideration as an environmental hazard;

– Studies of recent seismotechnical processes, and of their activation as a result of human influence. This is a critical issue in regard to the construction of new nuclear power stations, as well as in the enlargement of the existing Kozlodui facility. This should include research on the storage sites for radioactive and other hazardous industrial waste material, on the geotechnologic development of the Mirovo salt deposit, and on the construction of any industrial, hydrotechnical, or other sites in the country;

– Evaluation of the potential results of establishing observation and control networks for the geologic environment and sources of pollution, as well as for the remediation of unfavorable ecological changes in Bulgaria, due mainly to geologic processes set off by human agency. Another term for such studies is "lithomonitoring". A major issue here is the need for prognosis, early warning and eventual damage control should the exploration, exploitation and processing of raw materials result in catastrophic geologic processes. Such a monitoring effort would complement the National Program for Monitoring and Information of the Environment, presently run by an agency of the Ministry of the Environment;

– Compilation of a complete set of maps, at scales of 1:10 000 to 1:50 000, and even at 1:5 000 where needed, of the rock substrate, of Quaternary deposits and the soil layer, covering all threatened areas of the country. Due to the intrinsic complexity of ecogeologic work, it is advisable that this work be carried out by specialized teams. A first step toward this goal would be the interpretation of geochemical data from primary and secondary dispersion haloes in the country, in order to establish geochemical background values and to determine the alterations which resulted from years of geochemical overloading of certain areas;

– Determine the status of geophenomena (also called "natural monuments" and "sites of geological interest"). Work on this item has been carried out for some time now. The long-term aim would be to enlarge the scope of work, by increasing the area and number of such sites, and to perform such studies as would be needed to ensure their protection against destruction by various natural agents (wind, rain, ongoing geologic processes, etc.). It goes without saying that particular protection will be needed from human activity, since "man with one hand creates and with the other blindly and unreasonably destroys and kills Nature" (as an ancient Greek philosopher said 2000 years ago). Complex as this issue is, its resolution is well within the reach of the experts presently active in all of the geologic institutes of the country. Geophenomena, like raw materials, are non-renewable, and their disappearance can be considered final, since there is no artificial or even natural way to re-create them.

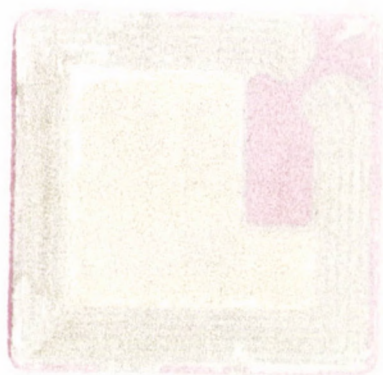
Conclusion

The ideas listed above constitute an ideal maximum program. The entire set could be realized if all scientific organizations and institutions were to coordinate their future activities in this direction. At present, due to personnel and equipment restraints, this is not possible. Therefore, it is advisable to propose a scaled-down version, stressing only the most important tasks to be fulfilled in each ecogeologic field.

In this paper the author is pursuing two main goals. The first is to enumerate the most important matters of ecogeologic concern, both globally and domestically. No less important is the second aim, which is to bring the existence of such a little-known subject as ecogeology to the public attention. The geologic aspects of the protection of the environment are hardly registered or discussed in Bulgaria, which explains why so little has been done in this field. Ecogeologic programs have not been addressed in the (locally) well-known Program of the Bulgarian Academy of Sciences, or in the National Program for the Protection and Restoration of the Environment by the year 2000 (or even later). The latter was organized by the Ministry of the Environment, and submitted for discussion at the end of 1989. This is a measure of the fact that the problems of pollution of the air, of surface waters and of soils, and their effect upon organisms (including humans), are more immediately obvious and in many ways easier to address. Changes in the lithosphere, however, are usually slower and less spectacular, and even largely invisible at first. Precisely for this reason, they are difficult to predict and even more difficult to correct. One needs only to remember the effects of such natural geologic forces as earthquakes or slumps, to visualize the ultimate effects of the rapacious exploitation of our natural wealth and the resulting ecological disasters in almost all areas where such activity was and is being carried out. The same holds true for localities where raw materials are being processed. This effectively summarizes the nature of ecogeologic problems, and shows how unwise it is to further ignore or underestimate them in future environmental studies. These studies should be undertaken as soon as possible, and be effectively included, in the nearest future, in the overall fabric of studies related to protecting the environment of Bulgaria.

Reference

- Todorov, T. 1991: Environmental Geology (Selected Bibliography). Ecogeoinvestconsult, Sofia, 123 p.



PRINTED IN HUNGARY
Akadémiai Kiadó és Nyomda, Budapest

GUIDELINES FOR AUTHORS

Acta Geologica Hungarica is an English-language quarterly publishing papers on geological topics. Besides papers on outstanding scientific achievements, on the main lines of geological research in Hungary, and on the geology of the Alpine–Carpathian–Dinaric region, reports on workshops of geological research, on major scientific meetings, and on contributions to international research projects will be accepted.

Only original papers will be published and a copy of the Publishing Agreement will be sent to the authors of papers accepted for publication. Manuscripts will be processed only after receiving the signed copy of the agreement.

Manuscripts are to be sent to the Editorial Office for refereeing, editing, in two typewritten copies, on floppy disk with two printed copies, or by E-mail. Manuscripts written by the following word processors will be accepted: MS Word, WordPerfect, or ASCII format. Authors are requested to sign and send to the Editor a Publishing Agreement after the manuscript has been accepted by the Editorial Board. Acceptance depends on the opinion of two referees and the decision of the Editorial Board.

Form of manuscripts

The paper complete with abstract, figures, tables, and bibliography should not exceed 25 pages (25 double-spaced lines with 3 cm margins on both sides).

The first page should include:

- the title of the paper (with minuscule letters)
- the full name of the author
- the name of the institution and city where the work was prepared
- an abstract of not more than 200 words
- a list of five to ten key words
- a footnote with the postal address of the author

The SI (System International) should be used for all units of measurements.

References

In text citations the author's name and the year of publication between brackets should be given. The reference list should contain the family name, a comma, the abbreviation of the first name, the year of publication, and a colon. This is followed by the title of the paper. Paper titles are followed – after a long hyphen – by periodical title, volume number, and inclusive page numbers. For books the title (English version), the name of the publisher, the place of publication, and the number of pages should be given.

Figures and tables

Figures and tables should be referred to in the text. Figures are expected in the size of the final type-area of the quarterly (12.6 x 18.6) or proportionally magnified 20–25% camera ready quality. Figures should be clear line drawings or good quality black-and-white photographic prints. Colour photographs will also be accepted, but the extra cost of reproduction in colour must be borne by the authors (in 1995 US\$ 260 per page). The author's name and figure number should be indicated on the back of each figure. Tables should be typed on separate sheets with a number.

Proof and reprints

The authors will be sent a set of proofs. Each of the pages should be proofread, signed, and returned to the Editorial Office within a week of receipt. Fifty reprints are supplied free of charge, additional reprints may be ordered.

Contents

Facies characteristics of the Lofer cycles in the Upper Triassic platform carbonates of the Transdanubian Range, Hungary. <i>J. Haas, A. Balog</i> .	1
Environmental significance of the Anisian Ostracoda fauna from the Forrás Hill near Felsőörs (Balaton Highland, Transdanubia, Hungary). <i>M. Monostori</i>	37
Crystallization conditions of pegmatites from the Velence Mts, western Hungary, on the basis of thermobarometric studies. <i>F. Molnár, K. Török, P. Jones</i>	57
Results of the research of the abiotic component of the environment in the Greater Bratislava area. <i>J. Hricko, J. Viskup, J. Vozár</i>	81
The main tasks of ecogeologic research in Bulgaria. <i>T. A. Todorov</i>	89

307216

5

Acta Geologica Hungarica

18.

VOLUME 38, NUMBER 2, 1995

EDITOR-IN-CHIEF

J. HAAS

EDITORIAL BOARD

GY. BÁRDOSSY (Chairman), **G. CSÁSZÁR**, **G. HÁMOR**,
T. KECSKEMÉTI, **GY. PANTÓ**, **GY. POGÁCSÁS**,
T. SZEDERKÉNYI, **Á. KRIVÁN-HORVÁTH** (Co-ordinating Editor),
H. M. LIEBERMAN (Language Editor)

ADVISORY BOARD

K. BIRKENMAJER (Poland), **M. BLEAHU** (Romania),
P. FAUPL (Austria), **M. GAETANI** (Italy), **S. KARAMATA** (Serbia),
M. KOVAČ (Slovakia), **J. PAMIĆ** (Croatia)



Akadémiai Kiadó, Budapest

ACTA GEOL. HUNG. 38 (2) 95-184 (1995) HU ISSN 0236-5278

ACTA GEOLOGICA HUNGARICA

A QUARTERLY OF THE HUNGARIAN ACADEMY OF SCIENCES

Acta Geologica Hungarica publishes original studies on geology, crystallography, mineralogy, petrography, geochemistry, and paleontology.

Acta Geologica Hungarica is published in yearly volumes of four numbers by

AKADÉMIAI KIADÓ
Publishing House of the Hungarian Academy of Sciences

H-1117 Budapest Prielle Kornélia u. 19-35

Manuscripts and editorial correspondence should be addressed to the

ACTA GEOLOGICA HUNGARICA

Dr. János Haas
Academical Research Group, Department of Geology, Eötvös Loránd University of Sciences
H-1088 Budapest, Múzeum krt. 4/a, Hungary
E-mail: haas@ludens.elte.hu

Orders should be addressed to

AKADÉMIAI KIADÓ
H-1519 Budapest, P.O. Box 245, Hungary

Subscription price for Volume 38 (1995) in 4 issues US\$ 92.00, including normal postage, airmail delivery US\$ 20.00.

Acta Geologica Hungarica is abstracted/indexed in Bibliographie des Sciences de la Terre, Chemical Abstracts, Hydro-index, Mineralogical Abstract

© Akadémiai Kiadó, Budapest 1995

Early Alpine shelf evolution in the Hungarian segments of the Tethys margin

János Haas, Sándor Kovács
*HAS Geological Research Group,
Eötvös Loránd University, Budapest*

Ákos Török
*Budapest Technical University,
Department of Geology, Budapest*

The pre-Neogene basement of the Pannonian basin is made up of structural units ("terranes") originating from different parts of Tethys, from the external to the internal zones.

A comparative study of the evolutionary history of these units offered us a chance to distinguish eustatic, tectonic and other controlling factors. In the studied units the facies evolution was controlled mainly by their paleogeographic setting and their actual position within the plate-tectonic cycle.

In the external Mecsek Unit the vicinity of the continental hinterland is crucial. In the intermediate Transdanubian Range Unit a delicate balance of the tectonic, eustatic and climatic factors determined the actual facies pattern. In the most internal Aggtelek–Rudabánya (South Gemer) Unit the extensional tectonism connected with oceanic rifting played a decisive role from the Middle Triassic onward.

Key words: Pannonian basin, Tethys, Late Paleozoic, Mesozoic, facies analysis, paleogeography

Introduction

In the Pannonian basin the basement beneath the Neogene cover consists of terranes of different origin. In the earliest phase of Alpine evolution (Late Permian–Triassic) they were situated relatively far from each other in various sectors of the north-western end of Tethys. They attained their present-day position as a result of sizeable plate-tectonic reorganisation processes during the Early Tertiary.

Evolution of the structural units was mainly controlled by large scale and local tectonism, climatic changes and global sea-level changes. A comparative study of the evolutionary history of some selected units offered us a chance to distinguish between the effects of the different controlling factors, and to determine the major ones.

Megatectonic setting

Present-day geological features and structural setting of the Pannonian basin are the final result of a multi-stage, complicated evolution in the contact zone of the European plate and the Apulian microplate.

Addresses: J. Haas, S. Kovács: H-1088, Budapest, Múzeum krt. 4/A, Hungary

Á. Török: H-1111, Budapest, Stoczek u. 2, Hungary

Received: 08 May, 1995

In the basement of the Neogene basins a collage of "terranes" is present, the individual units of which show varying geohistory, reflecting their different position within the margins of Tethys during Late Paleozoic–Mesozoic–Early Tertiary times (Kázmér and Kovács 1985; Balla 1988; Csontos et al. 1992). Basic structural pattern of the pre-Tertiary basement is presented in Fig. 1.

Paleogeographic setting

Based on the fitting of the Permian–Triassic facies zones which were defined and distinguished in the individual units a reconstruction for the early Alpine period was compiled (Fig. 2). Trend of facies changes, facies transitions and interfingerings were also considered. According to this interpretation parts of the Pelso Megaunit (Transdanubian Range Unit, Mid-Transdanubian Unit, Bükk Unit) were situated in the south-western margin of the Tethys embayment, whereas the Aggtelek–Rudabánya (South Gemer) Unit was located in the southern part of the northern margin and the Tisza Megaunit was also part of the northern margin, to the east of the Inner West Carpathian Units. This pattern persisted only until the Middle Jurassic when, as a consequence of the opening of new oceanic branches (e.g. the Penninic oceanic system), relationships markedly changed (Haas et al. 1990).

Discussion

The most important factors controlling the evolution of the individual units were:

- 1) structural setting, which includes both the plate-tectonic evolutionary stage (position in time) and actual location of the given area within the Tethys realm (position in space);
- 2) the sediment supply, which was controlled by the climate, the relief and the position of the sediment accumulation area relative to the source area;
- 3) global eustatic sea level changes.

Comparative analysis of the geohistoric evolution of the Pannonian "terranes" offered us a chance to distinguish between the different controlling factors. Due to their significantly different paleo-position, structural setting and distance of continental source area, the various structural units show markedly different histories of evolution. However, eustatic sea-level changes and climatic changes may have provided signals in every unit.

For the purposes of comparison three units were chosen:

- the Mecsek Unit, representing the most external zone of the Tisza Megaunit, i.e. the external zone of the northern margin of Tethys
- the Transdanubian Range Unit which preserved a nearly complete cross-section of the broad Triassic shelf of Tethys
- the Aggtelek–Rudabánya Unit which was situated in the internal belt of the northern margin of Tethys.

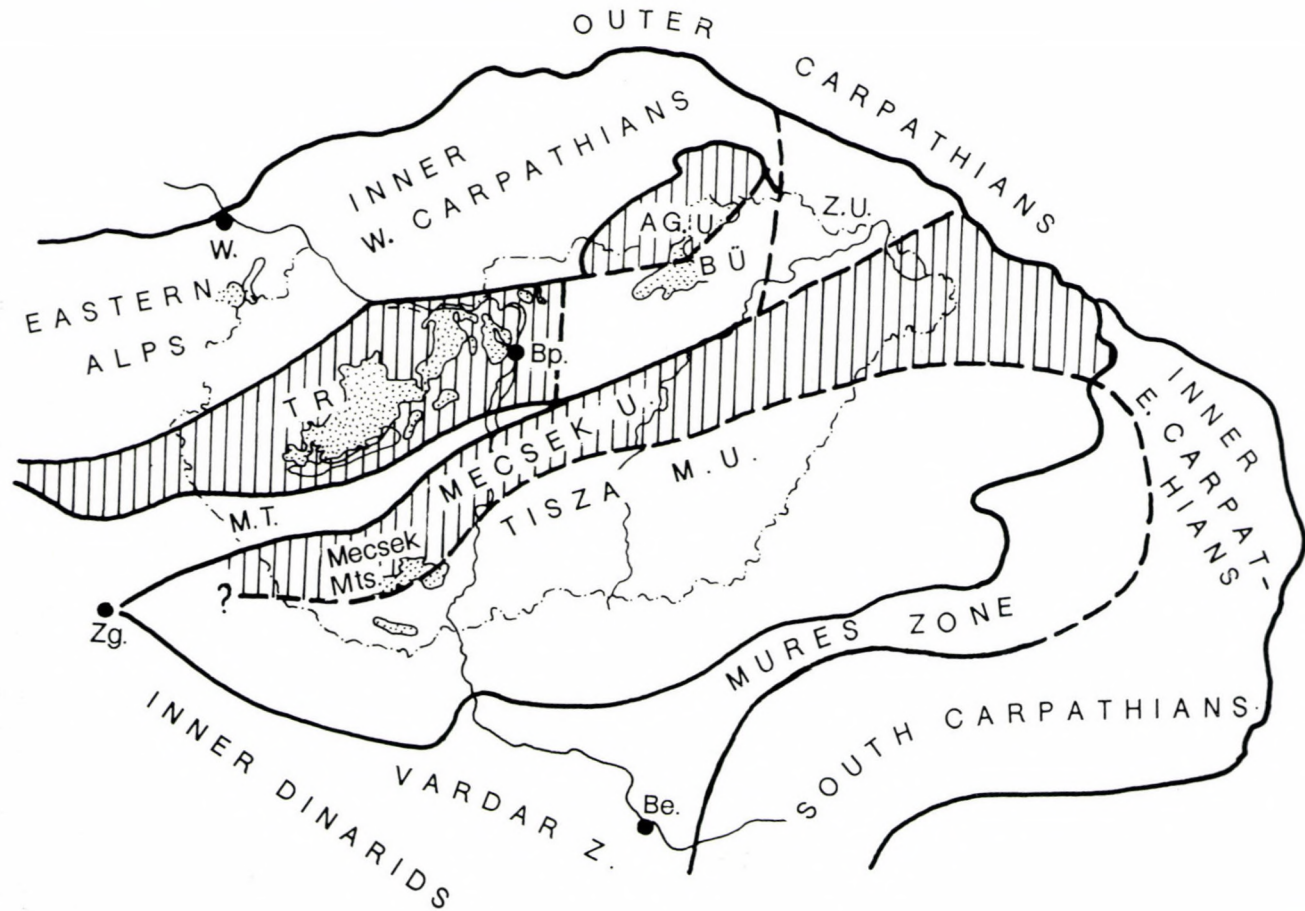


Fig. 1

Basic structural pattern of the pre-Tertiary basement of the Pannonian Basin and its surroundings, showing the position of terranes discussed in the text. TR - Transdanubian Range, AG.U - Aggtelek-Rudabánya Unit, BÜ - Bükk Unit, Z.U. - Zemplén Unit, M.T. - Mid-Transdanubian Unit, W. - Vienna, Bp. - Budapest, Zg. - Zagreb, Be. - Belgrad

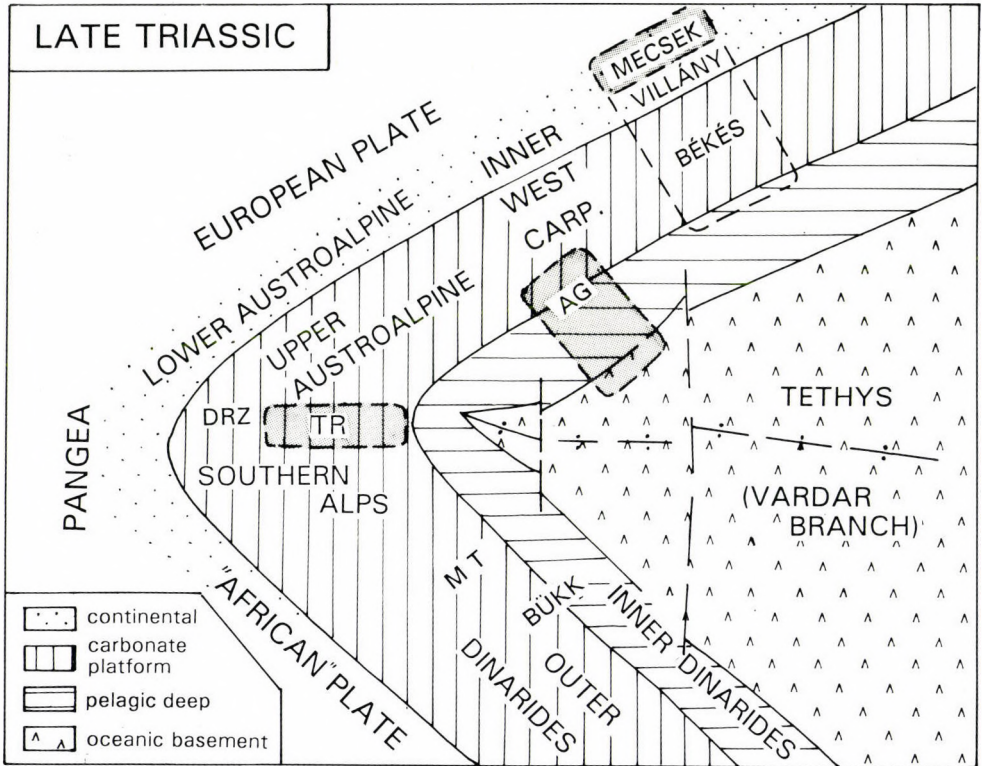
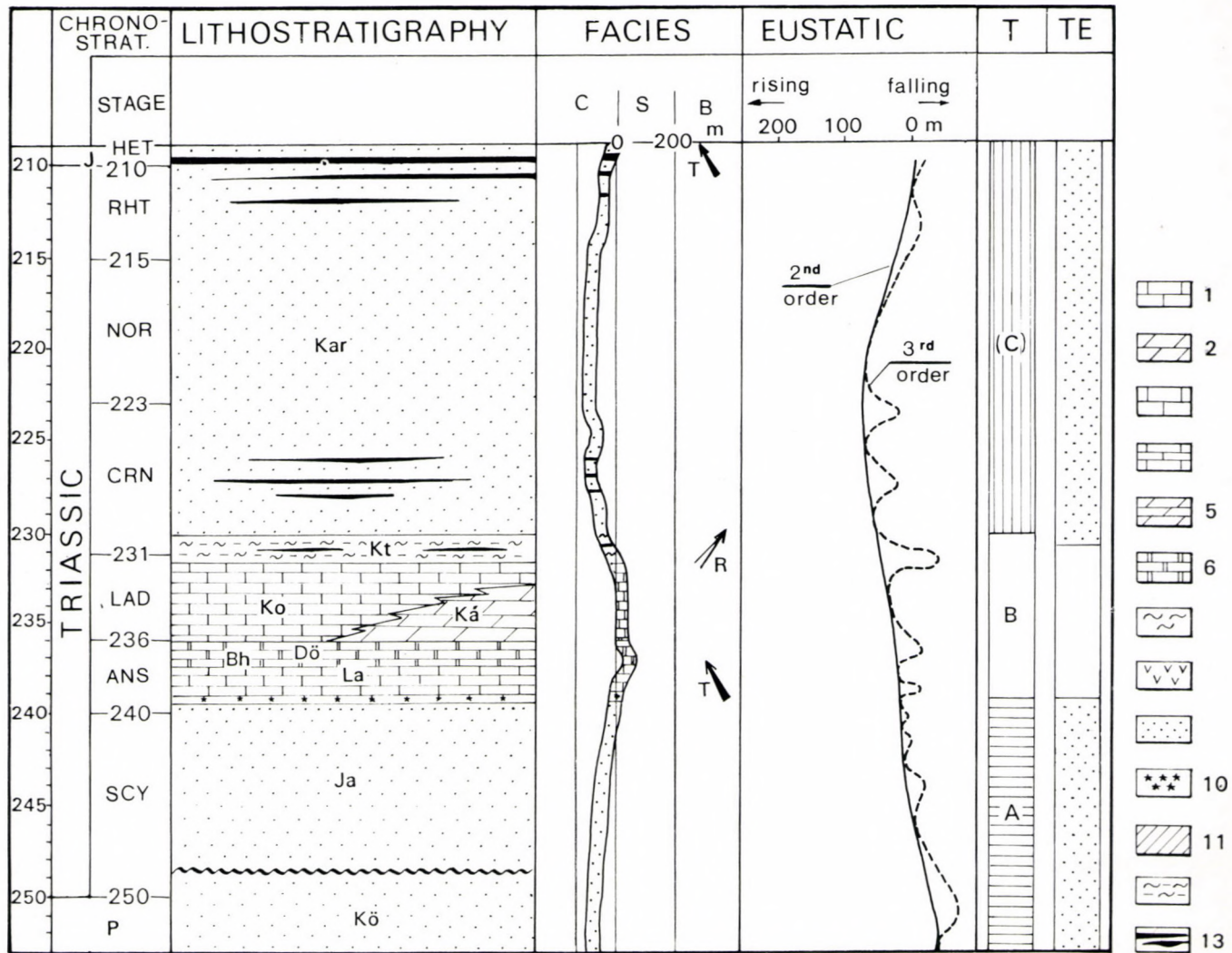


Fig. 2
Late Triassic (Norian) paleogeographic position of the terranes discussed in the text. TR – Transdanubian Range, AG – Aggtelek–Rudabánya Unit, DRZ – Drauzug, MT – Mid-Transdanubian Unit

The geohistory of the studied units is presented in Figs 3, 5 and 7. In these Figures, besides the relationships of the lithogenic units and gaps, plate tectonic setting, intervals of significant terrigenous input, and the global eustatic curve (after Haq et al. 1987) are also indicated. Relative sea-level changes and

Fig. 3 →
Triassic stratigraphy and facies evolution of the Mecsek Unit (lithostratigraphy after Rálisch-Felgenhauer, in press). Eustatic curve after Haq et al. 1987. 1. platform limestones; 2. platform dolomites; 3. platform dolomitic limestones; 4. shallow water limestones (non-platform facies); 5. shallow water dolomites (non-platform facies); 6. basinal limestones; 7. marls and pelites; 8. volcanics; 9. sandstone; 10. evaporites; 11. radiolarites; 12. brackish- and fresh-water marls; 13. coal seams; Kő – Kővágószőlős Sandstone Fm.; Ja – Jakabhegy Sandstone Fm.; Pa – Patacs Siltstone Mb. + Magyarürög Evaporite Mb. + Hetvehely Dolomite Mb. + Viganvár Limestone Mb.; La – Lapis Limestone Fm.; Bh – Bertalanhegy Limestone Mb.; Dö – Dömörkapu Limestone Mb.; Ko – Kozár Limestone Mb.; Ká – Kán Dolomite Mb.; Kt – Kantavár Formation; Kar – Karolinavölgy Sandstone Fm; C – continental; S – shelf; B – pelagic basin; T – transgression; R – regression; TECT – stages of tectonic evolution; A – continental rifting; B – moderate gradual subsidence; (C) – initial rifting; TE – interval of intense terrigenous input



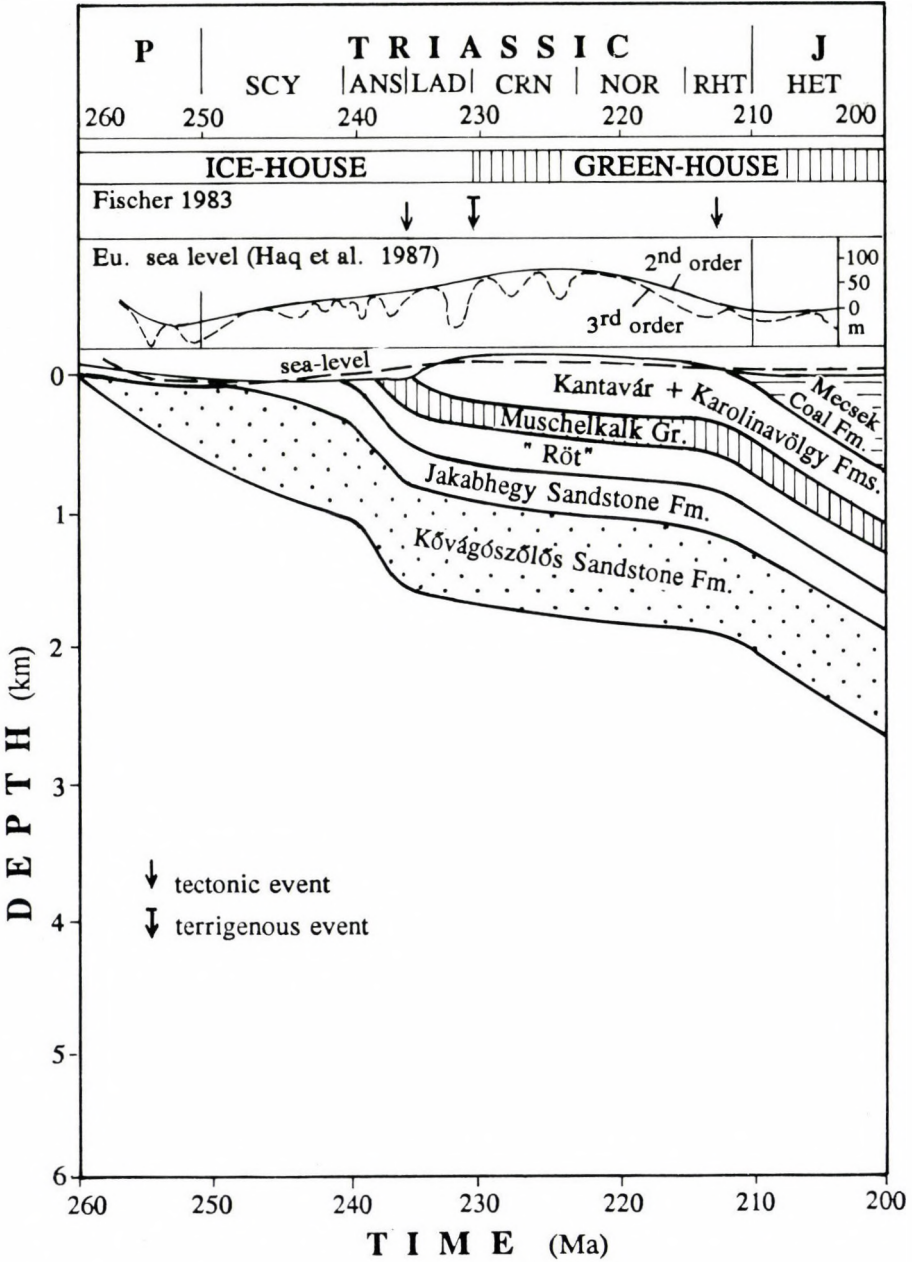


Fig. 4
Relative sea-level changes and significant tectonic and terrigenous events in the Mecsek Mountains. Cumulative formation-thickness curve, refers to changes in subsidence rate

cumulative formation – thickness curves indicative of the changes in the subsidence rate are shown in Figs 4, 6 and 8.

The main characteristics of the Early Alpine (Late-Permian–Early-Jurassic) evolution of the studied units are briefly summarised below.

Mecsek Unit

- A continental rifting phase began in the Early Permian. It was characterised by acidic volcanism and fluvial–lacustrine sedimentation.

- Buntsandstein-type Scythian overlaps the previous Late Variscan structures (Freytet and Cros 1984).

- Following an initial sabkha phase in the Early Anisian a storm-influenced carbonate ramp evolved from the Middle Triassic onward, probably indicating climatic and minor tectonic changes (Török 1993).

- The Middle Triassic is characterised by the accumulation of a relatively thick carbonate sequence (Nagy 1968).

- Siliciclastic fluvial-lacustrine and delta facies prevail in the Late Triassic and Gresten-type Early Jurassic sediments.

After the Permian continental rifting phase a clastic to carbonate ramp evolved in the Early–Middle Triassic. It is characterised by a moderate subsidence rate (Fig. 4). The sedimentation rate increased slightly in the Anisian, reflecting a coeval acceleration of subsidence and sea-level rise.

A significant increase in the subsidence rate started in the Late Triassic as a result of a new rifting phase. In the Mecsek Mountains the accumulation of an extremely thick Gresten sequence indicates extensional half-graben and ridge formation (local tectonism – Nagy 1969). A drastic decrease in the terrigenous input took place only in the Middle Jurassic (Galács 1984), as a result of the separation of the Tisza Megaunit from the European margin. It is also demonstrated by the differentiation of the ammonite fauna (Géczy 1984). The predominance of siliciclastic sedimentation in the Mecsek zone in the early

←Fig. 5

Triassic stratigraphy and facies evolution of the Transdanubian Range Unit. Eustatic curve after Haq et al. 1987. Sequence boundaries after Haq et al. 1987 and Aigner and Bachman 1992. Bf – Balatonfelvidék Red Sandstone Fm.; Ta – Tabajd Evaporite Fm.; Di – Dinnyés Dolomite Fm.; Kö – Köveskál Dolomite Fm.; Ar – Arács Marl Fm.; Al – Alcsútdoboz Limestone Fm.; Hs – Hidegkút Sandstone Fm.; Hd – Hidegkút Dolomite Mb.; Cs – Csopak Marl Fm.; As – Aszófő Dolomite Fm.; lh – Iszkahegy Limestone Fm.; Me – Megyehegy Dolomite Fm.; Ta – Tagyon Limestone Fm.; Fö – Felsőörs Limestone Fm.; Bu – Buchenstein Fm.; Bö – Budaörs Dolomite Fm.; Fü – Füred Limestone Fm.; Ve – Veszprém Marl Fm.; Ed – Ederics Limestone Mb.; No – Nosztor Limestone Mb.; Sv – Sédvölgy Dolomite Mb.; Ma – Mátyáshegy Limestone Fm.; Fh – Feketehegy Limestone Fm.; Da – Dachstein Limestone Fm.; Kö – Kössen Fm.; Kr – Kardosrét Limestone Fm.; Pi – Pisznice Limestone Fm.; C – continental; S – shelf; B – pelagic basin; 1) meter-scale cyclicity; T – transgression; R – regression; TECT – stages of tectonic evolution, B₁ – moderate gradual subsidence, B₂ – accelerated subsidence, C₁, C₂, C₃ – extensional tectonics, TE – interval of intense terrigenous input

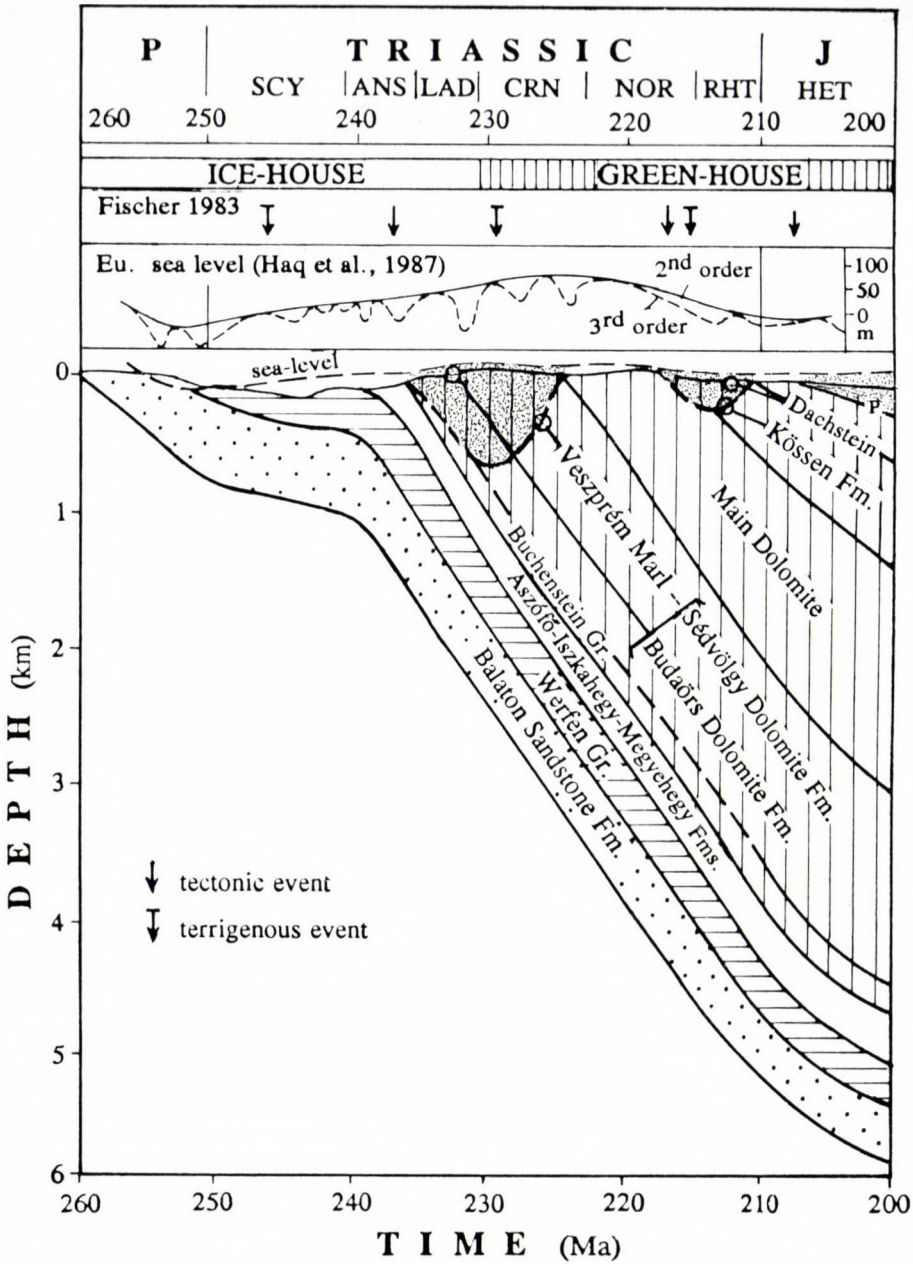


Fig. 6
Relative sea-level changes and significant tectonic and terrigenous events in the Transdanubian Range. Cumulative formation-thickness curve, refers to changes in the subsidence rate

stages of the Alpine evolution is a consequence of the proximity of the continental hinterland.

Transdanubian Range Unit

– Transgression occurred in two phases: in the Late Permian and at the Permian–Triassic boundary (Majoros 1980; Haas et al. 1988)

– Werfen-type Scythian – shallow ramp of mixed (siliciclastic + carbonate) sedimentation (Haas et al. 1988). Facies changes reflect 3rd order sea-level changes and/or climatic changes (e.g. Campil event – Broglio-Loriga et al. 1990).

– Carbonate platforms evolved in a larger number of phases from the Middle Triassic to the Early Jurassic (Budai and Vörös 1992; Haas 1988, 1994). They show meter-scale orbitally forced peritidal–lagoonal cyclicity as a rule (Haas 1992).

– Intraplatform basins of extensional origin were formed in the Late Anisian–Ladinian, in the Middle Carnian and in the Late Norian, respectively (Budai and Vörös 1992; Haas 1993, 1994). Infilling of these basins by fine terrigenous material was triggered by climatic changes ("Raibl event" and "Kössen event") (Haas 1993, 1994)

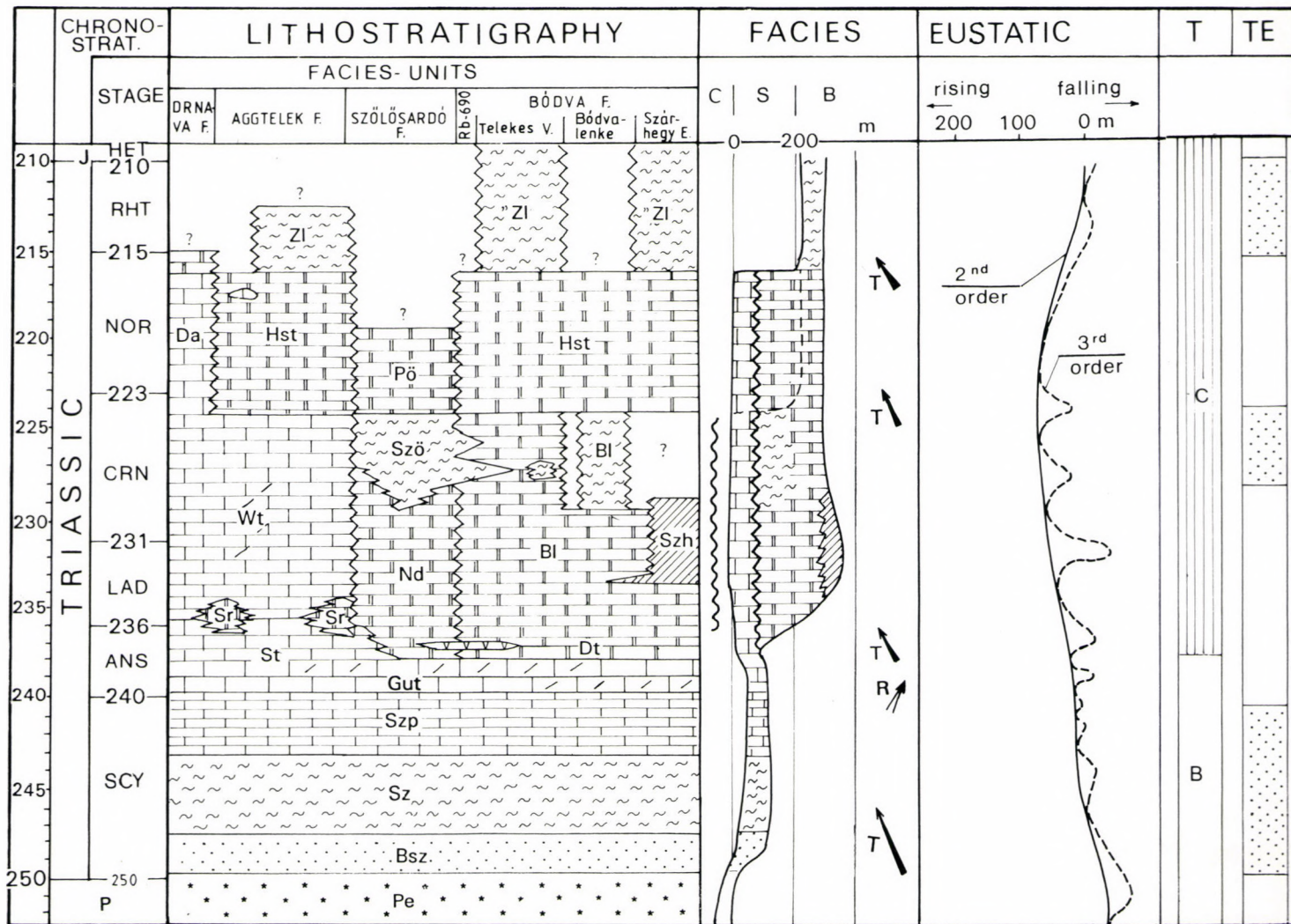
– Disruption of the platforms took place in the Early Jurassic (Late Hettangian–Early Sinemurian – Galácz 1988).

Due to the inner shelf position of the Transdanubian Range Unit, its evolution was controlled by a delicate balance of tectonic, eustatic and climatic factors.

A significant general increase in the subsidence rate occurred in the Middle Anisian (Fig. 6), with coeval segmentation of the platforms. In the extensional basins, where platform evolution terminated, deep, pelagic environments came into being, whereas on the platforms carbonate sedimentation was able to keep pace with the subsidence. The deep basins could have been filled up only during intervals of increased terrigenous input, which was generally followed by rapid progradation of carbonate platforms.

Fig. 7 →

Triassic stratigraphy and facies evolution of the Aggtelek–Rudabánya Unit, completed with the Drnava Facies in Slovakia (after Mello and Bystricky 1973). Eustatic curve after Haq et al. 1987. Pe – Perkupa Evaporite Formation; Bsz – Bódvaszilas Sandstone Fm.; Sz – Szín Marl Fm.; Szp – Szinpetri Limestone Fm.; Gut – Gutenstein Limestone Fm.; St – Steinalm Limestone Fm.; Dt – Dunnatető Limestone Fm.; Sr – Schreyeralm and Reifling Limestone Fm.; Wt – Wetterstein Limestone Fm.; Nd – Nádaska Limestone Fm.; Bl – Bódvalenke Limestone Fm.; Szh – Szárhegy Radiolarite Fm.; Szö – Szőlőszárdó Marl Fm.; Da – Dachstein Limestone Fm.; Zl – Zlambach Fm.; C – continental; S – shelf; B – pelagic basin; 1. meter-scale cyclicity (Lofer cycles); T – transgression; R – regression; TECT – stages of tectonic evolution; B – gradual, moderate subsidence; C – extensional tectonics (rifting); TE – interval of intense terrigenous input



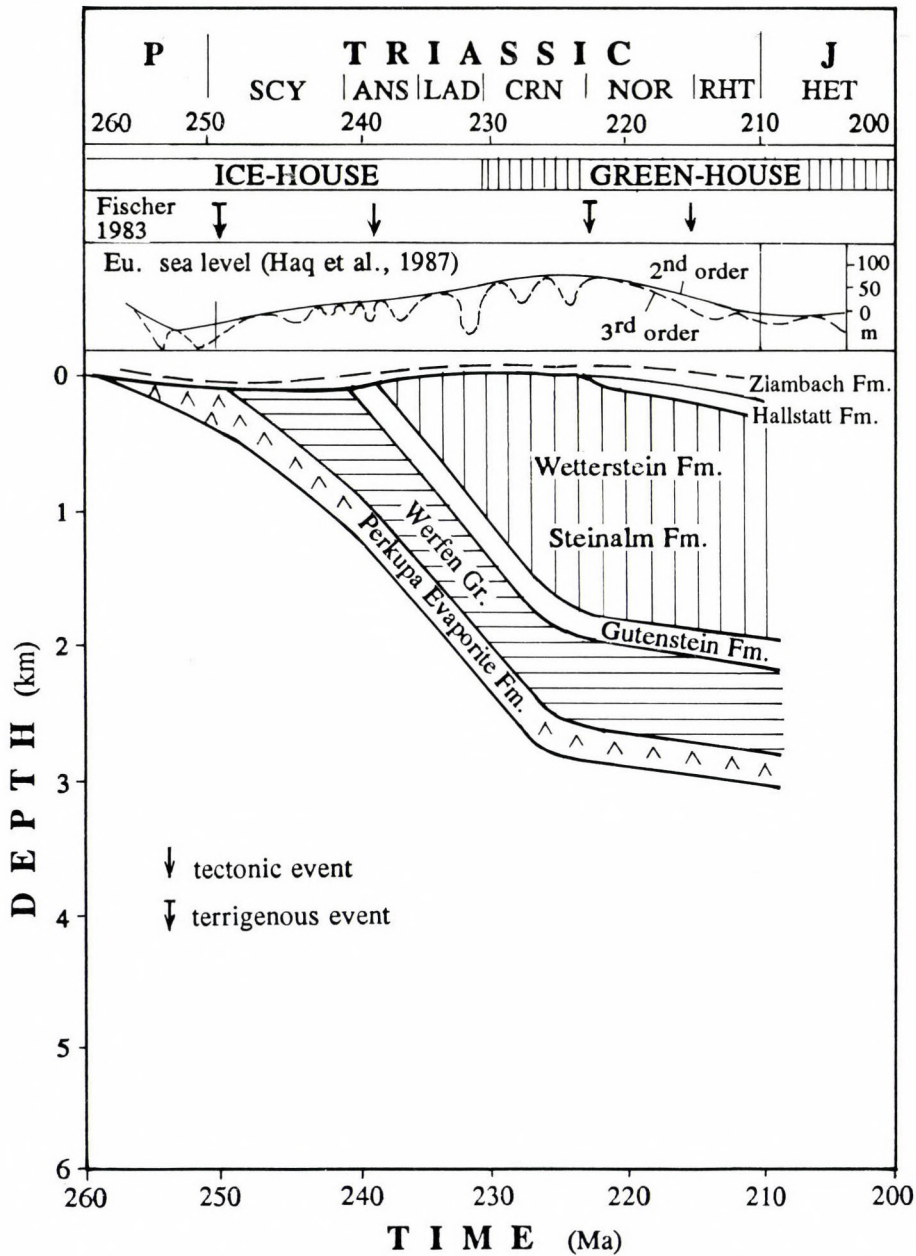


Fig. 8
Relative sea-level changes and significant tectonic and terrestrial events in the Aggtelek facies unit (Aggtelek-Rudabánya Unit). Cumulative formation-thickness curve, refers to changes in subsidence rate

Aggtelek–Rudabánya Unit

– Transgression initiated in the Late Permian – coastal sabkha zone with hypersaline lagoon came into being (Balogh 1981).

– Werfen-type Scythian-shallow ramp of mixed sedimentation was formed with upward decreasing siliciclastic supply (Hips pers. com.).

– Carbonate platform evolution was initiated in the Anisian, but due to oceanic rifting the platforms were drowned (in most of the unit) already in the Middle Anisian, when the most marginal part of the continental margin (i.e. most proximal to the opening oceanic basin) collapsed. A characteristic facies differentiation developed in the Ladinian from the outer shelf/shelf margin (Aggtelek facies unit) through the slope (Szőlősardó facies unit) into the deep basin with attenuated continental crust (Bódva facies unit), and then with oceanic crust (Meliata Unit, Tornakápolna facies unit – Kovács 1984; Kovács et al. 1989).

– Changes in the composition of the basin-filling sediments (limestone vs. shale) may reflect climatic changes ("Raibl and Kössen events", respectively). Coeval carbonate platforms were not affected by the terrigenous influx. Even in the Carnian, the evolution of dasycladacean flora was uninterrupted and served as evidence for the continuous build-up of carbonate platforms in the Aggtelek facies unit. Siliciclastic material was transported through intraplatform channels onto the slopes and into the eupelagic environments (Szőlősardó and Bódva facies units), in which deep-water sedimentation persisted throughout the rest of the Triassic.

Representing the most internal (marginal) zones of the shelf, the evolution of this unit was governed mainly by backstepping marginal rifting, from the Middle Triassic (Fig. 7) onward.

Tectonic control of sedimentation was evident throughout the Middle–Late Triassic:

– Middle–Late Anisian: disruption of the formerly uniform carbonate ramp, initiation of oceanic rifting;

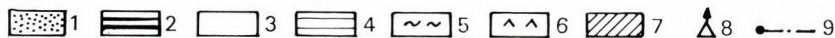
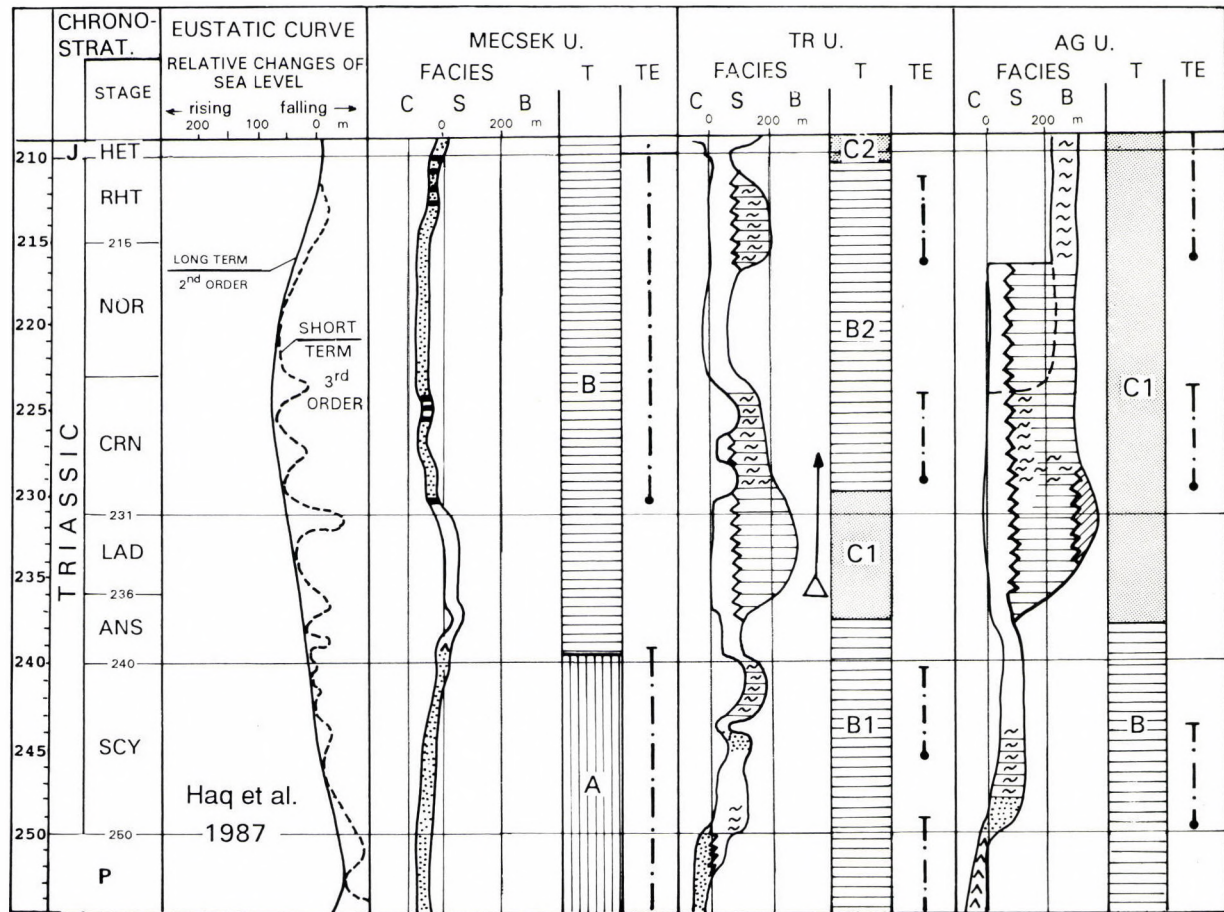
– Late Carnian: breakdown of the outer shelf–shelf margin (Aggtelek facies), back-stepping of the reef margin to the north (Drnava facies in Slovakia – Mello and Bystricky 1973).

– Late Norian: drowning of the Drnava platform, but without clastic influx, which, on the other hand, manifested itself in basinal environments (Mello and Bystricky op. cit.; Nádor 1990).

Conclusions

1. The main trends of the shelf evolution and basic facies characteristics are controlled primarily by paleo-position of the given area within the Tethys shelf.

The distance of terrestrial source-areas is of critical importance:



Mecsek Unit – adjacent to the continental hinterland – a trap for terrigenous sediments

Transdanubian Range Unit – inner shelf

Aggtelek–Rudabánya Unit – outer shelf – shelf margin.

2. Within the studied units the facies distribution is governed mainly by local tectonics which resulted in the formation of extensional basins.

Main phases of the basin formation:

– Middle–Late Anisian

– Middle Norian

– Early Jurassic

3. The features of the sedimentary sequences are significantly influenced by the climate.

Three major, most probably climate–influenced terrigenous events are detectable in every unit:

– the Scythian – "Campil event"

– the Carnian – "Raibl (or Lunz or Reingraben) event"

– the Late Norian – "Kössen event"

4. Eustatic sea-level changes are responsible for the cyclicity of certain formations. Effects of the 3rd order sea-level changes were demonstrated in the Transdanubian Range's Scythian and Carnian. 4th–5th order (Milankovitch) cyclicity is reflected in the Lofer-cycles of the Middle and Late Triassic platform carbonates in the Transdanubian Range and in the Aggtelek facies unit.

Acknowledgement

This project was financially supported by the Hungarian Scientific Research Fund (OTKA No. 2671).

Fig. 9 ←

Facies evolution and major controlling factors in the Triassic for the studied units. 1. siliciclastics; 2. coal; 3. shallow-marine carbonates; 4. deep-sea carbonates; 5. shales; 6. evaporites; 7. radiolarites; 8. volcanic activity; 9. terrigenous input

References

- Aigner, T., G.H. Bachman 1992: Sequence stratigraphy of the Triassic in the intra-Cratonic German Basin. – Sequence Stratigraphy of European Basins, Dijon, Abstracts pp. 108–109.
- Balla, Z. 1988: On the origin of the structural pattern of Hungary. – Acta Geol. Hung., 31, 1–2, pp. 53–63.
- Balogh, K. 1981: Correlation of the Hungarian Triassic. – Acta Geol. Hung., 24, 1, pp. 3–48.
- Broglio-Loriga C., F. Góczán, J. Haas, K. Lenner, C. Neri, A. Oravec-Scheffer, R. Posenato, I. Szabó, A. Tóth-Makk 1990: The Lower Triassic sequences of the Dolomites (Italy) and

- Broglio-Loriga C., F. Góczán, J. Haas, K. Lenner, C. Neri, A. Oravec-Scheffer, R. Posenato, I. Szabó, Á. Tóth-Makk 1990: The Lower Triassic sequences of the Dolomites (Italy) and Transdanubian Mid-Mountains (Hungary) and their correlation. – *Mem. Sci. Geol.*, XLII, pp. 41–103.
- Budai, T., A. Vörös 1992: Middle Triassic history of the Balaton Highland: extensional tectonics and basin evolution. – *Acta Geol. Hung.*, 35, 3, pp. 237–250.
- Csontos, L., A. Nagymarosy, F. Horváth, M. Kovác 1992: Tertiary evolution of the Intra-Carpathian area: a model. – *Tectonophysics*, 208, pp. 221–241.
- Freytet, P., P. Cros 1984: Sedimentological approach of some Upper Permian and Lower Triassic sections in the Transdanubian Central Range and in the Mecsek Mts. (Hungary). – *Acta Geol. Hung.*, 27, 3–4, pp. 277–288.
- Galács, A. 1984: Jurassic of Hungary: a review. – *Acta Geol. Hung.*, 27, 3–4, pp. 359–378.
- Galács, A. 1988: Tectonically controlled sedimentation in the Jurassic of the Bakony Mountains (Transdanubian Central Range, Hungary). – *Acta Geol. Hung.*, 31, 3–4, pp. 313–328.
- Géczy, B. 1984: Jurassic Ammonite Provinces of Europe. – *Acta Geol. Hung.*, 27, 1–2, pp. 67–71.
- Haas, J. 1988: Upper Triassic carbonate platform evolution in the Transdanubian Mid-Mountains. – *Acta Geol. Hung.*, 31, 3–4, pp. 299–312.
- Haas, J. 1993: Formation and evolution of the "Kössen Basin" in the Transdanubian Range. – *Földt. Közl.*, 123, 1, pp. 9–54.
- Haas, J. 1994: Carnian Basin evolution in the Transdanubian Central Range, Hungary. – *Zentralblatt für Geologie und Paläontologie Teil I*. H.11/12. pp. 1233–1252.
- Haas, J., G. Császár, S. Kovács, A. Vörös 1990: Evolution of the western part of the Tethys as reflected by the geological formation of Hungary. – *Acta Geol. Geoph. Mont. Hung.*, 25, 3–4, pp. 325–344.
- Haq, B.U., J. Hardenbol, P.R. Vail 1987: Chronology of fluctuating sea levels since the Triassic. – *Science*, 235, pp. 1156–1167.
- Kázmér, M., S. Kovács 1985: Permian–Paleogene paleogeography along the eastern part of the Insubric–Periadriatic lineament system: evidence for continental escape of the Bakony–Drauzug unit. – *Acta Geol. Hung.*, 28, 1–2, pp. 71–84.
- Kovács, S. 1984: North Hungarian Triassic facies types: a review. – *Acta Geol. Hung.*, 27, 3–4, pp. 251–264.
- Kovács, S., Gy. Less, O. Piros, Zs. Réti, L. Róth 1989: Triassic formations of the Aggtelek–Rudabánya Mountains (Northeastern Hungary). – *Acta Geol. Hung.*, 32, 1–2, pp. 31–63.
- Majoros, Gy. 1980: A permii üledékképződés problémái a Dunántúli Középhegységben. Egy ösföldrajzi modell és néhány következtetés (Problems of the Permian sedimentation in the Transdanubian Central Range: a paleogeographical model and some conclusions). – *Földt. Közl.*, 110, 3–4, pp. 323–341.
- Mello, J., J. Bystricky 1973: Drnava. – In: Bystricky, J. (Ed.) *Triassic of the West Carpathians Mts. Guidebook to Excursion D, Xth Congr. Carpatho-Balkan Geol. Assoc.*, pp. 52–59, GùDS Bratislava.
- Nagy, E. 1968: Die Triasbildungen des Mecsek Gebirges. – *Ann. Inst. Geol. Publ. Hung.*, 51, 1, pp. 1–198. Budapest (in Hungarian with German abstract).
- Nagy, E. 1969: Unterlias – Kohlenserie des Mecsek Gebirges – *Paläogeographie*. – *MÁFI Évkönyve*, 51, 2, pp. 307–317.
- Nádor, A. 1990: A Dél-Gömörikum triász-jura határképződményei (). – *MÁFI Évi Jel.* 1988-ról, I, pp. 35–59.
- Török, Á. 1993: Storm influenced sedimentation in the Hungarian Muschelkalk – in: Hagdorn, H. und Seilacher, A. (Eds): *Muschelkalk. Schöntaler Symposium 1991. (Sonderbände der Gesellschaft für Naturkunde in Württemberg 2).*, Korb (Goldschneck), pp. 133–142, Stuttgart.

Contribution to the Upper Triassic geology of the Keszthely Mountains (Transdanubian Range), western Hungary*

Gábor Csillag, Tamás Budai,
László Gyalog, László Koloszar
Hungarian Geological Institute, Budapest

A considerable part of the thick and extensive dolomite complex of the eastern Keszthely Range, formerly assigned to the Hauptdolomit, belongs to the Ederics platform of Middle to Late Carnian age. The Ederics Formation (Sédvölgy Dolomite Mb.) immediately underlies the Hauptdolomit. According to analogies with the Balaton Highland, the Ederics platform came into being in the early Julian. Representing the marginal facies of the Julian basin, Buhimvölgy Breccia shows the western limit of the platform in the Keszthely Range. Progradation of the platform started in the late Julian; this has resulted in the deposition of an intertidal–supratidal sequence above the reef facies (Ederics Mountain).

The Upper Norian Rezi Dolomite Formation of restricted basin facies forms several kilometre long range at the western and northern margins of the aforementioned Carnian platform, with tectonic contact. Southeast of the Rezi Dolomite range, bedded or thick-bedded dolomites with Dasycladaceae and Megalodontidae represent subtidal environment, belongs to the Hauptdolomit. This member of the Hauptdolomit (Pad-kő Dolomite) is coeval with the middle-upper part of the Rezi Dolomite.

Key words: Carnian, Norian, paleoenvironment, paleogeography, stratigraphy, Keszthely

Introduction

Within the scope of geological mapping of the Balaton Highland, detailed field work in the Keszthely Mountains was carried out in 1982–1983 at the scale of 1:10 000. However, the lithostratigraphic assignment of the Triassic units has become very contradictory for lack of a proper and uniform stratigraphic and palaeogeographic frame. Under- and overlying formations of the Hauptdolomit have appeared on the map as independent small patches inside the widespread area of the Hauptdolomit.

After completing the mapping, several authors dealt with stratigraphic and paleo-environmental interpretation (Budai and Kovács 1986; Gyalog et al. 1986). Plotting geological maps on the scale of 1 : 20 000 and describing the core samples caused a reevaluation of the distribution and lithostratigraphy of the Rezi Dolomite (Budai and Koloszar 1987). In addition, a dolomite sequence

Addresses: G. Csillag, T. Budai, L. Gyalog, L. Koloszar: H-1143, Budapest, Stefánia út 14, Hungary

Received: 26 May, 1995

* Lecture was given in the Hungarian Geological Society on the 16th of March 1993.

was detected in the Keszthely Range which is older than the Hauptdolomit, situated below or beside the Carnian Veszprém Marl (Császár et al. 1989).

During the final plotting of the maps on the scale of 1: 50 000 (Budai and Koloszár 1990) more steps were taken to clarify the Upper Triassic buildup of the Keszthely Range:

- the dolomite complex of the Szabad hill plateau belongs not to the Hauptdolomit but to the Ederics Formation;
- dolomites occurring west of this area belong to the Rezi Dolomite.

Carnian basin and platform facies of the Keszthely Range

The Ederics Limestone of peri-reef facies occurring in the hills above Balatonederics and marls of Carnian basin facies in the Szent Miklós valley were first recorded by Lóczy (1913, 1916).

In regard to the stratigraphic and paleogeographic knowledge of the Carnian units of the Keszthely Range, the study of the section of borehole Hévíz-6. (Fig. 1) is of crucial importance (Góczán et al. 1983).

On the basis of fieldwork and fossil evidence, Gyalog et al. (1986) assigned the Carnian coral-bearing dolomite of the eastern plateau to the Hauptdolomit. The sequence which is built up by an alternation of limestone and dolomite layers was interpreted as a direct transition between the Ederics Limestone and the Hauptdolomit. Nevertheless, this interpretation is inconsistent with the following facts:

- The Carnian age of the dolomite does not contradict the definition of the Hauptdolomit, but its corals (*Thecosmilia* sp.) and microfacies, showing a reef environment, are closer to the Ederics Limestone than to the Hauptdolomit.
- The evidence of boreholes Vát-4 and Vát-5 shows that the dolomite of the eastern plateau underlies the Veszprém Marl, in opposition to former assumptions (Bohn 1979; Gyalog et al. 1986).

In the Szent Miklós valley (Fig. 2), outcrops of the Buhimvölgy Breccia are indicative of an interfingering contact between the Carnian basin (Veszprém Marl) and the coeval carbonate platform (Ederics Formation). This situation is similar to that of the Southern Alps where the blocks of Cipit Limestone (Cipit boulders) up to several metres in size (derived from the coeval platform) are found within the Cassian beds of basin facies (Biddle 1980; Bosellini and Neri 1991).

According to the latest interpretation our lithostratigraphic classification, based on mapping, differs in the following two respects from the "official" one of the Hungarian Commission on Stratigraphy (Haas and Császár 1993):

- Within the Veszprém Marl Formation, in addition to the Mencshely Marl, Nosztor Limestone, and Csicsó Marl Members, the Buhimvölgy Breccia Member is also distinguished as a proximal slope facies of the Ederics and Sédvölgy platforms, coeval facies of the upper two basinal members. Megabreccias and

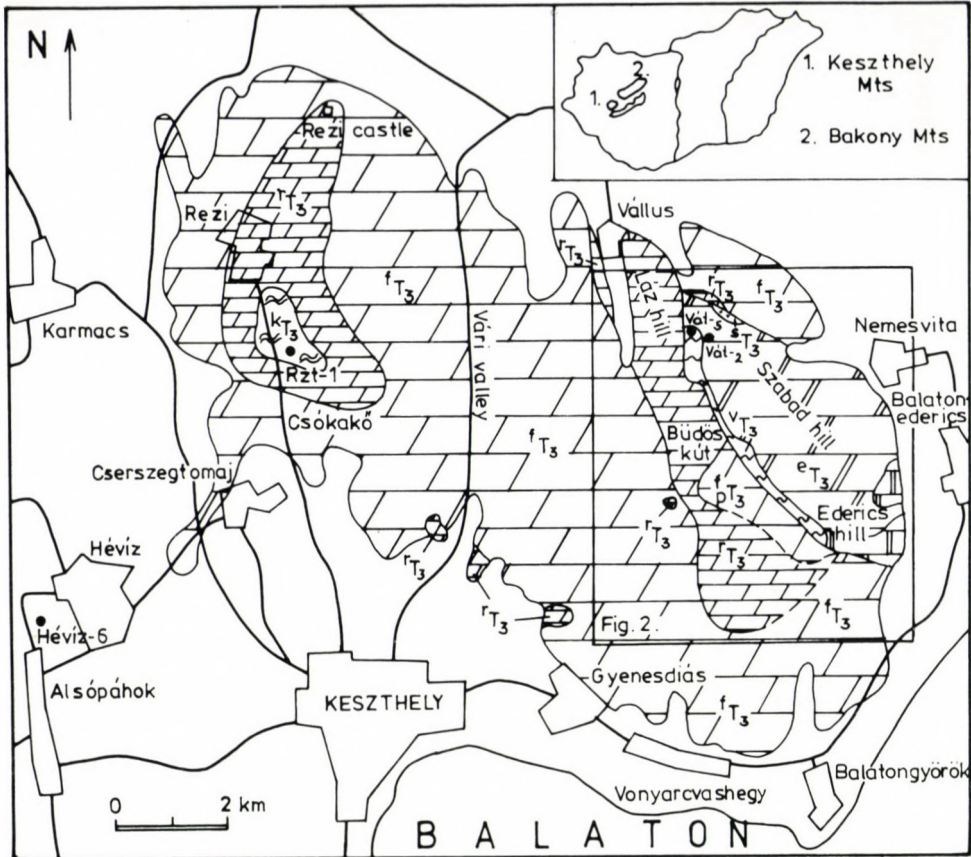


Fig. 1
Upper Triassic surface of the Keszthely Mts. kT_3 - Kössen Formation; rT_3 - Rezi Dolomite Formation; f_pT_3 - Hauptdolomit Formation, Pad-kő Dolomite Member; fT_3 - Hauptdolomit Formation; sT_3 - Sándorhegy Formation; vT_3 - Veszprém Marl Formation; eT_3 - Ederics Formation

allodapic bioclats, ooids, oncoids and limestone clasts from 0.5 to 40 cm size (Csillag 1991), originating from the platform, represent this member.

- Within the Ederics Formation, the Sédvölgy Dolomite Member has already been defined on the Balaton Highland, whereas the reef limestone is called Ederics Formation. In the Keszthely Range the presence of this dolomite member was only supposed previously, however, later it was found on greater areal extent than the reef limestone.

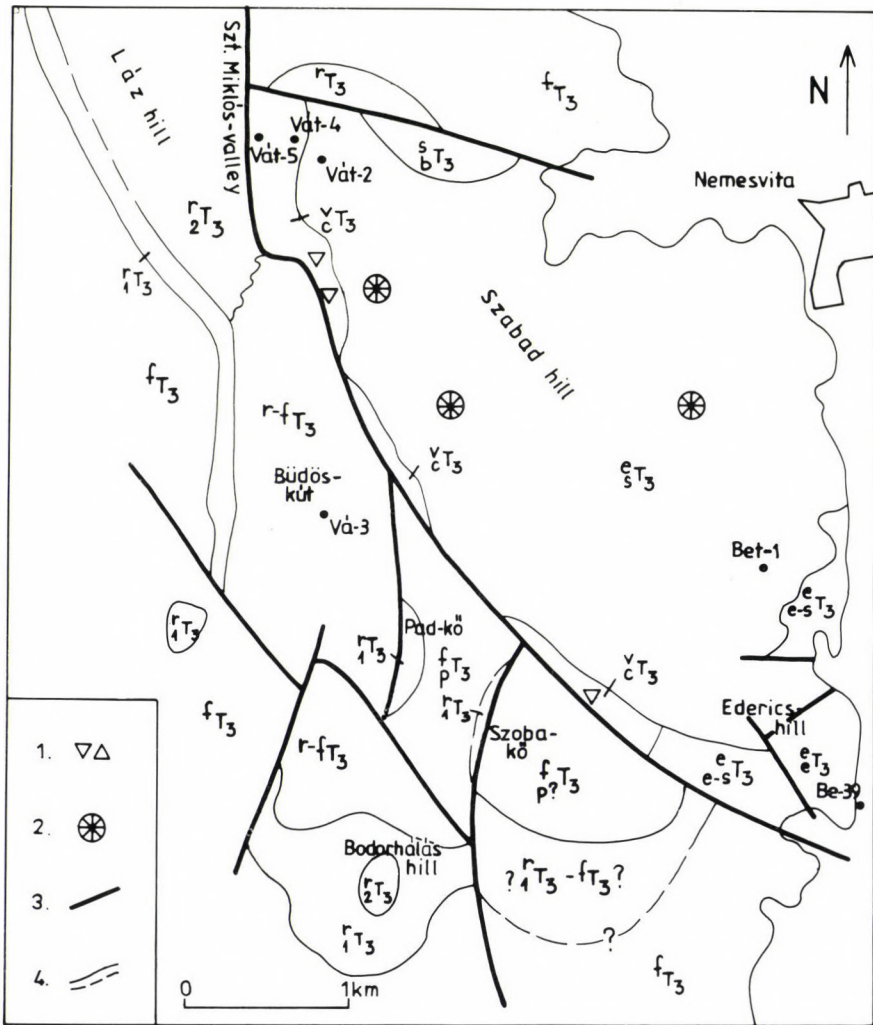


Fig. 2
Upper Triassic build-up of the Eastern part of the Keszthely Range. rT_3 – Rezi Dolomite Formation (r_2T_3 – middle member; r_1T_3 – lower member); $r-fT_3$ – transition between Rezi Dolomite and Hauptdolomit; f_pT_3 – Hauptdolomit Formation ("Pad-kő Dolomite Member"); fT_3 – Hauptdolomit Formation; s_bT_3 – Sándorhegy Formation, Barnag Member; v_cT_3 – Veszprém Marl Formation, Csicsó Marl Member; Ederics Formation: e_sT_3 – Sédvölgy Dolomite Member; e_eT_3 – Ederics Limestone Member; $e-e_sT_3$ – transition between Ederics Limestone and Sédvölgy Dolomite Member; 1. megabreccia (Veszprém Formation, Buhimvölgy Breccia Member); 2. corals; 3. tectonic boundary; 4. stratigraphic boundary

Evolution of the Ederics platform

By analogy with the Balaton Highland (Budai 1991; Csillag 1991) and the Veszprém area (Peregi 1979), the Ederics platform probably emerged in the Julian. Likewise, in the Southern Alps the Cassian dolomites became much more extensive in the Middle Carnian, forming the main mass of the Sella, Nuvolau and Lagazuoi platforms. Bosellini (1984, Fig. 1) Masetti et al. (1991, Fig. 1) and De Zanche et al. (1993, Plate 1) clearly illustrated the intensive progradation of the Cassian Dolomite (so-called Upper Cassian Dolomite or Cassian Dolomite 2) in the Middle Carnian (Julian substage). The evolution of the Balaton Highland fits better with this history than with the continuous progradation of the Cassian dolomite from the Ladinian, as advocated by Bizzarini and Braga (1987).

In spite of the general analogy in the evolution of the two areas, there are some differences in the lithologic and stratigraphic buildups. The Wengen Formation of the Southern Alps, underlying the San Cassian Formation is absent in the Balaton Highland, and is substituted by the Buchenstein Formation. The sequence, overlying the Julian platform-basin complex is also different in the two regions. In the Dolomites the Dürrenstein Dolomite is deposited on the San Cassian Formation and the Cassian Dolomite, as the intraplateau basins were filled up and the paleotopography was levelled (Bosellini 1982; De Zanche et al. 1993). However, the lithofacies of the Sándorhegy Formation is different, its depositing situation on the Ederics and Veszprém Marl Formation is quite similar (Csillag 1991).

In the south-eastern part of the Ederics platform (Ederics hill) the reef margin facies types can be found which were not dolomitized. Further west-northwest, up to the platform margin, the carbonate "bank" is generally composed of dolomite. A considerable part of the dolomite was presumably formed diagenetically late, i. e. the material of the large allodapic blocks (up to 10 m in size) and boulders (5–40 cm) of reef-facies is limestone on the fore-reef slope (Buhimvölgy Breccia). Because of the poor exposure it cannot be decided whether these are megabreccias or small platform-marginal patch reefs, a question which has also been raised for the Dolomites (Wendt and Fürsich 1980).

In the next period of platform development peritidal (?dolomitic) sedimentation with early diagenetic dolomitization took place, according to evidence from borehole Vállus Vát-2 which has penetrated the Sédvölgy Dolomite sequence in a thickness of 200 m. Supratidal breccias, palaeo-karst fissure infills (Plate I, 1) and "bioturbation" structures, probably caused by roots, indicate supratidal depositional environment. However, the thickness of the Ederics Limestone, reaching several hundred metres, leads to the conclusion that a reef must have survived in the southern zone of the platform.

The third evolutionary period of the Ederics platform is marked by a 100 to 150 metre thick sequence of limestones alternating with dolomites. This

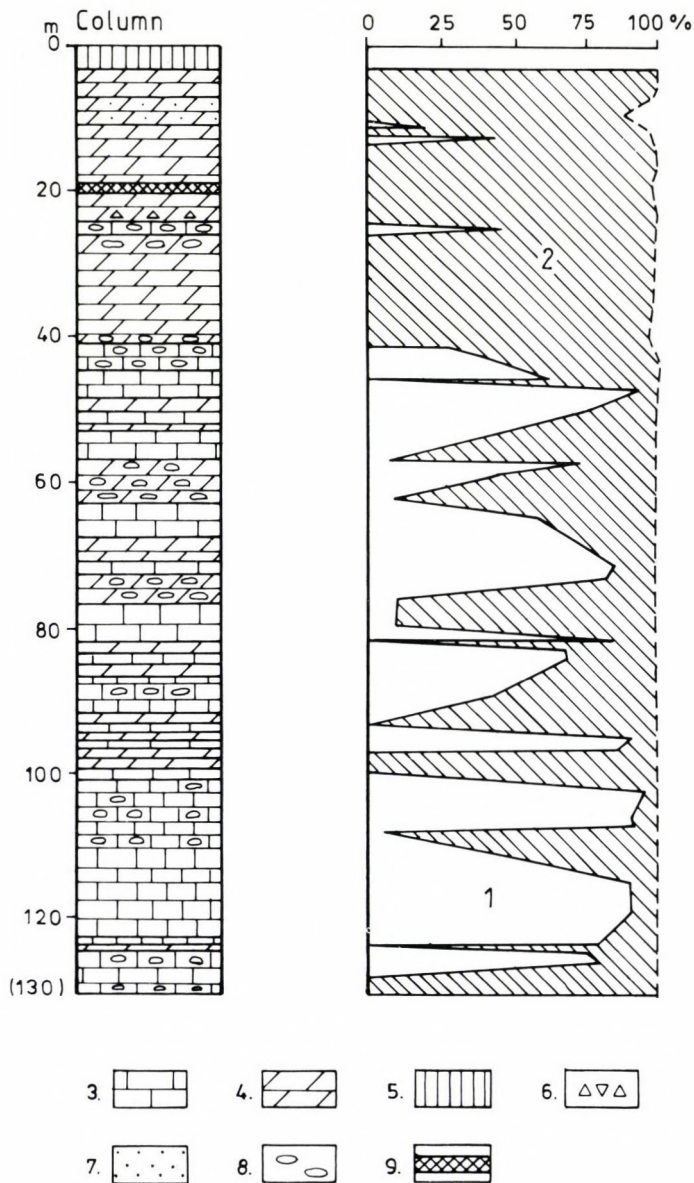


Fig. 3
 Section of the borehole Balatonederics Bet-1 with log of calcite/dolomite ratio 1. calcite; 2. dolomite; 3. limestone; 4. dolomite; 5. soil; 6. breccia; 7. "pulverized" dolomite; 8. intraclasts; 9. tectonic zone

sequence, overlying the pure reef-limestone of the Ederics hill indicates a peri-reef environment with high energy in the reef zone (borehole section Balatonederics Bet-1). The dolomite layers, deposited in the peritidal zone, become more frequent upwards; in the upper 40 m of borehole section Bet-1 only dolomite is found (Fig. 3). This trend could be explained with the advance of the platform margin, following the former reef area replaced by shallow-lagoon facies of the back-reef (Fig. 4). This process is assigned to a strong progradation, began around the Julian/Tuvalian boundary (Góczán et al. 1983), as is the case in the Balaton Highland (Csillag 1991) and in the Dolomites (De Zanche et al. 1993).

No overlying units are known in the central part of the Ederics platform in the Keszthely Range. Limestones and marls of the Sándorhegy Formation (Barnag Member), with several centimetres large oncooids can be detected only in a faulted zone on the western margins of the Szabad hill plateau (Szent Miklós valley). This special facies could be traced as an overlying unit above prograding platforms both in the Balaton Highland (Budai 1991) and in the Bakony Range (Sümege-Sáska), as well. In the northern foreground of the Keszthely Range (borehole Héviz-6) bioclastic, large-oncoidic marls overlying the Ederics Formation show a backstepping platform margin during the Late Tuvalian (Fig. 4).

The relationship between the Ederics and the Sédvölgy platform is an open question. Up to now there are no useful data to decide if the Ederics Formation around Veszprém and in the Keszthely Range belongs to a large single platform, or to separate ones.

Upper Norian units of the Keszthely Range

The Rezi Dolomite of restricted basin facies is much more extensive in the Keszthely Range than it was previously believed. According to the latest mapping records and data interpretation, the Rezi Dolomite and the Kössen Formation are found in the following four areas of this region (Fig. 1):

1. Western part of the Keszthely Mts.: Rezi basin and the surrounding areas;
2. Eastern part of the Keszthely Mts.: between Vállus and Balatongyörök;
3. Northeastern part of the Keszthely Mts: East of Szent Miklós valley;
4. Isolated patches on the SW margin of the Keszthely Range.

1. The surroundings of Rezi

Modern classification of the Rezi Dolomite Formation has been based mainly on the geological sections of this area (Budai and Koloszár 1985, 1987). Even here, we found the extent of the Rezi Dolomite greater than is shown in the map compiled by Budai and Koloszár (1987, Fig. 1), in accordance with the views of Szentes (1953).

Hévíz

NE Keszthely Mts

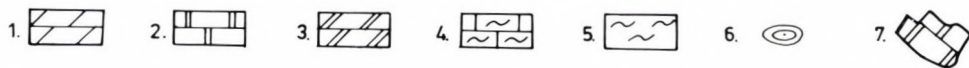
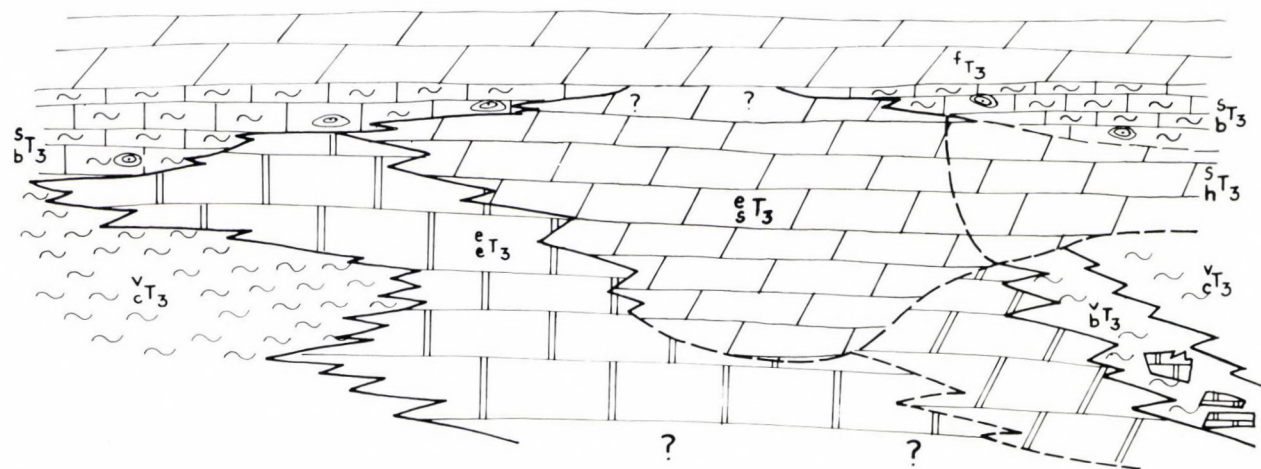
SW Balaton
Highland

Fig. 4

Generalized sketch of the Carnian lithostratigraphic units in the surroundings of the Keszthely Mts.: f_{T_3} - Hauptdolomit Formation; Sándorhegy Formation: s_{bT_3} - Barnag Member; s_{hT_3} - Hénye Dolomite Member; Veszprém Marl Formation: v_{cT_3} - Csicsó Marl Member; v_{bT_3} - Buhimvölgy Breccia Member; Ederics Formation: e_{sT_3} - Sédvölgy Dolomite Member; e_{lT_3} - Ederics Limestone Member; 1. dolomite; 2. limestone; 3. dolomitized limestone; 4. marly limestone; 5. marl; 6. large (1-3 cm) oncooids; 7. megabreccia

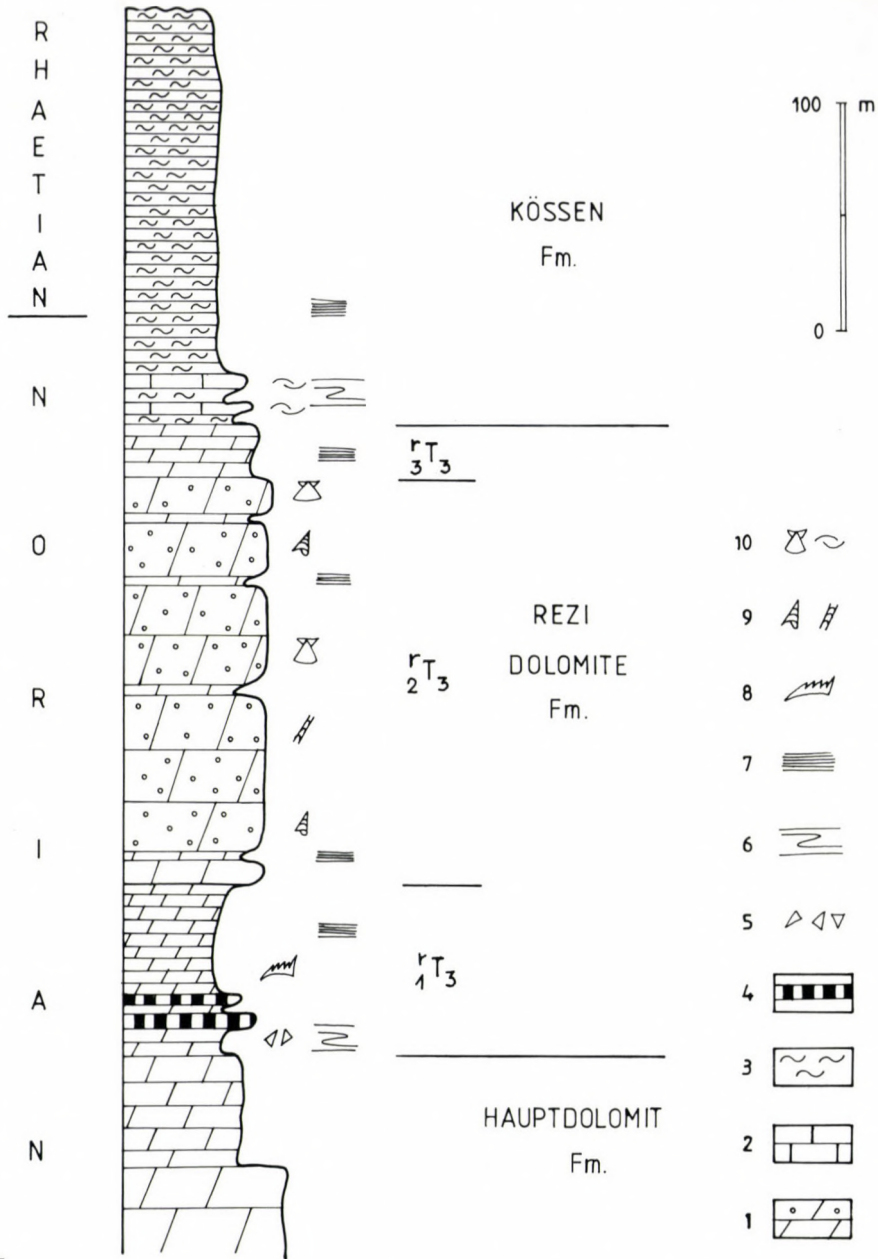


Fig. 5

Lithostratigraphy of the uppermost Triassic formations in the Keszthely Range (after Budai and Koloszář 1987, Fig. 5). Rezi Dolomite Formation: r_3T_3 - upper member; r_2T_3 - middle member; r_1T_3 - lower member; 1. dolomite, porous dolomite; 2. limestone; 3. marl; 4. chert; 5. breccia; 6. slump; 7. parallel lamination; 8. Conodonta (*Metapolygnathus slovakensis*); 9. gastropod, Dasycladacea; 10. bivalve, lumachelle

In the type locality of the Rezi Dolomite a threefold division of the formation is feasible (Fig. 5).

In general, a lithostratigraphic boundary between the Hauptdolomit and the Rezi Dolomite is hard to trace. The upper zone of Hauptdolomit consists of well-bedded bituminous dolomite in which intraclastic lenses and bed intercalations may also occur. Where the Hauptdolomit–Rezi Dolomite boundary is not indicated by bedding and bitumen content, it is now drawn where the appearance of slump structures makes it clear that the depositional environment of Hauptdolomit ceased to exist.

The lower member of the Rezi Dolomite consists of bituminous, well-bedded, often laminated, brecciated intraclastic rocks with chert layers or lenticular intercalations. Slump structures are characteristic (Plate I, 2; Plate II, 1). In some localities a monospecific Conodont-assemblage was found with *Metapolygnathus slovakensis* of Middle–Late Norian age (Budai and Kovács 1986).

The middle member of the formation is made of cellular, bedded dolomite (Plate II, 2), in which gastropod and bivalve fossils are frequent. The fauna collected at Csókakő quarry has been determined by Detre (in Budai and Koloszár 1985):

Gastropoda: *Naticella* sp. (frequent), *Loxonema* sp., *Pleurotomaria* sp.

Bivalvia: *Entolium hellii* (Emmr.), *Modiola minuta* (Goldf.), *Placunopsis* sp., *Protocardia* (?) sp., *Nucula* (?) div. sp.

According to Detre, this assemblage is characteristic of the Kössen facies. The high frequency of gastropods indicates relatively shallow water, however, the specimens seem to be reworked. The upper member is built up of laminated, marly dolomite, which is conformably overlain by the Kössen Formation.

2. Between Vállus and Balatongyörök

In areal extent the Vállus–Balatongyörök range of the Rezi Dolomite is similar to that of the Rezi basin. While the surroundings of Rezi are the type locality for the basin facies of the formation, in the middle part of this range there are deposits representing the heterotropical carbonate platform and transitional beds to the basin. The best and most characteristic outcrop of the lower member of Rezi Dolomite can be found near Vállus, from where the *Metapolygnathus slovakensis* assemblage first described (Budai and Kovács 1986). Further to the southeast the laminated, strongly bituminous lower member shows slump structure.

In the upper part of the member the following fauna was found near Büdöskút (determined by Detre, pers. com.):

Bivalvia: *Entolium discites* (Schl.), *Halobia* sp., *Mysidioptera* (?) sp., *Myophoria* (?) sp.

Brachiopoda: *Rhaetina* sp.

On the Láz hill the formation is represented by cellular, thick-bedded lithofacies, typical for the middle member in the Rezi basin. However, fragments of fossils are abundant here (mainly gastropods and calcareous algae), from where rich assemblage was collected in some outcrops (Detre 1983; Gyalog et al. 1986).

Worthenia oldae (Stopp.) is also found in the classic locality of Sümeg (Haas et al. 1984, p. 16), moreover in the Kössen Beds near Szentgál (Végh 1964, p. 46). From the frequent and large Dasycladaceae Piros determined the following Norian species (in Gyalog et al. 1986): *Gyroporella vesiculifera* (Gümbel) Pia, *Gryphoporella curvata* (Gümbel) Pia.

South of Láz hill, the middle member is substituted by the transitional beds between the Rezi Dolomite and the coeval Hauptdolomit. Further to the south the middle member appears again by its typical facies known in the Rezi basin. The upper member which is known in the Rezi basin is absent between Vállus and Balatongyörök. Fossils of the transitional beds and the Megalodon-bearing dolomite have been described as definitely Norian assemblage of the Hauptdolomit (Detre 1983, and in Gyalog et al. 1986). Doubts emerged later about this definition, when some contradictions were discovered, plotting the maps. It became obvious that placing these two dolomite units into the Rezi Dolomite would require unorthodox structural solutions. Several arguments prove the point:

- the Norian age, in itself, does not necessarily imply superposition of either formation. After all, the Rezi Dolomite is also entirely Norian in age (Budai and Koloszar 1985, 1987);

- southward of Búdös-kút, the lower member of the Rezi Dolomite dips to the east, under the so-called Megalodon-bearing dolomite;

- the same Dasycladacea species are present both in the Rezi Dolomite of Láz hill and the Megalodon-bearing dolomite of Pad-kő (Gyalog et al. 1986);

- "*Pecten*" div. sp., *Halobia* sp., *Nucula* sp. and *Gonodus* sp. was found in a quarry near Búdös-kút (Detre 1983; Gyalog et al. 1986) which are not characteristic of the Hauptdolomit. On the other hand, to the south, in the vicinity of Pad-kő the dolomite contains a Megalodon fauna characteristic of the upper part of the Hauptdolomit (Detre 1983; Gyalog et al. 1986): *Megalodon complanatus* ssp. and *M. cf. boeckhi* (Frech);

- northwest of Búdös-kút the lower member is overlain by algal and molluscan dolomite with brecciated texture. These strata may have formed in the transitional zone, on the slope between the Rezi basin and the Hauptdolomit platform.

Summing up, in the Búdös-kút–Pad-kő–Szoba-kő area it is possible to distinguish above the lower member of the Rezi Dolomite a light-brown, thick-bedded dolomite containing many molluscs (Megalodons) and Dasycladacea flora. In our opinion, this dolomite can be divided in two members by the environment of deposition. The thick-bedded Megalodon-bearing dolomite of Pad-kő and Szoba-kő represents the prograding wedge of the Hauptdolomit platform, surviving coevally with the Rezi basin (Fig. 6). It has been distinguished as Pad-kő Dolomite Member (f_pT_3), as an independent subunit within the Hauptdolomit Formation.

Around Búdös-kút the bedded or thin-bedded dolomite with bituminous intercalation contains *Halobia*, *Pecten* and *Nucula*. It is considered as the

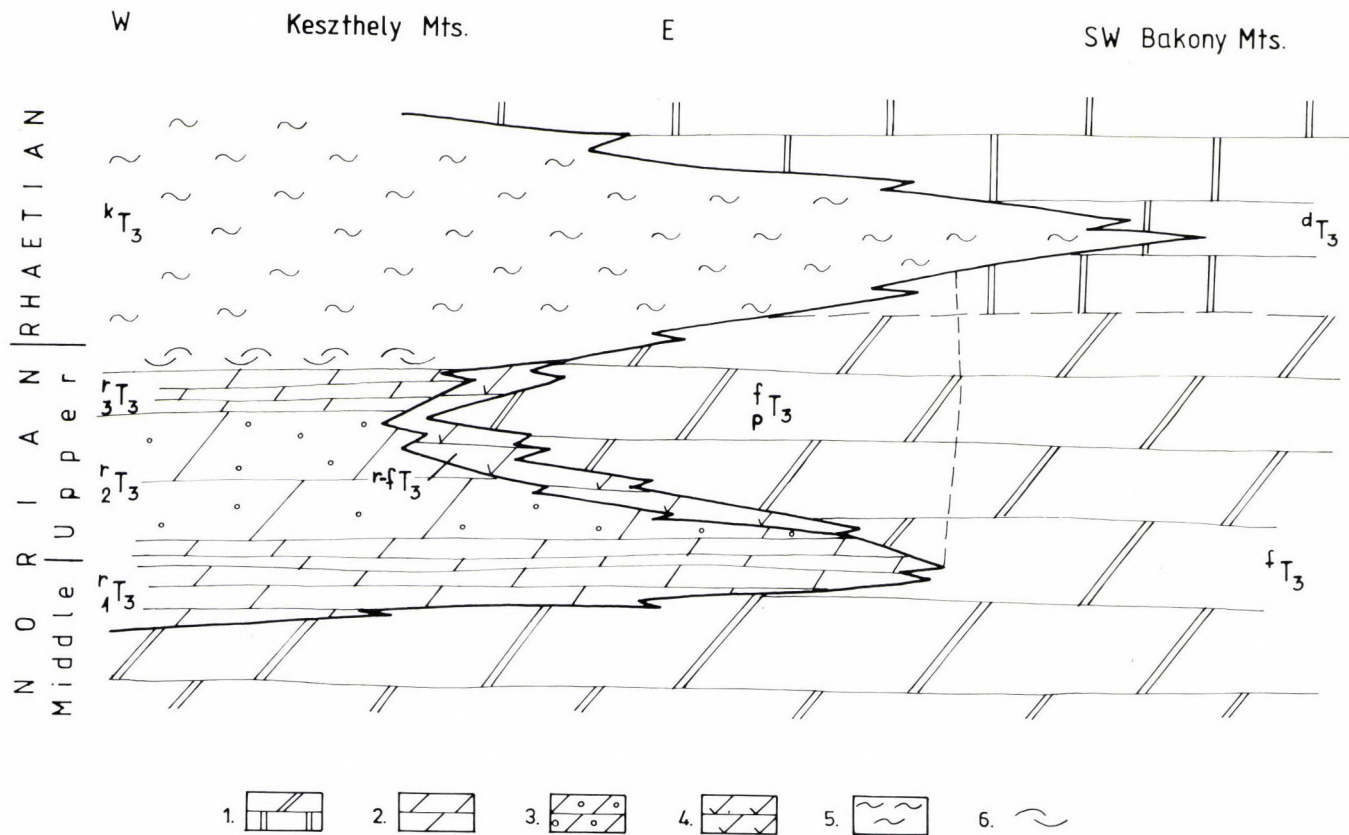


Fig. 6

Schematic section of the Middle Norian to Rhaetian formations in the Keszthely Range and their connection to the SW Bakony Mts. dT_3 – Dachstein Limestone Formation; kT_3 – Kőssen Formation; *Rezi Dolomite Formation*: r_3T_3 – upper member; r_2T_3 – middle member; r_1T_3 – lower member; $r-fT_3$ – transition between the Rezi Dolomite and Hauptdolomit; pT_3 – Hauptdolomit Formation, Pa-dkő Dolomite Member; fT_3 – Hauptdolomit Formation; 1. platform carbonates (Hauptdolomite, Dachstein Limestone); 2–6. basal sediments: 2. laminated, bituminous dolomite; 3. porous dolomite with "Kőssen-type" molluscs; 4. well-bedded dolomite with pseudoplanktic bivalves; 5. marls; 6. lumachelle with *Cardita* assemblage

marginal facies of the Rezi Dolomite and was deposited in the zone just behind the Hauptdolomit platform (r^fT_3).

3. The northeastern part of the Keszthely Range

A series of outcrops of the Rezi Dolomite Formation forms a line to the east of Szent Miklós valley, separated by a significant fault from the Carnian dolomite complex of the Szabad hill plateau. The thin-bedded, laminated, frequently, bituminous dolomite is intercalated with breccia of mm-sized fine debris, together with slumping structures.

4. The southwestern margin of the Keszthely Range

The Rezi Dolomite is found in a few outcrops in the region of Cserszegtomaj and Gyenesdiás (Fig. 1). Only the lower member is represented in all locations which can be distinguished from the underlying Hauptdolomit by chert lenses. In a quarry on the east side of the Vári valley beds of coarse breccia are considered to platform-slope facies (Plate III, 1).

Palaeogeographic relationships of the Rezi Dolomite and the heteropical Hauptdolomit

The nearest outcrops of the Rezi Dolomite to the Keszthely Range are found in the vicinity of Sümeg (SW Bakony). Lóczy (1913, p. 186) first mentioned this locality in his monograph. He considered the top horizon of the Hauptdolomit containing *Dicerocardium incisum* to be very close in age to the Rhaetian Dachstein Limestone. He also expressed the opinion (pp. 178 and 186) that the Rhaetian dolomite (=Rezi Dolomite) and the upper horizon of the Hauptdolomit are heteropical to each other. In this facies arrangement we can recognize the facies of the Vállus-Balatongyörök range of the Keszthely Mts.

For further paleogeographic relationships of the Rezi Dolomite comparison can be made with the Northern Limestone Alps (Budai and Koloszár 1985; Budai and Kovács 1986; Haas 1993). According to Tollmann (1976) the North-alpine Plattenkalk (of the same stratigraphic position as the Rezi Dolomite) is a cyclic sedimentary complex developed in a subtidal to supratidal environment. In our opinion, this depositional environment was shallower than that of the Rezi Dolomite.

Comparing Lombardian sections with the Keszthely Range the correlation seems to be much closer. Similar lithofacies to the Rezi Dolomite have been described from the Norian of the Bergamo Prealps by Jadoul (1985) and from the region west of Lake Garda by Stefani and Golfieri (1989). The sedimentation model of Jadoul (1985, Fig. 13) is nearly identical with that shown in Fig. 6. In our opinion, Dolomia Zonate, belonging to the Aralalta Group and the Rezi Dolomite were formed under very same conditions of a restricted intraplatform basin, only in the initial period of the tectonically controlled dissection of the Hauptdolomit

platform. However, neither platform-marginal patch reefs nor coarse-brecciated units are present in the Keszthely Range, although thick beds of coarse breccia were exposed in the Csókakő quarry, south of Rezi (Plate III, 2).

According to Stefani and Golfieri (1989) the sedimentation of the Hauptdolomit proceeded coevally with the Riva di Solto Argillite and the Zu Limestone of basin facies in the Norian and Rhaetian west of Lake Garda. This facies differentiation came to an end as the deposition of the Conchodon dolomite began, similarly to the Keszthely-Sümege area (Fig. 6).

Conclusions

The latest observations about the Upper Triassic of the Keszthely Range are summarized as follows:

– The dolomite formerly assigned to the Hauptdolomit in the eastern part of the region belongs to the Ederics platform. By analogy with the Balaton Highland, the development of this platform started in the Julian. Progradation began in the late Julian resulted in the deposition of a peritidal sequence above the Ederics reef.

– The blocks of Buhimvölgy Breccia are detached fragments of the Ederics platform and were deposited on the talus against the Carnian basin (Veszprém Formation). The Buhimvölgy Breccia is quite similar to the South-Alpine Cipit Limestone.

– The Rezi Dolomite and Hauptdolomit is partly heteropic with each other. In the transitional zone two facies can be distinguished: a "Rezi-type" dolomite containing pelagic bivalves and a Megalodon-bearing dolomite belonging to Hauptdolomit (Pad-kő Member).

Plate I

- 1 a–b Paleokarst fissure infill. Borehole Vát-2 at Vállus;
- 1c Supratidal breccia on top of dolomite, with fissures filled with the material of the cover rock. Borehole Vát-2 at Vállus (Ederics Formation, Sédvölgy Dolomite Member)
- 2 Slump structure in Csókakő quarry, S to Rezi (Rezi Dolomite Formation, lower member)

Plate II

- 1 Slump structure in Csókakő quarry (Rezi Dolomite Formation, lower member) (Photo Lénárt 1989)
- 2 Boundary of the lower, laminitic and the middle, cellular and thick-bedded member of the Rezi Dolomite in Csókakő quarry (Photo Lénárt 1989)

Plate III

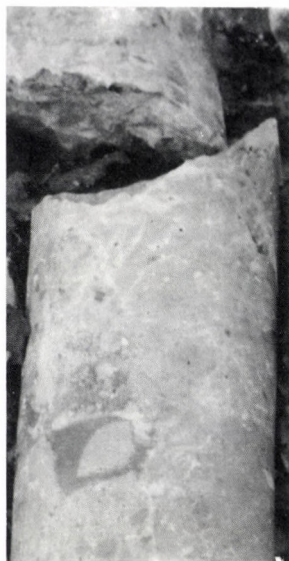
Beds with coarse breccia (slope facies) in the Rezi Dolomite

- 1 Breccia in the lower member of the Rezi Dolomite in the quarry near the southern end of Vári valley
- 2 Breccia in the middle member of the Rezi Dolomite in the quarry of Csókakő

Plate I



1a



1b

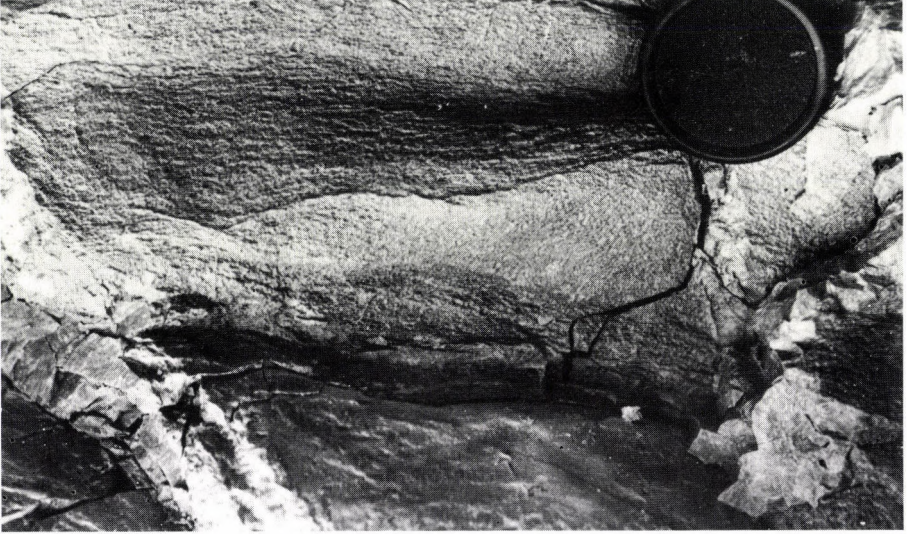


1c

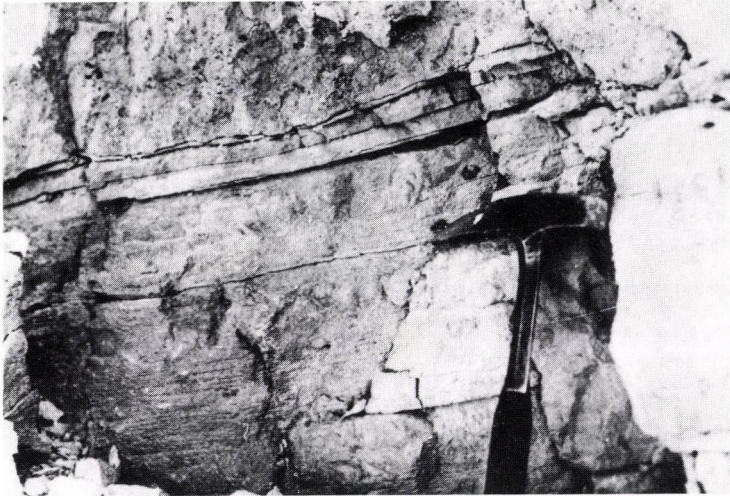


2

Plate II

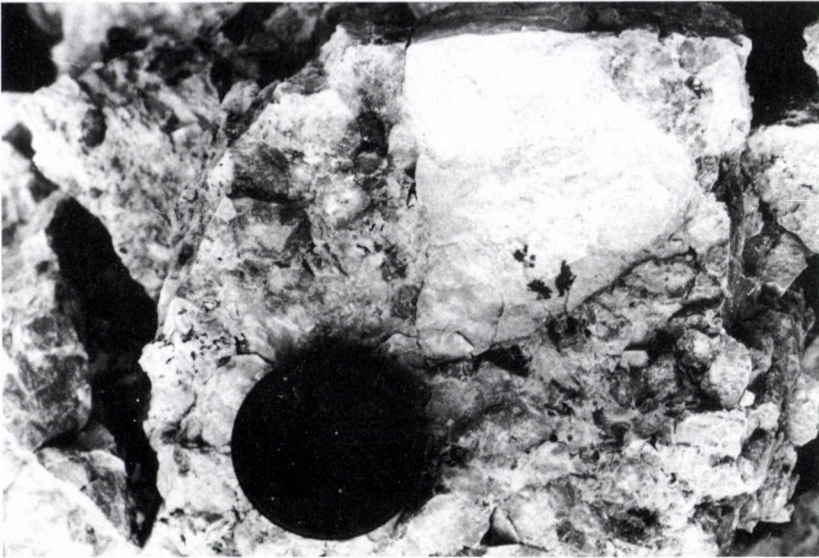


1

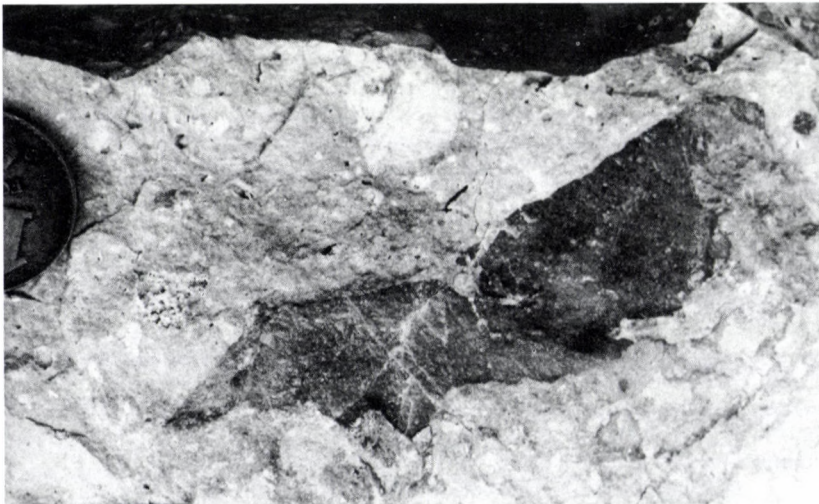


2

Plate III



1



2

References

- Biddle, K. T. 1980: The basinal Cipit boulders: indicators of Middle to Upper Triassic buildup margins, Dolomite Alps, Italy. – *Riv. Ital. Paleont. Strat.*, 86, 4, pp. 779–794.
- Bizzarini, F., G. Braga 1987: Considerazioni bio e litostratigrafiche sulla Formazione di S. Cassiano (Dolomiti Nord-Orientali, Italia). – *Studi Trentini di Scienze Naturali*, 64, pp. 39–56.
- Bohn, P. 1979: A Keszthelyi-hegység regionális földtana (The regional geology of the Keszthely Mountains). – *Geol. Hung. ser. geol.*, 19, 197 p.
- Bossellini, A. 1982: Guida dei Passi dolomitici circostanti il Gruppo di Sella. – Guida alla Geol. del Sudalpino centro-orientale, pp. 267–272.
- Bossellini, A. 1984: Progradation geometries of carbonate platform: examples from the Triassic of the Dolomites, northern Italy. – *Sedimentology*, 31, pp. 1–24.
- Bossellini, A., C. Neri 1991: The Sella Platform (Upper Triassic, Dolomites, Italy). – Dolomieu Conference on Carbonate Platform and Dolomitization, Guidebook Excursion B, pp. 3–30, Ortisei
- Brukner-Wein, A., T. Budai, Cs. Detre, F. Góczán, M. Hetényi, L. Koloszar, H. Lőrincz, A. Oravecz-Scheffer, L. Pápay, Zs. Peregi 1987: Összefoglaló jelentés a Rezi Rzt-1. fúrás vizsgálati eredményeiről (Comprehensive report on the investigations of borehole Rezi Rzt-1). – manuscript (in Hungarian). Hung. Geol. Surv. Doc. center
- Budai, T. 1991: Újabb adatok Felsőörs környékének geológiai felépítéséről (Contributions to the knowledge of the structural geology of Felsőörs, Balaton Upland). – *Ann. Rep. Hung. Geol. Inst.*, 1989, pp. 17–33.
- Budai, T., L. Koloszar 1985: A Keszthelyi-hegység legfelső-triász képződményeinek földtani vizsgálata (Geology of the uppermost Triassic formations of the Keszthely Mountains). – manuscript (in Hungarian). Hung. Geol. Surv. Doc. center
- Budai, T., L. Koloszar 1987: A Keszthelyi-hegység nőri-raeti képződményeinek rétegtani vizsgálata (Stratigraphic investigation of the Norian-Rhaetian formaions in the Keszthely Mountains). – *Bull. Hung. Geol. Soc.*, 117, pp. 121–130.
- Budai, T., L. Koloszar (ed.) 1990: A Balaton-felvidék földtani térképe. Fedett változat. M=1:50 000 (Geological map of the Balaton Highland. Scale: 1:50 000). – manuscript.
- Budai, T., S. Kovács 1986: A Rezi Dolomit rétegtani helyzete a Keszthelyi-hegységben (Contributions to the stratigraphy of the Rezi Dolomite Formation [Metapolygnathus slovakensis (Conodonta, Upper Triassic) from the Keszthely Mts (W Hungary)]). – *Ann. Rep. Hung. Geol. Inst.*, 1984, pp. 175–191.
- Császár, G., G. Csillag, T. Budai, L. Koloszar, D. Bihari 1989: A Keszthelyi-hegység és a Balaton-felvidék térképezésének eddigi eredményei (Preliminary result of mapping in the Keszthely Mountains and the Balaton Highland). – *Ann. Rep. Hung. Geol. Inst.*, 1987, pp. 85–93.
- Csillag, G. 1991: Mencshely környékének földtani felépítése (Geological buildup of Mencshely environs). – manuscript (in Hungarian).
- Detre, Cs. 1983: Jelentés a Keszthelyi-hegységi földtani térképezéshez kapcsolódó triász megalopaleontológiai vizsgálatokról (Report on macropaleontological investigations connecting with the geological mapping of the Keszthely Mts). – manuscript (in Hungarian). Hung. Geol. Surv. Doc. center.
- De Zanche V., P. Gianolla, P. Mietto, Ch. Siorpaes 1993: Triassic sequence stratigraphy in the Dolomites (Italy). – *Mem. Sci. Geol.*, 45, pp. 1–27.
- Góczán, F., J. Haas, H. Lőrincz, A. Oravecz-Scheffer 1983: Keszthelyi-hegységi karni alapszelvény faciológiai és rétegtani értékelése (Hévíz-6. fúrás). (Faciological and stratigraphic evaluation of a Carnian key section [borehole Hévíz-6] Keszthely Mts, Hungary). – *Ann. Rep. Hung. Geol. Inst.*, 1981, pp. 263–293.
- Gyalog, L., A. Oravecz-Scheffer, Cs. Detre, T. Budai 1986: A fődolomit és feküképződményeinek rétegtani helyzete a Keszthelyi-hegység K-i részén (Stratigraphic position of the

- Hauptdolomit and of the rocks underlying in the E Keszthely Mountains). – Ann. Rep. Hung. Geol. Inst., 1984, pp. 245–272.
- Haas, J. 1993: Formation and evolution of the "Köessen Basin" in the Transdanubian Range. – Bull. Hung. Geol. Soc., 123, 1, pp. 9–54.
- Haas, J. 1994: Carnian basin evolution in the Transdanubian Central Range, Hungary. – Zbl. Geol. Paläont., Teil 1. 1992 H. 11/12, pp. 1233–1252.
- Haas, J., E. Jocha-Edelényi, L. Gidai, M. Kaiser, M. Kretzoi, J. Oravecz 1984: Sümeg és környékének földtani felépítése (Geological buildup of Sümeg). – Geol. Hung. ser. geol., 20, 353 p. (in Hungarian)
- Haas, J., G. Császár (ed.) 1993: Magyarország litosztratigráfiai alapegységei. Triász (Lithostratigraphic units of Hungary. Triassic). – Hung. Geol. Surv. (in Hungarian), 278 p.
- Jadoul, F. 1985: Stratigrafia e paleogeografia del Norico nelle Prealpi Bergamsche occidentali. – Riv. It. Paleont. Strat., 91, 4, pp. 479–512.
- Lóczy, L. sen. 1913: A Balaton környékének geológiai képződményei és ezeknek vidékek szerinti telepedése (). – A Balaton. tud. tanulmányai. 1, 1, 617 p.
- Láczy L. sen 1916: Die geologischen Formationen der Balatongegend und ihre regionale Tektonik. – Resultate der wissenschaftlichen Erforschung des Balatonsees, 1, 1, 716 p., Wien, 1916)
- Masetti, D., C. Neri, A. Bosellini 1991: Deep-water asymmetric cycles and progradation of carbonate platforms governed by high-frequency eustatic oscillations (Triassic of the Dolomites, Italy). – Geology, 19, 4, pp. 336–339.
- Oravecz-Scheffer, A. 1987: A Dunántúli-középhegység triász képződményeinek Foraminiferái (Triassic Foraminifers of the Transdanubian Central Range). – Geol. Hung. ser. paleont., 50, 331 p.
- Peregi, Zs. 1979: A Veszprém környéki karni képződmények (Karnische Bildungen in der Umgebung von Veszprém [Transdanubia]). – Ann. Rep. Hung. Geol. Inst., 1977, pp. 203–216.
- Stefani, M., A. Golfieri 1989: Sedimentologia e stratigrafia della successioni retiche al confine fra Lombardia e Trentino. – Riv. It. Paleont. Strat., 95, 1, pp. 29–54.
- Szentes, F. 1953: Jelentés az 1952. évben Magyarországon a Keszthelyi-hegységben végzett bauxitkutató munkálatokról (Report on the bauxit research in the Keszthely Mts, Hungary, during 1952). – manuscript (in Hungarian). Hung. Geol. Surv. Doc. center.
- Tollmann, A. 1976: Analyse des klassischen nordalpinen Mesozoikums. – Wien, Franz Deuticke. 580 p.
- Végh, S. 1964: A Déli-Bakony raeti képződményeinek földtana (Geologie der Rhätischen Bildungen des südlichen Bakonygebirges in Ungarn). – Geol. Hung. ser. geol., 14., 109 p.
- Wendt, J., F. Th. Fürsich 1980: Facies analysis and paleogeography of the Cassian Formation, Triassic, Southern Alps. – Riv. Ital. Paleont., 85, 3–4, pp. 1003–1028.

Different types of orogens and orogenic processes, with reference to Southern and Central Europe



Greg Zolnai

Several types of orogenic belts exist, each with their own specific fabrics, formed by active tectonic forces, the composition and thickness of the sedimentary series involved, and by the structural influence of the basement. Not all orogenic belts are located along an active margin and not all folds are due to crustal shortening normal to the fold axes.

Orogenic events also affect basement-controlled areas where the tectonic push is transmitted through the basement. Readjustments between basement-blocks most frequently involve wrenching. Small-amplitude displacements at depth may thus generate spectacular superficial effects.

Many of the deformations encountered in the Southern and Central European realms, within the limits of the Alpine foldbelt(s) and in the platforms in between the orogenic forelands can be better accounted for by small to medium-scale basement adjustments than by the usual, well-known foldbelt mechanisms.

The South-European realm has undergone several phases of orogenic deformations since Proterozoic times. The best-known Alpine events were superimposed upon a consolidated, continuous basement complex. This structural inheritance strongly influenced later evolution.

In the Permian to Lower Cretaceous period passive-margin evolution with extension and left-lateral shearing dominated, mainly along the mega-shear belt formed between the European and African plates ("break up").

From mid-Cretaceous to the present, oblique convergence and collision dominated: the previously extended, loosened blocks of the African and South European margins were compacted again ("round up").

An alternative scheme is proposed here, with simpler, para-autochthonous paleogeography and limited internal movements, which avoids large-scale horizontal displacements and multiple subduction zones, difficult to fit into a regional context. This simplified interpretation using relative autochthonous domains may be useful when carrying out everyday applied exploration.

Key words: orogeny, folding, faulting, wrenching, rifts, gravity tectonics, tectonic inversions, flysh, oceanic basins, regional geology

Introduction

"Orogenesis" literally means mountain forming and it includes a large array of phenomena. The most significant orogenic belts are formed along the (active) edges of continents, during collisional periods (Figs 1–3). They are characterized by compressive folding due to crustal shortening. Such first order orogenic belts imply plate movements in the order of thousands of kilometers and are

Address: G. Zolnai: 11. av. des Sayettes PAU (64000) France

Received: 20 January, 1994

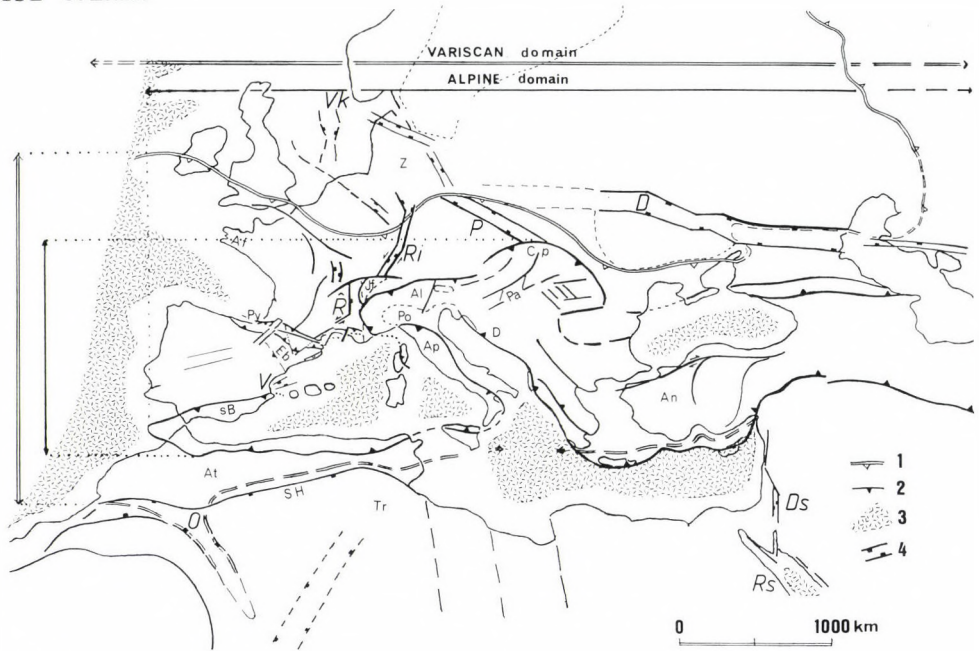


Fig. 1

Selected structural elements: *Europa and North Africa*. 1. Variscan (Hercynian) fronts; 2. Alpine fronts; 3. oceanic domains and basins; 4. rifts; *Foldbelts*: Ar – Armorican foldbelt; Al – Alps; Ap – Apennines; An – Anatolian domain; At – Atlas; Cp – Carpathians; D – Dinarides; Jf – Jura foldbelt; Py – Pyrenees; sB – sub-Betic; SH – Saharan (South Atlas) hingeline; *Basins*: Eb – Ebro; Pa – Pannonian; Po; Tr – Triassic (East Saharan); Z – Zechstein; *Rifts*: D – Don–Dnieper aulacogen; Ds – Dead Sea; O – Ougarta "chain"; P – Polish trough; Ri – Rhine graben; R – Rhône (Saône) graben; Rs – Red Sea rift; V – Valencia trough; Vk – Viking graben (Based on UNESCO 1976; B.R.G.M. 1986a and 1986b maps)

always related to collision and/or subduction. Forming high reliefs, they offer good outcrops, attract the attention of researchers and thus are extremely well studied (Central Alps, Canadian Rockies, Andes).

However, important (although less spectacular) mountain ranges or reliefs and subsurface structures are also generated within the continents, in areas remote from active margins, and also during time intervals not considered "orogenic". The latter are due either to moderate convergence of formerly extended crustal zones, or are related to small to medium-scale lateral adjustments between somewhat loose continental nuclei. These adjustments are also able to generate superficial folds and form considerable relief, which are not necessarily due to local crustal shortening, perpendicular to the fold axes. Although the dominant structural direction(s) within these second-order fold complexes or fault systems may be parallel to those of the nearby major orogenic belts, their mechanisms are different, since they primarily depend on the behaviour of the underlying basement. The competency and the structural fabric of the basement is always of prime importance. Such movements can

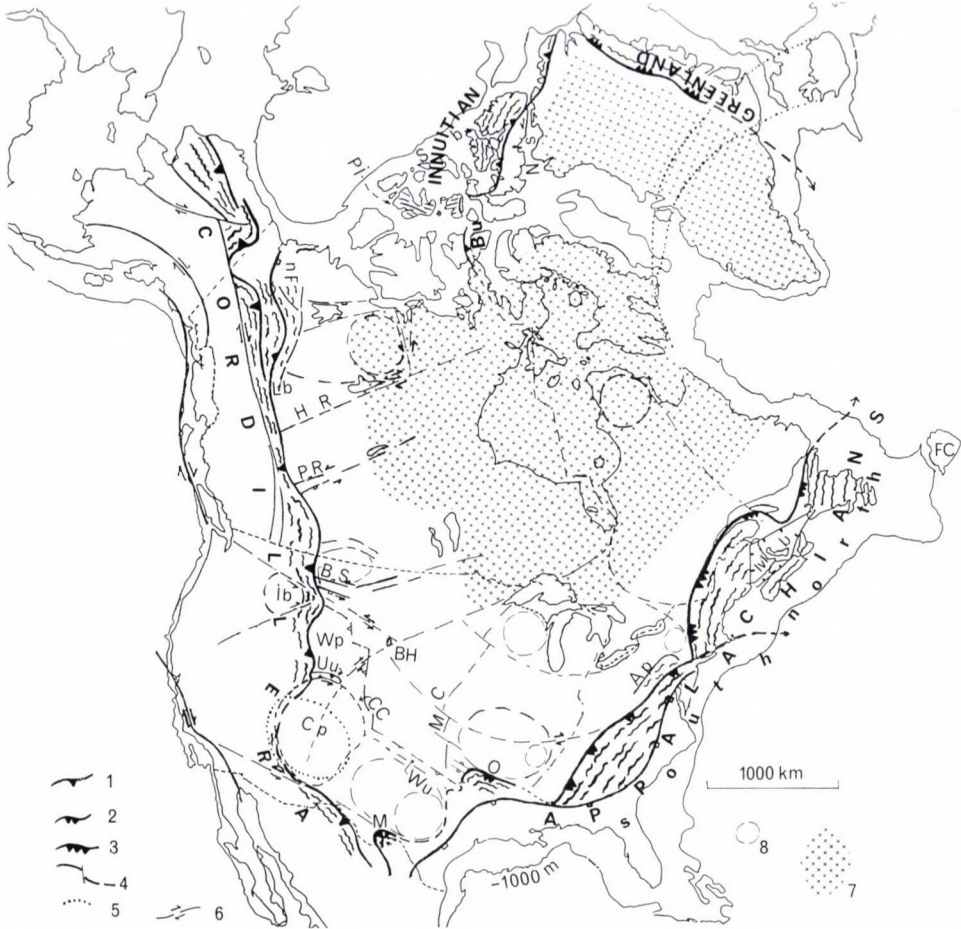


Fig. 2
 Selected structural elements: *North America*. 1. Tertiary foldbelts: Cordilleran and Inuitian; 2. Late Paleozoic (Variscan equivalent) foldbelts: South Appalachians etc.; 3. Early Paleozoic (Caledonian eq.) foldbelts: North Appalachians and Greenland; 4. trans-continental fault systems; 5. volcanic arches; 6. proven major shear faults; 7. outcrops of Canadian and Greenland shields; 8. major basement "nuclei"; Ap - Allegheny plateau; Bu - Boothia Uplift (Paleozoic and Tertiary); BH - Black Hills uplift (Tertiary); BS - Big Snowy system (Precambrian to Tertiary); CC - Central Colorado trough (Variscan, Tertiary); Cp - Colorado Plateau (Proterozoic); HR - Hay River fault; Id - Idaho batholith (Mesozoic); Mb - Magdalen Basin (Carboniferous); MC - Mid-Century rift system and geophysical anomaly (mostly Proterozoic); nF - Northern Franklin Mountains foldbelt (Tertiary); Ns - Nares Strait (Tertiary-Present day); O - Ouachita Orogen (Variscan, Tertiary?); PI - Parry Island foldbelt (Paleozoic, Tertiary?); PR - Peace River Arch (Precambrian-Tertiary); Sb - Sverdrup Basin (Paleozoic-Tertiary); Uu - Uinta Uplift (Precambrian, Tertiary); Wp - Wyoming Province (Archaean-Tertiary); Wu - Wichita Uplift (Variscan, Tertiary?). Using: USGS 1972; Cook 1983; G.S.C.1991 etc.)

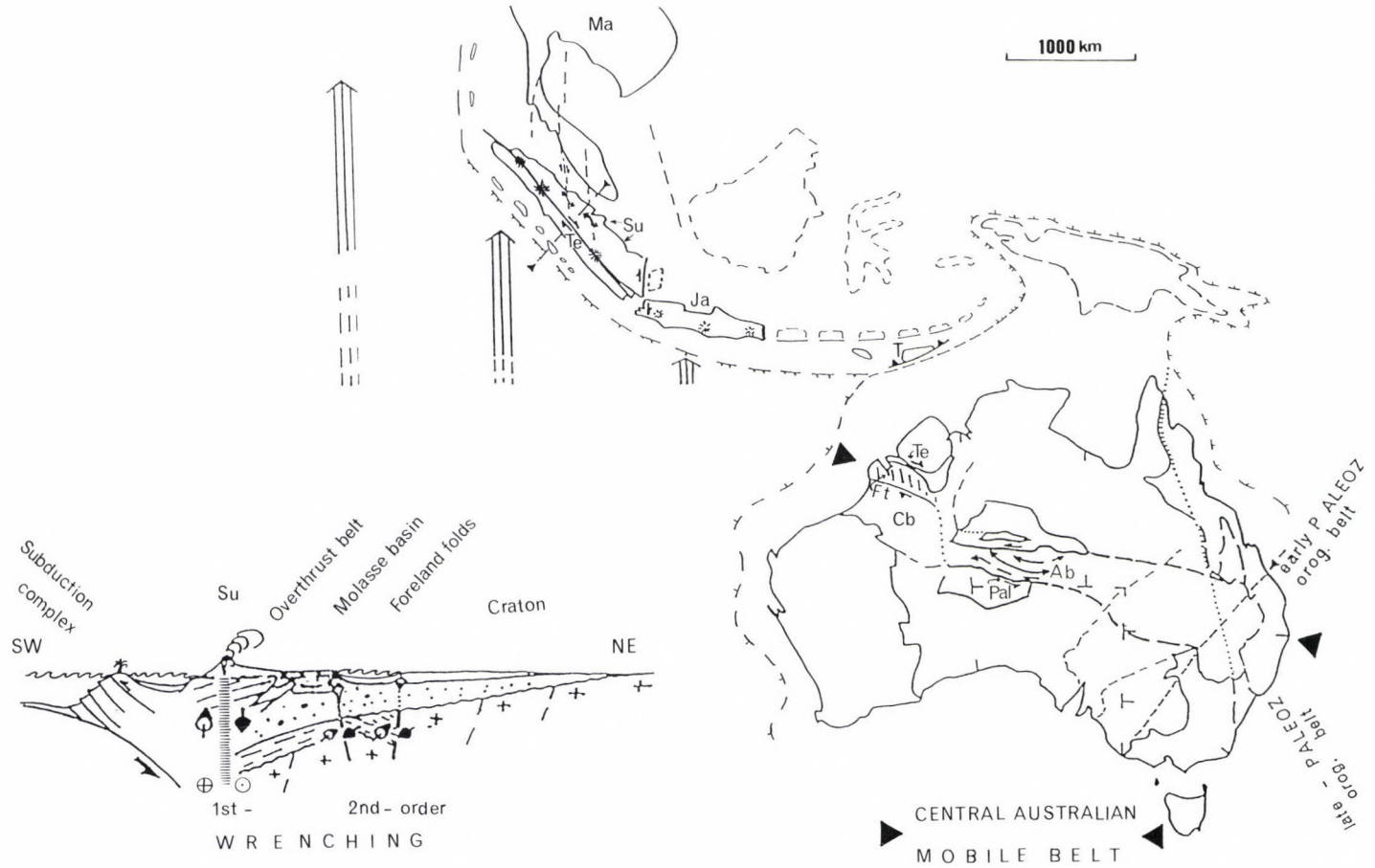


Fig. 3

Selected structural elements: *Southeast Asia and Australia*. Ab – Amadeus Basin; Cb – Canning basin; Ft – Fitzroy trough; Ja – Java; Ma – Malaysia; Su – Sumatra; T – Timor. Pal, Te – age of major shearing (Using UNESCO 1976; BMR 1970, 1981 maps and reports; Zolnai 1991)

occur during periods of relative quiescence such as continental drifting, even though some of the intracontinental deformations are synchronous with major diastrophisms.

Secondary foldbelts, as well as faulted structures and intramountain tabular zones, are best dealt with by establishing their own structural processes, rather than applying models borrowed solely from the classical, even though more spectacular, first-order orogenic complexes. Some of the secondary belts fall in line with or are extremely close to segments of primary belts: Pyrenees, North Franklin Mountains, Wyoming province, Carpathians. They should nevertheless be treated separately.

Orogenic styles

Collisional orogens, like the American Cordilleras, the Alps, the Indonesian Arch or the Appalachian Belt (Figs 1–3) exhibit, in addition to their "free folds", many volcanic and intrusive rocks, obducted ophiolitic complexes and rafted terranes; penetrative metamorphism is always present.

If an orogenic, active margin has initially been a quiet subsiding platform (e.g. a passive margin), not contaminated by erosional products from remote active belts, the sediments are mostly thick, homogeneous carbonates. If the time lapse between deposition and orogeny is long, it allows full diagenesis, resulting in very compact, brittle lithologies. If, furthermore, the continental margin (basement) remains essentially flat and undisturbed by earlier movements, the competent sedimentary sequence is laterally thrust and folded into stacked, folded overthrust sheets, over the gently dipping orogenic foreland or craton edge. Tightly set anticlinal trends (duplexes) dominate: for instance large segments of the *North American Cordillera* (Fig. 4).

In the "South Canadian Rockies" portion of the Cordilleran Foldbelt (Fig. 4) the typical duplex structures (or folded faults, "piggybacks" Dahlstrom 1970; McMechan and Thompson 1989, top and middle rows) are characteristic only of the approx. 100 km wide frontal strip, along the eastern, leading edge of the 1 000 + km-wide orogen (Monger 1989, bottom row). The basement surface is extremely flat and virtually undisturbed, the basal thrust-plane is continuous. Both basement surface and basal thrust plane dip gently towards the west, i.e. the inner zones of the foldbelt which are downwarped. This structural style is predominant only in the segment between lat. 40° and 56°N, i.e. in the Idaho–Wyoming (Montana) Overthrust Belt, and the South Canadian Rockies, or between the transversal structures of the Uinta Range and the Peace River Arch. Each of these major, old transverse lineaments introduces changes in the structural style of the Cordillera itself.

If, on the other hand, the basement of the continental margin undergoes early faulting due to passive extension and/or shearing, faulted basins, rift systems as well as block uplifts are formed. The Alpine belt *sensu lato* is such an example. Local clastic sediments fill nearby troughs (flysch), while shales and evaporites are deposited during periods of relative structural quiescence and in more confined basins or on intermediate platforms. The paleogeography of such zones is extremely complex and the sedimentary column(s) very varied. During subsequent compressive periods some of the earlier normal basement faults

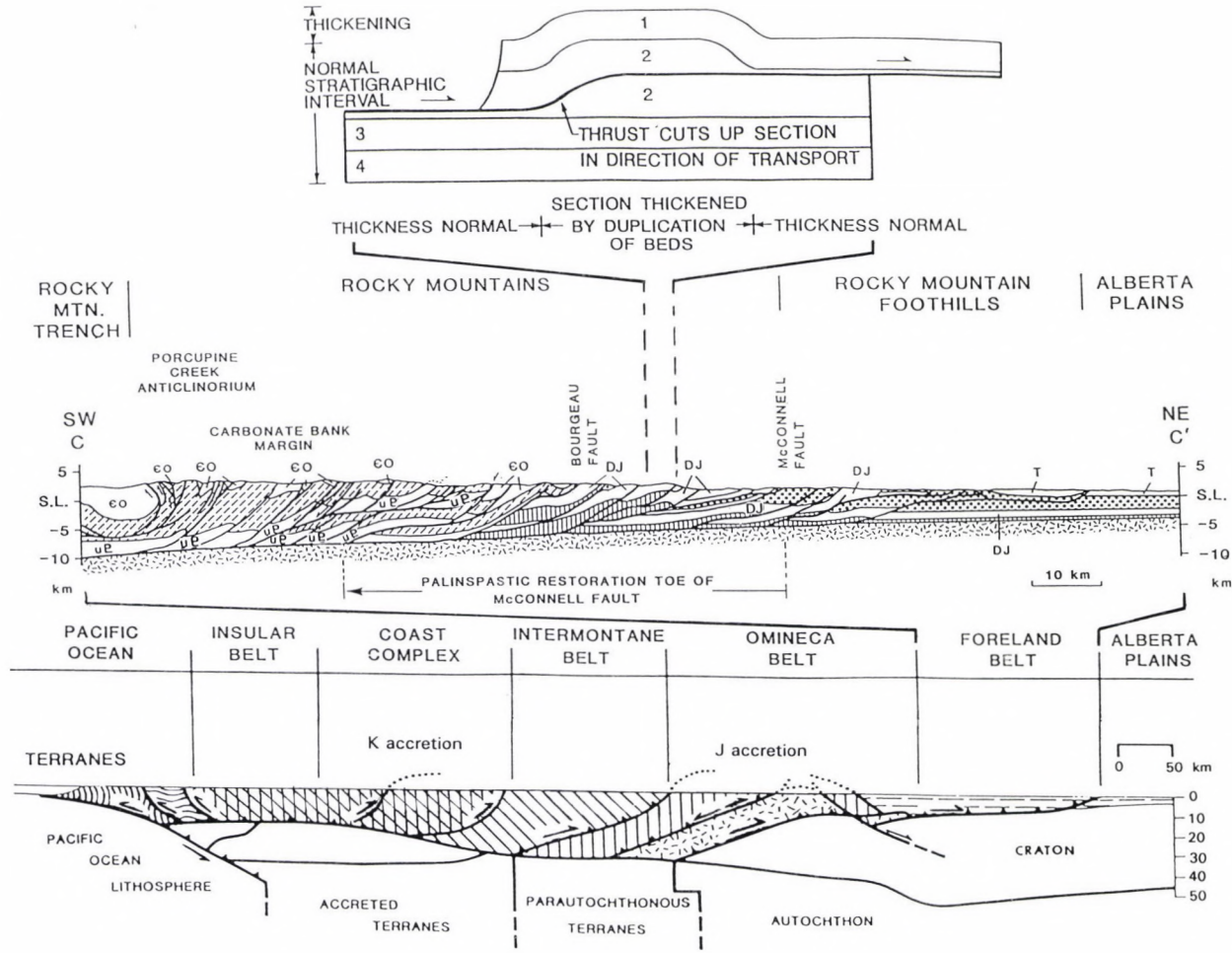


Fig. 4 E-W section across the Cordillera of North America (Canada, near the USA border) (Using Dahlstrom 1970; McMechan and Thompson 1989; Monger 1989)

are rejuvenated and changed into overthrust faults. Such structural inversions pour the contents of earlier furrows (as yet unconsolidated soft sediments, such as shales and flysches) towards and onto the orogenic foreland, resulting in syncline-dominated tectonic complexes (Fig. 5).

The basement of the *Alps sensu lato* is broken up (Fig. 5, see also Fig. 7); some of the faults cross the Alpine superstructure as well as the Variscan basement. Among the folds, synclines are wider than anticlines. The main thrust planes are undulating and uneven. Gravity tectonics mainly occur in the presence of mobile shaly and/or evaporitic décollement layers.

Zones of convergence are formed within continental domains (plate interiors) in belts which have first undergone important crustal stretching, like the *Aquitaine basin–Pyrenees* (part of the Alpine system) or the *Amadeus Basin* in Central Australia (Figs 3, 6, 7). Such zones, after receiving great thicknesses of sediments, also undergo orogenic crustal shortening but to a lesser extent (in the order of tens to one hundred kilometers), the folding being partially caused by lateral movements (wrenching) occurring between the neighbouring continental landmasses.

In the *Amadeus Basin*, Australia (Fig. 3) the superficial fold-groups are possibly due to deep *sinistral* shearing, during the mid-Paleozoic orogeny. – The *Canning Basin/Fitzroy Trough* exhibit N–S oriented fractures, which are best explained by regional *dextral* wrenching, related to the Miocene collision between Australia and the Indonesian Arc (Timor). – The folds of the *Sumatra Basin(s)*, Indonesia (Fig. 3, inset), are of the foreland foldbelt-type. They are due to a deep, N–S oriented dextral wrench-mechanism, during the Tertiary–present-day continent–ocean collision, which rejuvenated old N–S fractures within the Malaysian basement.

In the case of the *Pyrenean foldbelt*, the NPF forms the actual limit between the Iberian sub-plate and the Aquitaine domain of Southwestern Europe. It separates the axial high chain with dominant Variscan basement capped by thin Cretaceous platform sediments (to the south) and the strongly subsident, rifted Aquitaine Basin (to the north). – Mesozoic extension affected the whole area (including the Parentis infrabasin), while Eocene, Alpine compression is limited here only to the South Pyrenean Zone, the North Pyrenean Zone and the basement in between. The platforms and basins beyond, although extended during the Permian–Lower Cretaceous, underwent only limited (wrench) faulting with subsequent salt diapirism (passive folds). – The thick lower Cretaceous shales and limestones and massive Late Cretaceous–Paleocene flysches (Kf – Fig. 7, inset) were deposited along the extended, rifted southern edge of the Aquitaine Basin, while the platforms to the north and the south were covered by thin carbonates (Kp). The maximal shortening occurred in the flysch furrow(s) along the NPF, the fill of which was poured out as much as thrust onto the quiet foreland, in conjunction with the successive compressions (Eocene–Miocene) and the late orogenic uplift (Pliocene?) of the axial zone.

Belts of compressive wrenching are known within the orogenic complexes themselves, in such zones which are already provided with a somewhat consolidated basement, formed during earlier orogenic phases. The Central Brittany Zone in westernmost France (Fig. 8) or the Magdalen Basin in easternmost Canada (part of the Appalachian foldbelt, Fig. 2) were both deformed during the Mid- to Late-Paleozoic orogenic events. Successive periods of extensional and compressive wrenching are responsible for intra-orogen furrow or pull-apart formation as well as for subsequent folding. The magnitude of these movements can be estimated to be of the ten-kilometer order. In both

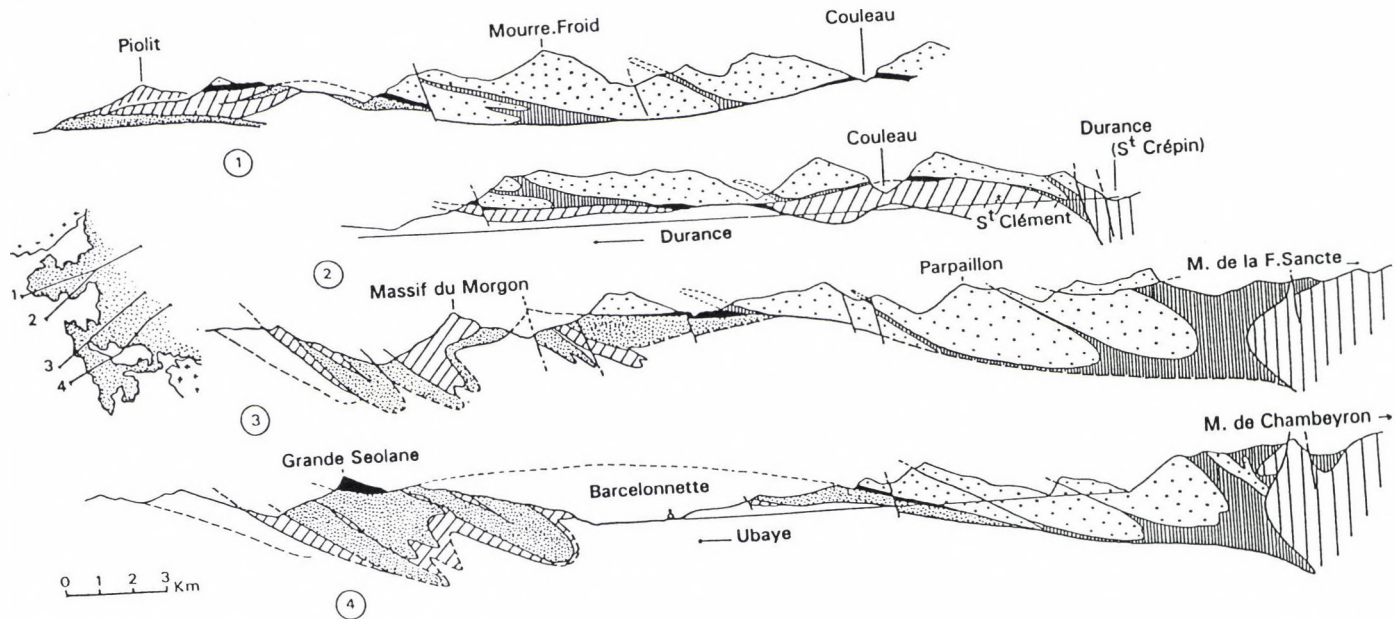


Fig. 5
Sections across the Western Alps. Position of sections on Fig. 6 (from Debelmas 1974)

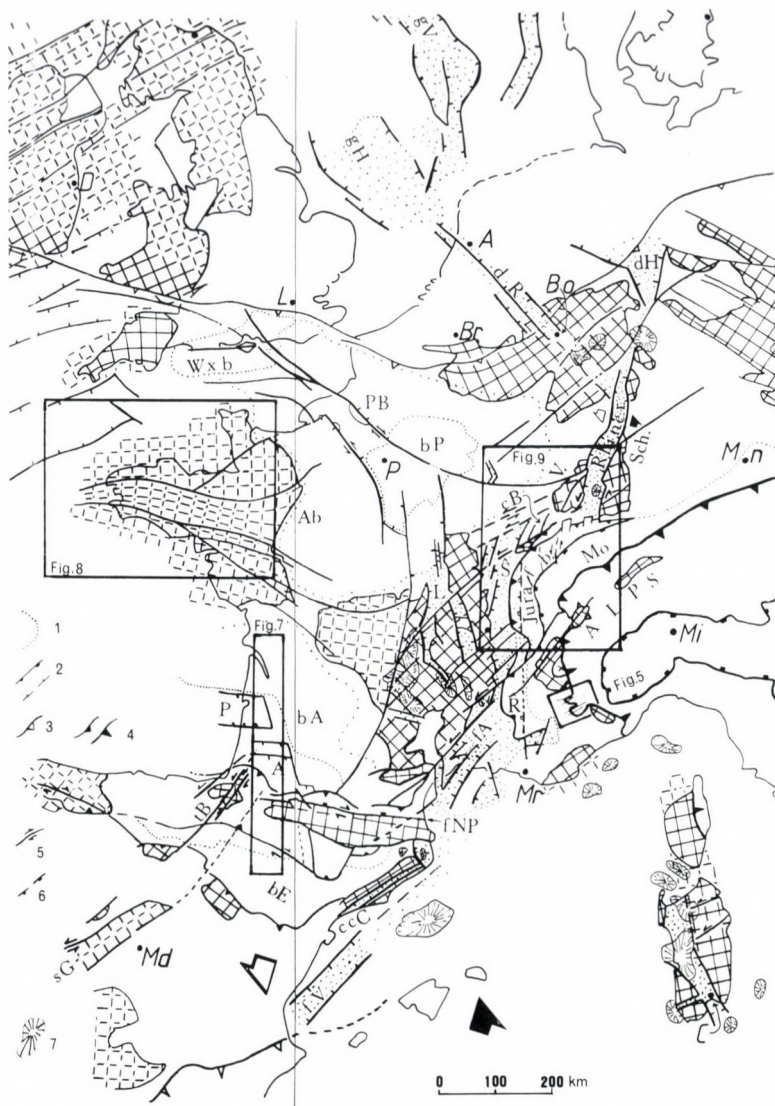


Fig. 6

Structural map of *Western Europe*. A – Amsterdam; Bo – Bonn; Br – Bruxelles; C – Cagliari; G – Geneva; L – London; Md – Madrid; Mi – Milan; Mn – Munich; Mr – Marseille; P – Paris; A – Arzacq (sub-)Basin; bA – Aquitaine Basin; Ab – (central) Armorican belt; fA – Alès Fault; cB – Belfort corridor; tB – Basque transverse zone; ccC – coastal chain of Catalonia; bE – Ebro basin; sG – Sierra da Guadarrama; dH – Hesse depression; gH – Holland graben; L – Limagne graben; Mo – Molasse Basin; fNP – North Pyrenean fault; P – Parentis (sub-)Basin; bP – Paris Basin; PB – Pays de Bray Fault/Structure; dR – Rhine depression; Sch – Schwarzwald (Black Forest) V – Vosges; gV – Viking graben; Wxb – Wessex Basin; 1. basin contours; 2. grabens, "West European Rift System"; 3. Variscan front; 4. Alpine front (s); 5. major shear faults; 6. major hinge-lines; 7. volcanic centers (Based on BRGM Chiron 1980; Autran and Prost 1986; Emberger 1986)

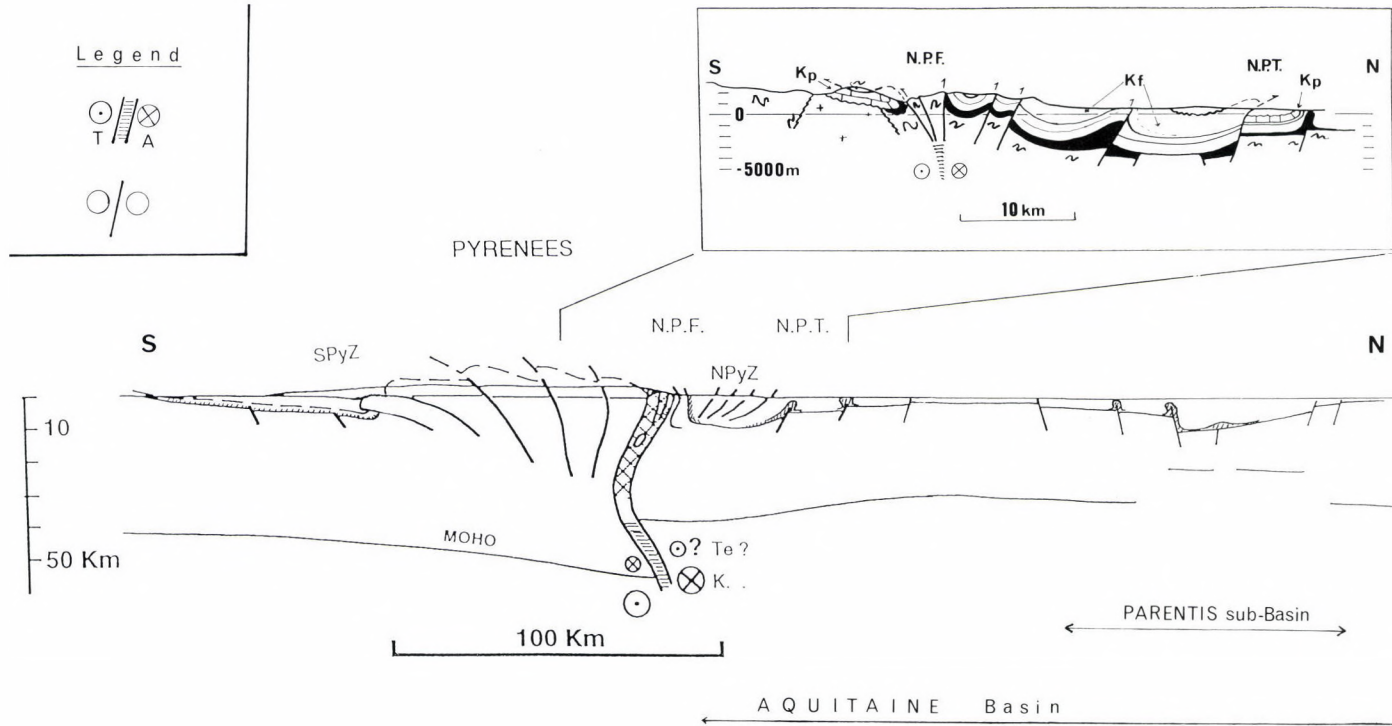


Fig. 7

N-S cross-section of the *Pyrenees* (Intra-continental foldbelts) SPyZ – South-Pyrenean Zone; NPyZ – North-Pyrenean Zone; NPF – North Pyrenean Fault; NPT – North Pyrenean Thrust; Inset, left: Symbols of wrench (shear, strike-slip) faults: A – Away, T – Towards, empty circles: direction unspecified or alternating. Position on Fig. 6 (using: Henry 1968; Zolnai 1971, 1975; Roure et al. 1989, modified in: Bourrouilh et al. 1995)

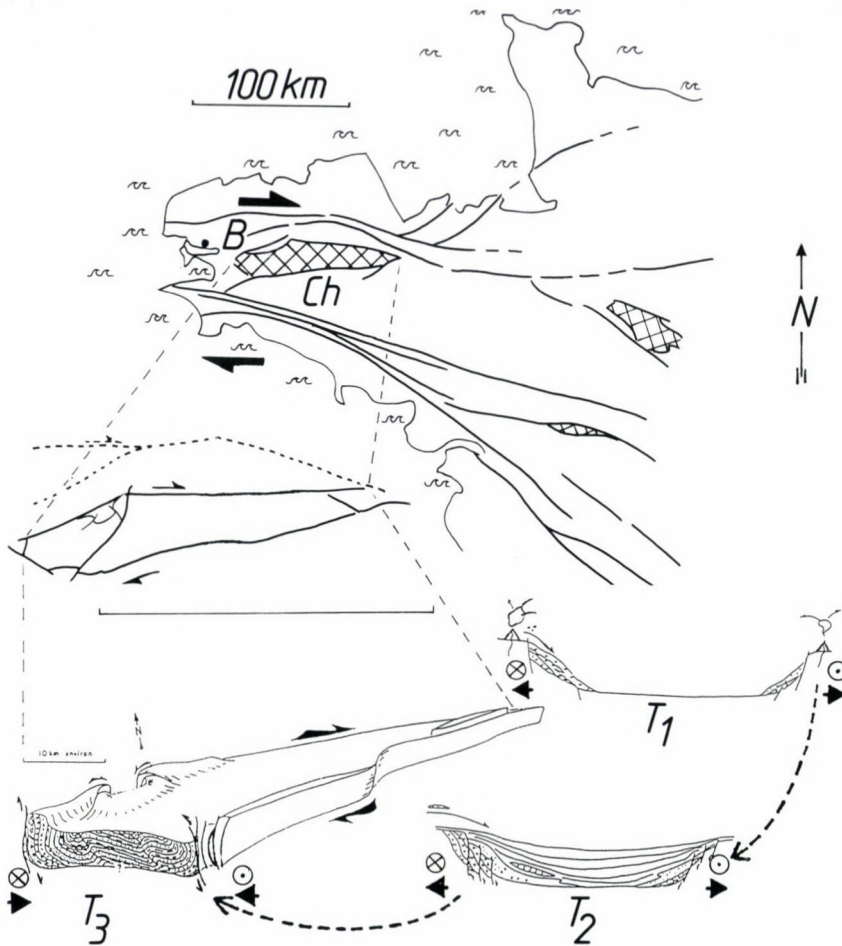


Fig. 8
Châteaulin Basin, western Brittany central foldbelt (Wrenching within orogens) B – Brest; Ch – Châteaulin Basin; T-1, T-2 – transtension; T-3 – transpression; Location on Fig. 6 (From Rolet 1984)

above-mentioned cases the transpressional fold-complexes are situated a few hundred kilometers behind the orogenic (overthrust) fronts.

The *Armorican Foldbelt* has undergone as much wrenching as compression during the Variscan orogeny. It is situated at abt. 350 km to the south of the northern Variscan overthrust front (Fig. 1). Successive phases of dextral transtension and transpression formed and deformed the synorogenic Carboniferous Châteaulin Basin. The amount of lateral displacement and crustal shortening are of the same order of magnitude: 10 km.

In orogenic forelands, folds and foldbelts can be better accounted for by wrench movements in the basement rather than through direct effects of the lateral

orogenic thrusts. Crustal shortening and basement adjustment movements may, however, be combined to form widely spaced fold networks with drape and drag-anticlines, including typical "box-folds". The *Jura foldbelt* in the foreland of the Western Alps (Figs 9, 10), the *Wyoming province* and the North Franklin Mountains to the east of the Cordilleran overthrust belt (Cook 1983), the *Saharan Atlas*, the fold-swarm of the Amadeus Basin in Central Australia (BMR 1970, 1981) and the *Sumatra basins* (Fig. 3 inset) are among the known examples of these foreland fold-complexes in which basement wrenching is essential (the Allegheny foldbelt to the west of the southern Appalachians may be yet another such case – Fig. 2).

The N–S oriented faults of the Vosges–Rhine Graben–Black Forest structural complex (Fig. 9) can be followed into and through the Jura Foldbelt. Left-lateral shearing is demonstrated in both areas; it caused different expressions at different structural levels. To the north huge arching uplifts in the competent Variscan basement (Vosges, Black Forest) are bordered by subvertical faults on one side: toward the Rhine Graben, many of which exhibit horizontal striation (Ruhland 1972). To the south, relatively incompetent Mesozoic–Tertiary sediments show swarms of superficial drag-folds, which are off-set by roughly N–S oriented fault zones (see Pavoni 1961a; Wegman 1961). – Tertiary clastic-filled rhomb-grabens between the Jura folds reflect combination of the recent N–S (Alpine?) direction and the typically Variscan ENE–WSW trend. The frontal thrust of the Jura over the neighbouring Tertiary grabens (Rhine and Rhône–Saône valleys) may be due to local gravity sliding.

The "*West European Rift System*" can be followed to the south into Sardinia and the Valencia off-shore Graben (Fig. 6). The sinistral strike-slip movement along the megashear is primary. It is remotely related to the northward push of the Apennine block during the Miocene (see also Figs 13, 28c, 29). – The basement uplifts of the Western Alps (Fig. 9) fall into line with straight fault lineaments which straddle the Rhône Graben (part of the rift system) and continue along the southern edge of the Massif Central.

The *folded Jura* (Fig. 10) is situated between two extensional systems: the Molasse Basin to the SE and the Rhine–Saône–Rhône rift-system to the N and the W. The widely spaced fold-trends, separated by tabular zones, can be accounted for by deep wrenching which affected the broken-up mosaic pattern of the basement and induced superficial drag-folds (see also Figs 13, 24 center). Regional compression, transferred from the High Alps to the southeast, may have been active, although the basement of the Molasse belt (separating the Jura from the Alps) only shows normal faulting. The northwest-oriented "oblique" regional compression may also have induced the basement shearing of the Jura, possibly a different basement domain, but the amount of shortening probably remains limited (a few to 10 km, same as the deep wrenching; middle row). – If a continuous basal detachment fault existed ("thin skin tectonics", top row) the spacing of the fold-arches would remain unexplained (i.e. contrary, among others, to the presently prevailing "Cordilleran model" see Figs 4, 13), as well as to sandbox experiments (Odonne and Viallon 1983) which favour the deep shear interpretation. Deep-focus earthquakes in the foreland of the Alps (Molasse basin–Jura foldbelt–Black Forest/Vosges compound, from Deichman 1992, bottom row) indicate basement involvement and favour "thick skin" tectonic interpretation. In the Alpine belt proper, shallower earthquakes abound, due to the movements within the stack of the multiple overthrust rafts.

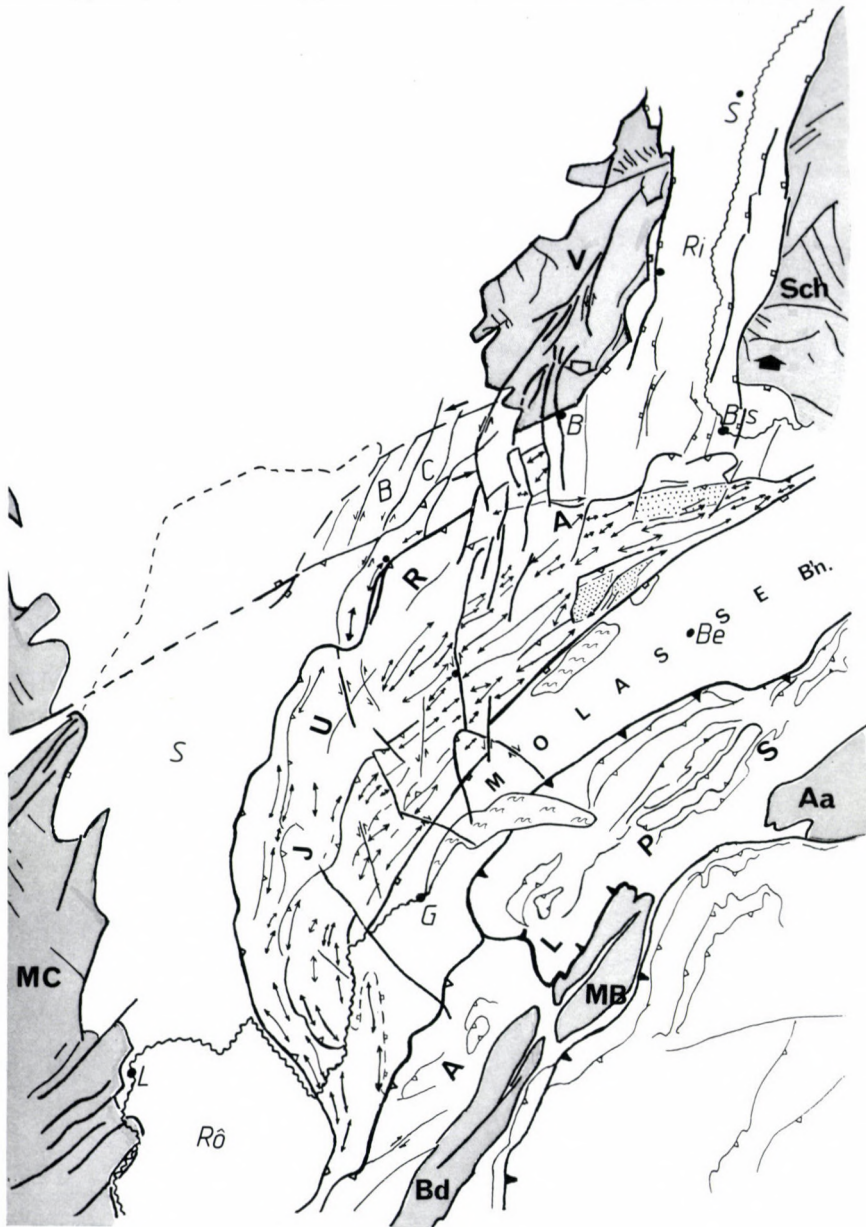


Fig. 9
 Structural map of the *Jura-Rhine Graben* area (Basement-dominated structures): B - Belfort; Bs - Basel; Be - Bern; G - Geneva; L - Lyon; S - Strasbourg; Ri - Rhine Graben; Rô - Rhône Graben; S - Saône Graben; BC - Belfort (wrensch) Corridor. Basement uplifts in the foreland of the Alps: MC - Massif Central; Sch - Schwartzwald (Black Forest); V - Vosges. Basement uplifts within the Alps: Bd - Belledone; MB - Mont Blanc; Aa - Aar. Location on Fig. 6 (Based on BRGM Chiron 1980)

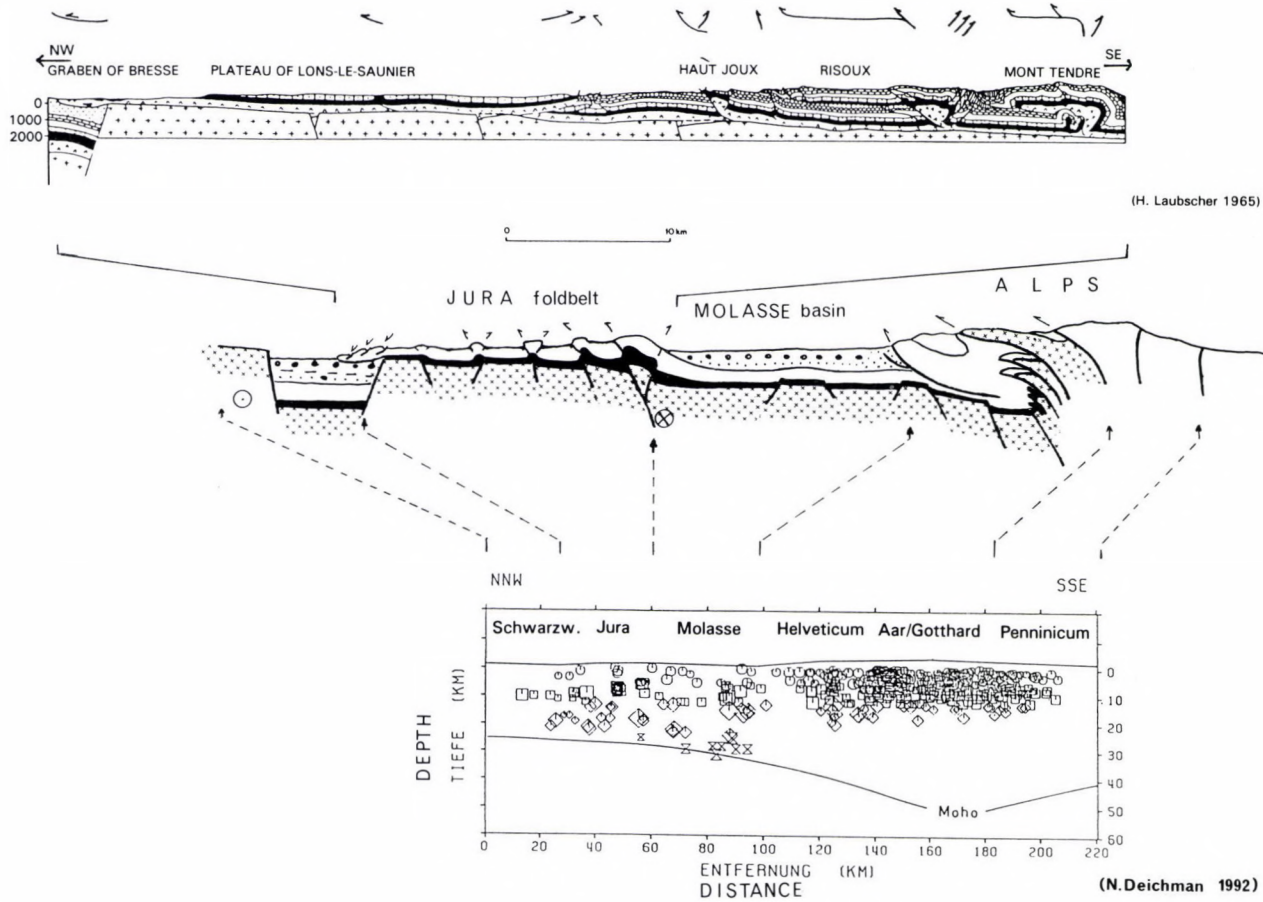


Fig. 10
Cross-section of Jura foldbelt (Basement-related folds) (using Laubscher 1965; Deichmann 1992; compare with Fig. 3 inset and 13/2-3)

Doming structures and block faulted uplifts of great magnitude (hundreds of kilometers long, tens of kilometers wide) and representing important vertical movements (> 10 km) are known in some orogenic forelands, usually striking the latter at high angles. The *Uinta Range*, the *Big Snowy Uplift*, the *Peace River Arch* in the foreland of the North American Cordillera, the Basque "*transversal*" in S.W. France, the *Ougarta Chain* in North Africa, or the doming structures of the eastern part of the Donbass Aulacogen were all formed through late, wrench-related relief inversions, over the trace of old transcontinental rift (trough) systems. Some of the grabens were filled with flysch-type sediments, derived from remote orogenic reliefs, e.g. *Uinta Range* (Fig. 11), indicating that all flysches are not situated within mobile, orogenic belts.

The huge *Uinta ridge* (Fig. 11), an east-west oriented structural arch, to the east of and perpendicular to the Cordilleran overthrust front, is due to the early Tertiary uplift or reversal of a Proterozoic clastic-filled graben (interbedded, extremely hard, slates and quartzites: originally flysches), situated between two very old basement-domains. The 250+km long, 50 km wide ridge was uplifted ± 16 km during the latest, Laramide phase of the Cordilleran orogenic suite. The left-lateral shear-component, responsible of the uplifting, can be estimated to ± 30 kilometers.

Such block-faulted uplifts form reliefs of great magnitude ("germano-type orogens") within stable, craton-type domains; these also can be accounted for by the mechanism of deep, *primary, wrenching*. They can be situated in immediate orogenic foreland areas (e.g. the *Vosges Uplift-Rhine Graben-Black Forest Uplift* compound, Fig. 9), within orogenic domains (*Little Carpathians* of western Slovakia) or at fair distances from the orogenic fronts (*Black Hills Uplift* in the northwestern USA, Fig. 2), or even along passive margins (*Boothia Uplift* in Arctic Canada). The minute strike-slip movements (hundreds of meters to a few kilometers) necessary to generate such vast reliefs, can be transmitted along transcontinental fault relays.

Mountain belts along sheared or passive margins are related to local block-adjustments, to basement-wrenching or to large-scale rotations induced by calved continental blocks. The Tertiary *Innuitian* (Eureka Sound) fold complex in Arctic Canada best illustrates this "orogenic" process (Fig. 12). The tightly-folded belt forms high reliefs (>3000 m) and exhibits wrench-related folding and faulting, in addition to compression-related overthrusting. Magmatic intrusions, large volcanoes, ophiolites and ophiolites, metamorphism and other subduction-related phenomena (Benioff zone) are, however, totally absent.

The northern edge of the North American continent, the *Arctic domain* (Fig. 12) has seen a passive-margin evolution since late Proterozoic times. In the Tertiary Innuitian Orogen, folding occurred through the rejuvenation of basement faults, consecutive to the breaking off, anti-clockwise rotation and northerly slippage of Greenland. Transpression dominated in the eastern Sverdrup Basin, resulting in tight overthrust-sheets and drag-folds, superposed upon the deep structural fabric. The checkerboard pattern of the Arctic Islands was (re)activated during the Tertiary sheared-margin evolution (continental drift to the west).

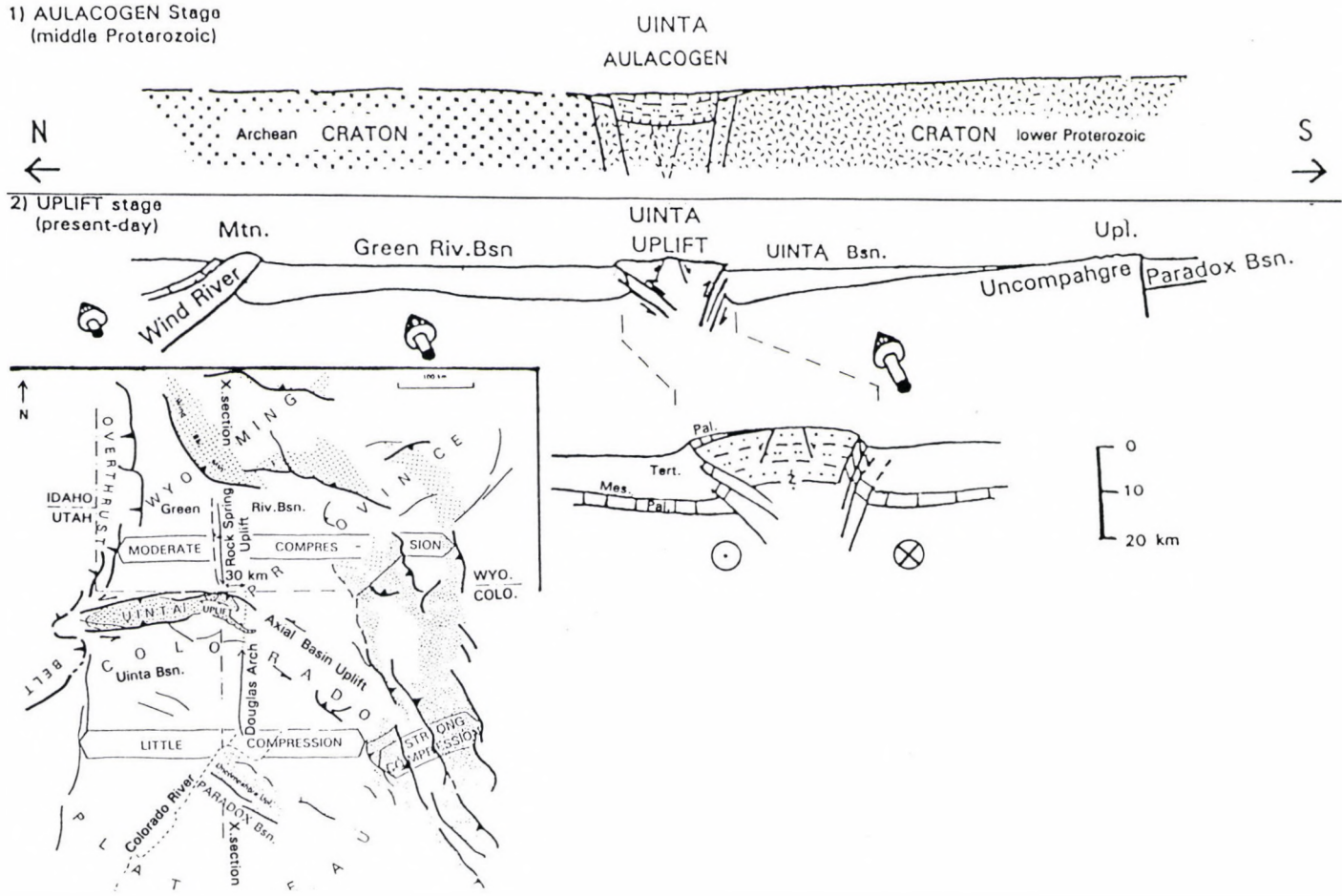


Fig. 11
 Uinta Range – western USA (Structural inversion in consolidated areas) from Zolnai 1986, 1991

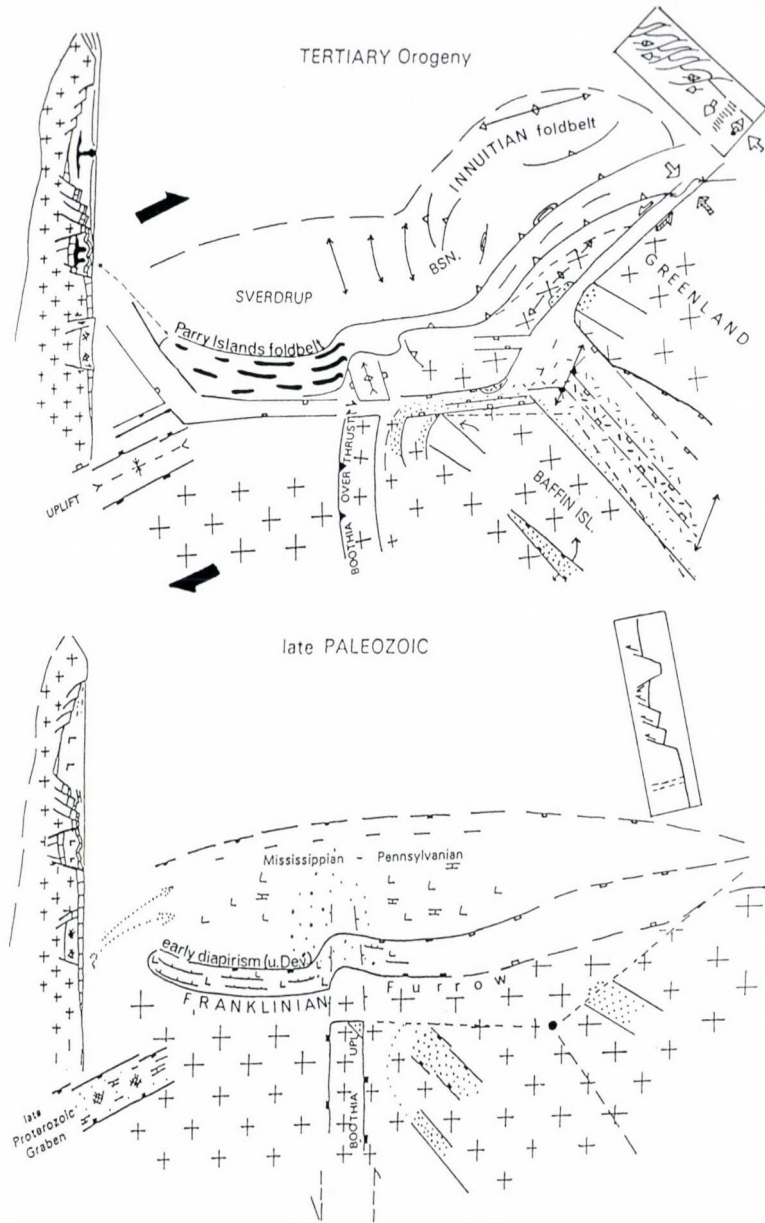


Fig. 12
 Inuitian foldbelt and Sverdrup basin: Arctic Canada, "passive tectonism" (from Zolnai 1991; using Fox 1985; Kerr 1980. Compare with Fig. 2, 14)

Salt diapirism generated the nearby *Parry Island* foldbelt, where very little to no compression can be demonstrated (Fig. 12). The visible set of evenly spaced parallel, Devonian folds with vertical fold axes were caused by non-piercing salt tectonism, under extensional and/or shearing movements (normal faulting with block tilting). These "passive" folds were formed along a trailing edge or a sheared margin, without crustal shortening, the active margin having been to the southeast of the continent during the mid-Paleozoic (continental drift to the southeast see Fig. 2).

Some of the above folding mechanisms may be misused if taken out of context, i.e. a) concentrating solely on the anatomy of the superficial folds, b) disregarding the structural heritage: the internal structure and the history of the basement and c) ignoring the role of the lithological composition of the cover (Fig. 13).

Ophites and ophiolites are frequently present on outcrops in orogenic belts. They are witnesses of subsea basic volcanism or they are remnants of (obducted) oceanic crust, or they may be fragments expelled from deeper horizons along shear-zones. "In situ" ophites/ophiolites are also frequent in intracontinental rifts, troughs and sea-arms; they are often emplaced at the moment of their opening. They indicate absence or thinning of the continental crust (partially oceanized basins, as opposed

Fig. 13 →

Resume of the *folding processes* in different tectonic settings.

1) Successive thrust-sheets are emplaced by a combination of lateral orogenic thrust and tectonic/sedimentary overloading of stacked overthrust rafts ("duplexes"). This time-transgressive process requires: a) flat, indurated and undisturbed basement-surface; b) very thin lubricating layer(s): ± 10 m, ("Sh"), and c) competent, fairly homogeneous and thick (3–5 000 m) sedimentary column, able to transfer horizontal tectonic thrust, and (d) syn-orogenic clastic wedges (increasing tectonic overburden). Neither salt/evaporites, nor volcanics are present. The succession of events is forward-stepping. E.g.: Southern part of the *Canadian Rockies* (Fig. 4).

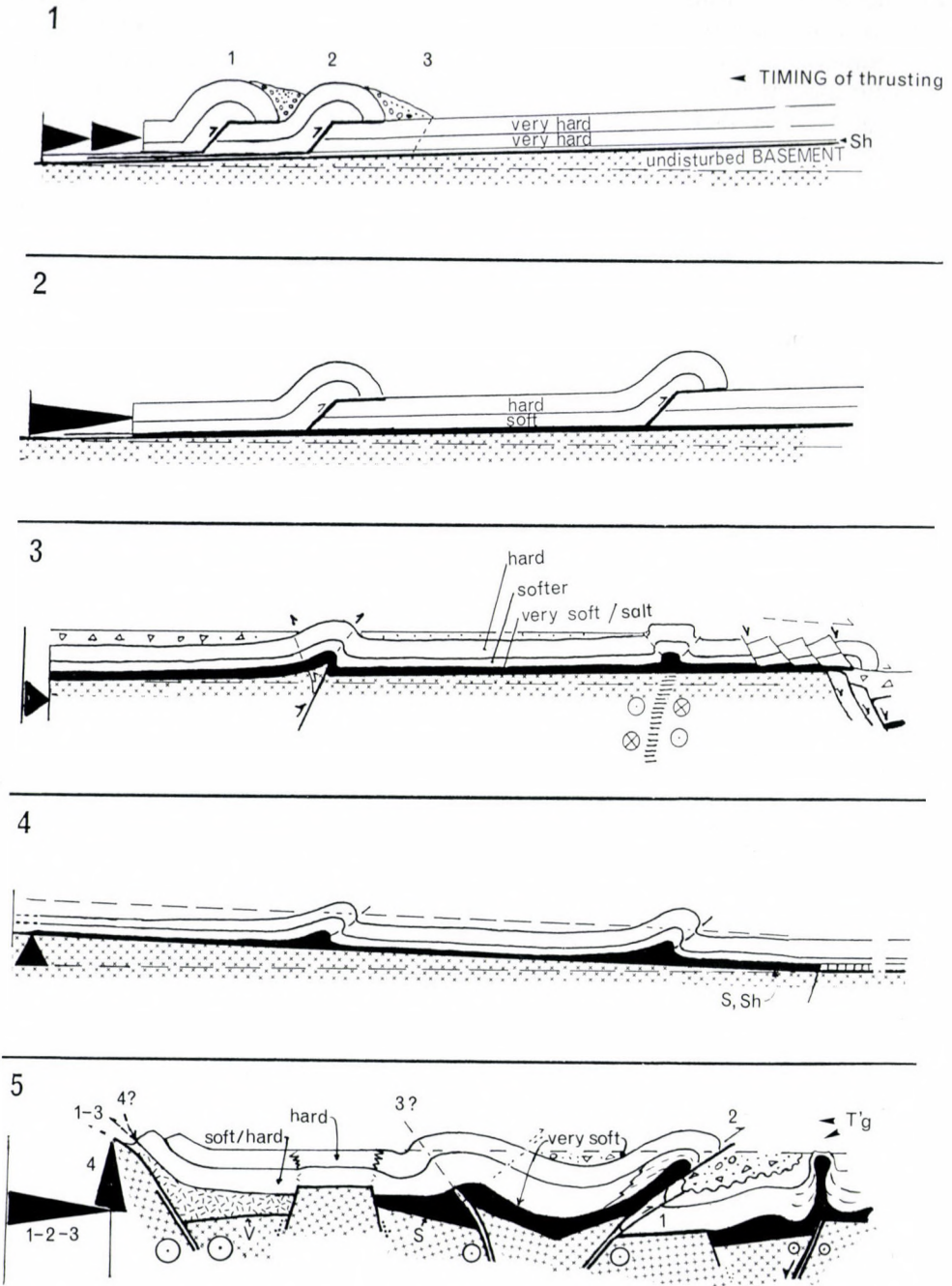
2) Simultaneous formation of equally-spaced anticlinal structures over vast areas, by simple lateral thrust and no basement involvement, over a thicker or thinner (10, 100 m-order) plastic horizon is a frequently used, yet *mechanically most unlikely hypothesis*.

3) In orogenic foreland areas or such zones where the basement is broken, drape- and drag-folds related to basement-level compression and/or wrenching are more likely. The drag-folds (right) are actually "flower structures"; both drape (left) and drag folds imply substantial thinning and fracturation (extension) of the sedimentary cover. E.g.: *Jura Foldbelt* (Fig. 10), North Franklin Mountains, northwestern Canada, Saharan Atlas, major segments of the Wyoming province, (foldbelt) etc.

4) Gravitational flow may trigger irregularly-spaced fold groups similar to (2) except for the opposite regional dip and the thinning of the sedimentary column. Large, flat-bottomed superficial synclines alternate with narrow, often very complex (recumbant) anticlinal structures. E.g: south flank of the Pyrenees, Catalanian Basin, *Atlas mountains*.

5) In areas with a) broken-up, uneven basement-surface, b) complex paleogeography gained through extensional/shearing phases, c) thick and incompetent décollement layers, d) varied, alternating hard-soft successions, and e) frequent facies-changes, orogenic compression deforms both basement and sedimentary column, producing anticlinal and synclinal structures which eventually become overthrusts. The succession and vergence of faulting are not necessarily uniform in the entire orogenic belt, since they start mostly by rejuvenation of the (most mobile?) basement fractures. Drape structures and recumbent synclines/anticlines abound. E.g.: major segments within the *Alpine Domain sensu lato*; *Northern Pyrenees* (see also Figs 5, 7).

In all cases the length of time a) between deposition and folding (i.e. the degree of diagenesis), and b) between successive tectonic phases, is of prime importance.



to true oceanic basins, Fig. 22 inset). Their presence is often inferred through geophysical anomalies (gravity and magnetism) rather than through direct observation. – The width of such geophysical anomaly-belts does nevertheless not indicate the amount of the "total" opening (offset), nor the distance between the walls of the separated continents or plates (e.g. the Baffin Sea – Fig. 14, or the Red Sea area). Furthermore, present-day true oceanic basins are also very deep (4000 meters and more) and receive specific sediments (mainly very fine clastics, excluding shallow platform deposits), while oceanized intra- or inter-continental domains or ocean arms are covered by shallower seas (< 2000 m) and receive thick, usually coarser clastic and volcanic sequences, which may nevertheless rapidly evolve towards carbonates. The high subsidence rates can be caused by the on-going crustal stretching. The response of the partially oceanized zones and of the purely oceanic domains during later compressive or collisional events is obviously different.

The oceanic floor of the Baffin Sea, as defined by geophysical anomalies, corresponds to a 1000 km long, 400 km wide rhomb-basin. The continental slippage demonstrated along the Nares Strait (i.e. along the short side of the lozenge) is nevertheless very limited (< 30 km, Dawes and Kerr 1982) and does not warrant the opening of an oceanic basin of the given dimensions by the simple pulling-apart mechanism ("wall-to-wall oceanic floor" see inset Fig. 22). Hence the necessity of admitting a partial oceanization process, where stretched and disbanded (disjoint) continental fragments are amalgamated, engulfed into the rising and intrusive volcanic masses (lavas, ophites and/or ophiolites?). – A similar although less developed set-up is known in the Red Sea–Gulf of Aqaba–Dead Sea–Gulf of Suez area (Figs 1, 28C).

Scattered ophitic/ophiolitic outcrops of limited extent and poor quality should therefore not be taken as evidence of former huge, true oceanic basins, but they can be valuable indicators of earlier extensional and/or sheared systems (e.g. Triassic ophiolites along the North Pyrenean Fault and probably most intra-Carpathian ophite/ophiolite complexes).

Calcareous sequences starting with truly deep marine (shaly-siliceous) sediments, but evolving rapidly (after only 1 000 ± meters) into neritic, shallow-sea carbonates, have therefore little likelihood of having been deposited in true oceanic basins (average depth: 4 000 m), even in the presence of ophitic/ophiolitic out(sub)crops nearby (e.g. Triassic–Jurassic calcareous sequences in the eastern Alpine–Carpathian domain). Chances are that they were generated rather in stretched, partially oceanized basins (pull-aparts, rifts, troughs, sag basins etc.) which may have been of any depth.

Volcanic phenoma often accompany the orogenic processes and contribute to "mountain-forming". Volcanism is nevertheless not exclusively related to any specific type of orogeny (e.g. to subduction-related arches along active margins) or to large-scale oceanic processes (oceanic rifts). The presence or chemical character of volcanoes is not diagnostic of any structural process or event. Volcanic complexes are present in basement dominated "craton"-type areas too,

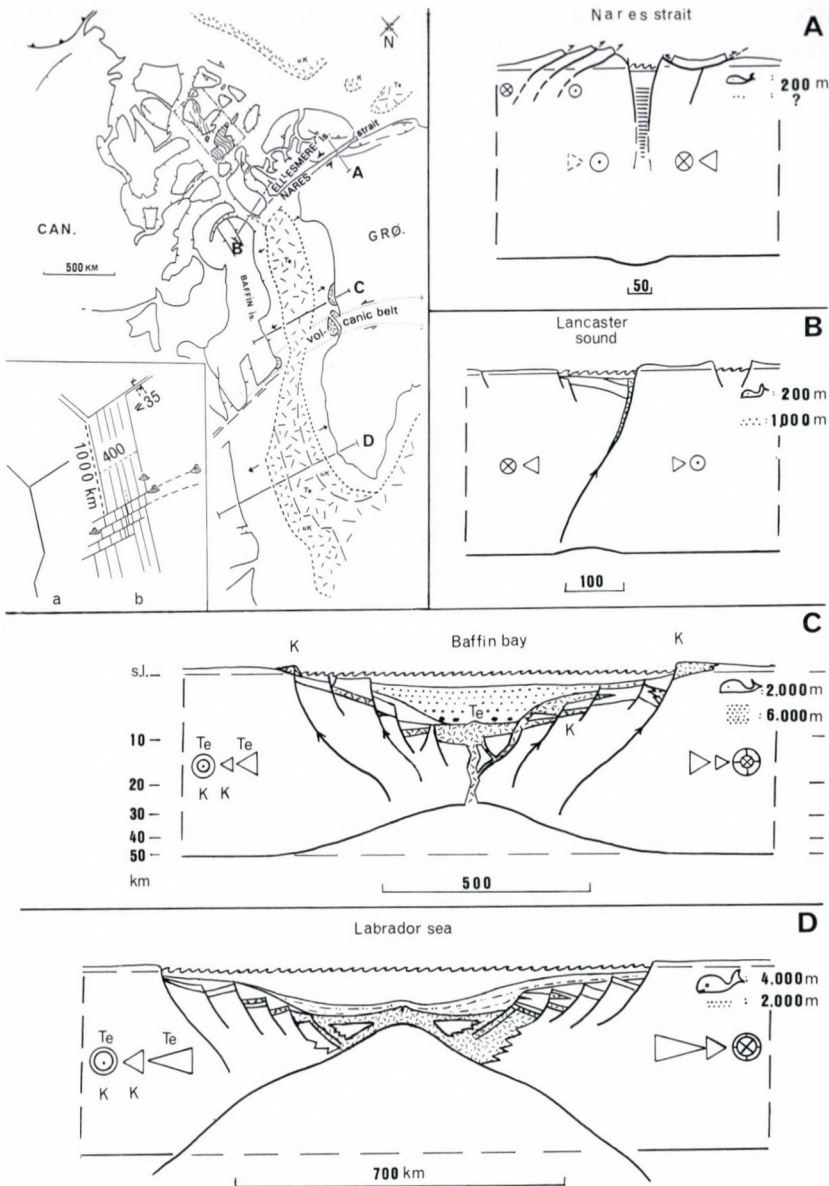


Fig. 14

Ocean arms - Oceanic basement, Canadian Arctic and Greenland area. Stages of evolution of continental break-up: A) Mega-shear zone: Nares Strait ("Wegener Fault"); B) Rift formed under extensional shearing, with some volcanism: Lancaster Sound; C) Ocean arm or mega-rift (system), with uneven, possibly discontinuous volcanic ocean floor (diffuse, irregular magnetic and gravity anomalies); D): True ocean with even, continuous, volcanic floor ("organized", regular magnetic anomalies); Inset, map: a) initial fault pattern, b) basin geometry of Baffin Bay. (Using Kerr 1980; Dawes and Kerr 1982)

especially where lateral displacements occur (continental rift-grabens and fault lineaments), since the major shear faults are mostly sub-vertical, deep-seated, and cut across the (upper) lithosphere thus tapping the deep magma sources.

Both acid and basic volcanism occurring around and across the diachronous *Intra-Carpathian volcanic systems* (Fig. 15) are more related to the basic fault-pattern of the basement checkerboard (Fig. 15a, also demonstrated by seismic phenomena), than to a hypothetical subduction-related island arch. In a similar way, the Proterozoic craton of the *Colorado Plateau* (Fig. 15b, inset) is surrounded and traversed by acid and basic volcanoes, which do not seem to be subduction-related, nor to form an "island-arc", since the Pacific Coast is at a distance of 700+km. – In both areas mineralization was very recent and related, among other factors to late, small-scale wrench movements (e.g. Colorado mineral belt and Baia Mare mineral lineament in the Carpathian realm).

Deformation mechanisms in basement-dominated areas

In areas underlain by an already established, consolidated basement of some thickness (20–30 kilometers or more), deformation mechanics are essentially different from those of active-margin type belts, from which most of our current tectonic models (and philosophy) are derived. The following are a few of these "different" mechanisms:

Small movements at basement level trigger *important anomalies* near the surface. The major deformations affect the continental crust to its full thickness (as demonstrated by gravity, magnetics and deep seismic results) and the total amount of volume changes are reflected to the surface and/or to the base. In most cases there is an obvious correlation between superficial and deep (Moho-level) anomalies. – The amount of crustal stretching or shortening needed to generate a sizeable basin or uplift is therefore much smaller in thick-crustal zones than in areas of thin basement (Figs 16, 17).

Rather small insignificant extensional or compressional movements can generate sizeable basins or uplifts (folds, ranges etc.) provided the continental crust is thick (Fig. 16, from Zolnai 1991). "*Mass balance diagrams*" demonstrate that to create similar size basins, the movement (offset, extension/compression) needed is much greater in thin crusted areas than in zones provided with thick crust. A mere 5 km extension can initiate a basin 25 km wide and 5 km deep, if the crust is 50 km thick. In an area with crustal thickness of only 10 km, 25 km of stretching is needed to reach the same basin geometry. The size of the virtual basin also depends upon its anatomy or its fault geometry (e.g 50 instead of 25 km width can be reached if the basin slope is progressive with step-by-step listric faults, replacing the sharp border-faults. – The upwelling of the "Moho" underneath of basins and rifts, as well as its downwarping under mountains are facts long known through geophysical methods (isostasy-gravity, magnetism, deep seismic). – The making of *lozenge-shaped pull-apart basin* (Fig. 17) does not take extensional or shear-movements of comparable magnitude to the edges of the basin, since the crust must be thinned on its full thickness ("thick skin tectonism"). – The timing of the faulting is often centrifugal; volcanism is current from the initial stages on.

In most *basement-controlled* deformation *shearing* appears to be the basic mechanism, since the thick and rigid basement blocks can more easily slip alongside than they can overthrust each other. Deep shearing introduces an

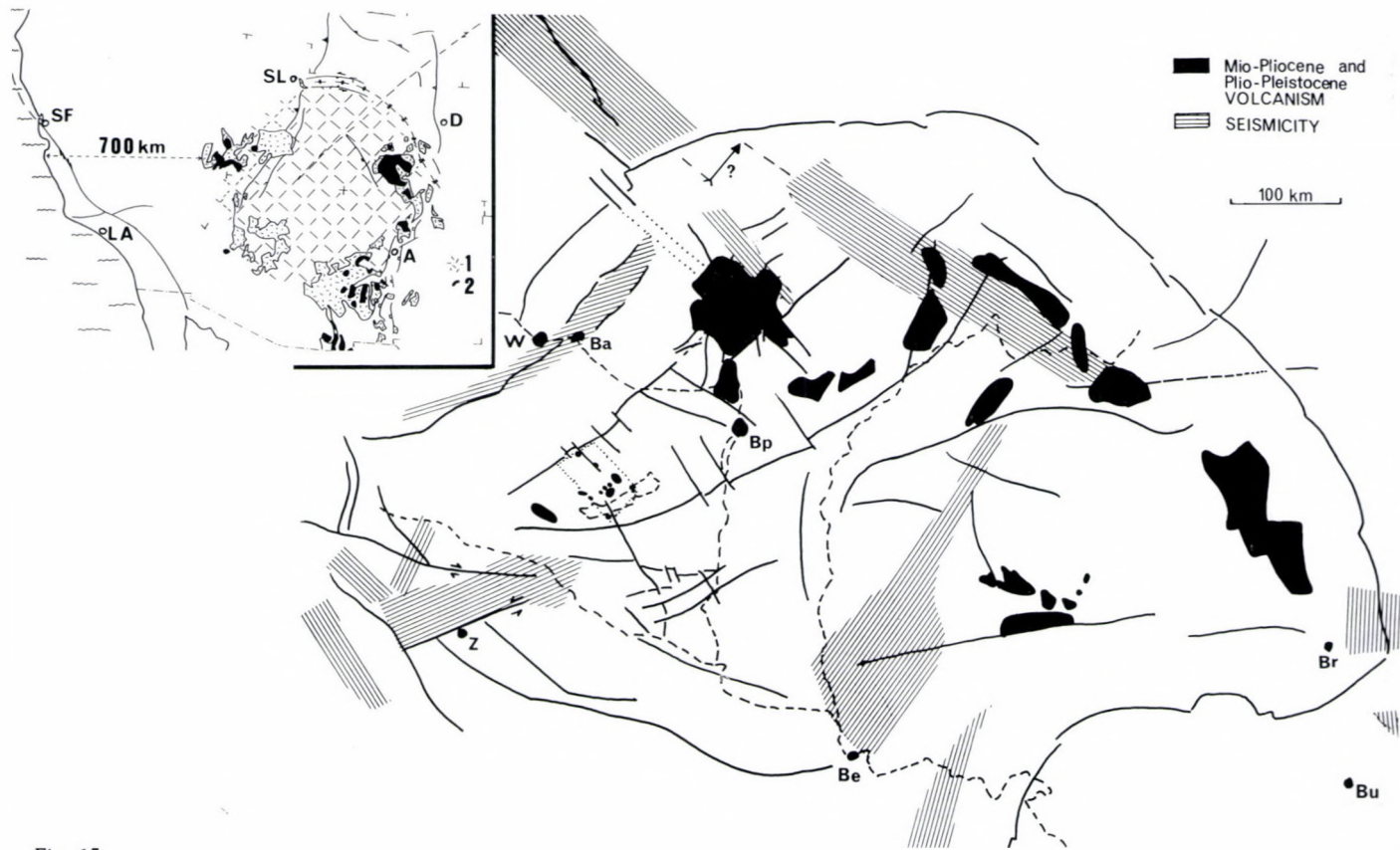


Fig. 15
 Volcanic arches: a) Carpatho-Pannonian area; b) (inset) Colorado plateau, USA. 1. acid ("felsic") volcanoes; 2. basic volcanoes; A - Albuquerque; D - Denver; LA - Los Angeles; SL - Salt Lake City; SF - San Francisco (Using Royden and Horváth 1988, King and Edmonston 1972)

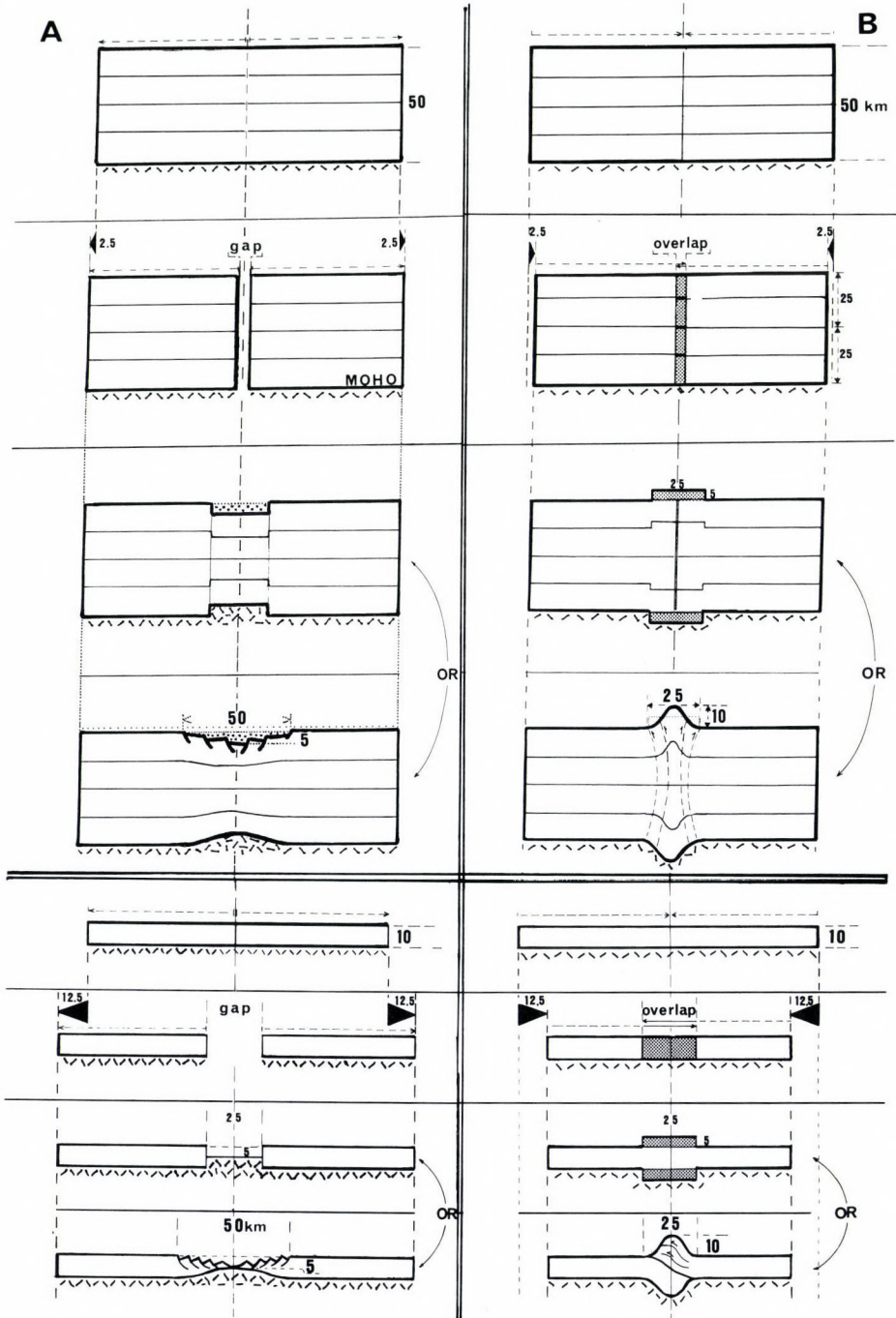


Fig. 16
Mass balance: A) extension, B) compression, upper part thick crust, lower part thin crust

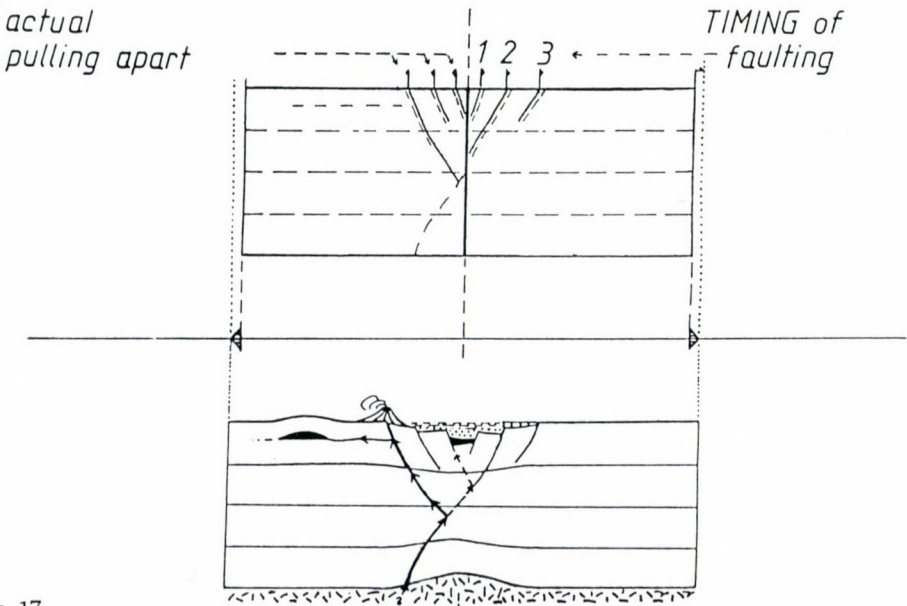
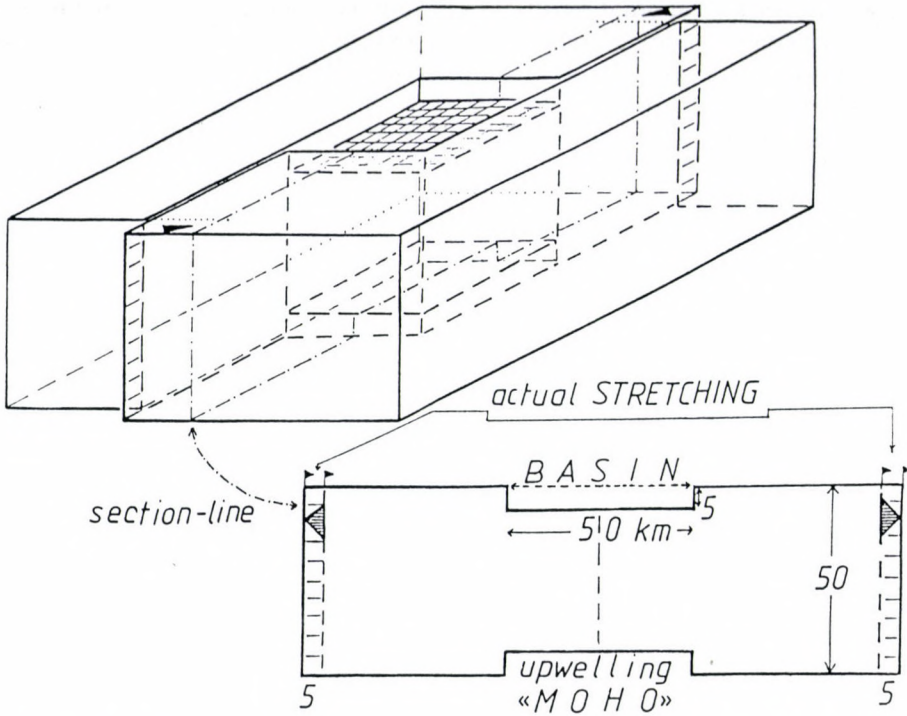


Fig. 17
Pull-apart basins in thick-crustal areas

array of superficial anomalies often in the opposite sense (positive *and* negative anomalies side-by-side), the mass balance thus being preserved. Such structural compounds are currently generated simultaneously ("coevally"), and not through alternating compressive and extensional phases. "Paired uplifts and basins" as well as "vaults and downwarps" are thus formed within the wrenching context (Figs 18, 19).

The evolution of a wrench-corridor (Fig. 18) depends on the lateral mobility of the area. In case of constant width, the blocks involved in the shearing are rearranged: some are uplifted, others pulled down; the mass-balance thus remaining unchanged (see also Figs 19, 20). (Zolnai 1991, after Walper 1977).

If a 10 km long "slab", limited by off-set faults (common in shear-systems where *en échelon*, oblique faults abound), is affected by a 0.2 km (200 m) horizontal displacement, an 800 m high structural *arch* (vaulted uplift) can be formed (Ruhland 1972), flanked by "pull-down" *sags* (due to mass balance, see lower right corner) which further accentuate the apparent structural contrast. The superficial drape structure, frequently enhanced by reverse faults, suggests E-W ("perpendicular-to-the-fold-axis") compression, whilst the real mechanism is deep N-S (longitudinal, left-lateral) wrenching. – Similar fault-relay, but with senestral offset and right-lateral strike-slipping, can produce identical structure. It is very hard not to see an 800 m high structure, on the surface or subsurface, whilst it is even harder to pinpoint a 200 m strike-slip movement at depth (hence the rarity of interpretations calling up such deep mechanisms to explain well-known superficial anticlines, gentle swells, bulges etc.).

The central belt of the Pannonian Basin exhibits typical examples of such wrench-related paired structures, but also most structures of the Paris and Aquitaine Basins as well as of the Saharan Triassic Basin are best accounted for in this way, especially since they are grouped in alignments.

Block rotations are often caused by small-scale wrenching. The generated local deformations (Figs 20, 22, 23) should not be systematically extrapolated over large areas around and taken as regional movements. Isolated outcrops scattered in basinal or platform areas usually appear in places of maximum deformation (e.g. at the corner of a rotated block or at the intersection of two fault-systems, Fig. 20a, b); they therefore stand for themselves alone, without being representative of large areas around them. *Tilted and/or uplifted blocks* may appear in an extensional and wrenching context too (Fig. 20c). They may become local sediment sources and be surrounded by uncomformable coarse clastic collars, which may or may not indicate major orogenic pulses (e.g. the "Sardinian Phase" of southern Europe has not the same structural signification as other phenomena of the Caledonian orogeny, which took place along the opposite continental margin). Some of the angular uncomformities of the general Alpine–Pannonian Basin area (e.g. near Sümeg in the Bakony Mountains of western Hungary), or those of the Eastern Pyrenees can be expressions of such (minor?) intra- or pre-orogenic block movements, and not of major orogenic phases. The Mecsek Mountains in southern Hungary and the Black Hills of the western part of the North American prairie region (Fig. 2) are both block uplifts taken into deep shear systems which generated local compressions and/or rotations.

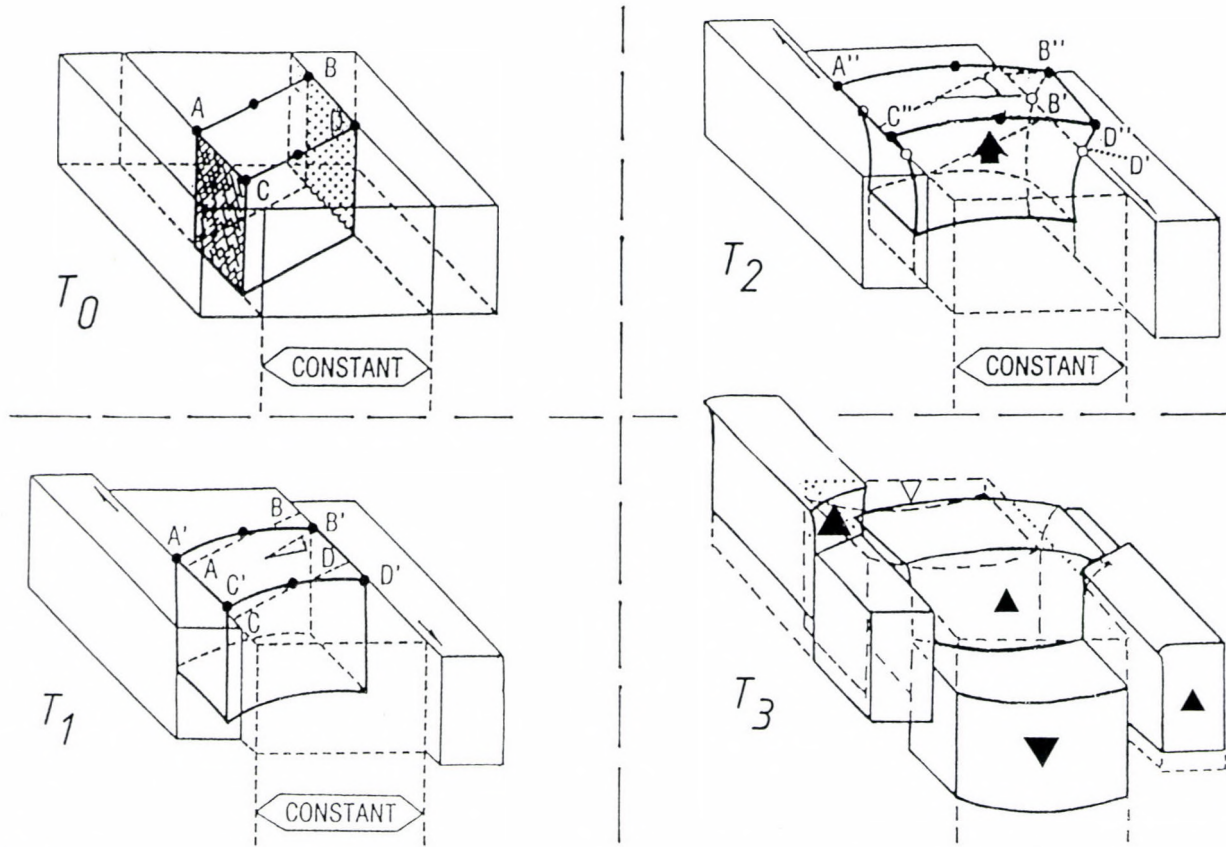


Fig. 18
 "Paired uplifts and basins". T_0 . Friction along the walls of basement blocks; at the beginning of wrenching; T_1 . Slight rotation and gentle vaulting of central block; T_2 . Uplift with bilateral slightly reverse faulting; T_3 . Blocks taken in the shearing process obtain chessboard pattern, with major subvertical border faults yet without internal crushing (frequent flat-top uplifts in spite of important lifting) See Walper 1977

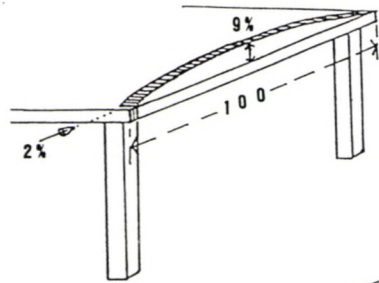
In an area which has undergone wrenching, sections (e.g. *seismic profiles* – Fig. 20b) may suggest synchronously-formed compressional and extensional structures (grabens, tilted blocks and imbricates) at close range, difficult to explain if the wrenching context is ignored. – Subsequent effects of *extensional tilting*, such as superficial drape folds and erosional unconformities can be mistaken for compressive phenomena, although they are due to minute extensions. The steep flanks of the drape-folds ("d.f.", Fig. 20c) may be substantially thinned. Saw-tooth patterns are favourable for reef growth which generate their own fore-and back dips. (up to 30°) which should be ignored when making structural reconstructions.

Wrench-corridors, composed by oblique, *en échelon* structures or slabs (parquets, floor-boards) taken into shearing may be widened by the "push-apart" effect of the rotating blocks, provided some lateral freedom exists in the area. (Figs 21, 22). Although local compressions and extensions will appear, regional subsidence may occur along the corridor, even if the initial wrenching itself was originated by overall compression (orogeny). This mechanism may have contributed to the generation of intra-orogenic sags, e.g. the Pannonian Basin during the Tertiary. If there is no lateral freedom, "paired uplifts and basins" are formed (Fig. 18), with constant mass balance. When the region undergoes major shortening, uplifted structural elements prevail and sets of imbricate ("*fishscale*") blocks predominate.

Dependent on the *basement's tectonic fabric*, and on the orientation and intensity of the overall stress-field, structural checkerboards or elongate parquet-systems may be raised during periods of renewed compressive, extensional or shearing deformation. Pull-apart basins, rifts and uplifts joining end-to-end or on corners eventually form *structural webs* as well as *wrench corridors* which remain loci of more intense deformation than the intervening nuclei (Fig. 22). Successive phases of movements in the extensional and/or wrenching modes can transform rifts and rift systems into mega-rifts, (aulacogens) which can eventually be oceanized and end up as new ocean-arms (Fig. 22 inset, see also Fig. 14).

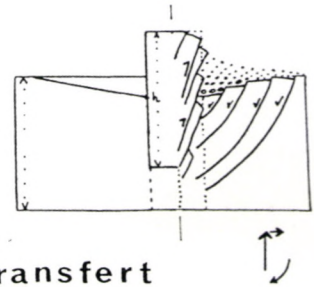
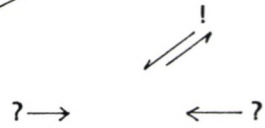
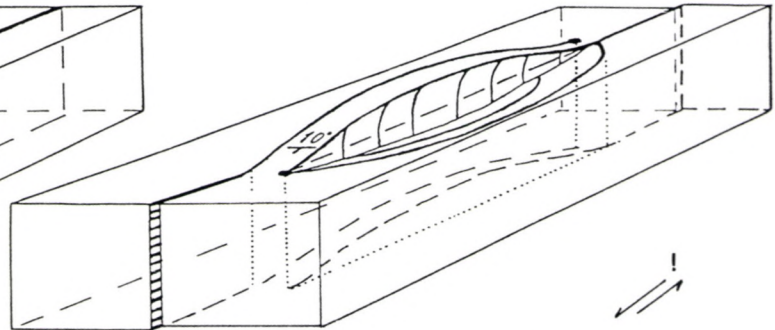
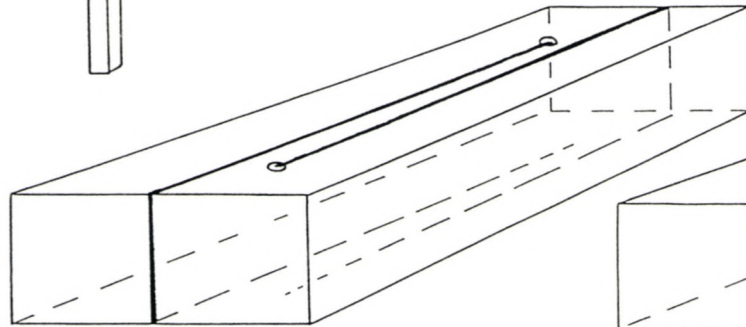
Structures with opposite signature can be formed in various segments of a wrench system, simultaneously or diachronously (e.g. in nascent systems), depending on the orientation of inherited (or newly-formed) faults, in conjunction with the regional stress-field or deformation pattern. Isolated basins can form almost anywhere ("*in the middle of nowhere*"). Gravity tectonics with klippen and nappes may be generated along uplifted basement-blocks, implying very small (if any) compression.

All stages between flat, undisturbed platforms, sag basins (usually at the crossing of rift systems, at "continental triple junctions", Zolnai 1986) deep troughs/rifts, and isolated pull-apart basins may thus be present simultaneously within the same intracontinental or passive-marginal area. Such wrench-related systems may cross whole continents and eventually form structural webs spread over entire plates. Intracontinental wrench systems also may remain active during a long time span, through repetitive but individually unimportant movements, frequently in opposing directions (e.g. the North Pyrenean Fault: Bourrouilh et al. 1995 or the Central Australian mobile belt; see also Muehlberger 1986).



the RULE of the RULER

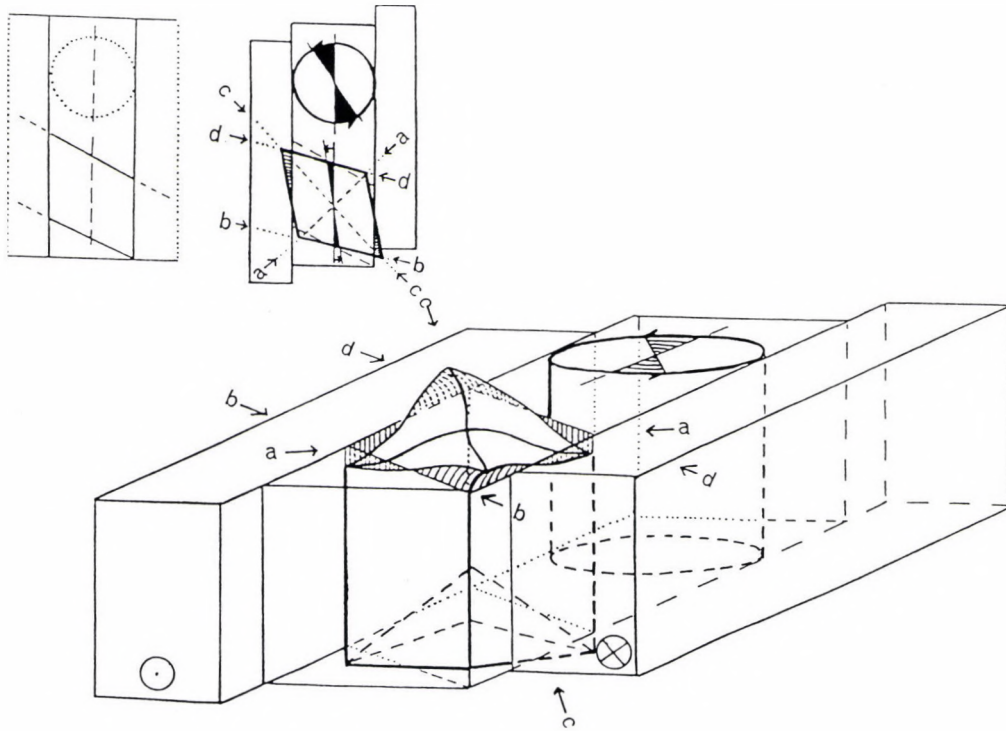
fault relay + wrenching = vault & sag



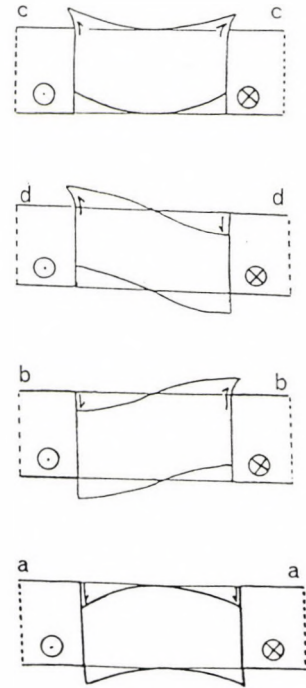
mass transfert

Fig. 19
Vaulted slabs ("the rule of the ruler") (from Zolnai 1991, using Ruhland 1972)

A: BLOCK ROTATIONS



B: consequences



C:

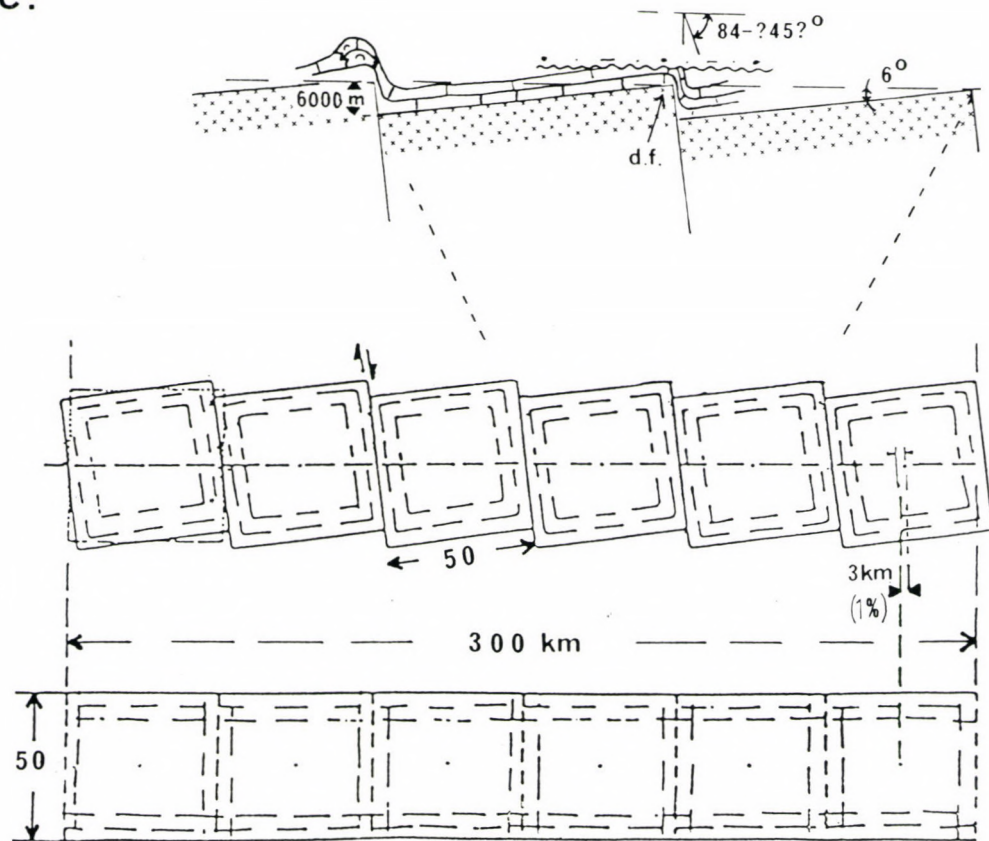


Fig. 20

Block rotations and tilting. A) Block-rotation caused by moderate-slip movement (e.g. Mecsek Mts, southern Hungary, basement blocks along the North Pyrenean Fault); B) Tilting under wrenching: cross-sections with apparently compressional and extensional features: tilted blocks and imbricate structures, situated at close range; C) Tilting under extension: geometry of basins generated through block tilting (here: West Canadian Platform, Rainbow basin: N of the Hay River fault, see Fig. 2). Note the extremely slight (1%) extension

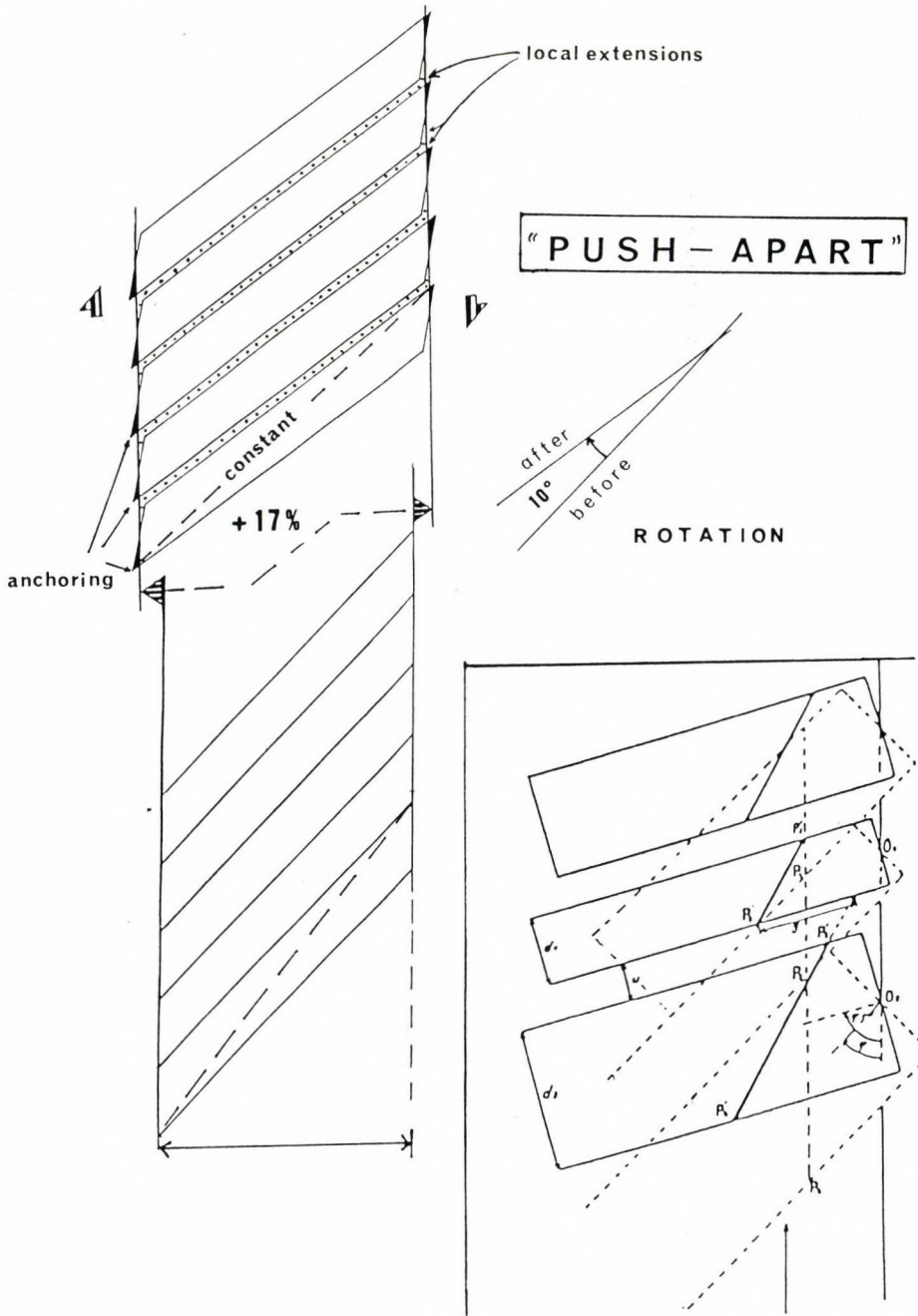


Fig. 21
"Push-apart" basins. Inset: Scheme proposed by Riedel, in 1929

WRENCH systems

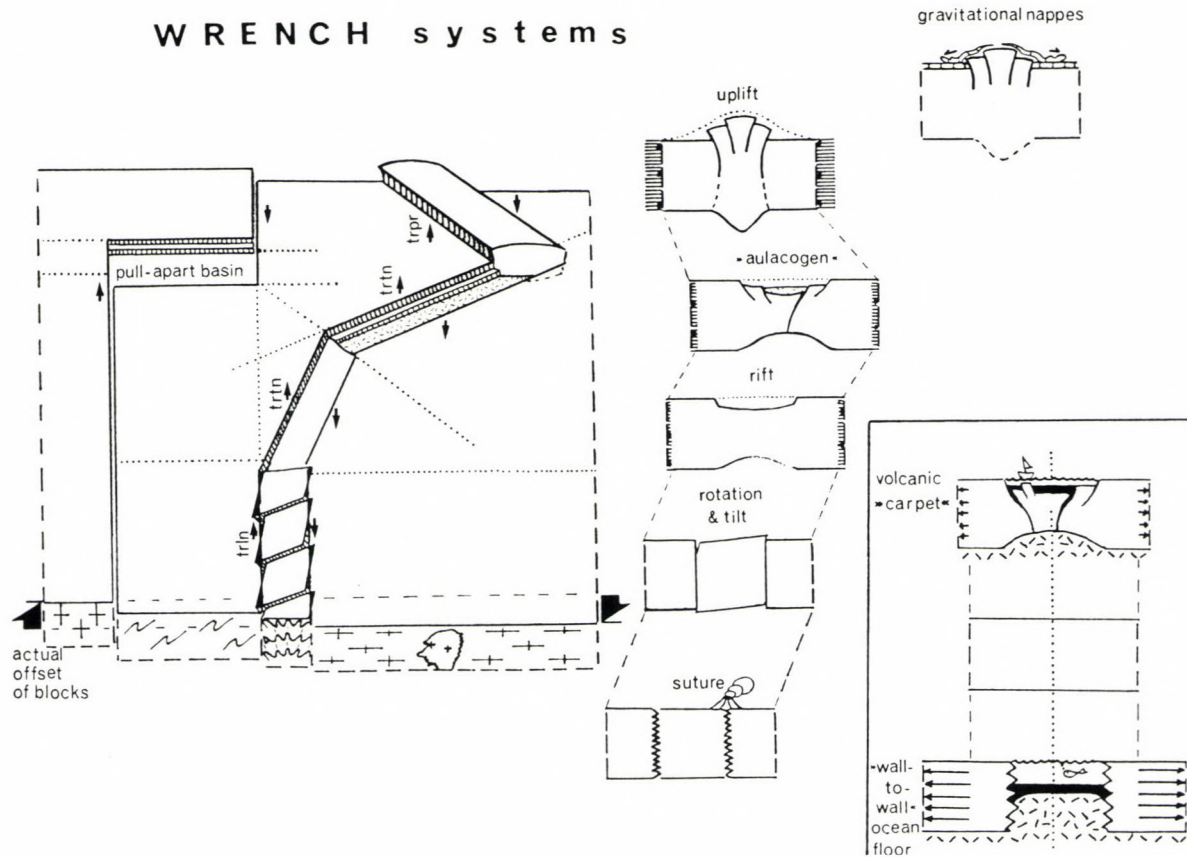


Fig. 22

Shear systems – wrench corridors. trln – translation (simple horizontal shift); trpr – transpression (wrenching with compression); trtn: transtension (wrenching with extension). *Inset, top*: partial oceanization through crustal stretching and diffuse subsea volcanism: thin and discontinuous "volcanic carpet" (frequent in areas of extensional wrenching); *Inset, bottom*: "wall-to-wall" oceanic floor caused by sudden rupture of continental blocks (e.g. West Mediterranean sea; compare with Fig. 14

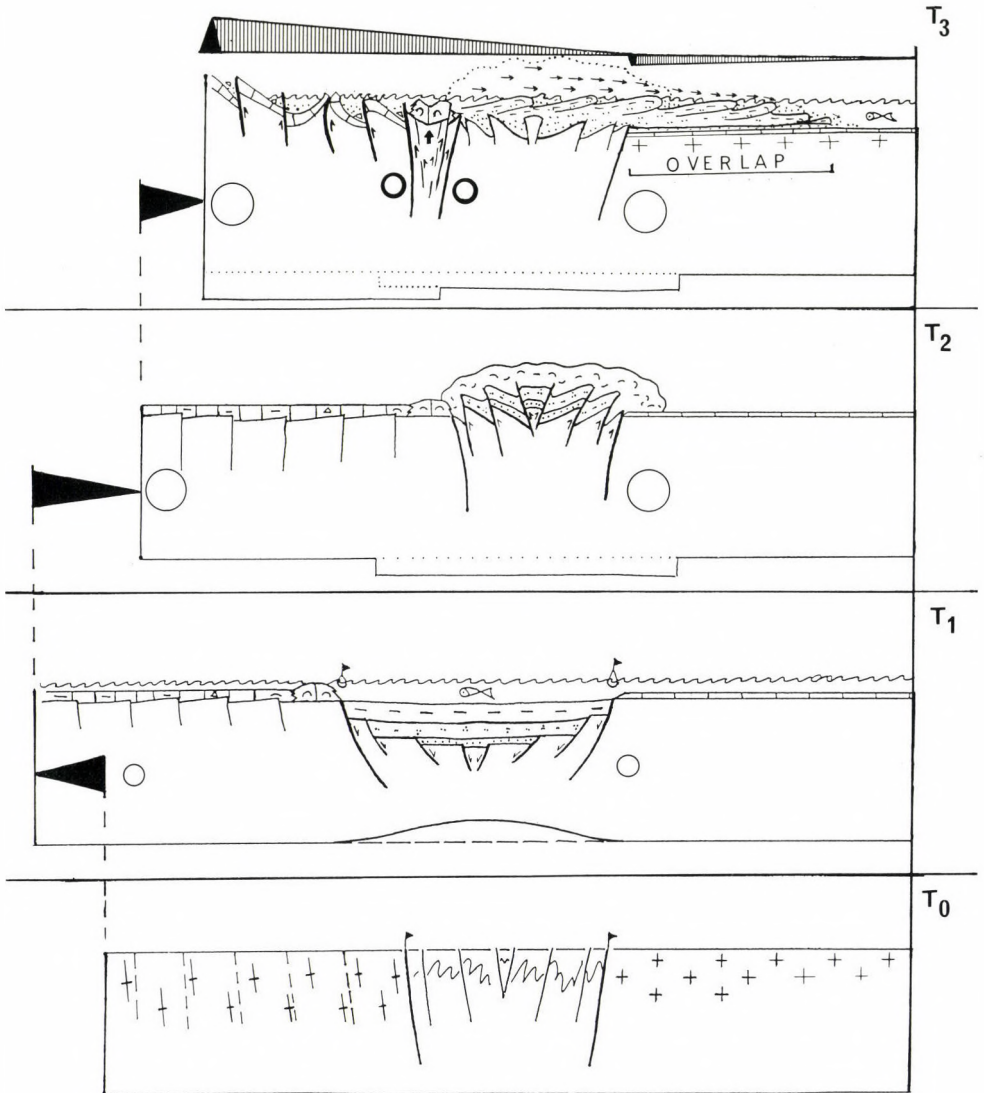


Fig. 23

Structural inversion in un-consolidated areas (flysch basins, gravity tectonics). T₀. initial situation; T₁. after extension (possibly transtension); T₂. after compression (transpression); T₃. after further transpression and uplift in the central orogen; note gravity flow of soft sediment fill. T₂ and T₃ may be coeval or a short interval. Direction and intensity of wrenching may change during the same orogenic cycle

Moderate extension and strike-slipping often results in the emplacement of basic, superficial or *subsea volcanics* in the continental interiors, frequently along the edges or within the rift- (later inversion-) systems (e.g. Albian basic subsea

volcanics, pillow lavas and volcanic sills inbedded into flysch series in the North Pyrenean furrow, or the individual superficial volcanoes of the Rhine Graben).

The simultaneous presence of volcanic and intrusive rocks and rhythmic sediments may thus lead to erroneous interpretations where the combination of horizontal (therefore supposedly large scale) movements with flysch and basic volcanics (attributed forcibly oceanic basements) are easily taken for (California-type) subduction-related "mélanges", which they are not necessarily.

Such *weakened zones remain mobile* and may undergo maximal subsidence (in the 5–10 000 meter range) as well as more intense deformation, including structural inversions. The Ougarta system, parts of the Don–Dneper aulacogen (Fig. 1) or the Big Snowy system and the Uintas (Figs 2, 11) demonstrate the vertical (as well as horizontal) mobility of such intracratonic mobile belts. Nevertheless, the actual sea-depth within these troughs does usually not exceed the 1–2 000 meter range.

In the case of *structural inversions* the resulting tectonic landscape depends not only upon the composition of the basin (rift) infilling but also of its degree of diagenesis. If the (usually clastic) sequences are competent, huge arches with sub-vertical or recumbent edges are formed and maintained after the relief inversion (as in the Uinta Range, where indurated Proterozoic flysch-type sediments were uplifted during the Laramide orogeny, starting in Paleocene time: Fig. 11). – If, on the other hand, the infill of the troughs or rifts is still incompetent at the time of the inversion (e.g. "viscosus" flysch series never uplifted above sea-level, see Henry 1969; Haller and Hammon 1993), structural "bulges" may occur (Cretaceous flysch in the subsurface of the Pannonian basin near Szolnok, Hungary). Should a regional dip exist at the time of the inversion, gravity tectonics may prevail and huge nappes ("*nappes d'écoulement*" or "*nappes de glissement*") can form, as in the Atlasic domain in North Africa, in Sicily–Italy (Mattauer 1980), on the slopes of the Pyrenees or, most probably, in the external (flysch) zones of the Carpathians (Fig. 23).

Gravitational tectonics also occur in areas of subvertical uplifting of basement blocks which were formerly capped by relatively competent sediments such as carbonates. The carbonates may thus be "scalped off" their basement, during or after the uplifting, and skip onto the younger sediments of the nearby downwarped basins (e.g. the Heart Mountain klippe in the Big Horn basin, Wyoming, western USA, or the allochthonous Tithonic limestones in the Lacu Rosu–Bicaz canyon area, in the East Carpathians (see Sandulescu et al. 1975). In such cases crustal shortening may be extremely limited or totally absent, and its magnitude cannot be related to the overlap of the nappes on the foreland nor to the internal complications of the allochthonous terrane. Balanced cross-sections are not credible in such cases. – Reefal banks situated in rifted zones (Fig. 23 center) may also become apparent "klippe"; actually they are pop-up (extrusion-) structures, emplaced under compressive wrenching, like in the "klippen belt" of the northern Carpathians. Carbonate build-ups and plateaus are common on rift edges and on hinge-lines between two furrows.

Although there is in most cases a correlation between rifting and major diastrophisms (orogenic events), the existence of flysch furrows does not necessarily indicate the presence or the proximity of orogens, in space or time.

Secondary folds and fold systems may take shape in the foreland zones, between the blocks of the continental basement, or on top of them, if the inherent fault-pattern of these basement mosaics is rejuvenated to some extent. These folds have their own structural logic, related to (but not identical with) that of the truly compressive fold-complexes of the nearby orogenic belts (e.g. the Jura foldbelt, in the foreland of the Alps: Figs 9, 10). – *Drape- and drag-folds* ("forced folds") are characteristic; they do not necessitate crustal shortening, but basement blockfaulting with shearing, uplifting and/or tilting (Fig. 24). Various superficial folds, situated at close range, may be interpreted as due to a succession of compressions and extensions of varied directions (and origins?), unless taking into account the fabric of the basement and the movements occurring at depth.

Many of these folds are actually flower structures, where local convergence ("sagging") and elongation ("stretching") of the strata are made possible by the thinning of the sediments (which replaces the "shortening"; see Zolnai 1991).

Wrench-related superficial reverse faults usually steepen rather than flatten out at depth, since deep shear systems always affect the entire (upper) crust. Given their frequent overthrust component they may easily be taken for emerging edges of nappes (Fig. 25).

Superficial structures parallel to overthrust belts are often interpreted as emerging overthrust sheets' leading edges. In the case of the foreland structures in North East British Columbia however (Fig. 25), applied exploration-work has demonstrated a vertical "pop-up" structure related to N-S compressive wrenching along an old, late Paleozoic graben (rif)-edge.

This is the high-angle "pop-up" structures versus flat detachment ("ski-tip") faults controversy, or the thick-skin versus thin-skin tectonic debate. – Some of the klippe or klippen-belts are actually extruded tectonic blocks or pop-up structures, emplaced in wrenching context (e.g. NW Carpathians). Individual horsts and horst-and-graben compounds can thus appear at close range with areas of collisional or convergence mechanisms.

The wrench-related uplifts are nevertheless usually straight, elongate systems, the superficial expression of which is little influenced by valleys crossing them (while the leading edges of thrusts are encroached at such intersections). The North Pyrenean Fault, the Bray Fault of the Paris Basin or the Murany Fault in Eastern Slovakia correspond to such steep to subvertical basement faults, rather than to emerging "nappe units".

Many of the space-problems raised through the exclusive use of strong orogenic compressions with large-scale crustal shortening, may be resolved by judiciously applying the basement-shear concept. The Western and Northern Pyrenees, the Amadeus Basin/Foldbelt in Central Australia, the foreland of the North American Cordillera, the Carpatho-Pannonic realm are but a few of the areas needing to be re-interpreted.

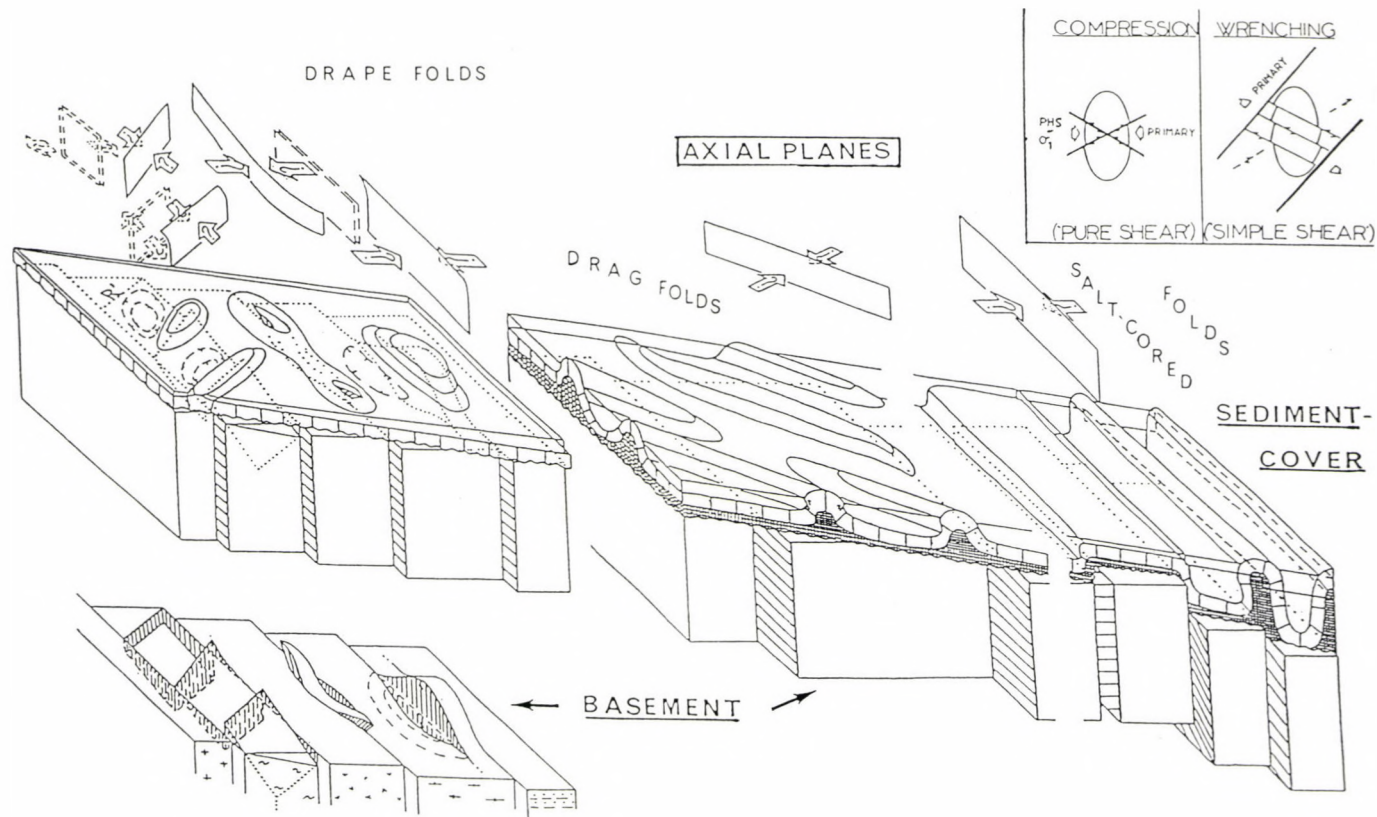


Fig. 24

Superficial folds versus deep faults (Drape- and drag-folds), (Where is the "Principal Horizontal Stress" or the "Sigma-1?"). Left block: Parallel drape-folds atop of a set of tilted basement blocks; Center: Drag-folds atop of flat-lying but wrenched basement "parquets"; Right: Anticlines due to diapirism, atop of deep dip-slip and/or strike-slip faults. Note: a) parallel basement faults, dextral wrenching in all cases; b) lubricating layer (salt) present in most drag-fold systems; in areas devoid of evaporites drape folds abound. Inset: Comparison of two similar folds and associated fault-patterns in compressive (left) and shearing (right) context. In case of shearing the set of fractures is a-symmetrical, non-conjugate ("en echelon") (Using Odonne and Viallon 1983)

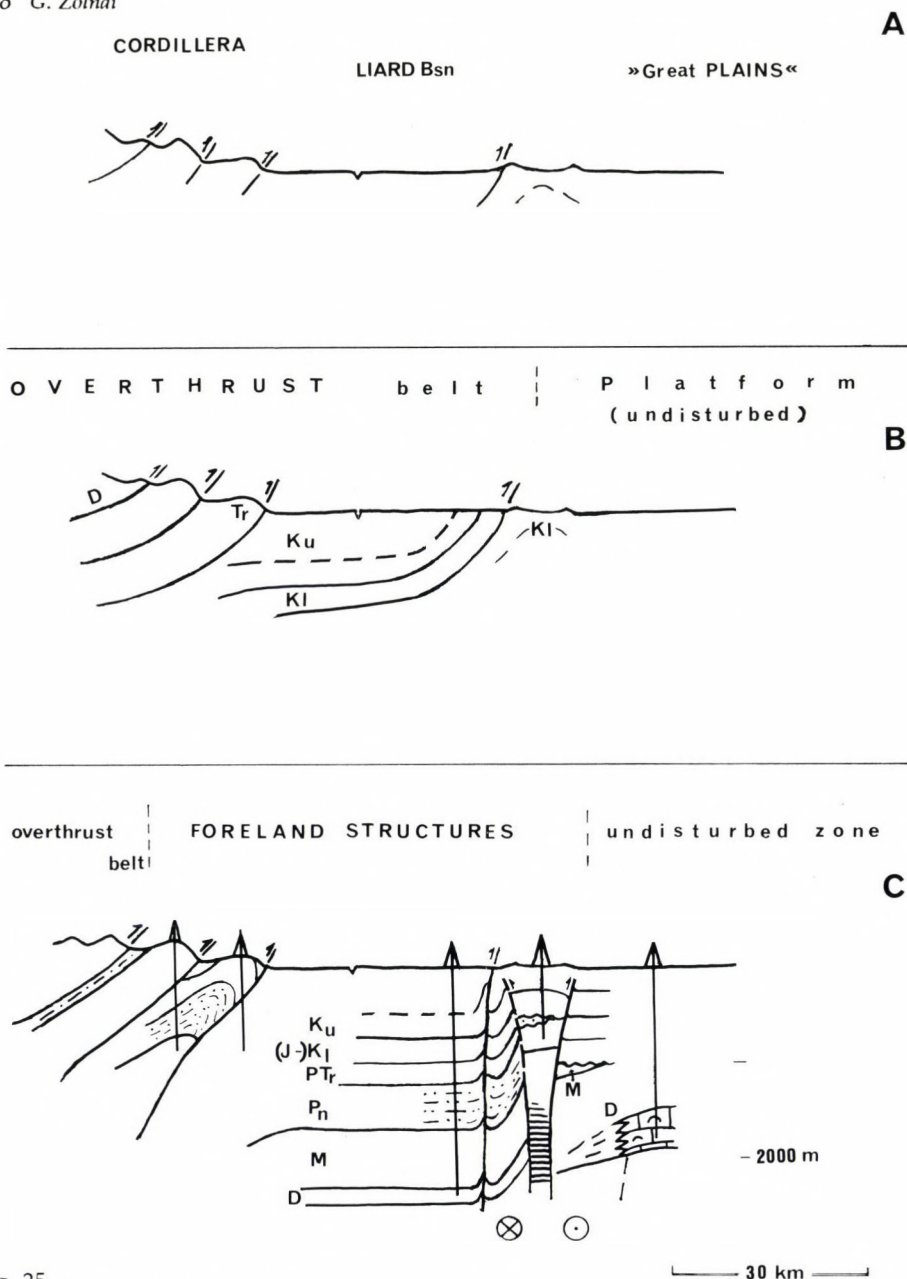


Fig. 25

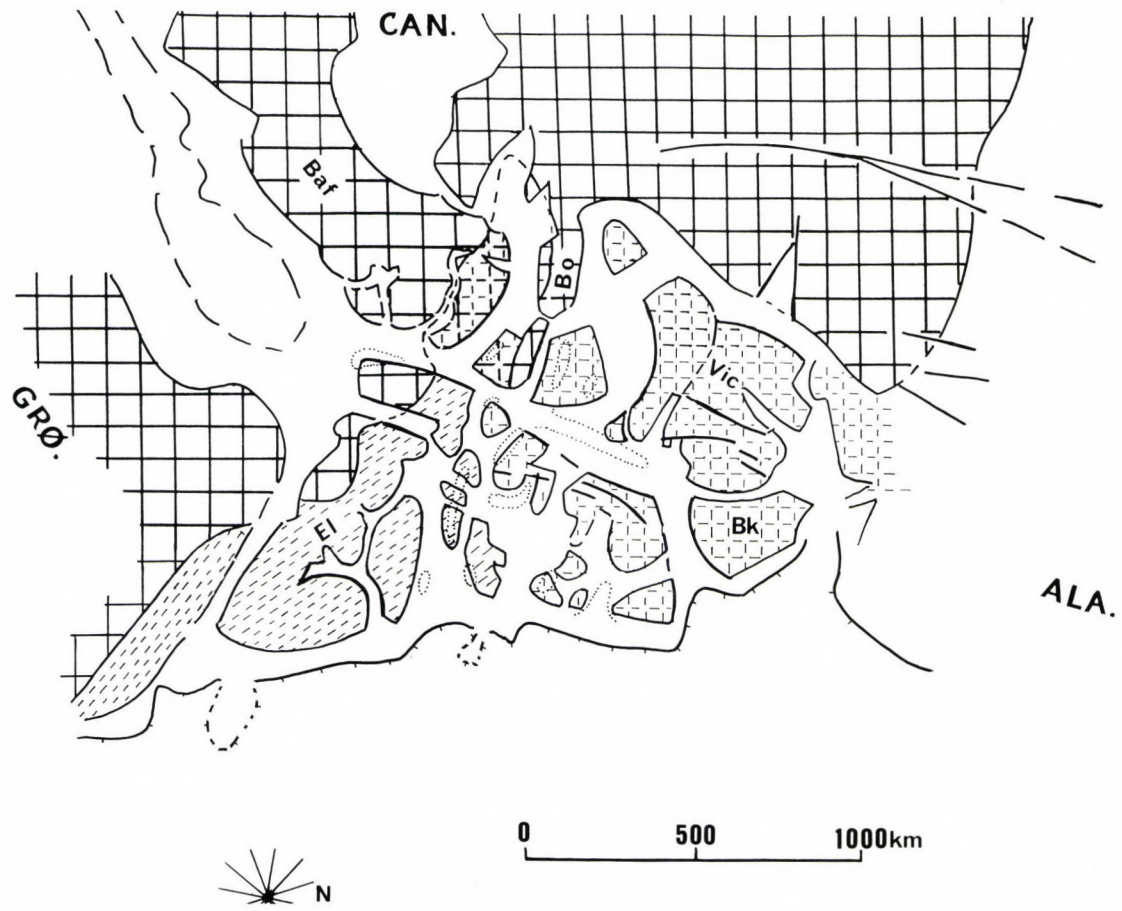
Steep-and-deep wrench-faults versus flat detachments. A) Field outcrops; B) Early interpretation, based on overthrust-theory, extrapolated from nearby foldbelt (flat detachment fault, thin-skin interpretation); C) Actual image, after seismic and exploration drilling (steep, deep-rooted shear-fault system: proven thick-skin tectonic). Ku – Upper Cretaceous; Kl – Lower Cretaceous; PTr – Permian and Triassic; Pn – Pennsylvanian (Upper Carboniferous) clastic rift-fill; M – Mississippian (Lower Carboniferous); D – Devonian. (North east British Columbia, Canada, the Liard Plateau/Basin area, Tadoo-Maxhamish structure. From Zolnai 1991, using unpublished Aquitaine C° of Canada documents.)

The role of tectonic *indenters* (Pavoni 1961a; Molnar and Tapponier 1975) may be predominant in the anatomy of foreland foldbelts as well as within the foldbelts themselves. If there is a basement of some consistency, the indenter will push pre-formed blocks of the underlying basement aside and may create calm pull-apart basins within the (compressive) foldbelt. The undisturbed intramountain successor-basins and high-lying, equally undisturbed plateaus encountered within orogenic zones (South Tyrol in the eastern Alps, Tertiary flysch basin in northeastern Slovakia) may also reflect the presence of hard cores (or rafts) at depth, blocks amalgamated into the orogenic complex, which move (escape) as such in front the indenters and ensure some structural immunity to the sequences immediately above them.

Paleogeographic patterns are extremely complex in the broken-up, extended and sheared passive margins. The trailing edges of the drifting plates are composed by discarded, sometimes calved blocks ("lost soldiers"), separated by grabens of varying dimensions which may or may not form continuous sea-arms and which can be partially or fully oceanized (ophites, ophiolites). Relays of lozenge-shaped grabens and uplifts can better account for the facies-distributions than classical cylindrical patterns, which extrapolate into elongate zones (parallel swells and furrows hundreds to thousands of kilometers long) which may have been only local depocenters, or a row of discontinuous (pull apart?) basins. – *Facies identity* (or similarity) alone cannot be taken as sufficient basis for paleotectonic reconstitutions, since *similar facies* are *not* necessarily due to *continuous depositional belts*. The study of similar yet separate paleogeographic domains in a parautochthonous mode may lead to more realistic interpretations than the large scale displacement of these blocks (for instance: the Permian of the Mecsek Mts, southern Hungary), aiming solely at the restitution or establishment of continuous paleogeographic zones. This is especially true in continental areas provided with a basement chequer, and distant from "free" oceanic domains of great lateral mobility. An example of such a mosaic-block arrangement is the present-day structural pattern of the Canadian Arctic Islands, a long-lived passive margin with still active rift-forming. A comparison may be attempted between the present-day geography of this area and what might have been the South European passive margin at Jurassic–lower Cretaceous time (Fig. 26).

In both cases (Fig. 26A, and B), the size of the blocks and the meandering pattern of the troughs ("rifts") inbetween is comparable; the nuclei decrease from the craton towards the oceanic domain. – In the Arctic area, in addition to the regular geographic pattern, gravity anomalies suggest nascent rift trends and indicate possible volcanic intrusions.

When relating the above mechanisms to orogenic events or to tectonic forces, the frontal collisional model, supposing straight and parallel continental edges, is but one of the possibilities. Plate edges can be arcuate and irregular (convex,



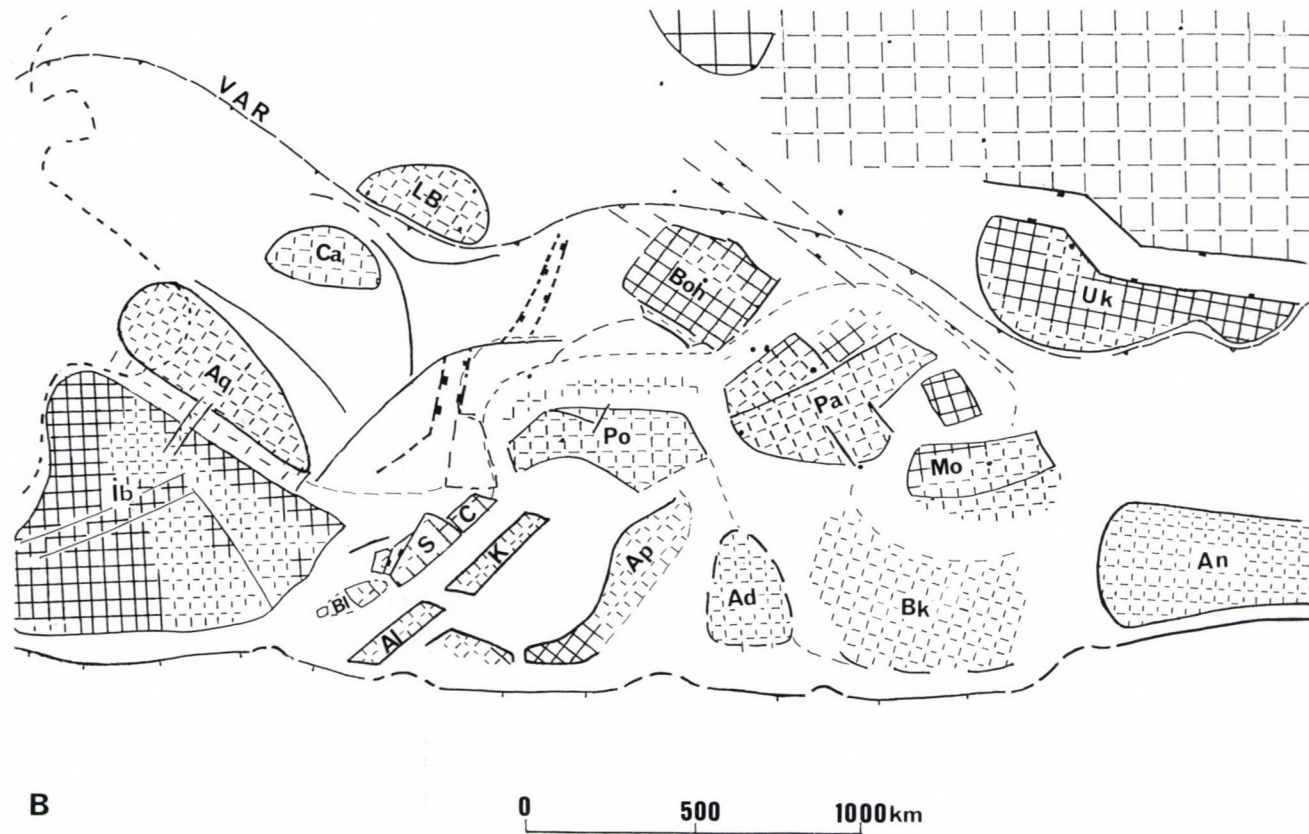


Fig. 26

Mosaic-structure of passive margins. A) Arctic Archipelago, Northern Canada, present day: ALA – Alaska, CAN – Canada, GRO – Greenland, N – North Pole; Baf – Baffin Island, Bk – Banks Is., Bo – Boothia Arch, El – Ellesmere Is., Vic – Victoria Is; B) Southern Europe during Jurassic-Early Cretaceous: Ad – Adriatic; Al – Alboran; An – Anatolian; Ap – Apulian; Aq – Aquitaine; Bl – Balearic; Bk – Balkanic; Boh – Bohemian; Ca – Cadomian; Ib – Iberian; K – Kabylia blocks; LB – London-Brabant Massif; Mo – Moesian platform; Pa – Pannonic; Pô; SC – Sicilian-Corsican; Uk – Ukrainian blocks; VAR – Variscan front

concave, broken, or saw-tooth lines) and they can be disposed in an *oblique way*. The resulting *orogens* may thus be *diachronous*.

Such diachronous orogens (Fig. 27) can be further complicated by the inclusion of loose, "suspect" oceanic or continental blocks, microcontinents or "terrane" ("lost soldiers" of earlier passive-margin evolutions, disposed between the converging plates, and amalgamated in the newly formed orogenic belt). In relation with the laterally sweeping orogenic deformation, primary shear can accompany the oblique collisional events and be responsible for the regional foreland deformations in the wrenching mode, also. Simple shear (off-set, en-échelon, "non-conjugate") fault patterns may thus dominate in the foreland platforms of these orogenic belts, while pure share (symmetrical, "conjugate") faults-networks may be typical of the classical collisions (Fig. 24, inset).

The above-mentioned mechanisms tend to demonstrate that most, if not all anomalies of such landlocked structural domains as the Pannonian Basin (as well as other basinal or basement-controlled zones within and around the Alpine system) can be accounted for by applying simple adjustment-processes occurring at basement level and necessitating only minor displacements, without calling for large-scale (100 km-order) deformations implying recurring internal movements s.as block migrations, rotations of huge domains and multiple subduction zones.

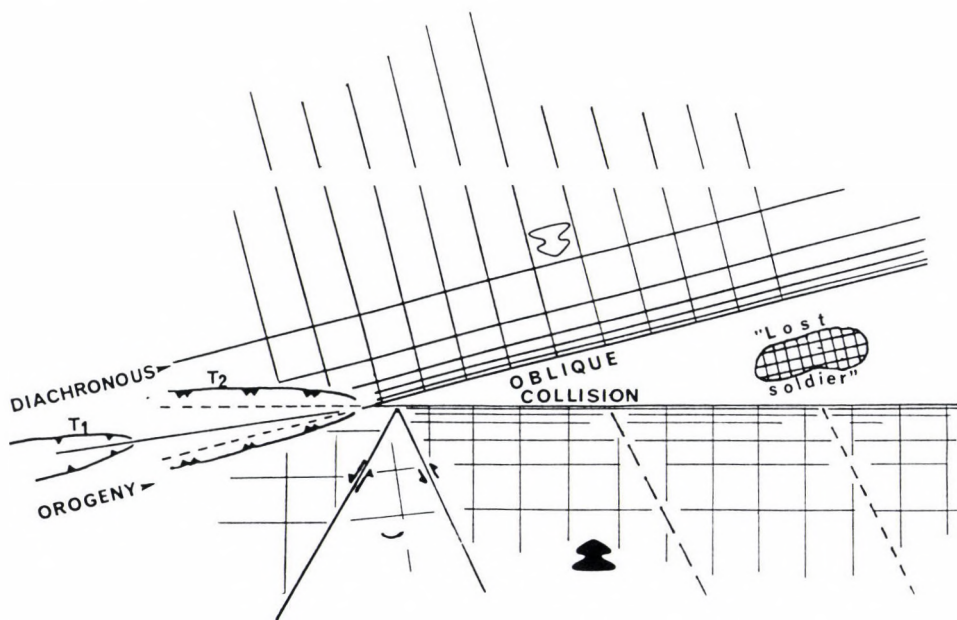


Fig. 27
Oblique collisions—diachronous orogenies

Evolution of the South European Margin, from Permian to present

The *South European Domain* has undergone several orogenic events during its evolution since Proterozoic times. The latest and best-known Alpine mountain-building period was thus superposed upon a basement of mostly Variscan (late Paleozoic: upper Carboniferous) age, which has included at least fragments of earlier orogenic belts. The European Alpine foldbelt is thus entirely contained within the limits of the Variscan (Hercynian) chain (Fig. 1). The existence of this Paleozoic complex is demonstrated by the presence of old massifs all along the "Alpine" foldbelt. In areas like the axial Pyrenees, the Little Carpathians in Western Slovakia or the Southern Carpathians in Romania, uplifted basement massifs bound by high-angle (wrench?) faults are the dominant elements. Furthermore, deep investigations (drilling, industrial and scientific seismic studies) carried out in basinal areas situated within the Alpine complex prove that the basins (with the exception of the Black Sea) all correspond to old basement mosaic-blocks (or clusters). Such intra-orogenic blocks carry a heritage compatible with that of the "cratons" situated outside of the Alpine belt itself. Thus, relatively quiet basement-dominated areas occupy approximately (at least) one half of the total surface of the South-European Alpine domain "*sensu lato*": the Po and Pannonian Basins, the Ebro Basin, etc. These tabular domains have undergone only minor shortening with moderate wrenching. Some of the basement blocks in these areas were affected by significant rotation (Mecsek Mts, blocks in the northern Pyrenees, Apulian Block etc.).

The east-west trending *Variscan belt* stretches between the Ural Mountains to the east and the Mauritanian-Appalachian belts to the west (Fig. 28a inset). Its northern edge is precisely known, while its southern limit is more speculative. It crosses northwestern Africa (no Variscan folds are known in Africa to the east of Tunisia or to the south of the Saharian hingeline), and continues eastwards along the northern edge of the "Paleo-Tethys", an ancient ocean-arm open to the East, which had not been closed during the late Paleozoic collisional events ("*Pangea*"). – The thickness of this old basement-complex might have been of the order of 30–40 km. It carried a structural fabric which influenced the later tectonic developments, both during the extensional and the compressive phases. In addition to fold- and thrust-structures it also included wrench-systems and was linked to rifts (aulacogens) which branched out into the neighbouring cratons to the north (Polish Trough, Don-Dnieper Aulacogen) and to the south (Ougarta system). The directions of these basement-features can also be detected inside the Alpine belt, suggesting a pre-existing, continuous basement-network which became consecutively deformed and disrupted in zones of maximal deformation (e.g. oceanized domains), but which were preserved in the more stable, internal platform domains. Some of the well-known "regional" basal faults cut across the recent foldbelts (NW and NE Carpathians; also Pyrenees and Western Alps) without showing very much offset. Most of the granites and much of the metamorphic

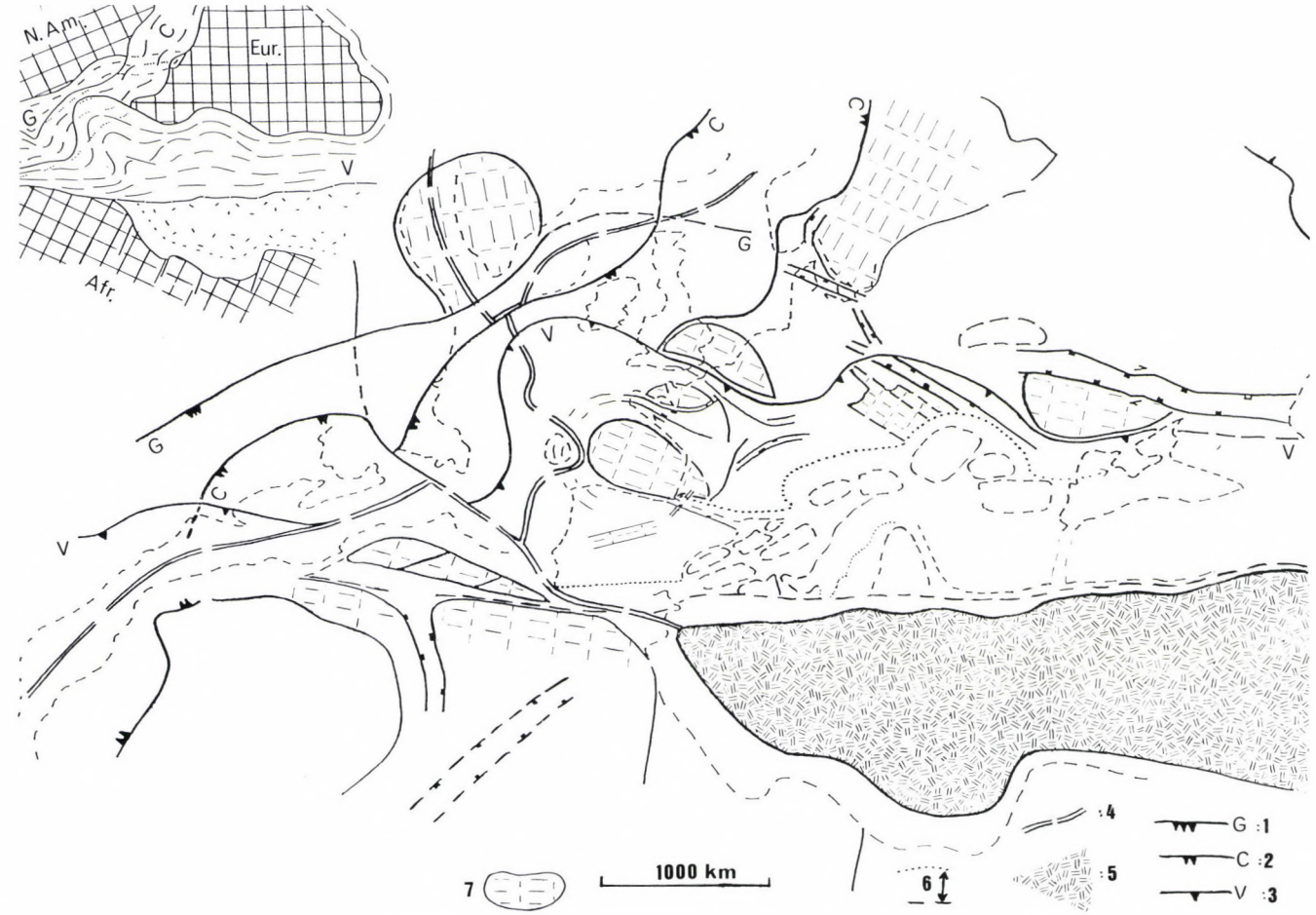


Fig. 28a
 Evolution of Southern Europe. Late Carboniferous ("Pangea fit"). 1. Grenville front; 2. Caledonian front; 3. Variscan front; 4. line of future continental break-up; 5. old oceanic basin; 6. South European Mobile Margin; 7. major old basement nuclei

complexes encountered in the Alpine foldbelt actually belong to this Variscan (and older) basement.

The *Alpine foldbelt* itself is limited to the south by a subduction complex only in its central segment: along the northern edge of the Eastern Mediterranean sea. To the east and the west continent-continent collision took place and the foldbelt abuts the North African and Arabian landmasses. The northern limit of the Alpine chain is formed by the stable European craton. This mostly Variscan foreland area underwent some deformation during the Mesozoic–Tertiary evolution too, in the form of basement block-faulting and related superficial folding, consecutive of minor wrenching (e.g. the Paris and Wessex Basins, the Jura foldbelt and the Rhine rift area).

Oceanic remnants are widespread within the Alpine belt, in form of pillow lavas, ophitic and ophiolitic masses. Although their present-day extent does not exceed a few percent of the total area, they may be representative of much larger domains, engulfed in depth during subductional events, or amalgamated into the basement-complex of strongly compressed zones. On the other hand, they may just as easily be remnants of only partially oceanized, restricted continental domains. The most important such ophiolitic zones are concentrated in the Balkans (Vardar zone), while the largest actually oceanized or oceanic area is evidently the Black Sea, which is surrounded by, or wedged into, the folded zones of the Alpine chain.

The *Mesozoic-Tertiary* (post-Carboniferous) evolution of the area has known two major tectonic periods: an extensional or transtensional period from Permian to middle Cretaceous (Fig. 28b), and a compressive – transpressive middle Cretaceous to present-day period (Fig. 28c).

During the *Permian-Triassic* epoch the entire North American–European–African supercontinent began to drift to the northwest, Pangea having been assembled (as well as broken up) in the Southern hemisphere (Irving 1977). Diffuse extension triggered rifting in the southern part of the relatively "fresh", post-Variscan zone, which corresponds to the present-day Alpine belt. Thus marine Permian sea arms radiated out to the north and northeast (i.e. in the northern Italian–South-Tyrolia domain and across the present-day Pannonian depression reaching northernmost Hungary, see Haas and Brezsnýánszky 1989). – Huge intracontinental sags were formed further inland (to the north the European Zechstein Basin and to the south the Saharan Triassic basin); the latter were connected to the oceanic domain through the Permian and Triassic rifts.

During the lowermost *Jurassic* the African block was cut off the rest and left behind, through the opening of the central Atlantic Ocean (Fig. 28b). The fragmentation along the trailing edge of the onward-moving South European passive margin proceeded, and an oceanic mega-shear zone was opened between the loosened Iberian–South European blocks on one side, and northwest Africa on the other. Since its very opening, the central Atlantic oceanic domain has been linked with the Tethys through this ocean arm. Due to the ongoing stretching of the southern, henceforth sheared margin of Europe (related to the dragging effect of

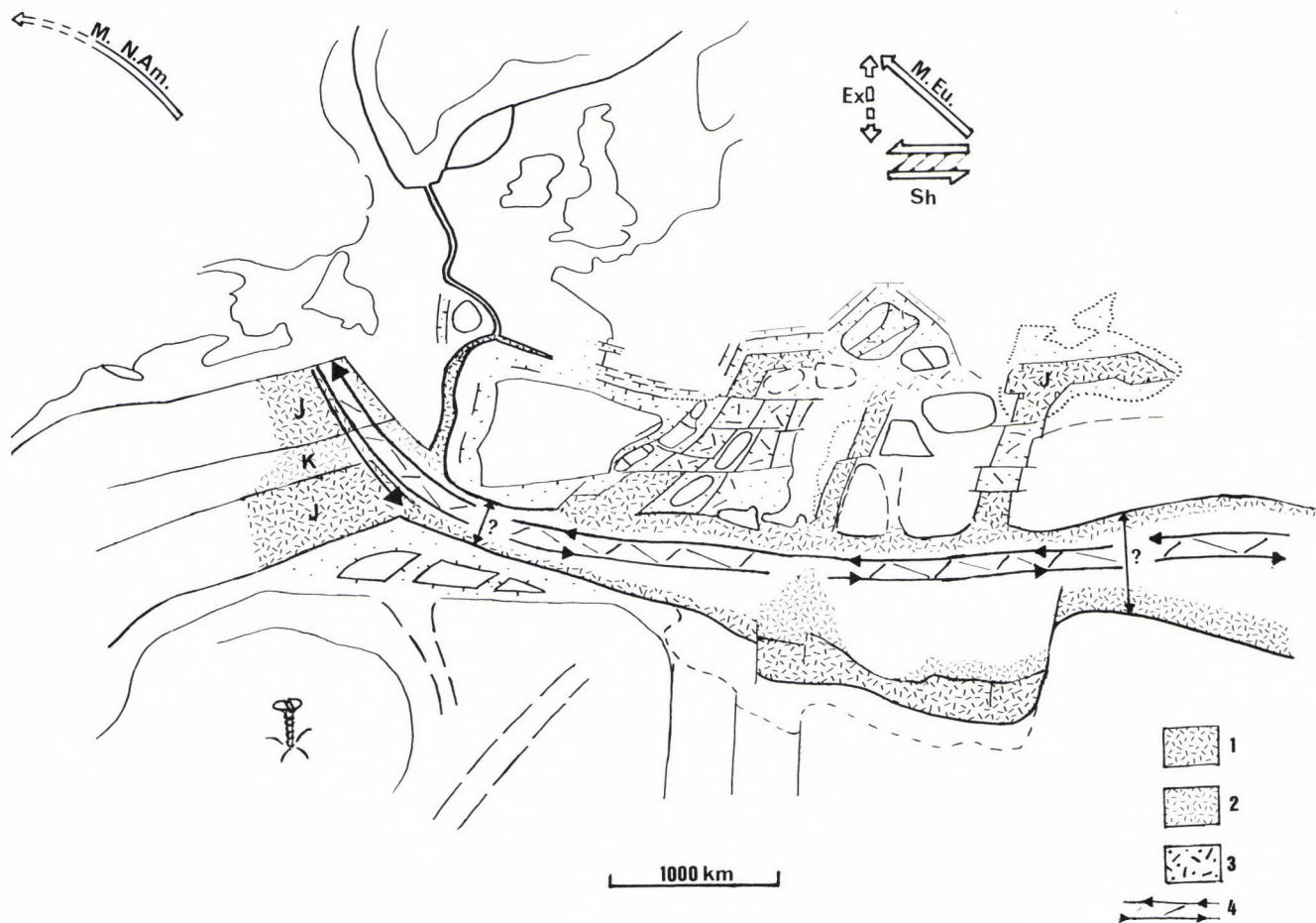


Fig. 28b

Evolution of Southern Europe. Permian to Lower Cretaceous ("break up") Oceanic basins. 1. Jurassic; 2. (Early) Cretaceous; 3. partial oceanization (mainly Jurassic?) 4. sinistral megashear; M.Eu. - Motion of Europa; Ex - Extension; Sh - Shearing; M.N.Am. - On-going motion of North America

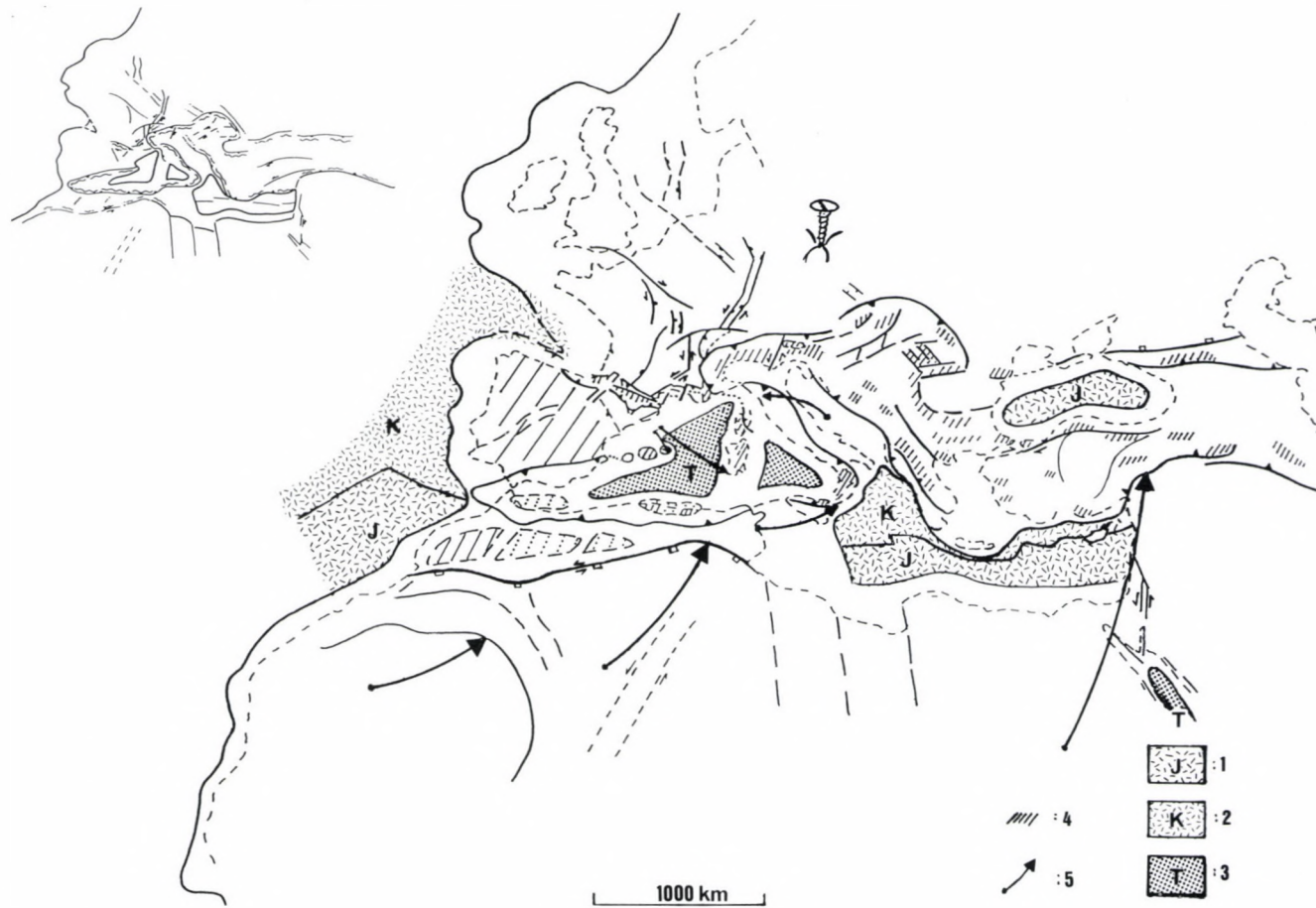


Fig. 28c

Evolution of Southern Europe. Mid-Cretaceous to present-day ("round up") Age of oceanic floor, 1. Jurassic; 2. Cretaceous; 3. Tertiary; 4. Paleozoic (Variscan) domains and nuclei; 5. motion of African plate. From Zolnai 1991;- Base maps: Carpathian-Balkan Association (1973), UNESCO (1976), and B.R.G.M. Emberger 1986 using Báldi-Beke and Báldi 1985; Pavoni 1961b; Irving 1977

the African plate?), deep NE-oriented oceanic rifts were split open, branching off the main NNW–SSE-oriented ocean-arm. The largest oceanic domain thus created during the Jurassic is the still present Black Sea; the more hypothetical Ligurian Ocean or Sea-arm might have been another. The main elements of the marginal mosaic pattern were thus emplaced, with relatively high-lying continental (or shallow-sea) plateaus separated by deep, stretched grabens or troughs some of which were oceanized. Each of these elements or zones developed their own sedimentary conditions. Some of the depressed "synclinal" zones, meandering across this paleogeographic pattern, correspond to the emplacement of the future fold-belts (Fig. 26b).

The *Jurassic-early Cretaceous* opening of the central Atlantic Ocean has resulted in a 1000+ kilometer (relative) easterly shift of Africa versus the South-European margin. Although this left-lateral movement has been partially compensated on the European side of the transform-system by the opening of the Jurassic rifts branching off the main ocean-arm (e.g. the Ligurian Sea/Ocean), the major part of the shearing must have been absorbed by the Tethys itself, since there is no evidence, and no space in the given framework, for the presence of oceanic domains of similar dimensions (1000 km width) in Southern Europe at this period. The main seaways have probably also been widened and deepened individually, during the lower to mid-Cretaceous period, as demonstrated by the appearance or presence of massive flysch deposits.

The first "Alpine folding" events are given as *mid-Cretaceous* (Albian?). Folds of this age could have also originated in response to the strong shearing and subsequent local block-rotations and local uplifts: "jammings" at the edges of the mobile domain (i.e. along the Central European stable margin which remained undeformed; the Carpathian Arch and the Pannonian domain, but also along the Pyrenean–Aquitaine boundary and the Southern Alps–Provence area). Such deformations ("Austrian phase") are not yet necessarily due to major, regional convergence or collision. Many of the structures within the Saharan Domain are dated Early- to Mid-Cretaceous, i.e. "pre-Alpine" (or early Alpine).

The dynamics of the system nevertheless radically changed during the (*Late*) Albian. Western Europe began to be split off the North American plate through the ongoing, progressive opening of the North Atlantic Ocean, while Africa began its north-easterly drifting. The sinistral shearing became more intense (North Pyrenean domain), while the South European loose blocks were pushed towards each other more strongly. This convergence resulted in further early-orogenic folds (e.g. Pyrenees during the Cenomanian). Part of this folding might also, however, been related to local block-adjustments, inducing uplifts and consequent gravity tectonics (Eastern Carpathians) as well as rifting and opening of pull-apart basins, with massive gravitational sedimentation (wildflysches in the Pyrenees).

The earliest plate-to-plate collision took place to the west, between Africa and Iberia, during the *Eocene* ("Pyrenean phase"). The diachronous orogenic wave propagated henceforth to the east. – The strongest orogenic event was in the *Miocene*, when collision occurred between Tunisia and Sicily. The Italian (Apulian

and Sicilian), blocks were hurt ("hooked") and pushed along by the north-easterly progression of North Africa; they were rotated anti-clockwise and violently pushed to the north. This sudden event led a) to the opening of the West Mediterranean oceanic basins, by the easterly migration (passive drift) of the Balearic, Corsican, and Sardinian blocks, and b) to the closure of the Ligurian "Ocean", through the strong push of Apulia towards the north, into the central Alpine domain. Blocks escaping to the west and the east in front of this *indenter* generated the West Alpine Arch, as well as contributed to the remobilization of vast foreland and intramountain areas (e.g. adjustments in the Paris–Wessex Basin, Vosges–Rhine–Black Forest areas; strong compaction of the Carpathian–Pannonian domain). – Ongoing ocean-continent collision compressed the Balkans, while the collision between the Arabian and Persian continental segments forced the Anatolian domain to escape to the west (Pavoni 1961b). – In a similar way the Iberian block was somewhat pushed to the west, regaining a position closer to that of its eastward displacement during the Albian.

The reactivation of the orogenic forelands occurred mainly in the wrenching mode. The "West European Rift System" (Rhine–Rhône–Valencia grabens and neighbouring uplifts) was generated through a left-lateral regional shear, while the Jura foldbelt gained its present-day geometry in the same general sinistral rearrangement of the foreland blocks (transpression). Secondary fold-structures were thus formed across the Ebro, Aquitaine and Paris–Wessex basins, in the Polish Trough and in the Central and Southern Atlasic domains etc. Some of these fault movements were practically continuous during the entire orogenic period (Eocene–Pliocene): Rhine–Rhône Grabens, faults within the Pannonian basin.

In the case of the Pannonian Basin the convergence of the continental blocks triggered internal wrench-movements, which on their turn caused block-rotations, relief inversions as well as on-going, coeval "paired" uplifts and basins. – The overall late-Miocene subsidence can, at least partially, be explained by extension due to the "push-apart" effects of rotating basement parquets, in both the Pannonian and Pô (intraorogenic) basins as well as in the Ebro (intracontinental) basin, in northern Spain. All these movements occurred in response to the Europe–Africa collision, which took place further to the south, the intensity of the movements decreasing from south to north (Fig. 29). – *In some areas however, the different orogenic mechanisms may have been combined and the resulting deformation effects (magnitudes) added.*

Conclusions

Within the huge South-European Mesozoic–Tertiary–Present-day (Alpine) orogenic belt several deformation mechanisms can be distinguished. The southernmost part of the central area (Eastern Mediterranean) is a still active subduction-zone. It is continued to the east and the west by two continent-continent collisional fold complexes, the earlier oceanic crust segments having been totally consumed. To the north of this collisional frontal belt, strong

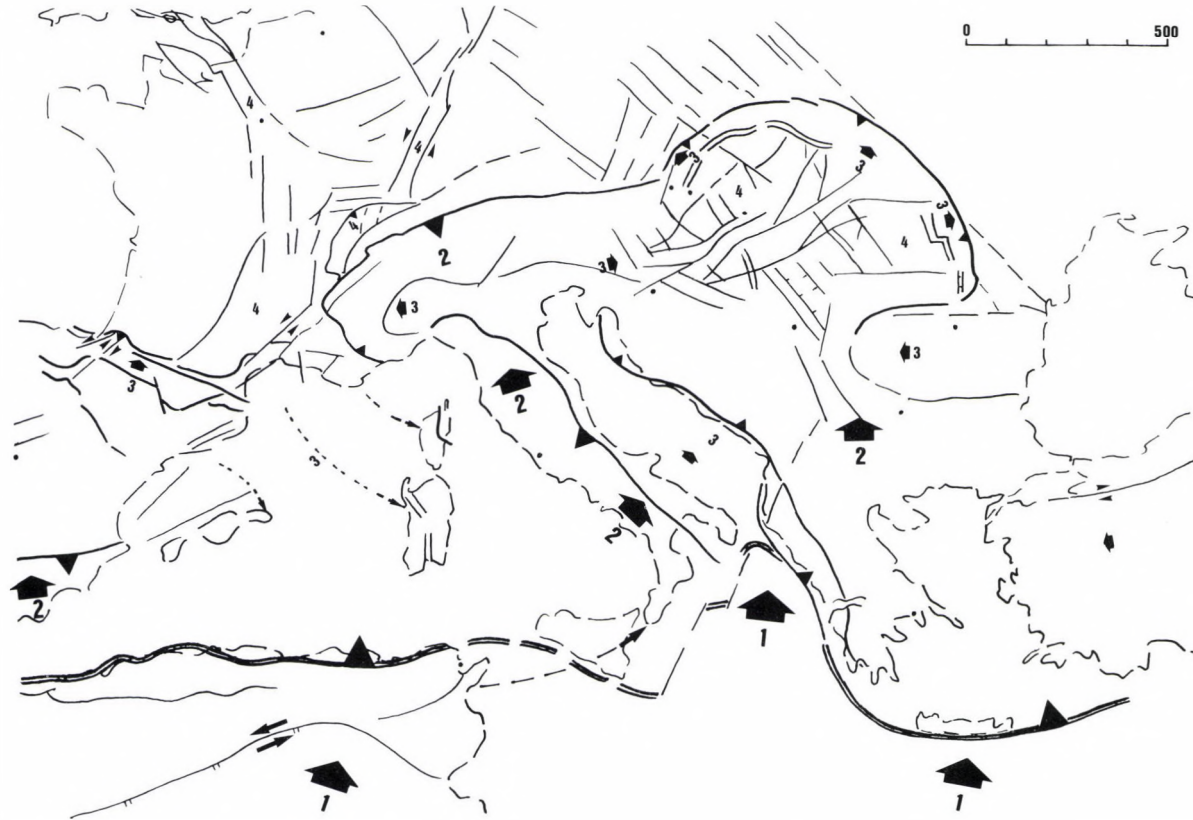


Fig. 29

Main movements during the Alpine orogeny in the South-European Domain. 1st order events (1000 km-order displacement): collision and subduction; 2nd order (100 km): large indenter of Italy–Apulia, triggering large overthrust systems: Northern Alps, Atlas Mountains; 3rd order (10 km): escaping blocks on both sides of indenter and convergent zones: Western Alps, Carpathians, Pyrenées Anatolia; 4th order (km): readjustment of continental blocks with wrenching and block-faulting; structural inversions of rifts and flysch-troughs, both superficial and deep. In some areas effects of various types of movements and deformation mechanisms may be combined and *added*

block-convergence issued the set of extremely complex, meandering orogenic foldbelts. Less mobile domains inside of the Alpine belt *sensu lato* were affected by internal shearing and consecutive, compressive block-faulting, which issued a set of imbricate structures. Close to the Central European platform margin, earlier rift-systems were inverted to form a now continuous folded flysch-belt. The klippen-belt has been emplaced by transpressive movements which affected a most mobile, most extended zone, thus extruding condensed deep-sea sediments as well as limestones of internal calcareous platforms.

The total regional orogenic shortening must have been of several hundreds of kilometers (or even more); it was preceded by extensional and/or lateral movements of similar magnitudes (Fig. 29). – There is no present-day evidence of major subduction zones inside of this broad belt (except for its southern active margin), and the basement nuclei within can be considered to have kept their *relative autochthonous position*.

The ophite/ophiolite "belts" can also result from only partial oceanization of some weakened (extended) segments of the continental crust, and are not necessarily indicators of earlier huge, continuous oceanic domains.

In the flysch belts the amount of convergence between continental blocks should not be much increased, only to make (satisfy) palinspastic reconstitutions. Balanced cross-sections are of little use in such zones of poor control in bed thickness and of no lateral competency of sediments. Inversion tectonics combined with wrenching and gravity flow may be more realistic. The clastic-filled grabens and rift-corridors having been stretched during earlier extensions, their weakened basement readily yielded to orogenic compression and/or transpression, without the amount of extension or compression being very strong.

In the basement-dominated areas between the mountain chains (Pannonian, Po, Ebro basins etc.) moderate, kilometer to ten-kilometer order basement wrenching can account for the observed superficial anomalies. Lateral shifts and consecutive, *in situ* block rotations thus resulted in basement uplifts and the emplacement of compressed and jammed "imbricate" structural units, rather than "nappe units". The local crustal convergence in these zones must not have exceeded the ten-kilometer magnitude either. The elements of the basement mosaic probably kept their relative positions during the structural evolution, although the distances between them and their individual orientations could have changed considerably. The present distribution of facies-belts is due to the extremely varied structural pattern during sedimentation, rather than to large-scale synorogenic lateral block-movements.

In the specific case of the Pannonian Basin, the dominant, recently rejuvenated "basic" NE-trending structural grain has only partly subdued another, NW-oriented basement fault group, which ties into the directions of the surrounding old ranges (Bohemia, Bihar), or that of the substratum of the Basin (Szeged area in Hungary and Eastern Slovakia). The long-lived Tertiary volcanism, as well as the distribution of seismicity follow the broken pattern of this basic fracture-network (NE, NW and E–W orientations) which also

formed a set of rectangular and rhomb-shaped blocks (e.g. Eastern Carpathians–Hargita area). Neither Tertiary volcanism nor present-day seismicity need to be subduction-related: no true structural arcs and no Benioff surfaces can be demonstrated within the Carpathian arch, itself a neotectonic envelope.

The foreland of the Carpathians forms a huge half-circle between Vienna and Brasov, which is remarkably continuous and relatively undisturbed. This precludes a theoretical "centripetal" (*per se* extremely unlikely) subduction of the old, thick, consolidated platform (craton) -margin under the more mobile, Pannonian basin (once a hypothetical oceanic basin, filled up by Mesozoic–Tertiary sediments and later pushed aside, or overridden by allochthonous terrane of southwesterly provenance). Such mechanisms would indeed necessitate major radial adjustments, as well as peripheric, hemi-circular compressions within the cratonic foreland, with consecutive deformations which are not present.

The above approach may help to establish a simpler structural framework and evolution model, especially useful for realistic, everyday exploration activity. Future synthesis work should aim at the elaboration of a genuine, specific model for the area, emphasizing the role of the early geological evolution: the heritage, and applying basement-tectonic mechanisms in basement-dominated areas, restraining the compressive "alpine" fold-mechanisms to those (limited) belts where major convergence actually took place.

References

- Báldi-Beke, M., T. Báldi 1985: The evolution of the Hungarian Paleogene Basins. – Acta Geol. Hung., 28, 1–2, pp. 5–28.
- Bourrouilh, R., JP. Richert, G. Zolnai 1995: The North Pyrenean Aquitaine Basin, France: Evolution and Hydrocarbons. – A.A.P.G. Bull., 79–6, pp. 831–853.
- B.R.G.M. 1986a (Bureau de Recherches Géologiques Géophysiques et Minières): Geological and Tectonic base maps of western Europe, scale 1 : 5 000 000, by A. Autran, A. Prost (unpublished documents).
- B.R.G.M. 1986b: Principaux gîtes minéraux de l'Europe et des pays limitrophes; scale: 1 : 18 750 000, compiled by A. Emberger.
- B.R.G.M. 1980: Carte Tectonique de la France, scale 1 : 1 000 000, J. Chiron coord.
- Carpathian–Balkan Association 1976: Tectonic Map of the Carpathian-Balkan mountain System and adjacent areas; scale 1: 1 000 000. – Tectonic commission, ed. M. Mahel. Edited by Geol. Institut. in Bratislava and UNESCO, Paris.
- Cook, D. 1983: The Northern Franklin Mountains, N.W.T., Canada – a scale model of the Wyoming Province. – Rocky Mtn. Assoc. Geol., J.D. Lowell, R. Griess eds: "Rocky Mountain Foreland Basins and Uplifts", Denver, pp. 315–338.
- Dahlstrom, C.D.A. 1970: Structural geology in the eastern margin of the Canadian Rocky Mountains. – Bull. Canad. Petr. Geol., 18, pp. 332–406.
- Dawes P.R., J.W. Kerr eds 1982: Nares Strait and the drift of Greenland: a conflict in plate tectonics. Meddeleser om Groenland. – Geoscience 8, 392 p, Odense, Denmark.
- Debelmas J., editor 1974: Géologie de la France. – 2 vols, 544 p, Doin, Paris.
- Deichman, N. 1992: Structural and rheological implications of lower-crustal earthquakes below northern Switzerland. – Physics of the Earth and Planetary Interiors, 69, pp. 270–280, (Note: Elsevier Science–NL kindly authorized the reproduction of one figure by N. Deichman 1992)

- Forman, D.J., D.W. Wales 1981: Geological evolution of the Canning Basin, Western Australia. – B.M.R., Bull. 210.
- Fülöp J. 1989: Bevezetés Magyarország geológiájába (Introduction to the geology of Hungary). – Akadémiai Kiadó, Budapest, 246 p.
- Fox, F.G. 1985: Structural geology of the Parry Island fold belt (Arctic Canada). – Bull. Can. Petr. Geol., 33–3, pp. 306–340.
- G.S.C. (Geological Survey of Canada), H.P. Trettin (Ed.) 1991: Geology of the Innuitian Orogen and Arctic Platform of Canada and Greenland. – "Geology of North America Vol. E" - "Geology of Canada no. 3", 569 p.
- Haas, J., K. Brezsnýánszky 1989: Maps and explanatory notes from the Hungarian Geological Institute, MÁFI.
- Haller, D., G. Hammon 1993: Meillon–St Faust gas field, Aquitaine basin. – In: J.R. Parker ed. Petroleum geology of north-west Europe: Proc. of 4th Conf. Geol. Soc. of London, pp. 1519–1526.
- Henry, G. 1969: Essai d'application des lois de la viscosité à la tectonique du flysch Aquitain. – Bull. du Centre de Rech. de Pau-SNPA, 3–1, pp. 65–98.
- Henry, J. 1968: Vallée d'Ossai. – In: Itinéraires d'initiation à la géologie des Pyrénées, éd. S.N.P.A. (Société Nationale des Pétroles d'Aquitaine) 17 p.
- Sandulescu, M., M. Muresan, G. Muresan 1975: Harta Geologica, Romania, 47d : Damuc, scale 1 : 50 000. Institut de Geologie si Geofizika, Bucharest.
- Irving, E. 1977: Drift of the major continental blocs since the Devonian. – Nature, 270, pp. 304–309.
- Kerr, J.W. 1980: Structural framework of Lancaster Aulacogen, arctic Canada. – Geol. Surv. of Canada, Bull. 319.
- Laubscher, H. 1985: Section through the eastern Jura mountains. – In: R. Trümpf (Ed.): Geology of Switzerland. Schweizerische Geol. Komm., pp. 1–104.
- Mattauer, M. 1980: Les déformations des matériaux de l'écorce terrestre. – Hermann Paris, 493 p. pp. 272–284.
- McMechan, M.E., R.I. Thompson 1989: Structural Style and History of the Rocky Mountain Fold and Thrust Belt. – In: Western Canada Sedimentary Basin, A case history (B.D. Ricketts editor), Canadian Society of Petroleum Geologists, Calgary, pp. 47–71.
- Molnar, P., P. Tapponier 1975: Cenozoic Tectonics of Asia: Effects of a Continental Collision. – Science, 189, pp. 419–426.
- Monger J.W.H. 1989: Overview of Cordilleran Geology. – In: Western Canada Sedimentary Basin. A case history (B.D. Ricketts ed.) C.S.P.G., pp. 9–32.
- Muehlberger W.R. 1986: Different slip senses of major faults during different orogenies: The Rule?. – In: Proc. 6th Int. Conf. on Basement Tectonics, pp. 76–81.
- Odonne, F., P. Viallon 1983: Analogue models of folds above a wrench fault. – Tectonophysics, 99, pp. 31–46.
- Pavoni, N. 1961a: Faltung durch Horizontalverschiebung. – Ecl. Geol. Helv., 54–2, pp. 515–534.
- Pavoni, N. 1961b: Die nordanatolische Horizontalverschiebung. – Geol. Rundsch., 51, pp. 122–132.
- Riedel, W. 1929: Zur Mechanik geologischer Brucherscheinungen. – Zentralblatt Min. Geol. Pal., – Abt. B.
- Rolet, J. 1984: Graben losangiques (pull-apart) en régime de décrochement. Le rôle des coulissements hercyniens dans l'individualisation des bassins carbonifères du Massif Armoricaïn. – Ann. Soc. Géol. Nord, CIII, pp. 209–220.
- Roure F., P. Choukroune, X. Berastéguy, J.A. Munoz, A. Villien, P. Matheron, M. Bareyt, M. Séguret, P. Camara, J. Deramond 1989: "ECORS" ("Etude de la croûte continentale et océanique par réflexion et réfraction sismiques") deep seismic data and balanced cross sections: geometric constraints on the evolution of the Pyrenees. – Tectonics, 8–1, pp. 41–50.
- Royden, L.H., F. Horváth (eds) 1988: The Panonian Basin – a study in basin evolution. – A.A.P.G. Memoir, 45, 394 p.

- Ruhland, M. 1972: Le rôle des décrochements dans le socle vosgien en bordure du Fossé Rhénan. – In: "Approaches to Taphrogenesis", proc. of Intern. Rift Symp., Karlsruhe, pp. 167–171.
- UNESCO – Commission for the Geological Map of the World 1976: Geological World Atlas scale 1 : 10 000 000, coordinators: G. Choubert and A. Faure-Muret
- U.S.G.S. – B. King, G.J. Edmonston 1972: Generalized tectonic map of North America, scale: 1: 15 000 000.
- Walper, J.L. 1977: Paleozoic tectonics of the southern margin of North America. – Proc. of the Gulf Coast Assoc. Geol. Soc., 27th ann. mtg., Austin (Tex.) pp. 230–241.
- Wegman, E. 1961: Anatomie comparée des hypothèses sur les plissements de couverture (le Jura plissé). – Bull. Geol. Institut. Univ. Uppsala (Sweden), 40, pp. 169–182.
- Wells, A.T., D.J. Forman, L.C. Ranford, P.J. Cook 1970: Geology of the Amadeus Basin, Central Australia. – B.M.R. (Bureau of Mineral Resources, Canberra – Australia), Bull. 100.
- Zolnai, G. 1971: Le front Nord des Pyrénées Occidentales. – In: Histoire Structurale du Golfe de Gascogne, 1, pp. 1–9, Editions Technip, RUEIL-MALMAISON.
- Zolnai, G. 1975: Sur l'existence d'un réseau de failles de décrochement dans l'avant-pays Nord des Pyrénées Occidentales. – Rev. Geogr. Phys. Géol. Dyn. XVII–3, pp. 219–238.
- Zolnai, G. 1986: Les Aulacogènes du Continent nord-américain. – Bull. Soc. Géol. France, 81, 5, pp. 809–818.
- Zolnai, G. 1991: Continental Wrench Tectonics and Hydrocarbon Habitat. – A.A.P.G. Cont. Educ. Course Note Ser. 30, 2nd ed. 286 p.



PRINTED IN HUNGARY
Akadémiai Kiadó és Nyomda, Budapest

GUIDELINES FOR AUTHORS

Acta Geologica Hungarica is an English-language quarterly publishing papers on geological topics. Besides papers on outstanding scientific achievements, on the main lines of geological research in Hungary, and on the geology of the Alpine–Carpathian–Dinaric region, reports on workshops of geological research, on major scientific meetings, and on contributions to international research projects will be accepted.

Only original papers will be published and a copy of the Publishing Agreement will be sent to the authors of papers accepted for publication. Manuscripts will be processed only after receiving the signed copy of the agreement.

Manuscripts are to be sent to the Editorial Office for refereeing, editing, in two typewritten copies, on floppy disk with two printed copies, or by E-mail. Manuscripts written by the following word processors will be accepted: MS Word, WordPerfect, or ASCII format. Authors are requested to sign and send to the Editor a Publishing Agreement after the manuscript has been accepted by the Editorial Board. Acceptance depends on the opinion of two referees and the decision of the Editorial Board.

Form of manuscripts

The paper complete with abstract, figures, tables, and bibliography should not exceed 25 pages (25 double-spaced lines with 3 cm margins on both sides).

The first page should include:

- the title of the paper (with minuscule letters)
- the full name of the author
- the name of the institution and city where the work was prepared
- an abstract of not more than 200 words
- a list of five to ten key words
- a footnote with the postal address of the author

The SI (System International) should be used for all units of measurements.

References

In text citations the author's name and the year of publication between brackets should be given. The reference list should contain the family name, a comma, the abbreviation of the first name, the year of publication, and a colon. This is followed by the title of the paper. Paper titles are followed – after a long hyphen – by periodical title, volume number, and inclusive page numbers. For books the title (English version), the name of the publisher, the place of publication, and the number of pages should be given.

Figures and tables

Figures and tables should be referred to in the text. Figures are expected in the size of the final type-area of the quarterly (12.6 x 18.6) or proportionally magnified 20–25% camera ready quality. Figures should be clear line drawings or good quality black-and-white photographic prints. Colour photographs will also be accepted, but the extra cost of reproduction in colour must be borne by the authors (in 1995 US\$ 260 per page). The author's name and figure number should be indicated on the back of each figure. Tables should be typed on separate sheets with a number.

Proof and reprints

The authors will be sent a set of proofs. Each of the pages should be proofread, signed, and returned to the Editorial Office within a week of receipt. Fifty reprints are supplied free of charge, additional reprints may be ordered.

Contents

Early Alpine shelf evolution in the Hungarian segments of the Tethys margin. <i>J. Haas, S. Kovács, Á. Török</i>	95
Contribution to the Upper Triassic geology of the Keszthely Mountains (Transdanubian Range), western Hungary. <i>G. Csillag, T. Budai, L. Gyalog, L. Koloszár</i>	111
Different types of orogens and orogenic processes, with reference to Southern and Central Europe. <i>G. Zolnai</i>	131

307216

Acta Geologica Hungarica

VOLUME 38, NUMBER 3, 1995

EDITOR-IN-CHIEF

J. HAAS

EDITORIAL BOARD

**GY. BÁRDOSSY (Chairman), G. CSÁSZÁR, G. HÁMOR,
T. KECSKEMÉTI, GY. PANTÓ, GY. POGÁCSÁS,
T. SZEDERKÉNYI, Á. KRIVÁN-HORVÁTH (Co-ordinating Editor),
H. M. LIEBERMAN (Language Editor)**

ADVISORY BOARD

**K. BIRKENMAJER (Poland), M. BLEAHU (Romania),
P. FAUPL (Austria), M. GAETANI (Italy), S. KARAMATA (Serbia),
M. KOVAČ (Slovakia), J. PAMIĆ (Croatia)**



Akadémiai Kiadó, Budapest

ACTA GEOL. HUNG. AGHUE7 38 (3) 185-283 (1995) HU ISSN 0236-5278

ACTA GEOLOGICA HUNGARICA

A QUARTERLY OF THE HUNGARIAN ACADEMY OF SCIENCES

Acta Geologica Hungarica publishes original studies on geology, crystallography, mineralogy, petrography, geochemistry, and paleontology.

Acta Geologica Hungarica is published in yearly volumes of four numbers by

AKADÉMIAI KIADÓ

Publishing House of the Hungarian Academy of Sciences

H-1117 Budapest Prielle Kornélia u. 19-35

Manuscripts and editorial correspondence should be addressed to the

ACTA GEOLOGICA HUNGARICA

Dr. János Haas

Academical Research Group, Department of Geology, Eötvös Loránd University of Sciences

H-1088 Budapest, Múzeum krt. 4/a, Hungary

E-mail: haas@ludens.elte.hu

Orders should be addressed to

AKADÉMIAI KIADÓ

H-1519 Budapest, P.O. Box 245, Hungary

Subscription price for Volume 38 (1995) in 4 issues US\$ 92.00, including normal postage, airmail delivery US\$ 20.00.

Acta Geologica Hungarica is abstracted/indexed in Bibliographie des Sciences de la Terre, Chemical Abstracts, Hydro-Index, Mineralogical Abstract

© Akadémiai Kiadó, Budapest 1995

AKADÉMIAI KIADÓ
HUNGARICA
1995

Data on the (Upper Permian) Foraminifer fauna of the Nagyvisnyó Limestone Formation from borehole Mályinka-8 (Northern Hungary)

Anikó Bérczi-Makk
MOL Plc, Budapest

László Csontos
Department of Geology, Eötvös Loránd University

Pál Pelikán
Hungarian Geological Institute, Budapest

The object of borehole Mályinka-8 was the study of the youngest (Djulfian–Midian) layers of the Northern Hungarian Nagyvisnyó Limestone Formation, which is overlain by the Gerennavár Limestone Formation. This upper part of the Nagyvisnyó Limestone Formation (Leptodus Member, Upper Mihalovits Member) is the equivalent of the *Bellerophon*-bearing layers of the Southern Alps and Dinarides.

The present paper reviews the results from the study of the species- and specimen-rich foraminifer fauna occurring alongside the biostratigraphically significant and rich algae, as well as ostracod and brachiopod remnants. In the foraminifer association, the species of the genus *Hemigordius* are the most frequent taxa: *Hemigordius abadehensis* Okimura et Ishii, *H. bronnimanni* Altiner, *H. giganteus* nov. sp., *H. guvenci* Altiner, *H. hungaricus* nov. sp., *H. mályinkai* nov. sp., *H. minutus* Pronina, *H. cf. reicheli* Lys, *H. zaninettiae* Altiner.

Key words: Foraminifer, taxonomy, biostratigraphy, Upper Permian, Djulfian–Midian, Bükk Mountains, Northern Hungary

Introduction

Borehole Mályinka (Má)-8 was drilled by the Hungarian Geological Institute (MÁFI) in 1982, on the northeastern margin of Mount Kemesnye (SE of Mályinka, Bükk Mountains; Fig. 1). It encountered the youngest layers of the Nagyvisnyó Limestone Formation and the type section of the Gerennavár Limestone Formation (Pelikán 1985; Haas et al. 1986, 1987). The palaeontological investigations performed for the borehole report described the rich ostracod material (Kozur 1985a), the algae as rock-forming components (Piros 1985), and the foraminifer assemblage (Bérczi-Makk 1985, 1987, this paper). A microfacies analysis was also carried out on the basis of thin sections (Csontos et al. 1983).

In borehole Mályinka-8, the upper part of the ca. 250 m thick Nagyvisnyó Limestone Formation (the Leptodus Member and the Upper Mihalovits

Addresses: A. Bérczi-Makk: H-1039 Budapest, Batthyany u. 45, Hungary

L. Csontos: H-1088 Budapest, Múzeum krt. 4/A, Hungary

P. Pelikán: H- 1143 Budapest, Stefánia út 14, Hungary

Received: 30 September, 1992

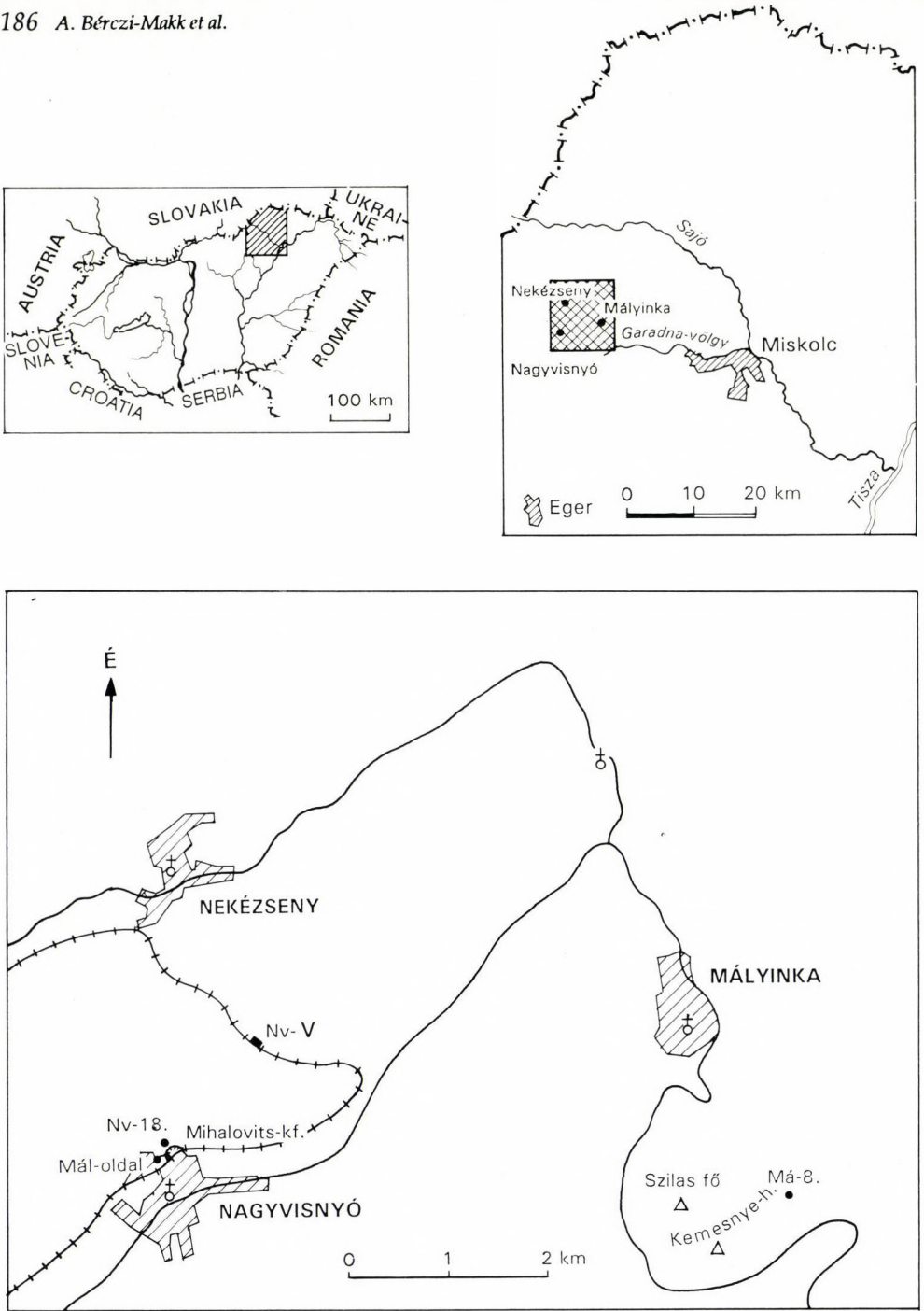


Fig. 1
Sketch map of borehole Mályinka-8 (Má-8)

Member, an equivalent of the *Bellerophon*-bearing layers of the Southern Alps and Dinarides) was described for the first time (Fülöp 1994).

The foraminifer assemblage, found together with a rich ostracod and brachiopod fauna of biostratigraphic significance, is also characterised by a great number of species and specimens. The study of this association was performed within the framework of the National Key Section Programme in 1984. The present paper includes the results of this work, dealing in greater detail with the taxonomic problems of the genus *Hemigordius*.

The authors would like to make use of this opportunity to express their thanks to late Dr. József Fülöp and to Dr. Pál Pelikán for making available the thin section sets from the borehole.

Stratigraphy

A. Lithostratigraphy (after Pelikán, P., 1985, with supplements)

In the unit underlying the Gerennavár Limestone Formation, borehole Mályinka-8 penetrated the youngest (Djulfian–Upper Midian) layers of the Northern Hungarian Nagyvisnyó Limestone Formation between 79.8 and 222.1 m (Fig. 10). Its composition (limestone, marly limestone, calcareous marl, marl) originated from alternating mixtures of calcareous and terrigenous clasts accumulated in a restricted shallow sea, bay or lagoon, a poorly ventilated, highly reducing development with high organic content, rich in pyrite, and thus indicating an anoxic environment. The rock owes its black colour to the fact that the accumulated organic matter had not been oxidised as a consequence of rapid burial and the lack of the oxidising currents.

The subdivision of the Upper Permian Nagyvisnyó Limestone in the borehole was made on the basis of the field macroscopic observations (after Pelikán, 1985):

79.8–89.5 m: dark grey, in some parts brownish, elsewhere black limestone, highly fractured, rich in fossils;

89.5–127.0 m: black limestone, often with slab jointing, with black calcareous intercalations and a rich fossil assemblage;

127.0–142.0 m: strongly tectonized, black brecciated limestone, with folded clay bands and red-brown marl intercalations, very poor in fossils;

142.0–162.0 m: a series consisting of alternating black limestone with marl streaks and black marl layers dipping at 20–30°. Rich coral fauna occurs in certain horizons (149 m);

162.0–168.0 m: unevenly distributed, tectonically disturbed dark grey limestone with red-brown spots, almost totally free of fossils;

168.0–222.0 m: black limestone with finely stratified black calcareous marl, marl, clay marl intercalations and rich fossil associations; in certain levels (202.5–209.3 m) with nodular marly limestone intercalations; the dip of the layer varies between 5 and 30°;

221.1 m (bottom of the borehole): black, calcareous marl

Among the petrologic features observable in thin sections the following are worth mentioning (after Csontos et al. 1983): orientation, pyritization, recrystallization, feldsparitization, silicification, stylolitization.

A definite orientation in the texture indicative of currents is frequent and characteristic. It is mainly due to the orientated position of alga stems and the lenticular arrangement of some components (mainly echinoderm shell fragments, e.g. 104.5 m, 105.5 m, 107.0 m, 107.5 m, 109.5 m, 110.0 m, 121.0 m, 133.5 m, 142.5 m, 178.5 m, 184.0 m, 203.0 m, 205.0 m, and 207.5 m). In other cases (e.g. 130.5 m, 140.0 m) the texture of the rock becomes orientated as a result of compressive tectonics.

Pyritization is a general phenomenon in the sequence. Pyrites occur in disseminated form (e.g. 86.0 m, 90.4 m, 95.5 m, 161.0 m, 179.0 m, 220.0 m) or in cube crystal form (e.g. 96.0 m; 143.0 m, 202.5 m). The black colour of the host rock (mostly shale) indicates high organic content as well as a poorly ventilated environment.

Recrystallization to a considerable degree can be found, mainly in heavily tectonized zones. As a consequence of intensive tectonic movements the rock is highly fractured. The fractured nature is a factor promoting recrystallization. The recrystallization of the Upper Permian sequence of borehole Mályinka-8 is of greater extent than in the limestones around Nagyvisnyó. Doubtlessly, this is due to the more intensive tectonic movements and denser crack network.

In some cases (e.g. 132.0 m, 132.5 m, 155.0–157.5 m) a remarkable amount of epigenetic feldspar appears in the micritic matrix, which is rich in small biogenic fragments. Feldspars occur in an idiomorphic crystal form with sharp edge.

Silicification is a frequent phenomenon. It predominantly affects the shells of ostracods, brachiopods, and among the algae, the vermiporellae, as well as the outer part of shell walls of taxa belonging to the genus *Hemigordius*, among the foraminifera. The silicified shell wall is of fibrous structure. Silicification is a phenomenon always spreading from outside inward and occurring over several generations. It can be complete or partial (Pl. XVI, Fig. 3; Pl. XVII, Fig. 5; Pl. XIX, Fig. 4; Pl. XX, Figs 1–2; Pl. XXI, Fig. 3) and may form an outer covering crust (Pl. XXII, Figs 1, 5).

In some places (126.8–131.0 m; 187.4–189.2 m) the rock is entirely interspersed with stylolites. Stylolitization perpendicular to stratification is the general rule.

B. Biostratigraphy

The biostratigraphic evaluation is based on the foraminifer fauna in 265 thin sections from the Upper Permian series. In general, thin sections were made of samples taken every half metre.

At 79.8 m in the borehole, the boundary of the Gerennavár Limestone and the Nagyvisnyó Limestone is marked by sharp lithological and microfaunal change.

The Earlandia microfacies (Bérczi-Makk 1987), of the greyish-brown to yellowish-brown, marl-banded limestone (Gerennavár Limestone Formation) penetrated in the bed directly overlying the Nagyvisnyó Limestone, between 75.5 and 79.8 m ("transitional" layers), indicates a depositional environment unfavourable for foraminifers. On the basis of the ostracod investigations, Kozur (1985a, b) assigns the part of the "transitional" limestone strata between 76.50 and 79.45 m to the *Indivisia buekkensis* zone of the uppermost Changxingian stage. According to him, however, the sudden lithological and microfaunal change between 79.45 and 79.80 m can be explained by a paraconformity (lack of Lower and Upper Changxingian). The lack of *Palaeofusulina* species may also indicate this.

Beneath the "transitional" layers, from 79.80 m to T.D., an Upper Permian series (Nagyvisnyó Limestone Formation) consisting of black limestone with calcareous marl and marl intercalations and characterised by a species- and specimen-rich foraminifer assemblage is known. The Nagyvisnyó Limestone in the borehole is made up of sediments deposited in a poorly ventilated, mostly restricted bay or lagoon, and exposed to currents of varying energy of a relatively shallow-water sea. On the basis of the rich benthic fossil association, the sea-floor may not have been of an extremely anoxic facies.

Among the small foraminifers of the Upper Permian, the species of the genus *Colaniella*, of biostratigraphic significance from the point of view of separating the Permian and Triassic periods, are almost totally missing from the borehole at Mályinka. Only one specimen belonging to the group *Colaniella minima* (96 m; Pl. I, Fig. 12) has been found, which however tends more toward the older Djulfian layers.

The *Palaeofusulina* species indicating the youngest (Changxingian) horizon of Upper Permian or a younger horizon of Djulfian (Dorashamian) age are totally missing from the sequence at Mályinka. However, within the area of Tethys (Kotlyar et al. 1991), among the *Codonofusiella* species characteristic of the Djulfian stage *Codonofusiella nana* Erk is widely distributed in the upper horizons (84.0–127.0 m) of the penetrated Nagyvisnyó Limestone.

The Nagyvisnyó Limestone of borehole Mályinka-8 can be divided into three parts on the basis of the foraminifer fauna (Fig. 2):

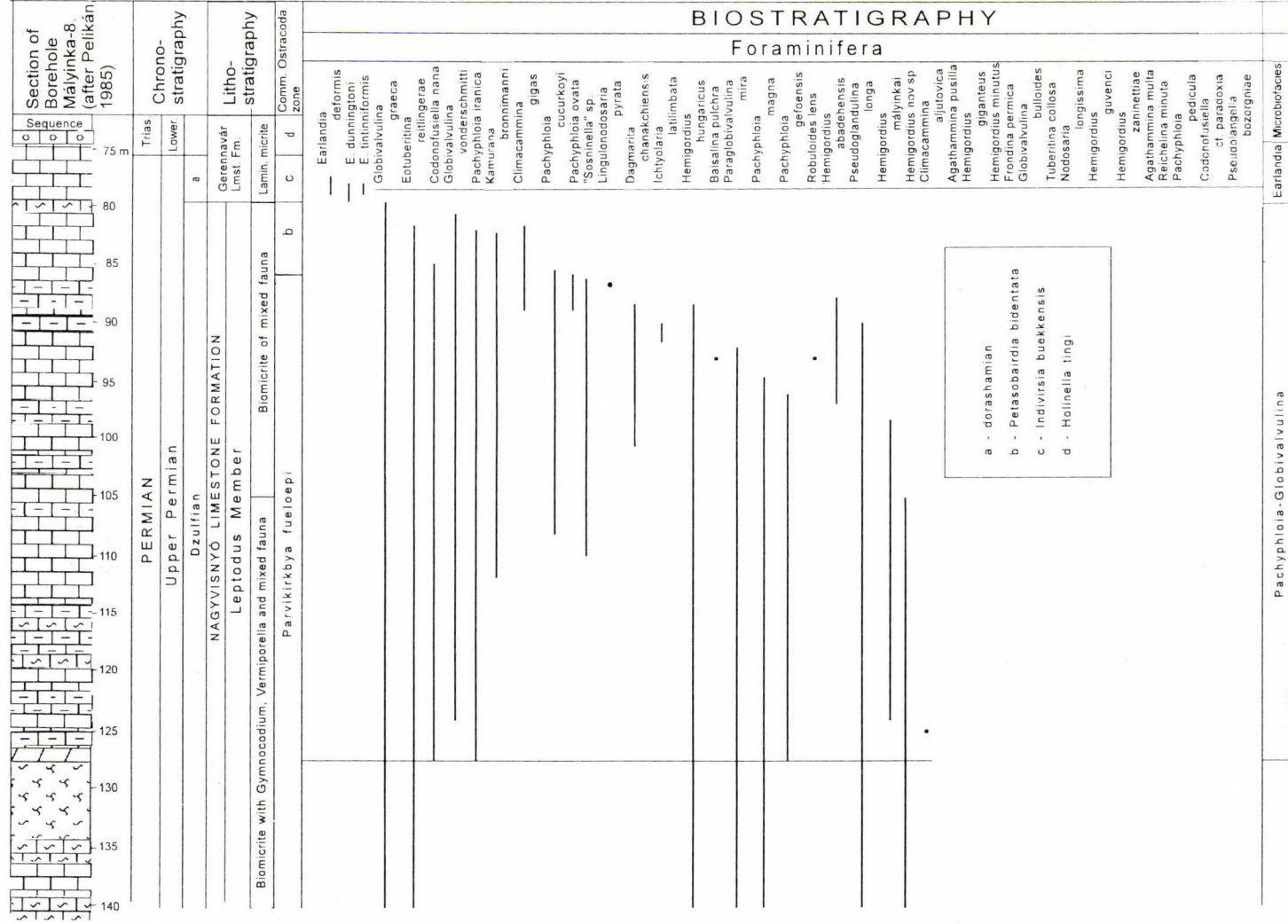
79.8–127.0 m (pachyphloia–globivalvulina microfacies)

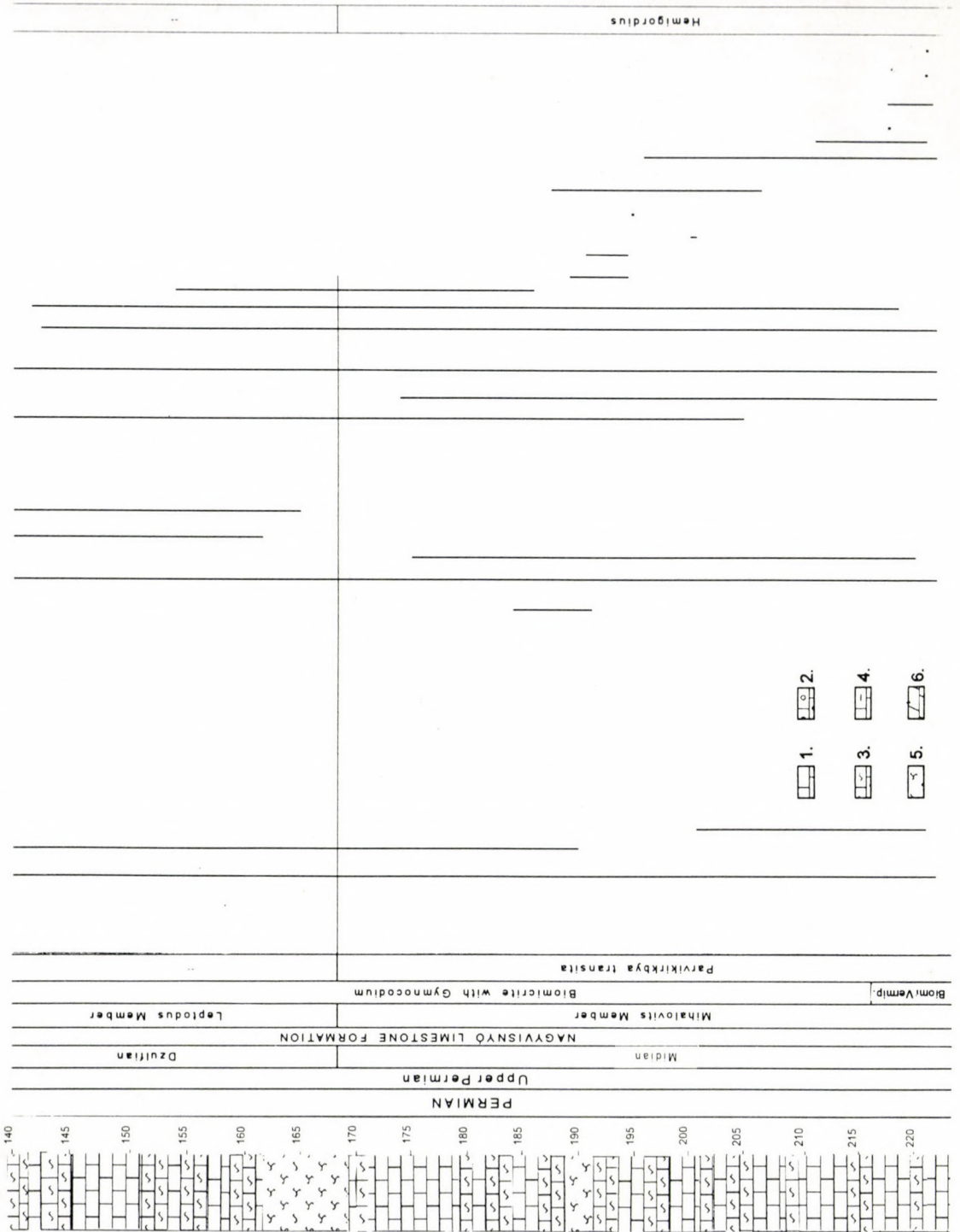
This is the horizon richest in fossils. Calcareous algae are widespread, the species of the individual genera (*Gymnocodium*, *Permocalculus*, *Vermiporella*) are represented by a great number of specimens. In the fossil association the most characteristic feature is the mass presence of brachiopod spines and shell fragments.

The foraminifer fauna is rich in species and specimens and is characterised by the frequency of the species of the genera *Pachyphloia*, *Globivalvulina*, *Climacammina*, and *Hemigordius*.

Fig. 2

Distribution of the Upper Permian foraminifer fauna of borehole Mályinka-8. 1. limestone; 2. ooidal limestone; 3. calcareous marl; 4. clay-banded limestone; 5 syngenic limestone breccia; 6. dolomite; a





The species *Climacammina major* Morozova and *Climacammina gigas* Sulejmanov are known from the younger layers (79.8–95.0 m) of the Nagyvisnyó Limestone, and are missing in the older Upper Permian ones.

Specimens of *Lingulonodosaria pyrula* (Sell. Civr. et Dess.) have been found exclusively in the youngest Upper Permian series (86.5 m) of the borehole.

The most frequent species are the following: the *Pachyphloia* species (*Pachyphloia cucurköyi* Sell. Civr. et DESS., *Pachyphloia gefoensis* (Mikl.-Makl.), *Pachyphloia iranica* Bozorgnia, *Pachyphloia ovata* Lange, and *Pachyphloia schwageri* Sell. Civr. et Dess.), "*Sosninella*" sp., and *Hemigordius hungaricus* nov. sp. The distribution of the taxa *Pachyphloia cucurköyi* Sell. Civr. et Dess. and "*Sosninella*" sp. is restricted exclusively to the section between 95.0 and 112.0 m. In all probability, the specimens of "*Sosninella*" sp. correspond to a *Pachyphloia* species' oblique sections perpendicular to the longitudinal axis, or enclosing a low angle within it.

The abundance of *Hemigordius hungaricus* nov. sp. specimens is remarkable in certain horizons (e.g. 89.0 m, 92.0 m, 96.0 m, 98.0 m, 101.0 m, and 104.0 m).

Globivalvulina vonderschmitti Reichel is known in this section of the borehole, while *Globivalvulina graeca* Reichel is widely distributed throughout its total length.

On the basis of the abundance of brachiopods, the occurrence of a sponge-rich horizon at 111.0 m, and the similarity of the foraminifer fauna, the strata between 80.7 and 126.5 m of this part of the borehole can be compared to the Nagyvisnyó Limestone of the railway cut No Nv-V.

127.0–168.0 m (microbiofacies of scattered foraminifers)

The Upper Permian sequence of this depth is disturbed by two significant tectonic zones (127.5–130.5 m; 162.5–168.0 m). The poverty of the fossil association in species and specimens is remarkable; certain layers are even entirely free of fossils. Calcareous algae occur sporadically, with only a few specimens to represent them. Brachiopod remnants are known only in the levels between 158.0 and 161.0 m.

The foraminifer fauna is very scattered; in certain horizons the foraminifer assemblage is formed by a few specimens of the species *Globivalvulina graeca* Reichel, *Eotuberitina reitlingerae* Mikl.-Makl., *Hemigordius giganteus* nov. sp., and *Agathammina pusilla* (Geinitz).

168.0–222.1 m (hemigordius microbiofacies)

A wide distribution of calcareous algae is characteristic. In certain horizons (178.5 m, 184.0 m, 196.5 m, 204.5 m, 210.0 m, 213.0 m, 215.5 m, 216.0 m, and 222.0 m) the mass occurrence of echinoderm shell fragments can be observed.

The foraminifer fauna can be characterised by a species- and specimen-rich *Hemigordius* assemblage (*Hemigordius brunnimanni* Altiner, *Hemigordius giganteus* nov. sp., *Hemigordius givenci* Altiner, *Hemigordius hungaricus* nov. sp.,

Hemigordius mályinkai nov. sp., *Hemigordius minutus* Pronina, and *Hemigordius zaninettiae* Altiner), by the abundance of the species *Agathammina* (*Agathammina pusilla* (Geinitz), *Agathammina multa* Pronina) and *Discospirella* (*Discospirella plana* Okimura et Ishii and *Discospirella minima* Okimura et Ishii), as well as by the occurrence of the species *Fronidina pernica* Sell. Civr. et Dess., *Pseudoglandulina longa* Mikl.-Makl., *Globivalvulina bulloides* Reichel, and *Baisalina pulchra* Reytlinger.

C. Microfacies (after Csontos et al., 1983 with supplements)

The Nagyvisnyó Limestone Formation penetrated in borehole Mályinka-8 is both macroscopically and microscopically homogeneous. All of the microfacies were formed in zones of different energies of the same environment, a more-or-less restricted, shallow, calm lagoon (Csontos et al. 1983).

1. Mudstone texture

The stratification appearing in biomicrites of mudstone texture indicates weak currents. In some places this microfacies type is dolomitized (e.g. 138.5 m, 139.0 m, 141.5 m) and feldsparized (e.g. 132.0 m, 132.5 m, 155.0 m, 155.5 m, 156.0 m, 156.5 m, 157.0 m, and 157.5 m), respectively.

2. Wackestone texture

The separation of microfacies of predominantly wackestone texture is carried out on the basis of some characteristic fossil groups.

The gymnocodium biomicrites are characterized by the dominance of *Gymnocodium*. Preferred orientation is frequent. The gymnocodia drifted together in lenses; patches of their occurrence indicate a transportation by moderate energy. Beside algae, echinoderms, and ostracods, the foraminifer species *Hemigordius*, *Agathammina*, and *Eotuberitina*, are present as general elements in the fossil association. In certain horizons (e.g. 143.0 m, 144.0 m, 144.5 m, 152.0 m, 153.5 m, 154.0 m, 181.5 m, 198.5 m, and 206.5 m) foraminifers represent 10–15% of the fauna.

In the microsparitic matrix of vermiporella biomicrites, the proportion of vermiporellae is large. Beside algae, echinoderms, ostracods and among foraminifer species *Agathammina*, *Baisalina*, *Pachyphloia*, and *Globivalvulina* have a major share. As accessory elements, brachiopod shell fragments, spines and biogenic fragments occur. The preferred orientation indicates a more intense current. The light requirements and encrusting nature of *Vermiporellae* indicates also those parts of the lagoon richer in currents (e.g. 85.0 m, 89.5 m, 102.5 m, 109.0 m, 125.0 m, 126.0 m, 161.0 m, 170.0 m, 217.0 m, and 219.0 m).

In the micritic or microsparitic matrix of biomicrites of mixed fauna, the proportion of robust algae (*Permocalculus*) is large, but gymnocodia and a few vermiporellae also occur. The proportion of brachiopod shell fragments and

spines is considerable (e.g. 85.5 m, 86.0 m, 88.0 m, 100.0 m, 108 m, 110.0 m, 124.0 m, 159.0 m, and 160.5 m). Because of their index horizon character, the sponges are worth mentioning (111.0 m). Among the foraminifers, the species *Agathammina*, *Hemigordius*, and *Globivalvulina* are frequent (102.0 m, 103.5 m, 142.0 m, and 174.0 m). The diversified fossil association originated in a well-ventilated part of the lagoon. The shells were slightly processed, drifting together by currents of low intensity.

In the matrix of brachiopodal biomicrites, the brachiopod shell fragments and spines are dominant. Besides these, echinoderm shell elements, a few alga fragments, and some foraminifers (*Agathammina*, *Hemigordius*, *Globivalvulina*, and *Eotuberitina*) can be found. The different water depth requirements of the elements of the fossil assemblage doubtlessly indicates reworking (95.0 m, 95.5 m, 96.0 m, 97.0 m, 99.5 m, 106.5 m, 108.5 m, 119.5 m, 123.0 m, and 123.5 m).

In the echinoderm biomicrites, the brachiopod, ostracod, mollusc shell fragments, and among the foraminifers the *Hemigordius* species, are frequent, apart from the dominance of echinoderm shell fragments. The enrichment of echinoderm shell fragments is a result of powerful currents in areas of high energy of the environment, near the wave base: 97.5 m, 141.0 m, 147.0 m, 204.5 m, and 216.0 m.

3. Grainstone texture

In the matrix of "alga pebbled" biosparite of grainstone texture, rounded, well-sorted, slightly oriented components indicating turbulent current can be found. The micritic margin of the components is probably due to the "corrosive" algae preferring a very shallow, nearshore environment (173.5 m).

Micropalaeontology

Within the rich fossil assemblage of the borehole, consisting of calcareous alga, foraminifer, ostracod, gastropod, mollusc, brachiopod, and echinoderm remnants, the rich ostracod fauna of biostratigraphic significance permitted the chronostratigraphic classification of the penetrated sequence (Fig. 10).

The ostracod fauna is extremely rich. The *Parvikirkbya transita* assemblage zone, assignable to the deeper (168–222 m) Upper Permian (Upper Midian) and the younger (79.5–168 m) Upper Permian (Djulfian) *Parvikirkbya fueleopi* assemblage zone, as well as the *Petasobairdia bidentata* zone, are represented by a rich ostracod assemblage (Fülöp 1994; Kozur 1985a, b).

The Upper Permian calcareous algae are the most common fossils of the borehole. Characteristic species are *Gymnocodium bellerophontis* (Rothpletz), *Mizzia velebitana* Schubert, *Permocalculus fragilis* (Pia), and *Vermiporella nipponica* Endo.

Beside ostracods and calcareous algae, a rich foraminifer association was found (Fig. 2). All the foraminifers are benthic forms and belong predominantly to the

vagile benthos. The taxa generally exhibiting a long range do not allow a stage-level classification similar to that of the ostracods. In greatest proportion, the species of the calcareous imperforate porcelaneous genus *Hemigordius* are present. In the Upper Midian layers of the borehole, the genus *Hemigordius* is remarkably rich in species and specimens (Fig. 8). The robust *Paraglobivalvulina mira* Reytlinger specimens are widely distributed in the Djulfian layers of the borehole. The species *Globivalvulina graeca* Reichel is present in the entire length of the borehole, while *Globivalvulina vonderschmitti* Reichel is a taxon determining the microfacies of the Upper Djulfian layers. The species- and specimen-rich assemblage of the genus *Pachyphloia* is characteristic of Upper Djulfian layers (Fig. 3). For that matter, this horizon represents the greatest depth of shallow marine formations of the Nagyvisnyó Limestone Formation (Fülöp J. 1994). The species *Kamurana bronnimanni* Altiner et Zaninetti, *Dagmarita chanakchiensis* Reytlinger were found exclusively in the younger Djulfian layers of the borehole. *Baisalina pulchra* Reytlinger, with a long range, can be traced throughout the total length of the borehole (Fig. 5). On the basis of the species *Codonofusiella* being present in the extremely poor Fusulinacea assemblage, the Upper Permian sequence penetrated by the borehole may not be older than the Upper Midian. The representatives of the family Ichthyleriidae containing mainly cosmopolitan taxa are remarkably rare in the Upper Permian section encountered by the borehole.

For the systematic classification of foraminifer taxa the authors used the system of Loeblich, R.A. et H. Tappan 1988 as a starting-point:

Family: Tuberitinae A.D. Miklukho-Maklay, 1958

Eotuberitina Miklukho-Maklay, 1958: *Eotuberitina reitlingerae* Miklukho-Maklay specimens (Pl. I, Fig. 10), overgrown on brachiopod, mollusc, and ostracod shell fragments (Pl. I, Fig. 14), were transported to their burial site by means of currents. They are common in biomicrites containing biogenic fragments, having mixed fauna, and indicating a nearshore environment.

Family: Pachyphloidae Loeblich et Tappan, 1984

Pachyphloia Lange, 1925: In borehole Mályinka-8, they are the species- and specimen-rich components of foraminifer associations of the *Pachyphloia* species (Fig. 3). The *Pachyphloia magna* (K.V. Miklukho-Maklay) specimens show a wide distribution in the Nagyvisnyó Limestone of the borehole (Pl. III, Figs 1–3). In the upper third of the Nagyvisnyó Limestone (79.5 m–127.0 m), *Pachyphloias* are present in a frequency determining the microfacies. The most common species are: *Pachyphloia iranica* Bozorgnia (Pl. IV, Figs 4–5) and *Pachyphloia cukurköyi* Sellier de Civrieux et Dessauvagie (Pl. III, Figs 6–7; Pl. IV, Fig. 3). Some specimens of *Pachyphloia gefoensis* (K.V. Miklukho-Maklay – Pl. IV, Fig. 4) are known in echinoderm micrites (105.5 m, 110.0 m). Specimens of *Pachyphloia ovata* Lange (Pl. IV, Figs 7–9) are frequent in the small biogenic clastic biomicrites of mixed fauna of the uppermost few metres (86.7–88.6 m) of the Nagyvisnyó Limestone. Some robust

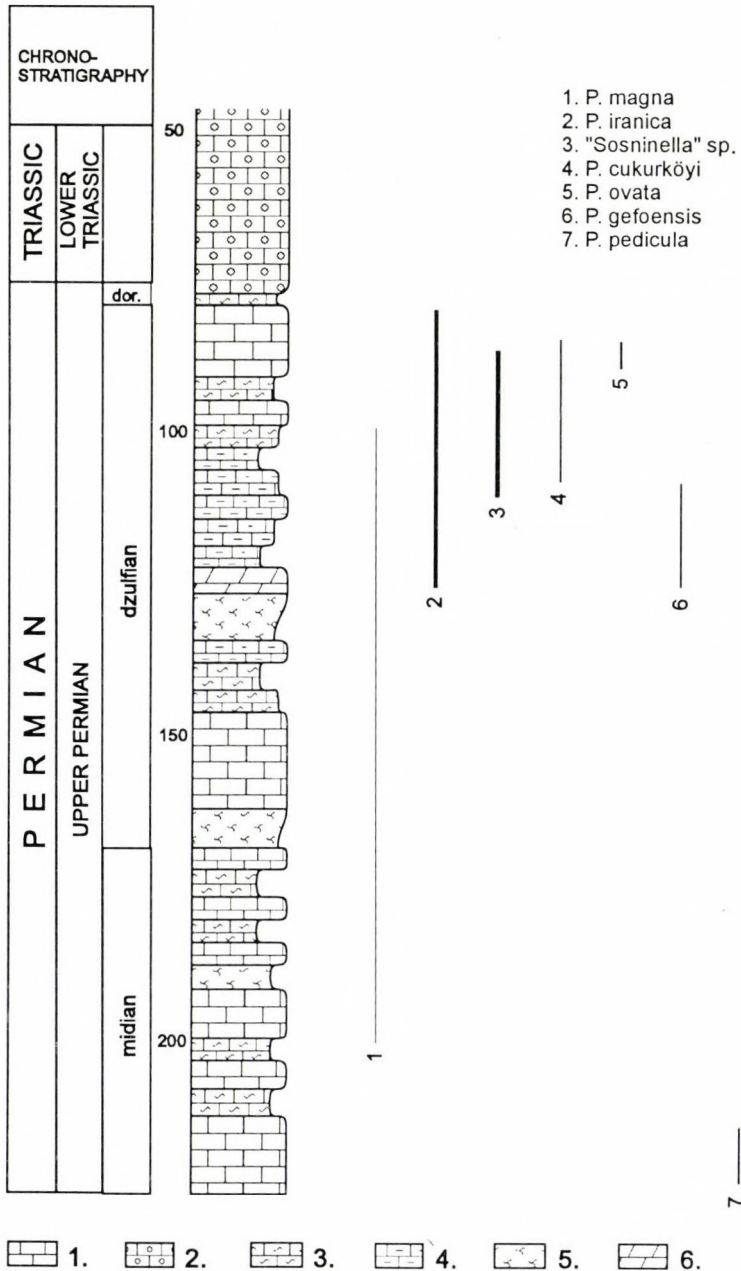


Fig. 3

Frequency and distribution of species of the genus *Pachyphloia*. 1. limestone; 2. oolitic limestone; 3. calcareous marl; 4. argillaceous limestone; 5. syngenically brecciated limestone; 6. dolomite

specimens of *Pachyphloia pedicula* Lange are known exclusively in the lowest formations of the borehole (Pl. II, Figs 6–8).

"*Sosninella*" Sellier de Civrieux et Dessauvage, 1965: The quotation-marks indicate that the taxonomic classification of the genus is uncertain. It cannot be excluded that the foraminifer sections of characteristic shape determined under this name (Pl. II, Figs 1–4) are special sections of a *Pachyphloia* species. Sosnina (1977b, 1978) described several new *Pachyphloia* species, presenting their "*Sosninella*" sp.-like oblique sections perpendicular to the longitudinal axis or enclosing an angle with it.

Family: Colaniellidae Fursenko, 1959

Colaniella Likharev, 1939: It is a taxon occurring very rarely in northern Hungarian Upper Permian formations. Some specimens are known from youngest Upper Djulfian layers of the Nagyvisnyó Limestone. In the Garadna Valley and in the railway cut No Nv-V (Sidó et al. 1974), as well as between 95–96 m of borehole Má-8 (Pl. I, Fig. 12), specimens of not determinable species with oblique section have been found.

Family: Palaeotextulariidae Galloway, 1933

Climacammina Brady, 1873: *Climacammina major* Morozova (Pl. V, Fig. 1) and *Climacammina* cf. *gigas* Sulejmanov (Pl. V, Fig. 3) specimens are known in the youngest Upper Permian complex (above 100 m – Fig. 6) of the borehole. In the geohistorical past, the preferred habitats of *Climacammina* species were the lagoons behind the reefs (Flügel 1981).

Family: Biseramminidae Chernysheva, 1941

Globivalvulina Schubert, 1921: Their common, specimen-rich species can be found throughout the Upper Permian sequence of the borehole (Fig. 4), with a significant frequency in the depth between 79.5–127.0 m. *Globivalvulina cyprica* Reichel (Pl. VI, Fig. 4) is the species with the smallest size. Some specimens of the species *Globivalvulina bulloides* (Brady), of small size and globular chamber, are known (Pl. VII, Fig. 5). *Globivalvulina graeca* Reichel is widely distributed in the Upper Permian layers of the borehole (Pl. VIII, Fig. 4). *Globivalvulina vonderschmitti* Reichel (Pl. VIII, Figs 1, 3), easily distinguished from the *Globivalvulina* species by its last chamber, of large size, is a species present in the upper third (79.5–127.0 m) of the Upper Permian series, in a frequency determining the microbiofacies.

Paraglobivalvulina Reytlinger, 1965: The robust *Paraglobivalvulina mira* Reytlinger specimens (Pl. VI, Figs 1–3, 5; Pl. VII, Figs 1–2) are widely distributed in the Djulfian layers of the borehole (Fig. 4).

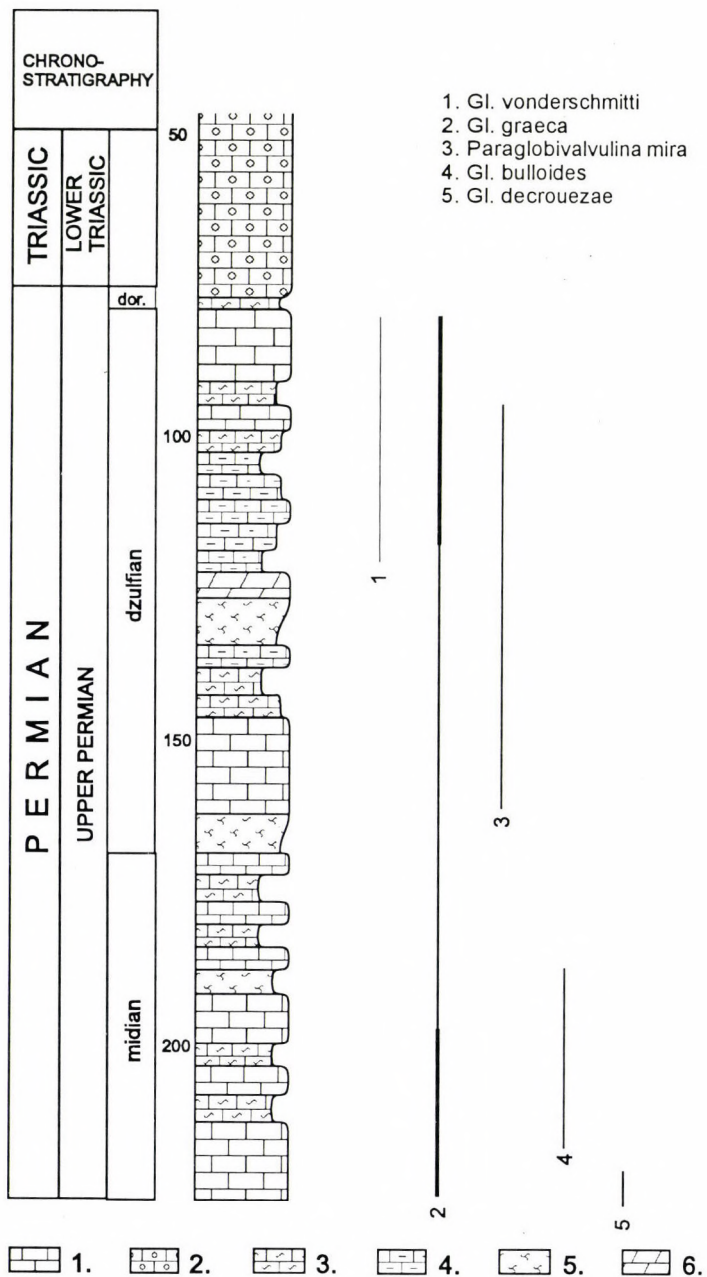


Fig. 4

Frequency and distribution of species of the genera *Globivalvulina* and *Paraglobivalvulina*. 1. limestone; 2. oolitic limestone; 3. calcareous marl; 4. argillaceous limestone; 5. syngenetically brecciated limestone; 6. dolomite

Dagmarita Reytlinger, 1965: Some *Dagmarita chanakchiensis* Reytlinger specimens (Pl. IX, Figs 1–3) were found in the Upper Djuflian developments (Fig. 5).

Family: *Ozawainella* Thompson et Foster, 1937

Reichelina Erk, 1942: As a representative of primitive Fusulinacea, the species *Reichelina minuta* Erk is known in from a single sample (217.5 m; Pl. XI, Fig. 3).

Family: Schubertellidae Skinner, 1931

Codonofusiella Dunbar et Skinner, 1937: In the extremely poor Fusulinacea assemblage of the Nagyvisnyó Limestone in the borehole, the representatives of the genus *Codonofusiella* show a wide distribution (84.2 m, 85.0 m, 88.6 m, 101.0 m, 103.5 m, 125.0 m, 126.5 m, 142.5 m, 202.0 m, 217.5 m, 218.0 m, 220.0 m, 220.5 m, 221.5 m). *Codonofusiella nana* Erk specimens (Pl. X, Figs 1–6) are more frequent, while a single specimen of *Codonofusiella* cf. *paradoxia* (Pl. XI, Fig. 1) is known only from 220.5 m.

Family: Hemigordiopsidae Nikitina, 1969

Hemigordius Schubert, 1908: Different authors have assigned more than 50 Palaeozoic species to the genus *Hemigordius*, indicating a great morphological variability. Studying these *Hemigordius* species from the extremely rich *Hemigordius* assemblage of the Upper Permian series of borehole Mályinka-8, it became obvious that taxonomic reassignment of several species described previously as *Hemigordius* is necessary.

At generic level, the manner of coiling (streptospiral, sigmoidal, trochospiral) of the second undivided tubular chamber, the nature of the whorls (involute, evolute), and the type of the calcareous shell (porcelaneous, hyaline, compound, micrograined, fibrous) should be taken into account.

Those species having an entirely planispiral second tubular chamber (*Hemigordius exsertus* Solovjeva in Krasheninnikov, 1965; *Hemigordius saidi* Solovjeva in Krasheninnikov, 1965; *Hemigordius grozdilova* Igonin; *Hemigordius brunsielloides* Kireeva; *Hemigordius tenuitecus* Kireeva; *Hemigordius umbilicatus* Kireeva) cannot be assigned to the genus *Hemigordius*.

The calcareous compound (dark inner, light outer) shell wall and entirely planispiral involute coiling of the second tubular undivided chamber of the species *Nummulostegina padangensis* Lange make its assignment to the genus *Permodiscus* Dutkevich unambiguous.

The calcareous micrograined shell wall and entirely planispiral involute coiling (with a last evolute whorl) of the second tubular undivided chamber of the species *Hemigordius nanus* Reytlinger is the reason for its assignment to the genus *Lapparentidiscus* Vachard.

At present (Loeblich and Tappan 1988), the genotype of *Hemigordius* is the species described as *Cornuspira schlumbergeri* by Howchin, W. in 1895, the oldest

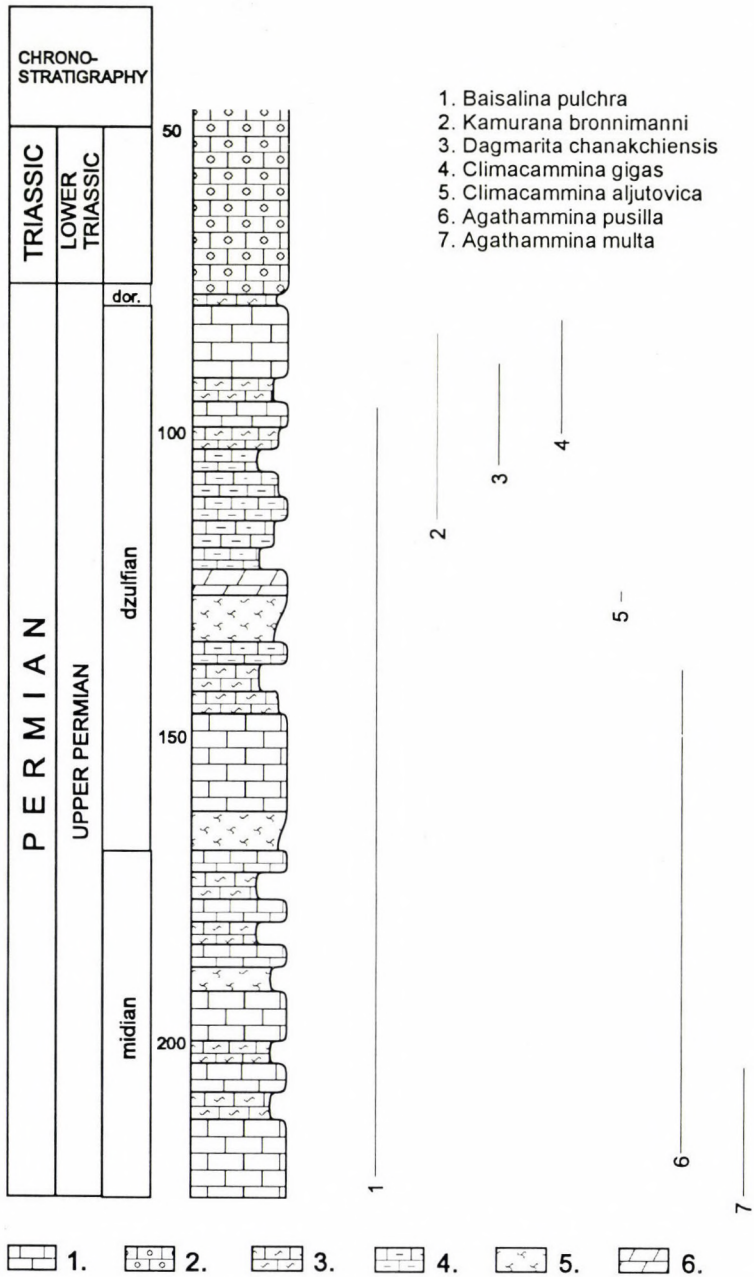


Fig. 5

Frequency and distribution of characteristic foraminifer species. 1. limestone; 2. oolitic limestone; 3. calcareous marl; 4. argillaceous limestone; 5. syngenetically brecciated limestone; 6. dolomite

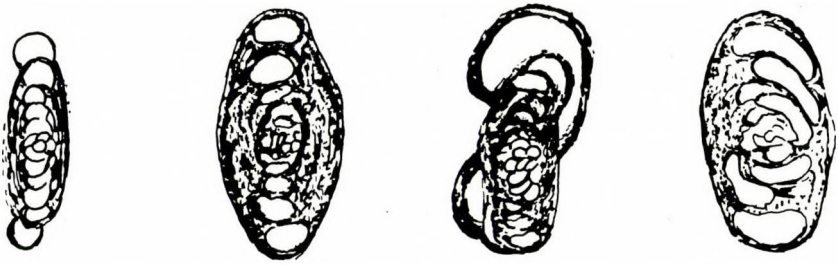
whorls of which are coiled streptospirally, similarly to those of *Glomospira gordialis* (Parker et Jones), while its younger whorls are coiled planispirally. According to Howchin (1895), however, the species *Cornuspira schlumbergeri* differs in two important properties from the generic features of *Cornuspira*. The first difference is the initial irregular coiling of the tubular second chamber, the second one is the stratified laminated shell wall.

In fact, on the basis of the (glomospiroid) coiling of the second tubular chamber and its (laminated) shell wall, *Cornuspira schlumbergeri* Howchin can be assigned neither to the *Cornuspira* nor the *Glomospira* genera. This is why in 1908 Schubert proposed the name *Hemigordius* for both the calcareous imperforate and sandy specimens.

The Palaeozoic calcareous-shelled small foraminifers consisting of a protoconch and a variably coiled (Fig. 6) undivided tubular second chamber are morphologically highly variable. It is hard to distinguish the morphologically identical calcareous porcelaneous, micrograined, or agglutinated homo-morphic varieties (Fig. 7). In the calcareous imperforate cases, the separation is rendered more difficult by frequent recrystallization. As a consequence of recrystallization the shell wall, built up of an agglomeration of small crystals, can show a micrograined structure (*Hemigordius irregulariformis* Zaninetti, Altiner, Catal); the wall, subsequently silicified, is of fibrous structure (Pl. XX, Figs 1-2). Due to the secondary depositions, the laminated shell wall is frequent in both the porcelaneous (*Hemigordius schlumbergeri* (Howchin), *Hemigordius harltoni* Cushman et Waters) and micrograined (*Neohemigordius maopingensis* Wang et Sun) cases. At generic level, a problem is caused by the imperforate nature of the species described originally as calcareous hyaline ones having a double-layered (inside dark thin, outside light thick) shell wall (e.g. *Hemigordius longus* Grozdilova; *Hemigordius ovatus* Grozdilova; *Hemigordius permicus* Grozdilova).

Within a certain *Hemigordius* population, several ecological varieties may occur within a single species (e.g. *Hemigordius irregulariformis* Zaninetti, Altiner, Catal). Probably, after a thorough *Hemigordius* revision, of the nearly 40 species known from the literature several could be merged due to polymorphism, such as *Hemigordius irregulariformis* Zaninetti, Altiner, Catal and *Hemigordius giganteus* nov. sp., or *Hemigordius grandis* (Ozawa), *Hemigordius hungaricus* nov. sp., and *Hemigordius umbilicatus* (Sosnina), or *Hemigordius changxingensis* Wang and *Hemigordius sigmoidalis* Wang, etc.

In the foraminifer association of the Upper Permian sequence of borehole Mályinka-8, the genus represented by the greatest number of species and specimens is *Hemigordius* (Fig. 8).



Streptospiral ↓ planispiral (involute-evolute)	Sigmoidal ↓ planispiral (involute-evolute)	Sigmoidal ↓ planispiral (involute) ↓ irregular spiral (evolute)	Trochospiral ↓ planispiral (involute)
<i>H. abriolensis</i> Luperto <i>H. amicus</i> Igonin <i>H. calcarea</i> Cush. et. Wat <i>O. campanula</i> Del. et Mar. <i>H. carbonarius</i> (Steinmann) <i>H. changxingensis</i> Wang <i>H. harltoni</i> Cush et Wat. <i>H. liratus</i> Cush et wat. <i>H. morillensis</i> Conkin <i>H. ovatus</i> Grozdilova <i>H. regularis</i> Plummer <i>H. reicheli</i> Lys <i>H. schlumbergeri</i> (Howchin)	<i>H. bronnimanni</i> Altiner <i>H. brunni</i> Lys <i>H. decorus</i> Lin <i>H. depressus</i> Luperto <i>S. Grandis</i> Ozawa <i>H. guvenci</i> Altiner <i>H. hungaricus</i> nov. sp. <i>H. japonica</i> Ozawa <i>H. longus</i> Grozdilova <i>H. nov. sp.</i> <i>Neoh. maopingensis</i> Wang <i>H. mályinkai</i> nov. sp. <i>H. minutus</i> Pronina <i>H. nalivkini</i> Grozdilova <i>H. pakistanus</i> Premoli-Silva <i>H. permicus</i> Grozdilova <i>H. planus</i> Pronina <i>H. pribyli</i> Vašíček et Ruzicka <i>H. regularis</i> Wang <i>H. rotundus</i> Wang <i>H. sigmoidalis</i> Wang <i>H. simplex</i> Reitlinger <i>A. umbilicata</i> Sosnina <i>H. zaninettiae</i> Altiner	<i>H. giganteus</i> nov. sp. <i>H. irregulariformis</i> Zan., Alt., Cat.	<i>H. abadehensis</i> Ok. et. Ish. <i>D. minima</i> Ok. et Ish. <i>D. plana</i> Ok. et Ish.

Fig. 6
 The types of coiling of the undivided tubular second chamber of Palaeozoic calcareous-shelled small foraminifers on the basis of the original species descriptions

		coiling of the second tubular chamber	material and structure of the wall			
			Streptospiral ↓ planispiral (involute-evolute)	Sigmoidal ↓ planispiral (involute-evolute)	Sigmoidal ↓ planispiral (involute) ↓ irregular spiral (evolute)	Trochospiral ↓ planispiral (involute)
calcareous, imperforate	porcelaneous	<i>H. amicus</i> Igonin <i>O. campanula</i> Deleau et Marie <i>H. reicheli</i> Lys	<i>H. bronnimanni</i> Altiner <i>S. grandis</i> Ozawa <i>H. guvenci</i> Altiner <i>H. japonica</i> Ozawa <i>H. nov. sp.</i> <i>H. malyinkai</i> nov. sp. <i>H. pribyli</i> Vašicek et Ruzicka <i>H. umbilicata</i> Sosnina <i>H. zaninettiae</i> Altiner			
	laminated, double	<i>H. calcarea</i> Cush. et Wat. <i>H. carbonarius</i> (Steinmann) <i>H. harltoni</i> Cush. et Wat. <i>H. liratus</i> Cush. et Wat. <i>H. morellensis</i> Conkin <i>H. regularis</i> Plummer <i>H. schlumbergeri</i> (Howchin)	<i>H. hungaricus</i> nov. sp.	<i>H. giganteus</i> nov. sp.	<i>H. abadehensis</i> Okimura et Ishii <i>D. minima</i> Okimura et Ishii <i>D. plana</i> Okimura et Ishii	
	microgranular agglomeration of minute calcite	<i>H. abriolensis</i> Luperto <i>H. changxingensis</i> Wang	<i>H. brunni</i> Lys <i>H. decorus</i> Lin <i>H. depressus</i> Luperto <i>H. minutus</i> Pronina <i>H. planus</i> Pronina <i>H. regularis</i> Wang <i>H. rotundus</i> Wang <i>H. sigmoidalis</i> Wang <i>H. simplex</i> Reitlinger	<i>H. irregulariformis</i> Zan., Alt., Cat.		
	secondary		<i>Neoh. maopingensis</i> Wang et Sun			
hyaline	bilamellar (inner: dark, outer: light)	<i>H. ovatus</i> Grozdilova	<i>H. longus</i> Grozdilova <i>H. nalikini</i> Grozdilova <i>H. pakistanus</i> Premoli-Silva <i>H. permicus</i> Grozdilova			

Fig. 7

Classification of calcareous-shelled Palaeozoic small foraminifers with an undivided tubular second chamber according to the material and structure

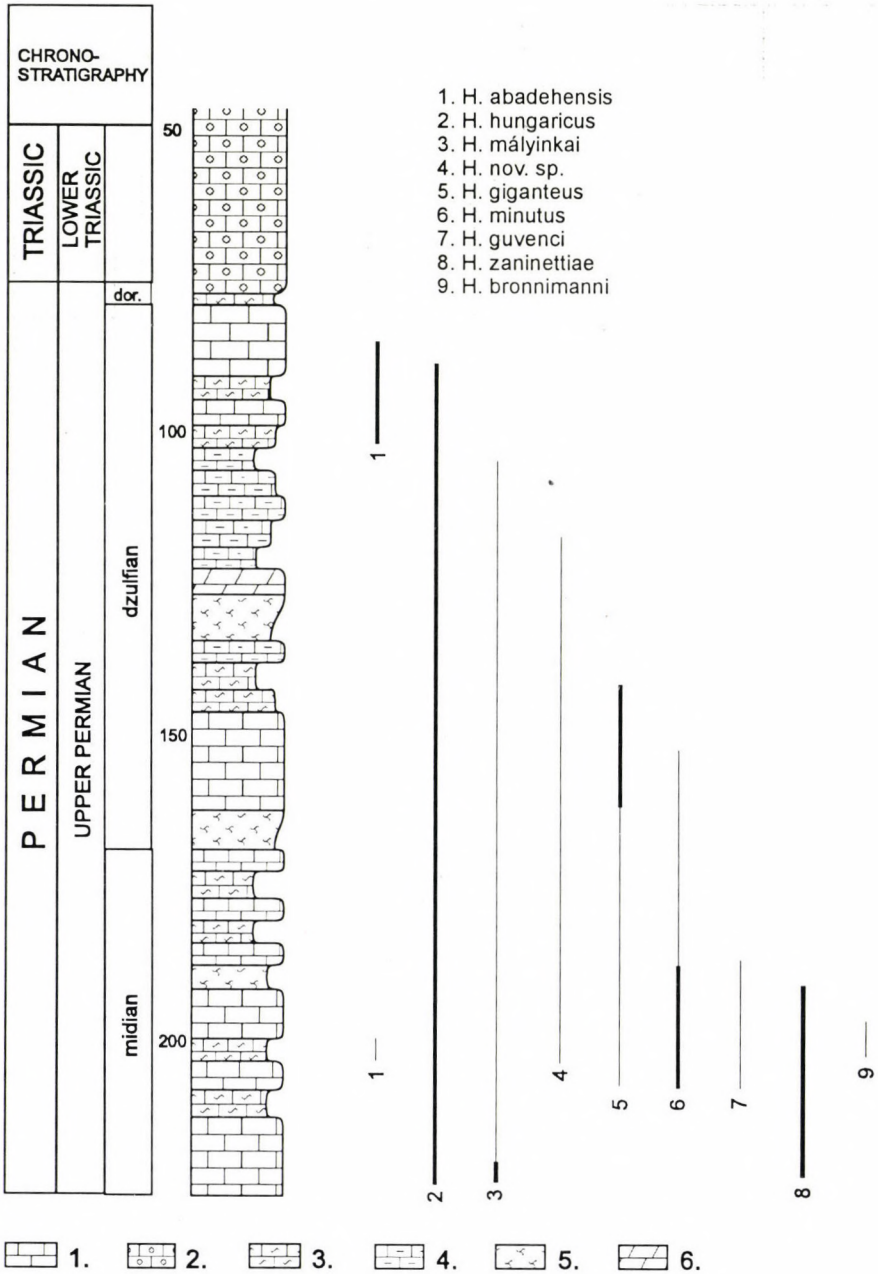


Fig. 8
Frequency and distribution of species of the genus *Hemigordius*. 1. limestone; 2. oolitic limestone; 3. calcareous marl; 4. argillaceous limestone; 5. syngenetically brecciated limestone; 6. dolomite

Hemigordius abadehensis Okimura et Ishii

Pl. XVI, Figs 1a, 2-4

Pl. XVII, Fig. 5

*Synonyms:*1981. *Hemigordius abadehensis* – Okimura, Y. et K.I. Ishii; p. 16, Pl. 1, Figs 19-201981. *Hemigordius abadehensis* – Taraz, H. et al. (not illustrated)1992. *Hemigordius abadehensis* – Bérczi-Makk, A.; Pl. 3, Fig. 12.1992. *Hemigordius cf. abadehensis* – Bérczi-Makk, A.; Pl. 6, Fig. 9, Pl. 13, Fig. 12

<i>Dimensions of the shell:</i>	Holotype	Má-8 borehole
diameter:	0.750 mm	0.550-0.730 mm
width:	0.320 mm	0.300-0.440 mm
width/diameter:	0.43	0.54-0.60
number of whorls:	6-8	6-7

Remarks: In two horizons (85.0-103.5 m, 202.5 m) of the borehole Má-8, it is a robust species represented by several specimens. It is strongly thickened at the umbilicus. It consists of 6-7 whorls, the width and length of which increases gradually. The initial trochospiral coil of the second tubular chamber is followed by a planispiral section, which inclines slightly to both sides. Its width (0.300-0.440 mm) is somewhat greater than that of the forms described in the Iranian Abadeh Formation. Accordingly, the width/diameter ratio is also a little greater. In some places, the calcareous, porcelaneous imperforate wall is recrystallized, and siliceous spines can be observed (Pl. XVI, Figs 3-4).

Hemigordius giganteus nov. sp.

Pl. XVII, Figs 1-4

Pl. XVIII, Figs 1-5, 6b

Derivatio nominis: after its robust size*Locus typicus:* borehole Mályinka-8, 143.0-215.5 m (Northern Hungary)*Stratum typicum:* Nagyvisnyó Limestone Formation, Upper Permian, Lower Djulfian-Upper Midian*Holotype:* in the micropalaeontological collection of the HAS Geological Research Group (Eötvös Loránd University)*Material:* 20 specimens

Description: The flat disc-shaped shell consists of a spherical protoconch and a tubular second chamber. The initial sigmoidal coil of the second chamber is followed by a planispiral section, resulting in thickening at the umbilicus. The last one or two whorls following this involute section are evolute. The height and width of the whorls increase. The width and height of the whorls of the evolute section increase abruptly as compared to those of involute whorls. The primary axis of the evolute whorls coincides with the axis of the planispiral whorls of the involute section. The wall is calcareous, porcelaneous, imperforate; in some places incipient silicification

(Pl. XVII, Figs 1–3) can be observed from the younger whorls toward the older ones. In a single specimen, the wall seems to be laminated (Pl. XVII, Fig. 2).

<i>Dimensions of the shell:</i>	Holotype	Paratypes
diameter:	0.850 mm	0.600–0.850 mm
width:	0.270 mm	0.170–0.270 mm
width/diameter:	0.31	0.28–0.31
number of whorls:	7	6–7

Differential diagnosis: The only species close to *Hemigordius giganteus* is *Hemigordius irregulariformis* Zaninetti, Altiner, Catal. The new species differs from *Hemigordius irregulariformis* in its much greater (about double) size and regular coiling of its evolute section.

Remarks: In the older Upper Permian (Lower Djulfian–Upper Midian) layers of borehole Má-8, the new species found in the depth between 142.0–215.5 m differs considerably from the specimens of the *Hemigordius* association of the borehole in its remarkably robust size and manner of coiling.

Foraminifer association: *Tuberitina collosa* Reytlinger, *Eotuberitina reitlingerae* Mikl.-Makl., *Hemigordius guvenci* Altiner, *Hemigordius hungaricus* nov. sp., *Hemigordius mályinkai* nov. sp., *Hemigordius minutus* Pronina, *Hemigordius zaninettiae* Altiner, *Hemigordius* sp., *Discospirella plana* Okimura et Ishii, *Baisalina pulchra* Reytlinger, *Pseudoglandulina longa* Mikl.-Makl.

Hemigordius guvenci Altiner

Pl. XIX, Figs 4–5

Pl. XXVII, Fig. 8

Synonyms:

- 1956. *Hemigordius* sp. – Grozdilova, L.P.; p. 527, Pl. 1, Fig. 8
- 1972. *Hemigordius* sp. – Bogusch, O.I.; Pl. 1, Figs 1–2
- 1978. *Hemigordius guvenci* – Altiner, D.; p. 28, Figs 15–17, 19
- 1980. *Hemigordius guvenci* – Altiner, D. et P. Broennimann (not illustrated)
- 1983. *Hemigordius guvenci* – Kotljar, G.V. et al.; Pl. 1, Fig. 10
- 1988a. *Hemigordius guvenci* – Pronina, G. (not illustrated)
- 1988b. *Hemigordius guvenci* – Pronina, G.; Pl. 2, Fig. 11
- 1991. *Hemigordius guvenci* – O. et J. Ferrière (not illustrated)
- 1992. *Hemigordius* cf. *guvenci* – Bérczi-Makk, A.; Pl. 13, Fig. 7

<i>Dimensions of the shell:</i>	Holotype	Má-8 borehole
diameter:	0.340–0.520 mm	0.300–0.540 mm
width:	0.190–0.250 mm	0.150–0.300 mm
width/diameter:	0.56–0.48	0.50–0.55
number of whorls:	7–8	6–7

Remarks: It is a species widely distributed in the older Upper Permian (Upper Midian) layers (183.0–207.0 m) of borehole Má-8. The initial sigmoidal coil of the second tubular chamber is followed by the planispiral coiling of the last whorls. It

is an involute form. The height of the whorls increases only very slightly, while their width increases rapidly during evolution. Its wall is calcareous, porcelaneous, and imperforate. Its size corresponds to that of the specimens described in Turkey.

Hemigordius hungaricus nov. sp.

Pl. XVI, Fig. 1b

Pl. XXIV, Figs 1a, 2–4

Pl. XXV, Figs 1–3, 5–11

Pl. XXVI, Figs 4, 8–10

Derivatio nominis: after its occurrence in Hungary

Locus typicus: borehole Mályinka-8, 88.5–220.5 m (Northern Hungary)

Stratum typicum: Nagyvisnyó Limestone Formation, Upper Permian, Djulfian–Midian

Holotype: in the micropalaeontological collection of the HAS Geological Research Group (Eötvös Loránd University)

Material: 210 specimens

Description: The shell is lens-shaped with parallel sides (one of the sides might be slightly concave) and widely rounded edges. The first, and possibly the second whorl of the second tubular chamber following the spherical protoconch are sigmoidally coiled, followed by 4–5 totally planispiral, involute coils. During evolution, the height of the tubular second chamber is almost unchanged or slightly increasing, while its width increases strongly. The wall is calcareous, porcelaneous, imperforate, rarely recrystallized, silicified (Pl. XXIV, Fig. 4; Pl. XXVI, Fig. 10) and appears to be laminated.

<i>Dimensions of the shell:</i>	Holotype	Paratypes
diameter:	0.370 mm	0.330–0.370 mm
width:	0.090 mm	0.090–0.130 mm
width/diameter:	0.24	0.24–0.35
number of whorls:	5	5–6

Differential diagnosis: It is a form close to the species *Hemigordius umbilicatus* (Sosnia) among the more than 50 Palaeozoic *Hemigordius* species published so far. However, it differs from it in its smaller size, different width/diameter ratio, and growth degree of the width of the second chamber. It cannot be excluded that after the revision of a Late Palaeozoic *Hemigordius* population these two species could be merged due to polymorphism.

Remarks: It is the most widely distributed foraminifer species in the entire Upper Permian (Djulfian–Upper Midian) series of borehole Má-8. Its frequency is remarkable in the depths between 88.5–104.5 m and 202.5–220.5 m (Fig. 7). It can be found in all foraminifer-rich assemblages of the borehole.

Foraminifer association: *Eotuberitina reitlingerae* Mikl.-Makl., *Pachyphloia ovata* Lange, *P. cukurköyi* Sell. Civr. et Dess., *P. pedicula* Lange, *Colaniella* sp., *Climacammina gigas* Sulejmanov, *Globivalvulina graeca* Reichel, *G. vonderschmitti* Reichel, *Para-*

globivalvulina mira Reytlinger, *Dagmarita chanakchiensis* Reytlinger, *Reichelina minuta* Erk, *Codonofusiella nana* Erk, *Agathammina pusilla* (Geinitz), *A. multa* Pronina, *Hemigordius minutus* Pronina, *H. giganteus* nov. sp., *H. mályinkai* nov. sp., *H. zaninettiae* Altiner, *Baisalina pulchra* Reytlinger, *Discospirella plana* Okimura et Ishii, *Kamurana bronnimanni* Altiner et Zaninetti, *Ichthyolaria latilimbata* Sell. Civr. et Dess., *Pseudoglandulina longa* Mikl.-Makl.

Hemigordius mályinkai nov. sp.

Pl. XXII, Figs 1–4

Derivatio nominis: after its occurrence at Mályinka (Northern Hungary)

Locus typicus: borehole Mályinka-8, 105–6.5–122.0 m; 175.0–222.0 m (Northern Hungary)

Stratum typicum: Nagyvisnyó Limestone Formation, Upper Permian, Djulfian–Midian

Holotype: in the micropalaeontological collection of the HAS Geological Research Group (Eötvös Loránd University)

Material: 56 specimens

Description: The shell is lens-shaped, towards the edges strongly compressed. The sigmoidal coiling of the first whorl of the second tubular chamber following the protoconch is followed by planispiral, involute and then evolute sections. The involute part is strongly thickened. In the involute part, the height and width of the tubular second chamber increases slightly. In the evolute section, its height and width increase abruptly and the form has a characteristic triangular cross-section. The wall is calcareous, porcelaneous, imperforate, sometimes with the signs of incipient recrystallization, and silicification (Pl. XXII, Figs 1–2).

<i>Dimensions of the shell:</i>	Holotype	Paratypes
diameter:	0.620 mm	0.470–0.620 mm
width:	0.200 mm	0.100–0.200 mm
width/diameter:	0.32	0.21–0.32
number of whorls:	4	3–4

Differential diagnosis: Regarding its size, this form is similar to the species *Hemigordius liratus* Cushman et Waters. However, while the latter has a sharp marginal edge, *Hemigordius mályinkai* nov. sp. has only a strongly compressed edge. In its cross-section and manner of coiling, this form is close to the species *Hemigordius simplex* (Reytlinger), but differs from it in the stronger thickening of the involute section as well as in its wall structure.

Remarks: It is a characteristic component of the rich *Hemigordius* assemblage in older Upper Permian (Upper Midian) layers (174.5–222.0 m) of borehole Má-8. It is present only sporadically in the Lower Djulfian.

Foraminifer association: *Globivalvulina graeca* Reichel, *Hemigordius hungaricus* nov. sp., *H. zaninettiae* Altiner, *Pseudoglandulina longa* Mikl.-Makl.

Hemigordius minutus Pronina

Pl. XXVIII, Figs 1–3, 5–7

Synonyms:

- 1988a. *Hemigordius minutus* Vuks – Pronina, G.; Pl. 1, Fig. 5
 1988b. *Hemigordius* (*H.*) *minutus* – Pronina, G.P.; p. 56, Pl. 2, Fig. 9
 1989. *Hemigordius minutus* – Kotljar, G.V. et al.; Pl. 4, Fig. 11
 1992. *Hemigordius minutus* – Bérczi-Makk, A.; Pl. 3, Figs 3–4, Pl. 6, Fig. 12

<i>Dimensions of the shell:</i>	Holotype	Má-8 borehole
diameter:	0.180–0.280 mm	0.170–0.230 mm
width:	0.110–0.150 mm	0.080–0.100 mm
width/diameter:	0.61–0.53	0.47–0.43
number of whorls:	3–5	3–5

Remarks: It is a species represented by a great number of specimens in the older Upper Permian (Lower Djulfian–Upper Midian) formations (154.0–205.5 m) of borehole Má-8. The spherical protoconch, of a large size compared to that of the small disc-shaped shell, is followed by the initially trochospiral, then planispiral coiling of the tubular second chamber. It is an involute form. The wall is calcareous and micrograined.

The Northern Hungarian specimens are somewhat flatter than those described in the Transcaucasian area.

Hemigordius zaninettiae Altiner

Pl. XIX, Fig. 1a, 2a–3

Pl. XX, Figs 1a, 2, 4a, 5

Pl. XXII, Fig. 6a

Synonyms:

1978. *Hemigordius zaninettiae* – Altiner, D.; p. 28, Pl. 1, Figs 7–14
 1978. *Hemigordius* aff. *H. ovatus* – Lys, M. et J. Marcoux; Pl. 1, Fig. 12
 1978. *Hemigordius reicheli*
 subsp. *sigmoidalis* – Lys, M. et J. Marcoux; Pl. 1, Fig. 11
 1980. *Hemigordius zaninettiae* – Lys, M. et al. (not illustrated)
 1980. *Hemigordius zaninettiae* – Altiner, D. et P. Broennimann
 (not illustrated)
 1981. *Hemigordius zaninettiae* – Zaninetti, L., D. Altiner et E. Catal
 (not illustrated)
 1983. *Hemigordius zaninettiae* – Sheng, J. Z. et Y. He; p. 58, Pl. 1,
 Figs 23–26
 1988b. *Hemigordius* (*Midiella*)
 zaninettiae – Pronina, G.P.; Pl. 2, Figs 19–20
 1988. *Hemigordius zaninettiae* – Noe, S. (not illustrated)
 1988. *Hemigordius zaninettiae* – Altiner, D. (not illustrated)

1989. *Hemigordius (Midiella) zaninettiae* – Kotljar, G.V. et al. (not illustrated)
 1989. *Hemigordius zaninettiae* – Köylüoğlu, M. et D. Altiner; Pl. 11, Figs 3–5

<i>Dimensions of the shell:</i>	Holotype	Má-8 borehole
diameter:	0.410–0.570 mm	0.380–0.600 mm
width:	0.180–0.330 mm	0.260–0.340 mm
width/diameter:	0.44–0.58	0.68–0.56
number of whorls:	6–7	5–6

Remarks: This species is present in great frequency in the older (Upper Midian) layers (195.0–220.5 m) of the Upper Permian series of borehole Má-8.

Initially, the tubular second chamber of the lens-shaped shell has a more-or-less regular sigmoidal, then planispiral coiling. It is an involute form. The planes of the whorls show a slight inclination compared to each other. The width and height of the second chamber increase quickly. In relation to the specimens found in Turkey, its width/diameter ratio is somewhat greater. It cannot be excluded that the subsequent silicification of the calcareous, porcelaneous wall of the younger whorls (Pl. XX, Figs 1–2) is the reason for the difference in the width/diameter ratio.

Family: Baisalinidae Loeblich et Tappan, 1968

Baisalina Reytlinger, 1965: As a juvenile, this form is similar to *Hemigordius*. It is streptospirally, later planispirally coiled. It can be distinguished from *Hemigordius* by the protosepta of the last whorl. *Baisalina pulchra* Reytlinger is a taxon with a long range (Upper Permian: Midian–Djulfian–Dorashamian). It can be traced in the entire length of the borehole (Fig. 5) (Pl. XIII, Figs 3–4, 6–7; Pl. XIV, Figs 4–5).

Family: Fischerinidae Millett, 1898

Discospirella Okimura et Ishii, 1981: It is not included in the foraminifer system of Loeblich and Tappan published in 1988. According to the authors, the species described in the Iranian Abadeh Formation can be distinguished from *Hemigordius* on the basis of its porcelaneous double-layered wall, the layered structure of which cannot be demonstrated because of the lateral thickening of the wall.

The few forms found in the Upper Permian series of borehole Má-8 and similar in size and cross-section to these Iranian forms can be regarded in all probability as belonging to the genus *Hemigordius* (Pl. XXVI, Figs 1–2, 5, 7, 11–13).

Family: Ichthylariidae Loeblich et Tappan, 1986

The representatives of this foraminifer family including mostly cosmopolitan genera are present sporadically; remarkably rarely in the Upper Permian sequence of the borehole (Fig. 9). Practically, their occurrence is restricted to two horizons of the explored complex, the youngest and the older ones.

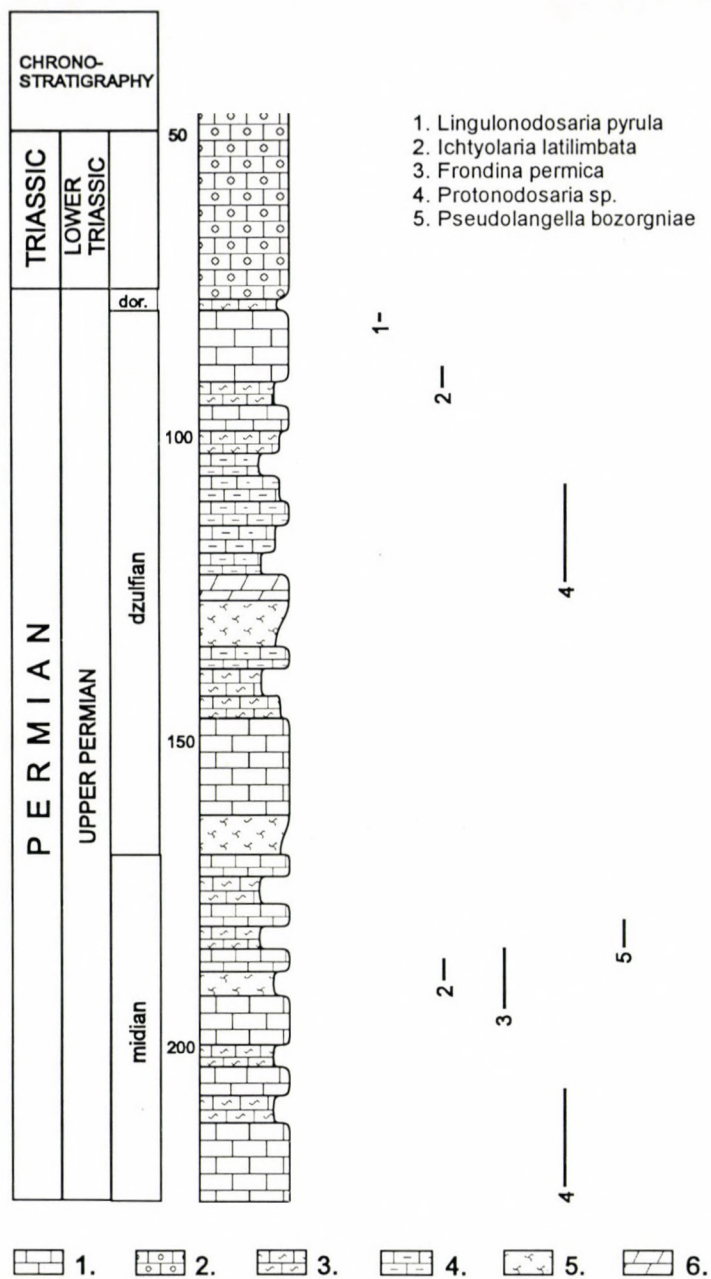


Fig. 9

Frequency and distribution of the taxa Nodosariidae and Ichthyolariidae. 1. limestone; 2. oolitic limestone; 3. calcareous marl; 4. argillaceous limestone; 5. syngenetically brecciated limestone; 6. dolomite

The specimens of *Lingulonodosaria pyrula* (Sell. de Civr. et Dess.) (Pl. XXIX, Fig. 2) were found exclusively in the youngest Upper Permian layer (86.5 m) of the borehole.

The representatives of *Ichthyolaria latilimbata* Sell. Civr. et Dess (Pl. XXVIII, Fig. 6) were encountered at two levels (91.5 m, 189.5 m).

The presence of *Fronidina permica* Sell. de Civr. et Dess. (Pl. XXVIII, Fig. 7) is restricted to a very narrow interval (184.0–196.0 m).

The *Protonodosaria* (Gerke, 1959) species are present sporadically in the Upper Permian formations of the borehole (Pl. XXVIII, Figs 4, 8).

The *Pseudolangella bozorgniae* Lys in Lys, M. et al. 1980 specimens (Pl. XXIX, Fig. 6) occur in the older Upper Permian layer (183.0 m). In the foraminifer system of Loeblich and Tappan (1988), the *Pseudolangella* Sell. de Civr. et Dess. taxon is a synonym of genus *Cryptoseptida* Sell. de Civr. et Dess. On the basis of priority, the name *Cryptoseptida* Sell. de Civr. et Dess is valid.

Family: Robuloididae Reiss, 1963

Robuloides Reichel, 1946: In the youngest layers of the Nagyvisnyó Limestone the *Robuloides lens* Reichel (Pl. IX, Fig. 5) specimens are frequent components of the foraminifer assemblages.

Family: Nodosariidae Ehrenberg, 1838

Generally, its Upper Permian taxa, occurring sporadically, are rare components of the foraminifer assemblages. An exception is the *Pseudoglandulina longa* Mikl.-Makl. species, the specimens of which (Pl. XXVIII, Figs 1–2) show a wide distribution in the entire section of the Nagyvisnyó Limestone drilled by the borehole.

Conclusions

The common occurrence of fossils of differing environmental demands points to the reworking activity of the currents:

- the optimal living conditions of calcareous algae grown on the sea floor and less sensitive to changes in salinity were in the shallow warm calm water of back-reef lagoons, in the sheltered locations of littoral bays. The frequency of the species *Vermiporella* indicates the surf zone of a high-energy environment.

- the back-reef lagoons are also indicated by foraminifer species belonging to the genus *Climacammina* (Flügel 1981).

- on the outer margin of the continental swell, on the part of the fore-reef slope exposed to surf, the brachiopod shell fragments and spine remnants of organisms living in great water depth could have reached the place of burial by intense currents.

- the reef building sponges and corals may occur also as a result of wash-over currents in the fossil associations of certain horizons.

– the presence of fusulinids (predominantly *Codonofusiella* and *Reichelina*), usually preferring deep water, in a shallow-water lagoon environment may also indicate wash-over currents.

– in some places, strong sea-water currents are indicated by the common occurrence of euryhaline fossils (*Gymnocodium*, *Hemigordius*) with stenohaline (*Fusulina*, *Globalvulina*) and open marine (*Pseudoglandulina*) organisms.

On the basis of the data of foraminifer stratigraphy, stage rank chronostratigraphic classification is not possible. Thus, the separation of Upper Permian stages in the borehole was carried out on the basis of the parastratigraphic data of the Ostracod fauna (Kozur 1985a, b).

– The optimal living conditions of the species belonging to the genus *Hemigordius* may have been in an environment of high energy and higher than normal salinity (Noé 1987). In most cases, they have a highly recrystallized (predominantly silicified) shell wall.

Plate I

1. *Earlandia dunningtoni* (Elliot), Má-8 79.0 m M: 65x
2. *Earlandia dunningtoni* (Elliot), Má-8 79.0 m M: 65x
3. *Earlandia dunningtoni* (Elliot), Má-8 79.5 m M: 100x
4. *Earlandia dunningtoni* (Elliot), Má-8 79.5 m M: 100x
5. *Tuberitiniidae* sp., Má-8 176.0 m M: 100x
6. *Earlandia* sp., Má-8 78.2 m M: 100x
7. *Earlandia* sp., Má-8 78.2 m M: 100x
8. *Earlandia dunningtoni* (Elliot), Má-8 79.0 m M: 100x
9. *Earlandia dunningtoni* (Elliot), Má-8 79.5 m M: 100x
10. *Eotuberitina reitlingeræ* Mikl.-Makl., Má-8 176.0 m M: 100x
11. *Tuberitina collosa* Reytlinger, Má-8 183.0 m M: 100x
12. *Colaniella* sp., Má-8 96.0 m M: 100x
13. *Glomospirella* sp., Má-8 93.5 m M: 100x
14. *Eotuberitina reitlingeræ* Mikl.-Makl. grown upon Brachiopoda shell fragment, Má-8 120.5 m M: 100x

Plate II

1. "*Sosnabella*" sp., Má-8 86.7 m M: 75x
2. "*Sosnabella*" sp., Má-8 98.0 m M: 100x
3. "*Sosnabella*" sp., Má-8 110.0 m M: 100x
4. "*Sosnabella*" sp., Má-8 86.7 m M: 100x
5. *Pachyphloia* sp., Má-8 118.5 m M: 75x
6. *Pachyphloia pedicula* Lange, Má-8 219.0 m M: 100x
7. *Pachyphloia pedicula* Lange, Má-8 217.5 m M: 100x
8. *Pachyphloia pedicula* Lange, Má-8 218.0 m M: 50x

Plate III

1. *Pachyphloia magna* (Mikl.-Makl.), Má-8 200.0 m M: 100x
2. *Pachyphloia magna* (Mikl.-Makl.), Má-8 99.5 m M: 100x
3. *Pachyphloia cf. magna* (Mikl.-Makl.), Má-8 164.5 m M: 100x
4. *Pachyphloia geyfoensis* (Mikl.-Makl.), Má-8 105.5 m M: 100x
5. *Pachyphloia* sp., *Hemigordius* sp., Má-8 126.0 m M: 100x
6. *Pachyphloia cukurköyi* Sell. Civr. et Dess., Má-8 88.6 m M: 100x
7. *Pachyphloia cukurköyi* Sell. Civr. et Dess., Má-8 85.5 m M: 100x

Plate IV

1. *Pachyphloia stricta* Sosnina, Má-8 110.0 m M: 100x
2. *Pachyphloia cf. elegans* Loriga, Má-8 103.0 m M: 90x
3. *Pachyphloia cf. cukurköyi* Sell. Civr. et Dess., Má-8 102.5 m M: 100x
4. *Pachyphloia iranica* Bozorgina, Má-8 126.5 m M: 85x
5. *Pachyphloia iranica* Bozorgina, Má-8 83.5 m M: 85x
6. *Pachyphloia iranica* Bozorgina, Má-8 86.7 m M: 85x
7. *Pachyphloia ovata* Lange, Má-8 86.7 m M: 100x
8. *Pachyphloia ovata* Lange, Má-8 88.6 m M: 100x
9. *Pachyphloia ovata* Lange, Má-8 86.7 m M: 100x

Plate V

1. *Climacammina major* Morozova, Má-8 88.6 m M: 50x
2. *Climacammina aljutovica* Reitlinger, Má-8 125.0 m M: 50x
3. *Climacammina cf. gigas* Sulejmanov, Má-8 84.2 m M: 30x

Plate VI

1. *Paraglobivalvulina mira* Reytlinger, Má-8 161.0 m M: 100x
2. *Paraglobivalvulina mira* Reytlinger, Má-8 111.5 m M: 50x
3. *Paraglobivalvulina mira* Reytlinger, Má-8 98.0 m M: 100x
4. *Globivalvulina cyprica* Reichel, Má-8 89.0 m M: 100x
5. *Paraglobivalvulina mira* Reytlinger, Má-8 97.0 m M: 100x

Plate VII

1. *Paraglobivalvulina mira* Reytlinger, Má-8 98.0 m M: 100x
2. *Paraglobivalvulina mira* Reytlinger, Má-8 94.5 m M: 100x
3. *Globivalvulina* sp., Má-8 219.0 m M: 100x
4. *Globivalvulina* sp., Má-8 124.0 m M: 100x
5. *Globivalvulina bulloides* Brady, Má-8 217.0 m M: 100x

Plate VIII

1. *Globivalvulina vonderschmitti* Reichel, Má-8 81.0 m M: 100x
2. *Globivalvulina* sp., Má-8 220.0 m M: 100x
3. a) *Paraglobivalvulina vonderschmitti* Reichel, b) *Rectoglandulina* sp., Má-8 220.5 m M: 100x
4. *Globivalvulina cf. graeca* Reichel, Má-8 96.0 m M: 150x

Plate IX

1. *Dagmarita chanakchiensis* Reytlinger, Má-8 89.5 m M: 100x
2. *Dagmarita chanakchiensis* Reytlinger, Má-8 102.5 m M: 100x
3. *Dagmarita chanakchiensis* Reytlinger, Má-8 88.6 m M: 100x
4. *Pachyphloia* sp. cf. *P. solita* Sosnina, Má-8 189.5 m M: 100x
5. *Robuloides lens* Reichel, Má-8 96.0 m M: 100x
6. *Pachyphloia* cf. *pedicula* Lange, Má-8 217.0 m M: 100x
7. *Pachyphloia* cf. *pedicula* Lange, Má-8 221.5 m M: 100x

Plate X

1. *Codonofusiella nana* Erk, Má-8 125.0 m M: 100x
2. *Codonofusiella nana* Erk, Má-8 218.0 m M: 100x
3. *Codonofusiella* cf. *nana* Erk, Má-8 126.5 m M: 100x
4. *Codonofusiella nana* Erk, Má-8 84.2 m M: 100x
5. *Codonofusiella nana* Erk, Má-8 202.0 m M: 100x
6. *Codonofusiella nana* Erk, Má-8 220.0 m M: 100x

Plate XI

1. *Codonofusiella* cf. *paradoxia* Dunb. et Skin., Má-8 220.5 m M: 80x
2. *Codonofusiella* sp.1., Erk, Má-8 88.6 m M: 100x
3. *Reichelina minuta* Erk, Má-8 217.5 m M: 100x
4. *Reichelina* sp., Má-8 101.0 m M: 100x
5. *Codonofusiella* sp.2, Má-8 221.5 m M: 50x
6. *Codonofusiella* sp.1, Má-8 142.5 m M: 100x

Plate XII

1. *Kamurana* sp., Má-8 98.0 m M: 100x
2. *Agathammina pusilla* (Geinitz), Má-8 202.0 m M: 80x
3. *Agathammina pusilla* (Geinitz), Má-8 143.0 m M: 80x
4. *Agathammina multa* Pronina, Má-8 217.5 m M: 80x
5. *Agathammina* sp., Má-8 97.5 m M: 100x
6. *Agathammina* sp., Má-8 160.5 m M: 100x

Plate XIII

1. a) *Agathammina* sp., b) Brachiopoda shell fragment, Má-8 102.0 m M: 50x
2. a) *Agathammina* sp., b) *Hemigordius* nov. sp., Má-8 153.5 m M: 100x
3. *Baisalina pulchra* Reytlinger, Má-8 202.5 m M: 100x
4. *Baisalina pulchra* Reytlinger, Má-8 217.0 m M: 100x
5. *Agathammina?* sp., Má-8 176.0 m M: 100x
6. *Baisalina pulchra* Reytlinger, Má-8 217.0 m M: 100x
7. *Baisalina pulchra* Reytlinger, Má-8 217.0 m M: 100x
8. *Agathammina multa* Pronina, Má-8 206.5 m M: 50x

Plate XIV

1. *Kamurana?* sp., Má-8 86.7 m M: 100x
2. *Kamurana?* sp., Má-8 89.0 m M: 100x
3. *Kamurana?* sp., Má-8 83.0 m M: 100x
4. *Baisalina pulchra* Reytlinger, Má-8 96.0 m M: 100x
5. *Baisalina pulchra* Reytlinger, Má-8 179.0 m M: 100x

Plate XV

1. *Foram. indet. sp.*, Má-8 101.0 m M: 100x
2. *Foram. indet. sp.*, Má-8 178.5 m M: 100x
3. *Foram. indet. sp.*, Má-8 198.5 m M: 100x
4. *Kamurana bronnimanni* Altiner et Zaninetti, Má-8 112.0 m M: 100x
5. *Hemigordius sp.*, Má-8 174.0 m M: 100x
6. *Baisalina cf. pulchra* Reytlinger, Má-8 201.0 m M: 100x

Plate XVI

1. a) *Hemigordius abadehensis* Okimura et Ishii; b) *Hemigordius hungaricus nov. sp.*, Má-8 98.5 m M: 100x
2. *Hemigordius abadehensis* Okimura et Ishii, Má-8 202.5 m M: 100x
3. *Hemigordius abadehensis* Okimura et Ishii, Má-8 102.0 m M: 100x
4. *Hemigordius abadehensis* Okimura et Ishii, Má-8 103.5 m M: 100x

Plate XVII

1. *Hemigordius giganteus nov. sp.* Holotype, Má-8 143.0 m M: 100x
2. *Hemigordius giganteus nov. sp.*, Má-8 178.5 m M: 100x
3. a) *Hemigordius giganteus nov. sp.*, b) *Hemigordius nov. sp.*, Má-8 178.5 m M: 100x
4. *Hemigordius giganteus nov. sp.*, Má-8 179.0 m M: 100x
5. *Hemigordius sp. aff. H. abadehensis* Okimura et Ishii, Má-8 85.0 m M: 80x
6. *Hemigordius sp.*, Má-8 154.0 m M: 120x

Plate XVIII

1. *Hemigordius giganteus nov. sp.*, Má-8 170.0 m M: 90x
2. *Hemigordius giganteus nov. sp.*, Má-8 174.0 m M: 90x
3. *Hemigordius giganteus nov. sp.*, Má-8 198.5 m M: 90x
4. *Hemigordius giganteus nov. sp.*, Má-8 174.0 m M: 90x
5. *Hemigordius giganteus nov. sp.*, Má-8 180.0 m M: 90x
6. a) *Hemigordius minutus* Pronina, b) *Hemigordius giganteus nov. sp.*, Má-8 215.5 m M: 90x

Plate XIX

1. a) *Hemigordius zaninettiae* Altiner, b) *Pseudoglandulina longa* Mikl.-Makl, Má-8 217.0 m M: 90x
2. a) *Hemigordius zaninettiae* Altiner, b) *Ammonovertella inversa* (Schellwien), Má-8 216.5 m M: 100x
3. *Hemigordius zaninettiae* Altiner, Má-8 217.0 m M: 100x
4. *Hemigordius guvenci* Altiner, Má-8 183.0 m M: 100x
5. *Hemigordius guvenci* Altiner, Má-8 206.0 m M: 80x

Plate XX

1. a) *Hemigordius zaninettiae* Altiner, b) *Hemigordius sp.*, Má-8 220.5 m M: 100x
2. *Hemigordius zaninettiae* Altiner, Má-8 209.0 m M: 100x
3. *Hemigordius sp.*, Má-8 142.0 m M: 90x
4. a) *Hemigordius zaninettiae* Altiner, b) *Agathammina pusilla* (Geinitz), Má-8 218.0 m M: 90x
5. *Hemigordius zaninettiae* Altiner, Má-8 202.0 m M: 100x
6. *Hemigordius sp.*, Má-8 179.0 m M: 100x

Plate XXI

1. *Hemigordius* cf. *reicheli* Lys, Má-8 103.5 m M: 50x
2. *Hemigordius* sp. cf. *H. abadehensis* Okimura et Ishii, Má-8 199.0 m M: 100x
3. *Hemigordius* cf. *reicheli* Lys, Má-8 107.0 m M: 50x
4. *Hemigordius* sp., Má-8 100.5 m M: 100x
5. *Foram. indet. sp.*, Má-8 205.5 m M: 100x
6. *Foram. indet. sp.*, Má-8 160.5 m M: 100x
7. *Foram. indet. sp.*, Má-8 202.5 m M: 100x
8. a) *Foram. indet. sp.*, b) *Hemigordius* sp., Má-8 179.0 m M: 100x

Plate XXII

1. *Hemigordius mályinkai* nov. sp. Holotype, Má-8 212.5 m M: 100x
2. *Hemigordius mályinkai* nov. sp., Má-8 107.0 m M: 100x
3. *Hemigordius mályinkai* nov. sp., Má-8 195.5 m M: 100x
4. *Hemigordius mályinkai* nov. sp., Má-8 175.0 m M: 100x
5. *Hemigordius bronnimanni* Altiner, Má-8 199.0 m M: 100x
6. a) *Hemigordius zaninettae* Altiner, b) *Hemigordius* sp., Má-8 217.5 m M: 100x

Plate XXIII

1. *Hemigordius* sp., Má-8 198.5 m M: 100x
2. *Hemigordius* sp., Má-8 119.5 m M: 100x
3. *Hemigordius* sp., Má-8 170.0 m M: 100x
4. *Hemigordius* sp., Má-8 202.5 m M: 100x
5. a) *Hemigordius sigmoidalis* Wang, b) *Hemigordius* sp., Má-8 174.0 m M: 100x
6. *Hemigordius* sp., Má-8 182.0 m M: 100x
7. *Hemigordius* sp., Má-8 193.5 m M: 100x
8. *Hemigordius* sp., Má-8 198.5 m M: 100x
9. *Hemigordius* sp., Má-8 195.5 m M: 100x

Plate XXIV

1. a) *Hemigordius hungaricus* nov. sp. Holotype, b) *Pachyphloia*, Má-8 98.0 m M: 100x
2. *Hemigordius hungaricus* nov. sp., Má-8 92.0 m M: 100x
3. *Hemigordius hungaricus* nov. sp., Má-8 193.0 m M: 80x
4. *Hemigordius hungaricus* nov. sp., Má-8 101.0 m M: 100x
5. *Hemigordius* sp., Má-8 206.5 m M: 100x
6. *Hemigordius* sp., Má-8 98.5 m M: 100x
7. *Foram. indet. sp.*, Má-8 96.0 m M: 100x

Plate XXV

1. a) *Hemigordius hungaricus* nov. sp., b) *Hemigordius* sp., Má-8 90.4 m M: 100x
2. *Hemigordius hungaricus* nov. sp., Má-8 89.9 m M: 100x
3. *Hemigordius hungaricus* nov. sp., Má-8 96.0 m M: 100x
4. *Hemigordius* sp. aff. *Discospirella* sp., Má-8 95.0 m M: 100x
5. *Hemigordius hungaricus* nov. sp., Má-8 178.5 m M: 100x
6. *Hemigordius hungaricus* nov. sp., Má-8 96.0 m M: 100x
7. *Hemigordius hungaricus* nov. sp., Má-8 96.0 m M: 100x
8. *Hemigordius hungaricus* nov. sp., Má-8 202.5 m M: 100x
9. *Hemigordius hungaricus* nov. sp., Má-8 88.6 m M: 100x
10. *Hemigordius hungaricus* nov. sp., Má-8 91.5 m M: 100x
11. *Hemigordius hungaricus* nov. sp., Má-8 89.9 m M: 100x

Plate XXVI

1. *Hemigordius* sp. aff. *Discospirella plana* Okimura et Ishii, Má-8 88.6 m M: 100x
2. *Hemigordius* sp. aff. *Discospirella plana* Okimura et Ishii, Má-8 195.0 m M: 100x
3. *Hemigordius* sp., Má-8 98.0 m M: 100x
4. *Hemigordius hungaricus* nov. sp., Má-8 89.0 m M: 100x
5. *Hemigordius* sp. aff. *D. minima* Okimura et Ishii, Má-8 205.5 m M: 100x
6. *Hemigordius* sp., Má-8 95.5 m M: 100x
7. *Hemigordius* sp. aff. *Discospirella plana* Okimura et Ishii, Má-8 91.5 m M: 100x
8. a) *Hemigordius hungaricus* nov. sp., b) *Hemigordius* nov. sp., Má-8 202.5 m M: 100x
9. *Hemigordius hungaricus* nov. sp., Má-8 205.0 m M: 100x
10. *Hemigordius hungaricus* nov. sp., Má-8 100.5 m M: 100x
11. *Hemigordius* sp. aff. *D. minima* Okimura et Ishii, Má-8 213.5 m M: 100x
12. *Hemigordius* sp. aff. *D. plana* Okimura et Ishii, Má-8 195.5 m M: 100x
13. *Hemigordius* sp. aff. *D. plana* Okimura et Ishii, Má-8 204.5 m M: 100x

Plate XXVII

1. *Hemigordius minutus* Pronina, Má-8 195.5 m M: 100x
2. *Hemigordius minutus* Pronina, Má-8 154.0 m M: 100x
3. *Hemigordius minutus* Pronina, Má-8 202.5 m M: 100x
4. *Hemigordius* cf. *hungaricus* nov. sp., Má-8 195.5 m M: 100x
5. *Hemigordius minutus* Pronina, Má-8 179.0 m M: 100x
6. *Hemigordius minutus* Pronina, Má-8 195.5 m M: 100x
7. *Hemigordius minutus* Pronina, Má-8 205.5 m M: 100x
8. *Hemigordius* cf. *guvenci* Altiner, Má-8 195.5 m M: 100x
9. *Hemigordius* microbiofacies, Má-8 207.0 m M: 100x

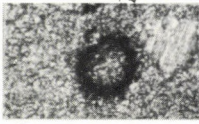
Plate XXVIII

1. a) *Hemigordius* sp., b) *Pseudoglandulina longa* Mikl.-Makl., Má-8 126.5 m M: 100x
2. *Pseudoglandulina longa* Mikl.-Makl., Má-8 217.0 m M: 100x
3. *Pseudoglandulina* sp., Má-8 193.0 m M: 100x
4. *Protonodosaria praecursor* (Rauser-Chernousova), Má-8 113.0 m M: 100x
5. *Nodosaria* cf. *sumatrensis* Lange, Má-8 124.0 m M: 100x
6. "*Ichtyolaria*" *latilimbata* Sell.Civr. et Dess., Má-8 184.5 m M: 100x
7. *Fronidina permica* Sell.Civr. et Dess., Má-8 184.5 m M: 100x
8. *Protonodosaria* sp., Má-8 217.0 m M: 100x
9. *Lunucammia* sp., Má-8 217.5 m M: 100x

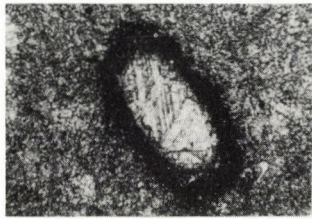
Plate XXIX

1. *Nodosaria mirabilis* Lipina, Má-8 144.0 m M: 100x
2. *Lingulonodosaria pyrula* (Sell.Civr. et Dess.), Má-8 86.7 m M: 100x
3. *Lingulonodosaria* sp., Má-8 210.5 m M: 100x
4. *Lingulonodosaria* sp., Má-8 182.5 m M: 50x
5. *Rectoglandulina* sp., Má-8 94.5 m M: 100x
6. *Pseudolangella bozorgiuae* Lys in Lys, M. et al. 1980, Má-8 183.0 m M: 100x

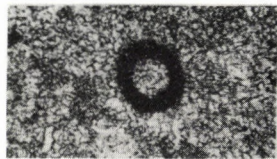
Plate I



1



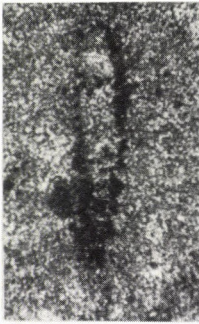
3



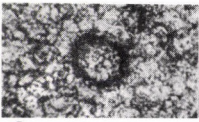
4



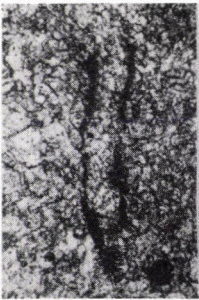
5



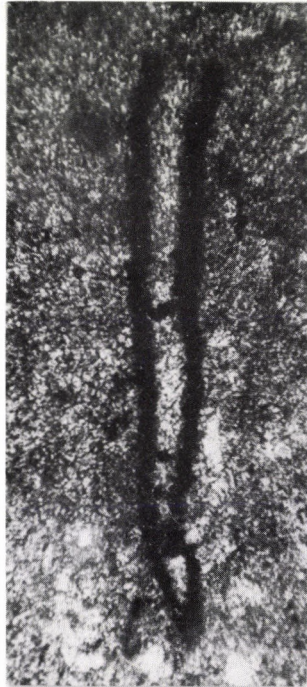
2



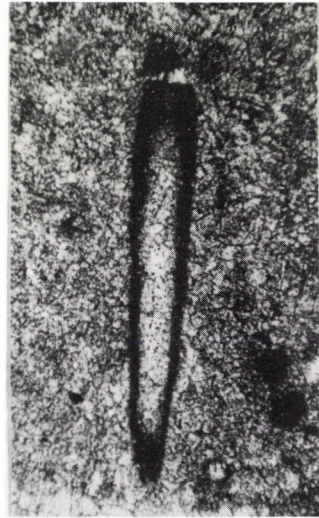
6



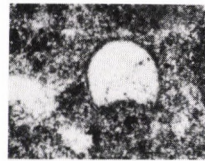
7



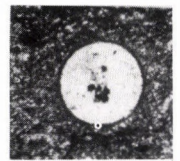
8



9



10



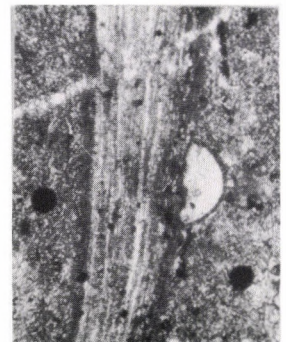
11



12

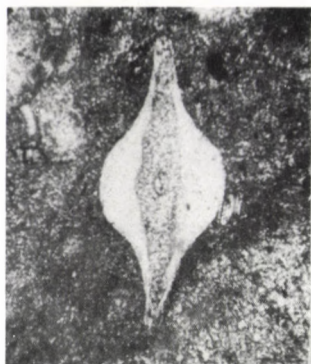


13



14

Plate II



1



2



3



4



5



6



7



8

Plate III



1



2



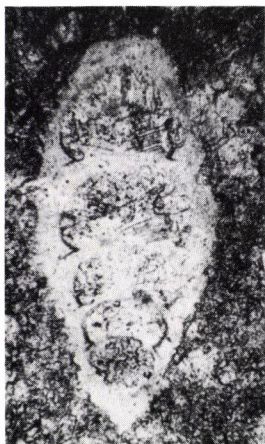
3



4



5

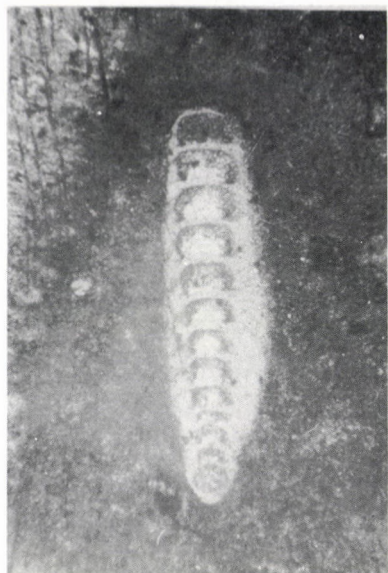


6

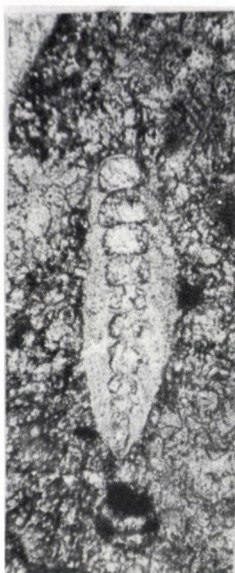


7

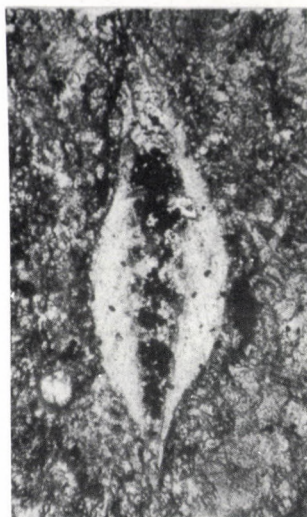
Plate IV



1



2



3



4



5



6



7



8



9

Plate V



1



2



3

Plate VI



1



2



3



4



5

Plate VII



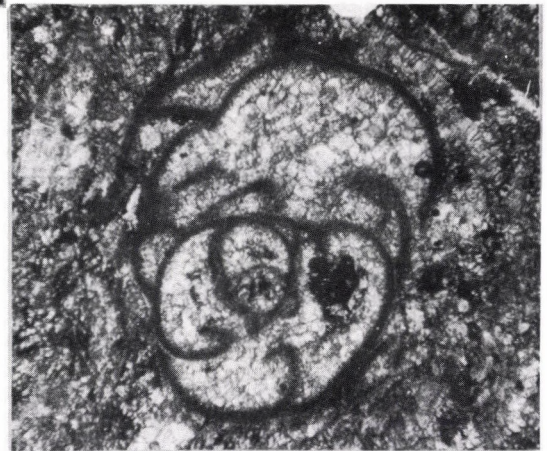
1



2



3



4



5

Plate VIII



1



2



3

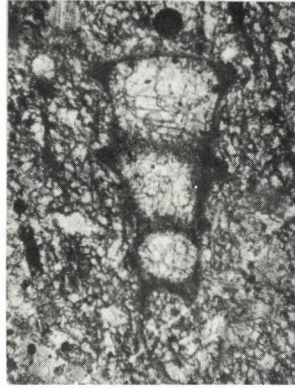


4

Plate IX



1



2



3



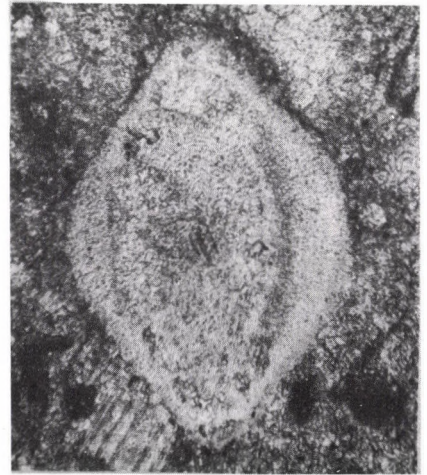
4



5



6

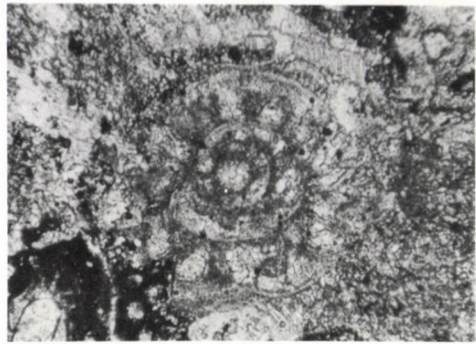


7

Plate X



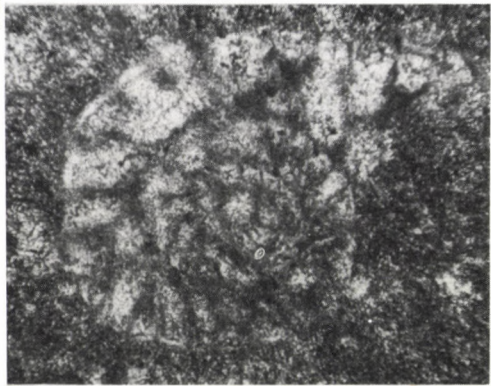
1



2



3



4

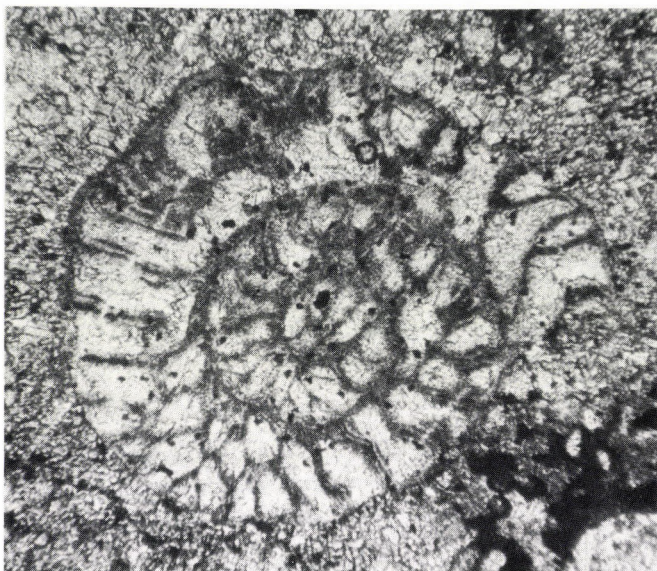


5



6

Plate XI



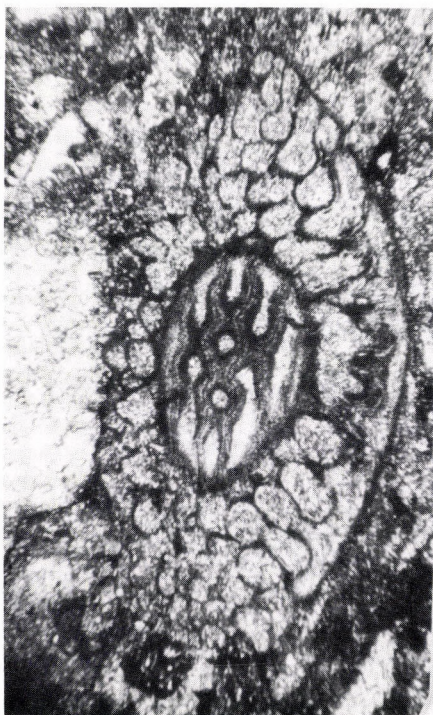
1



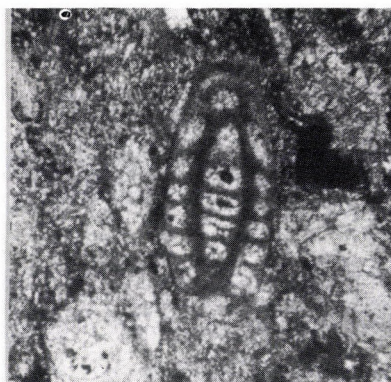
2



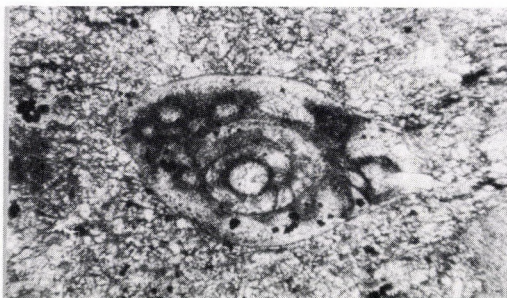
3



5

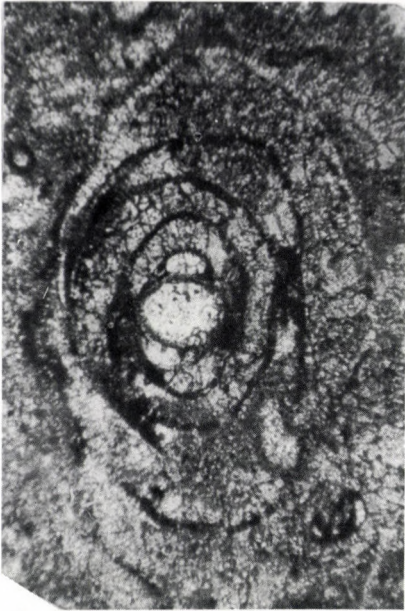


4



6

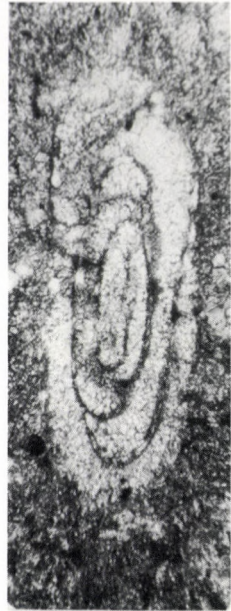
Plate XII



1



2



3



4

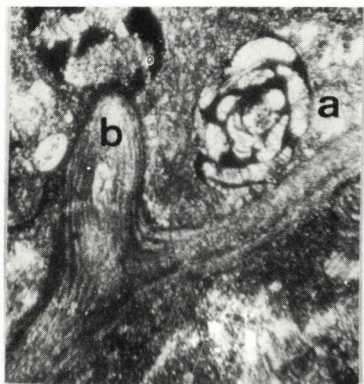


5



6

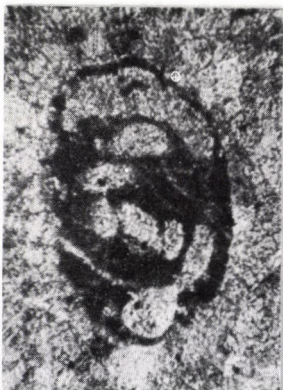
Plate XIII



1



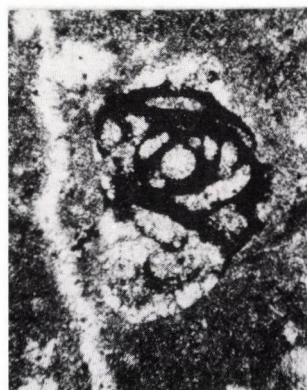
2



3



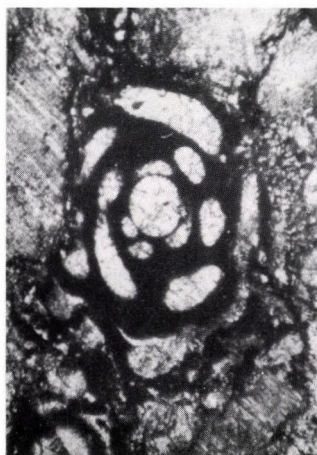
4



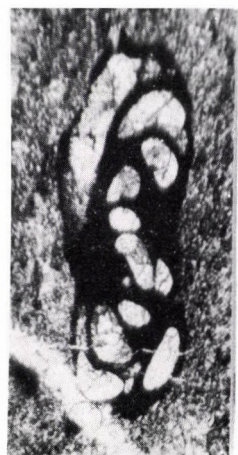
5



6



7

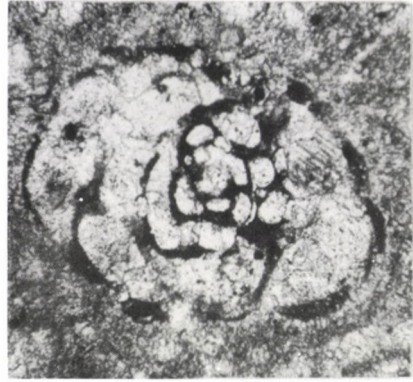


8

Plate XIV



1



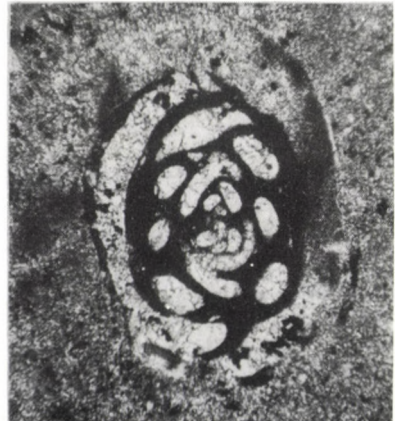
3



2



4

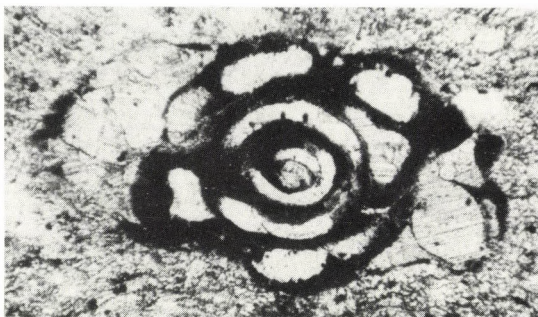


5

Plate XV



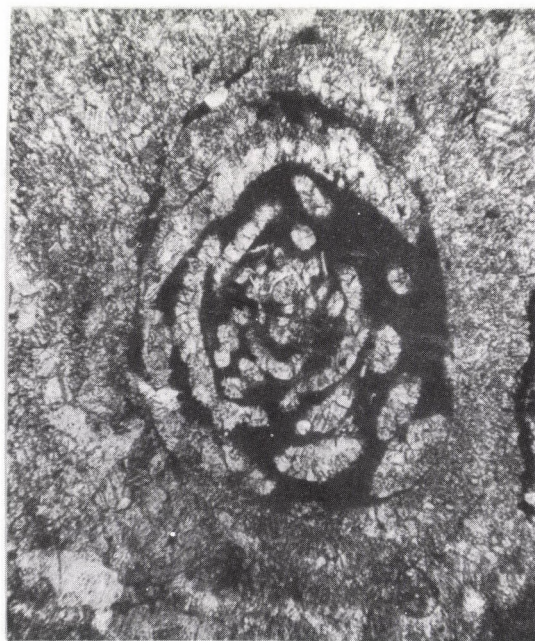
1



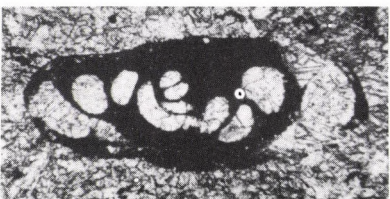
2



3



4



5



6

Plate XVI

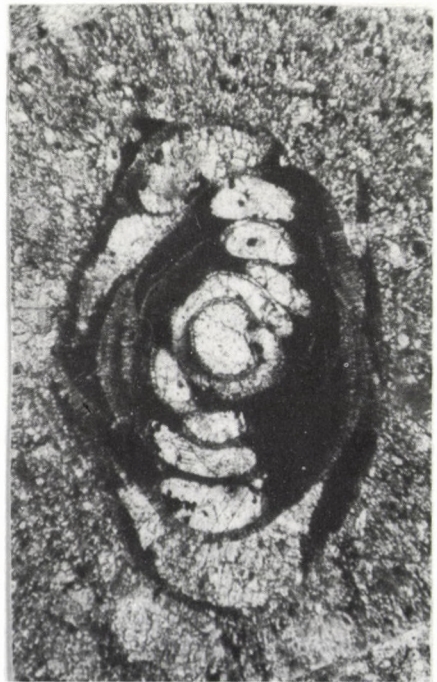
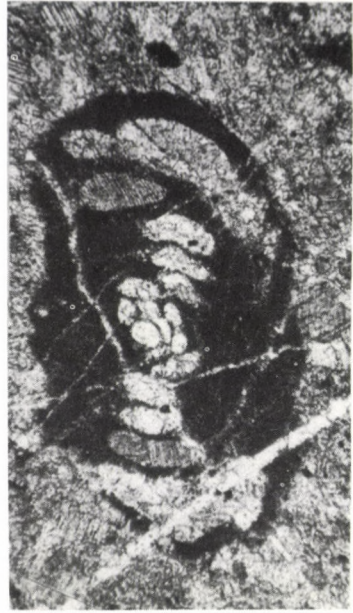


Plate XVII



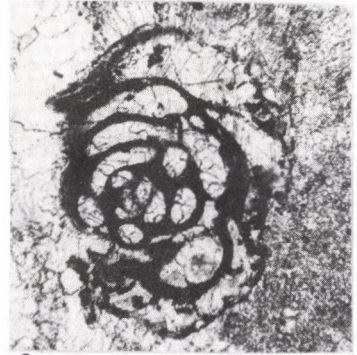
1



2



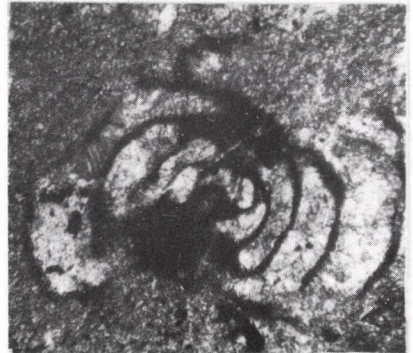
3



4



5



6

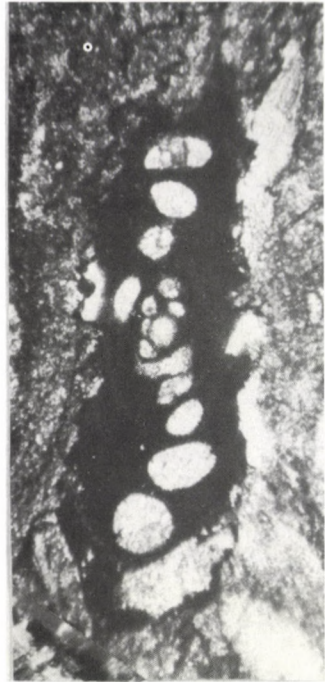
Plate XVIII



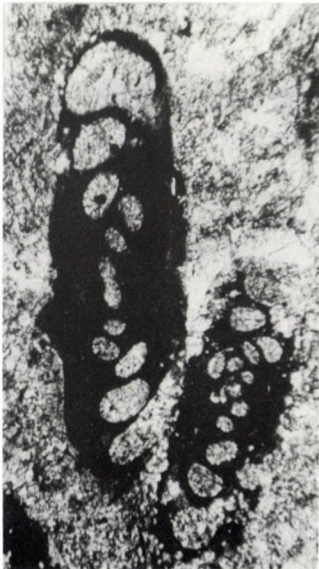
1



2



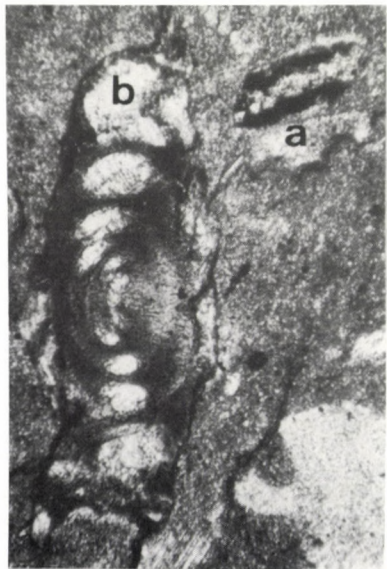
3



4



5



6

Plate XIX

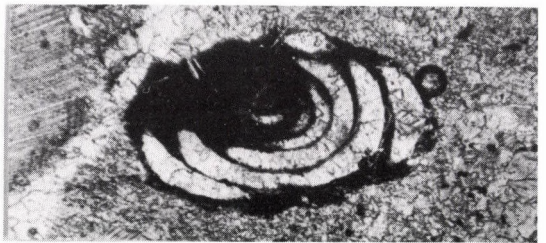
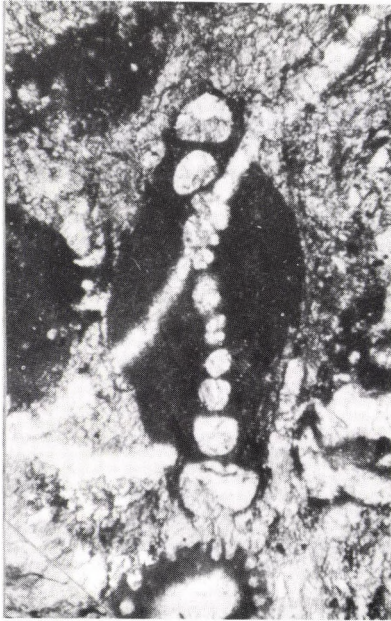
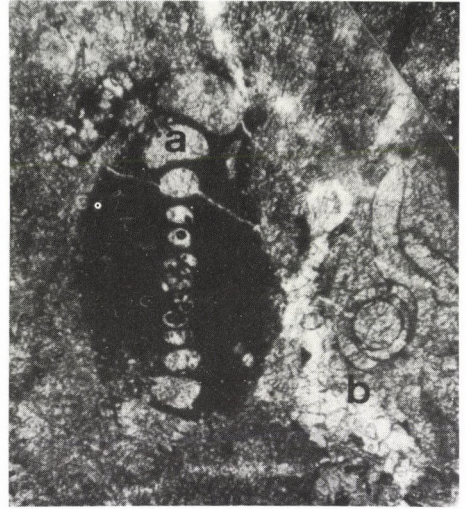
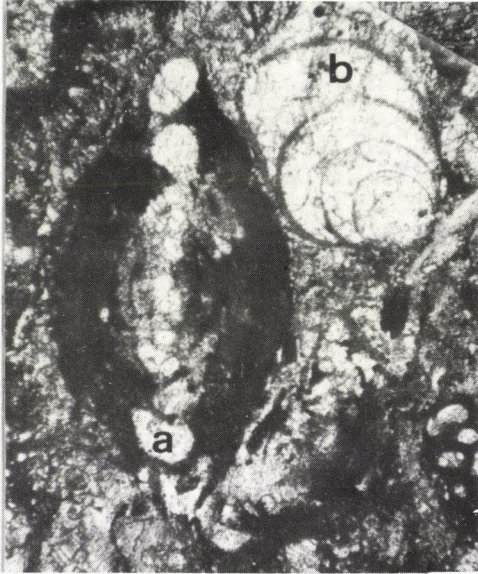
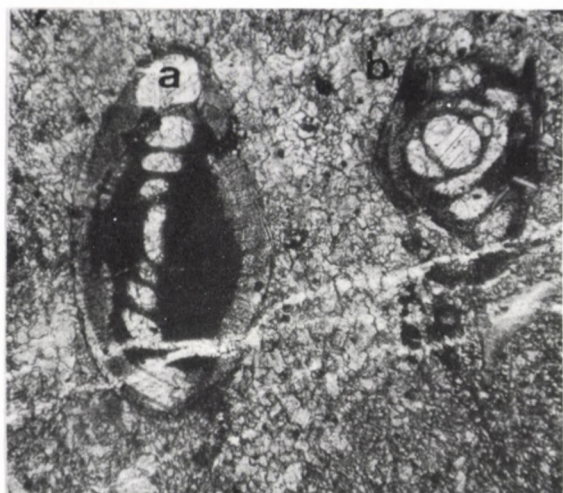


Plate XX



1



2



3



4



5

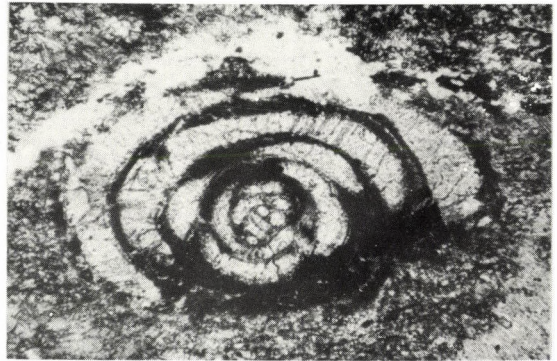


6

Plate XXI



1



2



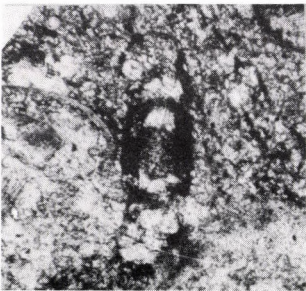
3



4



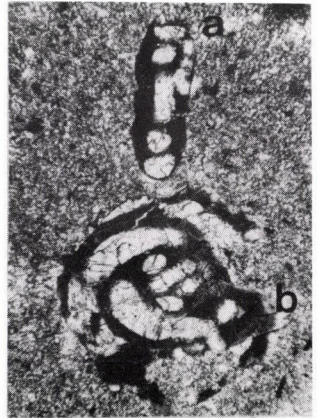
5



6

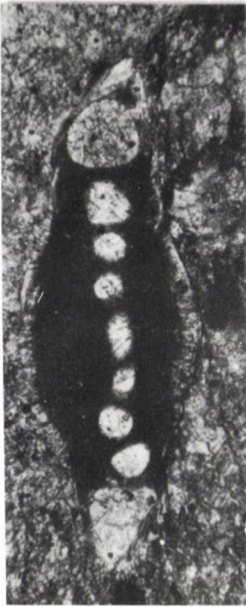


7



8

Plate XXII



1



2



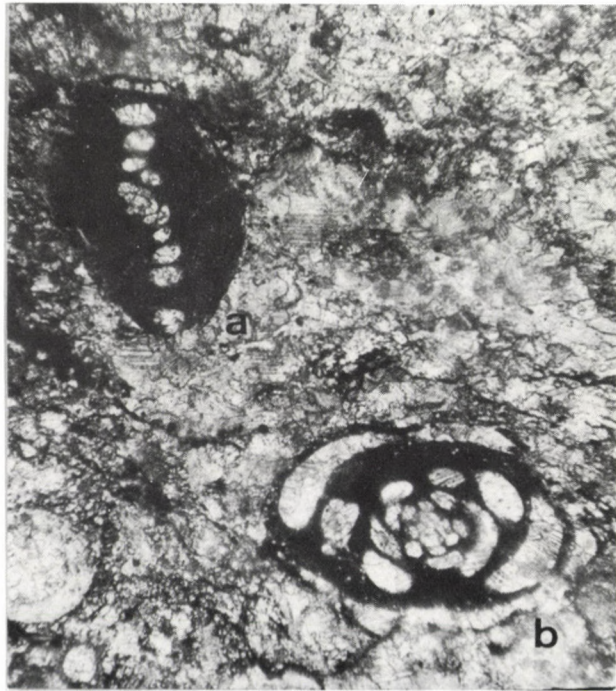
3



4



5



6

Plate XXIII



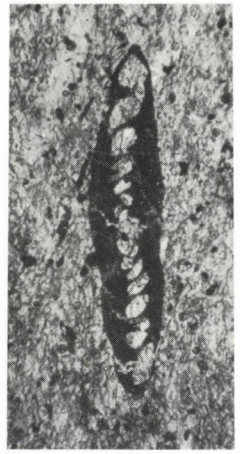
1



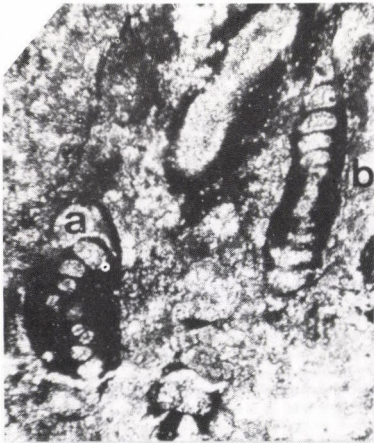
2



3



4



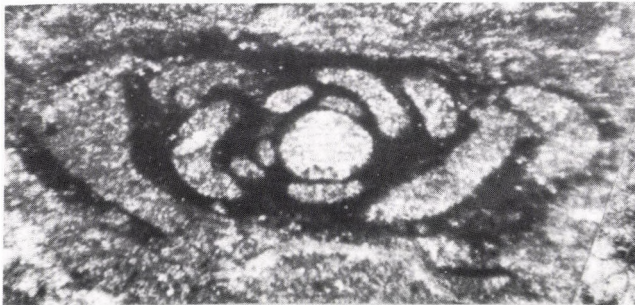
5



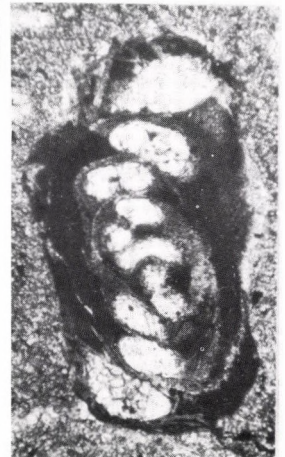
6



7

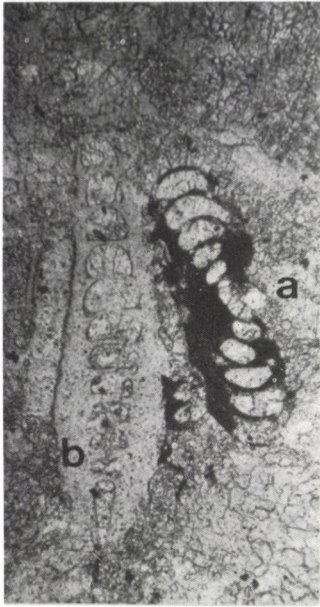


8

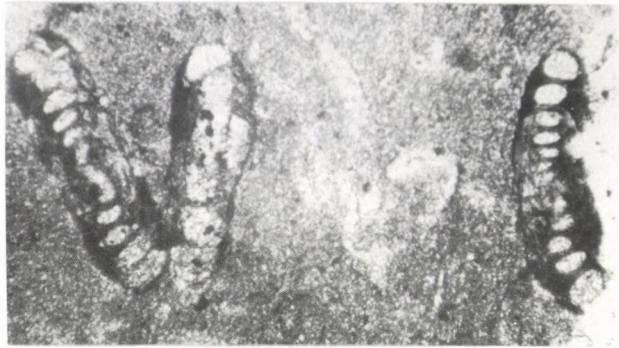


9

Plate XXIV



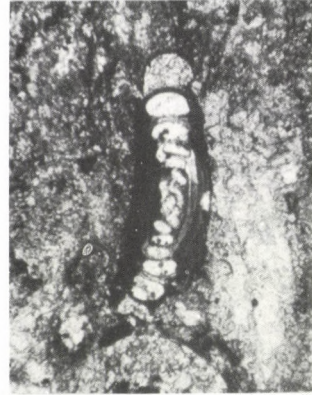
1



2



3



4



5

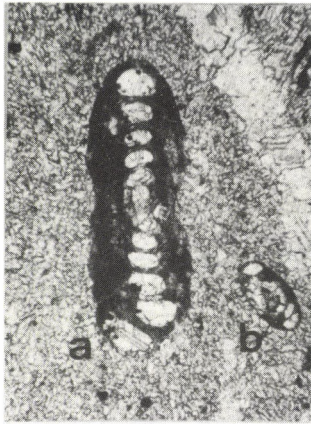


6

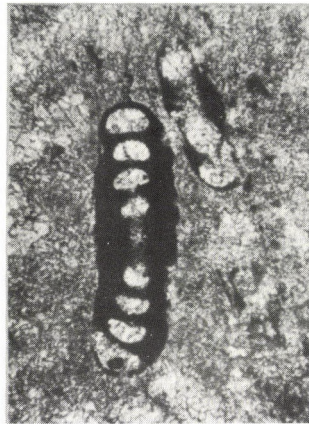


7

Plate XXV



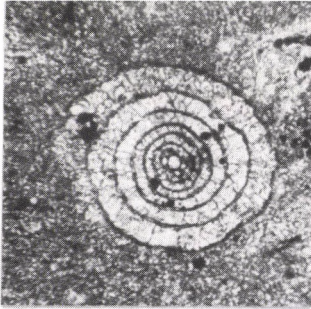
1



2



3



4



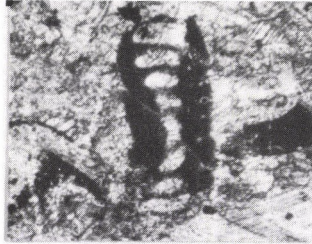
5



6



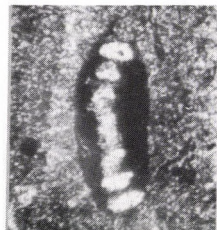
7



8



9

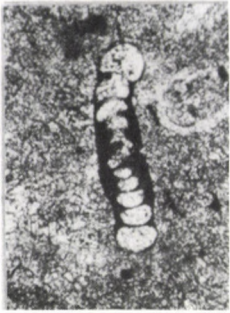


10

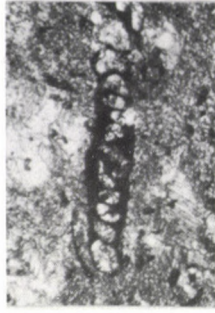


11

Plate XXVI



1



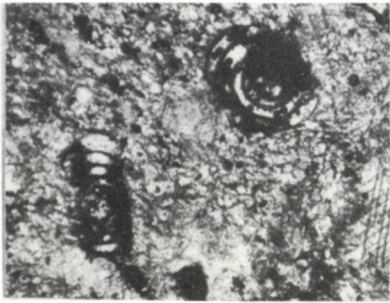
2



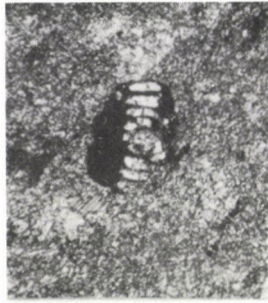
3



4



5



6



7



8



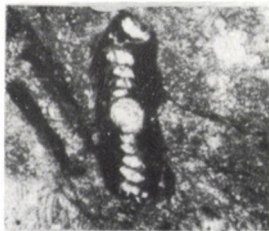
9



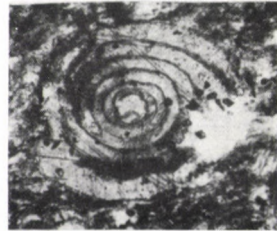
10



11



12



13

Plate XXVII



1



2



3



4



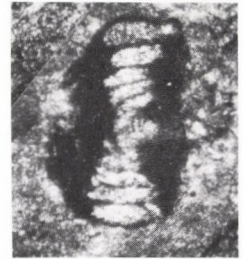
5



6



7

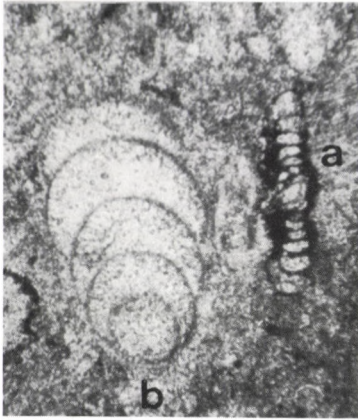


8



9

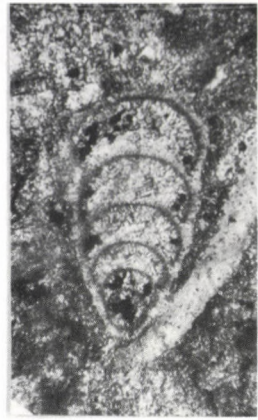
Plate XXVIII



1



2



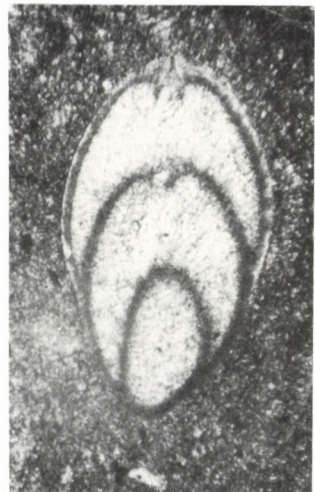
3



4



5



6



7



8



9

Plate XXIX



1



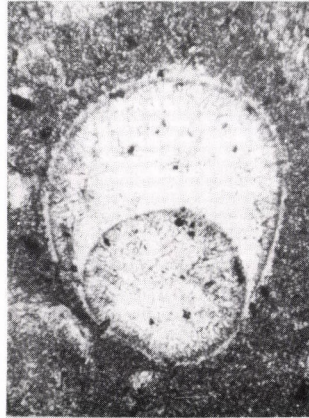
2



3



4



5



6

References

The works mentioned in the micropalaeontological part are listed in the References to the systematic work of Loeblich et Tappan (1988).

- Altiner, D. 1978: Trias nouvelles espèces du genre Hemigordius (Foraminiférel du Permien supérieur de Turquie (Taurus oriental). – Notes Lab. Paléontol., Univ. Genève, 2, 5, pp. 27–31.
- Altiner, D., P. Brönnimann 1980: Lousietta elegantissima, n. ge., n. sp. un nouveau foraminifère du Permien supérieur du Taurus oriental (Turquie). – Notes Lab. Paléontol., Univ. Genève, 6, 3, pp. 39–43.
- Bérczi-Makk, A. 1985: A Mályinka-8 fúrás foraminifera faunájának értékelése (Evaluation of the foraminifer fauna of borehole Mályinka-8). – In: Pelikán, P. A Mályinka-8 fúrás értékelő jelentése (Report on Study of Borehole Mályinka-8). MÁFI Doc Centr. 2109/1, Manuscript
- Bérczi-Makk, A. 1987: Észak-magyarországi Earlandia (Foraminifera) fajok a perm-triász határról (Northern Hungarian Earlandia (Foraminifer) species from the Permian/Triassic boundary). – MÁFI Évi Jel. 1985-ről, pp. 215–226.
- Bérczi-Makk, A. (in press): A Nagyvisnyó-18 sz. fúrás (Észak Magyarország) foraminifera faunája (perm-felső-karbon) (The foraminifer fauna [Permian–Upper Carboniferous] of borehole Nagyvisnyó-18 [Northern Hungary]). – MÁFI Évi Jel.
- Bérczi-Makk, A. (in press): A Mál-oldali (Észak-Magyarország) Nagyvisnyói Mésző Formáció foraminifera faunája (felső-perm) (The foraminifer fauna [Upper Permian] of the Nagyvisnyó Limestone Formation on the Mál side [Northern Hungary]). – MÁFI Évi Jel.
- Bogush, O.I. 1972: On the secondary changes of the testwall of some Paleozoic Foraminifera. – Vop. Mikropal., 15, pp. 19–24. (in Russian)
- Csontos, L., L. Félegyházi, S. Szabó, P. Varga 1983: Jelentés a Mályinka-8 számú fúrás mikrofácies vizsgálatáról (Nagyvisnyói Mésző Formáció) (Report on the microfacies study of borehole Mályinka-8 [Nagyvisnyó Limestone Formation]). – Manuscript, KFH 801/83, Budapest.
- Flügel, E. 1981: The Permian of the Carnic Alps –depositional environments and microfacies. – International Symposium Central European Permian, 1978 Warsaw, pp. 84–94.
- Fülöp, J. 1994: Magyarország geológiája. Paleozoikum II. (Geology of Hungary. Palaeozoic II). Akadémiai Kiadó, Budapest
- Grozdilova, L.P. 1956: Miliolidae of the Upper Artinskian (Lower Permian) of the western slope of the Urals. –VNIGRI, Microfauna of the USSR, n.s., 8, pp. 521–532, Leningrad (in Russian).
- Haas, J., F. Góczán, A. Oravecz-Scheffer, Á. Barabás-Stuhl, Gy. Majoros, A. Bérczi-Makk 1986: Permian–Triassic boundary in Hungary. – Mem. Soc. Geol. It., 34, pp. 221–241.
- Haas, J., F. Góczán, A. Oravecz-Scheffer, Á. Barabás-Stuhl, Gy. Majoros, A. Bérczi-Makk 1987: Perm–Triász határ Magyarországon. (The Permian/Triassic boundary in Hungary) – Ősl. Víták (Discussiones Palaeontologicae), 34, pp. 3–29, Budapest, (in Hungarian with English abstract).
- Howchin, W. 1885: Carboniferous Foraminifera of Western Australia with descriptions of new species. – Roy. Soc. South Australia Trans. et Proc., 19, pp. 194–198.
- Kotljar, G.V., G.S. Kropacheva, G.P. Pronina 1991: Upper Permian Zonal Scales of the South USSR and Possibilities of their Correlation. – Saito Ho – on Kai Spec. Publ, No 3, pp. 353–358, Sendai
- Kotljar, G.V., Yu.D. Zakharov, G.S. Kropatcheva, G.P. Pronina, I.O. Chedija, V.I. Burago 1989: Evolution of the latest Permian Biota. Midian regional stage in the USSR. – NAUKA, p. 185, Leningrad (in Russian).

- Kotljar, G.V., Yu.D. Zakharov, B.V. Koczyrkevich, G.S. Kropatcheva, K.O. Rostovcev, I.O. Chediya, G.P. Vuks, E.A. Guseva 1983: Evolution of the latest Permian Biota. Dzulfianand Dorashamian regional stages in the USSR. – NAUKA, p. 199, Leningrad (in Russian).
- Kovács, S., Cs. Péro 1983: Report on stratigraphical investigations in the Bükkium (Northern Hungary). – In: Sassi, F., T. Szederkényi (Eds) IGCP Project No. 5, Newsl., 5, pp. 58–65, Padova–Budapest.
- Kozur, H. 1985a: A Mályinka-8. sz. fúrás Ostracoda vizsgálata (Ostracod investigation of borehole Mályinka-8). – In: Pelikán, P. A mályinka-8 sz. fúrás értékelő jelentése (Report on Study of Borehole Mályinka-8), MÁFI Doc. Centre, 2109/1, Manuscript, Budapest.
- Kozur, H. 1985b: Biostratigraphic of the Upper Paleozoic conodonts, ostracods and holothurian sclerites of thye Bükk Mts. Part II, Uppper Paleozoic ostracods. – Acta Geol. Hung., 28, 3–4, pp. 225–256, Budapest.
- Köylüoğlu, M., D. Altiner 1989: Micropaleontologie (Foraminiferes) et Biostratigraphie de Permien superieur de laregion d'Hakkari (SE Turquie). – Rev. Paléobiol., 8, 2, pp. 467–503, Geneve.
- Loeblich, A.R., H. Tappan 1988: Foraminiferal genera and their classification. – VNR Company, New York, I, p. 970, II, p. 212. Plates 1–847.
- Lys, M., M. Colochen, J.P. Bassoullet, J. Marcoux, G. Mascle 1980: La biozone Colaniella parva du Permien superieur et sa microfaune daba le bloc calcaire exotique de Lamayuru, Himalaya du Ladakh. – Rev. Micropal., 23, 2, pp. 76–108, Paris.
- Lys, M., J. Marcoux 1978: Les Niveaux du Permien superieur des Nappes d'Antalaya (Taurides occidentales, Turquie). – C.R. Acad. Sci. 286, s.D, 20, pp. 1417–1420, Paris.
- Noé, S.U. 1987: Facies and Paleogeography of the Marine Upper Permian and of the Permian–Triassic boundary in the Southern Alps (Bellerophon Formation, Tesero Horizon). – Facies, 16, pp. 89–142, Erlangen.
- Okimura, Y., K.I. Ishii 1981: Smaller Foraminifera from the Abadeh Formation, Abadehian Stratotype, Central Iran. – Geol. Survey of Iran, Report. 49, pp. 7–28.
- Pelikán, P. 1985: A mályinka-8. sz. fúrás értékelő jelentése (Report on study of borehole Mályinka-8). – MÁFI Doc Centre, 2109/1 Manuscript, Budapest.
- Pesic, L., A. Ramovs, J. Sremac, S. Pantic-Prodanovic, I. Filipovic, S. Kovács, P. Pelikán 1986: Upper Permian deposits of the Jadar region and their position within the Western Paleotethys. – Mem. Soc. Geol. It., 34, pp. 211–219.
- Piros, O. 1985: A Mályinka-8. sz. fúrás alga vizsgálata (Alga investigation of borehole Mályinka-8.). – In: Pelikán, P. A Mályinka-8 sz. fúrás értékelő jelentése (Report on study of borehole Mályinka-8), MÁFI Doc. Centre 2109/1, Manuscript, Budapest.
- Pronina, G. 1988: The Late Permian Miliolata of Transcaucasus. – In: Classification, ecology and stratigraphy of Miliolata (Foraminifera). – Proc. Zool. Inst., Acad. Sci. USSR., 184, pp. 49–63. Leningrad (In Russian).
- Sheng, J.Z., Y. He 1983: Permian Shanita–Hemigordius (Hemigordiopsis) (Foraminifera) fauna in Western Yunnan, China. – Acta Palaeont. Sinica, 22, 1, pp. 55–59.
- Sidó, M., B. Zálányi, Z. Schréter 1974: Neue Paläontologische ergebnisse aus dem Oberpaläozoikum des Bükkgebirges. – Akadémiai Kiadó, Budapest, p. 311.
- Schubert, P.J 1908: Zur Geologie des österreichischen Velebit. – Jahrb. k.k. geol. Reichsanstalt, 58, 2, pp. 345–386.
- Taraz, H. et al (Iranian–Japanese Research Group) 1981: The Permian and Lower Triassic Systems in Abadeh Region, Central Iran. – Mem. Fac. Sc. Kyoto Un., s. Geol. Mineral. 47, 2, pp. 66–133, Kyoto.
- Zaninetti, L., D. Altiner, E. Catal 1981: Foraminifères et biostratigraphie dans le Permien supérieur du Taurus oriental, Turquie. – Notes Lab. Paleont. Univ Genève, 7, 1, pp. 1–38.

Clay mineralogy of Jurassic carbonate rocks, Central Transdanubia, Hungary

István Viczián

Hungarian Geological Survey, Budapest

X-ray diffraction was used to study the insoluble residues of about 100 samples of Jurassic rocks (limestone, marl and clay). The samples were collected from 10 outcrops in the Transdanubian Central Range and from 4 boreholes reaching the Mesozoic basement of the Neogene Zala Basin.

Jurassic rocks of the Transdanubian Central Range are free of major diagenetic alteration. Clay mineralogy varies with stratigraphic age: Lias and Bajocian are characterized by the dominance of illites and moderately expanded mixed-layer illite/smectites. Clays connected with Toarcian manganese ores are rich in smectite. In the Callovian and Malm smectite and mixed-layer illite/smectites are abundant. Kaolinite and chlorite are usually present in low amounts, increasing somewhat in a northeasterly direction.

Processes of diagenesis, environmental relations of deposition and Alpine analogies are discussed.

Key words: clay mineralogy, Jurassic, carbonate rocks, paleoenvironment, diagenesis, X-ray diffraction, Transdanubian Mountain Range, Zala Basin

Introduction

Mesozoic formations of Central Transdanubia form a predominantly marine carbonate sequence. This study deals with the Bakony, Gerecse and Pilis areas of the Transdanubian Mountain Range (Table 1) as well as as the Jurassic basement of the Neogene Zala Basin SW of the Bakony Mts. (Fig. 1).

In the Jurassic period the entire area under study was part of the sedimentation basin of Tethys and participated in its evolution. During the Lias the initial shallow carbonate platform was subdivided into seamounts and partial basins by block-faulting and differential subsidence. The greatest water depths prevailed in the Middle Jurassic (radiolarites) while in the Upper Jurassic a gradual uplift took place (Galács and Vörös 1972, see also Fig. 10).

Clay mineral data either of single Jurassic samples or of groups of samples from specific formations (especially sedimentary manganese ores in the Upper Liassic) were published by Szabó-Drubina (1962), Bárdossy and Csajághy (1966), Grasselly et al. (1969), Bernoulli and Peters (1970), Bausch (1971), Fülöp (1975), and Nemezc (1981, "blue illite", p. 517).

This paper considers mineralogical composition of insoluble residues as a function of stratigraphy and depth.

Address: I. Viczián: H-1143 Budapest, Stefánia út 14, Hungary

Received: 23 March, 1995

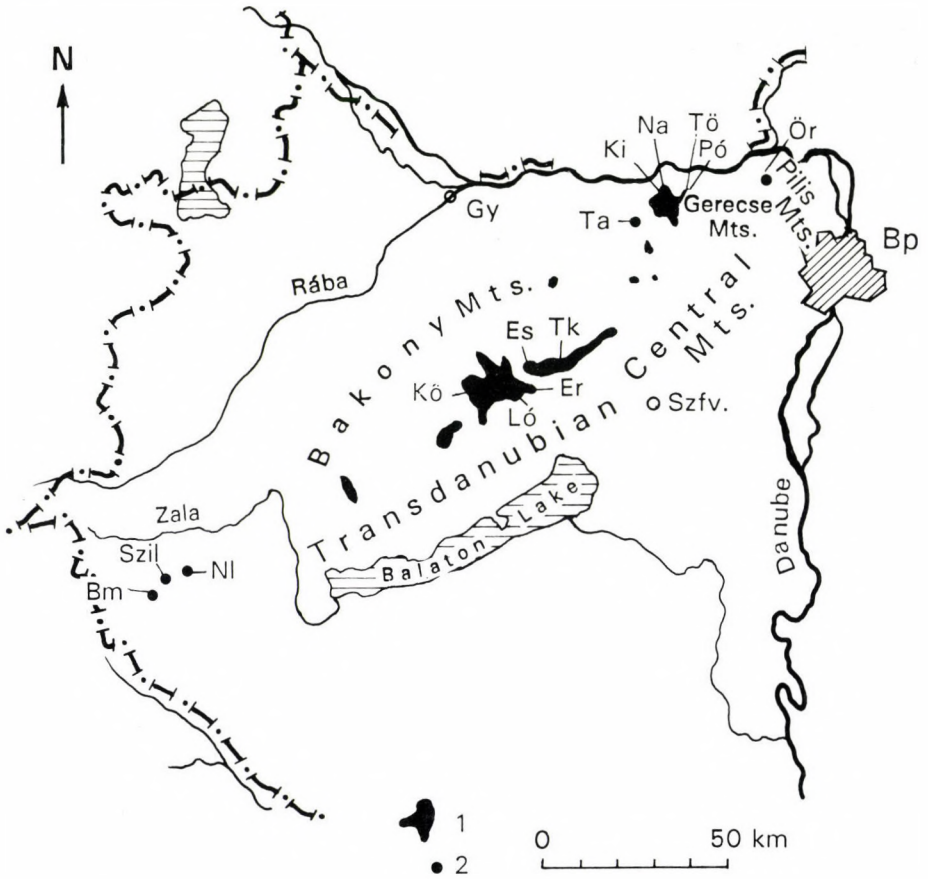


Fig. 1
 Locality map. Jurassic formations in the Transdanubian Central Range are shown according to Fülöp (1971, with additions). See Table 1 for abbreviations of the geological sections and references describing the geological relations of the sections. Abbreviations of major cities on the map: Gy - Győr; Bp - Budapest; Szfv - Székesfehérvár; 1. Jurassic; 2. borehole

Clay content of the samples

The majority of the samples studied were pure limestones with very low clay content. Some samples were collected from marl and clay horizons (e.g. from Upper Liassic manganese ores) and shaly intercalations in cherts (in the Callovian and Malm, see Fig. 3 to 6).

Special care was taken to observe textural characteristics of the samples. Each sample was studied visually and in thin section in order to determine the proportions of the clay material and the carbonate components of the particular rock. The following types can be distinguished:

Table 1
Studied geological sections

Area	Abbreviation in Fig. 1	Name of the section	References of field description
Pilis Mts	Ör	Kesztölc, Öregszirt (Velka Skala)	Dosztály (1988), Konda (1988a, MGA No. 84)
Gerecse Mts	Ta	Tata, borehole TVG-50	Fülöp (1975)
	Na	Nagypisznice Quarry	Konda (1985, MGA No. 07)
	Ki	Kisgerecse Quarry	Konda (1986, MGA No. 10)
	Tö	Lábatlan, Tölgyháti Quarry	Fülöp (1971), Konda (1988b, MGA No. 80)
Bakony Mts	Pó	Lábatlan, Póckő	Konda (unpubl.)
	Kö	Hárskút, Közöskúti-árok	Konda (1970), Fülöp (1971)
	Ló	Lókút, Lókút Hill	Vörös (1982), Konda (1970), Konda (1987, MGA No. 67)
	Es	Olaszfalú, Eperkés Hill	Konda (1970), Fülöp (1971)
	Tk	Bakonycsernye, Tűzköves-árok	Fülöp (1969), Konda (1989, MGA No. 117)
Zala Basin	Ep	Eplény, Mn deposit	Grasselly et al. (1969)
	Nl	Borehole Nagylengyel-358	Kőrössy (1988)
	Szil	Boreholes Szilvagy-32, -33	Kőrössy (1988), Bérczi-Makk (1980)
	Bm	Borehole Bárszentmihályfa-I	Kőrössy (1988), Jámbor et al. (1976)

"MGA" = Magyarország geológiai alapszelvényei (see: References)

1) The clay component is dispersed more or less homogeneously in the carbonate matrix of the limestones.

2) There are thin (a few mm thick) clay or marl layers between the limestone beds.

3) Red nodular limestones which represent a special textural type of Jurassic limestones of the Tethys area. These appear, for instance, in the Upper Lias and Bajocian of the Gerecse Mts. According to Jenkyns (1974), nodular texture is due to the early diagenetic rearrangement of the carbonate material, while clay minerals may be left unchanged by this process. According to my observations the clay mineral composition of the interior of the nodules is virtually identical with that of their clayey or marly envelope.

The clay mineralogy of each of these three textural types is considered to be representative of the original clay material deposited in the bottom of the Jurassic sea.

4) Clay occurring as coatings of small cavities in the limestones or present in the tests of fossils as well as the clay matrix of synsedimentary limestone breccias are presumably syngenetic or epigenetic neoformations.

5) Sometimes clay is concentrated in minute cracks. This type occurs especially among the samples taken from great depths in the basement of the

Zala Basin. This textural type is presumably the result of local rearrangement of dispersed clay material. However, it may indicate some degree of diagenetic transformation of the original composition.

Methods of investigation

Carbonate minerals were dissolved in 3% HCl.

Considering the very fine grained nature of the insoluble residues (Fülöp 1975, Table 1 to 3), no further separation of grain fractions seemed necessary. The μm grain size fraction was separated only from clay samples of Öregszirt and Póckő (Fig. 3). Insoluble residues were analysed by X-ray diffractometry. Oriented mounts were prepared by the smear-on-glass method. Untreated, ethylene glycol treated and heated (at 300 °C or 490 °C for 1 hour) mounts were X-rayed. Typical X-ray patterns are shown in Fig. 2.

Clay minerals were identified primarily by the position of their basal reflections. Specific values were used for detailed characterization of individual clay mineral types such as width of the 001 reflection of kaolinite and illite (Kübler index, "degree of crystallinity") as well as d position and intensity of the 001/001 reflection of mixed-layer illite/smectites.

Potassium feldspar appeared to be monoclinic, whilst plagioclases were identified as low-albites.

Semi-quantitative X-ray determination of clay minerals was carried out using the standard method of Rischák and Viczián (1974). Percentage values obtained by this method are usually reproducible within the limits of a few percent.

Results

Figures 3 and 4 show semi-quantitative clay mineralogical compositions expressed as mean values for individual stages of the Jurassic of the Pilis, Gerecse and Bakony, respectively. The two most complete sections occur in the Tűzköves-árok (Bakony Mts) and in the Tölgyháti Quarry (Gerecse Mts), both representing the entire Jurassic period. In addition, stratigraphically incomplete sections are exposed in the Közöskúti-árok and in the Eperkés Hill (both in the Bakony Mts). It is assumed that in these locations a continuous marine sedimentation took place during the Jurassic and the lack of certain stratigraphic horizons is most probably due to post-depositional submarine erosion. Other studied sections, Lókút (in the Bakony Mts), Kisgercse and Nagypisznice Quarries (in the Gerecse Mts) represent only a limited period of uninterrupted Jurassic sedimentation. A single locality in the Pilis Mts represents shales intercalated in radiolarian chert and underlying limestone of Malm age (Dosztály 1988).

Illites and mixed-layer illite/smectites of various degrees of expandability are almost always the dominant clay minerals in all the formations studied. Illite is usually of low crystallinity, values of the Kübler index vary in the range of 0.5 to 1.1 $^{\circ}2\theta$ (CuK α) in the Gerecse Mts and 1.3 to 2.0 $^{\circ}2\theta$ in the Pilis Mts (<2 mm fraction).

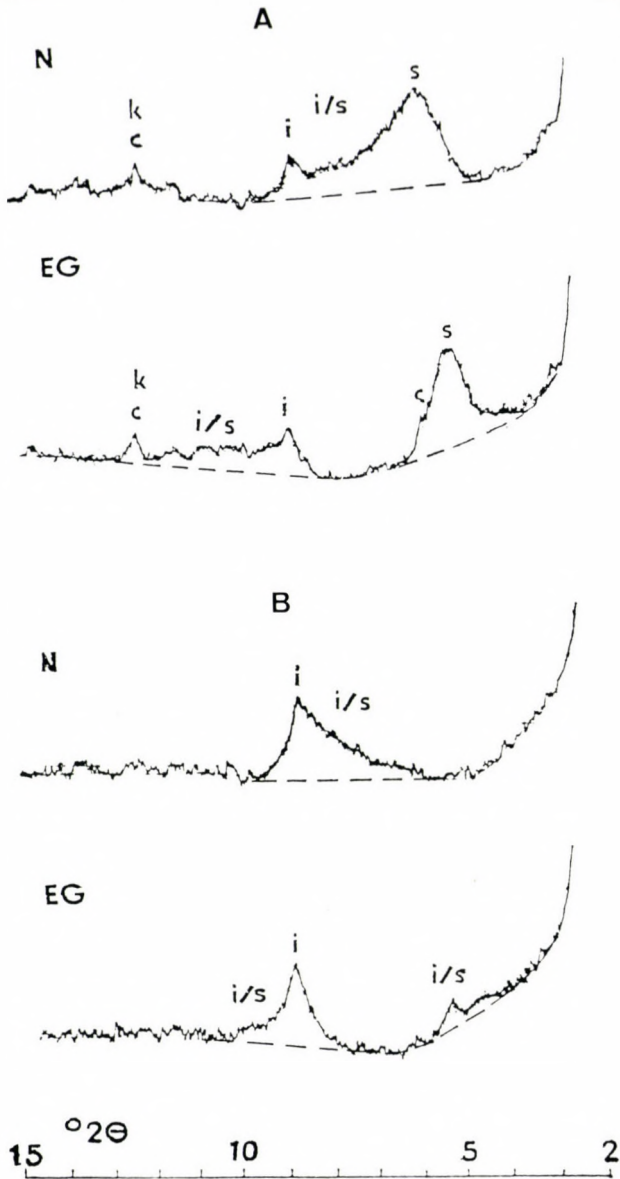


Fig. 2

Typical X-ray diffraction patterns of the insoluble residue of Jurassic limestones in the Tűzkőves-árok sequence (Bakony Mts). A. Kimmeridgian non-layered, massive, light grey limestone, B. Hettangian/Sinemurian, Dachstein-type yellowish grey limestone. Stratigraphic position of the samples is shown in Fig. 10. N - untreated; EG - ethylene glycol treated sample, oriented specimens, $\text{CuK}\alpha$ radiation; i - illite; i/s - mixed-layer illite/smectite; s - smectite, k - kaolinite; c - chlorite

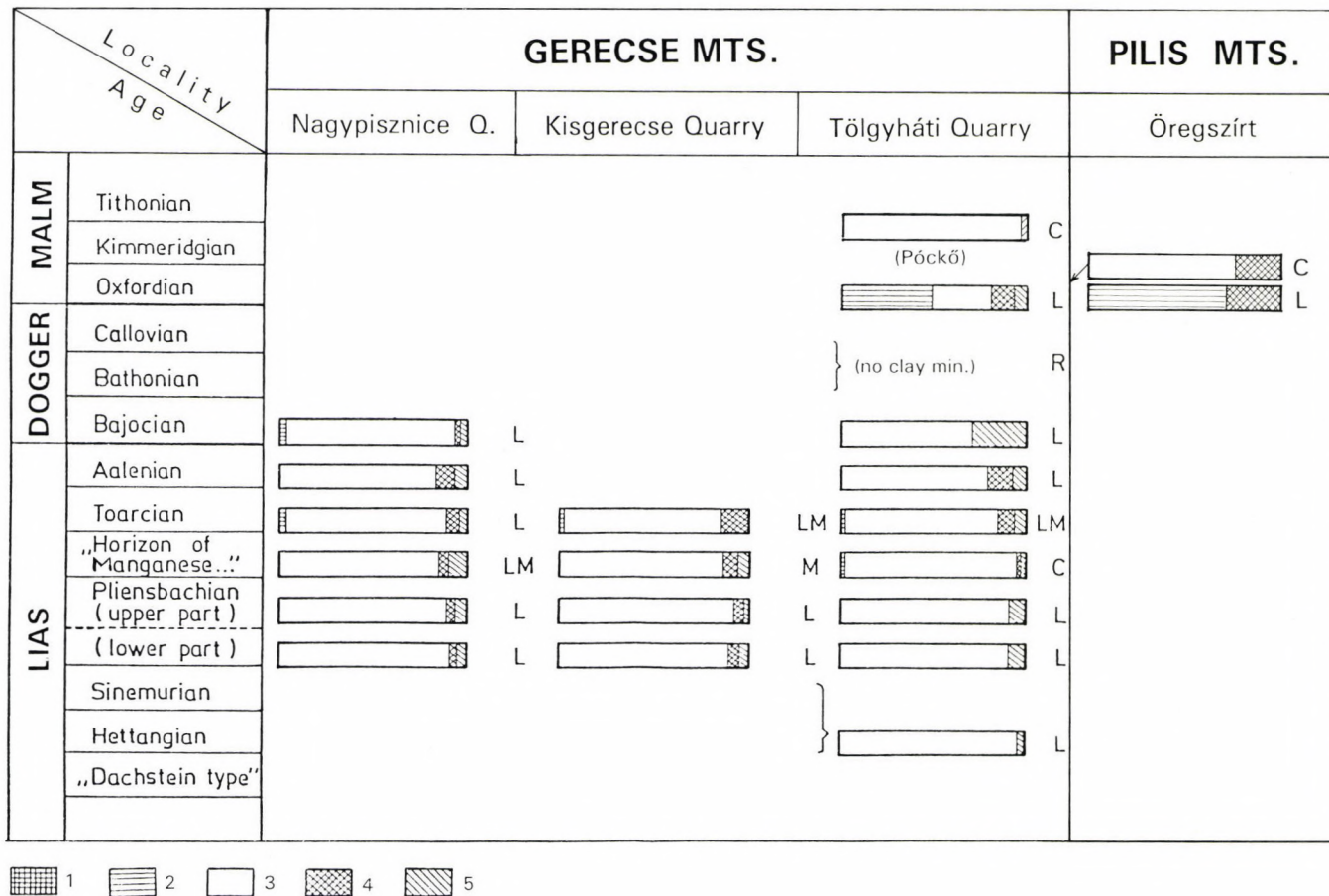


Fig. 3

Semi-quantitative clay mineral composition of insoluble residues of Jurassic carbonate rocks in the Gerecse and Pilis Mts. C – clay; L – limestone; LB – limestone breccia; LM – calcareous marl; M – marl; R – (Radiolarian) chert, 1. smectite + mixed-layer illite/smectite (smectite:illite 2/3 to 1); 2. mixed-layer illite/smectite (smectite:illite 1/3 to 2/3); 3. illite; 4. kaolinite; 5. chlorite

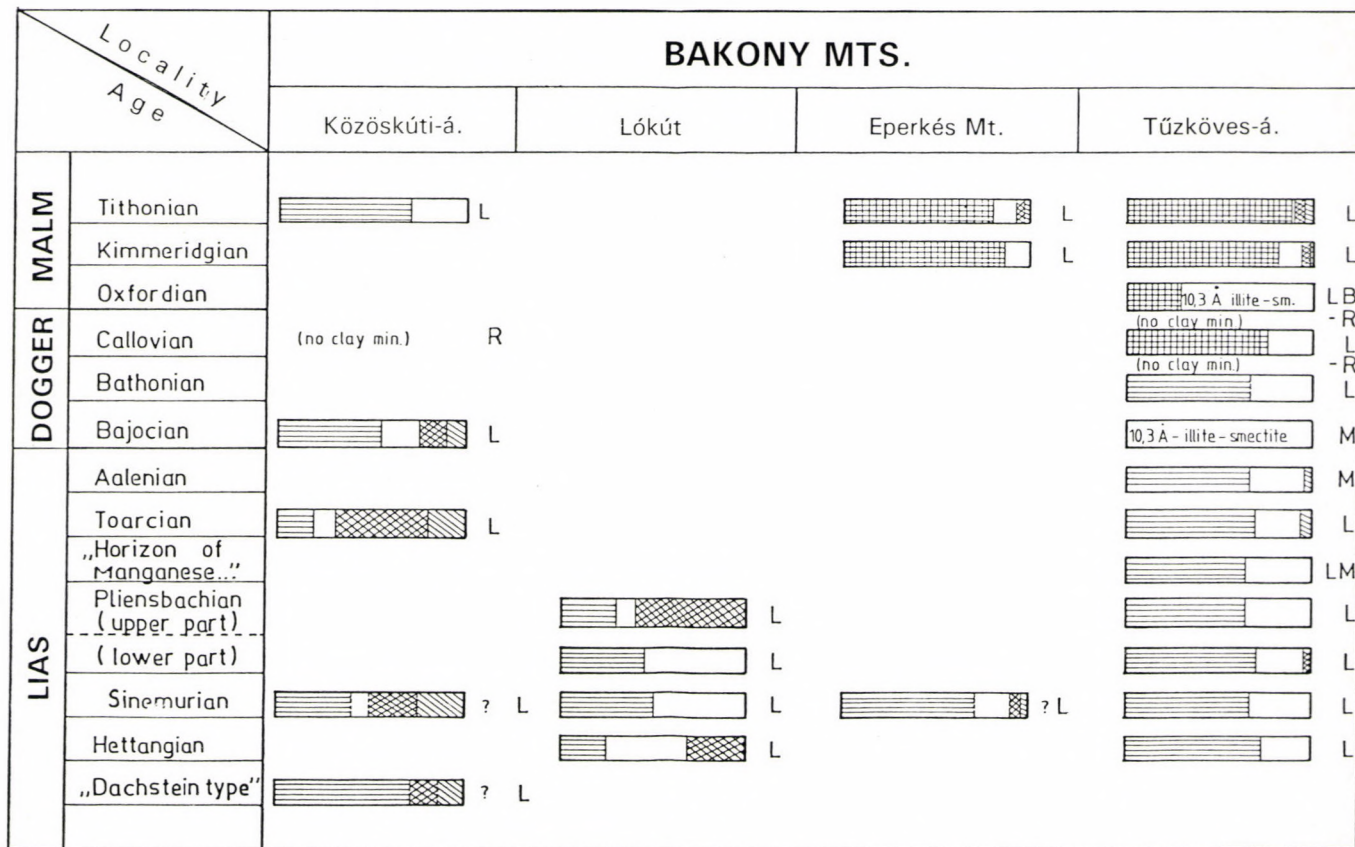


Fig. 4

Semi-quantitative clay mineral composition of insoluble residues of Jurassic carbonate rocks in the Bakony Mts. Legend and abbreviations as for Fig. 3

On the other hand, in most of the samples from the Bakony Mts Kübler indexes cannot be determined due to the presence of more expanded mixed-layer phases. Illite polytypes are most frequently of 1Md, though the 2M type was also clearly observed.

The contents of expandable layers in mixed-layer minerals vary systematically with the stratigraphic and geographic position of the samples. Clays in the Gerecse Mts are less expanded than those in the Bakony Mts. In addition, in the Bakony Mts and probably also in the Gerecse Mts the amount of expanding components is higher in the Callovian and Malm than in the Lias.

There is a remarkable clay horizon in the limestone series at the base of the Upper Liassic (Toarcian) which is stratigraphically equivalent to the manganese deposits of Úrkút and Eplény in the Bakony Mts (Grasselly et al. 1969; Konda 1970). The contents of expanded clay minerals are exceptionally high in this clay horizon, in the immediate vicinity of the manganese deposits. In other occurrences, however, its mineralogical composition resembles to that of the insoluble residue of the next limestone samples in the section (Fig. 5).

Contents of kaolinite and chlorite are rather low throughout the study area. There are only sporadic indications of somewhat higher kaolinite contents in the sections

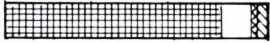
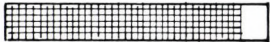
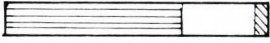
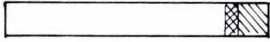
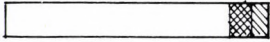
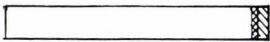
BAKONY MTS.	
Eplény, Mn dep (Mine)	 C
Eplény, Mn dep (Kávás Mt.)	 C
Tűzköves-á.	 LM
TATA	
Borehole TVG - 50	 C
GERECSE MTS.	
Nagypisznice Quarry	 LM
Kisgerecse Quarry	 M
Tölgyháti Quarry	 C

Fig. 5
Semi-quantitative clay mineral composition of clays belonging to the Toarcian Horizon of Manganese Ores in the Transdanubian Central Mts. Legend and abbreviations as for Fig. 3

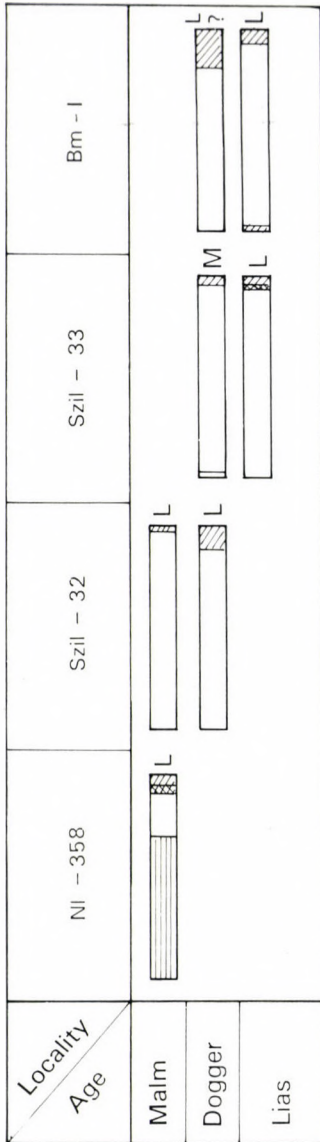


Fig. 6
Semi-quantitative clay mineral composition of insoluble residues of Jurassic carbonate rocks in the Mesozoic basin floor formations of Zala Basin. Boreholes: see Table 1. Legend and abbreviations as for Fig. 3

treated: 10.60 Å, heated at 490 °C: 9.80 Å). This mineral can be interpreted to contain about 20 per cent smectite component.

of Közöskúti-árok and Lókút while the rocks of Eperkés Hill and Tűzköves-árok (Bakony Mts) are virtually free of these minerals. In the Gerecse Mts both kaolinite and chlorite appear in almost all samples but always in small amounts. The locality of Malm at Öregszirt in the Pilis Mts seems to have the highest kaolinite contents.

The clay mineral assemblage of the Jurassic basement of the Zala Basin is similar to that of the mountain areas. The differences are in the expandability and in the kaolinite contents. Illite is very abundant, mixed-layer illite/smectites area much less widespread and kaolinite is practically absent. Malm limestones in borehole Nagylengyel-358 represent a transitional composition between the deeply buried rocks and those of near surface occurrences in the mountain area (Figs 6, 7). They contain a few percent of kaolinite and a moderately expanded mixed-layer mineral (illite:smectite 1/3 to 2/3).

Clays of supposedly syn- or epigenetic origin show special mineralogical compositions:

In small cavities of limestones the clay mineral association resembles the dispersed argillaceous material in the adjacent rocks, except that it contains more kaolinite.

Between the fragments of Oxfordian limestone breccia in Tűzköves-árok, the clay matrix is composed of smectite and abundant "10.3 Å illite/smectite", a special type of mixed-layer illite/smectites, different from those found elsewhere. It is characterised by sharp, symmetrical basal reflections (untreated: 10.37 Å, ethylene glycol

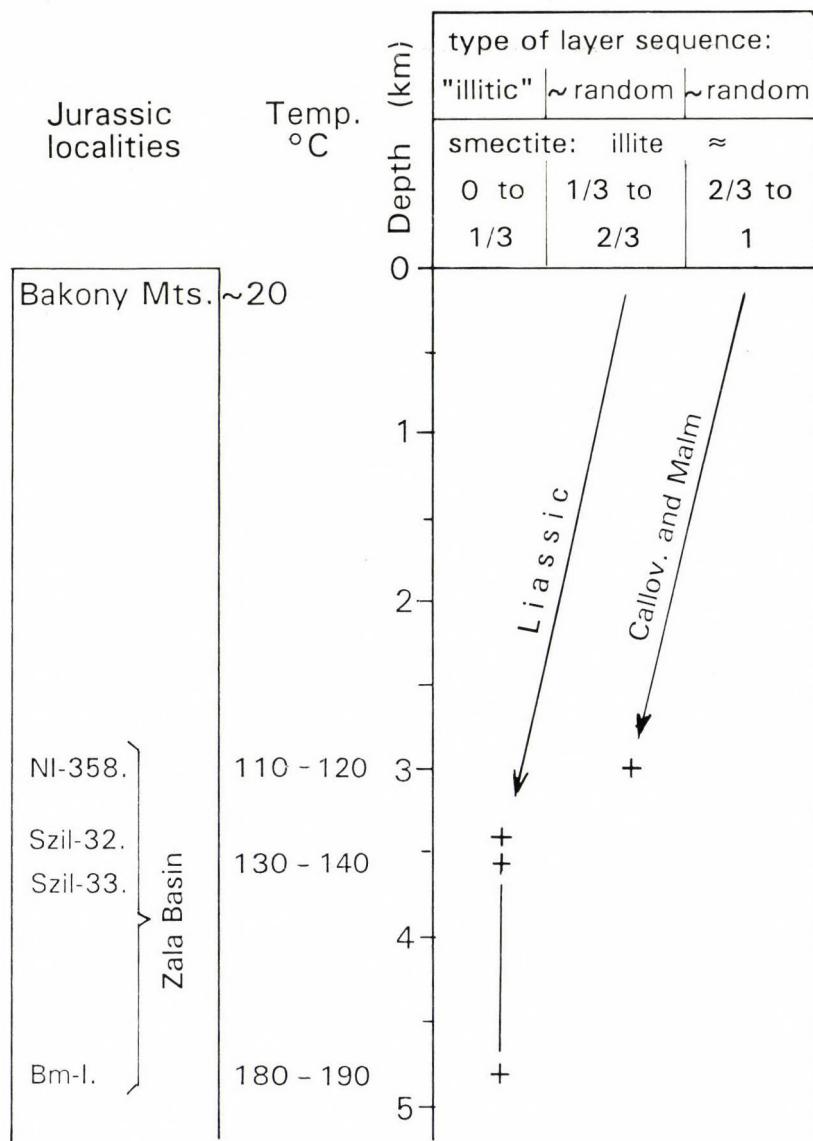


Fig. 7

Subsurface depth of Jurassic formations in boreholes of Zala Basin, temperatures measured in boreholes and schematic summary of diagenetic transformation of expanded 2:1 clay minerals. Note the distinct trends of diagenetic transformations for Liassic and for Callovian to Malm rocks

It is interesting to note that in the Tűzköves-árok Bajocian marls, having an otherwise normal, homogeneous texture, contain the same type of mixed-layer mineral (Fig. 10).

Discussion

Diagenesis in the Zala Basin

Differences in mineralogy between rocks of surface localities and deep-seated formations in the Zala Basin may be consequences of diagenetic processes (Fig. 7). However, when interpreting these differences, some caution is needed because they may also be due to lateral variations in the original composition of the sediment. Therefore, the Zala Basin was only compared to the adjacent Bakony Mts. In addition, variations due to different stratigraphic positions have been taken into account, thus Callovian + Malm formations and Liassic samples were compared separately.

The subsurface position of Jurassic strata, recovered in boreholes in the Zala Basin, are shown in the first column of Fig. 7. Their depths of burial vary between 3.4 and 5.0 km. Column 2 of Fig. 7 summarizes processes of diagenetic transformation of mixed-layer clay minerals of moderate to high expanding layer content. Details of the transformation of 2:1 type clay minerals as well as sharpening of the 002 chlorite reflection are shown in Fig. 8.

Rocks situated near the present-day surface contain monoclinic potassium feldspar but no albite. On the other hand, in the borehole Bárszentmihályfa Bm-I where Jurassic is at depths of nearly 5 km, plagioclase (low-albite) is rather abundant. Feldspar is absent at shallower levels in the borehole samples (Fig. 9). K-feldspar probably dissolves in deeper zones of diagenesis and serves as a source of K^+ for illitization. In accordance with Bausch and Poll (1976), the appearance of albite may indicate intensive diagenesis of Jurassic limestones in a similar manner as in the Eastern Alps. The lowest values of Kübler indices for illites (0.45 to 0.60 $^{\circ}2\theta$) correspond to the highest contents of low-albite in borehole Bm-I, indicating the highest degree of diagenetic transformation at subsurface depths of 4.8 km and temperatures at 180 to 190 $^{\circ}C$. Present-day temperatures measured in the boreholes are considered to be maximum temperatures reached by the sedimentary column. The actual maximal temperatures, however, may have been even slightly higher considering erosional periods during and after the Neogene sedimentation.

It is interesting to note that a single sample from the most intensively transformed rocks (a Toarcian red nodular limestone) contains hematite. In other subsurface samples goethite and hematite were not encountered and only pyrite was present due to the reduced nature of the subsurface samples.

Stratigraphic and regional variations in the mountain areas

In the entire Lias the clay mineralogy is remarkably constant in the continuous stratigraphic sequences, such as at Tűzköves-árok and in sequences of the Gerecse. It is also remarkable that small differences in the mineralogical composition (e. g. differences of kaolinite and chlorite contents) persisted for long periods among the depositional areas of the individual sections. All of

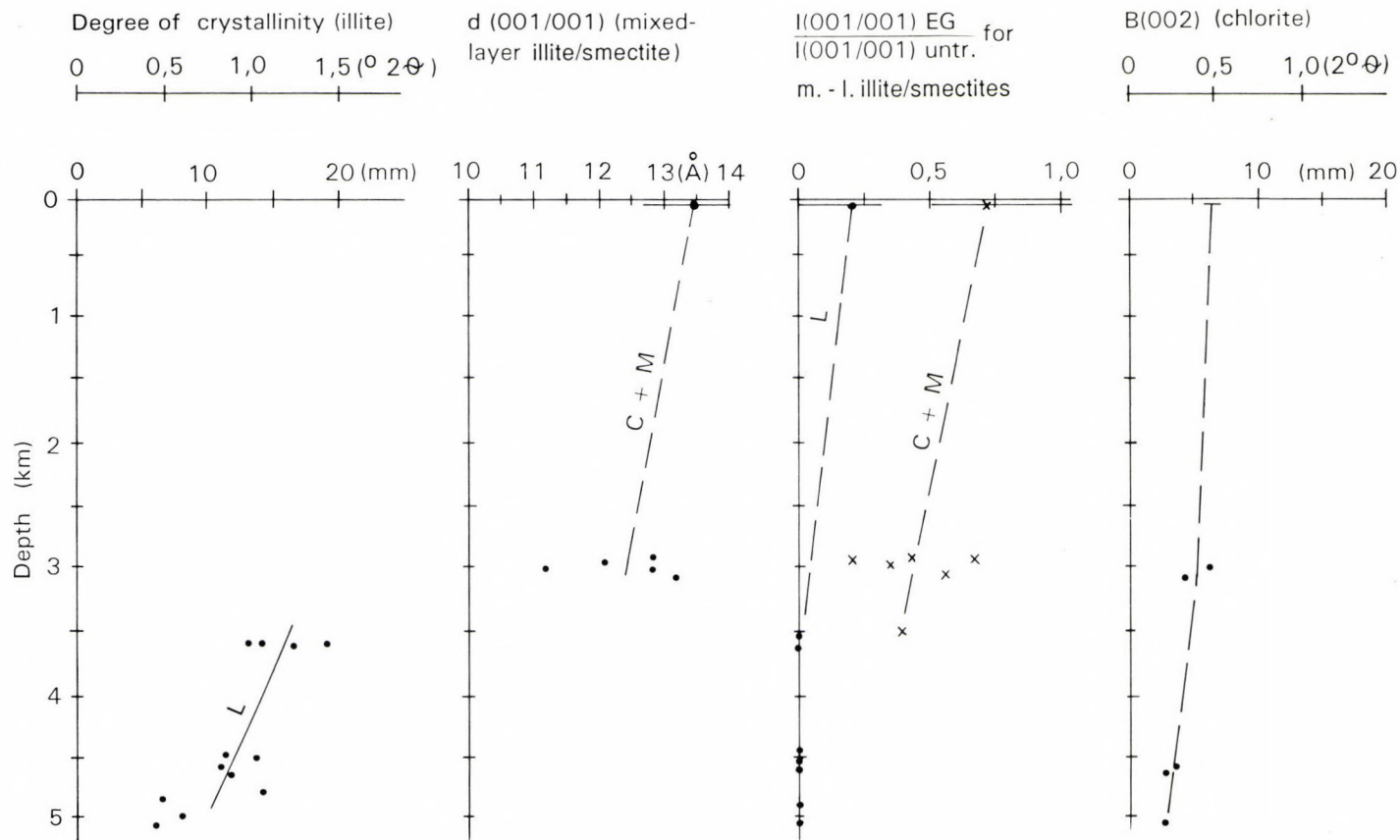


Fig. 8

Details of diagenetic transformation of clay minerals in the Zala Basin as compared with the Bakony Mts (range of the values measured in the Bakony samples is shown by horizontal lines at 0 km depth). Degree of illite crystallinity values in the Bakony Mts are 1.5 $^{\circ}2\theta$ (containing expanded phases together with illite). d(001/001): see Fig. 10. I - intensity (peak area); EG - ethylene glycol treated sample, untr.: untreated sample, B(002): width of the 002 basal reflection of chlorites ($d=7\text{\AA}$) at half height ("chlorite crystallinity"); L - Liassic samples, C+M: Callovian to Malm samples

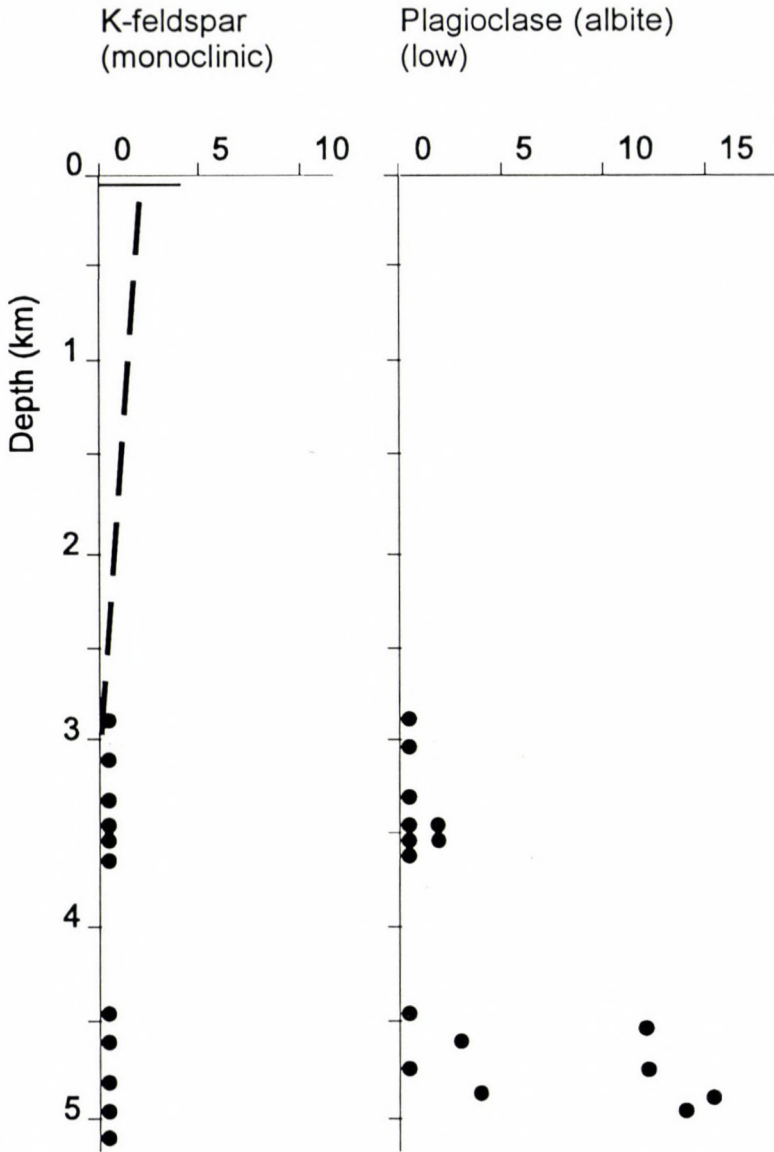


Fig. 9
 Variation of the feldspar contents in the insoluble residue of Jurassic limestones in Zala Basin and in Bakony Mts (range of the values measured in the Bakony samples is shown by horizontal line at 0 km depth)

this points to a long period of sedimentation, lasting until the Middle Jurassic, with little or no change in the environmental conditions. The Lókút section represents an exception with its highly variable kaolinite contents in the Lias.

Increasing kaolinite contents should indicate the direction of the ancient source area, approximately the coastline. Considering the differences between the individual sections, however, no particular direction can be established. Kaolinite seems to increase both in northeasterly and southwesterly directions, starting from a central minimum represented by the Tűzköves-árok sequence. The increase northeastward seems to be more systematic.

The evolution of the expanding-type 2:1 clay minerals during the Jurassic period is reflected by the variation of the value of $d(001/001)$ in the various stratigraphic horizons (Fig. 10). This figure shows that there is a sudden change in the proportions of the expanded component in the Middle Dogger. Lias and Bajocian are characterised by moderately expanded types (Fig. 2B), the Callovian and Malm by highly expanded ones (Fig. 2A). Analyses of samples from the Közöskúti-árok have revealed similar highly expanded types in the Lower Cretaceous limestones. The sudden break in the curve, representing the expanded nature of the 2:1 minerals, coincides with the rapid deepening of the basin (see bathymetric curve of Géczy, 1961 in Fig. 10).

In a similar manner as in the Bakony, two main periods of clay sedimentation took place in the Gerecse, indicated by a less expanded type before the Middle Jurassic and a more expanded one after this time. The rather high contents of illite/smectite and kaolinite in clays interbedded in the Oxfordian limestones of the Pilis Mts are similar to those in the Gerecse Mts. However, no older Jurassic formations were recovered in the Pilis area. The overall character of the Gerecse and Pilis material is somewhat less expanded than that of the corresponding Bakony horizons. This is expressed by the distinct trend lines of $d(001/001)$ in Fig. 10. The trend line of Gerecse (and Pilis) Mts occupies a transitional position between those of the Bakony Mts. and the Zala Basin. The most probable explanation is the slightly stronger diagenetic alteration of Gerecse (and Pilis) than that of the Bakony. Probably the thickness of the Cretaceous and Paleogene cover was higher in the Gerecse area.

Clays in Lower Toarcian manganese ores

The clays connected with the Lower Toarcian manganese ores represent an exception from the overall trend of the evolution of clay mineral assemblages of the study area (Fig. 10). There are controversial opinions regarding the genesis of these stratiform manganese ores. Many authors consider them to be of detrital origin (e.g. Konda 1970). However, the local enrichment of smectites within a limited time interval can hardly be explained simply by processes of differential sedimentation. More recently Szabó et al. (1981) considered a volcanogenic-sedimentary origin to be more feasible. This view is supported by the mineralogical analysis made by Kaeding et al. (1983). According to these authors iron-rich montmorillonites and

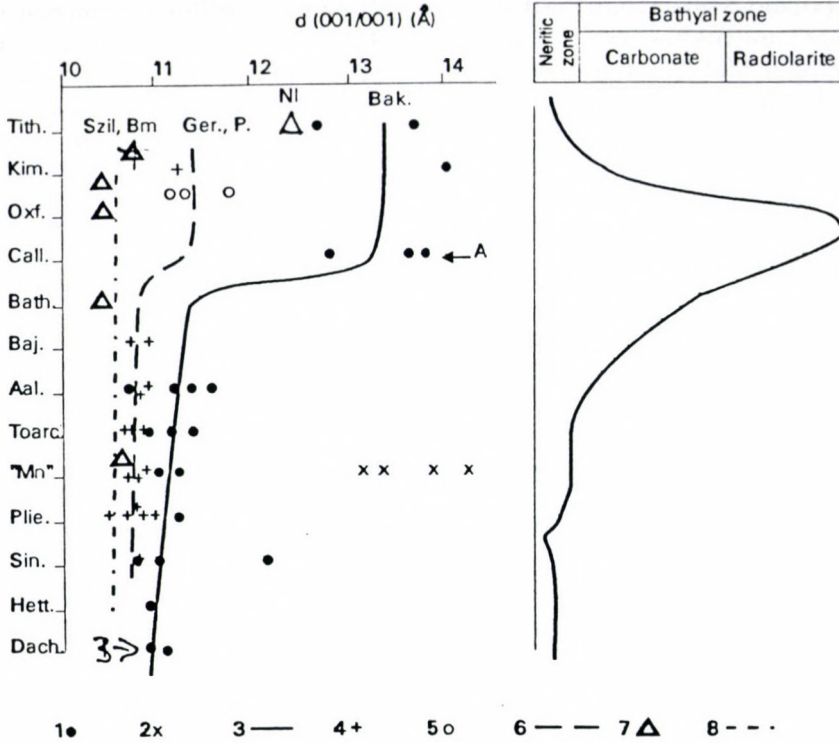


Fig. 10
 Character of expanding clay minerals (mixed-layer illite/smectites and smectites) by the position of their first order basal reflection, $d(001/001)$. Variation of $d(001/001)$ is compared with the bathymetric curve of Géczy (1961). 1. Bakony Mts; 2. clays in Lower Toarcian manganese deposits; 3. trend line for limestones and marls in Bakony Mts ("Bak."); 4. Gerecse Mts; 5. Pilis Mts; 6. trend line for Gerecse ("Ger.") and Pilis ("P.") Mts; 7. boreholes Szil, Bm and NI (Zala Basin); 8. trend line for boreholes Szil and Bm. Arrows indicate the samples A and B, the X-ray patterns of which are shown in Fig. 2

celadonites were formed by the adsorption of silica onto Fe-hydroxides and mixed Fe-Al gels as a consequence of submarine volcanogenic hydrothermal activity. Polgári (1993) considered iron-rich clay minerals as diagenetic products formed following sulphate reduction in the sediments. The present study can add one new aspect to these considerations, namely the local occurrence of these high-smectite clays in the immediate vicinity of the manganese deposits. This fact points to a close genetic connection between these formations.

Comparison with the Jurassic of the Lombardian Basin

A similar tendency of the evolution of clay mineral composition of Jurassic carbonate rocks was observed in the Lombardian Basin (Southern Alps) by Deconinck and Bernoulli (1991). In the hemipelagic / pelagic sequence of the Breggia

valley (Ticino, Switzerland) the dominant clay minerals are illite and smectite while kaolinite contents are very low. In the Lias illite is more abundant than smectite while upper Middle Jurassic to Lower Cretaceous sediments are rich in smectite. In the Lombardian Basin smectite is generally more abundant than in Central Transdanubia. According to the authors, this may be explained by two factors: (1) Lombardian sediments seem "not to be altered much by burial diagenesis". (2) Smectite may be derived from smectite rich soils developing in distant, tectonically stable source areas of the Tethyan margins under a warm and seasonally humid climate. Volcanogenic origin is considered to be possible but less probable.

Similar means of smectite genesis may be supposed for the Transdanubian area, although no detailed mineralogical analysis of the smectite was carried out so far. Considering the great distances from the ancient coasts and examples of Upper Jurassic volcanism in the Tethyan realm the volcanogenic origin seems to be more probable.

Conclusions

1. In the Lias illites and illite/smectites are mostly detrital. Sporadic enrichment of kaolinite may indicate restricted source areas with a kaolinitic weathering crust. Kaolinite contents slightly increase northeastward (and perhaps southwestward), with a minimum in the central areas.

2. In the Middle and Upper Jurassic smectite becomes abundant synchronously with the deepening of the basin.

3. In the Mesozoic of the Zala Basin diagenetic processes were connected with the subsidence of the area in the Neogene. Kaolinite, smectite proportion in mixed-layer illite/smectites and potassium feldspar disappear at depths greater than 3.5 km corresponding to temperatures higher than 110–120 °C. The association illite+chlorite+low-albite+quartz appears in the insoluble residue of limestones around 5 km depth and 180–190 °C temperature, indicating the zone of deep burial diagenesis.

4. The diagenetic transformation of the Bakony area seems to be less advanced than that of the Gerecse Mts.

5. Clays of the Toarcian manganese deposits contain much smectite. In other areas, however, in the same stratigraphic horizon the normal clay mineral assemblage is found.

6. The character of the clay mineral assemblage and the variation of the ratio of illite to smectite with the stratigraphic position is similar to that in the Lombardian Basin (Southern Alps).

Acknowledgements

The author wishes to express his thanks to József Konda and Attila Vörös for help in collecting samples and for information on the sections studied. Hans Füchtbauer (Bochum, Germany), Maria Mange-Rajetzky and Tamás Jaskó gave valuable comments and helped to improve the English text of the paper.

References

- Bárdossy, Gy., G. Csajághy 1966: Geochemical data on the Mesozoic of Hungary. – *Acta Geol. Hung.*, 10, pp. 233–248.
- Bausch, W. M. 1971: Tonmineralprovinzen im europäischen Malm. – *Annals of Hung. Geol. Inst.*, 54, 2, pp. 333–334.
- Bausch, W. M., K. G. Poll 1976: Nichtkarbonatische Rückstände von Malmkalken der Ostalpen. – *Geol. Rundsch.*, 65, pp. 579–592.
- Bérczi-Makk, A. 1980: Triassic to Jurassic microbiofacies of Szilvágy, southwestern Hungary. – *Földt. Közl.*, 110, 1, pp. 90–103.
- Bernoulli, D., T. Peters 1970: Traces of rhyolitic-trachytic volcanism in the Upper Jurassic of the Southern Alps. – *Ecl. Geol. Helv.*, 63, pp. 609–621.
- Deconinck, J.F., D. Bernoulli 1991: Clay mineral assemblages of Mesozoic pelagic and flysch sediments of the Lombardian Basin (Southern Alps): implications for palaeotectonics, palaeoclimate and diagenesis. – *Geol. Rundsch.*, 80, 1, pp. 1–17.
- Dosztály, L. 1988: A paleontological study of the Öregszirt radiolarites in the Pilis Mountains. – *Annual Rept. of the Hung. Geol. Inst.*, 1986, pp. 229–233.
- Fülöp, J. 1969: Geology of the Transdanubian Central, Mecsek and Villányi Mountains. Excursion Guide. – *Coll. on Mediterranean Jurassic*, Budapest, 1969. Hungarian Geological Institute, Budapest.
- Fülöp, J. 1971: Les formations Jurassiques de la Hongrie. – *Annals of the Hung. Geol. Inst.*, 54, 2, pp. 31–46.
- Fülöp, J. 1975: Blocks of the Mesozoic basement formation at Tata. – *Geol. Hung., Ser. Geol.*, 16, pp. 1–225.
- Galác, A., A. Vörös 1972: A sketch of the Jurassic development of the Bakony Mts. on the basis of the interpretation of principal sedimentological phenomena. – *Földt. Közl.*, 102, 2, pp. 122–135.
- Géczy, B. 1961: Die jurassische Schichtenreihe des Tűzköves-Grabens von Bakonycsérnye. – *Annals of the Hung. Geol. Inst.*, 49, 2, pp. 507–567.
- Grasselly, Gy., Z. Szabó, Gy. Bárdossy, J. Cseh Németh 1969: Data on the geology and mineralogy of the Eplény manganese ore deposit. – *Acta Min.-Petr. Szeged*, 19, pp. 15–43.
- Jámbor, Á. et al. 1976: Geological evaluation of the borehole Bárszentmihályfa Bm I. – Unpublished report (in Hungarian). Hung. Geol. Survey, Budapest.
- Jenkyns, H. C. 1974: Origin of red nodular limestones (Ammonitico Rosso, Knollenkalke) in the Mediterranean Jurassic: a diagenetic model. – In: K. J. Hsü, H. C. Jenkyns (Eds) *Pelagic sediments: on land and under the sea*. Spec. Publ. of IAS 1, pp. 249–271.
- Kaeding, L., O. Brockamp, H. Harder 1983: Submarin-hydrothermale Entstehung der sedimentären Mangan-Lagerstätte Úrkút/Ungarn. – *Chem. Geol.*, 40, 3–4, pp. 251–268.
- Konda, J. 1970: Lithologische und Fazies-Untersuchung der Jura-Ablagerungen des Bakony-Gebirges. – *Annals of the Hung. Geol. Inst.*, 50, 2, pp. 154–260.
- Kőrössy, L. 1988: Hydrocarbon geology of the Zala Basin in Hungary. – *Ált. Földt. Szemle*, 23, pp. 3–162. (in Hungarian).
- Nemecz, E. 1981: Clay minerals. – Akadémiai Kiadó, Budapest.
- Magyarország geológiai alapszelvényei (MGA) (Geological key sections of Hungary) 1985–1989. – Series published by the Hung. Geol. Inst. (MÁFI), Budapest.
- Polgári, M. 1993: Manganese geochemistry – reflected by black shale formation and diagenetic processes. Model of formation of the carbonatic manganese ore of Úrkút. – Publ. by Hung. Geol. Inst., Budapest.
- Rischák, G., I. Viczián 1974: Mineralogical factors influencing the intensity of basal reflections of clay minerals. – *Annual Rept. of the Hung. Geol. Inst.*, 1972, pp. 229–256.
- Szabó, Z., Gy. Grasselly, J. Cseh-Németh 1981: Some conceptual questions regarding the origin of manganese in the Úrkút deposit, Hungary. – *Chem. Geol.* 34, 1–2, pp. 19–29.

- Szabó-Drubina, M. 1962: Die liassischen Manganlagerstätten vom Bakony. – *Annals of the Hung. Geol. Inst.*, 49, 4, pp. 1171–1179.
- Viczián, I. 1980: Clay mineralogy of Mesozoic carbonate rocks of Central Transdanubia (Hungary). – *Fourth Meeting of the European Clay Groups, Freising, 1980. Abstracts* p. 163.
- Vörös, A. 1982: Stratigraphic evaluation of the Pliensbachian brachiopod fauna of the Bakony Mts. (Hungary). – *Földt. Közl.* 112, 4, pp. 351–361.

Petrophysical characteristics of the Mamura Formation (Lower Cretaceous), Western Desert, Egypt



Abdel Moktader A. El Sayed
Geophysics Dept., Ain Shams Univ., Cairo, Egypt

A number of petrophysical parameters were measured in laboratory on 32 core samples obtained from three wells; all samples are from the Mamura Formation (Lower Cretaceous). Several crossplot variations were tested for lithologic discrimination: the grain density–porosity relation was found to be the most effective combination.

Measured formation parameters such as porosity, formation factor, permeability, compressive strength, matrix conductivity, mounce potential, packing index and rock density were studied for these core samples; consequently, reliable reservoir relationships were obtained.

Using multi-regression analysis techniques, statistical models for storage capacity were created in order to predict and delineate reservoir porosity from other routine parameters.

Key words: petrophysical model, packing index, Mamura Fm., Egypt

Introduction

The Western Desert comprises an area of about 700 000 sq.km (two thirds of the area of Egypt). It extends 1000 km from the Mediterranean Sea to the Sudanese border in the south and 600 to 800 km from the Nile valley to the Libyan border to the West. The study area is located in the northern part of the Western Desert; northeast of the Qattara Depression and northwest of Wadi El Natrun (Fig. 1). The sedimentary section of the northern part of the Western Desert ranges from Lower Paleozoic to Recent; the sequence rests on the basement complex. This sequence exhibits four major transgressive cycles in Carboniferous, Upper Jurassic, Middle and Late Cretaceous, Middle Miocene and Pliocene times. A widespread unconformity is recorded at the Jurassic–Cretaceous boundary. From the hydrocarbon production point of view, all of the producing horizons of the Western Desert are Cretaceous in age.

The Cretaceous sediments were mainly transitional, shallow marine to deltaic in nature (Norton 1967; Abdine and Deibis 1972; Abu El-Naga 1983 and Barakat and Darwish 1984). The studied samples were collected from the Lower Cretaceous (Mamura Formation). The lower part of this formation is composed mainly of sandstone and argillaceous sandstone of transitional, shallow marine to deltaic facies, while the upper part consists mainly of carbonates deposited in restricted marine to lagoonal environments (Fig 2).

Addresses: A. M. A. El Sayed: Ain Shams Univ., Fac. of Sci., Dept. of Geophysics, Cairo, Egypt
Received: 15 October, 1993

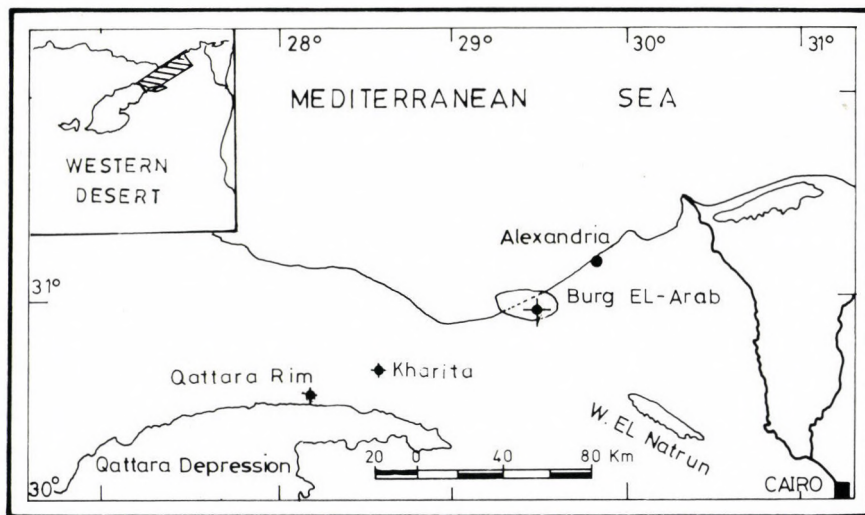


Fig. 1
Location map

Thirty-two core samples representing these two lithological facies were collected from three wells: Qattara Rim, Kharita and Burg El-Arab (Fig 1). In the present work, an attempt was made to study the reservoir properties of the Mamura Formation. The creation of an ultimate storage capacity model was an objective as well.

Methods and technique

The selected rock samples were cut into standard plugs of 2.5 cm diameter and 5.0 cm length for petrophysical analysis. Laboratory measurements of both rock porosity and horizontal permeability (Table 1) followed methods outlined by Anderson (1975). Porosity data were determined by using both a mercury pump universal porosimeter (Ruska Inst. C. No. 101A) for bulk volume (V_b) determination and a helium porosimeter with matrix cup core holder (Corelab. c. No: 7542-500) for grain volume (V_g) estimation. Hence, porosity is calculated as:

$$\varnothing = (1.0 - (V_g/V_b)) \times 100 \quad (1)$$

Where: \varnothing = porosity, %

Gas permeability measurements (Table 1) were conducted with Hassler-type core holder in which samples of 2.5 cm diameter and 5.0 cm length were subjected to dry nitrogen gas with pressure of 2.0 Mpa (El Sayed 1986). The permeability is calculated using a Corelab. type permeameter as:

$$K = C \cdot Q \cdot hw \cdot L^2 / 200 \times V_b \quad (2)$$

Where : K = Gas permeability, (m.d).
 C = Orifice value
 hw = Orifice manometer reading
 L = Sample length, cm
 V_b = Sample bulk volume, cm³

The electrical resistivity of the core samples was measured using the Corelab. resistivity bridge (cat. No. 100A). The measuring techniques were outlined by Hassan and El Sayed (1983a and 1983b). The electrical resistivity of samples previously fully saturated with a brine solution (R₀) was measured three times for three different successive brine concentrations (R_w= 2. 11,1. 66 and 0. 186 ohm.m). The Resistivity Index is calculated using the stepwise centrifuge method (Slobed et al. 1951; El Sayed 1976, 1990); after each desaturation step, the amount of expelled brine and the true resistivity (R_t) of the samples were measured.

Thirty-two cylindrical samples were selected for uniaxial compressive test measurements (compressive strength). They were selected so as to cover not only all lithologic variations but also the difference in both porosity and permeability. Grain density was measured with the pycnometer method (Kobranova 1962 and Keller, 1969) as:

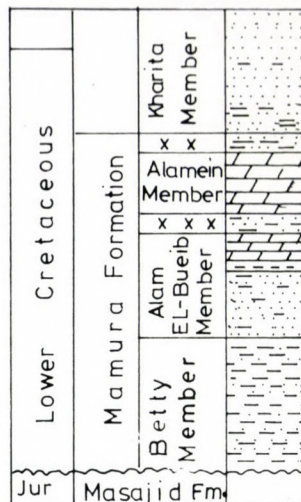
$$pg = [Wd/Ww - Ws] / [1.0 - (Ww - Wd)/(Ww - Ws)] \tag{3}$$

Where : pg = Grain density gm/cc
 Wd = Weight of dry sample, gm
 Ww = Weight of saturated sample, gm
 Ws = Weight of suspended sample, gm

Results and discussion

The measured petrophysical parameters of the Mamura Formation (Table 1) were plotted in order to throw light on some effective combinations capable of:

- a) Discriminating carbonate from sandstone samples
- b) Estimating important special reservoir parameters from routine elements
- c) Determining the most significant parameters affecting the reservoir storage capacity. Subsequently these parameters were used for constructing porosity models using the multi-regression analysis techniques.



xx Undifferentiated Aptian
 xxx Unnamed Unit

Fig. 2
 Lithostratigraphic succession of the Mamura Formation in the study area (according to Norton 1967)

Table 1
The measured and the computed petrophysical parameters for the Mamura

S.N.	Well	D(m)	Lith.	$\Delta\emptyset$	T	\emptyset	K (md)	$\lg \frac{K}{\emptyset}$	Vg	Vp	Vp/Vg	pb
1.	B. Arab	3051	Ss.	2.70	2.2	0.220	94.38	2.63	11.4	3.21	0.280	1.9
2.	B. Arab	3053	Ss.	2.65	2.7	0.230	176.00	2.88	11.2	3.23	0.288	2.3
3.	B. Arab	3056	Ss.	2.44	3.0	0.218	1507.00	3.84	15.0	4.20	0.279	1.9
4.	B. Arab	3057	Ss.	2.88	2.6	0.218	1231.00	3.75	16.3	4.55	0.279	2.1
5.	B. Arab	3180	Ss.	2.80	2.7	0.200	1073.00	3.73	16.0	4.05	0.252	1.9
6.	B. Arab	3181	Ss.	2.74	2.5	0.199	561.00	3.45	13.5	3.36	0.248	2.1
7.	B. Arab	3286	Ss.	2.85	2.4	0.210	813.00	3.59	10.2	2.73	0.266	1.9
8.	B. Arab	3408	Ss.	4.23	1.8	0.009	0.03	0.52	8.56	0.08	0.009	2.5
9.	B. Arab	3481	Ss.	2.48	2.6	0.204	668.00	3.52	14.2	3.65	0.256	1.9
10.	B. Arab	3482	Ss.	3.68	2.7	0.095	0.47	0.79	18.7	1.98	0.106	2.3
11.	B. Arab	3483	Ss.	3.32	2.1	0.120	17.74	2.17	14.3	1.95	0.136	2.2
12.	B. Arab	3544	Ss.	3.66	2.7	0.100	0.40	0.60	10.4	1.22	0.116	2.2
13.	B. Arab	3802	Ss.	2.96	2.1	0.197	414.00	3.32	11.2	2.74	0.245	2.0
14.	B. Arab	3843	Ss.	3.89	2.6	0.194	180.00	2.97	7.96	1.91	0.240	2.0
15.	B. Arab	4040	Ss.	3.29	2.5	0.160	259.00	3.21	13.0	2.44	0.187	2.1
16.	B. Arab	4050	Ss.	3.34	2.4	0.156	402.00	3.41	11.8	2.18	0.184	2.2
17.	Q. Rim	2041	D.Ls.	1.38	3.2	0.010	0.07	0.89	16.2	0.13	0.008	2.7
18.	Q. Rim	2042	D.Ls.	1.32	3.0	0.008	0.06	0.89	13.6	0.11	0.008	2.7
19.	Q. Rim	2048	D.Ls.	1.06	3.4	0.024	0.04	0.19	15.7	0.39	0.025	2.6
20.	Q. Rim	2050	D.Ls.	1.09	3.3	0.028	0.08	0.43	10.5	0.30	0.028	2.7
21.	Kharita	3001	D.Ls.	1.21	5.3	0.064	0.08	0.08	15.5	1.06	0.068	2.5
22.	Kharita	3002	D.Ls.	1.60	7.1	0.078	0.15	0.28	9.80	0.82	0.084	2.5
23.	Kharita	3003	D.Ls.	1.23	5.4	0.082	0.09	0.03	21.6	1.92	0.089	2.5
24.	Kharita	3004	D.Ls.	1.02	3.8	0.038	50.00	3.12	9.46	0.37	0.039	2.6
25.	Kharita	3013	D.Ls.	1.33	4.2	0.054	0.18	0.77	17.8	1.03	0.058	2.6
26.	Kharita	3014	D.Ls.	1.35	5.4	0.064	0.25	0.60	10.7	0.73	0.068	2.6
27.	Kharita	3015	D.Ls.	1.23	3.7	0.020	0.09	0.65	19.5	0.45	0.023	2.7
28.	Kharita	3016	D.Ls.	1.36	4.7	0.450	0.07	0.01	14.0	0.66	0.047	2.7
29.	Kharita	3032	D.Ls.	1.13	2.0	0.008	0.10	1.08	20.9	0.18	0.009	2.7
30.	Kharita	3033	D.Ls.	1.22	3.0	0.016	0.13	0.92	15.0	0.24	0.016	2.7
31.	Kharita	3034	D.Ls.	1.08	2.7	0.021	0.10	0.66	13.7	0.29	0.021	2.7
32.	Kharita	3035	D.Ls.	1.12	2.9	0.024	0.14	0.75	14.4	0.35	0.024	2.7

Symbols: B. Arab – Burg Al-Arab Well, Q. Rim – Qattara Rim Well; Ss. – Sandstone; D. Ls. – Dolomitic Limestone

Formation

pg	Co	F1	F2	F3	Fav	F _{lim}	lg F _{lim}	lg Fa/lg F _{lim}			σ_m	SSA
2.61	98.6	14.9	17.4	22.2	18.2	36	1.56	0.754	0.797	0.87	18.6	0.361
2.62	0.0	14.1	17.0	21.7	17.7	32	1.51	0.764	0.826	0.89	18.8	0.620
2.64	92.0	11.5	17.6	23.9	17.7	42	1.62	0.654	0.768	0.85	29.8	0.282
2.64	88.0	17.8	20.8	25.5	21.4	37	1.57	0.798	0.841	0.90	13.7	0.328
2.64	56.0	16.5	19.8	21.9	19.4	36	1.56	0.783	0.833	0.86	15.5	0.351
2.62	0.0	15.6	21.2	24.2	20.3	32	1.51	0.794	0.882	0.92	15.4	0.458
2.65	79.0	17.2	20.3	22.9	20.1	28	1.45	0.854	0.903	0.94	10.6	0.425
2.61	559.0	68.5	71.5	147.	95.9	35	2.54	0.722	0.729	0.85	5.55	1.498
2.63	164.0	17.1	21.3	25.2	21.2	33	1.52	0.813	0.875	0.92	13.3	0.429
3.63	309.0	39.7	42.4	53.4	45.2	75	1.88	0.853	0.868	0.92	5.59	1.327
3.61	0.0	25.3	30.3	33.1	29.6	38	1.58	0.889	0.938	0.96	6.20	1.560
2.58	421.0	38.9	39.9	51.8	43.5	70	1.55	0.862	0.868	0.93	5.41	1.360
2.66	118.0	19.2	18.8	26.7	21.6	48	1.60	0.764	0.759	0.85	14.7	0.444
2.65	180.0	23.1	25.1	28.2	25.4	36	1.55	0.876	0.900	0.93	7.34	0.600
2.63	85.0	27.3	29.6	31.1	29.3	38	1.58	0.910	0.932	0.95	4.85	0.542
2.63	0.0	609.7	30.6	32.8	30.4	37	1.57	0.926	0.942	0.97	3.91	0.484
2.83	907.0	573.0	625.6	721.	652.3	100	3.00	0.928	0.932	0.95	3.62	1.219
2.84	0.0	411.0	634.9	754.	654.2	110	3.04	0.907	0.922	0.95	4.01	1.236
2.81	749.0	337.0	428.0	434.	424.9	480	2.68	0.975	0.981	0.98	24.3	1.424
2.82	0.0	291.5	361.0	368.	355.5	390	2.59	0.976	0.987	0.99	1.30	1.355
3.95	236.0	216.6	343.4	354.	329.6	440	2.64	0.932	0.959	0.96	3.85	1.334
2.84	421.0	219.0	223.0	437.	262.2	650	2.81	0.830	0.835	0.90	2.45	1.189
2.85	309.0	321.3	232.0	267.	239.3	350	2.54	0.920	0.930	0.95	8.80	1.349
2.84	605.0	321.0	327.0	328.	325.6	380	2.58	0.972	0.975	0.98	3.12	0.450
2.81	710.0	339.0	328.0	450.	390.3	600	2.78	0.911	0.929	0.96	5.72	0.532
2.80	0.0	298.0	327.5	343.	337.8	450	2.65	0.933	0.969	0.96	2.79	0.521
2.82	348.0	456.0	516.9	560.	511.1	700	2.84	0.935	0.954	0.96	3.05	1.246
2.82	415.0	258.0	409.6	352.	340.4	510	2.70	0.891	0.965	0.94	2.90	1.639
2.83	927.0	455.0	484.0	513.	484.1	530	2.72	0.976	0.986	0.99	1.07	1.274
2.83	0.0	333.0	337.0	407.	359.5	570	2.75	0.916	0.917	0.94	2.17	1.222
2.80	499.0	315.0	325.0	340.	327.1	360	2.55	0.978	0.983	0.99	1.78	1.328
2.82	0.0	254.0	281.4	285.	273.7	350	2.54	0.945	0.963	0.96	4.20	1.287

Lithologic discrimination

Lithologic discrimination based on petrophysical properties is sometimes difficult when using well logs, especially if only one measured parameter is available. In order to resolve this problem, different crossplots were constructed to choose the most effective one.

Out of more than 30 combinations, only 4 crossplots were reliable for discriminating carbonates (dolomite or limestone) and sandstones (Fig 3a-d). The most effective one is the grain density versus porosity relationship. This may be due to the narrow grain density range of both the carbonate rock samples ($\rho_g = 2.78$ to 2.85) and the sandstones ($\rho_g = 2.58$ to 2.63).

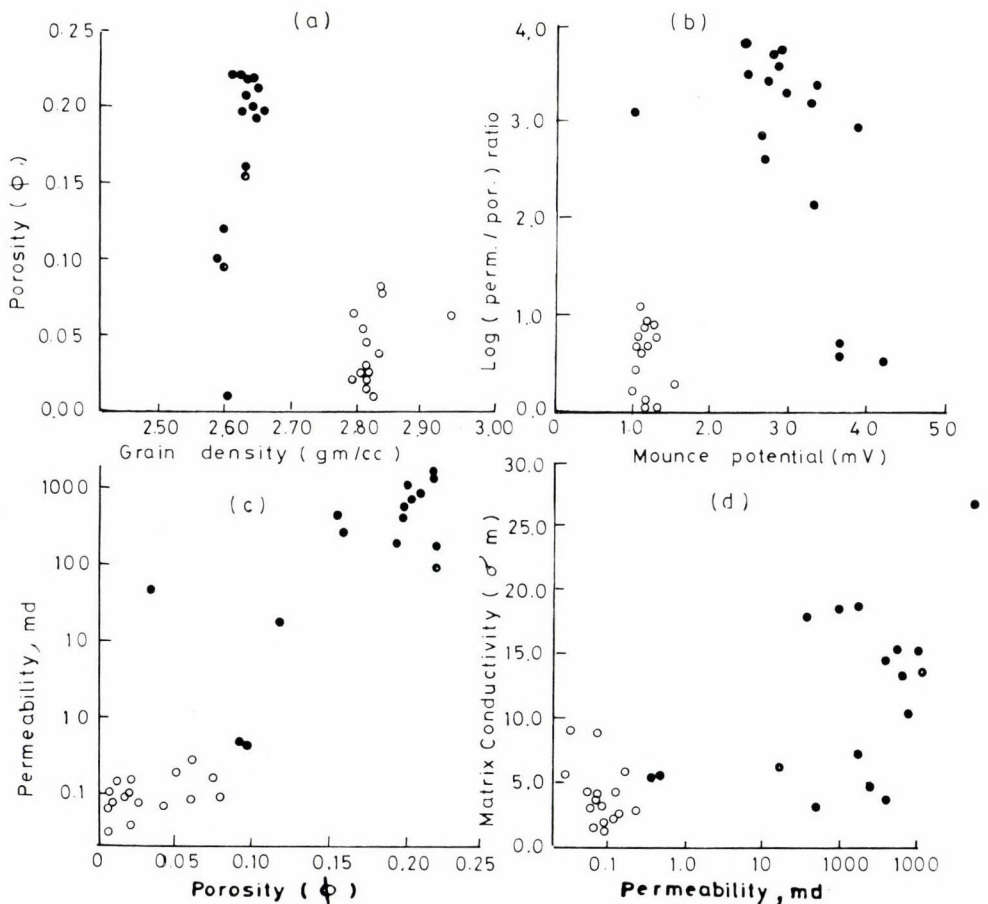


Fig. 3

The relationship of porosity vs. grain density (a) log (perm./poro) vs. Mounce potential (b) permeability vs. porosity (c) and Matrix conductivity vs. permeability (d) ● sandstone; ○ carbonate

Mounce potential versus $\lg(K/\emptyset)$ ratio crossplot also appears to be effective. This is attributed to the rule of the conductive solids (sandstone with specific clay minerals), usually associated with pore spaces as authigenic cement and/or matrix material.

Therefore the lithology of the Mamura Formation could be easily distinguished by using the compensated Formation density log in combination with either sonic or neutron logs.

Resistivity Index

The Resistivity Index (RI) is given directly as the ratio of the true resistivity of an unknown bed to that of the water-bearing one (Wyllie 1963). It has been noted quantitatively that the greater the resistivity index (RI), the more oil or gas can be expected to be present in the pores of a given rock, because in such a case the total conductivity will be reduced (i.e. the true resistivity R_t increases, while R_o remains constant). Figure (4a) shows that the RI of the Mamura samples is largely affected by rock porosity. It ranges from 1.0–3.0; 1.0–20.0 and 1.0–100 for rock porosities of 9.6%, 15–19% and 21.8% respectively. Figure (4b) exhibits the resistivity index-water saturation relation for the studied samples of the Mamura Formation. This relationship (Fig. 4b) is represented by the regression equation:

$$RI = 1.23 S_w^{-1.14} \quad (4)$$

Where : S_w = water saturation.

The calculated saturation exponent (n) in this equation equals 1.14. It indicates that the studied samples are entirely water wet.

Packing Index Versus Compressive Strength

In the present work, the packing index (PI) is calculated as the ratio of (ρ_g/ρ_b). It could be predicted from the relationships represented in Figs (5a, b).

Figure (5a) exhibits the compressive strength–packing index relationship. For sandstone samples, the relationship is controlled by a reliable regression line equation as:

$$Co = -1334.7 (PI) + 1874.8 \quad (5)$$

On the other hand, the calculated regression line equation which controls the carbonates is :

$$Co = -3654.99 (PI) + 4434.5 \quad (6)$$

Where : Co = Compressive strength Kg/cm^2
 PI = Packing index.

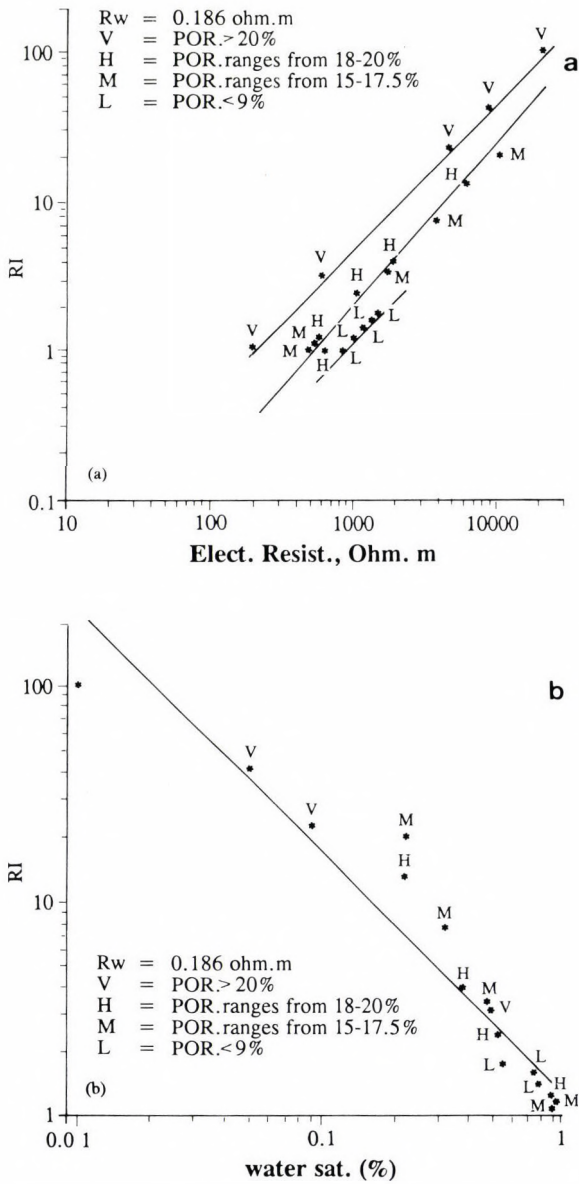


Fig. 4
Resistivity index vs. electrical resistivity (a), and water saturation (b)

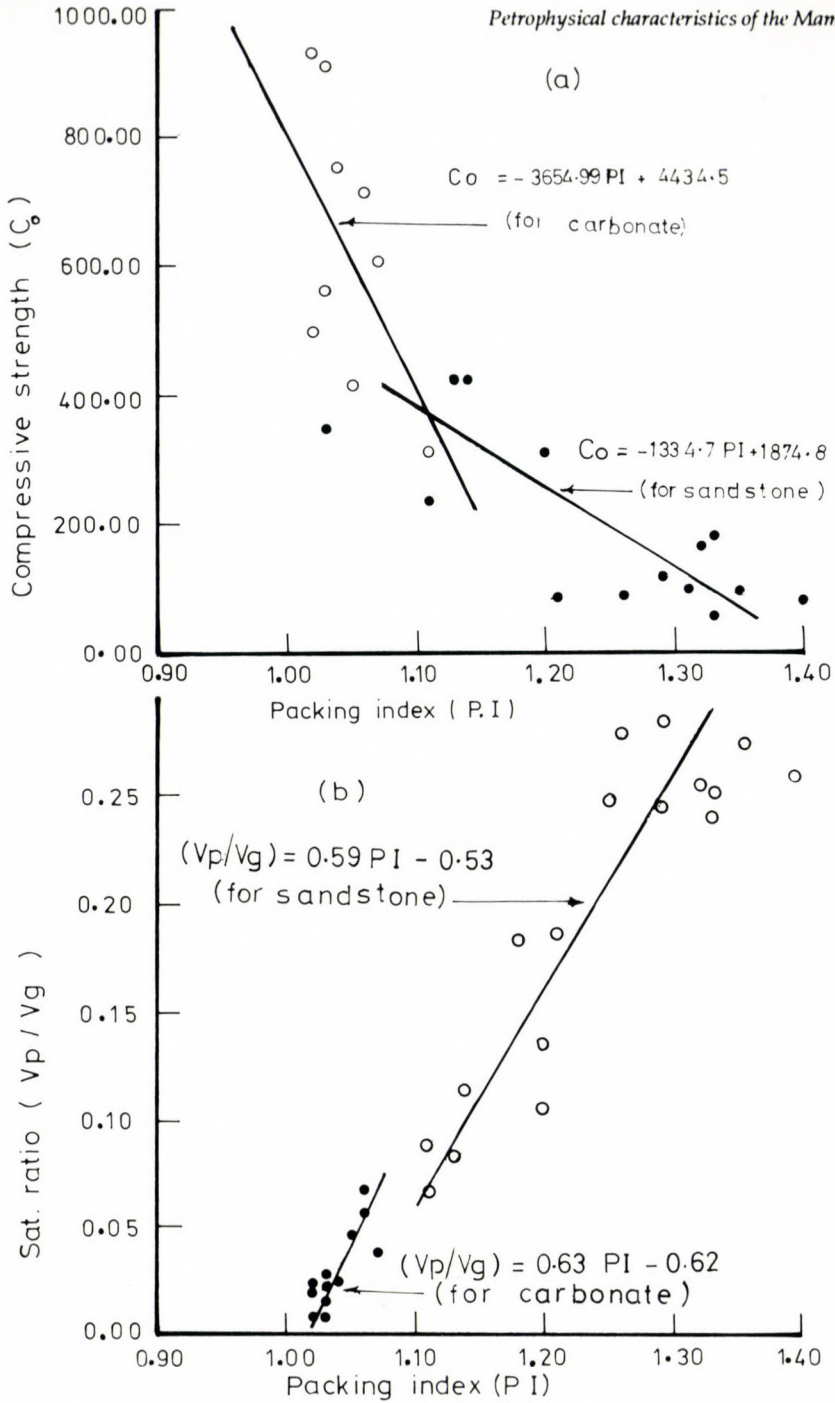


Fig. 5
Packing index vs. compressive strength (a) and sat. ratio (b)

These two equations are characterized by moderately high correlation coefficients: they are equal to (-0.71) for sandstone and (-0.74) for carbonate samples, respectively.

Packing index versus saturation ratio

The saturation ratio in this work is defined as the ratio between V_p to V_g , where V_p and V_g are the sample pore volume and grain volume, respectively. The saturation ratio-packing index relationship (Fig 4b) is controlled by two linear equations. The first one is calculated for sandstone samples as:

$$\text{Saturation ratio } (V_p/V_b) = 0.59 (\text{PI}) - 0.53 \quad (7)$$

and for carbonate samples as:

$$\text{Saturation ratio } (V_p/V_b) = 0.63 (\text{PI}) - 0.62 \quad (8)$$

The correlation coefficient (r) for the two relations were reasonably high, equal to (0.87) and (0.89) for sandstone and carbonate samples, respectively. Therefore, the packing index (PI) and/or the compressive strength (C_o) could be predicted from the routine laboratory measurements of pore and grain volume.

Saturation ratio versus $Lg(K/\emptyset)$

The $lg(K/\emptyset)$ versus saturation ratio (V_p/V_b) relationship (Fig. 6) proved to be of great significance for both lithologic discrimination (between sandstones and carbonates) and permeability prediction.

Moderate correlation coefficients were obtained for these relations. they equal to (0.78) for sandstone and (-0.66) for carbonate samples of the Mamura Formation. The equation representing the sandstone lithology is:

$$\text{Saturation ratio } (V_p/V_b) = 0.079 + 0.04959 \log (K/\emptyset) \quad (9)$$

while for the carbonate lithology, the following equation is obtained:

$$\text{Saturation ratio } (V_p/V_b) = 0.0653 - 0.04264 \log (K/\emptyset) \quad (10)$$

These two equations could be used for permeability prediction in the Mamura Formation.

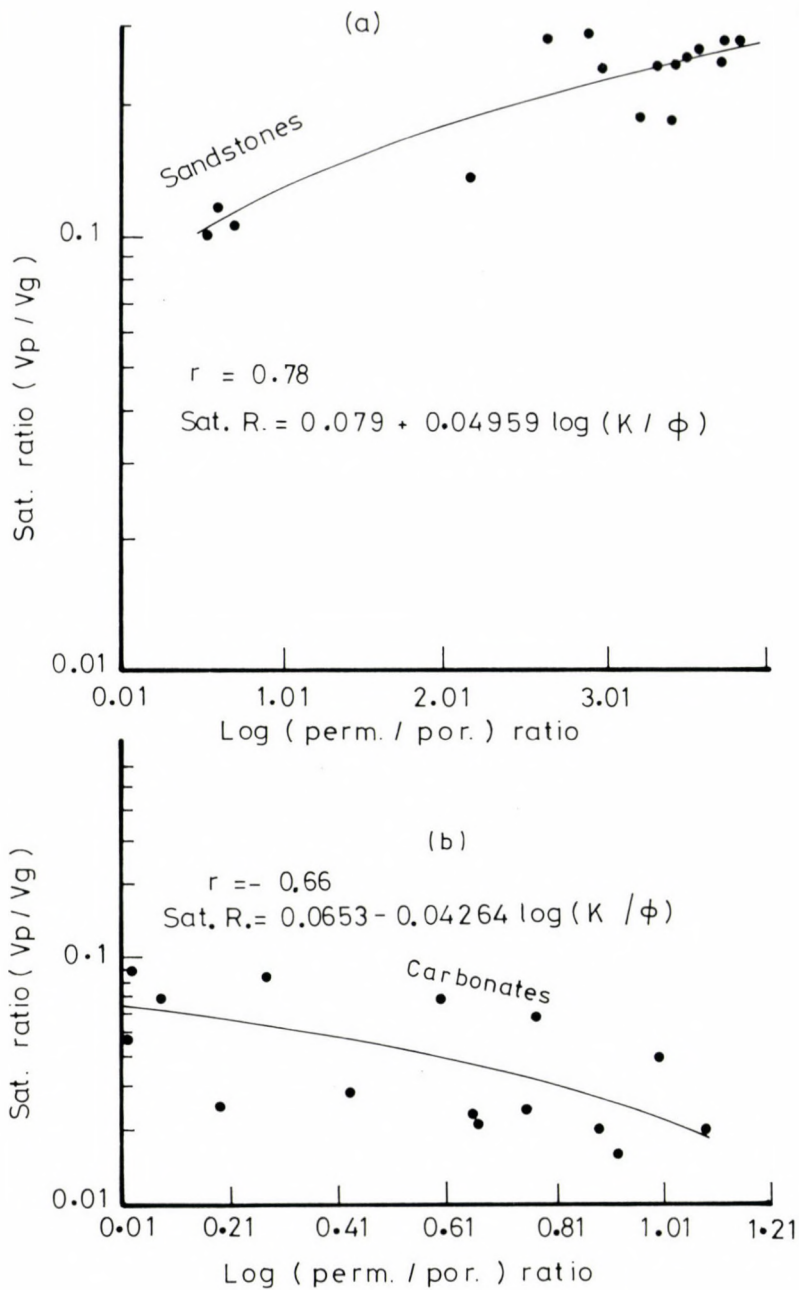


Fig. 6
Saturation ratio vs. log (perm./por.)

Porosity

The essential feature of any reservoir rock is its porosity. The reservoir rock must contain pores and/or voids of such size and character as to permit the storage of hydrocarbon fluids.

In the present work, an attempt was made to create some porosity models for the studied rock samples of the Mamura Formation. The multi-regression analysis technique was used for model element calculations. The formation parameters used in this study are listed in Table 2. The calculated coefficients of correlation were found to be variable. Accordingly, porosity models are constructed using only the parameters significantly affecting porosity. Thereinafter, the stepwise regression methods were used to obtain the most reliable model.

Three porosity models established, one of them related to the textural parameters, the second model related to the electrical properties, while the third to both (textural and electrical parameters).

The porosity model related to the measured textural parameters is represented by the equation:

$$\varnothing = 0.781 (V_p/V_b) + 6.235 \times 10^{-3} \rho_g - 0.114 \quad (11)$$

This model is characterized by a multiple coefficient of correlation, $r = 0.998$.

The second model, which is related to the electrical parameters (Table 1) is represented by the equation:

$$\varnothing = 0.02\tau + 9.05 \times 10^{-5} F_{lim} + 1.59 \times 10^{-3} \sigma_m - 0.03 \log S_{por} - 0.17 \log F_{lim} + 0.4 \quad (12)$$

Where: τ = Tortuosity factor
 F_{lim} = True formation resistivity factor
 σ_m = Matrix conductivity
 S_{por} = Surface area of rock pore space

This is controlled by a multiple correlation coefficient ($r = 0.988$).

The third model is related mainly to both electric and textural parameters and is represented by the equation:

$$\varnothing = 0.69 (V_p/V_b) + 4.23 \times 10^{-3} \tau - 0.02 \log F_{lim} + 0.047 \quad (13)$$

This model is characterized by a very reliable multiple coefficient of correlation $r = 0.999$. Using these models it was possible to outline the storage capacity of the Mamura Formation.

Table 2
Formation parameters of the Mamura Formation

Variable	Mean	St. Dev.	Minimum	Maximum	N
Ro1	400.00	400.96	24.34	1286.50	32
F1	188.07	189.60	11.54	609.70	32
Ro2	332.15	336.94	28.90	1054.00	32
F2	207.92	206.93	17.00	634.90	32
Ro3	42.24	41.76	4.04	140.40	32
F3	230.25	226.44	21.72	754.80	32
Fav	208.77	206.91	17.70	654.23	32
F _{lim}	305.74	304.20	28.00	1100.00	32
lg F _{lim}	2.17	0.58	1.45	3.04	32
lg (F _{lim} /F1)	0.87	0.08	0.65	0.98	32
lg (F _{lim} /F2)	0.90	0.07	0.73	0.99	32
lg (F _{lim} /F3)	0.93	0.04	0.85	1.00	32
σ^m	8.39	7.29	1.07	29.80	32
lg S _{por}	0.91	0.45	0.28	1.56	32
$\Delta\phi$	2.20	1.04	1.02	4.23	32
τ	3.28	1.19	1.77	7.12	32
Shaliness	0.07	0.11	0.01	0.65	32
ϕ	0.11	0.08	0.01	0.23	32
K _{md}	240.27	410.09	0.03	1507.00	32
lg (K/ ϕ)	1.77	1.43	0.02	3.84	32
Vg	13.83	3.54	7.96	21.60	32
Vp	1.68	1.40	0.08	4.55	32
Vg/Vp	0.13	0.11	0.01	0.29	32
ρ_b	2.40	0.31	1.90	2.78	32
ρ_g	2.82	0.32	2.59	3.95	32
co	349.03	276.77	0.00	927.00	32

Conclusions

1. The most effective crossplot for lithologic discrimination was the porosity-grain density relationship.

2. The compressive strength of the studied samples of the Mamura Formation could be calculated from the standard laboratory measurements of both the grain and bulk densities.

3. Both the saturation ratio and the packing index are proven to be important reservoir parameters, especially for formation evaluation.

4. The permeability of the Mamura samples could be predicted by use of equations 8 and 9, based on the routine laboratory measurements of both the pore volume and grain volume during sample porosity determination.

5. The porosity model based on textural parameters and electrical parameters gave the best calculation method of porosity determination of the Mamura Fm. samples.

References

- Abdine, A. S., S. Deibis 1972: Lower Cretaceous Aptian sediments and their oil properties in the North Western Desert of Egypt. – 8th Arab pet. cong. Algiers.
- Anderson, G. 1975: Coring and core analysis hand book. – Pet. Publishing Company, Tulsa, 200 p.
- Abu El-Naga, M. 1983: North Western Desert stratigraphic summary, A CONOCO'S chart compiled from different official, sources. – CONOCO, Egypt internal. report.
- Barakat, M. G., M. Darwish 1984: Contribution to the lithostratigraphy of the Lower Cretaceous sequence in Marsa Matruharea, North Western Desert, Egypt. – 20th Am. petro. Geol. Soc. Egypt.
- El Sayed, A.M.A. 1976: Petrophysical studies from UM EL Yasr oil field Eastern Desert, Egypt. – Msc. Thesis, Ain Shams Univ., Cairo, 137 pp.
- El Sayed, A.M.A. 1986: Formation parameters of the Lower Eocene rocks. – Qatar Univ., Sci. Bull., 6, pp. 229–345.
- El Sayed, A.M.A. 1990: Variation of saturation exponent in the Miocene oolitic limestone of Qatar (Arabian Gulf). – Egypt J. Geol., 32, (1–2) pp. 159–172.
- Hassan, N.M., A.M.A. El Sayed 1983a: Electrical properties of Umm El Yasr oil field, Egypt, as an aid for determination of their storage capacity properties-Egypt. – Geophys. Soc. Ann. Meet., pp. 108–128.
- Hassan, N.M., A.M.A. El Sayed 1983b: Storage capacity of El-Yasr sandstones (Umm Yasr oil field) Egypt, and its relation to their textural properties-Egypt. – Geophys. Soc 2nd Ann. Meet., pp. 86–107.
- Keller, G.V. 1969: Electrical resistivity of modern reef sediments from Midway Atoll, Hawaii. – 10th Ann. Logging Symp. SPWLA.
- Kobranova, M. 1962: Physical properties of rocks. – Gostoptechizdat. Moscow, p. 490 (in Russian).
- Norton, P. 1967: Rock stratigraphic nomenclature of the Western Desert, Egypt. – Int. Report G. P. C. p. 18.
- Slobed, R.L., A. Chambers, W.L. Perhn 1951: Use of centrifuge for determining connate water, residual, oil and capillary pressure curves of small core samples. – Trans AIME, 192, pp. 127–135.
- Wyllie, M.R.J. 1963: The fundamentals of well log interpretation. – Acad. Press, New York, 3rd edition, 238 pp.

Book review

Amos Salvador (Ed.) 1994: International Stratigraphic Guide.

A Guide to Stratigraphic Classification, Terminology and Procedure, 2nd edition, 214 p.

The volume is an exhaustively revised and enlarged edition of the first edition published under the same title in 1976. It summarizes the results of ten years international efforts in the framework of the International Subcommittee on Stratigraphic Classification. It consists of ten numbered and four unnumbered chapters. It is stated in the Introduction that the purpose of the new edition is to "develop an internationally acceptable stratigraphic terminology and rules of stratigraphic procedure" emphasizing that the Guide is a recommended approach and not a "code". More attention is paid in the new edition to the igneous and metamorphic rocks trying to give expression to their special features.

Separate chapters are dedicated to the Magnetostratigraphic Polarity Units and to the Unconformity Bounded Units that were missing from the 1st edition.

Among lithostratigraphic units, the Flow, a new distinctive category is introduced for distinguishing the basic units of volcanic rocks from sedimentary and metamorphic rocks. An

other new category is the lithozone that is suggested to use for thin markers or just surfaces between larger units.

The biostratigraphic chapter reflects the changes the biostratigraphic nomenclature and even terminology underwent. Separate sub-headings denote the special treatment of the Precambrian and the Quaternary chronostratigraphic units. The great variety of stratigraphic units gave reason for inserting a new chapter that enlightens the relation between the different kinds of stratigraphic units. The Glossary of Stratigraphic Terms is an important part of the volume that contains 376 terms. The inquiry within the volume is promoted by the Index at the end of the Guide.

As stratigraphy is a basic subject for all branches of geology, in addition to stratigraphers the Guide can be a useful Bible for every geologist.

Géza Császár

copublished by the
Geological Society of America (GSA) and the International Union of Geological Sciences (IUGS)

International Stratigraphic Guide:

A Guide to Stratigraphic Classification, Terminology, and Procedure, 2nd edition

edited by Amos Salvador, 1994

Here is the most up-to-date statement of international agreement on concepts and principles of stratigraphic classification, and a guide to international stratigraphic terminology. The first edition, published in 1976, was a significant contribution toward international agreement and improvement in communication and understanding among earth scientists worldwide. This revised, second edition updates and expands the discussions, suggestions, and recommendations of the first edition, expansions necessitated by the growth and progress of stratigraphic ideas and the development of new stratigraphic procedures since release of the first edition. A valuable tool for every earth scientist writing for an international audience.

GSA publication No. IUG001, hardbound, 220 pages in 6" x 9" format, indexed, ISBN 0-8137-7401-2, \$48.50, postpaid surface mail.

ORDER DIRECTLY FROM THE GEOLOGICAL SOCIETY OF AMERICA

PUBLICATION SALES, P.O. BOX 9140, BOULDER, CO 80301 USA FAX 303-447-1133



The Geological Society of America



PREPAYMENT REQUIRED. MAJOR CREDIT CARDS ACCEPTED

PRINTED IN HUNGARY
Akadémiai Kiadó és Nyomda, Budapest

MAGYAR
TUDOMÁNYOS AKADÉMIA
KÖNYVTÁRA

GUIDELINES FOR AUTHORS

Acta Geologica Hungarica is an English-language quarterly publishing papers on geological topics. Besides papers on outstanding scientific achievements, on the main lines of geological research in Hungary, and on the geology of the Alpine–Carpathian–Dinaric region, reports on workshops of geological research, on major scientific meetings, and on contributions to international research projects will be accepted.

Only original papers will be published and a copy of the Publishing Agreement will be sent to the authors of papers accepted for publication. Manuscripts will be processed only after receiving the signed copy of the agreement.

Manuscripts are to be sent to the Editorial Office for refereeing, editing, in two typewritten copies, on floppy disk with two printed copies, or by E-mail. Manuscripts written by the following word processors will be accepted: MS Word, WordPerfect, or ASCII format. Authors are requested to sign and send to the Editor a Publishing Agreement after the manuscript has been accepted by the Editorial Board. Acceptance depends on the opinion of two referees and the decision of the Editorial Board.

Form of manuscripts

The paper complete with abstract, figures, tables, and bibliography should not exceed 25 pages (25 double-spaced lines with 3 cm margins on both sides).

The first page should include:

- the title of the paper (with minuscule letters)
- the full name of the author
- the name of the institution and city where the work was prepared
- an abstract of not more than 200 words
- a list of five to ten key words
- a footnote with the postal address of the author

The SI (System International) should be used for all units of measurements.

References

In text citations the author's name and the year of publication between brackets should be given. The reference list should contain the family name, a comma, the abbreviation of the first name, the year of publication, and a colon. This is followed by the title of the paper. Paper titles are followed – after a long hyphen – by periodical title, volume number, and inclusive page numbers. For books the title (English version), the name of the publisher, the place of publication, and the number of pages should be given.

Figures and tables

Figures and tables should be referred to in the text. Figures are expected in the size of the final type-area of the quarterly (12.6 x 18.6) or proportionally magnified 20–25% camera ready quality. Figures should be clear line drawings or good quality black-and-white photographic prints. Colour photographs will also be accepted, but the extra cost of reproduction in colour must be borne by the authors (in 1995 US\$ 260 per page). The author's name and figure number should be indicated on the back of each figure. Tables should be typed on separate sheets with a number.

Proof and reprints

The authors will be sent a set of proofs. Each of the pages should be proofread, signed, and returned to the Editorial Office within a week of receipt. Fifty reprints are supplied free of charge, additional reprints may be ordered.

Contents

Data on the (Upper Permian) Foraminifer fauna of the Nagyvisnyó Limestone Formation from borehole Mályinka-8 (Northern Hungary). <i>A. Bérczi-Makk, L. Csontos, P. Pelikán</i>	185
Clay mineralogy of Jurassic carbonate rocks, Central Transdanubia, Hungary. <i>I. Viczián</i>	251
Petrophysical characteristics of the Mamura Formation (Lower Cretaceous), Western Desert, Egypt. <i>A. M. A. El Sayed</i>	269

Book review

Amos Salvador (Ed.) 1994: International Stratigraphic Guide. <i>G. Császár</i> .	283
--	-----

307216

Acta Geologica Hungarica

18

5

VOLUME 38, NUMBER 4, 1995

EDITOR-IN-CHIEF

J. HAAS

EDITORIAL BOARD

**GY. BÁRDOSSY (Chairman), G. CSÁSZÁR, G. HÁMOR,
T. KECSKEMÉTI, GY. PANTÓ, GY. POGÁCSÁS,
T. SZEDERKÉNYI, Á. KRIVÁN-HORVÁTH (Co-ordinating Editor),
H. M. LIEBERMAN (Language Editor)**

ADVISORY BOARD

**K. BIRKENMAJER (Poland), M. BLEAHU (Romania),
P. FAUPL (Austria), M. GAETANI (Italy), S. KARAMATA (Serbia),
M. KOVAČ (Slovakia), J. PAMIĆ (Croatia)**



Akadémiai Kiadó, Budapest

ACTA GEOL. HUNG. AGHUE7 38 (4) 285-376 (1995) HU ISSN 0236-5278

ACTA GEOLOGICA HUNGARICA

A QUARTERLY OF THE HUNGARIAN ACADEMY OF SCIENCES

Acta Geologica Hungarica publishes original studies on geology, crystallography, mineralogy, petrography, geochemistry, and paleontology.

Acta Geologica Hungarica is published in yearly volumes of four numbers by

AKADÉMIAI KIADÓ

Publishing House of the Hungarian Academy of Sciences

H-1117 Budapest Prielle Kornélia u. 19-35

Manuscripts and editorial correspondence should be addressed to the

ACTA GEOLOGICA HUNGARICA

Dr. János Haas

Academical Research Group, Department of Geology, Eötvös Loránd University of Sciences

H-1088 Budapest, Múzeum krt. 4/a, Hungary

E-mail: haas@ludens.elte.hu

Orders should be addressed to

AKADÉMIAI KIADÓ

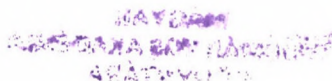
H-1519 Budapest, P.O. Box 245, Hungary

Subscription price for Volume 38 (1995) in 4 issues US\$ 92.00, including normal postage, airmail delivery US\$ 20.00.

Acta Geologica Hungarica is abstracted/indexed in Bibliographie des Sciences de la Terre, Chemical Abstracts, Hydro-Index, Mineralogical Abstract

© Akadémiai Kiadó, Budapest 1995

PRINTED IN HUNGARY
Akadémiai Kiadó és Nyomda, Budapest



On the present state of geological research in Hungary

György Bárdossy
Hungarian Academy of Sciences, Budapest

Márta Csongrádi
Hungarian Geological Survey, Budapest

János Haas
*Geological Research Group,
Eötvös Loránd University, Budapest*

Tibor Kecskeméti
Hungarian Natural History Museum, Budapest

In the last few years, Hungarian geologic research has undergone radical structural and financial changes, about which foreign scientific and practical professional circles have not generally obtained proper knowledge. The aim of the present study is to offer a brief survey of the new structure of geologic research in Hungary, of research work under way and the main objectives. Our review covers only the traditional branches of geology (general and applied geology, tectonics, stratigraphy, palaeontology, mineralogy, petrology, sedimentology and geochemistry), as we do not feel entitled to evaluate geophysics.

Basic research

Up to the end of the eighties, prospecting for raw materials, the geologic mapping and the description of the so-called "key sections" had provided voluminous material to be scientifically elaborated for basic research in Hungary. In the nineties, Hungarian researchers, reduced considerably in number, work on the elaboration and interpretation of this material. The main directions and results can be summarized as follows:

Stratigraphy has been regenerating all over the world; "sequence stratigraphy", heavily supported by geophysical methods, has become a borderland between stratigraphy and sedimentology. In the sequence stratigraphy of the Tertiary formations of the Pannonian Basin, Hungarian researchers have achieved considerable results, some of them working together with their American colleagues who developed the method. Under the guidance of the Hungarian Commission on Stratigraphy, the new summary table of the Hungarian stratigraphical units has been compiled and publishing of the series introducing the individual units has begun.

Addresses: Gy. Bárdossy: H-1051 Budapest, Roosevelt tér 9, Hungary
M. Csongrádi: H-1143 Budapest, Stefánia út, 14, Hungary
J. Haas: H-1088 Budapest, Múzeum krt. 4/a, Hungary
T. Kecskeméti: H-1370 Budapest, Múzeum krt 12-14, Hungary

Received: 17 November, 1995

In 1993, an international conference on the Balaton Highland was organized in order to designate one of the boundaries of the Global Chronostratigraphic Scale. If the international board of experts decides in favour of the Balaton Highland, it will be the first "golden spike" the boundaries of the world scale in Hungary.

In the field of *tectonics*, considerable advances have been made concerning the interpretation of structural development and geodynamics of the extremely complex basement of the Pannonian Basin. As a result, nowadays the Pannonian Basin is regarded globally as the basic type of intramountain basins. Besides studying the phenomena of structure development embracing entire mountains and basins, a school based on measuring and statistically evaluating the meso- and microtectonic elements was established. Methods of remote sensing also joined the routine methods of evaluation in Hungary.

In the field of *sedimentology*, the elaboration of the model of Late Tertiary infilling of the Pannonian Basin, the analysis of the development and cyclicity of Mesozoic carbonate platforms, as well as basic bauxite geologic research (and palaeokarst and palaeosol investigations), have yielded results of even international importance.

Mineralogy, petrology and geochemistry have achieved considerable advances through the study of the Tertiary volcanism of the Pannonian Basin, the investigation of the Mesozoic magmatites and the Palaeozoic granitoid rocks as well as the analysis of the processes of low-grade metamorphism. In the field of geochemistry, organic geochemical research activities are outstanding and the application of methods based on the investigation of stable isotopes have evolved.

In *palaeontology*, palaeocommunity investigations and palaeobiogeographical research has been stressed. Besides studying some fossil groups on traditionally high levels, macroflora investigations and the study of some stratigraphically important microfossil groups can be considered as advances.

In the past years, the institutional network of geological research has been significantly transformed. Previously, the Hungarian Geological Institute played a determinative and coordinating role in basic geologic research. It elaborated national programmes of geologic mapping and basic research. The coordinating role of the Hungarian Geological Institute has been terminated; it has also given up a significant part of its programmes because of the considerable decrease in number of researchers.

In other fields of basic research, the research groups of universities, public collections (museums) and the Academy can generally carry on activities only by means of international cooperations. OTKA (the National Science Foundation) has become almost the only source of financing, but it does not allow for programmes of greater volume and comprehensive character to be realized.

Connections with the researchers of the neighbouring countries is lively within the framework of bilateral cooperation of academies, universities as well as state research institutions. An appropriate example of multilateral cooperation is the Alps-Carpathians-Pannonian Basin programme (ALCAPA). Participation in the International Geological Correlation Programme (IGCP) proved to be the most

suitable form of multilateral cooperation, in which several Hungarian researchers take part in leading projects as well.

Applied geologic research

Within the framework of the economic system based on central planning, applied geologic research in Hungary had predominantly been directed towards prospecting for raw materials and the geologic support of mining. Research work had been continued under the authoritative supervision of the Central Geological Office. Prospecting for mineral raw materials had been carried out for the hydrocarbon and aluminium industries as well as for certain coal mining companies with large output. These activities had been undertaken at an appropriate professional level, even in comparison to Western Europe. Between 1987 and 1990, the Central Geological Office had executed the so-called "programme of modernization" in the entire professional field of applied geologic research, in order to introduce to and adapt for Hungary the research methods applied in the most developed industrial countries. Within it, high priority was given to the application of computer technology and methods of advanced mathematics.

The level of prospecting for bauxite and hydrocarbons in Hungary enjoys remarkable international recognition. This is proved by the international conferences and symposiums organized during the last ten years in our country, as well as by positions held in international organizations.

In the field of applied geology, the structural switch-over to a market economy had been ended only by late 1993. The research institutions of industry have been considerably shrunk, or totally dissolved, especially in the field of coal and mineral mining. Today, prospecting for mineral raw materials is carried out in the framework of a single department in the Hungarian Geological Institute. It deals primarily with the geologic preparations of prospecting for energy-bearing mineral raw materials, as well as the modeling of certain raw material deposits.

The geologic organization of prospecting for hydrocarbon has been best preserved within the framework of the MOL, Hungarian Oil and Gas Company. Its activity ranges from the mineralogical-petrographic and geochemical investigations applied to the basin analysis. It also plays an important role in developing a petroleum system models for concession areas.

Hydrogeology is one of the most important fields of applied geologic research in Hungary. Within its framework, a national hydrogeologic water level detecting network was established, and the results of measurements are stored and evaluated by modern computer methods. A great importance is attached to the elaboration of the hydrogeologic computer model of Szigetköz (NW Hungary), a cooperation between the Geological Institute and the Danish Hydraulic Institute. This area is examined and evaluated jointly by Austrian and Slovakian experts ("DANREG" programme), as well.

Regional offices of the Hungarian Geological Survey have organized the control of the professional waste disposal. An especially difficult question, requiring multilateral research, is the disposal of radioactive waste material. Since 1992

organized work has been in progress, under the guidance of the National Atomic Energy Commission, to solve this problem, in which the Geological Institute, the Mecsek Uranium Mining Company and different research institutions of the Hungarian Academy of Sciences also take part.

To summarize, the role of prospecting for raw materials has been diminished within applied geologic research. On the other hand, the role of hydrogeology, engineering geology and environmental geology has been increased. The wider and wider application of computer and space technology is regarded as a positive fact. Postgraduate training and the rapid adaptation of new research methods elaborated in the most developed industrial countries will help to solve the problem.

Size of staff and proportion of graduated researchers

During the reorganizations of the last years, the number of active employees has been considerably reduced in the field of geology. Many of them have retired, many have found jobs elsewhere and, unfortunately, there are unemployed geologists as well. As against the 310 active employees of 1995, the number of active geologists had ranged from 800 to 900 persons in the eighties. Most of them work in the Geological Institute today. In addition, there are industrial companies, among which the role of the MOL, Hungarian Oil and Gas Company is the most important.

Today, the training of geologists at university level continues in the Eötvös Loránd University of Budapest and the University of Miskolc. In the former 155, and in the latter 230 students had received diplomas of geology between 1984 and 1994. This adds up to 385 new graduates, which is more than the total number of geologists employed today.

Among the geologists, 5 are members of the Hungarian Academy of Sciences, 28 are "academic doctors" (D.Sc), 68 are "candidates" (approximately equivalent to the Ph.D.) for that title, and 190 are university doctors. The new academic and higher educational laws will make it possible to introduce scientific degrees usual in the western countries, such as "Ph.D."

Activity of scientific associations

In Hungary, the oldest scientific association is the Hungarian Geological Society. It was founded in 1848 and it has 954 members today. The Society, with its 8 thematic and 5 regional organizations, provides a forum for becoming acquainted with new Hungarian and foreign accomplishments through proceedings, conferences, symposiums, workshops in oral form, and, by means of the *Földtani Közlöny* (Bulletin of the Hungarian Geological Society) and other publications, in a written form. Some of the more important events organized by the Society in the last years were the 10th Conference of the International Association of Sedimentologists (1989), the 21st European Micro-palaeontological Colloquium (1989), the 1st International Meeting of Young Geologists (1991), the 8th Meeting of the Association of European Geological Societies (1993) and the 64th Conference of the German Palaeontological Society (1994).

Fruitful cooperation has been established with several foreign – mainly Austrian, German and French – geological associations, principally on the basis of personal contacts. The international recognition of Hungarian geology is marked by the honorary positions as well as the memberships in the scientific councils, executive boards and editorial of different geological associations.

Publications

In the last years, the possibilities of geologic publishing in Hungary have been significantly narrowed down. With difficulty, it was possible to preserve the bulletin of the Hungarian Geological Society, *Földtani Közlöny*, which is beginning its 123rd volume. In addition, the English language quarterly of the Hungarian Academy of Sciences, *Acta Geologica Hungarica*, and some periodicals of universities and public collections, appear regularly. At the same time, *Földtani Kutatás* (Geological Prospecting), with an applied geologic theme, as well as publications of a review character of the Geological Society, have been terminated, and the publishing activity of the Geological Institute has been practically stopped. This is an irrecoverable loss, as the publication of monographs of greater volume has become almost impossible, to say nothing of the maps.

Simultaneously, the publication of manuals, school-books and university lecture notes has shown a positive trend. Works of outstanding level have appeared. The list of Hungarian technical books on geology published since 1989 in Hungarian or foreign edition is given in Appendix I. Among them, "Sedimentology", published in three volumes under the editorship of Kálmán Balogh, who died recently, is worth emphasizing. It represents a milestone for both Hungarian basic research and university education.

Despite the difficulties, a surprisingly great number of geological publications, altogether 1132, have appeared in Hungarian technical journals between 1989 and 1994. This is, however, the total of 5 years, and the annual distribution shows an unambiguously decreasing character because of the narrowing down of the publication possibilities.

Papers of several Hungarian geologists are also published in foreign journals. A complete review of them is almost impossible because of the great number of technical journals. Therefore, we selected 21 journals, regarded by us as the most respected ones, and counted the number of publications of Hungarian geologists which appeared in them between 1989 and 1994 (Table I). It is a remarkably great number (50) and, in our opinion demonstrates the international recognition of Hungarian geology.

International recognition

The most generally used means of assessing international recognition is the *Scientific Citation Index* (SCI), compiled by the Institute of Scientific Information, Philadelphia, USA, which processes more than 3500 technical journals of the world. Unfortunately, geology is represented only by 95 journals in this index,

and there is no representative of a Central European edition among them. Therefore, within the scope of the SCI, this gives a more unfavourable impression of Hungarian geology than is justified.

Table I

Publications of Hungarian authors in respected foreign journals

Title of the journal	1989	1990	1991	1992	1993	1994	
AAPG Bulletin		1				1	2
Applied Geochemistry				1		1	2
Comptes Rendus de l'Acad. des Sciences Sciences de la Terre	1						1
Cretaceous Research		1			2		3
Eclogae Geologicae Helvetiae				2		1	3
Episodes				1			1
Geochimica et Cosmochimica Acta				1			1
Journal of Geology			1				1
Journal of Petrology	1						1
Journal of Sedimentary-Petrology			1			1	2
Lithos		1		1		1	3
Micropaleontology		1				1	2
Neues Jahrbuch für Mineralogie, Geologie und Paleontologie	3	1	2		1		7
Organic Geochemistry		4				2	6
Palaeogeography, Palaeoclimatology, Palaeoecology		1	2				3
Revue de Micropaleontologie	1						1
Sedimentary Geology					1	2	3
Sedimentology						1	1
Societe Geologique de France		1	1				2
Tectonophysics			2				2
Terra Nova		1	1	1	1		4
							50

Unfortunately, the degree of being referred to is not even satisfactory in the computerized referring systems of geologic topics. In order to prove this numerically, we asked ten well-known Hungarian geologists to make available to us a complete list of their publications for the years between 1989 and 1994. The sum total was 65 publications in Hungary and 82 abroad. The computer database "Geoarchive" of Baltimore, USA, had registered only 25% of these publications. The "Georef" referring computer database of Washington recognizes only 39% of the publications.

International recognition, however, can be indirectly defined by means of the positions held in international scientific associations. Hungarian geologists hold offices in 12 international associations of geologic scope of interest.

A good example of the international recognition of Hungarian geological research is the December 1995 issue of the central journal of the International Union of Geological Sciences, *Episodes*, on the front-page of which a view of Budapest can be seen, and in which Hungarian and foreign authors offer a brief survey of the Hungarian geologic institutions and their research achievements.

Conclusions

1. During the last years, Hungarian geology has taken substantial steps toward the conditions of a free market economy. It is regrettable that, because of the difficult economic situation of the country, instead of establishing a rational staff number, an excessive or total reduction in the number of geologists has occurred in several places.

2. Within geologic research, the amount of prospecting for mineral raw materials and geologic mapping has been considerably diminished; in turn, the role of environmental geology, hydrogeology and engineering geology has increased.

3. Positive developments are the increased international relations and cooperations.

4. A significant development has taken place in the application of computer and space-related technology in Hungarian geology.

5. Presence in international references of geologic technical journals is regrettably deficient. Concerted steps have been taken to remedy this situation, benefiting also by international collaboration. In the meantime, we strive to develop a *publication strategy*, which will provide more referencing of Hungarian

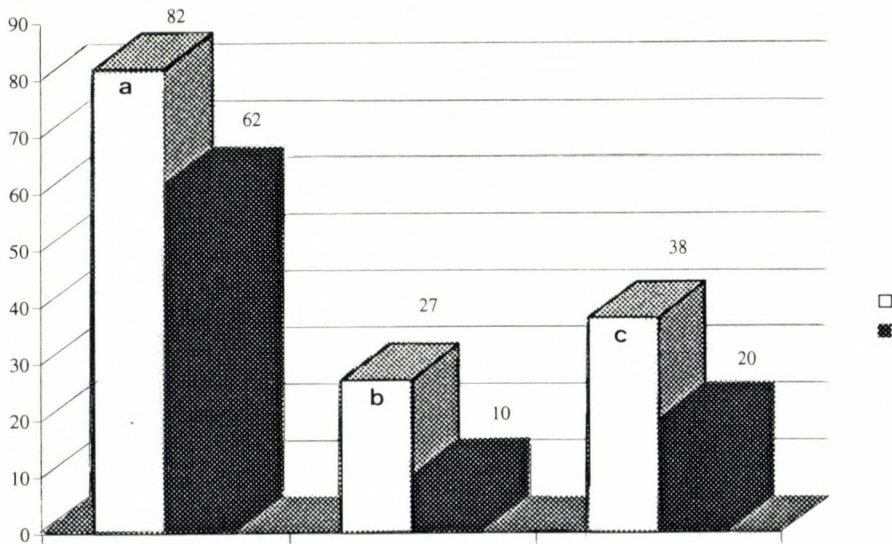


Fig. 1
Representative sampling from the publications which appeared between 1989 and 1994. a) own publication; b) among them those listed in the "Geoarchive" database; c) among them those listed in the "Georef" database; □ foreign; ■ Hungarian

geologists' publications which have appeared in a global language in the present-day data bases.

6. In the interest of national and international comparability, we want to rely to a greater degree on the methods of scientometry, and we have already taken the initial steps in this respect.

To summarize, we are of the opinion that despite the economic difficulties, Hungarian geologic research has preserved its capacity to survive and, in looking for new possibilities, produces significant results in certain fields.

Appendix I

Technical books of geologic topics published between 1989 and 1995

- Balogh, K. (Ed.): Szedimentológia I–III (Sedimentology I–III) – Akadémiai Kiadó, Budapest, Vol. I: 1991, 546, Vol. II: 1991, 355 p., Vol. III: 399 p. (in Hungarian).
- Bárdossy, Gy., G.J.J. Aleva: Lateritic bauxites. – Elsevier Science Publishers, Amsterdam–Oxford–New York, 1990, 629 p.
- Bárdossy, Gy., G.J.J. Aleva: Lateritic bauxites. – Liaoning Science and Technology Publishing House, Peking 1990, 541 p. (in Chinese)
- Bognár, L.: Ásványnévtár. (Catalogue of minerals). – Eötvös University Press, Budapest, 1995, 345 p. (in Hungarian).
- Egerer, F., P. Kertész: Bevezetés a közetfizikába (Introduction to petrophysics. – Akadémiai Kiadó, Budapest, 1993, 424 p. (in Hungarian).
- Erdélyi, M.: Hydrogeology of the Hungarian upper Danube section (before and after damming the river). – Hungarian Natural History Museum, Budapest, 1994, 115 p.
- Fülöp, J.: Bevezetés Magyarország geológiájába (Introduction to the Geology of Hungary). – Akadémiai Kiadó, Budapest, 1989, 249 p. (in Hungarian).
- Fülöp, J.: Magyarország geológiája. Paleozoikum I (Geology of Hungary. Paleozoic I). – Magyar Állami Földtani Intézet, Budapest, 1990, 325 p. (in Hungarian)
- Fülöp, J.: Magyarország geológiája. Paleozoikum II (Geology of Hungary. Paleozoic II). – Akadémiai Kiadó, Budapest, 1994, 445 p. (in Hungarian).
- Géczy, B.: Ósállattan Vertebrate Paleontologia. – Tankönyvkiadó, Budapest, 1993, 502 p. (in Hungarian).
- Géczy, B.: Ósállattan Invertebrate Paleontologia. – Tankönyvkiadó, Budapest, 1993, 595 p. (in Hungarian).
- Haas, J.: Jelenkori tengeri üledékképződési környezetek. (Recent marine sedimentary environments). – Tankönyvkiadó, Budapest, 1991, 150 p. (in Hungarian)
- Kretzoi, M., V. T. Dobosi (Eds): Vértesszőlős site, Man and Culture. – Akadémiai Kiadó, Budapest, 1990, 554 p.
- Kubovics, I.: Kőzetmikroszkópia (Petrologic microscopy). – Tankönyvkiadó, Budapest, Vol. I. 1993, 361 p. Vol. II. 1994, 596 p. (in Hungarian).
- Molnár, B.: A Föld és az élet fejlődése (Evolution of the Earth and life). – Tankönyvkiadó, Budapest, 1990, 360 p. (in Hungarian)
- Szádeczky-Kardoss, E.: Introduction in cycle view. – Akadémiai Kiadó, Budapest, 1991, 211 p.
- Szádeczky-Kardoss, E.: A jelenségek univerzális kapcsolódása (Universal linkage of phenomena). – Akadémiai Kiadó, Budapest, 1989, 289 p. (in Hungarian)
- Szakáll, S., I. Gatter: Magyarországi ásványfajok. (Mineral varieties of Hungary). Fair System Kft, Miskolc, 1993, 211 p. (in Hungarian).
- Szőőr, Gy. (Ed.): Fáciesanalitikai, paleobiogeokémiai és paleoökológiai kutatások (Facies analytical, palaeobiogeochemical and palaeoecological researches). – MTA Debreceni Akadémiai Bizottság, Debrecen, 1992, 263 p. (in Hungarian).

Biotite in a Paleozoic metagreywacke complex, Mecsek Mountains, Hungary: Conditions of low-T metamorphism deduced from illite and chlorite crystallinity, coal rank, white mica geobarometric and microstructural data

Péter Árkai, Csaba Lantai

Géza Nagy,

*Laboratory for Geochemical Research,
Hungarian Academy of Sciences, Budapest*

Gyöngyi Lelkes-Felvári

*Natural History Museum, Dept. of Mineralogy
and Petrography, Budapest*

The investigated borehole Szalatnak-3 (with continuous core material) penetrated a Silurian metagreywacke complex, which is overlain by Triassic sediments. Basic dykes cut across the sequence; moreover, a syenite body was found in the bottom of the borehole. Microstructural observations prove that regional (dynamothermal) metamorphism was overprinted by a contact (thermal) event.

The application of the illite crystallinity (IC) method for determining metamorphic zones of the metagreywacke samples, which contain di- and trioctahedral mica phases in strongly varying proportions, gave misleading results. In contrast, chlorite crystallinity (ChC) indicates transitional "anchi-/epizonal" (ca 350–400°C) metamorphism. ChC data fit fairly well with conclusions obtained from chlorite geothermometric and coal rank data. On the basis of the $d_{331,060}$ parameter of illite-muscovite, the complex was metamorphosed in a high thermal gradient regime.

Newly formed (metamorphic) biotite is widespread in the whole metagreywacke sequence. Microstructural observations and mineral chemical data refer to non-equilibrium transformations of detrital biotite → chlorite → newly formed biotite. Based on its post-tectonic (partly fissure filling) nature, the formation of biotite is attributed to the contact metamorphic heat effect and/or to an eventual infiltration metasomatism connected to the intrusion of syenite.

Key words: greywacke, low-T metamorphism, biotite, illite crystallinity, chlorite crystallinity, coal rank, anchizone, epizone, white mica geobarometry, Hungary

Introduction

The appearance of biotite in progressively metamorphosed terrains is generally considered to be an important indicator of temperature (biotite zone, biotite isograd, "biotite + muscovite in" isograd, see Miyashiro 1973 and Winkler 1979). Depending on the lithology-controlled mineral associations, various biotite-producing reactions are known, the equilibrium temperatures of which differ significantly.

Addresses: P. Árkai, Cs. Lantai, G. Nagy: H-1112 Budapest, Budaörsi út 45, Hungary,
Gy. Lelkes-Felvári: H-1088 Budapest, Baross u. 13, Hungary

Received: 23 May, 1995

In the present study the occurrence of biotite in a metagreywacke sequence is characterized by microstructural, mineral paragenetic and mineral chemical observations. To determine the physical conditions of the formations of biotite, illite and chlorite crystallinity, coal rank and white mica b_0 geobarometric data were used. In this way, the effect of trioctahedral mica, being present in varying proportions, on illite crystallinity was demonstrated, and the applicability of chlorite crystallinity, as an additional, complementary, metamorphic zone-indicating parameter was tested.

Geology, previous data on metamorphism

The Silurian metagreywacke complex of the Mecsek Mts (Southern Transdanubia, Hungary) belongs to the Tisza Unit or "Tisia microplate" (Fig. 1), which proved to be one of the most stable, resistant lithosphere fragments during the Alpine tectonocycle (Árkai 1991a). The Tisza Unit derived from the northern, European border of the Tethys, and occupied its present tectonic position by meso-Alpine horizontal displacements (Géczy 1973; Kovács 1982; Kázmér and Kovács 1985).

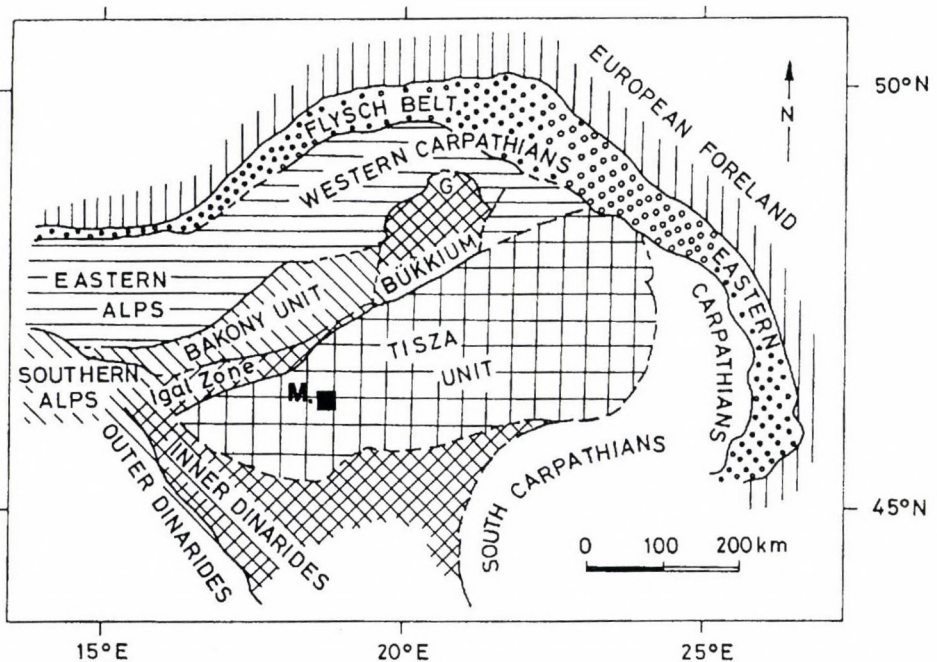


Fig. 1
Tectonic position of the Mecsek Mountains (M) within the Alpine-Carpathian-Dinaric frame.
G - Gemer Unit

The crystalline basement of this area records two main phases of pre-Alpine metamorphism. In medium-grade rocks – known only from boreholes – a kyanite-bearing mineral assemblage was overprinted by an andalusite-bearing Hercynian metamorphic event (Lelkes-Felvári and Sassi 1981; Árkai 1984). Hercynian low- to medium-grade rocks outcrop in the eastern part of the Mecsek Mts (Mórágý area), being in tectonic contact with Hercynian granitoids (Szederkényi 1975; Jantsky 1979).

North of the Mecsek Mts., in a structural high covered by Triassic sediments, several boreholes encountered a slightly metamorphosed series, for which paleontological findings proved a Silurian sedimentation age (Kozur 1984). The Sz-3 borehole at the village of Szalatnak, which was found to be representative of the entire series, was investigated in detail.

The schematic geologic column of the Szalatnak-3 borehole is presented in Fig. 2. The Silurian metagreywacke complex is overlain by Lower Triassic, red bed-type sandstone and conglomerate, and rests on porphyric syenite with a narrow biotite-plagioclase hornfels aureole, which is separated tectonically from the metagreywacke complex. The metagreywacke was folded and also strongly faulted, i.e. brecciated. It consists of numerous thin slate, metachert and volcanoclastic intercalations, and a relatively thick, polymictic volcanic breccia-agglomerate horizon. The contacts of the different layers within this volcanosedimentary complex are sharp. Some coarser beds show gradation. Load clasts, mudstone clasts in sandstone and sandstone lenses in mudstone are not rare. In forms of dispersed, minute parts or coherent seams, high organic matter content is characteristic for the complex.

The available petrographic data on the metamorphism of the metagreywacke complex are sporadic and rather controversial. Based on the presence of prehnite in veinlets, "low-grade metamorphism" (Szederkényi 1975), "zeolite zone metamorphism" (Szederkényi 1982), "zeolite facies" (Lelkes-Felvári and Sassi 1981) was described. The age of the regional metamorphism is Hercynian. In the surroundings of the Hercynian late-kinematic syenite intrusion, contact metamorphism also affected the complex (Szederkényi in Szederkényi et al. 1991). The whole rock Rb-Sr model age of the syenite is 330 ± 25 Ma, while the Rb-Sr cooling age of the magmatic biotite is 227 ± 59 Ma, as analyzed by Kovách (unpublished data). Kozur (1984), referring to the petrographic observations of L. Ravasz-Baranyai, concluded that the complex had not suffered dynamothermal metamorphism; only traces of a slight contact metamorphic effect could be proven.

Methods

In addition to mesoscopic and petrographic microscopic observations, the following methods were applied.

Illite crystallinity (IC, more precisely, IC(002), i.e., half-height width of the first, 10Å basal reflection of illite-muscovite) was determined by X-ray diffractometric (XRD) method, using the techniques of Kübler (1967, 1975, and

1990). Rock samples were disaggregated under standard conditions using a jaw crusher followed by crushing in a mortar mill (type Pulverisette 2, Fritsch) for 3 minutes. Previous experiments showed that this short-term pulverization has no measurable effects on the IC values. Final disaggregation was achieved by repeated shaking in deionized water. The $<2 \mu\text{m}$ grain-size fraction was separated from aqueous suspension based on differential settling of grains of different diameters. Aqueous suspensions of the given fraction were pipetted and dried at room temperature on glass slides to produce thin-layer, highly oriented preparations with a density of $1\text{--}3 \text{ mg/cm}^2$. The half-width values of the first (14\AA) and second (7\AA) basal reflections of chlorite indicated as ChC(001) and ChC(002) were determined in a similar way, from the same preparations.

A Philips PW-1730 diffractometer was utilized at $45 \text{ kV}/35 \text{ mA}$, with $\text{CuK}\alpha$ radiation, graphite monochromator, proportional counter, divergence and detector slits of 1° , goniometer speeds of $2^\circ/\text{min}$ and $0.5^\circ/\text{min}$, time constant of 2 s , and chart speed of 2 cm/min . At these instrumental parameters, the

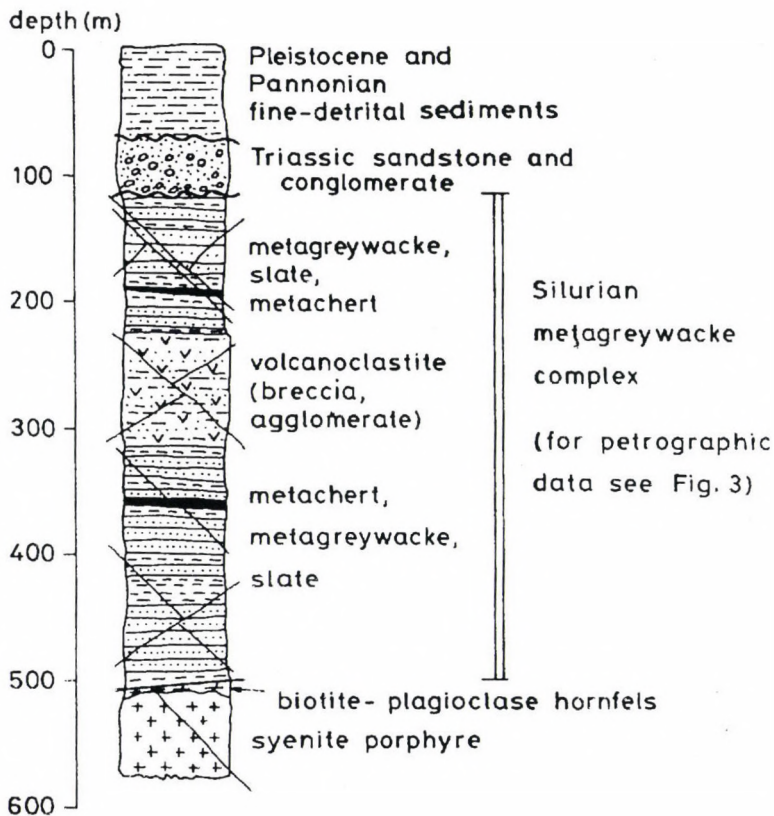


Fig. 2
Schematic geological profile of the Szalatnak-3 borehole

standard deviations of the half-height width measurements were $s = 0.012 \Delta^{\circ}2\Theta$ ($n = 10$) for an IC of $0.259 \Delta^{\circ}2\Theta$ using $2^{\circ}/\text{min}$, and $s = 0.008 \Delta^{\circ}2\Theta$ ($n = 10$) for an IC of $0.215 \Delta^{\circ}2\Theta$ using $0.5^{\circ}/\text{min}$ goniometer speeds.

The calibration of IC values against those of Kübler's laboratory (where the $0.25\text{--}0.42 \Delta^{\circ}2\Theta$ boundary values of the anchizone were established) was made using standard rock slabs (series Nos. 32, 34 and 35) kindly provided by B. Kübler. Smaller scale, temporal instrumental changes were corrected by the repeated use of a calibrated standard rock slab series (Nos. Á-1, -2 and -3) of the Laboratory for Geochemical Research, Budapest. Applying the least-squares' method, the calibration equations are

IC(Kübler) = $1.124 \times \text{IC (present work)} - 0.069$ at $2^{\circ}/\text{min}$, and
 IC(Kübler) = $1.164 \times \text{IC (present work)} - 0.038$ at $0.5^{\circ}/\text{min}$ goniometer speeds.

Thus, IC values of 0.284 and $0.435 \Delta^{\circ}2\Theta$ measured at $2^{\circ}/\text{min}$, as well as 0.247 and $0.393 \Delta^{\circ}2\Theta$ at $0.5^{\circ}/\text{min}$ goniometer speed correspond to Kübler's original anchizone boundaries in the present paper. However, the "diagenetic", "anchi-" and "epizone" were re-defined by Árkai (1983, 1991b), using the correlations between IC, clay mineral assemblages, vitrinite reflectance and metabasite mineral facies. The IC boundaries of this "anchizone" are $0.25\text{--}0.34 \Delta^{\circ}2\Theta$ at $2^{\circ}/\text{min}$ and $0.20\text{--}0.30 \Delta^{\circ}2\Theta$ at $0.5^{\circ}/\text{min}$ goniometer speed in the present work, and correspond to $0.21\text{--}0.31 \Delta^{\circ}2\Theta$ on Kübler's original scale. This "anchizone" is correlated roughly with the pumpellyite-actinolite facies and with the medium- and high-T parts of the prehnite-pumpellyite facies, and is characterized by vitrinite reflectance ranges of $R(\text{random})$ $5.0\text{--}3.0\%$ and $R(\text{max})$ $6.0\text{--}3.5\%$. The estimated temperature range of Kübler's anchizone is ca $200\text{--}300^{\circ}\text{C}$, while that of the re-defined "anchizone" corresponds to ca $250\text{--}350^{\circ}\text{C}$ (see Frey 1986; Kisch 1987; Árkai 1991b). These re-defined zones (indicated by quotation marks) are used in the present paper (For further details concerning the theoretical and methodological problems of the determination of zone boundaries see Kisch 1990 and Árkai 1991b).

The $d_{331,060}$ spacing of illite-muscovite was determined from whole rock non-oriented powder mounts.

Vitrinite reflectance (R) data of the dispersed, coalified particles were measured in the Institute of Coal and Petroleum of the Technical University Aachen, Germany, by means of a Zeiss microscope with an EPI 40x lens in oil immersion [$n(23^{\circ}\text{C}, e) = 1.518$], under standardized conditions.

Chemical analyses of minerals were carried out by a JEOL JCSA-733 electron microprobe equipped with 3 WDS, using the measuring program of Nagy (1984, 1990). The measuring conditions were: 15 kV, 30 nA, defocused electron beam with a diameter of $5\text{--}10 \mu\text{m}$, measuring time 5×5 s. Matrix effects were corrected using the method of Bence and Albee (1968). The following standards were used for quantitative analysis: orthoclase (Si, Al and K), synthetic glass (Fe,

Mg and Ca), spessartine (Mn), rutile (Ti) and albite (Na). Statistical errors expressed as 1σ are as follows: SiO_2 : ± 0.3 , TiO_2 : ± 0.05 , Al_2O_3 : ± 0.05 , FeO : ± 0.2 , MgO : ± 0.1 , MnO : ± 0.05 , CaO : ± 0.1 , Na_2O : ± 0.03 , and K_2O : ± 0.02 %.

IR absorption spectra were obtained by a Pye-Unicam SP 1000 spectrophotometer, using pressed KBr pastilles that contain 1 mg of investigated materials.

Rock types, microstructure and modal composition

Metasandstone, slate, metachert and metavolcanite clasts (the latter from the agglomerate) were investigated. These rocks display weak metamorphic foliation. In general, the cleavage planes are parallel to bedding. Less frequently, cleavage planes cross the bedding plane at various angles.

The medium-, dark grey *metasandstone* displays slightly developed, rough cleavage. The cleavage surfaces form widely spaced, short seams. Foliation is caused by the dimensional preferred orientation of quartz + mica + chlorite overgrowths ("beards") around detrital grains, while the preferred orientation of the detrital grains is rather weak. The proportion of rock occupied by cleavage domains is low. Fracture cleavage and conjugate cleavage are subordinate. Refraction of cleavage on the boundary with pelitic and silty layers is rarely observed. Sometimes cleavage seams truncate thin silty layers.

The detrital components of the metasandstone are: quartz, plagioclase, muscovite, biotite and lithoclasts. K-feldspar clasts are very rare. Besides quartz grains with undulatory extinction, crystals of volcanic origin also occur. The detrital plagioclase is usually represented by zoned grains that are partially altered to white mica. Rarely, "chess-board" albite is also present. Based on the electron microprobe analyses, the An content of the detrital plagioclase varies between 16 and 36%, the Or content is generally $< \text{or} = 1$ %, in certain cases reaching 4–5 % (Table 1). The sporadic K-feldspar is perthitic in certain cases, and displays "cross-scratch" twinning. Muscovite and biotite flakes are deformed, or kinked; the latter are also opacitic and partially chloritized. Besides subordinate fragments of quartzite and a plutonic rock consisting of quartz and feldspar, a wide variety of volcanic rock fragments forms the majority of the lithoclasts. The latter are characterized by aphanitic, variolitic, trachytic and pilotaxitic textures. Sometimes they contain quartz and/or feldspar and/or biotite phenocrysts. The ratio of the plagioclase detritus and the lithoclasts is highly variable, while the muscovite and biotite clasts are subordinate.

The recrystallized matrix of the metasandstones consists of quartz, albite, chlorite, biotite, coalified organic matter, pyrite carbonate minerals (dolomite, siderite and calcite in varying proportions) and white mica. "Spine-like" overgrowth microstructures consisting of quartz "beards" intergrown with micas and chlorite are characteristic around the clastic quartz grains.

Table 1
Representative electron microprobe analyses of plagioclase from metagreywacke

sample	141.9m		170.2 m			172.7 m	
SiO ₂	67.12	62.84	61.12	58.56	59.56	62.10	60.48
Al ₂ O ₃	24.21	23.28	24.41	25.61	25.92	21.89	24.90
CaO	5.25	4.07	5.01	7.32	7.26	3.17	5.70
Na ₂ O	8.53	9.24	8.27	7.04	7.39	8.31	7.78
K ₂ O	0.13	0.12	0.12	0.13	0.11	0.89	0.72
<i>total</i>	100.29	99.55	98.93	99.07	100.24	96.36	99.58
numbers of cations on the basis of 8 (O)							
Si	2.74	2.78	2.73	2.65	2.65	2.81	2.69
Al	1.26	1.22	1.29	1.36	1.36	1.17	1.31
Ca	0.25	0.19	0.24	0.35	0.35	0.15	0.27
Na	0.73	0.79	0.72	0.61	0.64	0.73	0.67
K	0.01	0.01	0.01	0.01	0.01	0.05	0.04
<i>total</i>	4.99	4.99	4.99	4.98	5.01	4.91	4.98

Considering the dark-grey colour, the reductive sedimentary environment, the abundant occurrence of (mainly magmatic) rock fragments and plagioclase clasts, the unsorted character of the clasts, the varying proportion of the pelitic-silty matrix and clasts, the rhythmic changes of grain-size and the scarcity (practically, lack) of K-feldspar detritus, this metasandstone can be classified as *metagreywacke* (see Pettijohn et al., 1987). The bulk rock modal composition of metagreywacke are characterized by the predominance of quartz and plagioclase. The quantities of the 10 Å phyllosilicates (illite-muscovite and biotite) and chlorite are also considerable, while those of dolomite, siderite, calcite, pyrite and coalified organic matter are subordinate.

The pelitic and silty *slates* display rough fracture cleavage. The typical slaty cleavage with weak silky sheen caused by the newly-formed phyllosilicates and the crenulation cleavage is rare. Preferred orientation (foliation) of white mica and chlorite in slates indicates recrystallization and/or deformation in anisotropic strain field. Slates also contain sporadic quartz, plagioclase and biotite detritus.

In addition to the dominant 10 Å phyllosilicates and chlorite, the < 2 µm grain-size fraction samples of the clastic rocks always contain quartz and plagioclase in small amounts, while subordinate kaolinite was observed only sporadically.

Metachert shows rough, splintery, conchoidal fracture cleavage.

Silty-psammitic detritus (mostly in the lower horizons) and altered volcanic ash (mostly in the upper levels) form the matrix of the *volcanogenic breccia* and *agglomerate*. The clasts of these rocks consist of mainly volcanic, subordinately subvolcanic and intrusive rock fragments of strongly varying chemical composition.

Crystallinity indices of 10Å phyllosilicates and chlorite

Changes of metamorphic grade (~temperature) indicating parameters of the phyllosilicates and the dispersed, coalified organic matter along the investigated profile of the metagreywacke complex are presented in Fig. 3.

The "IC" values of the mica-like phyllosilicates strongly vary, both in the whole rock and in the < 2 µm fraction samples. The changes of ChC values do not follow the variations of "IC". The majority of the "IC" values falls in the "diagenetic zone" of the illite crystallinity scale. This is in disagreement with the microstructural observations and the coal rank data.

Similarly remarkable, but – comparing with the changes of "IC" values – opposite variations were observed in the intensity ratios of the first two basal reflections of the 10Å phyllosilicates (Fig. 4). Since the intensity of the 5Å reflection of the trioctahedral micas is very weak, the $I(5\text{Å})/I(10\text{Å})$ ratio was also used for discriminating the di- and trioctahedral micas and mica-like structures by XRD (Esquevin 1969; Kübler and Rey 1982). With decreasing intensity ratio the "IC" increases (Fig. 4), which is in agreement with the earlier statements of Esquevin (1969), Dunoyer de Segonzac (1970) and others.

Consequently, "IC" values of samples with $I(5\text{Å})/I(10\text{Å}) > \text{ or } = 0.25$ (which is characteristic of illite-muscovite) may only be used for an approximately realistic estimation of the illite crystallinity zone of the alteration, supposing that the proportion of the trioctahedral micas and mica-like structures in these samples is negligible. (It is obvious that the disturbing effect of the trioctahedral mica cannot be ruled out perfectly.) Thus, the "IC" average obtained by this way may be used only for the rough estimation of the possible minimal temperature of the transformation. The "IC" values of the samples that satisfy the above mentioned criterion are

0.289–0.346 $\Delta^{\circ}2\Theta$, n = 2 at 2°/min, and

0.219–0.260 $\Delta^{\circ}2\Theta$, n = 2 at 0.5°/min, using whole rock samples, and

0.251–0.262 $\Delta^{\circ}2\Theta$, n = 3 at 2°/min, and

0.149–0.252 $\Delta^{\circ}2\Theta$, n = 3 at 0.5°/min, measured on < 2 µm fraction samples.

The majority of these "IC" values falls within the range of the "anchizone".

As the "IC" method provided rather uncertain, inconsistent results, the chlorite crystallinity values were also determined for the metagreywacke complex. In order to determine the metamorphic zones, the boundary values established by Árkai (1991b) for a pelitic-silty series were applied, because

(i) based on the intensity ratios of the first three basal reflections and the electron microprobe data (Table 2), the chemistry of the chlorites of the metagreywacke complex is homogeneous and rather similar to that of chlorite investigated by Árkai (1991b);

(ii) calculating the total iron as Fe^{2+} , the sum of the cations in the chlorite cell containing 28 oxygen is very near to 20. Thus, the chlorite in question is trioctahedral chlorite, the Fe^{3+} content of which is negligible. (This is supported also by the reductive nature of the rocks.)

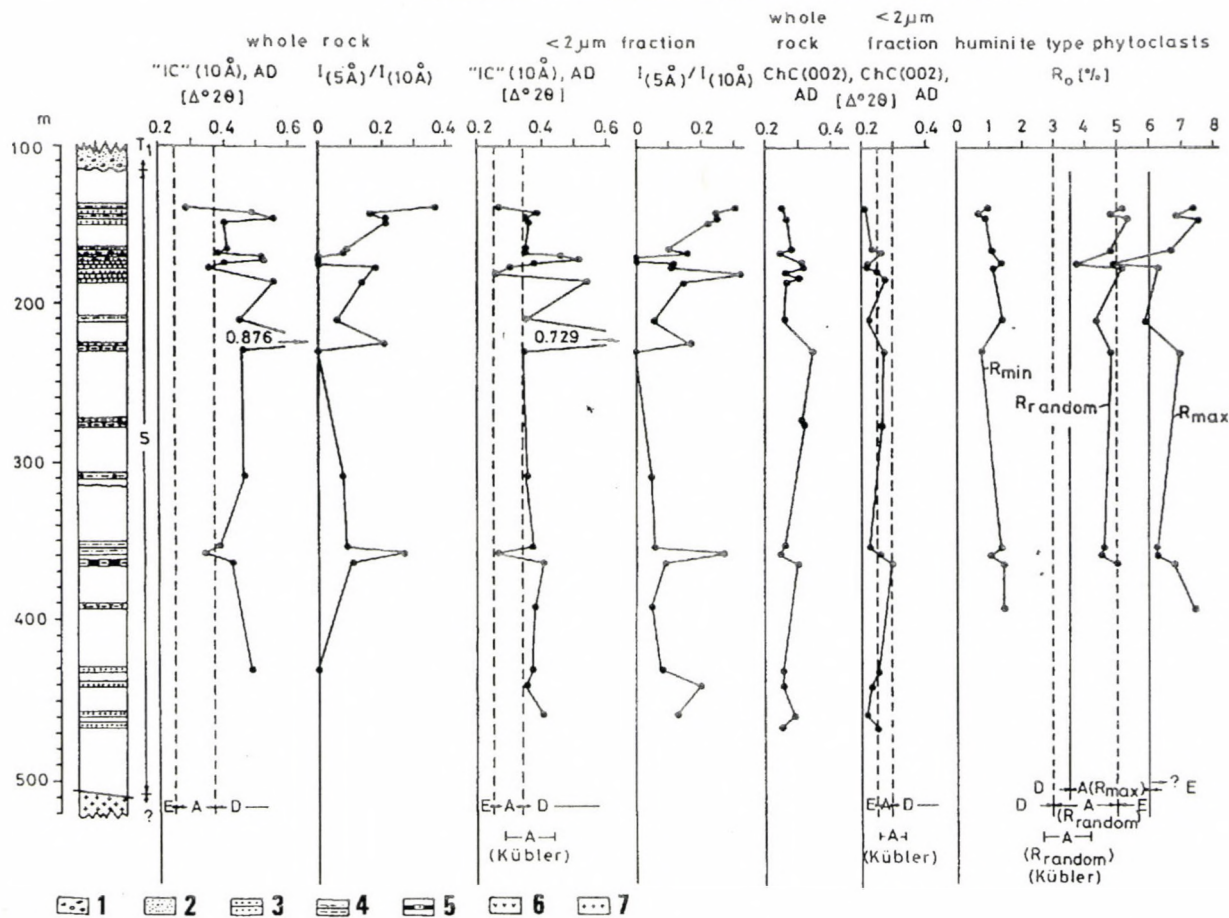


Fig. 3

Changes of the crystallinity indices of the 10 Å phyllosilicates ("IC"), chlorite (ChC), the intensity ratio of the 5 and 10 Å basal reflections of the micas and the reflectance (R) of the huminite type organic matter in the Silurian metagreywacke complex. The ranges of diagenetic, anchi- and epizones in the sense of Kübler (1967, 1990), and those, re-defined by Árkai (1983, 1991b) are also indicated. XRD measurements were carried out on air-dried (AD) samples. 1. conglomerate; 2. sandstone; 3. metasandstone; 4. slate (silty, pelitic); 5. metachert with psammitic bands; 6. volcanoclastics (metamorphosed); 7. syenite porphyre; T₁ - Lower Triassic; S - Silurian; D, A, E, (present work): D - diagenetic zone; A - anchizone; E - epizone

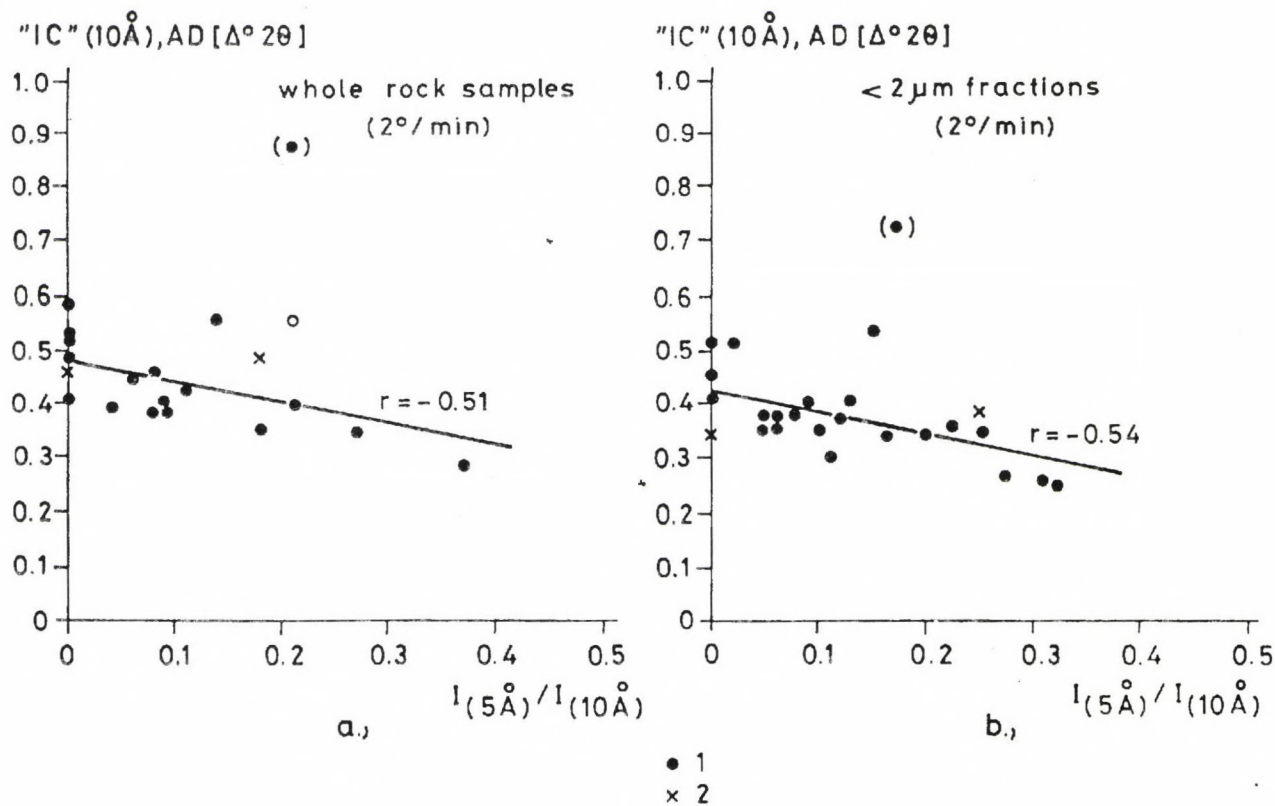


Fig. 4 Relationship between the half-height width of the first basal reflection ("IC") and the intensity ratio of the second and first basal reflections of micas, measured on air-dried (AD) preparations. 1. rocks of psammitic, silty and pelitic origin; 2. metavolcanoclastic rocks

The following ChC averages were obtained for the metagreywacke complex:

whole rock samples:

ChC(002), $2^\circ/\text{min} = 0.281\Delta^{\circ}2\Theta$, $s = 0.032$, $n = 21$;

< 2 μm fraction samples:

ChC(001), $2^\circ/\text{min} = 0.262\Delta^{\circ}2\Theta$, $s = 0.044$, $n = 16$;

ChC(002), $2^\circ/\text{min} = 0.246\Delta^{\circ}2\Theta$, $s = 0.025$, $n = 18$;

ChC(002), $0.5^\circ/\text{min} = 0.201\Delta^{\circ}2\Theta$, $s = 0.021$, $n = 17$.

For determination of metamorphic zones the ChC(001) and ChC(002) values of the < 2 μm fraction samples measured at $2^\circ/\text{min}$ were used. Taking also into consideration the standard errors of the averages ($0.011\Delta^{\circ}2\Theta$ for ChC(001) and $0.006\Delta^{\circ}2\Theta$ for ChC(002)), the ChC(001) average falls within the "epizone", and the ChC(002) average on the boundary between the "anchi-" and "epizones", which corresponds to ca 350 $^\circ\text{C}$ (see Árkai 1983, 1991b). Applying the chlorite- Al^{IV} geothermometer of Cathelineau (1988) to the chlorites of the metagreywacke complex (Table 2), similar (somewhat higher, 355–400 $^\circ\text{C}$) temperature was calculated. This proves that chlorite crystallinity method is a reliable tool for indicating metamorphic thermal zones.

Coal rank

The average maximal, minimal and random reflectance values and bireflectance of the huminite-type, coalified particles are summarized in Table 3. The variations of these data are also displayed in Fig. 3. The R_{max} average indicates "epizonal", while the R_{random} average "anchizonal" conditions. In the latter case the average is close to the boundary of the "anchi- / epizones". Thus, satisfactory agreement exists between the ChC and R data. The bireflectance is rather high. This is due to maturation of organic matter in an anisotropic stress field, i.e., in dynamothermal rather than static thermal conditions. Considering the reflectance data, the organic matter is transitional between metaanthracite and semigraphite (see the diagrams of Ragot 1977; Teichmüller and Teichmüller 1981).

Several samples are characterized by R_{max} histograms with two or three maxima. To explain this, two mechanisms are available:

1) the coal particle population with lower R_{max} can be considered as "autochthonous", while the population(s) with higher R_{max} represent(s) "inherited", detrital particles, characterized by a higher R_{max} already at the time of sedimentation;

2) different types of organic matter were metamorphosed, and the effects of the original chemical differences of the various organic substances on the maturation processes were preserved.

Table 2
Representative electron microprobe analyses of phyllosilicates

type sample	detrital, partially chloritized biotite [Bt ₁ →(Chl)]			newly formed, metamorphic biotite (Bt ₂)			
	141.9 m	170.2 m	172.3 m	141.9 m	170.2 m	172.3 m	353.0 m
n	2	4	8	15	11	8	7
SiO ₂	34.99	33.13	30.97±1.82	35.63±1.28	35.49±1.05	37.31±1.50	35.81±1.16
TiO ₂	0.93	1.00	0.63±0.29	1.15±0.17	1.63±0.50	1.35±0.19	1.56±0.23
Al ₂ O ₃	18.24	19.00	20.06±1.31	19.78±1.34	19.10±0.51	18.37±1.59	19.08±0.58
★FeO	18.04	18.00	18.49±1.69	17.55±0.77	16.87±1.33	16.53±1.90	20.11±0.58
MnO	0.13	0.09	0.11±0.03	0.11±0.03	0.08±0.02	0.07±0.02	0.12±0.01
MgO	11.53	15.07	16.52±1.84	11.95±0.67	12.48±0.69	12.72±0.48	9.60±0.27
CaO	0.04	0.06	0.05±0.04	0.02±0.02	0.03±0.02	0.03±0.03	0.02±0.01
Na ₂ O	0.03	0.00	0.02±0.01	0.04±0.01	0.03±0.01	0.15±0.28	0.04±0.01
K ₂ O	7.74	3.69	2.46±0.93	7.34±0.96	8.62±1.46	8.66±0.77	8.21±0.74
<i>total</i>	91.65	90.04	89.31	93.55	94.33	95.19	94.55

	numbers of cations per unit cells on the basis of								
	22(0)	22(0)	28(0)	22(0)	28(0)	22(0)	22(0)	22(0)	22(0)
Si	5.46	5.16	6.56	4.86±0.23	6.19±0.29	5.40±0.14	5.37±0.12	5.56±0.21	5.46±0.12
Al ^{IV}	2.54	2.84	1.44	3.14±0.23	1.81±0.29	2.60±0.14	2.63±0.12	2.44±0.21	2.54±0.12
Al ^{VI}	0.81	0.64	3.00	0.57±0.19	2.91±0.24	0.92±0.19	0.77±0.07	0.78±0.14	0.89±0.06
Ti	0.11	0.12	0.15	0.07±0.03	0.09±0.04	0.13±0.02	0.18±0.06	0.15±0.02	0.18±0.02
★Fe ²⁺	2.36	2.34	2.98	2.43±0.27	3.10±0.35	2.22±0.12	2.13±0.18	2.06±0.24	2.57±0.09
Mn	0.02	0.01	0.02	0.01±0.00	0.02±0.01	0.01±0.00	0.01±0.00	0.01±0.00	0.02±0.00
Mg	2.68	3.50	4.45	3.86±0.40	4.92±0.51	2.70±0.19	2.81±0.17	2.83±0.13	2.18±0.06
Σ Oct	5.98	6.61	10.60	6.94±0.24	11.04±0.31	5.98±0.16	5.90±0.22	5.83±0.20	5.84±0.13
Ca	0.01	0.01	0.01	0.01±0.01	0.01±0.01	0.00±0.00	0.01±0.00	0.01±0.00	0.00±0.00
Na	0.01	0.00	0.00	0.01±0.00	0.01±0.01	0.01±0.00	0.01±0.00	0.04±0.08	0.01±0.00
K	1.54	0.73	0.94	0.49±0.18	0.62±0.23	1.42±0.19	1.66±0.27	1.65±0.15	1.60±0.12
Σ int.l.	1.56	0.74	0.95	0.51±0.18	0.64±0.22	1.43±0.19	1.68±0.27	1.70±0.16	1.61±0.12
<i>total</i>	15.54	5.35	19.55	15.45	19.68	15.41	15.58	15.53	15.45

Table 2 (continuation)

type sample	biotite (Bt ₂) + chlorite intergrowths		chlorite		detrital muscovite (Ms ₁)	
	141.9 m	353.0 m	170.2 m	353.0 m	141.9 m	170.2 m
n	3	4	2	3	1	2
SiO ₂	35.67	28.71	26.23	25.88	47.10	47.62
TiO ₂	1.24	0.49	0.13	0.10	0.00	0.29
Al ₂ O ₃	21.18	21.19	21.94	21.80	32.02	31.70
★FeO	17.59	24.10	21.33	25.72	4.27	1.86
MnO	0.09	0.21	0.13	0.27	0.03	0.00
MgO	11.70	12.35	16.85	13.72	2.17	2.04
CaO	0.02	0.06	0.04	0.01	0.06	0.06
Na ₂ O	0.02	0.08	0.00	0.02	2.50	0.17
K ₂ O	5.83	2.28	1.81	0.31	8.63	10.06
<i>total</i>	93.35	89.47	88.46	87.83	96.78	93.80

numbers of cations per unit cells on the basis of

	22(0)	22(0)	28(0)	28(0)	28(0)	22(0)	22(0)
Si	5.35	4.63	5.90	5.41	5.45	6.26	6.43
Al ^{IV}	2.65	3.37	2.10	2.59	2.55	1.74	1.57
Al ^{VI}	1.09	0.70	3.06	2.75	2.87	3.27	3.47
Ti	0.14	0.06	0.07	0.02	0.02	0.00	0.03
★Fe ²⁺	2.21	3.27	4.16	3.68	4.53	0.47	0.21
Mn	0.01	0.03	0.04	0.02	0.05	0.00	0.00
Mg	2.62	2.99	3.80	5.18	4.31	0.43	0.41
Σ Oct	6.07	7.05	11.13	11.65	11.78	4.17	4.12
Ca	0.00	0.01	0.01	0.01	0.00	0.01	0.01
Na	0.01	0.02	0.03	0.00	0.01	0.64	0.04
K	1.12	0.47	0.59	0.48	0.08	1.46	1.73
Σ int.l.	1.13	0.50	0.63	0.49	0.09	2.11	1.78
<i>total</i>	15.20	15.55	19.76	20.14	19.87	14.28	13.90

Symbols: n: number of analysed grains; if n < 5, averages; if n ≥ 5, averages and standard deviations are given; ★: total Fe is given as FeO and Fe²⁺, respectively; Σ Oct: sum of the octahedrally coordinated cations; Σ int.l.: sum of cations in the interlayer space

Table 3
Reflectance values of the huminite type, coalified, dispersed organic matter

sample	n	R_{\max} x	(%) S	R_{\min} x	(%) S	ΔR (%)	* R_{random} (%)	r ($R_{\max}-R_{\min}$)	r ($R_{\max} - \Delta R$)
137.4 m	30	7.315	1.170	0.923	0.201	6.393	5.184	0.46	0.99
141.9 m	13	6.819	0.664	0.695	0.108	6.125	4.777	-0.20	0.99
142.4 m	5	7.506	1.234	0.894	0.335	6.612	5.302	0.43	0.96
170.2 m	30	6.682	0.648	1.056	0.357	5.626	4.807	0.37	0.84
170.6 m	6	4.942	0.529	1.312	1.008	3.630	3.732		
172.7 m	50	6.320	1.181	1.144	0.393	5.170	4.594	0.00	0.95
210.0 m	20	5.904	1.052	1.381	0.599	4.523	4.396	-0.23	0.90
227.0 m	16	6.975	0.704	0.719	0.120	6.256	4.889	-0.31	0.99
353.0 m	15	6.214	2.335	1.323	0.625	4.891	4.584	-0.04	0.97
357.4 m	9	6.277	1.700	1.048	0.387	5.229	4.534	0.54	0.98
362.7 m	9	6.774	2.702	1.481	0.886	5.293	5.009	0.65	0.96
391.7 m	15	7.435	1.176	1.128	0.559	6.307	5.332	-0.14	0.92
averages of the mean values:	12**	6.597	0.727	1.092	0.254	5.505	4.762		

Symbols: n: number of measurements; x: mean value; S: standard deviation; ΔR : $R_{\max}-R_{\min}$ (%) – bireflectance; * R_{random} (calculated): $(2xR_{\max}+R_{\min})/2$; r: linear correlation coefficient; **: number of samples

Considering the increasing chemical homogenization of the organic substances with advancing maturation (see Teichmüller 1987), version (1) seems to be more probable.

Pressure character of metamorphism

The b_0 cell parameter ($b_0 = 6d_{33\bar{1},060}$) of the K white mica (illite-muscovite) of the metaclastic rocks with mineral assemblage of quartz, plagioclase, illite-muscovite, biotite, chlorite, pyrite and small amounts of carbonate minerals is 9.001 \AA ($s=0.010 \text{ \AA}$, $n=13$). Using the barometer of Sassi (1972), improved by Sassi and Scolari (1974) and Guidotti and Sassi (1976, 1986), this average indicates low pressure type (high thermal gradient) metamorphism.

Occurrence and identification of biotite in metagreywacke

As to the microscopic observations, deformed detrital flakes of partially chloritized biotite, and rarely, muscovite were observed. The small ($< 20 \mu\text{m}$ long and $1\text{--}2 \mu\text{m}$ wide) illite-muscovite ("sericite") flakes forming coherent seams with chlorite parallel to the cleavage planes are common mostly in the pelitic-silty rock types, but can also be found in the coarser-grained variants. The metagreywacke usually contains post-tectonic, newly-formed (metamorphic) mafic mica, the maximal length and width of which vary between $30\text{--}100$ and $2\text{--}20 \mu\text{m}$, respectively. This mica is strongly pleochroic: β and $\gamma =$ dark greenish brown, $\alpha =$ light greyish green. The larger flakes are idio- or hypidioblastic, while in the recrystallized matrix irregular aggregates of small ($< 1 \mu\text{m}$), xenoblastic grains are also common. Based on preliminary XRD data, celadonite was found in the metagreywacke complex by Viczián (in Lelkes-Felvári, 1983), however, glauconite and biotite may also be taken into account as possible phases.

The overlapping reflections of the illite-muscovite (being present in varying proportions) and other rock-forming phases made the identification of this phase by XRD rather uncertain. For the distinction between glauconite, celadonite and biotite, samples devoid of illite-muscovite characterized by the lack of the 5 \AA reflection were selected as most probable candidates. Using disoriented powder preparations, the d_{060} reflections characteristic of the glauconite and celadonite at $1.511\text{--}1.517 \text{ \AA}$ and $1.507\text{--}1.510 \text{ \AA}$ could not be observed, while that of the biotite at $1.53\text{--}1.54 \text{ \AA}$ was covered by the strong (211) reflection of quartz, which is always present in considerable quantities. Comparing our results to the corresponding data of the JCPDS system, several (hkl) and (hk0) reflections characteristic of the glauconite and celadonite could not be observed. On the infrared absorption spectra of the samples, the splitting of the OH-bands characteristic of the celadonite was not proven either. This phase in question was only partially dissolved in boiling 10% HCl after 30 minutes.

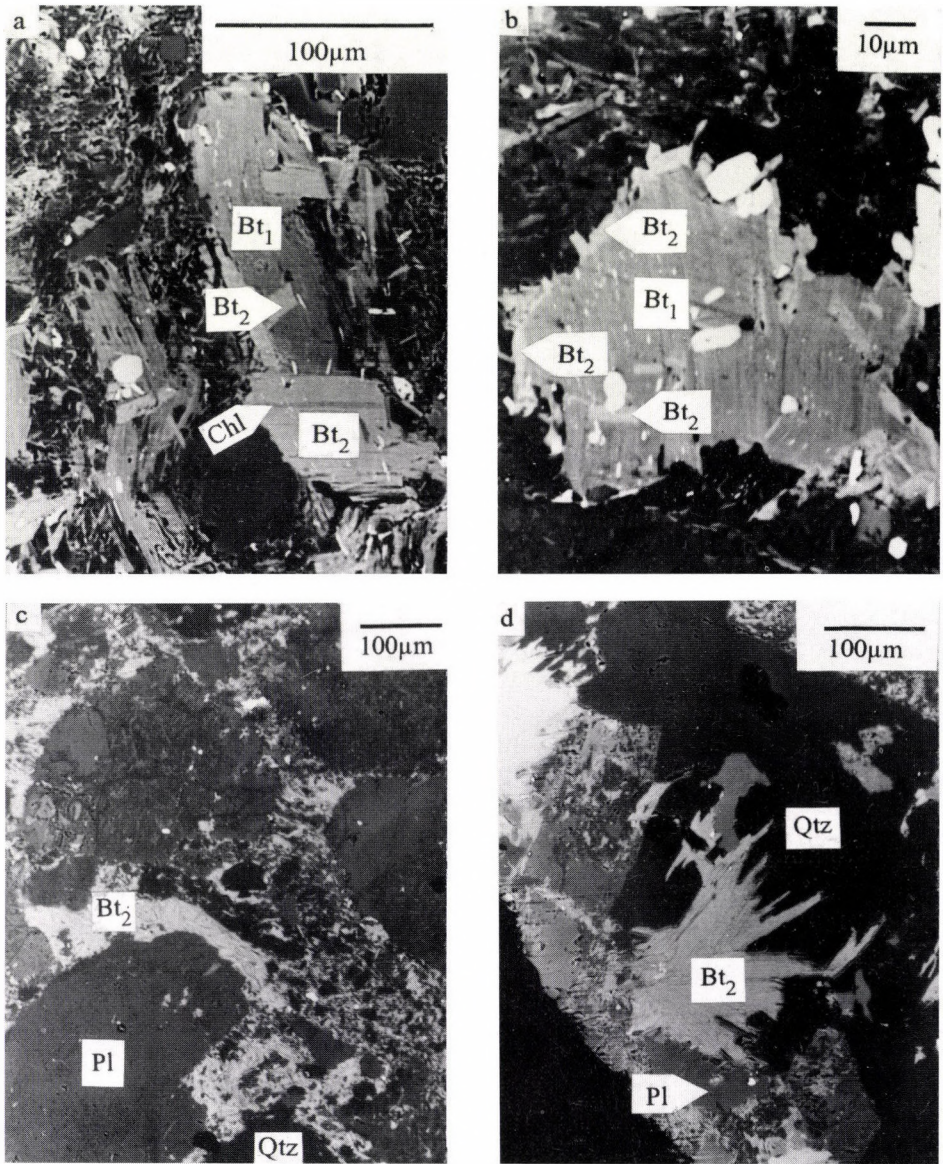


Fig. 5
 Back scattered electron (BSE) images of greywacke from borehole Szalatnak-3. a) large, deformed, partially chloritized, detrital biotite (Bt_1), with newly-formed (metamorphic), smaller biotite flakes (Bt_2), and biotite-chlorite (Chl) intergrowths, cross-cutting the older micas. Sample 170.2 m. b) Deformed, partially chloritized detrital biotite (Bt_1) with metamorphic overgrowths at the rim and cross-mica type smaller biotite flakes (Bt_2) within the detrital biotite. Sample 172.7 m. c) Small-grained metamorphic biotite cement (Bt_2) fills the intergranular space between detrital plagioclase (Pl) and quartz (Qtz) grains. Sample 141.9 m. d) Fissure filling that contains quartz (Qtz), biotite (Bt_2) and plagioclase (Pl) in sample 170.2 m

Based on the anhydrous oxide sum, the Si, Al, interlayer K contents and the number of cations that occupy the octahedral position, the phase in question is biotite, the chemical composition of which differs significantly from those of celadonite and glauconite. Figure 5a shows detrital, deformed, partially chloritized biotite flakes, the chemical composition of which are found in Table 2. The metamorphic biotite generation is found at the rims (Fig. 5b) or within the detrital, partially chloritized biotite flakes (Figs 5a–b), forming post-tectonic "cross-micas", characteristic of crystallization in strain-free medium. The major part of the metamorphic biotite fills in the space between the detrital grains, forming quasi-monomineralic aggregates of fine-grained flakes (Fig. 5c) or mechanical mixtures with chlorite. In addition, newly-formed biotite is often found in association with quartz, chlorite, plagioclase and rare K-feldspar as fissure fillings (Fig. 5d), indicating post-tectonic crystallization in open system.

Figure 6 displays the variations of chemical components of the different types of biotite and chlorite in function of their SiO₂ content (all in weight-%). The chemical compositions of the detrital (not altered) and the newly-formed (metamorphic) biotites seem to be similar (the number of analyses of the former type is relatively small). From biotite to chlorite, i.e., with decreasing SiO₂ content, the K₂O and TiO₂ contents decrease continuously, and the amounts of Al₂O₃, FeO and MgO increase with relatively large scattering.

The relation of the chemical composition of the phyllosilicates can also be studied in Fig. 7. There are no signs of the eventual illitization of detrital biotite, which – according to Morad and Aldahan (1986) – is also a possible, common way of degradation of biotite. In the triangular diagram suggested by Velde (1985), the projections of both the detrital and the newly-formed biotites differ significantly from the fields of celadonite and glauconite (Fig. 8). Even supposing considerable amounts of Fe³⁺ – which is very unlikely because of the reductive nature of the rocks – the projection points could not be shifted to the fields of celadonite and glauconite. Both biotite and muscovite are characterized by small-scale deficiencies of interlayer cations. This phenomenon seems to be general in the low-T range of metamorphism (see also Hunziker et al. 1986, Wang and Banno 1987). The projection points of biotite, chlorite and the intermediate, complex phases occupy a relatively narrow belt within the triangle of Fig. 8, between the fields of ideal biotite and chlorite.

There are two possible mineralogical explanations for the wide, continuous, transitional range of chemical compositions between biotite and chlorite:

1) mixed-layer biotite/chlorite or biotite/vermiculite ("hydrobiotite") was formed, presumably by weathering of the detrital biotite (see Maresch et al. 1985; Götzinger 1986);

2) preferentially intergrown biotite and chlorite lamellae, that form aggregates (mechanical mixtures) composed of these discrete mineral phases (see Aldahan and Morad, 1986). In this case the diameter of the electron beam used for analyses is larger than the widths of the mineral lamellae, and consequently, the obtained compositions reflect different, arbitrary proportions

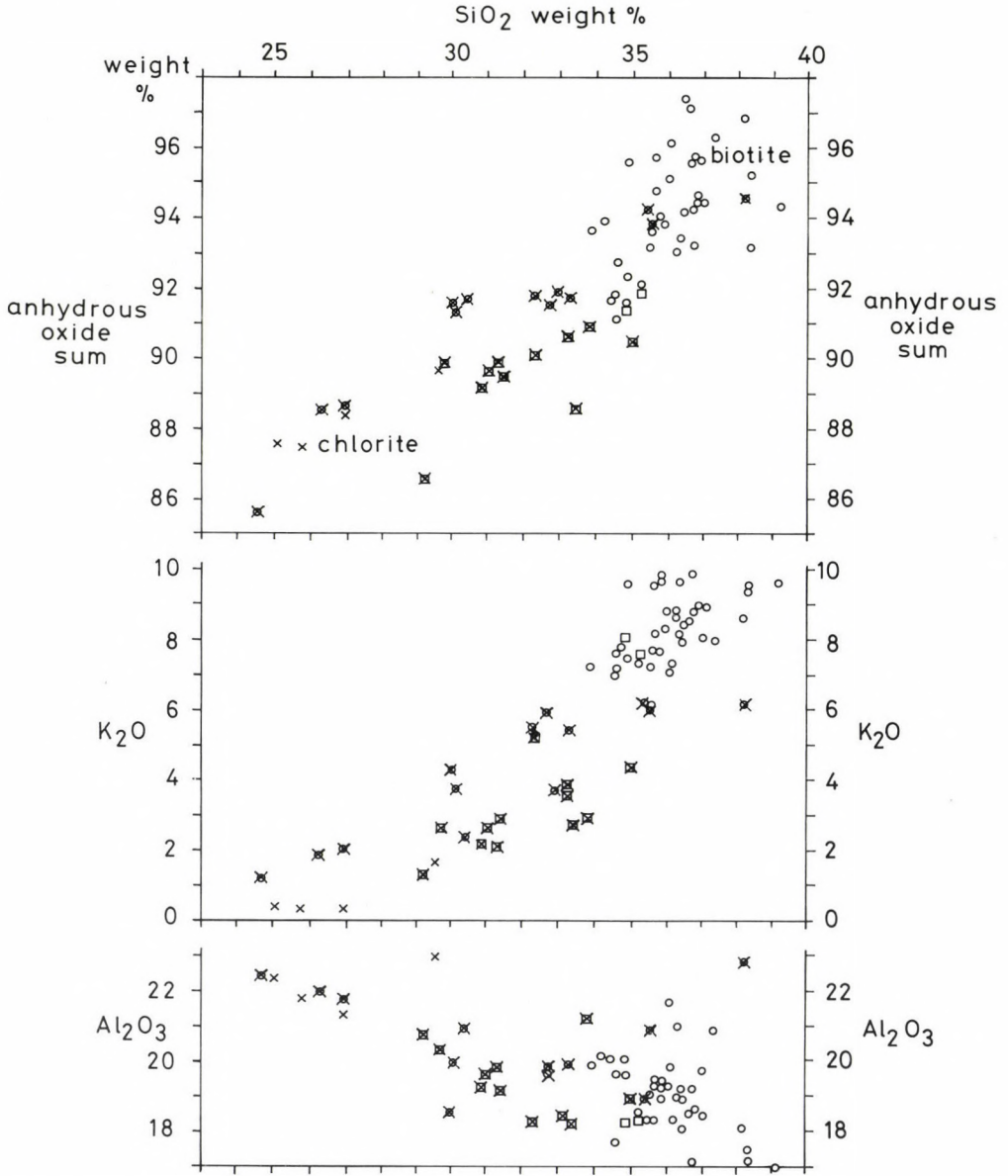


Fig. 6
 Variation of the chemical composition of mafic phyllosilicates in function of their SiO₂ contents. (Data from electron microprobe analyses. Total Fe calculated as FeO.) 1. detrital (inherited) biotite; 2. partially chloritized detrital biotite; 3. metamorphic (newly formed) biotite; 4. averages of metamorphic, intergrown, orientated biotite and chlorite flakes (mixtures of small, discrete phases), being present in varying proportions; 5. metamorphic (newly formed) chlorite

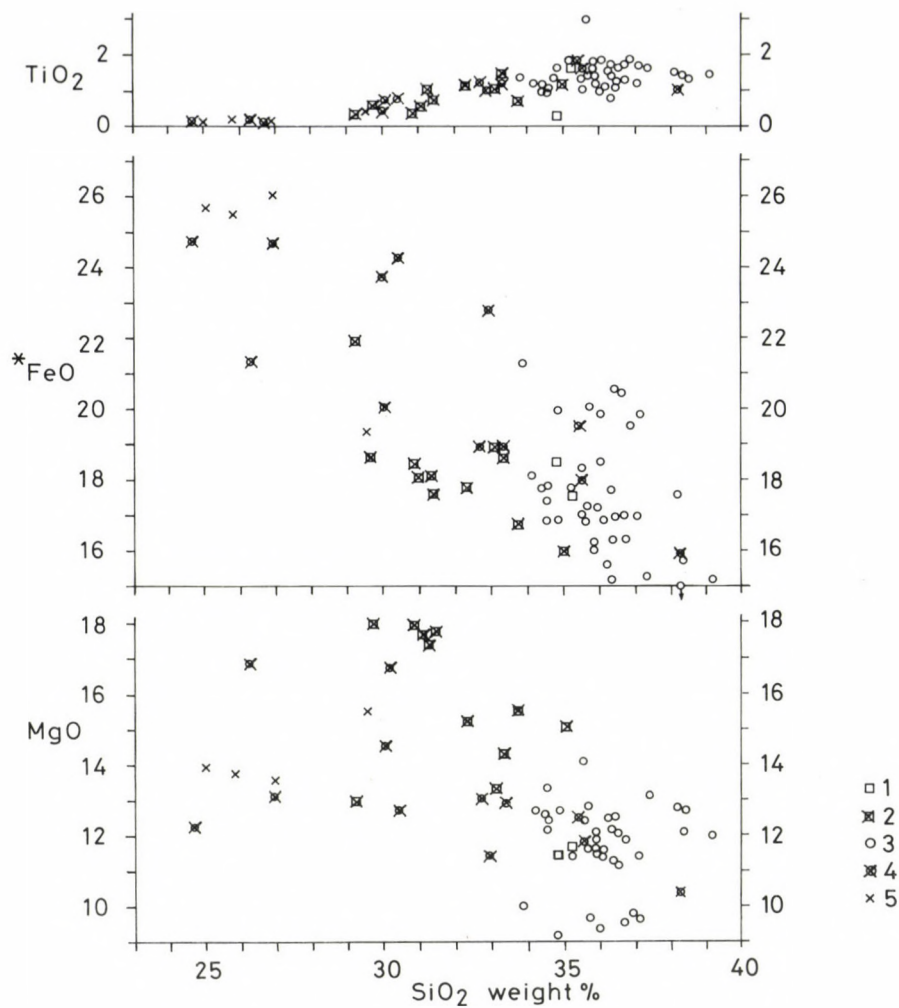


Fig. 6 (cont.)

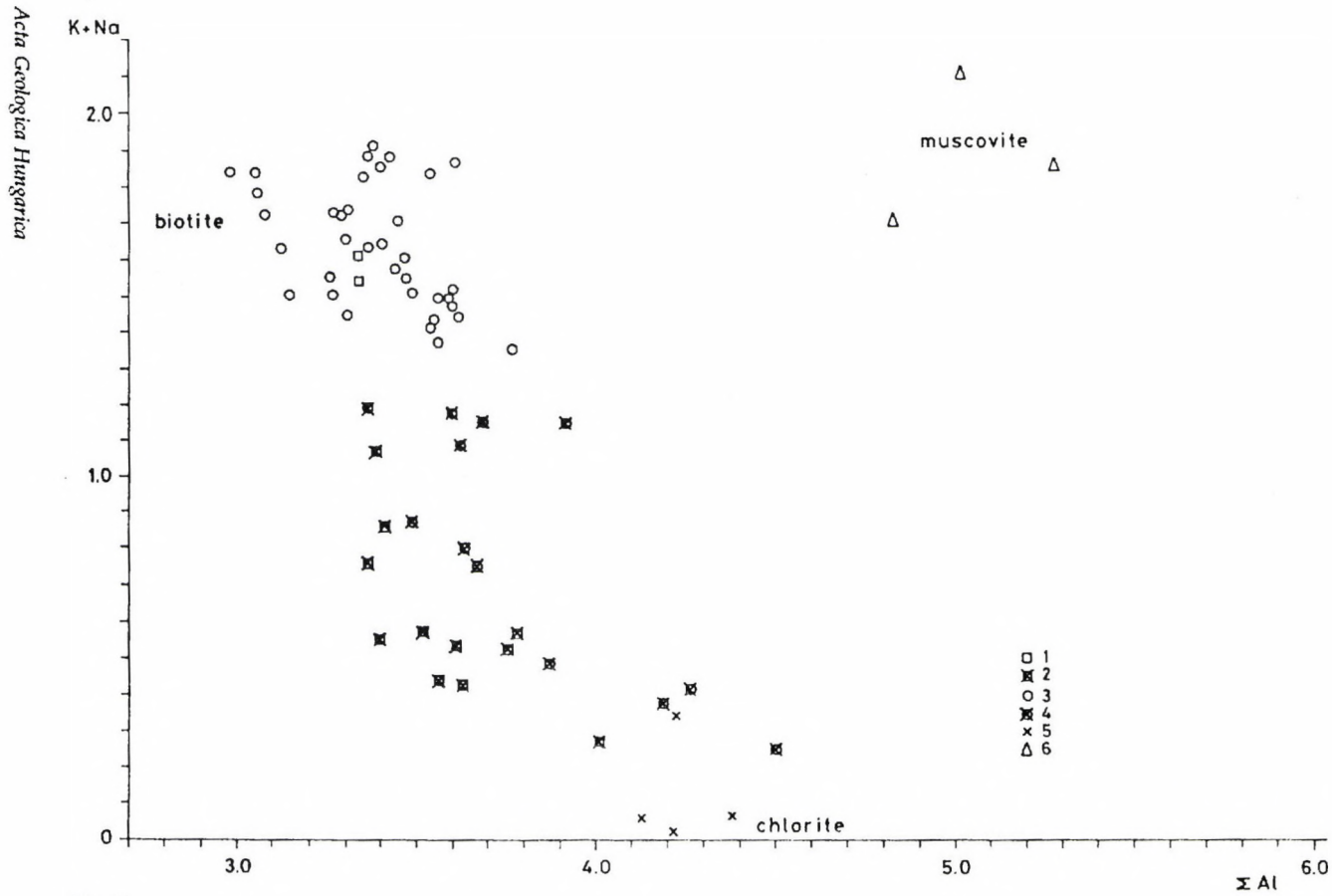


Fig. 7

The distribution of phyllosilicates from the metagreywacke complex in the (K+Na) vs. Al diagram after Morad and Aldahan (1986). Cation numbers calculated on the basis of 44⁻ charge, i.e., for 22 oxygen ions. Legend: for 1 to 5 see Fig. 6, 6. detrital muscovite

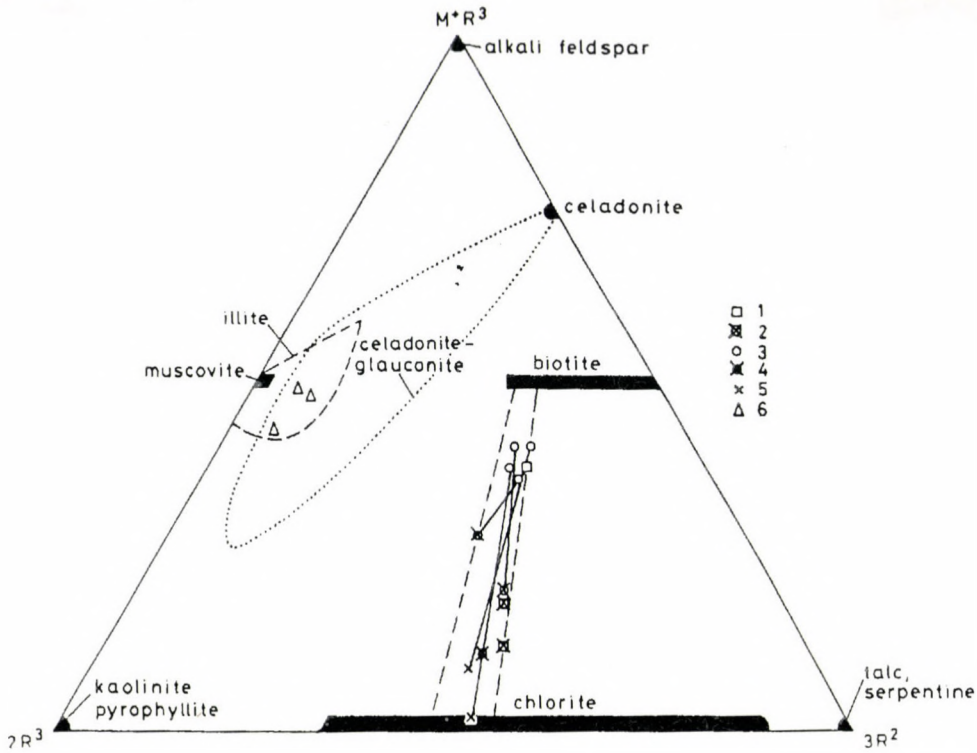


Fig. 8
Distribution of the phyllosilicates in the $M^+R^3 - 2R^3 - 3R^2$ triangular diagram after Velde (1985), slightly modified. $M^+R^3 = Na + K + 2Ca$, $2R^3 = (Al + Ti - M^+R^3)/2$, $3R^2 = (Fe^{2+} + Mn^{2+} + Mg)/3$. Total Fe was calculated as Fe^{2+} . Legend: for 1 to 5 see Fig. 6, 6. detrital muscovite

of the two phases analyzed simultaneously. These chlorite + biotite aggregates might form by weathering of the detrital biotite, by prograde alteration of chlorite to biotite, or by simultaneous (quasi-equilibrium) crystallization of the two phases. As the XRD reflections characteristic of the mixed-layer phases are lacking, version (2), i.e., the mechanical mixture of discrete chlorite and biotite phases is the single, acceptable explanation for both the chloritization of detrital biotite and the formation of metamorphic biotite in the present case.

Possible mechanisms of formation of biotite

The formation of biotite at relatively low (ca 340–350 °C) temperature (i.e., at the estimated metamorphic temperature of the metagreywacke complex) is rather rare. According to a summary by Miyashiro (1973), in certain, low-P type terrains the first appearance of biotite coincides with the beginning of metamorphic recrystallization, while in other, low or medium-P areas the

chlorite zone precedes the biotite zone. Biotite often forms in the contact aureoles around granitoid intrusions. Thus, Wirth (1985) described biotite±chlorite±oligoclase assemblages in metasedimentary rocks. Maresch et al. (1985) determined a transformation series of chlorite → irregular and regular mixed-layer chlorite/biotite → biotite in low-K metabasic rocks caused by hydrothermal solutions associated with intrusion of granite. Frey et al. (1973) demonstrated a stilpnomelane → biotite reaction in glauconite-bearing meta-marls in very low-grade conditions. This reaction was correlated with the pumpellyite zone of the intercalated greywacke. The possible reactions are: stilpnomelane + phengite → biotite + chlorite + quartz + H₂O or – according to Brown (1975) – stilpnomelane + chlorite + K-feldspar → biotite + quartz + H₂O. According to Winkler (1979) the formation of biotite with the participation of stilpnomelane in very low-grade conditions should be clearly distinguished from the "classic" reaction in normal metapelites, in which biotite forms from the common phyllosilicates: phengite + chlorite → muscovite + biotite + quartz + H₂O. The temperature range of this "muscovite + biotite in" isograd is 420–450 °C, depending on pressure.

Ferry (1984) explained the formation of biotite in marly rocks by H₂O infiltration, decarbonation and desulfidation reactions (muscovite + ankerite + rutile + pyrite + graphite + siderite (or calcite) → biotite + plagioclase + ilmenite). Quartz, chlorite and pyrrhotine may be reacting phases or products, as well. The equilibrium temperature of this reaction at P=3.5 kbar and X(CO₂) = 0.02–0.04 is 400°C.

According to Mather (1970) and Wang et al. (1986), biotite forms earlier (at lower temperature) in K-feldspar-bearing psammitic rocks than in metapelites by the reaction K-feldspar + chlorite → biotite + muscovite + quartz + H₂O or K-feldspar + chlorite + phengite → biotite + muscovite + quartz + H₂O. As Wang and Banno (1987) stated, in the prograde evolution of di- and trioctahedral micas, the "illitic" substitution ($\square^{\text{Xii}}[\text{vacancy}] + \text{Si}^{\text{iv}} \leftrightarrow \text{K}^{\text{Xii}} + \text{Al}^{\text{iv}}$) plays also an important role, in addition to the Tschermak's substitution ($\text{Mg}^{\text{vi}} + \text{Si}^{\text{iv}} \leftrightarrow \text{Al}^{\text{vi}} + \text{Al}^{\text{iv}}$).

Based on the textural observations and mineral chemical data, the temporal sequence of detrital biotite → partially chloritized detrital biotite → chlorite → newly formed (metamorphic) biotite can be set up in the investigated metagreywacke complex. The common occurrence of the various mineral phases characteristic of the different stages refers to the non-equilibrium nature of these processes. On the other hand, however, the chemical compositions of these phases formed in the retrograde and prograde paths of alteration are similar. This may indicate chemical homogenization of chlorite and biotite, presumably in the prograde phase.

There is no direct evidence on the biotite-producing reaction in the investigated complex. The close spatial and chemical relations of biotite and chlorite indicate that chlorite might take part in the formation of biotite. The necessary K, Si, and Ti might derive from detrital K-feldspar, from detrital and

metamorphic illite-muscovite and from accessory Ti-minerals, formed mostly by the chloritization of detrital biotite. The scarcity of K-feldspar may be due to this reaction. (As no stilpnomelane was found, there is no reason to suppose the participation of this phase in the reaction.)

As far as the microstructural observations are concerned, biotite formed in static conditions devoid of deviatoric stresses, after the dynamothermal (regional) metamorphism that produced schistosity. The post-tectonic crystallization of biotite is proven by the distribution of biotite grains without preferred orientation and by the frequent occurrence of "cross micas" penetrating the planes of foliation. Thus, biotite might form in a low pressure-type, partially open system, in which the migration of K- and Si-bearing hydrothermal fluids should also be taken into consideration (fissure fillings with quartz, biotite, chlorite and plagioclase, infiltrations in the matrix, producing biotite-rich parts). The scale of this hydrothermal-metasomatic process, however, is not known; it may vary from several millimeters to several hundred meters.

Most probably, this post-tectonic crystallization of biotite may be due to the contact (conductive and convective) heat effects and to the K- and Si-bearing hydrothermal metasomatic fluids, which were mobilized by the syenite intrusion encountered at the bottom of the investigated borehole. There are several facts that seemingly contradict this hypothesis, for instance that there are no systematic changes in the amount, grain size and chemistry of biotite, in the crystallinity indices of phyllosilicates and in coal rank with decreasing distance from the border of the syenite intrusion in the ca. 350 m thick metagreywacke complex. (The thin biotite-plagioclase hornfels contacting the syenite is separated by a fault from the metagreywacke.) This contradiction can be satisfactorily explained by the highly tectonized, faulted, brecciated nature of the complex: the original position and the relation of the clastic sequence and the intrusion were severely disturbed by the younger tectonic movements. Thus, the lack of a continuous, prograde zonation does not contradict the contact metamorphic-metasomatic effects in this strongly disturbed geologic environment.

Conclusions

Based on microstructural observations, the low-T regional (dynamothermal) metamorphism of the Silurian metagreywacke and associated slate, metachert and volcanogenic clastic rocks of the Mecsek Mountains were overprinted by an other, low-T, contact metamorphic-metasomatic event, presumably caused by the Hercynian syenite intrusion. Disregarding the microstructural features and the formation of biotite, only the resultant P- and T-indicating parameters could be determined, emphasizing that no considerable P and T differences need be considered between the two events.

The illite crystallinity (IC) method gave misleading results in rocks containing mixtures of di- and trioctahedral micas in varying proportions. Instead, the

chlorite crystallinity (ChC) method provided reliable information on the grade (~T) of metamorphism. The conclusions obtained by the ChC method are consistent with the chlorite-Al^{IV} geothermometric, and coal rank data, and also with the microstructural features, which all indicate metamorphic temperatures of ca 350–400 °C, i.e., to conditions corresponding to the epizone of Kübler (1967, 1990) or to the boundary of the "anchizone" and "epizone" as re-defined by Árkai (1983, 1991b).

Applying the white mica barometer of Sassi (1972), the metamorphism occurred in a low-P type (high thermal gradient) system.

The mineralogical and chemical characteristics of the non-equilibrium transformations in the series detrital biotite → chlorite → newly formed (metamorphic) biotite were determined. Based on the post-tectonic, partly fissure-filling, infiltrational nature of the newly formed biotite, the formation of this mineral may be attributed to the Hercynian contact metamorphic-metasomatic effect of the underlying syenite intrusion.

Acknowledgements

Cs. Lantai is indebted to Prof. Dr. M. Wolf (Technical University Aachen, Germany) for providing facilities for the reflectance measurements and for consultations. The authors thank the Mecsek Ore Mining Company, Kővágószőlős for allowing sampling and investigation of the Szalatnak-3 borehole. Thanks are due to Prof. T. Szederkényi and dr. I. Viczián for reviewing and improving the manuscript. The present work forms parts of the research programs of P. Árkai, sponsored by the Hungarian Scientific Research Fund (OTKA, Budapest), Project Nos 284/1987–1991 and T007211/1993–1996.

References

- Aldahan, A.A., S. Morad 1986: Mineralogy and chemistry of diagenetic clay minerals in Proterozoic sandstones from Sweden. – *Amer. J. Sci.*, 286, pp. 29–80.
- Árkai, P. 1983: Very low- and low-grade Alpine regional metamorphism of the Paleozoic and Mesozoic formations of the Bükkium, NE-Hungary. – *Acta Geol. Hung.*, 26, pp. 83–101.
- Árkai, P. 1984: Polymetamorphism of the crystalline basement of the Somogy-Dráva Basin (South-western Transdanubia, Hungary). – *Acta Miner. Petr. Szeged*, 26, pp. 129–153.
- Árkai, P. 1991a: Alpine regional metamorphism of the different tectonic domains in the Hungarian part of the Pannonian Basin. – In: Baud, A., P. Thelin, G. Stampfli (Eds): Paleozoic geodynamic domains and their alpidic evolution in the Tethys. – ICGP Project No. 276 Newsletter No. 2. *Mémoires de Géologie (Lausanne)* No. 10, pp. 5–13.
- Árkai, P. 1991b: Chlorite crystallinity: an empirical approach and correlation with illite crystallinity, coal rank and mineral facies as exemplified by Palaeozoic and Mesozoic rocks of northeast Hungary. – *J. Metamorph. Geol.*, 9, pp. 723–734.
- Bence, A.E., A. Albee 1968: Empirical correction factors for electron microanalysis of silicates and oxides. – *J. Geol.*, 76, pp. 382–403.
- Brown, E.H. 1975: A petrogenetic grid for reactions producing biotite and other Al-Fe-Mg silicates in the greenschist facies. – *J. Petrol.*, 16, pp. 258–271.
- Cathelineau, M. 1988: Cation site occupancy in chlorites and illites as a function of temperature. – *Clay Minerals*, 23, pp. 471–485.
- Dunoyer de Segonzac, G. 1970: The transformation of clay minerals during diagenesis and low-grade metamorphism: a review. – *Sedimentology*, 15, pp. 281–346.

- Esquevin, J. 1969: Influence de la composition chimique des illites sur leur cristallinité. – Bull. Centre Rech. Pau, – S.N.P.A. 3, pp. 147–153.
- Ferry, J.M. 1984: A biotite isograd in South-Central Maine, U.S.A.: mineral reactions, fluid transfer, and heat transfer. – J. Petrol., 250, pp. 871–893.
- Frey, M. 1986: Very low-grade metamorphism of the Alps: an introduction. – Schweiz. Mineral. Petrogr. Mitt., 66, pp. 13–27.
- Frey, M., J.C. Hunziker, P. Roggwiler, C. Schindler 1973: Progressive niedriggradige Metamorphose glaukonitführender Horizonte in den helvetischen Alpen der Ostschweiz. – Contrib. Mineral. Petrol., 39, pp. 185–218.
- Géczy, B. 1973: The origin of the Jurassic faunal provinces and the Mediterranean plate tectonics. – Ann. Univ. Sci. Budapest. R. Eötvös Nom. Sect. Geol., 16, pp. 99–114.
- Götzinger, M.A. 1986: Continuous biotite–hydrobiotite–vermiculite transitions in the original specimen "Hydrobiotit", Schrauf (1882), from the serpentinites near Kremze, CSSR. – N. Jb. Miner. Mh., pp. 163–171.
- Guidotti, C.V., F.P. Sassi 1976: Muscovite as a petrogenetic indicator mineral in pelitic schists. – N. Jb. Miner. Abh., 127, pp. 97–142.
- Guidotti, C.V., F.P. Sassi 1986: Classification and correlation of metamorphic facies series by means of muscovite b_0 data from low-grade metapelites. – N. Jb. Miner. Abh., 153, pp. 363–380.
- Hunziker, J.C., M. Frey, N. Clauer, R.D. Dallmeyer, H. Friedrichsen, W. Flehmig, K. Hochstrasser, P. Roggwiler, H. Schwander, 1986: The evolution of illite to muscovite: mineralogical and isotopic data from the Glarus Alps, Switzerland. – Contrib. Mineral. Petrol., 92, pp. 413–427.
- Jantsky, B. 1979: Géologie du socle cristallin granitique de la montagne Mecsek. – Annals Hung. Geol. Inst., 60, pp. 1–385.
- Kázmér, M., S. Kovács 1985: Permian–Paleogene paleogeography along the Eastern part of the Insubric–Periadriatic lineament system: evidence for the continental escape of the Bakony–Drauzug Unit. – Acta. Geol. Hung., 28, pp. 71–84.
- Kisch, H.J. 1987: Correlation between indicators of very low-grade metamorphism. – In: Frey, M. (Ed.): Low temperature metamorphism, pp. 227–300, Blackie, Glasgow, London.
- Kisch, H.J. 1990: Calibration of the anchizone: a critical comparison of illite 'crystallinity' scales used for definition. – J. Metamorph. Geol., 8, pp. 31–46.
- Kovács, S. 1982: Problems of the "Pannonian Median Massif" and the plate tectonic concept. Contributions based on the distribution of Late Paleozoic–Early Mesozoic isopic zones. – Geol. Rundschau, 71, pp. 614–640.
- Kovács, S. 1989: Major events of the tectono-sedimentary evolution of the North Hungarian Paleozoic: history of the northwestern termination of the Late Paleozoic–Early Mesozoic Tethys. – In: Sengör, A.M.C. (Ed.): Tectonic evolution of the Tethyan region. Kluwer Academic Publishers, Dordrecht, pp. 93–108.
- Kozur, H. 1984: Some new stratigraphical and paleogeographical data in the Paleozoic and Mesozoic of the Pannonian Median Massif and adjacent areas. – Acta Geodaet. Geophys. et Montanist. Hung., 19, pp. 93–106.
- Kübler, B. 1967: La cristallinité de l'illite et les zones tout a fait superieures du métamorphisme. – In: Étages tectoniques, Colloque de Neuchâtel 1966, pp. 105–121, A La Baconniere, Neuchâtel.
- Kübler, B. 1975: Diagenese - anchimétamorphisme et métamorphisme. – Institut national de la recherche scientifique - Pétrole, Quebec.
- Kübler, B. 1990: "Cristallinité" de l'illite et mixed-layers: breve révision. – Schweiz. Mineral. Petrogr. Mitt., 70, pp. 89–93.
- Kübler, B., J.P. Rey 1982: Identification des micas des series sedimentaires par diffraction X a partir de la serie harmonique (001) des preparations orientees. – Cahiers de l'Institut de Géologie, Université de Neuchâtel, pp. 1–12.

- Lelkes-Felvári, Gy. 1983: Report on the petrographic investigation of the borehole Szalatnak-3. – Manuscript, Hung. Geol. Inst., Budapest (in Hungarian).
- Lelkes-Felvári, Gy., F.P. Sassi 1981: Outlines of the pre-Alpine metamorphism in Hungary. – In: Karamata, S., F.P. Sassi (Eds.): IGCP Project No. 5 Newsletter No. 3, pp. 89–99.
- Maresch, W.V., H.J. Massone, M. Czank 1985: Ordered and disordered chlorite/biotite interstratifications as alteration products of chlorite. – *N. Jb. Miner. Abh.*, 152, pp. 79–100.
- Mather, J.D. 1970: The biotite isograd and the lower greenschist facies in the Dalradian rocks of Scotland. – *J. Petrol.*, 11, pp. 253–277.
- Miyashiro, A. 1973: *Metamorphism and metamorphic belts*. – George Allen, Unwin Ltd., London.
- Morad, S., A.A. Aldahan 1986: Discussion and comments on the paper: electron optical studies of phyllosilicate intergrowths in sedimentary and metamorphic rocks. – *Mineral. Mag.*, 50, pp. 340–343.
- Nagy, G. 1984: Computer programs for quantitative electron microprobe analysis developed for geological applications. – EUREM '84: Proc. 8th Eur. Congr. on Electron Microscopy, Budapest, pp. 1041–1042.
- Nagy, G. 1990: Quantitative analysis by electron microprobe: Methods and applications in the Laboratory for Geochemical Research. – *Izotóptechnika, Diagnosztika*, 33, pp. 133–139 (in Hungarian).
- Pettijohn, F.J., P.E. Potter, R. Siever 1987: *Sand and sandstone*. – 2nd ed. Springer, New York, Berlin, Heidelberg.
- Ragot, J.P. 1977: Contribution à l'étude de l'évolution des substances carbonées dans les formations géologiques. – Thèse Univ. P. Sabatier, Toulouse.
- Sassi, F.P. 1972: The petrologic and geologic significance of the b_0 value of potassic white micas in low-grade metamorphic rocks. An application to the Eastern Alps. – *Tschermaks Mineral. Petrogr. Mitt.*, 18, pp. 105–113.
- Sassi, F.P., A. Scolari 1974: The b_0 value of the potassic white micas as a barometric indicator in low-grade metamorphism of pelitic schists. – *Contrib. Mineral. Petrol.*, 45, pp. 143–152.
- Szederkényi, T. 1975: Rare element research of the Early Paleozoic formations in SW-Transdanubia. – C.Sc. Thesis, Budapest (in Hungarian).
- Szederkényi, T. 1982: Lithostratigraphic division of the crystalline mass in South Transdanubia and the Great Hungarian Plain. – In: Sassi, F.P., I. Varga (Eds.): IGCP Project No. 5 Newsletter No. 4, pp. 101–106.
- Szederkényi, T., P. Árkai, Gy. Lelkes-Felvári 1991: Crystalline basement of the Great Hungarian Plain and South Transdanubia, Hungary. – In: Karamata, S. (Ed.): Geodynamic evolution of the Pannonian Basin. – *Serb. Acad. Sci. Arts, Acad. Conf.*, 62, Dept. Nat. and Math. Sci., 4, pp. 261–273, Beograd.
- Teichmüller, M. 1987: Organic material and very low-grade metamorphism. – In: Frey, M. (Ed.): *Low temperature metamorphism*. Blackie, Glasgow, London, pp. 114–161.
- Teichmüller, M., R. Teichmüller 1981: The significance of coalification studies to geology – a review. – *Bull. Centre Rech. Expl. Prod. ELF-Aquitaine*, 5, pp. 491–534.
- Velde, B. 1985: *Clay minerals (A physico-chemical explanation of their occurrence)*. – *Developments in Sedimentology*, Vol. 40, Elsevier, Amsterdam, Oxford, New York, Tokyo.
- Wang, G.F., S. Banno 1987: Non-stoichiometry of interlayer cations in micas from low- to middle-grade metamorphic rocks in the Ryoke and the Sanbagawa belts, Japan. – *Contrib. Mineral. Petrol.*, 97, pp. 313–319.
- Wang, G.F., S. Banno, K. Takeuchi 1986: Reactions to define the biotite isograd in the Ryoke metamorphic belt, Kii Peninsula, Japan. – *Contrib. Mineral. Petrol.*, 93, pp. 9–17.
- Winkler, H.G.F. 1979: *Petrogenesis of metamorphic rocks*. – 5th ed. Springer, New York.
- Wirth, R. 1985: Dehydration and thermal alteration of white mica (phengite) in the contact aureole of the Traversella Intrusion. – *N. Jb. Miner. Abh.*, 152, pp. 101–112.

Palynostratigraphy of the Upper Triassic formations in the Mecsek Mts (Southern Hungary)

József Bóna

The Upper Triassic sequence of the Mecsek Mts is characterized by hiatuses. The thin black coal seams, coal veins, as well as the disseminated organic materials occurring in the stratigraphic column are strongly carbonized, especially in the Kantavár Formation. For this reason, the state of preservation of the spore and pollen exines is very bad.

Characteristic spore and pollen guide-forms correlating well with the pollen stratigraphic horizons of the Transdanubian Range and the Western Europe, are mostly lacking or have not been yet found.

Separation of substages by palynologic methods cannot be yet realized at present. In the Karolinavölgy Sandstone Formation, the great proportion of pollen genera *Duplicisporites* and *Partitisporites* refers to the Julian substage. In the upper part of the formation and above it, in the Rhaetian part of the Mecsek Coal Formation, the common presence of *Ovalipollis pseudoalatus* (Thiergart) Sch. and *Triancoraesporites ancorae* (Reinh.) Sch. indicates the Rhaetian stage. Photographed forms are shown in Plates I–X.

Key words: Mecsek Mountains, Upper Triassic, palynostratigraphy

Introduction

The palynologic investigation of the Upper Triassic formations in the Mecsek Mts was in close connection with black coal exploration. The first investigations made on the samples taken from the coal seams of active mines were carried out primarily in order to identify the seams (Góczán 1956; Bóna 1963). They allowed the recognition of the Lower Liassic assemblages. Later also the seams penetrated by exploratory wells were investigated with the aim of long-distance identification of the seams and seam groups. The exploratory drillings were successful when they penetrated the complexes with seams, and drilled into the Rhaetian sandstone complex lacking seams, known today as the Karolinavölgy Formation. However, many times it was difficult to say with certainty by the macroscopic investigation of the cores, whether the machine was really already drilling in Rhaetian formations – or still in Liassic ones. This was the case also in 1961 with the Nagymányok-12 structure exploratory well. It did not penetrate any black coal seams, since below the Miocene it immediately entered rocks similar to the Upper Triassic footwall; however, the

Address: J. Bóna: 7300 Komló, Gorkij u. 37, Hungary

Received: 16 March 1994

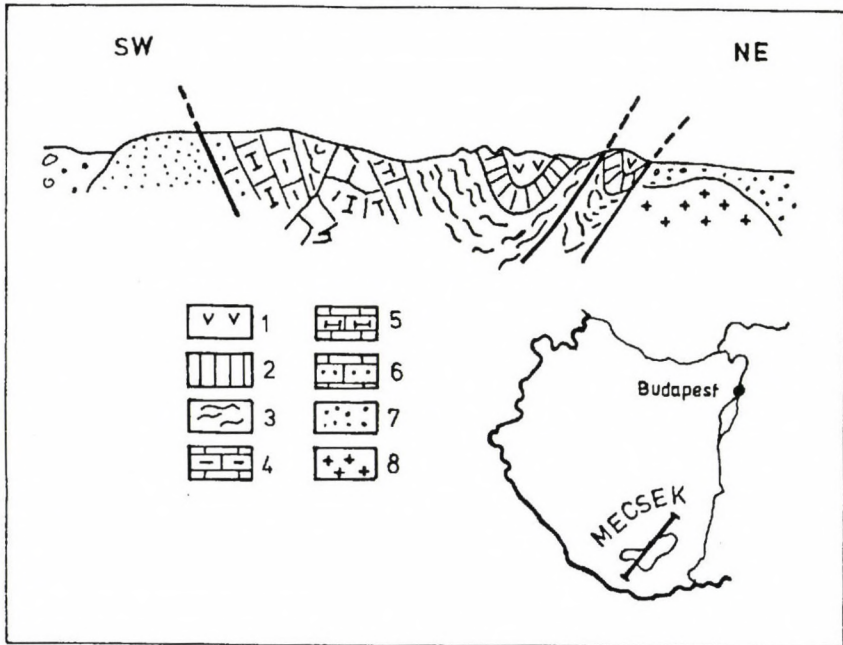


Fig. 1a
 Transversal section through the Mecsek Mts (after J. Dercourt et al., 1984). 1. volcanogenous Late Cretaceous; 2. Upper Jurassic; 3. Liassic (partly Upper Triassic); 4. Upper Triassic; 5. Middle Triassic; 6. Lower Triassic; 7. Permian; 8. basement

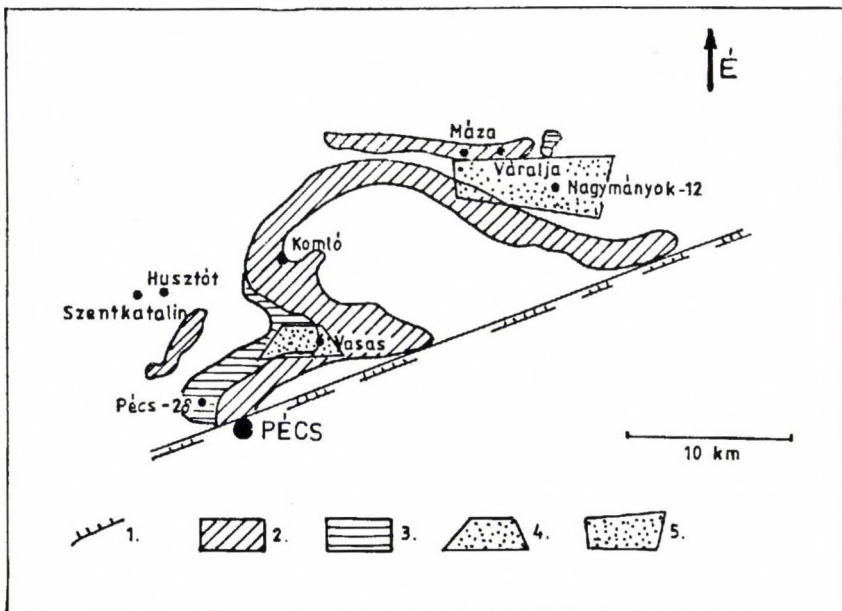


Fig. 1b
 Distribution of the Upper Triassic–Lower Liassic coal-bearing layers of the Mecsek Mts. 1. thrust fault, tectonic zone; 2. coal-bearing layers under the surface; 3. Upper Triassic on the surface; 4. Vasas-Rücker exploitation and exploratory area; 5. Máza-South exploratory area

age could not be unanimously and satisfactorily determined. This is why it was then proposed by the geologist Némedi-Varga to try solving the problem by palynologic methods as well. With this aim, I collected samples from the siltstone layers with plant remnants of the sandstone complex. With the samples deriving from the interval between 368.6 and 537.3 m, it was possible to determine such spores and planktonic remnants which so far had not been known from the Liassic in the Mecsek Mts. Among the spores even the species *Aulisporites astigosus* (Leschik) Klaus was found, which indicates the deeper horizons of the Upper Triassic.

After it had been proven that the palynologic investigation of the Upper Triassic sediments could be successful even in the Mecsek Mts, E. Nagy collected samples with this aim from the Upper Triassic key sections of the Mecsek Mts, in boreholes P-28 and P-39. With these samples began the systematic palynologic investigation of the Triassic formations. Later, the palynologic method became systematically and effectively used even for material testing of the Triassic part of coal exploratory wells. However, its efficiency was often reduced by the high degree of carbonization of the disseminated organic material and by the complicated structure. The supply of data was often made difficult, mainly due to the high carbonization degree of pollen grains, and impossible by the vitrification. However, the investigation of the large number of samples resulted in contributing to the better understanding of the Upper Triassic in the Mecsek Mts on a palynologic basis, as well.

So far, few data have been published in the literature on the palynologic investigation of the Upper Triassic in the Mecsek Mts. The first data were submitted by Nagy (1968) and Némedi Varga (1968). Afterwards, Bóna (1973, 1974, 1979, 1983, 1984) demonstrated mainly the palynologic methods of drawing the Rhaetian/Liassic boundary, in short communications. Wéber (1990) published palynologic data on the northern foreland of the Mecsek Mts with respect to the Ladinian and Upper Triassic.

Short description of the Upper Triassic formations

The Upper Triassic in the Mecsek Mts is composed of an approximately 600–800 m thick, predominantly clastic complex. It overlies, generally continuously, sometimes unconformably, the Ladinian sequence. In the lower part of the complex the Kantavár Formation, in the middle one the Karolinvölgy Formation can be separated. At the top, the lower seam group of the Mecsek Coal Formation represents the closing section of the Upper Triassic. In the Triassic–Liassic boundary sequence, tuffite layers are intercalated which according to the observations of Szilágyi (1987) can be traced over a great area and considered an isochronous horizon (Fig. 2).

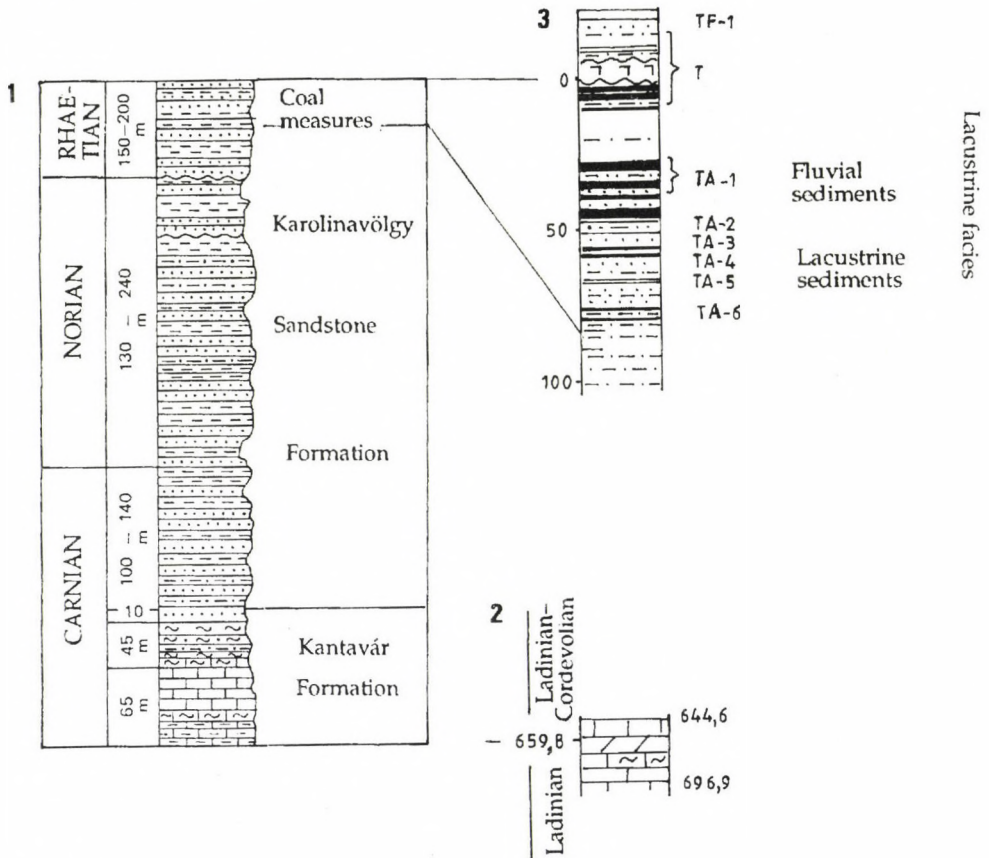


Fig. 2
 1. Standard section of the Upper Triassic of the Mecsek Mts. according to Balogh (1981); 2. Section of Ladinian-Cordevolian boundary layers in borehole Husztót-2 (Wéber, 1990); 3. General section of Upper Triassic coal seams beneath the tuffite level in the exploratory area Váralja-South, according to Szilágyi (1987). TF-1: Liassic coal seam No. 1 above the tuffite; TA-1: Triassic coal seam No. 1 beneath the tuffite; T: tuffitic marker bed

The Kantavár Formation

It is predominantly built up by dark grey-black limestone, clayey limestone, calcareous marl, marl, calcareous siltstone, and coal layers. Its development indicates anoxic depositional conditions. Sometimes the rocks are of thin-bedded, laminitic structure. The formation represents the lowermost part of the Upper Triassic in the Mecsek Mts, the lower part of the Carnian stage (Balogh 1981). Lithologically, it can be well separated though at the top it grades into the Karolinavölgy Formation without a sharp boundary. According to Weber (1990), the whole of the "Ladinian-Carnian" regressive series can be assigned to this formation.

The Karolinavölgy Sandstone Formation

It is composed mainly of grey, greenish-grey, rarely brownish-grey and purple spotted sandstone, siltstone, and mudstone beds. Sometimes conglomerates of limestone and dolomite material, carbonaceous mudstones, and coals also occur in it. According to Nagy (1968), it was formed in restricted lagoonal, lacustrine, and deltaic environments. The upper part begins with the sediments of river-beds formed on the surface during the Rhaetian emersion, which are followed by deltaic and lacustrine facies. The formation represents the upper part of the Carnian stage and the uncertain parts of the Norian and Rhaetian stages. Its subdivision still can hardly be carried out at present.

The lower part of the Mecsek Coal Formation

The formations of the lower seam group of the coal complex belong here. It is made up of similar rocks as the Karolinavölgy Formation, and cannot be sharply separated from it. In this formation, the sandstone, siltstone, and mudstone layers have already lost their red and purple spotted color. The occurrence of coal veins and seams is more frequent. According to Némedi Varga (1969), at Komló the coal complex – taking into account its lithologic nature – still belongs to the Rhaetian stage. He draws the boundary at the coal-free "index interval" developed above the lower seams and consisting of unstratified greenish-grey siltstones and sandstones, which was still formed in the Rhaetian. Szilágyi (1987) also assigns the lower coal seams to the Rhaetian stage in the area of Máza-South and Váralja-South, as well as in the Vasas and Rucker shafts near Pécs. He draws the Triassic/Jurassic boundary at the predominantly thin but isochronous tuffite horizon observable in the complex with seams.

The palynostratigraphic results of the investigation of the formations

Footwall of the Kantavár Formation

In connection with the Kantavár Formation the question arises of drawing the boundary towards the footwall. Therefore, investigations were carried out in the formations of the footwall. One part of the samples was collected by myself, another part was offered by E. Nagy (Hungarian Geological Institute) and B. Wéber (Mecsek Ore Mining Company). Nagy collected four samples from borehole Pécs-28 from the Ladinian limestone layers penetrated between 591.8 and 646.5 m. These samples proved to be pollen-free. The samples which I collected in borehole Pécs-57 from the interval between 785.6 and 950.0 m were also pollen-free. According to geologist S. Platsek, this was the footwall of the Kantavár Formation. The samples collected by Wéber for me in the structure exploratory well Husztót-2 from the directly underlying layers of the coal-bearing Upper Triassic were positive. On the basis of the six samples

deriving from the interval between 652.0 and 688.0 m, I determined the following spore and pollen taxa:

Protodiploxipinus potoniei (Mädler) Scheuring
Triadispora obscura Scheuring
Lunatisporites fsp.
Lunatisporites acutus (Leschik) Scheuring
Ovalipollis div. fsp.
Ovalipollis pseudoalatus (Thiergart) Schuurman
Cuneatisporites radialis Leschik
Striatoabietites aytugii Visscher
Triadispora fsp.
Platisaccus fsp.

Aratrisporites fimbriatus (Klaus) Payf. et Dettm.
Aratrisporites tenuispinosus Playf.
Aratrisporites fsp.
Alisporites fsp.
Infernopollenites parvus Scheuring
Porcellispora longdonensis (Clarke) Scheuring
Verrucosisporites div. fsp.
Punctatisporites fsp.
Concentricisporites fsp. (fragmen())
Dictyophyllidites harrisii Couper

The details are included in Table 1.

Table 1

Palynologic data of the Ladinian-Carnian layers of the borehole Husztót-2

Samples	<i>Ovalipollis pseudoalatus</i>	<i>Triadispora obscura</i>	<i>Lunatisporites</i> fsp.	<i>Lunatisporites acutus</i>	<i>Ovalipollis</i> fsp.	<i>Cuneatisporites radialis</i>	<i>Striatoabietites aytugii</i>	<i>Triadispora</i> fsp.	<i>Platisaccus</i> fsp.	<i>Aratrisporites fimbriatus</i>	<i>Aratrisporites</i> fsp.	<i>Aratrisporites tenuispinosus</i>	<i>Alisporites</i> fsp.	<i>Infernopollenites parvus</i>	<i>Porcellispora longdonensis</i>	<i>Verrucosisporites</i> div. fsp.	<i>Punctatisporites</i> fsp.	<i>Concentricisporites</i> fsp. fragment	<i>Dictyophyllidites harrisii</i>	<i>Protodiploxipinus potoniei</i>	<i>Sporites</i> indet.	pine pollen with respiratory cavity indet
643,50 - 647,40																						+
652,00 - 655,00	+	+					+	+					+	+	+	+	+	+	+			+
659,00 - 663,90	++	+					+			+		+	+	+	+			+				+
688,80	+	+	+	+	+	+	+	+	+	+	+	+	+	+	+				+			+

Wéber (1990) also describes a macrofauna here, in which *Gervilleia socialis* and *Myophoria goldfussi*, observed between 659.8 and 644.6 m, are age indicators. On the basis of these, he points out that the age of the carbonate layers above 659.8 m may already be even Carnian (Fig. 2). In the pollen assemblage of the sample collected from the depth between 652.0 and 655.0 m, I observed a *Concentricisporites* fsp. fragment as well. According to the observations made until now, the form group *Concentricisporites* Antonescu occurs only in the Middle Triassic. Taking into account, however, that I could observe and

photograph only a fragment of the spore, it cannot be considered decisive from the point of view of the age, as it may be reworked. At present, it can be said about the assemblage with great certainty that it is of Ladinian or Carnian age. More precisely, it indicates a higher horizon of the Ladinian stage or the Cordevolian substage.

In the exploratory area of Máza-South-Váralja-South, only one well penetrated the Kantavár Formation: borehole Váralja-21. It drilled into the Misina Group, in the Kozár and Mánfa Members of which I examined samples from the interval between 623.4 and 654.0 m. The result is practically negative, since besides some fractured and undistinctive pine pollen and indeterminate spores it did not contain other remnants. According to Szilágyi and Villám (1985), here the formation boundaries are tectonic.

The Kantavár Formation

I examined the formation on the basis of four occurrences. I received 12 samples from E. Nagy from borehole Pécs-28. It was also he who collected samples in the valley of Andor Spring near Kozár from the clayey, vitrite-banded lime marls (still assigned at that time to the Ladinian). In these samples, no valuable pollen were found. Only in Pécs-28 could I find some strongly carbonized and fractured pine pollen. Nagy also obtained the material of a coal vein from samples collected at Andor Spring, examined from coal petrologic point of view. Referring to Mrs. A. Paál, he pointed out that 99.5% of the coal veins are composed of homogeneous vitrite. In the Pécs area, the degree of carbonization of coal seams is generally high. They reach or exceed the "fat coal state". From such coals no pollen can be obtained anymore, since the exines have also reached the vitrite state. However, in the barren rocks where the sand grains had absorbed the pressure to a certain extent, sometimes the pollen were still preserved, though the exines are strongly carbonized even in these samples. However, by means of hydrofluoric and hydrochloric exposure they can be released; nitric treatment would not be withstood by the exines. By such methods we were able to obtain pollen from the layers of the Kantavár Formation penetrated by boreholes Pécs-57 and Váralja-21. According to Platsek, in Pécs-57 the Middle Triassic limestone complex is overlain by a regressive sequence composed of siltstones and marl layers. Between these layers there is also a 0.5 m-thick coal seam. This regressive sequence and the overlying limestone, lime marl, and marl layers were assigned by Platsek to the Kantavár Formation. He drew the boundary with the Karolinavölgy Sandstone Formation at 594.6 m. Here for the first time a greater amount of more or less determinable pollen grains could be obtained from the Kantavár Formation. Out of the 29 samples collected from the interval between 595.5 and 780.9 m, 13 contained sporomorph material and 16 were pollen-free. In the positive samples, besides the pollen I also found *Michystridium* alga cysts of marine origin. The explored assemblage differs significantly from the

Ladinian-Cordevolian assemblage known from borehole Husztót-2. Its composition is very similar to that of the assemblages of the lower part of the Karolinavölgy Sandstone Formation and it cannot be separated from them. The dominant forms are the Gymnosperma pollen belonging to the Cycas-type Gymnosperma and the Klaus' *Singulipollenites* form group. An important element of the assemblage is the spore *Leptolepidites reissingeri* (Reinh.) Lund which appears in the Middle Keuper. A similar assemblage was also found in the Kantavár Formation penetrated by borehole Váralja-21. According to the summary report on coal exploration in the area of Máza-South-Váralja-South, the well penetrated the formation, composed of well-bedded dark grey, black calcareous siltstone, clayey marl, marl, lime marl, and clayey limestone layers, in a thickness of 74.7 m. The spore *Leptolepidites reissingeri* (Reinh.) Lund also appeared here. In the lower part of the formation, between 578.0 and 618.6 m there were only negative samples. In the middle part, between 564.2 and 572.0 m I found more pollen but they were strongly carbonized and hardly determinable. Here, the representatives of the pine pollen with respiratory cavity and the *Singulipollenites* are predominant. Between 549.0 and 560.0 m, I found sporadic spores and pollen grains. This sporadic occurrence and a similar species composition are characteristic in the lower part of the overlying Karolinavölgy Sandstone Formation, as well.

The spore-pollen flora demonstrated in two localities was mostly gathered from the upper marly, silty layers of the formation. The upper part, which constitutes a continuous transition into the Karolinavölgy Formation, is considered by Balogh (1981) to belong to the Julian substage. This can be only confirmed by the palynologic data. Mass occurrence of pollen belonging to Klaus's *Singulipollenites* form group is characteristic of the lower part of Middle Keuper.

Spore and pollen taxa demonstrated in the Kantavár Formation are as follows:

<i>Triadispora</i> fsp.	<i>Anemiidites spinosus</i>
<i>Cuneatisporites radialis</i>	<i>Chordasporites australiensis</i>
<i>Alisporites</i> div. fsp.	<i>Todisporites minor</i>
<i>Dictyophyllidites harrisii</i>	<i>Conbaculatisporites mesozoicus</i>
<i>Duplicisporites</i> fsp.	<i>Inaperturopollenites reisingeri</i>
<i>Singulipollenites</i> form group Klaus	<i>Punctatosporites scabratus</i>
<i>Cycadopites</i> div. fsp.	<i>Cyathidites minor</i>
<i>Vitreisporites pallidus</i>	<i>Duplexisporites problematicus</i>
<i>Alisporites robustus</i>	<i>Ephedripites tortuosus</i>
<i>Monosulcites minimus</i>	<i>Anaplanisporites telephorus</i>
<i>Trachisporites</i> div. fsp.	<i>Concavisporites</i> (O.) <i>jurienensis</i>
<i>Leptolepidites reissingeri</i>	<i>Calamospora uathorstii</i>
<i>Granulatasporites</i> div. fsp.	<i>Retusotriletes</i> div. fsp.
<i>Toroisporites</i> (T.) <i>mesozoicus</i>	<i>Retitriletes</i> div. fsp.
<i>Cyclinasporites glabrus</i>	

Aquatic organisms:

<i>Micrhystridium</i> sp.	<i>Schizosporis parvus</i>
---------------------------	----------------------------

The spore-pollen and microplankton flora demonstrated in the Kantavár Formation is well-complemented by the fossilized plant macroremnants found in these layers. They are summarized horizon by horizon in the monograph of Nagy (1968). It is the basis for the following flora list:

<i>Equisetites arenaceus</i> Brongh.	<i>Thaumatopteris münsteri</i> Göpp.
<i>Equisetites</i> sp.	<i>Podozamites lanceolatus</i> Brauns
<i>Macropterigium bronni</i> Schenk	<i>Baiera</i> sp.
<i>Clatopteris reticulatus</i> Kuhn	<i>Schizoneura paradoxa</i> Schimp et Moug.
<i>Anotopteris distans</i> Presl	<i>Crossothea</i> sp.
<i>Phlebopteris angustilobatus</i> (Presl)	<i>Voltzia</i> sp.
<i>Todites roesserti</i> Krist.	<i>Abies</i> sp.
<i>Norimbergia</i> sp.	<i>Dioonitocarpidium</i> sp.

This list was complemented by Nagy (1968) with a questionable fruit remnant and the remnants known as *Stigmaria*, all collected in the valley of the Andor Spring near Kozár. He also presented photos of both plants. Judging by the photos, the questionable fruit reminds me of *Nilssonia* seeds, while the "*Stigmaria*" findings may be the root nodules of the horsetail species *Equisetites arenaceus* Brongh. which are common in the European Keuper layers (Mägdefrau, 1956, p. 231). An important element of the plant macroremnants is the occurrence of *Thaumatopteris* restricted to the Upper Triassic and the Lower Jurassic. Nagy I.Z. (in Nagy, 1968) believes the assemblage to be older than the Rhaetian-Liassic flora.

The Karolinavölgy Sandstone Formation and the Rhaetian part of the Mecsek Coal Formation

Its key section was marked out by Nagy in the sequences of borehole Pécs-28 drilled in the Karolinavölgy near Pécs, and of the neighbouring borehole Pécs-39. He separated it into the Carnian, Norian, and Rhaetian stages on the basis of fauna and flora investigations, as well as facies analysis. I carried out the palynologic investigation in all of these stages. In this area, in borehole Pécs-57, I examined those formations which were compared by Platsek with the certain parts of the key section. In the Western Mecsek, Wéber collected material in boreholes Husztót-2 and Szentkatalin-2. From the palynologic point of view, the investigation of the above formations was the most successful in the coal exploratory areas Máza-South-Váralja-South. Generally, the exploratory drillings penetrated into the upper, seam-free sandstone layers of the Karolinavölgy Sandstone Formation, since they represent the footwall of the coal complex. The lower seam group of the coal complex is lithostratigraphically already assigned already to the Mecsek Black Coal Formation; chronostratigraphically, however, it still belongs to the Triassic.

Carnian part of the Karolinavölgy Sandstone Formation

To this time unit belongs primarily the part of borehole Pécs-28 between 270.0 and 457.2 m. The results of the analysis of its samples were used by Nagy (1968) to determine the age of the complex. He pointed out that, first of all, the pollen play an ageindicating role here. Though the pollen grains are also strongly carbonized here, it is not as strongly as those in the Kantavár Formation, and even their state of preservation is better. However, most of them can be determined only at generic level.

The assemblage contains a lot of pollen belonging to Klaus's *Singulipollenites* form group. They are representatives of the genera *Duplicisporites* and *Partitisporites* (syn: *Paracirculina*). Their dominance is characteristic of the Carnian stage. Both genera became extinct in the Norian; at the end of that stage they cannot be found anymore. I was able to make photos and determinations mainly from the assemblages of the samples obtained between 311.3 and 311.8 m, and 351.5 and 352.4 m. These samples derive from the layers separated by Nagy (1968) as "Semionotus-bearing beds" and thought by him to be correlatable with the Middle Keuper. The determined and illustrated assemblage consists of the following species and genera (in Nagy 1968; Plate XII):

Conbaculatisporites fsp.
Microreticulatisporites fsp.
Anemioidites spinosus Mädlér
Apiculatisporites fsp.
Retusotriletes fsp.
Simplicesporites fsp.

Aulisporites fsp.
Duplicisporites fsp.
Partitisporites fsp. (Syn.: *Paracirculina*)
Circulina fsp.
Singulipollenites div. gen. et. fsp.

Later, I also succeeded in determining *Micrhystridium* alga cysts from the assemblage, which indicate a marine connection.

A similar assemblage was encountered in borehole Pécs-57. According to Platsek (pers. comm.), in this borehole the Karolinavölgy Formations begins at 594.60 m. It is made up of clastic rocks, principally siltstones and sandstones, among which are locally intercalated conglomerates and gravelly sandstones, and in the interval between 529.8 and 531.3 m a 1.5 m thick carbonaceous mudstone horizon. On the basis of its lithology and spore-pollen composition, the complex can be compared and correlated with the phyllopod- and *Semionotus*-bearing Carnian sequence of borehole Pécs-28. On a palynologic basis, the upper boundary of the Carnian stage can be emplaced at 419.5 m, since the assemblage *Leptolepidites reissingeri* (Reinh.) Lund, *Aratrisporites scabratus* Klaus, and *Triadispora hyalina* (Mädlér) Scheuring can be traced to that point. *L. reissingeri* appears in the Middle Keuper, while the two latter pollen are found in the Carnian stage for the last time.

I was even able to separate an assemblage of palynologically provable Carnian age in borehole Váralja-20. In the interval between 703.8 and 738.0 m, this assemblage can be found in the beds assigned by Szilágyi and Villám (1985) to the Karolinavölgy Sandstone Formation in the summary report on the coal

exploration in the area of Máza-South-Váralja-South. According to their data, the average thickness of the Carnian part of the formation is 61.8 m in this area. Its facies is similar to that of the Pécs area. It contains coal seams only exceptionally, which is why it can be regarded as the direct footwall of the complex with seams. On the basis of their differing colours, the rocks can be distinguished as follows: Rhaetian formations of greenish-grey colour overlying Carnian-Norian formations of brown spotted, and sometimes red-brown, purple spotted colour.

In borehole Váralja-20, on a lithologic basis the boundary was drawn at 677.8 m, at the first rhythmic wash-out surface above which greenish-grey, and beneath which red-brown spotted sediments were deposited. The borehole was drilled one km away from borehole Nagymányok-12 in which I determined the first spores indicating the Carnian. In this borehole, I found just such an assemblage in the interval between 703.8 and 738.0 m. Between 704.00 and 704.70 m, I determined the taxa *Striatoabieites aytugii* Visscher, *Triadispora hyalina* (Mädler) Scheuring, and *Duplicisporites* fsp. in the assemblage. Their presence together with the spore *Leptolepidites reissingeri* (Reinh.) Lund refers to the Carnian stage. In the samples below this depth – probably due to the strong oxidation conditions – I could hardly find intact pollen. However, in the greenish-grey complex above the wash-out surface there were still grains older than the Rhaetian, probably belonging to the Norian stage: *Duplicisporites* fsp. and *Undulatosporites lucens* Leschik. Consequently, the first rhythmic wash-out surface appears still in the Norian stage. According to the observations of Platsek (pers. comm.), there occur red spotted layers even in this part of the borehole sequence, though much more rarely than below 670 m.

In borehole Váralja-21, above the Kantavár Formation as far as the Miocene cover, the Karolinavölgy Sandstone Formation was penetrated by the well. Out of the 30 samples taken from this part, 19 proved to be pollen-free. Due to the small amount of remnants, I could establish only that part of the borehole from 595.8 m up to 473.0 m – on the basis of the *Aratrisporites* fsp. and *Duplicisporites* fsp. – belongs to the Carnian or the Norian stage. The samples taken in the upper part of the formation were practically pollen-free.

I have also found a pollen assemblage occurring both in the Carnian and Norian stages in the beds of the coal footwall penetrated by borehole Máza-21. Below the Miocene cover, the well entered directly into Triassic formations. It penetrated three coal seams and then drilled into the Karolinavölgy Sandstone Formation. According to the geologic summary report on the area, at 531.8 m in the coal footwall sequence a wash-out surface was observed. The overlying Rhaetian and the underlying Norian formations were separated at this surface. On the basis of the palynologic investigations, the sequence below the coal seams, throughout the interval between 390.3 and 611.8 m, contains a pollen assemblage of Carnian-Norian character. Probably the wash-out surface also occurs in the Norian stage here.

Spore and pollen taxa demonstrated in the Carnian part of the Karolinavölgy Sandstone Formation are as follows:

<i>Ovalipollis</i> div. fsp.	<i>Concavisporites</i> (<i>O.</i>) <i>jurienensis</i>
<i>Aratrisporites</i> fsp.	<i>Calamospora</i> <i>nathorstii</i>
<i>Porcellispora</i> <i>longdonensis</i>	<i>Retusotriletes</i> div. fsp.
<i>Triadispora</i> fsp.	<i>Triadispora</i> <i>hyalina</i>
<i>Striatoabietites</i> <i>aytugii</i>	<i>Lophotriletes</i> div. fsp.
<i>Cuneatisporites</i> <i>radialis</i>	<i>Lophotriletes</i> <i>verrucosus</i>
<i>Ovalipollis</i> <i>pseudosalatus</i>	<i>Contignisporites</i> <i>dunrobiensis</i>
<i>Alisporites</i> div. fsp.	<i>Lycopodiacidites</i> cf. <i>frankonense</i>
<i>Dictyophyllidites</i> <i>harrisii</i>	<i>Convolutispora</i> <i>klukiforma</i>
<i>Duplicisporites</i> fsp.	<i>Aratrisporites</i> <i>scabratus</i>
<i>Singulipollenites</i> (form group Klaus)	<i>Klausipollenites</i> cf. <i>schaubergeri</i>
<i>Cycadopites</i> div. fsp.	<i>Reticulatasporites</i> <i>adunctus</i>
<i>Vitreisporites</i> <i>pallidus</i>	<i>Undulatasporites</i> <i>angueus</i>
<i>Alisporites</i> <i>robustus</i>	<i>Zebbrasporites</i> <i>corneolus</i>
<i>Monosulcites</i> <i>minimus</i>	<i>Partitisporites</i> fsp.
<i>Trachisporites</i> div. fsp.	<i>Undulatasporites</i> <i>lucens</i>
<i>Leptolepidites</i> <i>reissingeri</i>	<i>Aulisporites</i> <i>astigmaticus</i>
<i>Granulatasporites</i> div. fsp.	<i>Nevesisporites</i> <i>limatulus</i>
<i>Toroisporites</i> (<i>T.</i>) <i>mesozoicus</i>	<i>Baculatisporites</i> <i>commaumensis</i>
<i>Cyclinasporites</i> <i>glabrus</i>	<i>Microreticulatisporites</i> <i>fuscus</i>
<i>Anemiidites</i> <i>spinus</i>	<i>Eucommiidites</i> div. fsp.
<i>Chordasporites</i> <i>australiensis</i>	<i>Corollina</i> fsp.
<i>Todisporites</i> <i>minor</i>	<i>Todisporites</i> <i>major</i>
<i>Conbaculatisporites</i> <i>mesozoicus</i>	<i>Inaperturopollenites</i> <i>flavus</i>
<i>Inaperturopollenites</i> <i>reissingeri</i>	<i>Cyathidites</i> <i>australis</i>
<i>Punctatosporites</i> <i>scabratus</i>	<i>Perinopollenites</i> <i>elatoides</i>
<i>Cyathidites</i> <i>minor</i>	<i>Conbaculatisporites</i> fsp.
<i>Duplexisporites</i> <i>problematicus</i>	<i>Cerebropollenites</i> fsp.
<i>Ephedripites</i> <i>tortuosus</i>	<i>Trachisporites</i> <i>asper</i>
<i>Anaplanisporites</i> <i>telephorus</i>	<i>Ginkgocycadophytus</i> fsp.

Aquatic organisms:

<i>Schizosporis</i> <i>parvus</i>	Plankton with one appendage
<i>Microhystridium</i> sp.	Microforaminifer

Norian part of the Karolinavölgy Sandstone Formation

The separation of the Norian stage in the formation is difficult from both lithologic and palynologic points of view. On the basis of the scattered sporomorphs found so far, it is not possible at all. The number of pollen restricted only to the Norian stage is small in general, both in the Alpine and Germanic facies areas. In the Mecsek Mts, I draw the Carnian/Norian boundary where *Aulisporites astigmaticus* (Leschik) Klaus and *Undulatasporites lucens* Leschik are still present in the sequence, and the microplankton *Hystrichosphaeridium magnum* determ. prov. appears. In the sporomorph-bearing sequence, the lower boundary is also marked by a reduction in the numerical proportion of the *Partitisporites* fsp. In connection with the Rhaetian stage of the Mecsek Mts.,

the main problem is that two important indicator pollen, namely the genera *Granuloperulatipollis* and *Rhaetipollis*, are lacking, or have not been detected so far. These pollen taxa occur consistently in the Kössen layers of the Transdanubian Range and there play an important role in the palynostratigraphy of the Upper Norian, Lower and Middle Rhaetian stages. Possibly, their absence in the Mecsek Mts. is due to the break of sedimentation at the end of the Norian, respectively at the beginning of the Rhaetian. This is, however, only one of the hypotheses, as these two pollen taxa are also absent from the Norian and Rhaetian layers in areas east of the Mecsek Mts. (Dhoneck Basin, Kazakhstan, Iran – Semenova 1973; Gluzhar 1973; Sakulina 1973; Achilles et al. 1984). Accordingly, their lack may be due to other reasons, as well.

The Norian key section of the Mecsek Mts. was established by Nagy (1968) in borehole Pécs-28 between 270.0 m and 67.0 m. He separated it on the basis of its facies, which is different from both the Carnian and Rhaetian intervals, and of its intermediate stratigraphic position. According to Balogh (1981), the section may represent the Lácian and Alaunian substages of the Norian stage. In its upper part, there are wash-out surfaces and the sediments of the Rhaetian stage also lie on an elevated surface. From the interval of the type section between 107.2 and 255.3 m, I examined 25 samples. In the assemblage found, representatives of the genera *Duplicisporites* and *Partitisporites* are still present, proving that the complex is older than Rhaetian. However, their numerical proportion is reduced. The pine pollen with respiratory cavity occur in a greater amount. The genera *Aulisporites*, *Undulatosporites*, and *Reticulatasporites* (described by Leschik in the Schilfsandstein group of the Keuper), appearing in the lower part of the formation, still appear here in certain samples in a greater amount and cannot be traced further into the Rhaetian layers.

In borehole Pécs-57, Platsek (pers. comm.) assigned the interval penetrated between 475.8 and 225.5 m to the Norian stage. He thought the stage boundaries provisional, since on a lithologic basis uncertainties prevailed. I drew the boundary (by palynologic methods) higher up, at 164.8 m, as far as the spore *Aulisporites astigosus* (Leschik) Klaus could be traced. Compared with the Carnian part, the numerical proportion of the *Duplicisporites* fsp. and *Partitisporites* fsp. is also strongly reduced in the Norian.

In borehole Váralja-26, under the Rhaetian part of the Mecsek Black Coal Formation, separated by a tectonic boundary, red-brown spotted beds were penetrated by the well. On the basis of their lithologic character, they could be assigned to the lower part of the Karolinavölgy Sandstone Formation. From a palynologic point of view, the same stratigraphic position could be determined: these formations are of Carnian or Norian age. I examined 17 samples taken from the red-brown spotted beds. Ten samples contained some spores and pollen, among them *Duplicisporites* fsp., as well.

The exploratory wells drilled in the Western Mecsek penetrated the sequence of the Karolinavölgy Sandstone Formation in several places. From these, I received from B. Wéber samples from Upper Triassic beds for examination. In

boreholes Husztót-2 and Szentkatalin-1, in the intervals between 384.2 and 393.2 m, and 386.2 and 436.5 m, respectively, I encountered pollen and spore assemblages of Norian age, containing *Aulisporites astigmaticus* (Leschik) Klaus, *Undulatosporites lucens* Leschik, and *Corollina meyeriana* Venk et Goczan.

Besides those mentioned so far, I found also a pollen assemblage referring to the Carnian/Norian stage between 233.5 and 465.2 m in the karst exploratory well Tettye-1. Here, the Upper Triassic rocks are highly fractured and dislocated. They are overthrust on each other as well as on Miocene-Pliocene formations.

Borehole Komló-20 also penetrated a highly tectonized Upper Triassic sequence. Below 380.6 m, the well passed from Miocene into Upper Triassic. Káli (1962) correlated the two penetrated thin coal seams with the level of the alpha seam, and assigned the sequence as far as 620.8 m to the Lower Liassic. He considered the rocks below 620.8 m to be of Rhaetian age. It was palynologically proven that both the layers with alpha seams and the underlying ones belong to the Upper Triassic. In the sporomorph assemblage, there occurred spore and pollen grains indicating the Carnian-Norian stages as well, e.g. *Zebrasporites corneolus* (Leschik) Klaus and *Duplicisporites* fsp. Nagy (1968) published a flora list and photos of the spores and pollen found in the borehole.

Spore and pollen taxa demonstrated in the Norian sequence of the Karolinavölgy Sandstone Formation are as follows:

<i>Cuneatisporites radialis</i>	<i>Klausipollenites</i> cf. <i>schaunberggeri</i>
<i>Alisporites</i> div. fsp.	<i>Reticulatasporites adunctus</i>
<i>Dictyophyllidites harrisii</i>	<i>Undulatosporites anguineus</i>
<i>Duplicisporites</i> fsp.	<i>Zebrasporites corneolus</i>
<i>Singulipollenites</i> form group Klaus	<i>Partitisporites</i> fsp.
<i>Cycadopites</i> div. fsp.	<i>Undulatosporites lucens</i>
<i>Vitreisporites pallidus</i>	<i>Aulisporites astigmaticus</i>
<i>Alisporites robustus</i>	<i>Microreticulatasporites fuscus</i>
<i>Monosulcites minimus</i>	<i>Eucommiidites</i> div. fsp.
<i>Trachisporites</i> div. fsp.	<i>Corollina</i> fsp.
<i>Leptolepidites reissingeri</i>	<i>Todisporites major</i>
<i>Granulatasporites</i> div. fsp.	<i>Inaperturopollenites flavus</i>
<i>Toroisporites</i> (T.) <i>mesozoicus</i>	<i>Cyathidites australis</i>
<i>Cyclinasporites glabrus</i>	<i>Perinopollenites elatoides</i>
<i>Anemiidites spinosus</i>	<i>Conbaculatisporites</i> fsp.
<i>Chordasporites australiensis</i>	<i>Cerebropollenites</i> fsp.
<i>Todisporites minor</i>	<i>Ginkgocycadophytus</i> fsp.
<i>Conbaculatisporites mesozoicus</i>	<i>Ricciisporites tuberculatus</i>
<i>Inaperturopollenites reissingeri</i>	<i>Tigrisporites microrugulatus</i>
<i>Punctatosporites scabratus</i>	<i>Corollina meyeriana</i>
<i>Cyathidites minor</i>	<i>Pinuspollenites minimus</i>
<i>Duplexisporites problematicus</i>	<i>Trachisporites tuberosus</i>
<i>Ephedripites tortuosus</i>	<i>Osmundacidites wellmannii</i>
<i>Anaplanisporites telephorus</i>	<i>Anapiculatisporites spiniger</i>
<i>Concavisporites</i> (O.) <i>juriensis</i>	<i>Laevigatisporites</i> fsp.
<i>Calamospora nathorstii</i>	<i>Granulatasporites ovaloides</i>
<i>Retusotriletes</i> div. fsp.	<i>Leptolepidites</i> fsp.

Aquatic organisms:

Michrystidium sp.
Hystriosphæridium magnum

Plankton with one appendage
Schizosporis parvus

*Rhaetian beds of the Karolinavölgy Sandstone Formation
 and the Mecsek Coal Formation*

The key section of the Rhaetian stage is represented in the Mecsek Mts by the interval 0.0 m to 67.0 m of borehole Pécs-28, and by the interval from 58.0 m to 220.0 m of borehole Pécs-39 (Nagy, 1968). In the key section, I investigated the interval between 85.9 and 219.6 m of borehole Pécs-39. In connection with the Carnian-Norian stages and the Liassic, I examined the Triassic-Jurassic formations of boreholes Pécs-57 and Váralja-26. The Rhaetian sequence extends from 28.5 m to 164.8 m in Pécs-57, and from 662.8 m to 1,270.0 m in Váralja-26. In their Rhaetian assemblages, the most remarkable features are the lack of the characteristic Carnian-Norian elements and the presence of certain triangular trilet microspores such as the genera *Anemiidites* and *Anapiculatisporites*. These spiny spores are absent in the Liassic of the Mecsek Mts.

In the coal exploratory areas of Komló, Máza-South, and Váralja-South, I examined a number of borehole sequences penetrating the lower (or "alpha") seam group and drilling to a certain extent into the Rhaetian footwall sandstone complex, as well. Among others, they included boreholes Máza-23 and Váralja-9, -15, -18, and -34, respectively. Their investigation made it possible to point out that the lower seam group still belongs to the Upper Triassic. Balogh (1981) interpreted the question of the Rhaetian/Liassic boundary in this sense. The reason for the palynologic uncertainty was the fact that at this time the pollen *Ephedripites tortuosus* Mädlér was known in other areas only in the Lower Liassic. Since then, it has been found in the Upper Triassic, not only in Hungary but also in areas farther afield (Lund 1977). From the group with alpha seams the pollen *Ovalipollis pseudoalatus* (Thiergart) Schuurman also became wellknown. This species appears in the Ladinian and becomes extinct in the Upper Triassic. The recognition of *Triancoraesporites ancorae* (Reinh.) Schulz was also of great importance. In Europe, this species is a zonal index form in the Rhaetian stage. Schulz (1967) reports it from the Middle and Upper Rhaetian. According to Visscher and Brugman (1981), it is restricted to the Upper Rhaetian. Antonescu (1973) also found it in the Hettangian, while according to Achilles et al. (1984), it is present in the whole of the Rhaetian.

The Rhaetian age of the group with alpha seams could be also proven recently in the coal exploratory areas Vasas-North and Rücker, in borehole sequences in which the Triassic/Jurassic boundary within the coal complex was also verified by the occurrence of tuffite horizons by Szilágyi, Hónig, Soós, and Németh. In the beds with coal seams below the tuffite horizon, I was able to detect pollen assemblages occurring in the Upper Triassic in the following boreholes: Vasas-35, -38, -39, -45, -52, -63, Rücker-27, -29, -31.

Spore and pollen taxa demonstrated in the Rhaetian stage are as follows:

<i>Ovalipollis pseudoalatus</i>	<i>Inaperturopollenites flavus</i>
<i>Ovalipollis</i> fsp.	<i>Cyathidites australis</i>
<i>Cuneatisporites radialis</i>	<i>Perinopollenites elatoides</i>
<i>Alisporites</i> div. fsp.	<i>Conbaculatisporites</i> fsp.
<i>Dictyophyllidites harrisii</i>	<i>Cerebropollenites</i> fsp.
? <i>Singulipollenites</i> form group Klaus	<i>Trachisporites asper</i>
<i>Cycadopites</i> fsp.	<i>Ginkgocycadophytus</i> fsp.
<i>Vitreisporites pallidus</i>	<i>Tigrisporites microrugulatus</i>
<i>Alisporites robustus</i>	<i>Corollina meyeriana</i>
<i>Monosulcites minimus</i>	<i>Pinuspollenites minimus</i>
<i>Trachisporites</i> div. fsp.	<i>Trachisporites tuberosus</i>
<i>Leptolepidites reissingeri</i>	<i>Osmundacidites wellmanii</i>
<i>Granulatasporites</i> div. fsp.	<i>Laevigatasporites</i> fsp.
<i>Toroisporites</i> (T.) mesozoicus	<i>Granulatasporites ovaloides</i>
<i>Cyclinasporites glabrus</i>	<i>Granulatasporites splendens</i>
<i>Anemiidites spinosus</i>	<i>Parcisporites annectus</i>
<i>Chordasporites australiensis</i>	<i>Chasmatosporites major</i>
<i>Todisporites minor</i>	<i>Toroisporites</i> (T.) parvulus
<i>Conbaculatisporites mesozoicus</i>	<i>Chasmatosporites apertus</i>
<i>Inaperturopollenites reissingeri</i>	<i>Chasmatosporites hians</i>
<i>Punctatosporites scabratus</i>	<i>Quadraculina anellaeformis</i>
<i>Cyathidites minor</i>	<i>Chasmatosporites elegans</i>
<i>Duplexisporites problematicus</i>	<i>Equisetosporites chinleanus</i>
<i>Ephedripites tortuosus</i>	<i>Zebraspores interscriptus</i>
<i>Anaplanisporites telephorus</i>	<i>Rogalskiasporites cicatricosus</i>
<i>Concavisporites</i> (O.) juriensis	<i>Apiculatisporites parvispinosus</i>
<i>Calamospora nathorstii</i>	<i>Lycopodiumsporites semimuris</i>
<i>Retusotriletes</i> div. fsp.	<i>Aratrisporites minimus</i>
<i>Retitriletes</i> div. fsp.	<i>Heliosporites altmarkensis</i>
<i>Nevesisporites limatulus</i>	<i>Triancoraesporites ancorae</i>
<i>Baculatisporites commaumensis</i>	<i>Monosaccites</i> indet.
<i>Microreticulatisporites fuscus</i>	<i>Pollenites</i> indet. (papillat)
<i>Eucommiidites</i> div. fsp.	<i>Patellina plicata</i>
<i>Corollina</i> fsp.	<i>Anapiculatisporites spiniger</i>
<i>Todisporites major</i>	

Acritarchs:

<i>Micrhystridium</i> sp.	Plankton with one appendage
<i>Hystrochosphaeridium magnum</i>	<i>Schyzosporis parvus</i>
<i>Dinoflagellata</i> indet.	Microforaminifer

The stratigraphic position of the spores *Triancoraesporites ancorae* (Reinh.)

E. Schulz and *Aratrisporites minimus* Schulz in the Rhaetian stage in the Mecsek Mts

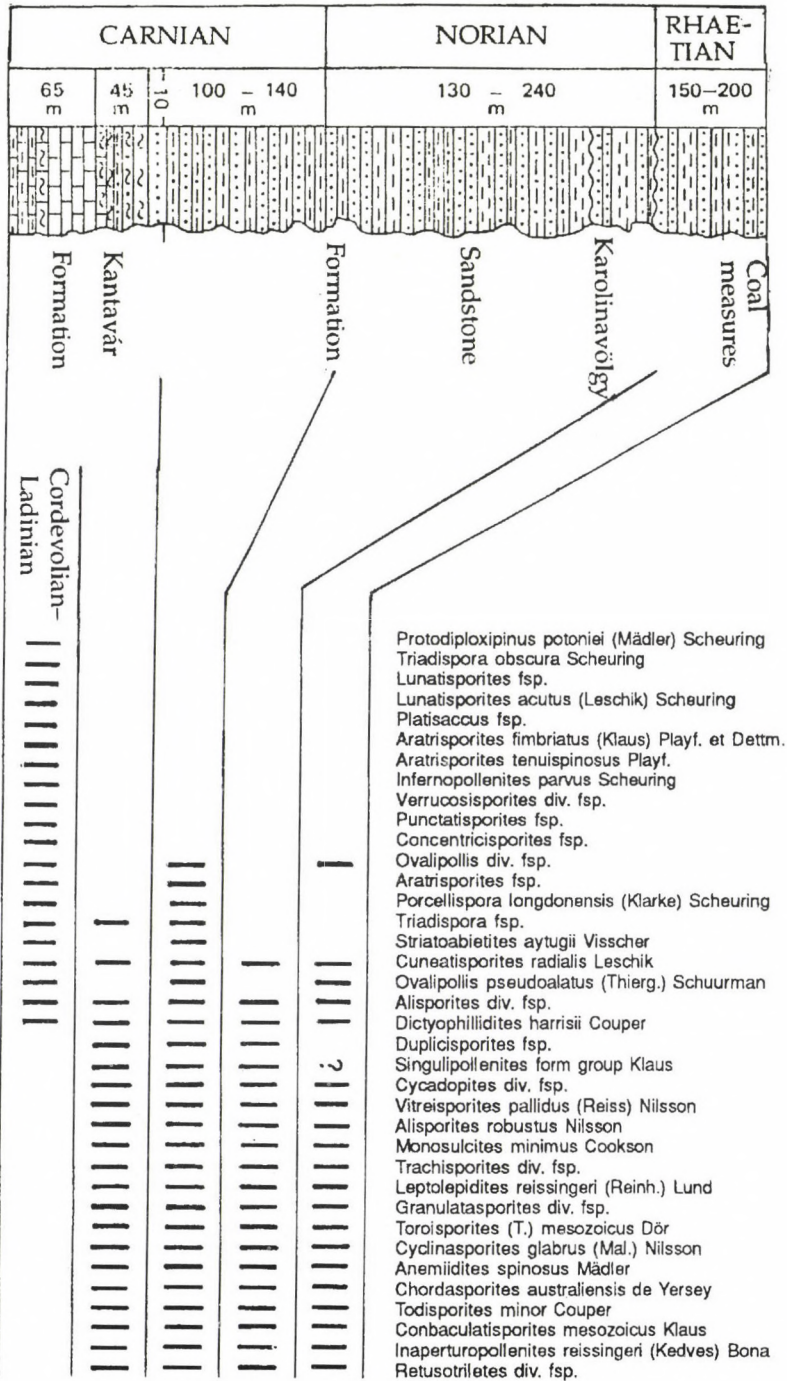
Triancoraesporites ancora fsp. was described by Reinhardt as *Waltzisporea ancorae* n. sp. in the Rhaetian formations of Thuringia in 1962. It was assigned to the genus *Triancoraesporites* by Schulz in 1967. Since then it has been included within the Germanic Triassic as one of the characteristic taxa of the Middle and Upper Rhaetian. Its occurrence in the entirety of the Rhaetian stage was referred to

only by Achilles et al. (1984). In the Transdanubian Range, it has not yet been found. In the Mecsek Mts., it is present in the coal exploratory area Váralja-South. In borehole Váralja-18, it appeared in the Upper Triassic part of the coal complex, and in borehole Váralja-15, in the underlying sandstone, with one specimen in each. In the unit overlying of the lower seam group, Váralja-15 penetrated tuffitic layers in the interval between 606.2 and 670.5 m where the Triassic/Jurassic lithologic boundary was drawn (Szilágyi and Villám 1985). Beneath the tuffites, four coal seams could be distinguished, with the lowermost one in the interval between 744.1 and 747.4 m. Between 693.3 and 901.0 m, I was able to identify the following characteristic Upper Triassic forms: *Ovalipollis pseudoalatus* (Thiergart) Schuurman, *Anemiidites spinosus* Mädlér, *Aratrisporites minimus* E. Sch., *Ephedripites tortuosus* Mädlér, *Triancoraesporites ancorae* (Reinhardt) E.Sch. *Triancoraesporites* was found in the interval 900.8 to 901.0 m, and the only specimen of *Aratrisporites minimus* Sch. in the interval 703.0 to 703.2 m, in the layers between the coal seams. E. Schulz (1967) described this spore in the Hettangian formations of borehole Wellnitz-1, and he found it in 7 further boreholes, also in the Hettangian. Investigating the Frankish Rhaeto-Liassic boundary layers, Achilles (1981) separated the *Concavisporites-Duplexisporites problematicus-Aratrisporites minimus* Zone, restricted to Liassic alpha 1+2. He correlated it with other sporomorph zones of the same age described in European areas, such as the *Pinuspollenites-Trachisporites* Zone of Lund. Achilles reckons the beginning of the Liassic from the appearance of *Aratrisporites minimus*. In our case, I consider the layers with seams beneath the tuffite as still belonging to the Upper Triassic, since *A. minimus* is accompanied here by spore-pollen and plankton forms which do not grade into the Liassic in the Mecsek. Lund (1977) also found the spore *A. minimus* in uppermost Triassic layers.

Conclusions

In the Upper Triassic of the Mecsek Mts., two formations are distinguished – the Kantavár Formation and above it the Karolinavölgy Sandstone Formation. Above the Karolinavölgy Sandstone Formation, the Mecsek Black Coal Formation is positioned. The latter unit's greater part belongs to the Liassic. Its lower seam group can be separated from the middle one by a tuffite horizon. It can be palynologically proven that the so-called lower seam group beneath the tuffite chronostratigraphically still belongs to the Upper Triassic. In the siltstones between the seams, *Ovalipollis pseudoalatus* (Thiergart) Sch., *Aratrisporites minimus* E. Sch., *Triancoraesporites ancorae* (Reinh.) E. Sch., *Parcisporites annectus* Leschik, diverse trilet spores with spiny ornaments, as well as the microplankton *Hystrichosphaeridium magnum* n. sp. (determ. prov.) can be found. Of these, only *A. minimus* extends into the Lower Liassic in the Mecsek Mts.

Table 2
Stratigraphic distribution of the Upper Triassic spore and pollen forms, as well as of microplankton with organic tests, in the Mecsek Mts



CARNIAN		NORIAN		RHAE- TIAN
—	—	—	—	Cyathidites minor Couper
—	—	—	—	Duplexisporites problematicus (Couper) Playf. et Dettm.
—	—	—	—	Ephedripites tortuosus Mädlér
—	—	—	—	Anaplanisporites telephorus (Pauts) Jans.
—	—	—	—	Concavisporites (O.) juriensis Balme
—	—	—	—	Calamospora nathorstii (Halle) Klaus
—	—	—	—	Retitriletes div. fsp.
—	—	—	—	Triadispora hialina (Mädlér) Scheuring
—	—	—	—	Lophotriletes div. fsp.
—	—	—	—	Lophotriletes verrucosus E. Sch.
—	—	—	—	Contignisporites dunrobiensis (Couper) E. Sch.
—	—	—	—	Lycopodiacidites cf. frankonense Achilles
—	—	—	—	Convolutispora klukiforma (Nilsson) E. Sch.
—	—	—	—	Aratrisporites scabratus Klaus
—	—	—	—	Klausipollenites cf. schaubergeri (Pot. et Klaus) Jans.
—	—	—	—	Reticulatasporites adunctus Leschik
—	—	—	—	Undulatasporites anguineus Leschik
—	—	—	—	Zebbrasporites corneolus (Leschik) Klaus
—	—	—	—	Partitisporites fsp.
—	—	—	—	Undulatasporites lucens Leschik
—	—	—	—	Aulisporites astigosus (Leschik) Klaus
—	—	—	—	Nevesisporites limatulus Playf.
—	—	—	—	Baculatisporites commaumensis (Cookson) R. Pot.
—	—	—	—	Microreticulatisporites fuscus (Nilsson) Morbey
—	—	—	—	Eucomiidites div. fsp.
—	—	—	—	Corollina fsp.
—	—	—	—	Todisporites major Couper
—	—	—	—	Inaperturopollenites flavus (Leschik) Nilsson
—	—	—	—	Cyathidites australis Couper
—	—	—	—	Perinopollenites elatoides Couper
—	—	—	—	Conbaculatisporites fsp.
—	—	—	—	Cerebropollenites fsp.
—	—	—	—	Trachisporites asper Nilsson
—	—	—	—	Ginkgocycadophytus fsp.
—	—	—	—	Riccisporites tuberculatus Lundbl.
—	—	—	—	Leptolepidites fsp.
—	—	—	—	Tigrisporites microrugulatus E. Sch.
—	—	—	—	Corollina meyeriana (Klaus) Venk. et Goczan
—	—	—	—	Pinuspollenites minimus (Couper) Kemp.
—	—	—	—	Trachisporites tuberosus Nilsson
—	—	—	—	Osmundacidites wellmanii Couper
—	—	—	—	Anapiculatisporites spiniger (Leschik) Reinh.
—	—	—	—	Laevigatasporites fsp.
—	—	—	—	Granulatasporites ovaloides Leschik
—	—	—	—	Granulatasporites splendens Leschik
—	—	—	—	Parcisporites annectus Leschik
—	—	—	—	Chasmatosporites major Nilsson
—	—	—	—	Toroisporites (T.) parvulus Dör.
—	—	—	—	Chasmatosporites apertus (Rog.) Nilsson
—	—	—	—	Chasmatosporites hians Nilsson
—	—	—	—	Quadraeculina ahellaeformis Mal.
—	—	—	—	Chasmatosporites elegans Nilsson
—	—	—	—	Equisetosporites chinleanus Daugherti
—	—	—	—	Zebbrasporites interscriptus (Thiery.) Klaus
—	—	—	—	Rogalskaiisporites cicatricosus (Rog.) Danze-Corsin et Lav.
—	—	—	—	Apiculatisporites parvispinosus (Leschik) E. Sch.
—	—	—	—	Lycopodiumsporites semimuris Danze-Corsin et Lav.
—	—	—	—	Aratrisporites minimus E. Sch.
—	—	—	—	Heliosporites altmarkensis E. Sch.
—	—	—	—	Triancoraesporites ancorae (Reinh.) E. Sch.
—	—	—	—	Monosaccites indet., Patellina plicata Mal.
—	—	—	—	Pollenites indet. (papillat)
—	—	—	—	Michrystidium sp.
—	—	—	—	Hystrichosphaeridium magnum determ. prov.
—	—	—	—	Dinoflagellata indet
—	—	—	—	plankton with one appendage
—	—	—	—	Schizosporis parvus Cookson et Dettm.
—	—	—	—	Microforaminifer

The Carnian age of the lower part of the Upper Triassic key section in the Mecsek Mts. can be also palynologically proven. Based on its spore-pollen and microplankton content, the upper part can be assigned to the Upper Rhaetian stage. Palynologically, the Norian stage can hardly be separated from the Rhaetian, partly because there is a sedimentation gap in the upper part of the Norian and in the Lower Rhaetian, partly because the taxa, palynologically usable in western and northern Europe both in the Upper Norian and the Lower Rhaetian, have not yet been found in the Mecsek Mts. Such elements are primarily *Granuloperculatipollis rudis* Venk. et Gócz. and *Rhaetipollis germanicus* E. Schulz, frequent in the Lower Rhaetian of *Classopollis* dominance, rare in the Upper Norian. Their absence so far, and the simultaneous more frequent presence of *Triancoraesporites ancorae* (Reinh.) E. Schulz in the Upper Rhaetian, do not exclude the possibility of other palaeophytogeographic relations.

Acknowledgements

This palynostratigraphical study is a part of the Hungarian National Scientific Research Fund (OTKA) theme "Mesozoic palaeogeographical setting of the tectonic units of Hungary". Hereby, I express my thanks to János Haas scientific adviser, project leader for making me possible to be a member of the palynological working group. As a result of my work, he helped in publishing this study in *Acta Geologica Hungarica*. I owe geologists Ferenc Góczán and Sándor Kovács special thanks for their help and valuable advice.

Plate I

1. *Lunatisporites acutus* (Leschik) Scheuring, Borehole Husztót-2, 659.0–663.9 m, Ladinian–Cordevolian
2. *Porcellispora longdonensis* (Clarke), Scheuring, Borehole Husztót-2, 688.80 m, Ladinian–Cordevolian
- 3–4. *Triadispora obscura* Scheuring, Borehole Husztót-2, 688.80 m, Ladinian–Cordevolian
5. *Infernopollenites parvus* Scheuring, Borehole Husztót-2, 688.80 m, Ladinian–Cordevolian
6. *Striatoabietites aytugii* Visscher, Borehole Husztót-2, 688.80 m, Ladinian–Cordevolian
Magnification: 750x

Plate II

1. *Triadispora* fsp., Borehole Husztót-2, 659.00–663.90 m, Ladinian–Cordevolian
2. *Verrucosiporites* fsp., Borehole Husztót-2, 652.00–655.00 m, Ladinian–Cordevolian
3. *Aratrisporites fimbriatus* Klaus, Borehole Husztót-2, 688.80 m, Ladinian–Cordevolian
4. *Ovalipollis pseudoalatus* (Thiergart) Schuurman, Borehole Husztót-2, 688.80 m, Ladinian–Cordevolian
5. *Ovalipollis* fsp., Borehole Husztót-2, 688.80 m, Ladinian–Cordevolian
6. *Protodiploxipinus potonie* (Mädler) Scheuring, Borehole Husztót-2, 688.80 m, Ladinian–Cordevolian
7. *Concentricisporites* fsp. fragment, Borehole Husztót-2, 652.00–655.00 m, Ladinian–Cordevolian
8. *Dictyophyllidites harrisii* Couper, Borehole Husztót-2, 659.00–663.90 m, Ladinian–Cordevolian
Magnification: 750x

Plate III

1. *Triadispora hyalina* (Mädler) Scheuring, Borehole Pécs-57, 441.50 m, Carnian
2. *Triadispora hyalina* (Mädler) Scheuring, Borehole Váralja-20, 704.00 m, Carnian
3. *Ephedripites tortuosus* Mädler, Borehole Váralja-20, 704.00 m, Carnian
4. *Triadispora* sp., Borehole Pécs-57, 442.00 m, Carnian
5. *Triadispora* sp., Borehole Váralja-20, 703.80–703.90 m, Carnian
6. *Aratrisporites scabratus* Klaus, Borehole Pécs-57, 457.7 m, Carnian
7. *Parcisporites annectus* Leschik, Borehole Máza-23, 1408.40–1408.50 m, Rhaetian, M=859x
8. *Granulatasporites ovaloides* Leschik, Borehole Pécs-57, 457.00 m, Carnian
9. *Leptolepidites reissingeri* (Reinh.) Lund, Borehole Pécs-57, 441.50 m, Carnian
10. *Todisporites major* Couper, Borehole Pécs-57, 457.70 m, Carnian
11. *Inaperturopollenites flavus* (Leschik) Nilsson, Borehole Pécs-57, 441.50 m, Carnian
Magnification: 750x, except Fig. 8

Plate IV

1. *Partisporites* sp., Borehole Szentkatalin-1, 393.20 m, Norian
2. *Duplicisporites* sp., Borehole Szentkatalin-1, 393.20 m, Norian
3. *Duplicisporites* sp., Borehole Váralja-20, 617.50–617.70 m, Norian
4. *Duplicisporites* sp., Borehole Váralja-26, 1271.00–1271.10 m, Carnian–Norian
5. *Corollina* sp., Borehole Szentkatalin, 393.20 m, Norian
6. *Corollina meyeriana* (Klaus) Venk. et Goczán, Borehole Váralja-20, 704.00 m, Carnian
7. *Aratrisporites minimus* E. Sch., Borehole váralja-15, 703.00–703.20 m, Rhaetian
8. *Granulatasporites splendens* Leschik, Borehole Váralja-26, 908.00–908.20 m, Rhaetian
9. *Aulisporites astigmus* (Leschik) Klaus, Borehole Pécs-57, 179.00 m, Norian
10. *Perinopollenites elatoides* Couper, Borehole Váralja-26, 838.30–838.40 m, Rhaetian
- 11–12. *Cycadopites* sp., Borehole Szentkatalin-1, 393.20 m, Norian
13. *Ovalipollis* sp., Borehole Váralja-26, 951.00–951.50 m, Carnian
- 14–15. *Equisetoporites chinleanus* Daugherti, Borehole Váralja-26, 951.00–951.5 m, Rhaetian
16. *Chasmatosporites hians* Nilsson, Borehole Váralja-26, 720.40–720.50 m, Rhaetian
Magnification: 750x

Plate V

1. *Striatoabietites aytugii* Visscher, Borehole Váralja-20, 704.00 m, Carnian
2. *Ovalipollis pseudoalatus* (Thierg.) Schuurman, Borehole Váralja-20, 704.00 m, Carnian
3. *Chordasporites australiensis* De Yerse massula, Borehole Váralja-20, 704.00 m, Carnian
4. *Undulatasporites anguineus* Leschik, Borehole Komló-120, 528.90–539.80 m
Carnian–Norian
5. *Klausipollenites* cf. *schaubergeri* (Pot. et Klaus) Jans., Borehole Szentkatalin-1, 393.20 m
Norian
6. *Ricciisporites tuberculatus* Lundbl., Borehole Szentkatalin-1, 393.20 m, Norian
7. *Undulatasporites lucens* Leschik, Borehole Váralja-20, 665.00 m, Carnian–Norian
8. *Undulatasporites lucens* Leschik, Borehole Váralja-20, 661.20–661.30 m, Carnian–Norian
Magnification: 750x

Plate VI

1. *Duplexisporites problematicus* (Couper) Playf. et Dettm., Borehole Váralja-20, 704.00 m, Carnian
 2. *Convolutispora klukiforma* (Nilsson) E. Sch., Borehole Váralja-20, 704.00 m, Carnian
 3. *Contiguisporites dunrobiensis* (Couper) E. Sch., Borehole Váralja-20, 704.00 m, Carnian
 4. *Lophotriletes verrucosus* E. Sch., Borehole Váralja-20, 704.00 m, Carnian
 5. *Lophotriletes* *fsp.*, Borehole Váralja-20, 704.00 m, Carnian
 6. *Microreticulatisporites fuscus* (Nilsson) Morbey, Borehole Váralja-20, 704.00 m, Carnian
 7. *Trachisporites tuberosus* Nilsson, Borehole Vasas-32, 52.00–52.20 m, Rhaetian
 8. *Trachisporites asper* Nilsson, Borehole Váralja-20, 704.00 m, Carnian
 9. *Tigrisporites microrugulatus* E. Sch., Borehole Szentkatalin-1, 393.20 m, Norian
 10. *Conbaculatisporites mesozoicus* Klaus, Borehole Váralja-20, 704.00 m, Carnian
 11. *Anapiculatisporites spiniger* (Leschik) Reinh., Borehole Váralja-26, 791.00–791.10 m, Rhaetian
 12. *Anaplanisporites telephorus* (Pauts) Jans., Borehole Váralja-20, 704.00 m, Carnian
 13. *Apiculatisporites parvispinosus* (Leschik) E. Sch., Borehole Váralja-20, 704.00 m, Carnian
 14. *Anemiidites spinosus* Mädlér, Borehole Váralja-26, 788.00–788.10 m, Carnian
 15. *Anemiidites spinosus* Mädlér, Borehole Vasas-52, 52.00–52.20 m, Rhaetian
 16. *Zebrasporites interscriptus* (Thierg.) Klaus, Borehole Vasas-63, 157.30–157.90 m, Rhaetian
 17. *Zebrasporites corneolus* Klaus, Borehole Tettye-1, 284.50–284.60 m, Carnian–Norian
- Magnification: 750x

Plate VII

1. *Alisporites robustus* Nilsson, Borehole Váralja-26, 1019.50–1019.60 m, Rhaetian
2. *Pinuspollenites minimus* (Couper) Kemp., Borehole Husztót-2, 561.10–564.00 m, Norian
3. *Cyathidites australis* Couper, Borehole Szentkatalin-1, 389.00 m Norian
4. *Osmundacidites wellmanii* Couper, Borehole Husztót-2, 561.10–564.00 m Norian
5. *Eucommiidites* *fsp.*, Borehole Pécs-57, 457.00 m, Carnian
6. *Quadraeculina anellaeformis* Mal., Borehole Váralja-15, 900.80–9.01.00 m, Rhaetian
7. *Eucommiidites* *fsp.*, Borehole Szentkatalin-1, 393.20 m, Norian
8. *Ginkgocycadophytus* *fsp.*, Borehole Szentkatalin-1, 393.20 m, Norian
9. *Schizosporis parvus* Cookson et Dettm., Borehole Váralja-20, 704.00 m, Carnian
10. *Retitriletes* *fsp.*, Borehole Vasas-52, 52.00–52.20 m, Rhaetian
11. *Cyathidites minor* Couper, Borehole Szentkatalin-1, 389.00, Norian
12. *Monosulcites minimus* Cookson, Borehole Husztót-2, 566.90–567.00 m, Norian
13. *Monosulcites* *fsp.*, Borehole Vasas-52, 52.00–52.20 m, Rhaetian
14. *Vitreisporites pallidus* (Reiss) Nilsson, Borehole Pécs-57, 441.50 m, Carnian
15. *Vitreisporites pallidus*, (Reiss) Nilsson, Borehole Váralja-26, 472.70–472.80 m, Rhaetian
16. *Punctatosporites scabratus* (Couper) Norris, Borehole Váralja-26, 800.40–800.50 m, Rhaetian

Plate VIII

1. *Nevesisporites limatulus* Playf., Borehole Váralja-20, 703.20–703.90 m, Carnian
2. *Reticulatasporites adunctus* Leschik, Borehole Váralja-20, 661.20–661.30 m, Carnian–Norian
3. *Calamospora nathorstii* (Halle) Klaus, Borehole Váralja-26, 951.00–951.10 m, Rhaeti
4. *Micrhystridium* sp., Borehole Pécs-57, 457.70 m, Carnian
5. *Conbaculatisporites* fsp., Borehole Váralja-26, 788.00–788.10 m, Rhaetian
6. *Rogalskaisporites cicatricosus* (Rog.) Danze-Corsin et Lav., Borehole Vasas-63, 157.30–157.90 m, Rhaetian
7. *Stereisporites* fsp., Borehole Váralja-20, 704.00 m, Carnian
8. *Cyclinasporites glabrus* (Mal.) Nilsson, Borehole Vasas-39, 43.50 m, Rhaetian
9. *Lycopodiacidites* cf. *franconense* Achilles, Borehole Váralja-20, 404.00 m, Carnian
10. *Triancoraesporites ancorae* (Reinh) E. Sch., Borehole Váralja-18, 586.70–586.80 m, Rhaetian
11. *Triancoraesporites ancorae* (Reinh) E. Sch., Borehole Váralja-15, 900.80–9.0.00 m, Rhaetian
12. *Retusotriletes* fsp., Borehole Váralja-20, 704.00 m, Carnian
13. *Inaperturopollenites reissingeri* (Kedves) Bóna, Borehole Pécs-57, 175.00 m, Norian
14. *Lycopodiumsporites semimuris* Danze-Corsin et Lav., Borehole Vasas-45, 32.0–33.50 m, Rhaetian
15. Plankton with one appendage, Borehole Váralja-26, 726.40–726.50 m, Rhaetian
16. *Hystrichosphaeridium magnum* determ. prov., Borehole Váralja-15, 838.30 m, Rhaetian
17. *Dinoflagellata* indet., Borehole Váralja-15, 900.80–901.00 m, Rhaetian

Plate IX

1. *Chasmatosporites major* Nilsson, Borehole Váralja-26, 735.70–735.80 m, Rhaetian
2. *Hystrichosphaeridium magnum* determ. prov., Borehole Váralja-26, 838.30 m, Rhaetian
3. *Hystrichosphaeridium magnum* determ. prov., Synonym: *Porcellispora magna* Bóna 1983, pp. 75–76, Borehole Nagymányok-12, 405.80 m, Norian
4. *Micrhystridium* sp., Borehole Pécs-57, 457.00 m, Carnian
5. *Micrhystridium* sp., Váralja-26, 466.40–466.50 m, Rhaetian
6. *Hystrichosphaeridium magnum* determ. prov., Borehole Váralja-34, 433.30–434.90 m, Rhaetian
7. *Microforaminifer*, Borehole Váralja-20, 704.00 m, Carnian
Magnification: 750x

Plate X

- 1–2. *Alisporites* fsp., Borehole Máza-23, 1408.40–1408.50 m, Rhaetian
3. *Patellina plicata* Mal., Máza-23, 1408.40–1408.50 m, Rhaetian
4. *Ovalipollis* fsp., Máza-23, 1408.40–1408.50 m, Rhaetian
5. *Chasmatosporites apertus* (Rog.) Nilsson, Máza-23, 1408.40–1408.50 m, Rhaetian
6. *Pollenites* fsp. (papillat), Borehole Váralja-9, 777.50–782.8 m, Rhaetian
7. *Monosaccites* indet., Borehole Váralja-9, 691.80–691.90 m, Rhaetian
Magnification: 850x

Plate I



Plate II

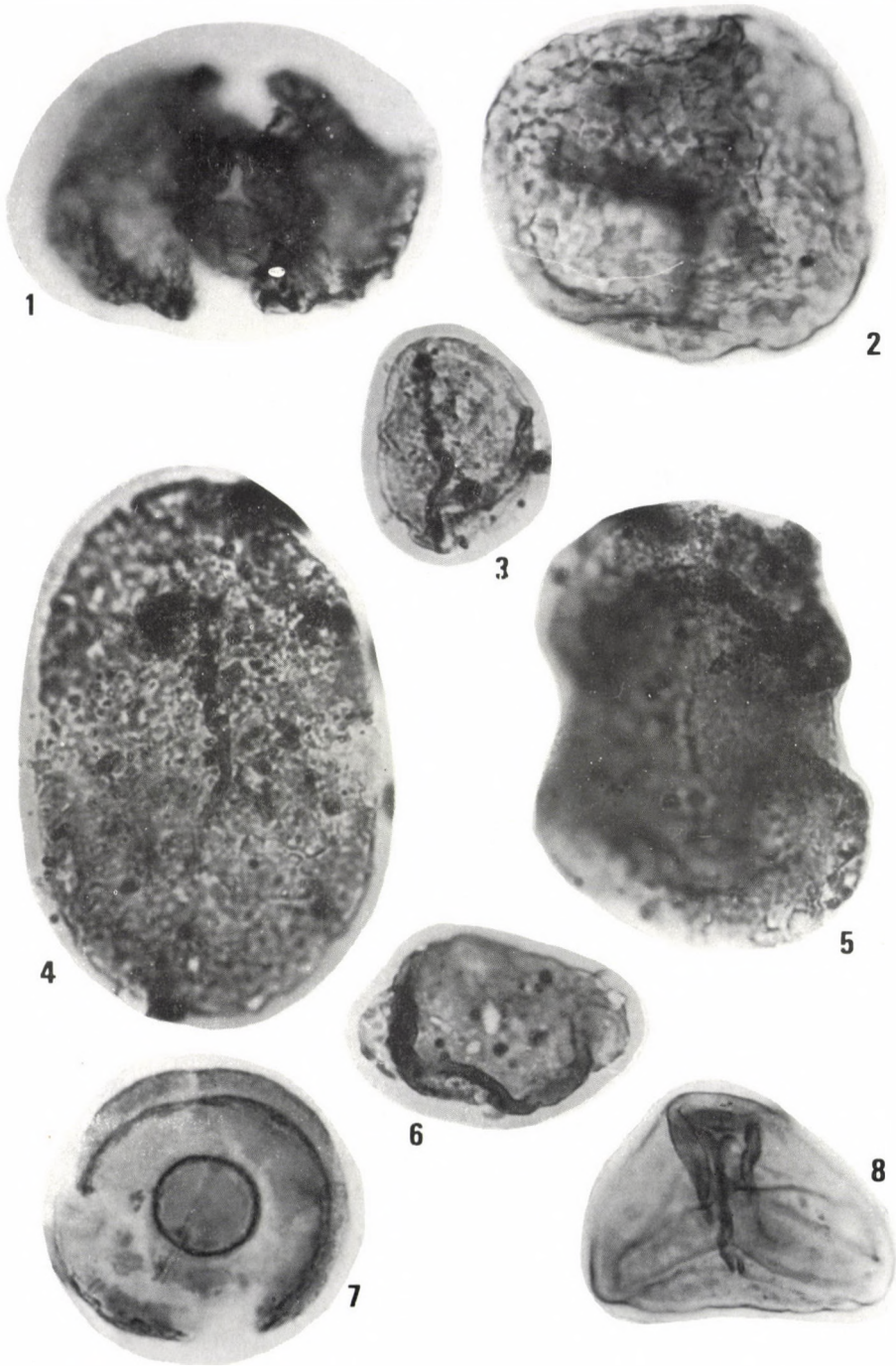


Plate III

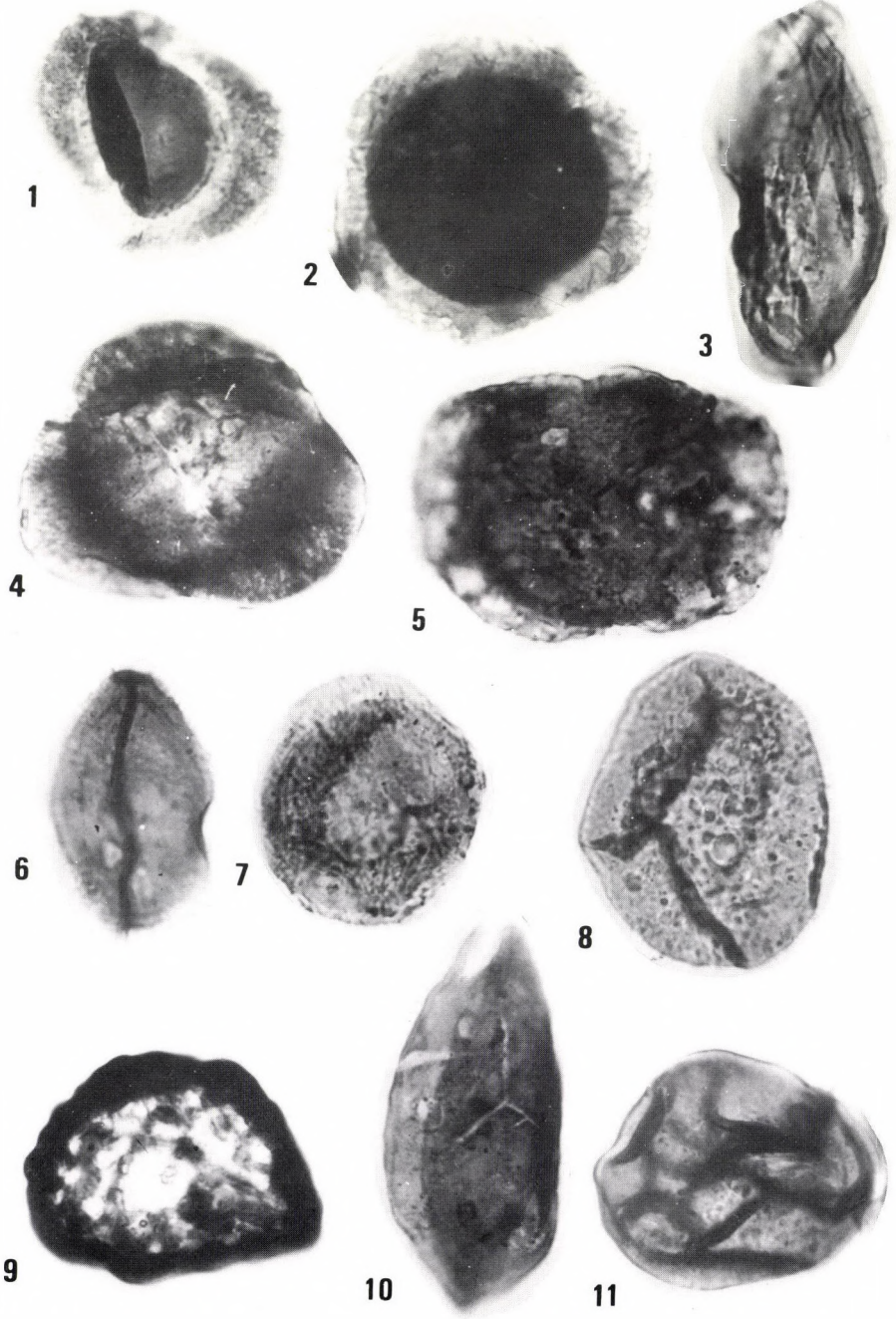


Plate IV

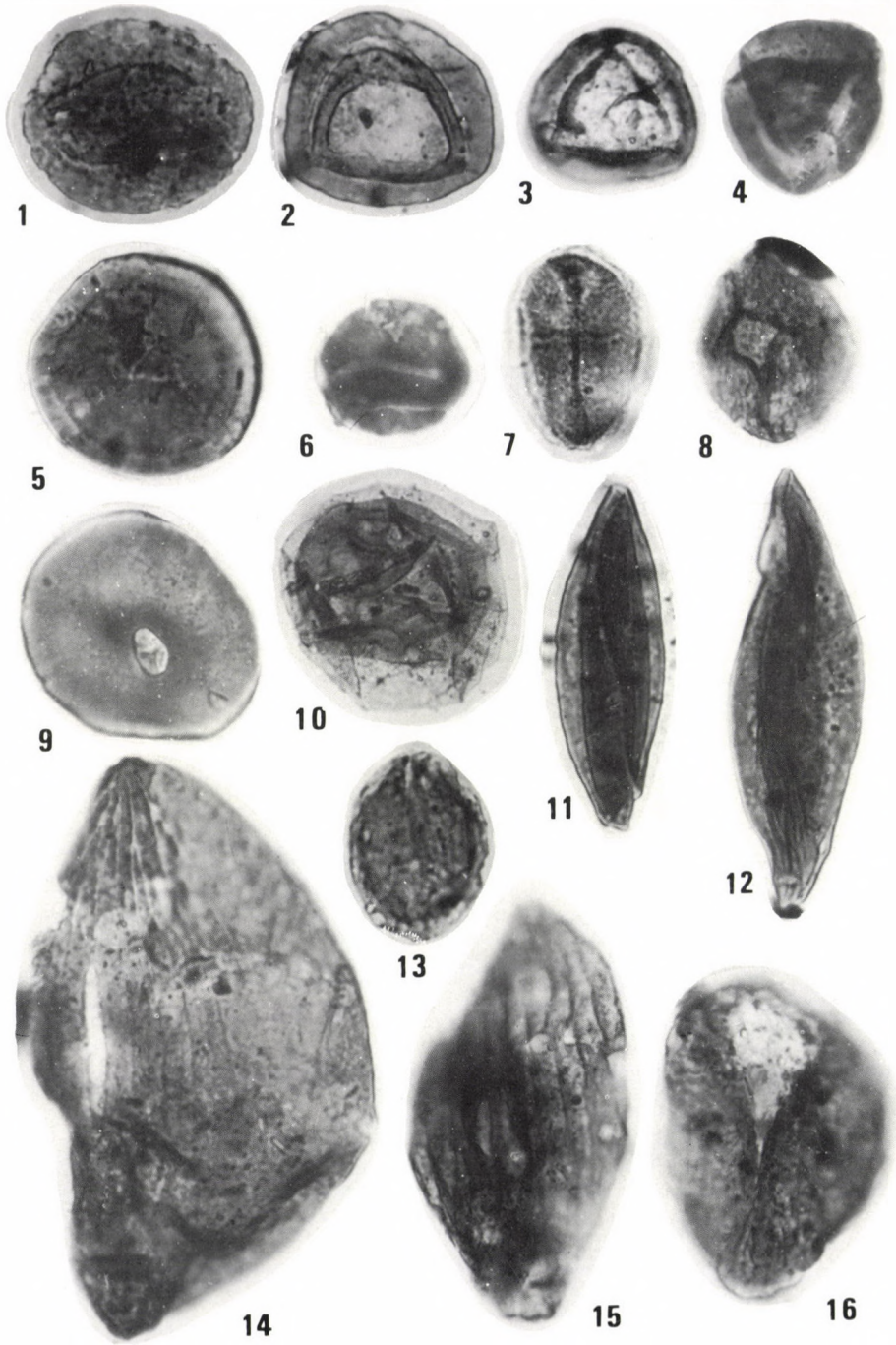


Plate V

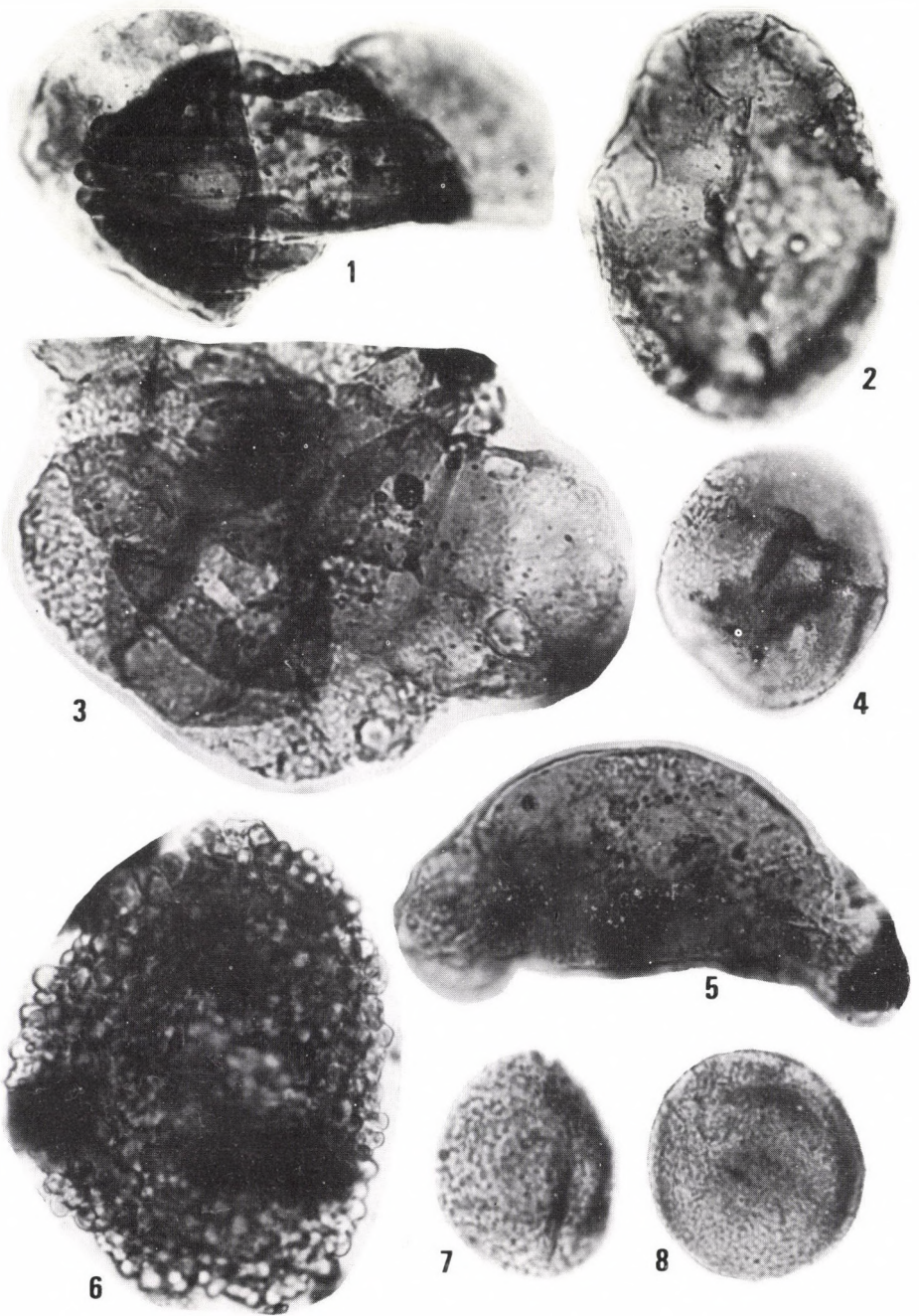


Plate VI

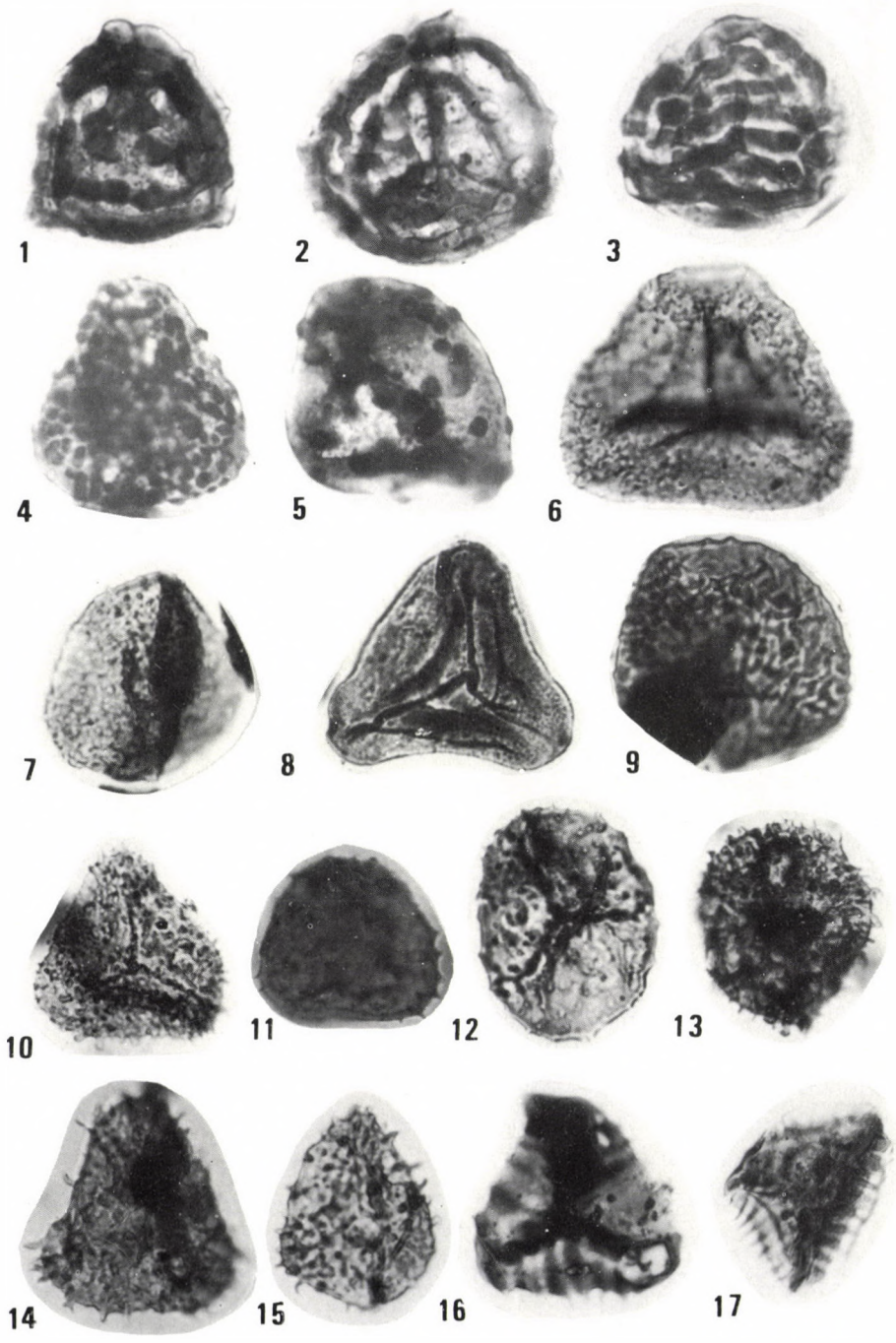


Plate VII

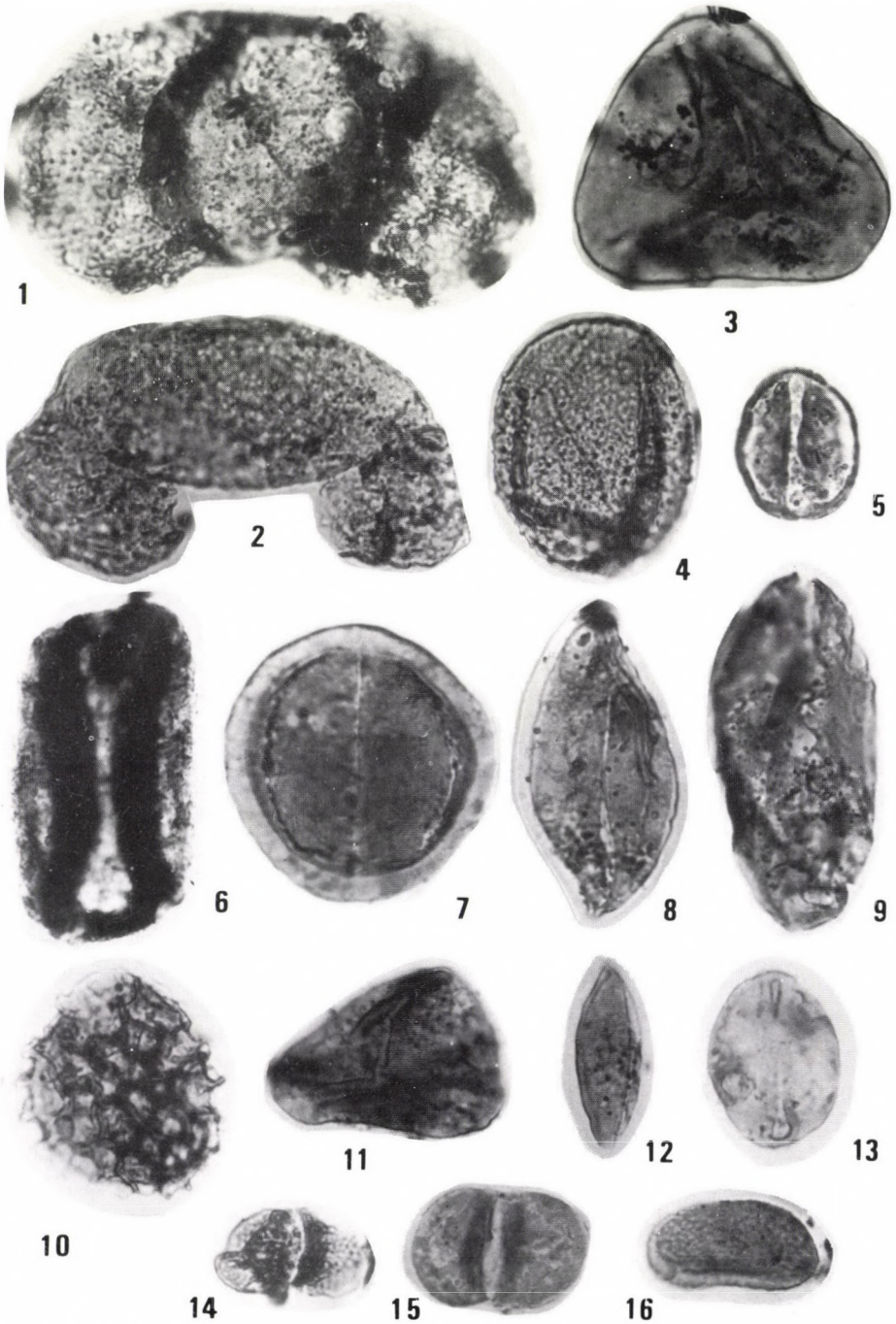


Plate VIII

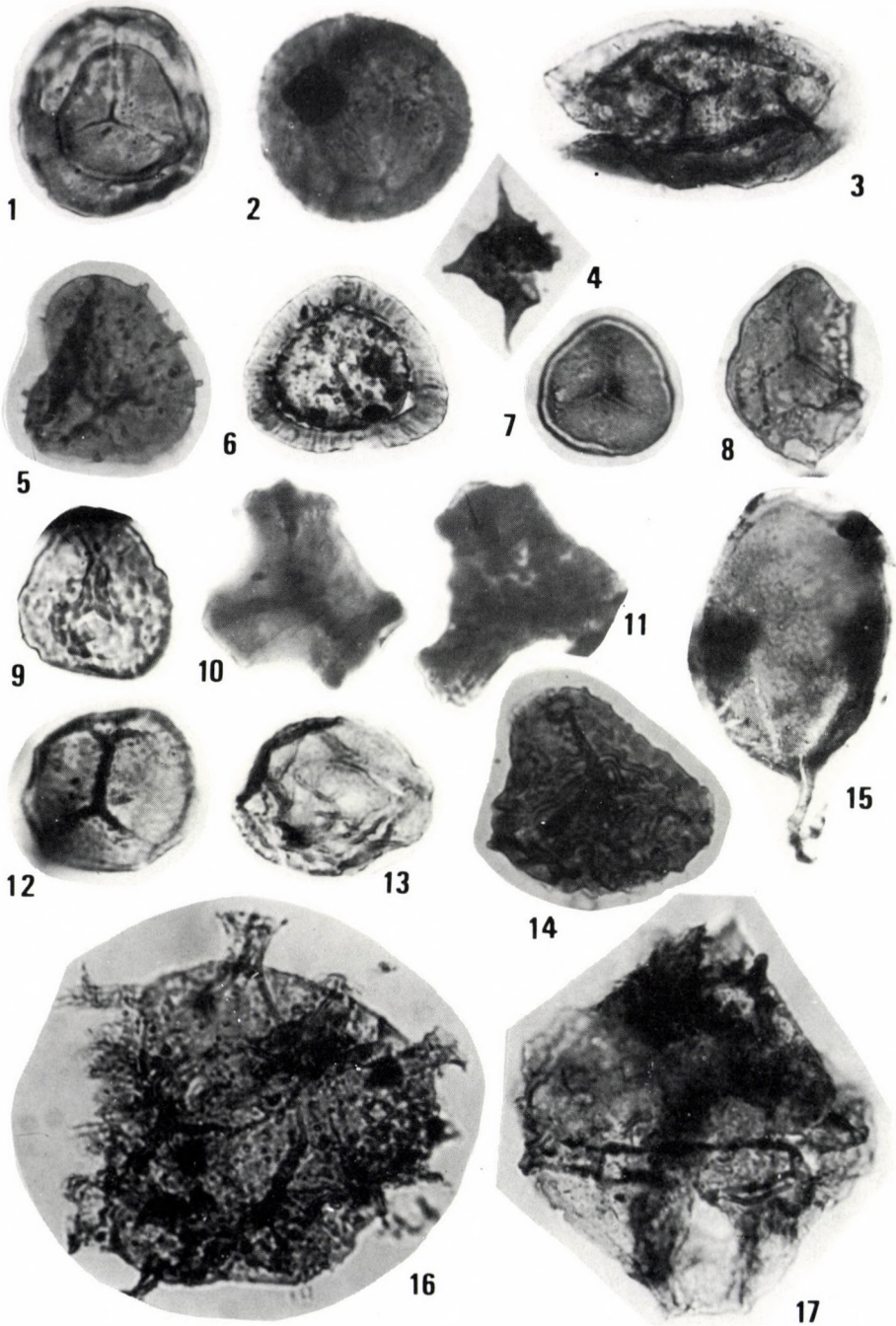


Plate IX

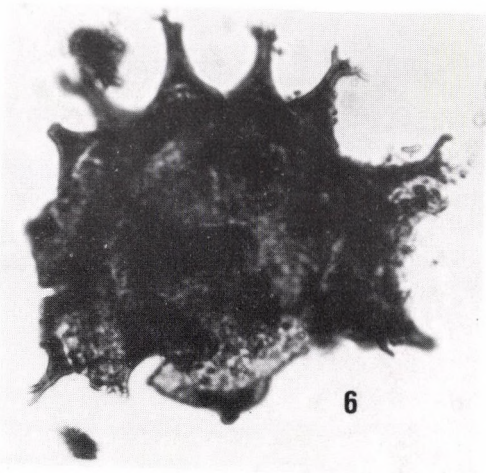
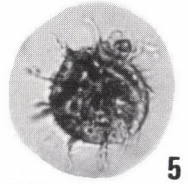
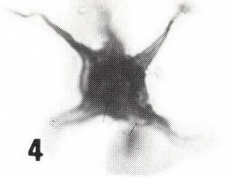
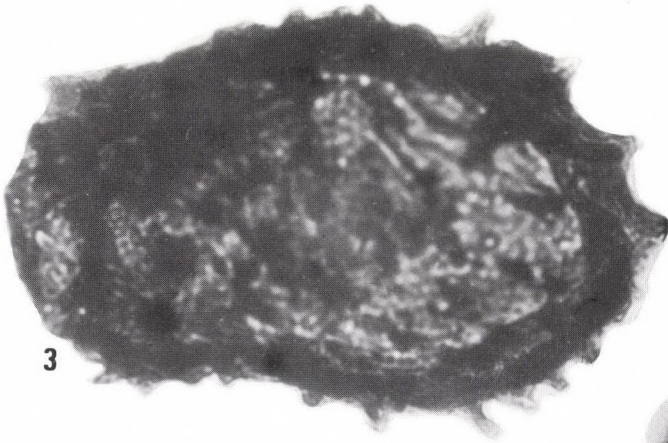
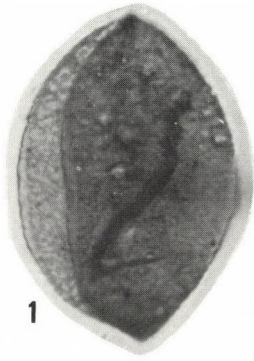
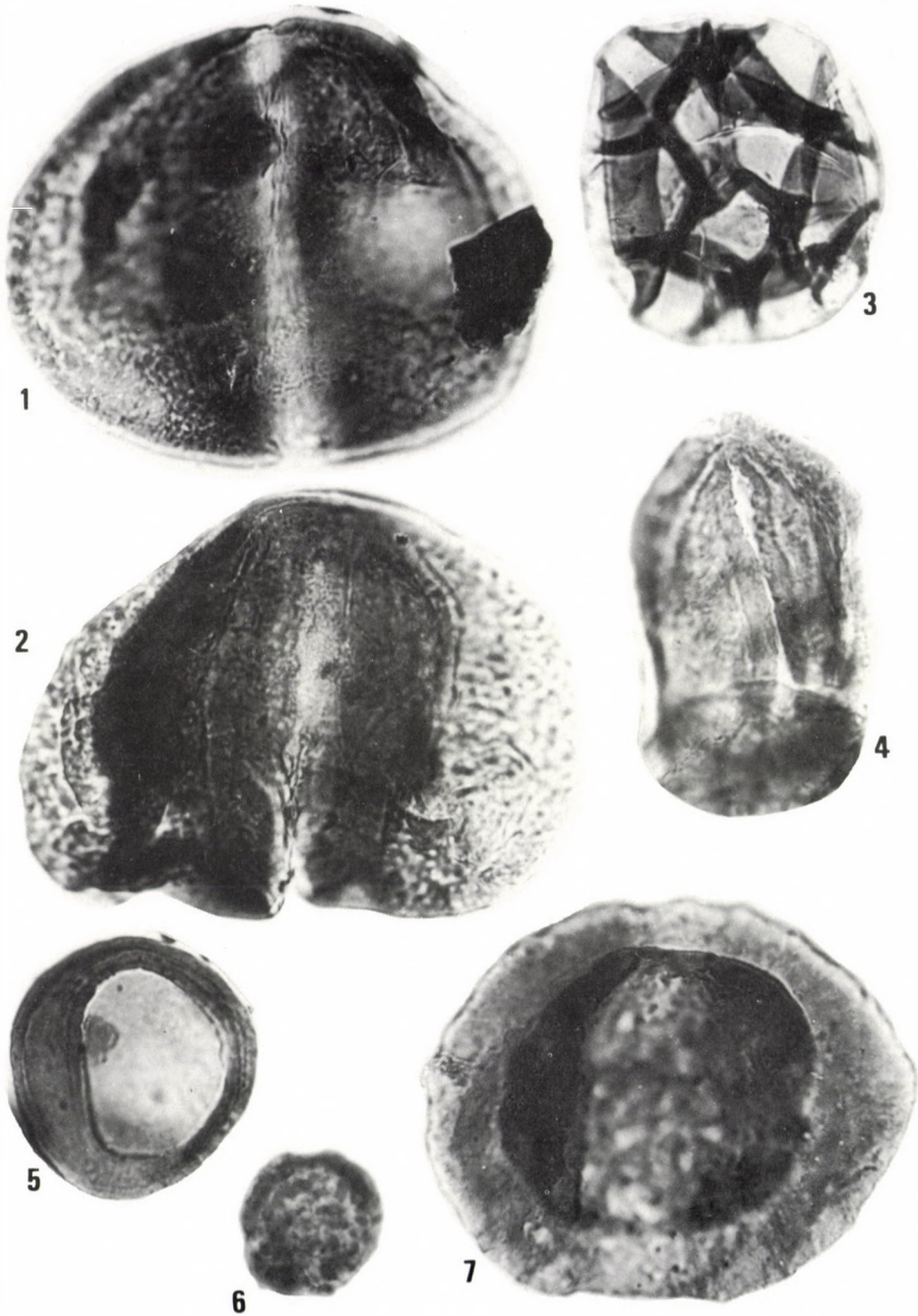


Plate X



References

- Achilles, A 1981: Die rätische und liassische Microflora Frankens. – *Palaeontogr., Abt. B.*, 179, pp. 1–86.
- Achilles, H., H. Kaiser, H.J. Sweitzer 1984: Die rätó-jurassischen Floren des Iran und Afganistans. 7. Die Microflora der obertriadisch–jurassischen Ablagerungen des Alborz-Gebirges (Nord-Iran). – *Palaeontogr., Abt. B.* 194, pp. 14–95.
- Antonescu, E. 1973: Quelques données sur la palynologie du lias sous faciès de Gresten de Rumanie. – In: Chlonova, A.F. (Ed.): *Palynology of Mezophyte. Proc. Int. Palynol. Conf. 3rd, Novosibirsk 1971*, pp. 53–57.
- Balla, Z. 1988: Late Eocene tectonic pattern of the Carpatho-Pannonian region and its bearing on the Mesozoic reconstructions of the Tethys. – *Földt. Közl.*, 118, pp. 11–26.
- Balogh, K. 1981: Correlation of the Hungarian Triassic. – *Acta Geol. Hung.*, 24, 1, pp. 3–48.
- Barabás-Stuhl, Á. 1981: Microflora of the Permian and Lower Triassic sediments of the Mecsek Mountains (South Hungary). – *Acta Geol. Hung.*, 24, 1, pp. 49–97
- Bóna, J. 1963: A mecseki liász feketekőszéntelegek távolazonosítására irányuló palynológiai vizsgálatok (Palynological investigations aimed at remote sensing the liassic black coal seams). – *Földt. Közl.*, 93, 1, pp. 15–23.
- Bóna, J. 1969: Palynologie. – In: Nagy, E. (Ed.): *Unterliás–Kohlenserie des Mecsek-Gebirges, Geologie. MÁFI Évk.*, 51, pp. 623–707.
- Bóna, J. 1973: Palynological practice i the investigation of liassic coal maesures in the Mecsek Mountains. – *Ösl. Viták (Discuss. Paleontologicae)*, 21, pp. 65–71, Budapest.
- Bóna, J. 1974: A mecseki feketekőszén-készlet palynológiai vizsgálatának eredményei (Results of palynological investigation of black coal measures in the Mecsek Mountains). – *Pécsi Műszaki Szemle*, 19, 1–2, pp. 17–18.
- Bóna, J. 1979: Telepcsoportok távolazonosítása a mecseki feketekőszén összletben palynológiai alapon (Remote identification of seam groups in the black coal measures of the Mecsek Mountains on palynological basis). – *Földt. Kut.*, 22, 4, pp. 29–32.
- Bóna, J. 1983a: Palynological studies on the Upper Triassic and Lower Liassic of the Mecsek Mountains. – *Ösl. Viták (Discuss. Paleontologicae)*, 29, pp. 47–57, Budapest
- Bóna, J. 1983b: A Máza-Dél–Váralja-Dél feketekőszén összlet pollenvizsgálati eredményei (Results of pollen investigation of the black coal measures of Máza-South, Váralja-South). – *Földt. Kut.*, 26, 2–3, pp. 73–80.
- Bóna, J. 1984a: Contributions to the palynostratigraphic division of the Upper Triassic and Lower Liassic in the Mecsek Mts. – *MÁFI. Évi jel. 1982-ről*, pp. 203–216.
- Bóna, J. 1984b: Szintjelző spórák és virágporszemek a kelet-mecseki felső triász kőszénfekü rétegekből (Spore and pollen guide forms in the Upper Triassic black coal footwall layers of the eastern Mecsek Mountains). – *Folia Comloensis*, 1, pp. 3–25.
- Dercourt, J., G. Bignot, P. Cros., P. DeWever, C. Guernet, G. Lachkar, J. Geissant, G. Lepvrier, F. Bergerat, B. Géczy 1984: Hungarian Mountains in Alpine framework. – *Acta Geol. Hung.*, 27, 3–4, pp. 213–221.
- Döring, H. 1965: Die sporen paläontologische gliederung des Wealden in Westmecklenburg (Struktur Werle). – *Geologie, Beih.*, 47, pp. 1–118.
- Dunay, R.E., M.I. Fischer 1974: Late Triassic palynofloras of North America and their European correlatives. – *Rev. Palaeobot. Palynol.*, 17, pp. 179–186.
- Dunay, R.E., M.I. Fischer 1979: Palynology of the Dockum Group (Upper Triassic). Texas. – *Rev. Palaeobot. Palynol.*, 28, pp. 61–92.
- Gluzbar, E.A. 1973: Correlation of several Lower Mesozoic geological sections of Europe based on palynological data. – In: Clonova A.F. (Ed.): *Palynology of Mesophyte. Proc. Int. Palynol. conf. 3rd. Novosibirsk 1971*, pp. 44–48.

- Góczán, F. 1956: A komlói liász feketekőszéntelepek azonosítására irányuló pollenanalitikai (palynológiai) vizsgálatok (Pollen analytical (palynological) investigations aimed at identifying the Liassic black coal seams of Komló. – *MÁFI. Évk.*, 45, 1, pp. 135–166.
- Góczán, F., J. Haas, H. Ióric, A. Oravec-Scheffer 1983: Faciological and stratigraphical evaluation of a Carnian key section (borehole Hévíz-6.). *MÁFI Évi Jel.* 1981-ről, pp. 263–293.
- Horowitz, A. 1973: Triassic miospores from Southern Israel. – *Rev. Palaeobot. Palynol.*, 16, 3, pp. 175–207.
- De Jersey, N.J. 1962: Triassic spores and pollen grains from the Rosewood coalfield. – *Queensland Govt. Min. J.*, 60, pp. 346–366.
- De Jersey, N.J. 1964: Triassic spores and pollen grains from the Bundaba groups. – *Publ. Geol. Surv. Queensl.*, 321, pp. 1–21.
- Klaus, W. 1960: Sporen der Karnischen Stufe der Ostalpinen Trias. – *Jahrb. Geol. Bundesanst. Sonderb.*, 5, pp. 107–184.
- Káli, Z. 1962: Üledékciklusosság a mecseki kőszéntelepes öszszletben. Komlói terület (Sediment cyclicity in the coal seam measures of Mecsek. Komló area). – *Földt. Kut.*, 5, 12, pp. 12–32, Budapest.
- Kovács, S. 1983: Az Alpok nagyszerkezeti áttekintése (Megastructural review of the Alps). – *Ált. Földt. Szemle*, 18, pp. 77–155, Budapest.
- Kovács, S. 1998: Tiszia-probléma és lemeztekonika – kritikai elemzés a koramezozoós fácieszónák eloszlása alapján (Tisia problem and plate tectonics critical analysis on the basis of the distribution of the Early Mesozoic facies zones). – *Földt. Kut.*, 27, 1, pp. 55–72.
- Krutzsch, W. 1955: Zur Bedeutung microbotanischer (sporen-paläontologischer) Untersuchungen für die praktische Geologie. – *Zeitschrift für angew. Geol.*, 3–4, pp. 137–145.
- Lachkar, G., J. Bóna, M.J. Pavillon 1984: The Liassic Gresten facies: palynological data and paleogeographical significance. – *Acta Geol. Hung.*, 27, 3–4, pp. 409–416.
- Leschik, G. 1955: Die Keuperflora von Neuwelt bei Basel II. Izo und Microsporen – *Schweiz Paleont. Abh.*, 62, pp. 1–70.
- Litwin, R.J. 1985: Fertile organs and in situ spores of ferns from the Late Triassic Chinle Formation of Arizona and New Mexico, with discussion of the associated dispersed spores. – *Rev. Paleobot. Palynol.*, 44, 2/1, pp. 101–146.
- Lund, J. 1977: Rhaetic to Lower Liassic palynology of the onshore south-eastern North Sea Basin. – *Geological Survey of Denmark, II. Series No.* 109.
- Maljavkina, V.S. 1953: Verhnyetriaszov e, nyizsyejurszkie i szrednyejurszkie szporovo-pülcevje komplexü vosztočno i zapadno Priuralja. – *Trudü VNIGRI*, 75, pp. 94–147.
- Mädler, K. 1964: Bemerkenswerte Sporenformen aus dem Keuper und unteren Lias. – *Fortschr. Geol. Rheinl. u. Westf.*, 12, pp. 169–200.
- Mägdefrau, K. 1956: Paläobiologie der Pflanzen. – Jena.
- Morbey, S.J., R. Neves 1974: A cheme of palynologically defines concurrent range zones and subzones from the Triassic Rhaetian stage (sensu lato). – *Rev. Paleobot. Palynol.*, 17, pp. 161–173.
- Nagy, E. 1968: Triasbildungen des Mecsek-Gebirges. – *MÁFI Évk.* 51, 1, pp. 1–198.
- Némédi-Varga, Z. 1968: Geologische und Gebirgsstructurelle Verhältnisse des Steinkohlengbietes von Hosszúhetény. – *Nehézipari Műszaki Egyetem Közl.*, 11, pp. 11–34.
- Némédi, V.Z. 1969: Geophysik. Bewertung der Karotageprofil. – In: Nagy, E. (Ed.): *Unterlias-Kohlenserie des Mecsek-Gebirges (Geologie)*. – *MÁFI Évk.* 51, 2, pp. 593–621.
- Nilsson, T. 1958: Über das Vorkommen eines mesozoischen Sapropelgestein in Schonen. – *Lunds Univ. Arss. Avd.*, 2, 54, 10, pp. 5–112.
- Norris G. 1965: Triassic and Jurassic micropores and Acritarchs from the Beacon and Ferrar Groups, Victoria Land, Antarctica. – *N. Z. Jl. Geol. Geophys.*, 8, pp. 236–277.
- Pedersen, K.R., J. Lund. 1980: Palynology of the plant-bearing Rhaetian to Hettangian Kap Stewart Formation, Scoresby Sund, East Greenland. – *Rev. Paleobot. Palynol.*, 31, pp. 1–69.

- Potonié, R. 1956, 1958, 1960, 1966: Synopsis der Gattungen der Sporae dispersae. Teil I, II, III, IV. – *Beih. Geol. Jb.*, 23, 31, pp. 39–72
- Sakulina G.V. 1973: Middle and Late Triassic miospores from South-Eastern Kazahstan. – In: Clonova, A.F. (Ed.): *Palynology of Mesophyte – Proc. Int. Palynol. Conf. 3rd, Novosibirsk (1971)*, pp. 33–38.
- Scheuring, B.W. 1970: Palynologische und palynostratigraphische Untersuchungen des Keupers in Bülchertunnel (Solothurner Jura). – *Schweiz. Pal. Abh.*, 88, pp. 1–119.
- Scheuring, B.W. 1978: Microfloren aus dem Mezidekalken des Mte. San Giorgio (Kanton Tessin). – *Schweiz. Pal. Abh.*, 100, pp. 1–100.
- Smit, D.G. 1974: Late Triassic pollen and spores from the Kapp Toscana Formation, Hopen Svalbard – a preliminary account. – *Rev. Paleobot. Palynol.*, 17, pp. 175–178.
- Schulz, E. 1967: Sporenpaläontologische Untersuchungen rätoliasischer Schichten im Zentralteil des germanischen Beckens. – *Paläontol. Abh.*, B, 2, 3, pp. 543–633.
- Schurmann, W.M.L. 1979: Aspect of Late Triassic Palynology. 3. Palynology of Latest Triassic and Earliest Jurassic deposits of the Northern Limestone Alps in Austria and Southern Germany, with special reference to a palynological characterization of the Rhaetian Stage in Europe. – *Rev. Paleobot. Palynol.*, 27, 1, pp. 53–75.
- Semenova, E.V. 1973: Correlation of the Upper Triassic of Donets basin and some European regions in according to miospores. – In: Clonova, A.F. (Ed.): *Palynology of Mesophyte. Proc. Int. Palynol. Conf 3rd, Novosibirsk (1971)* pp. 42–44.
- Szilágyi, T. 1987: A Mecseki kőszén Formáció faciológiai és teleptani értékelése a Máza-Váralja-Dél területen (Faciological and economic geological evaluation of the Mecsek Coal Formation in the Máza-South, Váralja-South area). – Manuscript
- Szilágyi, T., E. Villám 1985: Összefoglaló jelentés a Máza-Dél-Váralja-Dél feketekőszénterület felderítő fázisú kutatásáról és készletszámításáról (Summary report on the preliminary survey of black coal area Máza-South, Váralja-South. – OFKfV Doc. centre, Váralpota (Manuscript).
- Van der Eem, J.G.L.A. 1983: Aspects of Middle and Late Triassic palynology. 6. Palynological investigations in the Ladinian and Lower Karnian of the Western Dolomites, Italy. – *Rev. Paleobot. Palynol.*, 39, pp. 189–300.
- Visscher, H., K.A. Brugman 1981: Ranges of selected palynomorphs in the Alpine Triassic of Europe. – *Rev. Paleobot. Palynol.*, 34, 1, pp. 115–128.
- Visscher, H., L. Krystun 1978: Aspects of Late Triassic palynology. 4. A. Palynological assemblage from ammonoid controlled Late Karnian (Tuvalian) sediments of Sicily. – *Rev. Paleobot. Palynol.*, 26, pp. 93–112.
- Venkatalacha, B.S., F. Góczán 1964: The spore-pollen flora of the Hungarian "Kössen facies". – *Acta Geol. Hung.*, 8, pp. 203–228.
- Warrington, G. 1974: Studies in the palynological biostratigraphy of the British Trias. I. Reference sections in West Lancashire and North Somerset. – *Rev. Paleobot. Palynol.*, 17, pp. 133–148.
- Wéber, B. 1978: Újabb adatok a Mecsek-hegységi anizuszi és ladini rétegek ismeretéhez (Newer data on the Anisian and Ladinia layers of the Mecsek Mountains). – *Földt. Közl.*, 108, 2, pp. 137–148.
- Wéber, B. 1990: Ladin és felső triász rétegek a Ny-Mecsek északi előterében (Ladinian and Upper Triassic layers in the northern foreland of the western Mecsek Mountains). – *Földt. Közl.*, 120, 3–4, pp. 153–180.
- Weiss, M. 1989: Die Sporenfloren aus Rät und Jura Südwest-Deutschlands und ihre Beziehung zur Ammonitenstratigraphie. – *Palaeontogr. Abt.*, B, 215, Lfg. 1–6, pp. 1–168.

Results of isotope-geochemical studies in sedimentological and environmental geologic investigations of Lake Balaton

Tibor Csernyi
Hungarian Geological Institute, Budapest

Ede Hertelendi
*Institute of Nuclear Research of
Hungarian Academy of Sciences, Debrecen*

Sándor Tarján
National Food Investigation Institute, Budapest

In the complex geological research of Lake Balaton, several new methods were introduced. Among these methods, the isotope-geochemical tests have proved to be very efficient, allowing us to have a better understanding of a few questions concerning the environmental status of Lake Balaton (rate of mud deposition, physical properties and underwater motion of mud, etc.), and to have a better knowledge of formerly known features (the age of Lake Balaton, reconstruction of the climate of its environment etc.).

According to the C^{14} -dating of the peat, the development of the Lake started at the beginning of the Late-Pleistocene (Bølling) and this process lasted approx. 1500 years.

The values of oxygen isotope ratios measured in the autochthonous carbonate deposits of the lake and on the carbonate test of gastropods allow us to trace the gradual warming-up of the climate which started in Holocene time.

Upon the comparative analysis of tendencies concerning the ^{18}O value of the water in Lake Balaton and the weather conditions can clearly be seen.

The artificial radio-isotopes entering the atmosphere since 1950 till today can be well traced in the lake's mud. Their occurrence and maximum peaks have allowed us to determinate the rate of mud development. Under undisturbed hydrological conditions, this value ranges from 0.5 cm/year to 1.4 cm/year, as function of the measurement point. The rate of mud development has shown a dramatically increasing tendency. In some points of Lake Balaton, underwater transport of the deposit, whereas in other sites accumulation of this transported deposit takes place.

Key words: Lake Balaton, limno-geology, isotope-geochemistry, environmental geology, Quaternary

Introduction

Lake Balaton, an important part of our valuable national treasures, is the largest shallow-water lake in Central Europe. A great number of experts have been involved in its investigations, including its surroundings, since the end

Addresses: T. Csernyi: H-1143 Budapest, Stefánia út, 14, Hungary
E. Hertelendi: H-4001 Debrecen, Bem tér 18/c, Hungary
S. Tarján: H-1097 Budapest, Gyáli út 3/a, Hungary

Received: 26 Jun, 1995

of the last century, from different but always new aspects (among many others, major milestones include: Lóczy 1913; Sebestyén 1951; Bulla 1958; Bendefy and Nagy 1969; Baranyi 1979; Marosi and Szilárd 1981; Mike 1980a, b; Herodek and Máté 1984; Máté 1987; Zólyomi 1952, 1969, 1987; Szesztay et al. 1966; Müller 1970; Müller and Wagner 1978; Rónai 1969; Somlyódy et al. 1983). Apart from always enriching the knowledge of scientists, the lake calls attention to itself more and more frequently with new problems (such as mud deposition, eutrophication, the upsetting of the ecological equilibrium, etc.), presenting a challenge for biologist, limnologist and geologist alike. Experts from the Hungarian Geological Institute have been investigating the lake and its catchment area since 1965, because the actual status of the lake depends on the geologic background (as a dead environment), the ecological changes in the water catchment area and the living world of the lake, and the age of the lake itself.

The investigation of Lake Balaton is of great importance due to the intensive mud deposition and eutrophication of the lake itself. Although the aging and filling-up of lakes is a natural process, it may be accelerated by some environmental (particularly, human) influences.

The aim of the limno-geological investigations which began in 1981 was to study the present sedimentological conditions and the diagenesis of shallow-water carbonate sediments. This project, which started as a methodological investigation, also aimed, from 1986, at a better understanding of the history of development of the lake and the changes in its ecological conditions. The over 370 km long geophysical (seismo-acoustic) log recorded during the investigation and a total of 33 boreholes drilled into the lake bed have allowed us to compile a mud thickness map and a seismo-acoustic tectonic map of the basement of Lake Balaton (at the scale of 1 : 50 000). Samples from some two-thirds of the boreholes have been subjected to complex material testing (sedimentological, soil-physical, mineralogical, petrologic, geochemical, and paleontological investigations – Miháltz-Faragó 1982; Bodor 1987; Bruckner-Wein 1982; Cserny 1987, 1990; Cserny and Corrada 1989; Cserny et al. 1991).

The aim of this paper is to give a brief description of the isotope geochemical investigations performed and the results obtained using this method, which relate to the geologic questions which have been of concern to us.

Müller and Wagner (1978) were the first to perform an isotope-geochemical investigation of Lake Balaton, and presented a reconstruction of climate on the basis of results of mineralogical, geochemical and isotope-geochemical examinations of Quaternary lacustrine sediments. The autochthonous carbonate deposit of the fraction of the samples finer than 0.2 mm was tested for ^{18}O isotope ratio. It was also noticed that the calcite lattice of some bed portions has a higher MgCO_3 concentration, and here an unarranged protodolomite is encountered, to which high Sr concentration and a positive ^{18}O value belong. It is normal that, in the case of an intensive evaporation, the ^{18}O value occurs in larger proportion in water, and this may lead to an isotope enrichment in

the calcareous deposits as well. Two well-distinguishable Mg maxima were observed in the borehole. After comparing them with the results from the palynological examinations performed by B. Zólyomi it has been determined that these sediments were deposited from shallow water, under dry and warm climatic conditions.

In the year 1987, Hertelendi performed radiocarbon dating on samples from a peat deposit in the lower portion of boreholes formerly drilled into the lake bed. The peat samples from the lower part of four boreholes were subjected to a pollen analysis performed by Nagy. The results show correlation, that is the results of pollen analysis indicate Allerød and Dyras III, whereas the radiocarbon dating indicates an age of 10 500 to 12 000 yrs BP, that is.

In our investigations, which began in 1981, further isotope-geochemical examinations were performed, on the one hand as a continuation and follow-up of the previous ones, and on the other hand, in order to perform other tasks by introducing new methods.

A contribution to the isotope geochemistry of the lake

^{14}C dating was performed on peat, on samples from an additional 7 boreholes, in order to obtain a dating of the lacustrine sediments. To give a paleo-climatological reconstruction, ^{13}C and ^{18}O dating were also performed on samples from the water in Lake Balaton, the autochthonous lacustrine carbonate mud, mollusc shells collected from the sediment, and on samples from the carbonate rocks and carbonate-bearing unconsolidated deposits in the catchment area of Lake Balaton. In addition, ^{137}Cs and ^{134}Cs dating were also performed, in order to determine the rate of underwater reworking of lacustrine deposits, including the rate of their sedimentation. Finally, gamma-gamma insitu measurements using an isotope source were also performed in Keszthely Bay in order to facilitate the planning of mud dredging.

Radiocarbon dating of peat samples from Lake Balaton

The ^{14}C dating method has played a very important role in dating the peat strata penetrated by boreholes drilled into the bed of Lake Balaton. Our starting point was that peat had been identified in one-third of the aforementioned boreholes, between the lithologically uniform, unconsolidated lacustrine lime mud and the compact, dominantly pelitic, Upper Pannonian deposits forming the lake basement (Fig. 1). The peat bed, with a thickness of 0.2 to 1.2 m was, in general, the first Quaternary bed to develop, after an intensive erosional and deflational denudation occurring in Pleistocene times in this region, under climatic conditions more favourable than previously, in an area inundated by water. Samples taken from the peat every 10 to 20 cm were subjected to radiocarbon dating.

The radiocarbon dating of peat samples allows us to draw several conclusions of great importance which are as follows: in the area of Lake Balaton the peat development began in the Late Pleistocene, during the Bølling warming-up period following the Oldest Dryas; however, this process lasted a long time in the area of the lake and was the most widespread during the Allerød following the Old Dryas. The youngest peat was formed during the Young Dryas. As shown by the radiocarbon dating of the thickest (1.2 m thick) peat bed penetrated by the boreholes, the peat development occurred over a period of 1200 to 1500 yrs.

Table 1

^{13}C value and radiocarbon age of samples penetrated by boreholes drilled into lake Balaton (the deb-No. refers to the international standard No. of the particular sample)

deb-No.	Borehole No.	Depth interval (in m)	^{13}C	BP age (yrs)
deb- 576	Tó-5	2.03–2.05	-27.85	11250±170
deb- 583	Tó-7	1.85–1.90	-28.62	12080±160
deb- 584	Tó-8	2.18–2.22	-29.30	11500±170
deb- 563	Tó-16	3.80–3.85	-28.68	10490±200
deb-1766	Tó-17	3.00–3.10	-29.28	10140±300
deb-1800	Tó-17	3.10–3.20	-29.19	10350±300
deb-1816	Tó-17	3.20–3.30	-29.00	10590±300
deb-1824	Tó-17	3.30–3.40	-28.10	10800±300
deb-1806	Tó-17	3.40–3.50	-27.96	11370±300
deb-2246	Tó-20	3.00–3.08	-29.56	11460±300
deb-2247	Tó-20	3.08–3.16	-30.95	11680±300
deb-2239	Tó-20	3.16–3.24	-30.83	11660±300
deb-2250	Tó-20	3.24–3.37	-29.15	11620±300
deb-1628	Tó-21	1.80–2.00	-29.14	11110±200
deb-1631	Tó-21	2.75–2.83	-29.74	12280±200
deb-1634	Tó-21	2.83–2.93	-22.60	12340±200
deb-1809	Tó-22	2.80–3.10	-29.18	10980±300
deb-1817	Tó-22	3.30–3.40	-28.67	11560±300
deb-1825	Tó-22	3.40–3.50	-28.93	11950±300
deb-1833	Tó-22	3.50–3.60	-29.00	12490±300
deb-1627	Tó-23	4.75–4.88	-30.2	11860±200
deb-1626	Tó-23	4.88–5.00	-29.49	11800±200
deb-1629	Tó-23	5.00–5.12	-28.65	12060±200
deb-1633	Tó-23	5.12–5.24	-30.53	12020±200
deb-1801	Tó-30	3.90–4.00	-29.28	10960±300
deb-1632	Tó-31	3.40–3.60	-29.56	12210±300
deb-1624	Tó-31	3.60–3.84	-31.79	12490±300
deb-1623	Tó-31	3.80–3.94	-30.24	12020±300

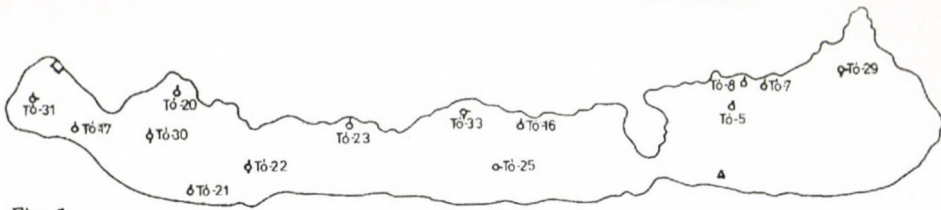


Fig. 1

A layout of boreholes and sampling sites. \odot peat-bearing borehole including radiocarbon dating; \circ borehole, with ^{13}C and ^{18}O tests; ϕ borehole, with ^{137}Cs isotope test; W- water sampling site, for regular ^{18}O test; D- site of experimental dredging

Measuring the stable isotope ratio in samples from the deposits and water of Lake Balaton

Using a mass spectrometer developed by ATOMKI and designed to measure isotope ratio (Hertelendi et al. 1986), measurements were made on the following types of samples in order to experimentally determine the ^{13}C and/or ^{18}O isotope ratios:

1. Carbonates in samples from the Quaternary lime mud penetrated by two boreholes
2. The pore water distilled from samples of the same two boreholes
3. The organic matter of core samples
4. Samples taken from the water of Lake Balaton once a week, over a period of nearly four years
5. Carbonate rocks and carbonate-bearing unconsolidated deposits collected from the catchment area of Lake Balaton (Fig. 1).

In regard to geology, the aim of the experimental measurements was to contribute to the paleoclimatological reconstruction of Lake Balaton and its surroundings by revealing the alternation of stable-isotope ratios including their rules. The following additional explanatory notes are appended to the results of measurements:

- 1) The two boreholes drilled into Lake Balaton were selected for deposits dominantly consisting of autochthonous carbonates. The boreholes were sampled at every 10 cm, and the results of measurements were plotted in a diagram (Figs 2 and 3), then in a co-ordinate system (Fig. 4). The varying character of the isotope ratios vs. depth is identical for both boreholes. Borehole Tó-31 drilled in Keszthely Bay has a less carbonate content than Tó-25, which clearly proves that in addition to the autochthonous carbonates, an enormous amount of allochthonous deposit was also accumulated in the bay. This intensive mud deposition is also the reason for the fact that the variation in isotope ratio vs. depth (thus, vs. time) is less visible in borehole Tó-31 than in borehole Tó-25. Of the curves, especially the ^{18}O curves, with their more positive values visible as a function of depth, well reflect the dry climatic stages (where the

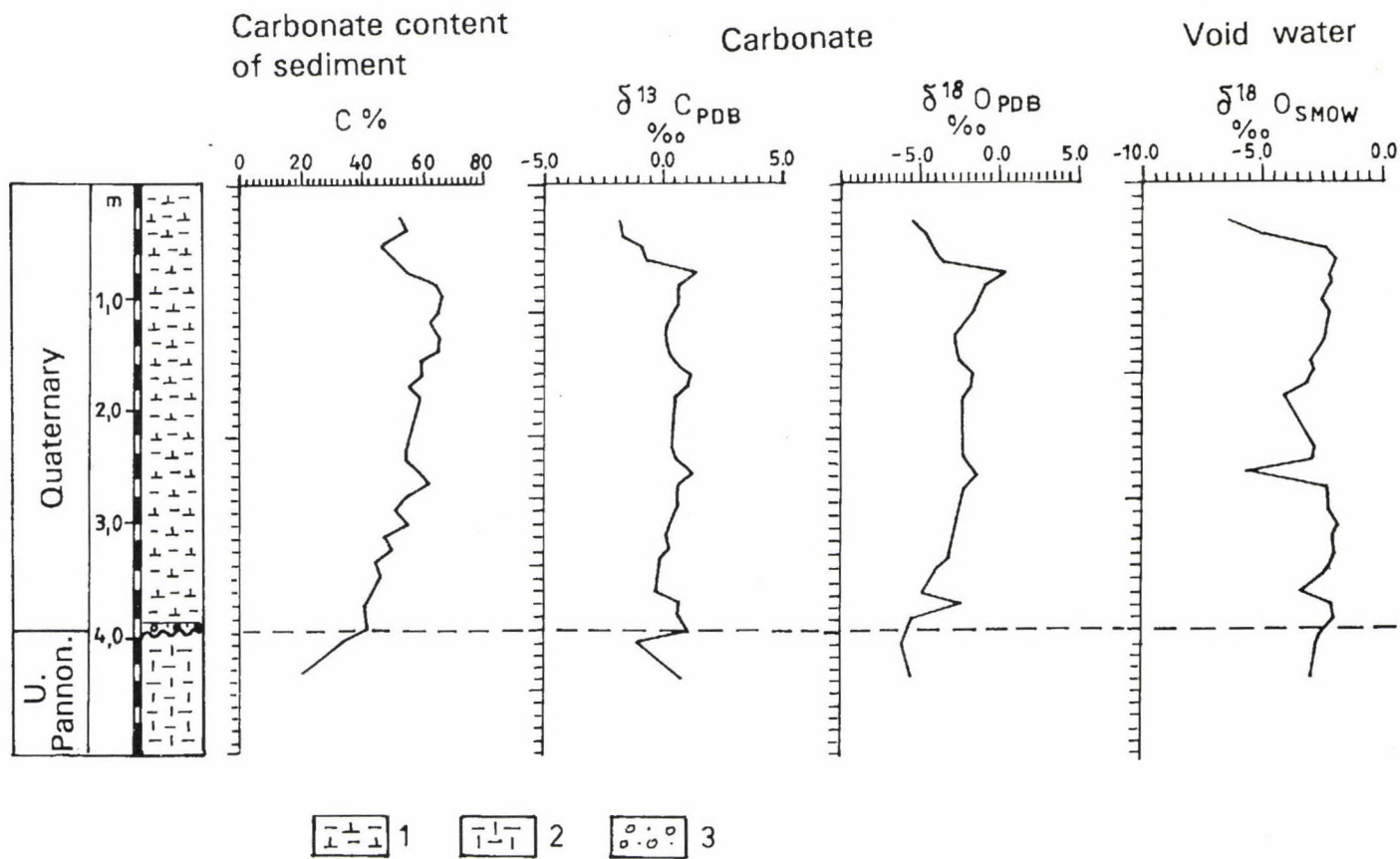


Fig. 2
The ^{13}C and ^{18}O values, vs. depth, measured in samples from borehole Tó-25. 1. calcareous mud; 2. aleurite; 3. sand, gravel

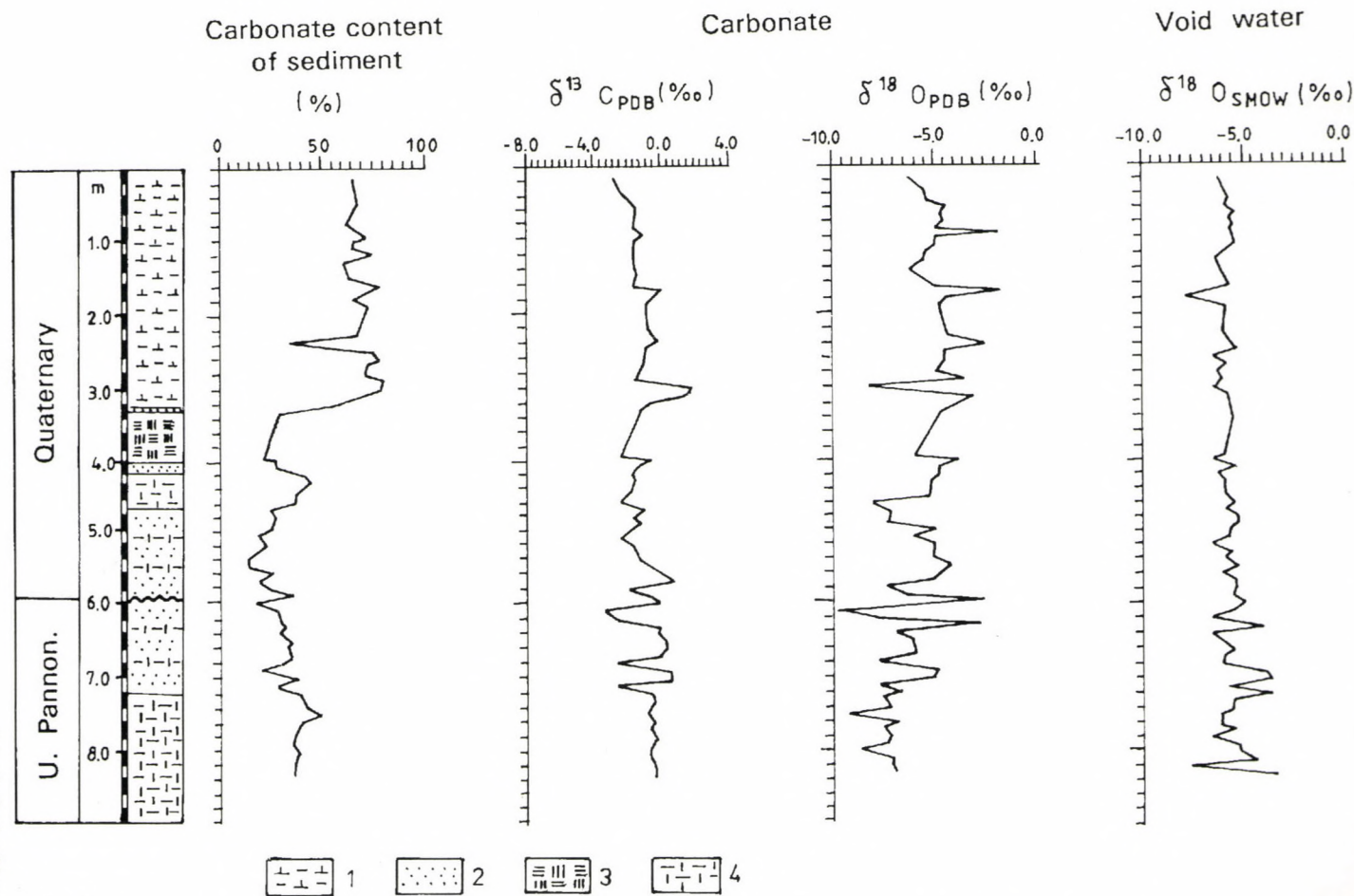


Fig. 3
The ^{13}C and ^{18}O values, vs. depth, measured in samples from borehole Tó-31. 1. calcareous mud; 2. sand; 3. peat; 4. aleurite

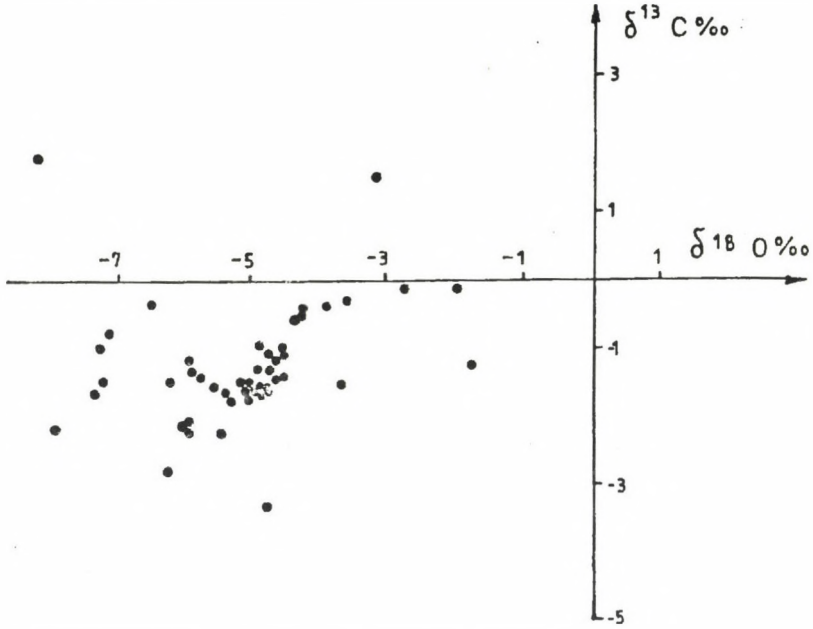


Fig. 4
Relationship between the ^{13}C and ^{18}O values in borehole T6-31

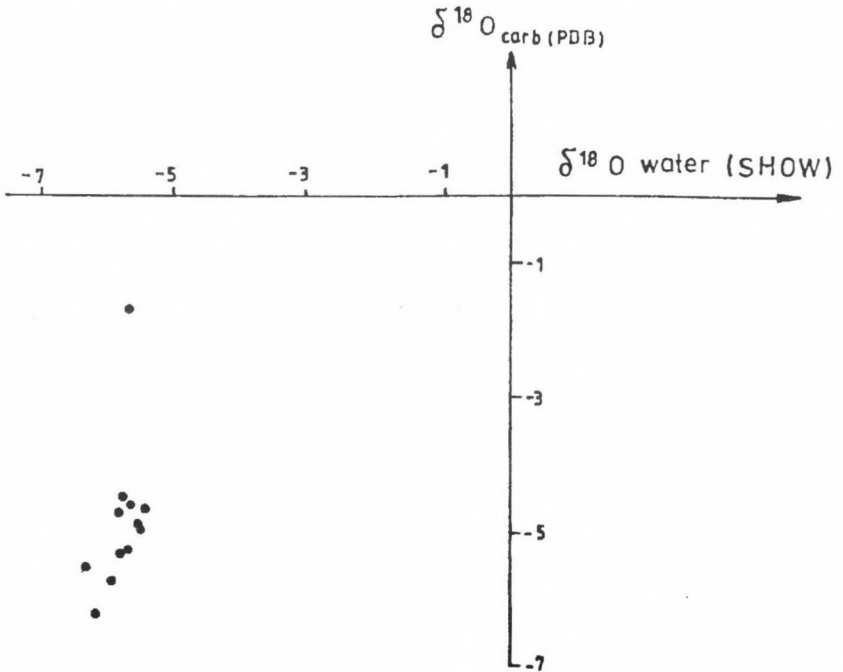


Fig. 5
Relationship between the ^{18}O values of the carbonate and the interstitial water in borehole T6-25

evaporation was intensive) of previous periods. A good correlation has been observed between the ^{13}C and ^{18}O isotope ratios measured on samples from Quaternary deposits.

2) When a common coordinate system is used for the representation of pore water distilled from the core samples and the ^{18}O values of carbonates (Fig. 5), some correlation is visible, although it is well known that the pore water streams upwards when the sediment with a very high water content, when subjected to deposition, becomes compacted, and thus mixed with the pore water deposited simultaneously with the sediment. The latter phenomenon is not too disturbing in the case of a parameter curve of a sequence of a few tens or hundred metres, where, although the transition between the measured values is not sharp, the tendency of changes can be well observed. As far as the sediment is concerned, with a thickness of a few metres (as in Lake Balaton), where the sampling interval of 10 cm can be compared, in regard to the order of magnitude, with the part of mixing with pore water, the correlation shown in Fig. 5 can be considered to be appropriate.

3) From several boreholes, gastropods were collected. Of these, the shells of the species *Lithoglyphus naticoides*, occurring throughout the borehole, and here and there in mass, were separated by P. Sümegi, because we assumed that if the ^{18}O and ^{13}C isotope ratios of the calcareous tests vary in the same way as the isotope ratios corresponding to the total carbonate of the deposits, then it would mean that the dominant, partly allochthonous carbonate content of the deposit, transported from the water catchment area, is negligible. Based on the isotope ratio of *Lithoglyphus* shell, three subdivisions have been established in the boreholes. Of these, only the middle one, that is, the Early Holocene one, was so rich in carbonate shells as to ensure that the measurements can be reliably evaluated. At this section (in which, by the way, the occurrence of gastropodal remains in mass was observed), the isotope ratios slowly shifted in a positive direction (Fig. 6). This indicates the increasing evaporation of the lake, due to the warming of the climate and a decrease in precipitation.

4) The organic matter in samples taken from borehole Tó-31 at intervals of 10 cm was subjected to ^{13}C measurement. In this examination, we again started from the fact that the change in ^{13}C isotope ratio of the organic matter (accumulated together with the deposit) showed a tendency similar to the corresponding values of the total carbonate of the deposit and the calcareous tests of the gastropods. The results were plotted vs. depth (Fig. 7). This clearly shows that a certain tendency can be observed in the ^{13}C isotope values of the organic matter. For peat beds, and beds with a high organic matter content, the ^{13}C values are much more negative. The explanation for this is the increased amount of carbon atoms which are present.

The ^{13}C values are more positive for the Upper Pannonian deposits forming the basement than for the Quaternary deposits. This supported the selection of the unconformity boundaries.

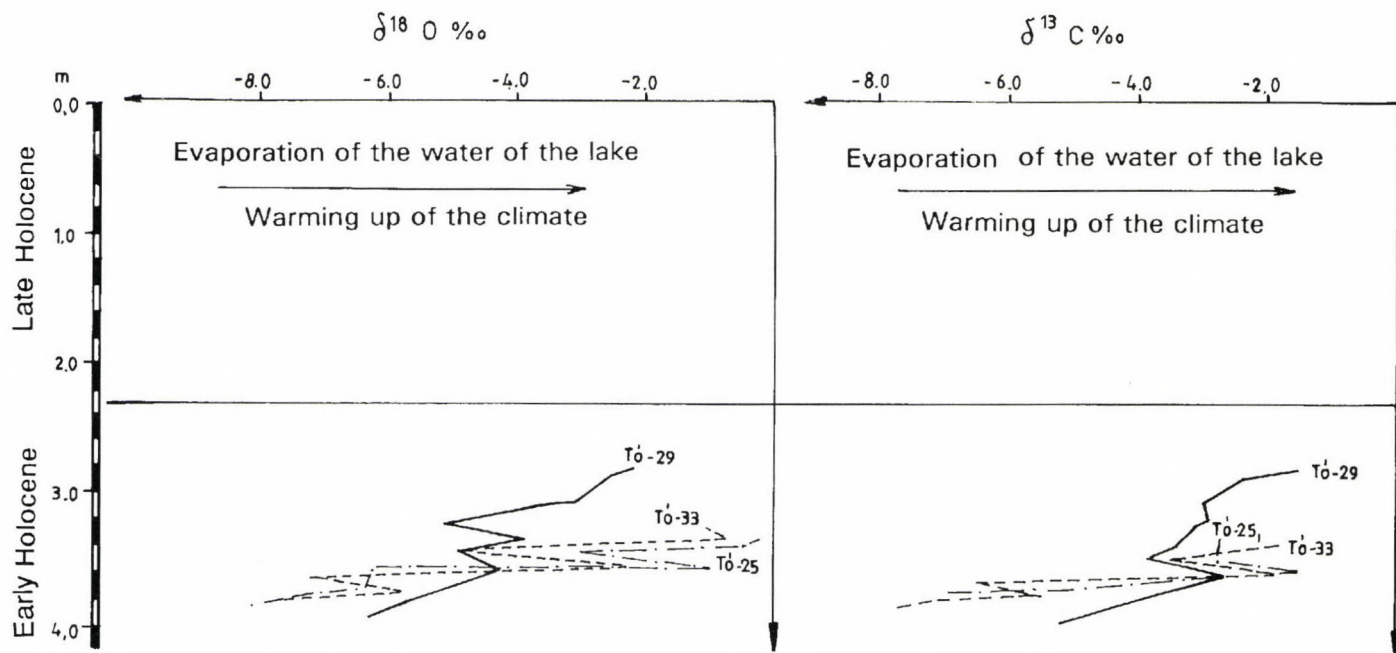


Fig. 6
The variation of ^{13}C and ^{18}O values vs. depth, in the carbonate test of *Lithoglyphus naticoides* (Gastropoda)

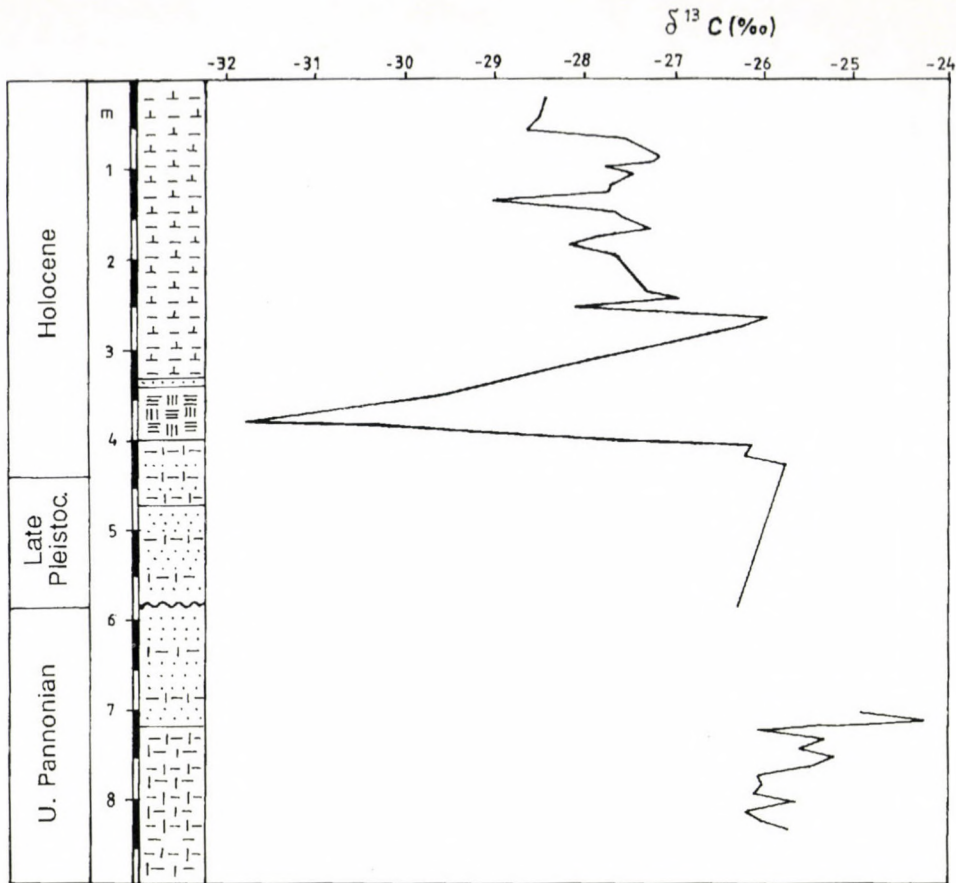


Fig. 7

The variation of ^{13}C value vs. depth, in the organic matter taken from borehole T6-31

5) During the period from July 1991 to January 1995, the water in Lake Balaton was sampled once a week, at Balatonszékplak, approx. 1 km off-shore. The aim of the series of measurement was to clarify the average ^{18}O value of water in Lake Balaton, the order of magnitude of its seasonal variation, and the influence of temperature and precipitation (the water level) on the tendency of oxygen isotope ratio of the water. Then, the values of ^{18}O and temperature of the present water in the lake and the ^{13}C and ^{18}O values of the recently formed carbonates would allow us to obtain a relationship between the temperature and the isotope ratios of carbonates, which also can be projected to the former stages of the lake. The results from the measurements were plotted in a diagram (Fig. 8). For the water samples, the ^{18}O value varied within the range of 0 to -2‰ , and, as shown by a polynomial matched to the curve, the amplitude of the variation was between 0.9 and 1.0‰ , attaining the most positive value at the

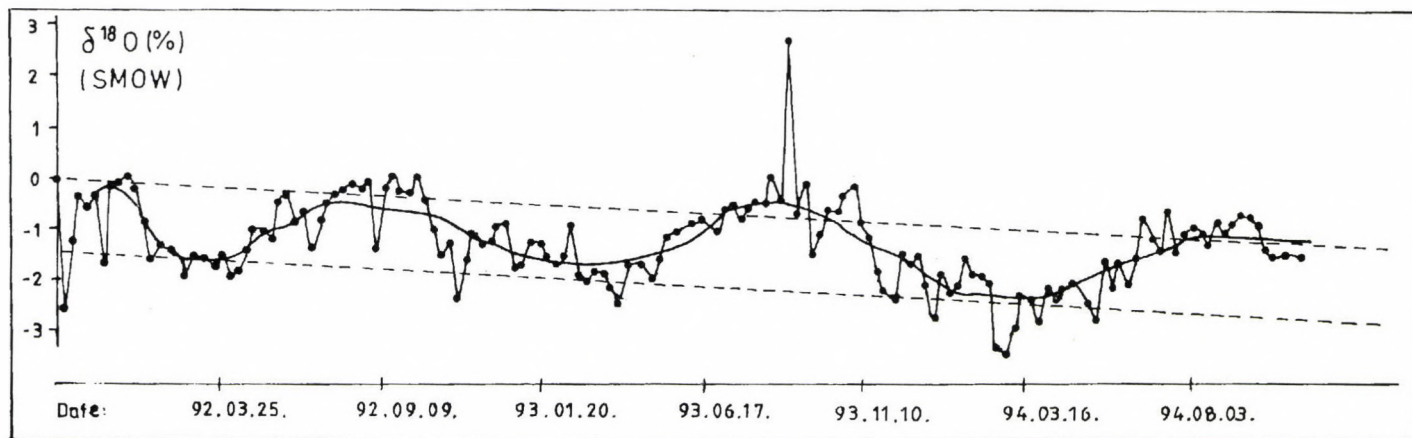


Fig. 8
The ^{18}O value of the water of Lake Balaton during 1991–1995.

end of the summer, and the most negative value in the beginning of springtime. This can be excellently correlated with the weather conditions prevailing in the area of the lake: in summertime the intensive evaporation from the lake surface (approx. 1 mm/day) and the great deficiency in precipitation causes the water of the lake to be enriched with heavy oxygen isotope, and the measured ^{18}O value becomes more positive. For the precipitation and waterflows in Hungary, the ^{18}O value varies in the range from -4 to -12 ‰. Moreover, in wintertime a thick ice layer also prevents the lake from evaporating; thus, it is easy to understand the more negative ^{18}O value measured during the abundance of water in springtime.

We have failed to find any correlation between ^{18}O values of the mud surface carbonates and the water. The explanation for this is that, on the one hand, the seasonal changes take place too rapidly, and on the other hand, that the sediment is whirled up, several times a year, by the storms over the lake.

6) The information content of isotope ratio values measured on the carbonates of the mud in the lake is greatly influenced by the fact that the carbonates are not formed *in situ* but are transported there from the catchment area. To eliminate this factor, it would be advisable to select, in general, a pilot area where the geologic background is free of carbonate. However, in the case of Lake Balaton this is impossible; therefore, the most widespread carbonate rocks and carbonate-bearing sediments in the catchment area were sampled and tested for isotope ratios, in order to have a knowledge of the ^{13}C and ^{18}O values of allochthonous carbonates, and to clarify their possible proportion in the Balaton mud. The measured values allow us to draw the following conclusion: the ^{13}C and ^{18}O values of potentially transported carbonates are separate from those of the Quaternary lacustrine deposits.

Testing the samples from boreholes drilled in lake Balaton, for artificial and natural isotopes

A brief description of the method applied

The distribution of radioactive isotopes of artificial or natural origin encountered in a particular geologic environment (as with the stable isotope ratio) preserves a great number of valuable pieces of information on recent, or former transport processes, or geochemical alterations.

Of the radioactive isotopes of artificial origin, in regard to its quantity and occurrence, the ^{137}Cs nuclide is of great importance. Due to nuclear explosions in the atmosphere and nuclear plant accidents, it is present in the northern and southern hemisphere alike, as an anthropogenic isotope contaminant. Its half-life (30 yrs) is a brief period on a geological scale. Thus, it only allows us to study, or trace, mainly surface processes which take place rapidly (for instance, sedimentary conditions in rivers, lakes).

During the Chernobyl nuclear accident, a mixture of 1:2 of ^{134}Cs isotope and ^{137}Cs isotope was released into the environment. During the period of a couple of years following this accident, an opportunity was provided to give an assessment of the ratio of isotope of Chernobyl origin (^{137}Cs new) and of the isotope (^{137}Cs old) originating from former nuclear weapon tests performed in the atmosphere.

Together with the determination of the artificial isotope ratios, a few natural radioactive isotopes were also measured. Of them, in regard to its occurrence, the ^{40}K nuclide, and the three radioactive decomposition series (uranium, thorium, actinium) are of greatest importance.

Results of our investigations

The measurements of natural and artificial isotopes were performed, on the request of the Hungarian Geological Institute, by the Department for Radiology at the National Food Investigation Institute. The uppermost, 50 to 80 cm thick mud layer of four boreholes were sampled, uniformly, at every 2 cm. The aim of the bed-by-bed radiological test of the samples was to determine the activity-concentration of the ^{134}Cs and ^{137}Cs isotopes and the gamma-radiating isotopes in the particular mud bed (see as a sample Fig. 9).

The results from the measurements were expected to give an answer to the following questions:

- 1) Can the maxima of fall-out concerning the nuclear test in the atmosphere and the Chernobyl accident be detected in the mud in Lake Balaton?
- 2) Should the above values be known, which is the mud development rate at the particular area?
- 3) Is the rate of mud development uniform throughout all of Lake Balaton?
- 4) What thickness of the upper part of the mud is stirred up during the storms over the lake?
- 5) Does any transport of underwater deposit take place in the lake?

In accordance with the specific topics, four of the boreholes drilled in 1989 were selected. In the selection, we were also helped by a Landsat satellite image showing the lake. The satellite image clearly showed the areas where the water contained a large amount of floating sediments (the area of borehole Tó-33), or where the amount of floating mud was average (boreholes Tó-22 and Tó-30), and where mud transport was likely (borehole Tó-29).

The activity values for borehole samples Tó-22, Tó-29 and Tó-30 show a similar trend, that is, gradual decrease with an increasing depth. This phenomenon may be linked with the greater organic matter content of the surface layers of the mud and with its higher capacity to absorb uranium and thorium. It can also be observed that the amounts of the three major isotopes of natural origin (^{238}U , ^{232}Th , ^{40}K) show a good correlation with one another throughout, which is in accordance with the conclusions deduced from the other sedimentological, soil physical, mineralo-petrological and geochemical

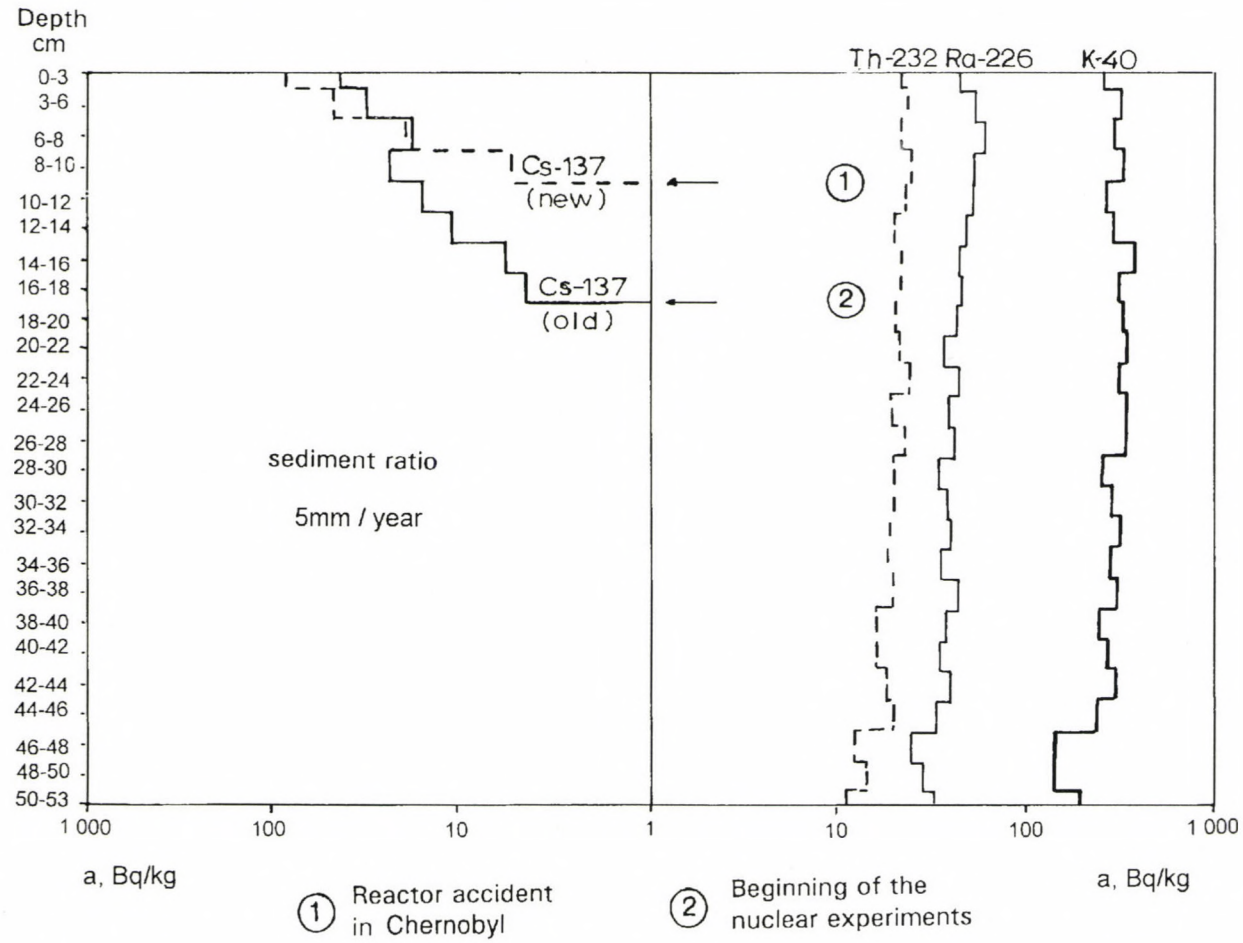


Fig. 9
The variation of natural and artificial isotopes vs. depth, in borehole Tó-22

parameters of the beds. All these show that the samples from these three boreholes were undisturbed.

For borehole Tó-33, the situation is different. The tendency observed in the examination of the other samples is reversed at a depth of 41 to 46 cm – with an adherence to the proportionality between the isotopes – and starts to increase, to 51 cm. Then, the activity concentration for all the three natural nuclides will remain constant. It should be noted that these stable values are similar to the values of subsurface ^{238}U , ^{232}Th and ^{40}K activities of samples from the other boreholes.

The variation of activity values for cesium which entered due to an anthropogenic contamination shows a completely different picture as compared to the natural isotopes. For samples from boreholes Tó-22 and Tó-30, although the curve of cesium activity concentration is similar, the depth at which the new and the old ^{137}Cs occur is essentially different. For borehole Tó-22, the $^{137}\text{Cs}(\text{new})$ and the $^{137}\text{Cs}(\text{old})$ appear at a depth of 11 cm and 21 cm, respectively, whereas for Tó-30, the $^{137}\text{Cs}(\text{new})$ and the $^{137}\text{Cs}(\text{old})$ appear at a depth of 31 cm and 55 cm, respectively. As far as the profile from Tó-29 is concerned, no ^{137}Cs isotope resulting either from the Chernobyl accident, or from atmospheric nuclear test explosions, could be detected. For sample Tó-33, the old cesium can be detected almost continuously, nearly in every section, however, new cesium only appears at a depth of 45 to 51 cm. Comparing this very surprising result with the distribution of natural isotopes vs. depth allows us to conclude that the profile is likely to preserve traces of an enormous reworking process.

As shown by the results from our measurements, it is possible to detect, in the mud of lake Balaton, the artificial radioactive isotope contaminations which entered the atmosphere from the 50s. In some cases, the peaks of radioisotope amounts associated with the nuclear test explosions in the atmosphere performed before the Nuclear Test Ban of 1962 (old ^{137}Cs), and with the amounts of radioisotopes which entered the atmosphere during the Chernobyl reactor accident (new ^{137}Cs), and then deposited, are well visible. Based on boreholes Tó-22 and 30, in the knowledge of the above results, the rate of mud development can be determined in the vicinity of the particular borehole. Under undisturbed hydrological conditions, this rate was, during the past forty years, 1.4 cm/year in the middle of Szigliget Bay, and 0.5 cm/year at the eastern boundary of the bay. The rate of mud development shows not only local differences but a variation of intensity in time as well: as shown by the occurrence of the contamination resulting from the Chernobyl accident, the intensity of mud deposition shows a rapidly increasing tendency: in the past 5 years these values were, for the aforesaid regions of Szigliget Bay, 6 cm/year, and 2 cm/year, respectively. Moreover, data on borehole Tó-29 indicate a transport of underwater depositions, whereas borehole Tó-33 indicates an additional depositional accumulation taking place in the lake. The occurrence of each ^{137}Cs isotope peak in the depth range of 2 to 3 m indicates that the storms over Lake Balaton cause an approx. 2 to 3 cm thick layer to mix up.

Case study of using ^{137}Cs isotope measurements

In recent decade, the eutrophication and mud development rate have shown an extraordinary increase in Lake Balaton, particularly in Keszthely Bay. The Water Control Authority has taken efficient and powerful measures (establishment of water reservoirs at Kis-Balaton, layer and deep dredging actions in the aforesaid bay), in order to save the lake.

When testing the dredging efficiency of a hydromechanical dredge equipped with a special head, and manufactured within the PHARE program, including its application in Keszthely Bay, it became necessary to perform several geologic, geophysical and geochemical analyses.

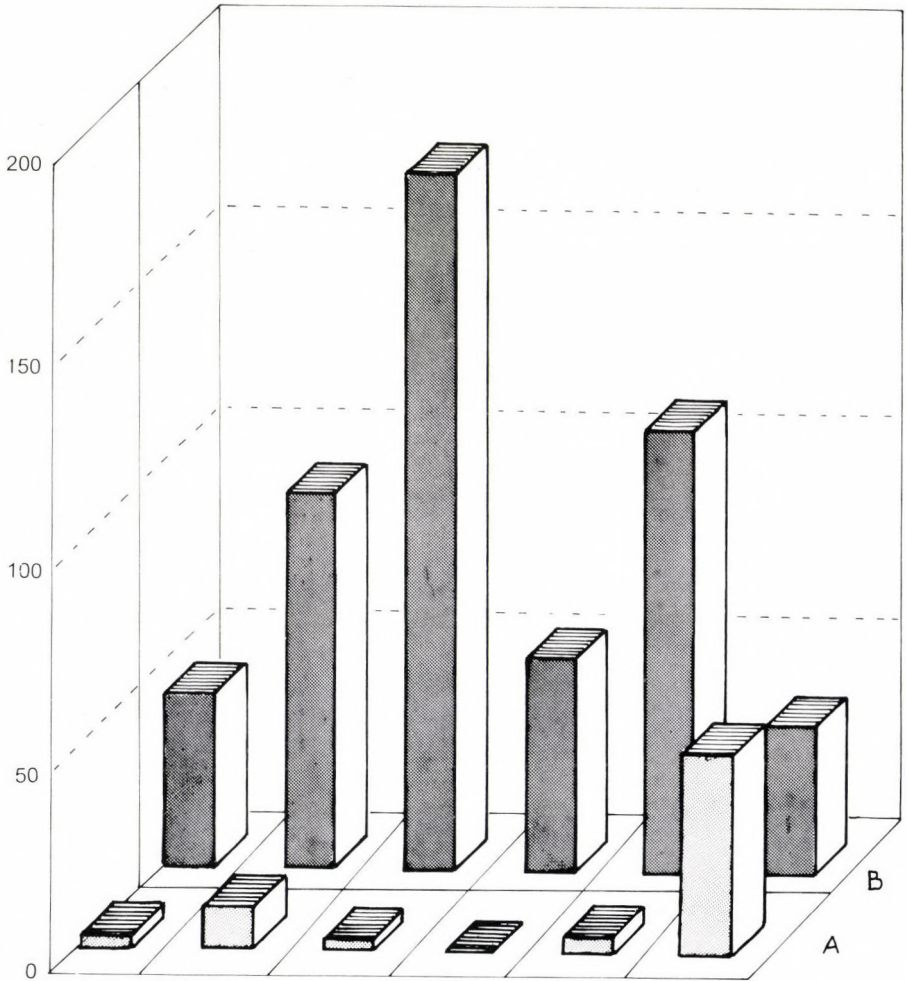
For this purpose, in-situ geophysical measurements and sampling were performed at 6 allocated sites in the dredging area, in order to have a better knowledge of the physical, mineralogical and geochemical properties of the sediments. The sampling and the insitu geophysical measurements were made twice, prior to and after dredging. The insitu measurement were performed using a ^{137}Cs isotope probe, parallel with sampling, by the Well-Logging Team of MAELGI.

The precise knowledge of mud density according to depth was an issue of great importance, in order to determine the amount of the dredged material and the dredging efficiency. As shown by the measurement, the boundary between the mud and the water is not sharp. The bulk density gradually increases from 1.0 g/cm^3 to 1.5 g/cm^3 , then, it is stabilized, for the latter value, within the measurement range of 1 m.

When examining the density values obtained after dredging, it can be observed that this feature of the mud reaches the limit of 1.5 g/cm^3 more rapidly towards depth. This has led us to the conclusion that a layer with a thickness of approx. 20 cm was removed by the dredging. The results from the in-situ measurements were also suitable for use in the follow-up of the result of a former geophysical survey. The colloidal mud thickness map compiled as a result of the seismo-acoustical logging performed in 1987 shows the thickness of this upper mud layer with a volumetric weight not exceeding 1.5 g/cm^3 .

At the points of in-situ geophysical measurements, samples were also taken for isotope-geochemical tests. The aim of these tests were (1) to control the success of dredging, (2) to make clear whether there is a natural mud motion at the boundary between the water and the deposit in the particular area, and (3) to assess the rate of mud accumulation in the particular region. The above tasks were solved by performing high sensitivity gamma-spectrometry tests on the lower and upper parts of 5 cm of the 30 cm thick samples collected at the sampling sites. At the Department for Radiology of the National Food Investigation Institute, the activity concentration of old and new ^{137}Cs isotopes and gamma-radiating isotopes of the samples were determined. The variation of activity of ^{137}Cs and of a few radioactive isotope of natural origin (^{210}Pb , ^{40}K) can be explained by the fact that the density of phytoplankton playing a

Activity concentration



sampling	1	2	3	4	5	6	dredging
	43,1	93,3	173	53,05	110	36,8 *	before
	3,36	10,4	2,9	0	4,62	49,83 *	A after

Fig. 10 ^{137}Cs isotope value, prior to and after experimental dredging, in Keszthely Bay. * - without dredging

major role in sedimentation is different in each subbasin of Lake Balaton, and that the chemical elements that were concentrated in their organism in considerable amounts, after their destruction, also accumulated over a corresponding extent.

The isotope-geochemical results concerning samples taken after dredging show that the dredging action was successful (Fig. 10), although the activity concentration values measured in the upper samples indicate that some mud is transported back to the formerly dredged area. In the surroundings of the area subjected to dredging (in the NNW area of Keszthely Bay, at a distance of some 1.5 to 2 km W of the Keszthely mole), the rate of deposition was approx. 1 cm/year.

Conclusions

In a complex geologic research project, several new methods were introduced in order to perform our scheduled tasks. Of these methods, the isotope-geochemical tests have proved to be very efficient, allowing us to have a better understanding of a few questions concerning the environmental status of Lake Balaton (rate of mud deposition, physical properties and underwater motion of mud etc.), and to have a better knowledge of formerly known items (the age of Lake Balaton, a reconstruction of the climate of its environment etc.). Of the results we have achieved, the major ones are as follows:

1) In the area of Lake Balaton, peat development started in the beginning of the Late-Pleistocene (Bølling), but this process lasted approx. 1500 years in the area of some subbasins of the lake and was the most widespread in the Allerød;

2) The oxygen isotope ratios measured on the autochthonous carbonate deposits in the lake and on the carbonate tests of gastropods are influenced mainly by the evaporation of water. In addition, the latter indirectly also depends on the climatic conditions of the particular region. The measured values of oxygen isotope ratios allow us to trace the gradual warming-up of the climate which began in Holocene times.

3) The major part of the carbonate content of deposits in the lake were formed *insitu*. Only a negligible part thereof was transported from the catchment area.

4) On the comparative analysis of tendencies of the ^{18}O value of the water in Lake Balaton and the weather conditions, it can be stated that the oxygen isotope ratio of the water in Lake Balaton, due to the intensive evaporation of the water, is close to that of sea-water and considerably differs from the relevant values of rivers and meteoric water in Hungary. In Hungary, the average ^{18}O value is -9.5% , for meteoric water, related to sea-water. In the oxygen isotope ratio of the water of Lake Balaton, well-visible seasonal changes can be observed.

5) Part of the organic matter included in the mud of the lake originates from the reuse of the biological carbon formerly accumulated. This process has been going on since the time the lake was developed, which implies a relative enrichment in ^{13}C .

6) The artificial radio-isotope contaminations entering the atmosphere from 1950 to present can be well traced in the mud of the lake. Their occurrence and maximum peaks have allowed us to determine the rate of mud development. Under undisturbed hydrological conditions, this value ranges from 0.5 cm/year to 1.4 cm/year, as a function of the measurement points. The rate of mud development varies vs. time, and in recent years, it has showed a dramatically increasing tendency (2 to 6 cm/year). At some points of Lake Balaton, an underwater transport of the deposit, at other point the accumulation of this transported deposit take place. As shown by our measurements, a 2 to 3 cm thick layer is mixed up by the storms over the lake.

Acknowledgements

Of the above investigations, the topics titled Radiocarbon dating on peat samples from lake Balaton, and Measurement of stable isotope ratio values on deposits in Lake Balaton or on older deposits, were financed by the Central Office of Geology, whereas the fund allowing us to perform the tasks referred to as the ^{18}O analysis of the water of Lake Balaton and the measurement of natural and artificial isotope ratios of deposits in Lake Balaton was provided by OTKA 550. The Siófok Office of KDT-VIZIG commissioned us to perform the work associated with environmental protection, in Keszthely Bay.

The authors wish to express their thanks to the aforesaid institutes for allowing them to achieve the results described in this paper.

References

- Baranyi, S. 1979: A Balaton hidrológiai viszonyai (Hydrology of Lake Balaton). – In: Baranyi, S. (Ed.) A Balaton kutatási eredményeinek összefoglalása () Vízügyi Gazd. Tájé., 112, VIZDOK, pp. 128–176.
- Bendefy, L., I. Nagy 1969: A Balaton évszázados partvonalváltozásai (Secular changes of the Lake Balaton's shore line). – Műszaki Könyvkiadó, Budapest (in Hungarian).
- Bodor, E. 1987: Formation of the Lake Balaton palynological aspects. – In: Pécsi, M., Kordos, L. (eds.). Holocene environment in Hungary. Budapest, Geogr. Res. Ins. Hung. Acad. of Sci. pp. 77–80.
- Bruckner-Wein, A. 1988: Az 1982. évi balatoni aktuálgeológiai kutatás során mélyült fúrások szervesgeokémiai vizsgálata (Actual geological drilling in Lake Balaton 1982: organic geochemistry). – Földt. Int. Évi Jel. 1986-ról, pp. 581–609 (Summary in English).
- Bulla, B. 1958: A Balaton és környéke földrajzi kutatásairól. (Geographical exploration of Lake Balaton and its surroundings). – Földr. Közlem., 6, 82, 4, pp. 313–324.
- Csernyí, T. 1984: Relation of clay content and some lithophysical characteristics of Upper Pannonian sedimentary rocks based on the evidence obtained in the course of mapping of the surroundings of Lake Balaton. – Proc. 6th Conference on Soil Mech. and Found. Eng., Budapest.
- Csernyí, T. 1987: Result of recent investigations of the Lake Balaton deposits. – In: Pécsi, M. and Kordos, L. (eds.). Holocene environment in Hungary. Budapest, Geogr. Res. Ins. Hung. Acad. of Sci. pp. 67–76.
- Csernyí, T. 1990: Some results of engineering geological mapping in the Lake Balaton region. – In: Price D. G. (Ed.): Proceedings Sixth International Congress International Association of Engineering Geology, 6–10 August 1990, Amsterdam, Netherlands, pp. 79–84.
- Csernyí, T., R. Corrada 1989: Complex geological investigation of Lake Balaton (Hungary) and its results. – Acta Geol. Hung., 32, 1–2, pp. 117–130.

- Cserny, T., E. Nagy-Bodor, M. Hajós 1991: Contributions to the sedimentology and evolution history of Lake Balaton. – In: Pécsi, M., F. Schweitzer, F. (Eds.) Quaternary environment in Hungary. Studies in Geography in Hungary 26, pp. 75–84, Akadémiai Kiadó.
- Friedman, I., J.R. O'Neil 1977: Compilation of stable isotope fractionation factors of geochemical interest. – In: Data of Geochemistry 6th, USGS Prof. Paper 440-KK
- Gonfiantini, R. 1983: Advisory group meeting on stable isotope reference samples for geochemical and hydrological investigations. – IAEA, Vienna, p. 19
- Herodek, S., F. Máté 1984: Eutrophication and its reversibility in Lake Balaton (Hungary). – Proceedings of SHIGA Conference'84 on Conservation and Management of World Lake Environment, Leccs (Japan), abstract.
- Hertelendi, E., J. Gál, A. Paál, S. Fekete, M. Györffi, I. Gál, Zs. Kertész, S. Nagy 1986: Stable isotope mass spectrometer. – In: Wand U., G. Strauch (Eds) Fourth Working Meeting Isotopes in Nature – Akademie der Wissenschaften der DDR, Zentralinstitut für Isotopen und Strahlenforschung, Leipzig, p. 323.
- Hertelendi, E., É. Csongor, L. Záborszky, J. Molnár, J. Gál, M. Györffi, S. Nagy 1989a: Counter system for high precision ¹⁴C dating. – Radiocarbon, 31, 3, p. 399.
- Libby, W.F. 1955: Radiocarbon Dating. – (The University of Chicago Press)
- Libby, W.F. 1967: Radioactive Dating and Methods of Low-level Counting (International Atomic Energy Agency, Vienna) p. 3
- Lingenfelter, R.E., R. Ramaty 1970: Radiocarbon Variations and Absolute Chronology. – Nobel Symp. 12, Ingrid U. Olsson (Ed.) Almqvist and Wiksell, Stockholm, p. 513
- Lóczy, L. sen. 1913: A Balaton tudományos tanulmányozásának eredményei. I. A Balaton környékének geológiai képződményei és ezeknek vidékek szerinti telepedése (Results of the scientific investigations of the Balaton region. I. Geological formations of the Balaton area and their regional distribution), pp. 541–567 (in Hungarian)
- Marosi, S., J. Szilárd 1981: A Balaton kialakulása (The formation of Lake Balaton). – Földrajzi Közl., 29, 1, pp. 1–30.
- Máté, F. 1987: A Balaton meder recens üledékeinek térképezése (Mapping of the recent sediments of the bottom of Lake Balaton). – Földt. Int. Évi Jel. 1985-ről, pp. 366–379.
- Miháltz-Faragó, M. 1982: Palynológiai vizsgálatok a Balaton fenékmintáin (Palynological examination of bottom samples from Lake Balaton). – Földt. Int. Évi Jel. 1981-ről, pp. 439–448.
- Mike, K. 1980a: Ósmedernyomok a Balaton környékén (Ancient traces of river beds around Lake Balaton). – Földr. Ér., 29, 2–3, pp. 313–332.
- Mike, K. 1980b: A Balaton környéki neotektonika (Neotectonic feature of the Lake Balaton surrounding). – Földr. Közlem., 28, 104, 3, pp. 185–204.
- Müller, G. 1970: High-magnesian calcite and protodolomite in Lake Balaton (Hungary) sediments. – Nature, 22, 5247 pp. 749–750.
- Müller, G., F. Wagner 1978: Holocene carbonate evolution in Lake Balaton (Hungary): a response to climate and impact of man. – In: Modern and ancient lake sediments. Blackwell Sci. Publ., pp. 57–81.
- Rónai, A. 1969: The geology of Lake Balaton and surroundings. – Mitt. Internat. Verein. Limnol., 17, pp. 275–281.
- Sebestyén, O. 1951: A Balaton biológiai kutatásának korszerű szempontjai (Modern aspects of biological investigations of Lake Balaton). – Hidr. Közl., pp. 20–23.
- Somlyódy, L. 1983: A Balaton eutrofizálódása (Eutrophication of Lake Balaton). – VITUKI Közl., 38, pp. 1–62.
- Szesztay, K. et al. 1966: A Balaton feliszapodásával kapcsolatos kutatások 1963–1964 (Investigations of the filling up of the Lake Balaton, 1963–1964). Manuscript (in Hungarian).
- Vörös, L., K. Balogh, F. Máté, L. Ligeti 1984: A feltöltődés meghatározása paleolimnológiai módszerekkel (Determination of the filling up by palaeolimnological methods). – Vízügyi Közl., 66, 1, pp. 104–113.
- Willkomm, H. 1976: Alterbestimmungen im Quartär. – (Verlag Karl Thieme, München)

- Zólyomi, B. 1952: Magyarország növénytakarójának fejlődéstörténete az utolsó jégkorszaktól (Evolution of vegetation in Hungary since the last glacial). – MTA Biol. Oszt. Közl. 1, 4, pp. 491–553.
- Zólyomi, B. 1969: A Balaton iszaprétegeinek kormeghatározása virágporvizsgálatok alapján (Dating of the mud-layers of Lake Balaton by Sporomorphs). – Tájékoztató az állóvizek hidrológiai feltárásáról. - VITUKI spec. paper.
- Zólyomi, B. 1987: Degree and rate of sedimentation in Lake Balaton. – In Pécsi, M. (Ed.): Pleistocene environment in Hungary – Contribution of the INQUA Hungarian National Committee to the XIIth INQUA Congress Ottawa, Canada, 1987, pp. 57–79.

**ACTA GEOLOGICA
HUNGARICA**

Editor-in-Chief

J. Haas

Volume 38

APR 11 1953
RECORDED TO 96/2153

ACTA GEOLOGICA HUNGARICA

Vol. 38

Contents

Number 1

Facies characteristics of the Lofer cycles in the Upper Triassic platform carbonates of the Transdanubian Range, Hungary. <i>J. Haas, A. Balog</i>	1
Environmental significance of the Anisian Ostracoda fauna from the Forrás Hill near Felsőörs (Balaton Highland, Transdanubia, Hungary). <i>M. Monostori</i>	37
Crystallization conditions of pegmatites from the Velence Mts, western Hungary, on the basis of thermobarometric studies. <i>F. Molnár, K. Török, P. Jones</i>	57
Results of the research of the abiotic component of the environment in the Greater Bratislava area. <i>J. Hricko, J. Viskup, J. Vozár</i>	81
The main tasks of ecogeologic research in Bulgaria. <i>T. A. Todorov</i>	89

Number 2

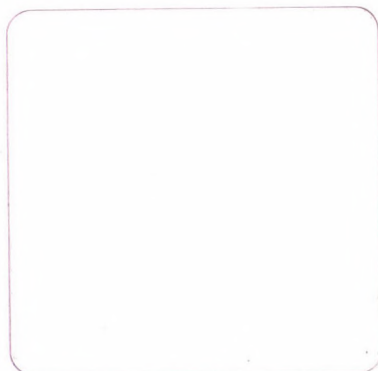
Early Alpine shelf evolution in the Hungarian segments of the Tethys margin. <i>J. Haas, S. Kovács, Á. Török</i>	95
Contribution to the Upper Triassic geology of the Keszthely Mountains (Transdanubian Range), western Hungary. <i>G. Csillag, T. Budai, L. Gyalog, L. Koloszfár</i>	111
Different types of orogens and orogenic processes, with reference to Southern and Central Europe. <i>G. Zolnai</i>	131

Number 3

Data on the (Upper Permian) Foraminifer fauna of the Nagyvisnyó Limestone Formation from borehole Mályinka-8 (Northern Hungary). <i>A. Bérczi-Makk, L. Csontos, P. Pelikán</i> ..	185
Clay mineralogy of Jurassic carbonate rocks, Central Transdanubia, Hungary. <i>I. Viczián</i> ..	251
Mamura Formation (Lower Cretaceous), Western Desert, Egypt. <i>A. M. A. El Sayed</i> ..	269
Amos Salvador (Ed.) 1994: International Stratigraphic Guide. <i>G. Császár</i>	283

Number 4

On the present state of geological research in Hungary. Gy. Bárdossy, M. Csongrádi, J. Haas, T. Kecskeméti	285
Biotite in a Paleozoic metagreywacke complex, Mecsek Mountains, Hungary: conditions of low-T metamorphism deduced from illite and chlorite crystallinity, coal rank, white mica geobarometric and microstructural data. P. Árkai, Cs. Lantai, Gy. Lelkes-Felvérdi, G. Nagy	293
Palynostratigraphy of the Upper Triassic formations in the Mecsek Mts (Southern Hungary). J. Bóna	319
Results of isotope-geochemical studies in sedimentological and environmental geologic investigations of Lake Balaton. T. Csérnyi, E. Hertelendi, S. Tarján	355



GUIDELINES FOR AUTHORS

Acta Geologica Hungarica is an English-language quarterly publishing papers on geological topics. Besides papers on outstanding scientific achievements, on the main lines of geological research in Hungary, and on the geology of the Alpine–Carpathian–Dinaric region, reports on workshops of geological research, on major scientific meetings, and on contributions to international research projects will be accepted.

Only original papers will be published and a copy of the Publishing Agreement will be sent to the authors of papers accepted for publication. Manuscripts will be processed only after receiving the signed copy of the agreement.

Manuscripts are to be sent to the Editorial Office for refereeing, editing, in two typewritten copies, on floppy disk with two printed copies, or by E-mail. Manuscripts written by the following word processors will be accepted: MS Word, WordPerfect, or ASCII format. Authors are requested to sign and send to the Editor a Publishing Agreement after the manuscript has been accepted by the Editorial Board. Acceptance depends on the opinion of two referees and the decision of the Editorial Board.

Form of manuscripts

The paper complete with abstract, figures, tables, and bibliography should not exceed 25 pages (25 double-spaced lines with 3 cm margins on both sides).

The first page should include:

- the title of the paper (with minuscule letters)
- the full name of the author
- the name of the institution and city where the work was prepared
- an abstract of not more than 200 words
- a list of five to ten key words
- a footnote with the postal address of the author

The SI (System International) should be used for all units of measurements.

References

In text citations the author's name and the year of publication between brackets should be given. The reference list should contain the family name, a comma, the abbreviation of the first name, the year of publication, and a colon. This is followed by the title of the paper. Paper titles are followed – after a long hyphen – by periodical title, volume number, and inclusive page numbers. For books the title (English version), the name of the publisher, the place of publication, and the number of pages should be given.

Figures and tables

Figures and tables should be referred to in the text. Figures are expected in the size of the final type-area of the quarterly (12.6 x 18.6) or proportionally magnified 20–25% camera ready quality. Figures should be clear line drawings or good quality black-and-white photographic prints. Colour photographs will also be accepted, but the extra cost of reproduction in colour must be borne by the authors (in 1995 US\$ 260 per page). The author's name and figure number should be indicated on the back of each figure. Tables should be typed on separate sheets with a number.

Proof and reprints

The authors will be sent a set of proofs. Each of the pages should be proofread, signed, and returned to the Editorial Office within a week of receipt. Fifty reprints are supplied free of charge, additional reprints may be ordered.

Contents

On the present state of geological research in Hungary. <i>Gy. Bárdossy, M. Csongrádi, J. Haas, T. Kecskeméti</i>	285
Biotite in a Paleozoic metagreywacke complex, Mecsek Mountains, Hungary: conditions of low-T metamorphism deduced from illite and chlorite crystallinity, coal rank, white mica geobarometric and microstructural data. <i>P. Árkai, Cs. Lantai, Gy. Lelkes-Felvári, G. Nagy</i> .	293
Palynostratigraphy of the Upper Triassic formations in the Mecsek Mts (Southern Hungary). <i>J. Bóna</i>	319
Results of isotope-geochemical studies in sedimentological and environmental geologic investigations of Lake Balaton. <i>T. Csernyei, E. Hertelendi, S. Tarján</i>	355